

COMMUNICATIONS

FACULTY OF SCIENCES
UNIVERSITY OF ANKARA

DE LA FACULTE DES SCIENCES
DE L'UNIVERSITE D'ANKARA

Series A1: Mathematics and Statistics

VOLUME: 72

Number: 4

YEAR: 2023

Faculty of Sciences, Ankara University
06100 Beşevler, Ankara-Turkey

ISSN 1303-5991 e-ISSN 2618-6470

C O M M U N I C A T I O N S

FACULTY OF SCIENCES
UNIVERSITY OF ANKARA

DE LA FACULTE DES SCIENCES
DE L'UNIVERSITE D'ANKARA

Series A1: Mathematics and Statistics

Volume: 72

Number: 4

Year: 2023

Owner (Sahibi)

Sait HALICIOĞLU, Dean of Faculty of Sciences

Editor in Chief (Yazı İşleri Müdürü)

Fatma KARAKOÇ (Ankara University)

Associate Editor

Arzu ÜNAL (Ankara University)

Managing Editor

Elif DEMİRCİ (Ankara University)

Area Editors

Nuri OZALP (Applied Mathematics)	Murat OLGUN (Functional Analysis, Fuzzy Set Theory, Decision Making)	Burcu UNGOR (Module Theory)	Halil AYDOĞDU (Stochastic Process-Probability)
Arzu ÜNAL (Partial Differential Equations)	Gülen TUNCA (Analysis-Operator Theory)	Elif TAN (Number Theory, Combinatorics)	Olçay ARSLAN (Robust Statistics-Regression-Distribution Theory)
Elif DEMİRCİ (Mathematical Modelling-Comput. Mathematics)	Mehmet UNVER (Analysis, Fuzzy Set Theory, Decision Making)	Ahmet ARIKAN (Group Theory)	Birdal SENOĞLU (Theory of Statistics & Applied Statistics)
Gizem SEYHAN OZTEPE (Differential Equations)	Oktay DUMAN (Summability and Approximation Theory)	Tuğçe ÇALCI (Ring Theory)	Yılmaz AKDİ (Econometrics-Mathematical Statistics)
Abdullah ÖZBEKLER (Differential Equations and Inequalities)	İshak ALTUN (Topology)	İsmail GÖK (Geometry)	Mehmet YILMAZ (Computational Statistics)
Hijaz AHMAD (Numerical Analysis-Mathematical Techniques)	Sevda SAĞIROĞLU PEKER (Topology)	İbrahim Ünal (Differential Geometry, Differential Topology)	Cemal ATAKAN (Multivariate Analysis)
Shengda ZENG (Mathematical modeling of physical systems, Applications of PDEs)			

Editors

P. AGARWAL Anand Int. College of Eng., INDIA	R. P. AGARWAL Texas A&M University, USA	M. AKHMET METU, TURKEY	A. ATANGANA University of the Free State, SOUTH AFRICA
A. AYTUNA METU, retired, TURKEY	E. BAIRAMOV Ankara University, TURKEY	H. BEREKETOĞLU Ankara University, TURKEY	H. BOZDOĞAN University of Tennessee, USA
C. Y. CHAN University of Louisiana, USA	A. EDEN Boğaziçi University, retired, TURKEY	A. B. EKİN Ankara University, TURKEY	D. GEORGIU University of Patras, GREECE
V. GREGORI Universitat Politècnica de València, SPAIN	V. S. GULIYEV Nat. Acad. of Sciences, AZERBAIJAN	A. HARMANCI Hacettepe University, TURKEY	F. HATHOUT Université de Saïda, ALGERIA
K. ILARSLAN Kırıkkale University, TURKEY	A. KABASINSKAS Kaunas Univ. of Tech. LITHUANIA	V. KALANTAROV Koç University, TURKEY	Sandi KLAVŽAR University of Ljubljana, SLOVENIA
A. M. KRALL The Pennsylvania State University, USA	H. T. LIU Tatung University, TAIWAN	V. N. MISHRA Indira Gandhi National Tribal University, INDIA	C. ORHAN Ankara University, retired, TURKEY
M. PITUK University of Pannonia, HUNGARY	S. ROMAGUERA Universitat Politècnica de València, SPAIN	H. M. SRIVASTAVA University of Victoria, CANADA	I. P. STAVROULAKIS Univ. of Ioannina, GREECE
S. YARDIMCI Ankara University, TURKEY			

This Journal is published four issues in a year by the Faculty of Sciences, University of Ankara. Articles and any other material published in this journal represent the opinions of the author(s) and should not be construed to reflect the opinions of the Editor(s) and the Publisher(s).

Correspondence Address:
COMMUNICATIONS EDITORIAL OFFICE
Ankara University, Faculty of Sciences,
06100 Tandoğan, ANKARA – TURKEY
Tel: (90) 312-2126720 Fax: (90) 312-2235000
e-mail: commun@science.ankara.edu.tr
<http://communications.science.ankara.edu.tr/index.php?series=A1>

Print:
Ankara University Press
İncitaş Sokak No:10 06510 Beşevler
ANKARA – TURKEY
Tel: (90) 312-2136655

C O M M U N I C A T I O N S

FACULTY OF SCIENCES
UNIVERSITY OF ANKARA

DE LA FACULTE DES SCIENCES
DE L'UNIVERSITE D'ANKARA

Series A1: Mathematics and Statistics

VOLUME: 72

Number: 4

YEAR: 2023

Faculty of Sciences, Ankara University
06100 Beşevler, Ankara-Turkey

ISSN 1303-5991 e-ISSN 2618-6470

C O M M U N I C A T I O N S

FACULTY OF SCIENCES
UNIVERSITY OF ANKARA

DE LA FACULTE DES SCIENCES DE
L'UNIVERSITE D'ANKARA

Series A1: Mathematics and Statistics

Volume: 72

Number: 4

Year: 2023

Research Articles

Semra YURTTANÇIKMAZ, On the curves lying on parallel-like surfaces of the ruled surface in E^3	867
Süleyman ŞENYURT, Davut CANLI, Elif ÇAN, Sümeyye GÜR MAZLUM, Another application of Smarandache based ruled surfaces with the Darboux vector according to Frenet frame in E^3	880
Fatma TOKMAK FEN, Mehmet Onur FEN, Modulo periodic Poisson stable solutions of dynamic equations on a time scale.....	907
Thatayaone MOAKOFI, Broderick OLUYEDE, The type I heavy-tailed odd power generalized Weibull-G family of distributions with applications.....	921
Esra BAŞARIR NOYAN, Yılmaz GÜNDÜZALP, Quasi hemi-slant pseudo-Riemannian submersions in para-complex geometry.....	959
Jeevitha KANNAN, Vimala JAYAKUMAR, Sustainable method for tender selection using linear Diophantine multi-fuzzy soft set.....	976
Nurettin IRMAK, A Diophantine equation including Fibonacci and Fibonomial coefficients.....	992
Babar SULTAN, Mehvish SULTAN, Ferit GÜRBÜZ, BMO estimate for the higher order commutators of Marcinkiewicz integral operator on grand variable Herz-Morrey spaces.....	1000
Asia K, Shahid KHAN, Demonstration of the strength of strong convexity via Jensen's gap.....	1019
Melike KARTA, Numerical approximation with the splitting algorithm to a solution of the modified regularized long wave equation.....	1034
Yıldırım ÇELİK, Renewed structure of neutrosophic soft graphs and its application in decision-making problem.....	1055
Özgül İLHAN, Osman Raşit IŞIK, Simge BOZKURT, Numerical analysis of a time relaxation finite difference method for the heat equation.....	1077
Hazal CEYHAN, Ebru YANIK, Zehra OZDEMİR, Anholonomic co-ordinates and electromagnetic curves with alternative moving frame via Maxwell evolution.....	1094
Çağla SEKİN, Mehmet Emin TAMAR, İlham ALİYEV, New proofs of Fejer's and discrete Hermite-Hadamard inequalities with applications.....	1110
Hesham MOUSTAFA, Mansour MAHMOUD, Ahmed TALAT, Some bounds for the k-generalized digamma function.....	1126
Güler Başak ÖZNUR, Güher Gülçehre ÖZBEY, Yelda AYGAR KÜÇÜKEVCİLİOĞLU, Rabia AKTAŞ, Miscellaneous properties of Sturm-Liouville problems in multiplicative calculus.....	1141
Angelın KAVITHA RAJ, S. N. Suber BATHUSHA, Satham HUSSAIN, Self centered interval-valued intuitionistic fuzzy graph with an application.....	1155
Nezaket JAVANSHIR, Filiz YILDIZ, Various results on some asymmetric types of density.....	1173
Cengiz GAZELOĞLU, Asuman ZEYTİNOĞLU, Nurullah YILMAZ, A new multidimensional model II regression based on bisector approach.....	1187
Tuğba YAVUZ, Şahsene ALTINKAYA, Sharp coefficient estimates for \mathfrak{S} -spirallike functions involving generalized q-integral operator.....	1201

ON THE CURVES LYING ON PARALLEL-LIKE SURFACES OF THE RULED SURFACE IN E^3

Semra YURTTANCIKMAZ

Atatürk University, Faculty of Science, Department of Mathematics, Erzurum, TÜRKİYE

ABSTRACT. In this paper, it has been researched curves lying on parallel-like surfaces M^f of the ruled surface M in E^3 . Using the definition of parallel-like surfaces it has been found parametric expressions of parallel-like surface of the ruled surface and image curve of the directrix curve of the base surface. Moreover, obtaining Darboux frames of curves lying on surfaces M and M^f , it has been compared the geodesic curvatures, the normal curvatures and the geodesic torsions of these curves.

1. INTRODUCTION

Ruled surfaces are surfaces that attract the attention of many researchers, especially differential geometers, and make them work on these surfaces from past to present. These surfaces have been obtained by the motion of a straight line on a curve in space, also called the directrix of the surface. Since ruled surfaces have a particularly simple structure, they are important for use in many fields such as architecture, engineering, mechanics, kinematics and CAD computer aided design, etc. as well as differential geometry [1, 3, 6, 7, 15].

Parallel-like surfaces are the surfaces obtained as a result of the generalization of parallel surfaces. These surfaces were first described by Tarakcı and Hacısalihoğlu in 2002 and named with surfaces at a constant distance from the edge of regression on a surface [17]. The authors have obtained by considering a surface instead of a curve in the paper written by Hans Vogler. He has defined notion of curve at a constant distance from the edge of regression on a curve. In 2004, Tarakcı and Hacısalihoğlu have computed for parallel-like surfaces some properties and theorems given for parallel surfaces [16]. After this work, it's made many articles by different authors on parallel-like surfaces. In 2010, Sağlam and Kalkan have

2020 *Mathematics Subject Classification.* 53A04, 53A05.

Keywords. Ruled surface, parallel-like surface, Darboux frame.

✉ semrakaya@atauni.edu.tr; 📞 0000-0001-6712-3687.

searched parallel-like surfaces in E_1^3 Minkowski space [12]. In 2015, Yurttañıkmağ and Tarakcı have established a relationship between focal surfaces and parallel-like surfaces. They have obtained focal surfaces using parallel-like surfaces, that is, an alternative way of finding focal surfaces of any surface via parallel-like surfaces was demonstrated [18]. From this point of view, the geometric structure of parallel-like surfaces has an important place in the field of line congruence and therefore in the field of visualization (see [5]). And finally, in 2023, Yurttañıkmağ and Tarakcı have researched image curves on the parallel-like Surfaces in E^3 [19].

In this study, the parametric expression of the parallel like surface of the ruled surface was obtained and the differences between these surfaces were examined in terms of differential geometric properties. In general, it has been shown that the parallel like surface of the ruled surface is also not a ruled surface, but if the directrix curve is selected as the parameter curve, this surface also preserves its characteristics of being a ruled surface.

Since curves lying on the surface have an important place in terms of the theory of curves, it has attracted the attention of many geometers [8, 10, 13, 14]. In the theory of surfaces, the Darboux frame constructed at any non-umbilical point of the surface can be viewed as an analog of the Frenet frame. In here, obtaining β image curve lying on M^f parallel-like surface of M ruled surface, Darboux frames of curve-surface pairs (α, M) and (β, M^f) have been calculated at any points P on M and $f(P)$ on M^f . Finally, it has been compared the geodesic curvatures, the normal curvatures, the geodesic torsions of reference curve α on M and its image curve β on M^f and expressed the relationships between these two curves.

2. PRELIMINARIES

Let α be a unit speed curve lying on a surface M in E^3 and s be arc length of the curve α , i.e. $\|\alpha'(s)\| = 1$. Suppose that Z is a unit normal vector of the surface M and T is unit tangent vector field of the curve α . Considering the vector field Y defined by $Y = Z \times T$, set of $\{T, Y, Z\}$ create orthonormal frame which is called Darboux frame for partner of curve-surface (α, M) .

Thus, the geodesic curvature κ_g , the normal curvature κ_n , the geodesic torsion t_r of the curve $\alpha(s)$ can be calculated as follows

$$\kappa_g = \langle \alpha''(s), Y \rangle \quad (1)$$

$$\kappa_n = \langle \alpha''(s), Z_{\alpha(s)} \rangle \quad (2)$$

$$t_r = -\langle Z'_{\alpha(s)}, Y \rangle. \quad (3)$$

Besides, the derivative formulas of the Darboux frame of (α, M) is given by

$$\begin{bmatrix} T' \\ Y' \\ Z' \end{bmatrix} = \begin{bmatrix} 0 & \kappa_g & \kappa_n \\ -\kappa_g & 0 & t_r \\ -\kappa_n & -t_r & 0 \end{bmatrix} \begin{bmatrix} T \\ Y \\ Z \end{bmatrix}. \tag{4}$$

In addition, given an arbitrary curve $\beta(s)$ on the surface M under the condition $\|\beta'(s)\| = C$, the geodesic curvature κ_g , the normal curvature κ_n , the geodesic torsion t_r of the curve $\beta(s)$ can be calculated as follows

$$\kappa_g = \frac{1}{C^2} \langle \beta''(s), Y \rangle \tag{5}$$

$$\kappa_n = \frac{1}{C^2} \langle \beta''(s), Z_{\beta(s)} \rangle \tag{6}$$

$$t_r = -\frac{1}{C} \langle Z'_{\beta(s)}, Y \rangle. \tag{7}$$

Furthermore, in the differential geometry of surfaces, for a curve $\alpha(s)$ lying on a surface M the followings are well-known

- i) $\alpha(s)$ is a geodesic curve $\iff \kappa_g = 0$,
- ii) $\alpha(s)$ is an asymptotic curve $\iff \kappa_n = 0$,
- iii) $\alpha(s)$ is a principal line $\iff t_r = 0$ [2,9,11].

3. PARALLEL-LIKE SURFACES

Definition 1. Let M and M^f be two surfaces in Euclidean space E^3 and Z_P be a unit normal vector and $T_P M$ be tangent space at point P of the surface M and $\{X_P, Y_P\}$ be an orthonormal bases of $T_P M$. Take a unit vector $E_P = d_1 X_P + d_2 Y_P + d_3 Z_P$, where $d_1, d_2, d_3 \in \mathbb{R}$ are constants and $d_1^2 + d_2^2 + d_3^2 = 1$. If there is a function f defined by,

$$f : M \rightarrow M^f, \quad f(P) = P + rE_P$$

where $r \in \mathbb{R}$, then the surface M^f is called parallel-like surface of the surface M .

Here, if $d_1 = d_2 = 0$, then $E_P = Z_P$ and so M and M^f are parallel surfaces. Now, we represent parametrization for parallel-like surface of the surface M . Let (ϕ, U) be a parametrization of M , so we can write that

$$\begin{aligned} \phi & : U \subset E^2 \mapsto M. \\ (u, v) & \mapsto \phi(u, v) \end{aligned}$$

In the case $\{\phi_u, \phi_v\}$ is a bases of $T_P M$, then we can write that $E_P = d_1 \phi_u + d_2 \phi_v + d_3 Z_P$. Where, ϕ_u, ϕ_v are respectively partial derivatives of ϕ according to u and v . Since $M^f = \{f(P) : f(P) = P + rE_P\}$, a parametric representation of M^f is

$$\psi(u, v) = \phi(u, v) + rE(u, v).$$

Thus, it's obtained

$$M^f = \{\psi(u, v) : \psi(u, v) = \phi(u, v) + r(d_1 \phi_u(u, v) + d_2 \phi_v(u, v) + d_3 Z(u, v))\}$$

and if we get $rd_1 = \lambda_1$, $rd_2 = \lambda_2$, $rd_3 = \lambda_3$, then we have

$$M^f = \left\{ \psi(u, v) : \psi(u, v) = \phi(u, v) + \lambda_1 \phi_u(u, v) + \lambda_2 \phi_v(u, v) + \lambda_3 Z(u, v), \right. \\ \left. \lambda_1^2 + \lambda_2^2 + \lambda_3^2 = r^2 \right\}$$

Calculation of ψ_u and ψ_v gives us that

$$\psi_u = \phi_u + \lambda_1 \phi_{uu} + \lambda_2 \phi_{vu} + \lambda_3 Z_u \quad (8)$$

$$\psi_v = \phi_v + \lambda_1 \phi_{uv} + \lambda_2 \phi_{vv} + \lambda_3 Z_v.$$

Here $\phi_{uu}, \phi_{vu}, \phi_{uv}, \phi_{vv}, Z_u, Z_v$ are calculated as like as [17]. Suppose that parameter curves are curvature lines of M and let u and v be arc length of these curves. Thus, following equations are obtained

$$\begin{aligned} \phi_{uu} &= -\kappa_1 Z \\ \phi_{vv} &= -\kappa_2 Z \\ \phi_{uv} &= \phi_{vu} = 0 \\ Z_u &= \kappa_1 \phi_u \\ Z_v &= \kappa_2 \phi_v. \end{aligned} \quad (9)$$

From [8] and [9], we find

$$\psi_u = (1 + \lambda_3 \kappa_1) \phi_u - \lambda_1 \kappa_1 Z$$

$$\psi_v = (1 + \lambda_3 \kappa_2) \phi_v - \lambda_2 \kappa_2 Z$$

and $\{\psi_u, \psi_v\}$ be a bases of $\chi(M^f)$. If we denote by Z^f unit normal vector of M^f , then Z^f is

$$Z^f = \frac{\psi_u \times \psi_v}{\|\psi_u \times \psi_v\|} = \frac{\lambda_1 \kappa_1 (1 + \lambda_3 \kappa_2) \phi_u + \lambda_2 \kappa_2 (1 + \lambda_3 \kappa_1) \phi_v + (1 + \lambda_3 \kappa_1) (1 + \lambda_3 \kappa_2) Z}{\sqrt{\lambda_1^2 \kappa_1^2 (1 + \lambda_3 \kappa_2)^2 + \lambda_2^2 \kappa_2^2 (1 + \lambda_3 \kappa_1)^2 + (1 + \lambda_3 \kappa_1)^2 (1 + \lambda_3 \kappa_2)^2}}$$

where, κ_1, κ_2 are principal curvatures of the surface M . If

$$A = \sqrt{\lambda_1^2 \kappa_1^2 (1 + \lambda_3 \kappa_2)^2 + \lambda_2^2 \kappa_2^2 (1 + \lambda_3 \kappa_1)^2 + (1 + \lambda_3 \kappa_1)^2 (1 + \lambda_3 \kappa_2)^2}$$

we can write

$$Z^f = \frac{\lambda_1 \kappa_1 (1 + \lambda_3 \kappa_2)}{A} \phi_u + \frac{\lambda_2 \kappa_2 (1 + \lambda_3 \kappa_1)}{A} \phi_v + \frac{(1 + \lambda_3 \kappa_1) (1 + \lambda_3 \kappa_2)}{A} Z.$$

Here in case of $\kappa_1 = \kappa_2$ and $\lambda_3 = -\frac{1}{\kappa_1} = -\frac{1}{\kappa_2}$ since ψ_u and ψ_v are not linear independent, M^f is not regular surface. We will not consider this case [17].

4. PARALLEL-LIKE SURFACES OF RULED-SURFACES

Ruled surfaces are surfaces formed by the movement of a straight line based on a curve called the directrix curve in space. This moving straight line is called a

”generator”. The parametric expression of the ruled surface M with the directrix curve $\alpha(u)$ and the direction vector $X(u)$ along the generator is

$$\phi(u, v) = \alpha(u) + vX(u). \tag{10}$$

Considering the definition of the parallel-like surface, it is clear that parametrization of the parallel-like surface of the ruled surface will be

$$\begin{aligned} \psi(u, v) &= \phi(u, v) + \lambda_1\phi_u(u, v) + \lambda_2\phi_v(u, v) + \lambda_3Z(u, v) \\ &= \alpha(u) + vX(u) + \lambda_1\left(\alpha'(u) + vX'(u)\right) + \lambda_2X(u) + \lambda_3\frac{\phi_u \times \phi_v}{\|\phi_u \times \phi_v\|}. \end{aligned} \tag{11}$$

Let’s assume that the directrix curve α of the ruled surface M is given by the arc parameter and the tangent vector X on the directrix is the unit vector for any parameter u . If the unit tangent vector of the directrix curve α is $\alpha'(u) = \frac{d\alpha}{du} = T$, the unit normal of the ruled surface M is Z and the curve α is chosen with the condition $\langle T, X \rangle = 0$, the triple $\{T, X, Z\}$ becomes an orthonormal basis along the directrix curve. In order to express the parameterization of the parallel-like surface of the ruled surface more simply, we will find the variation of the triple $\{T, X, Z\}$ along the curve α , that is, the covariant derivatives of each tangent vector with respect to T . If the covariant derivatives of both sides of the equations $\langle T, T \rangle = \langle X, X \rangle = \langle Z, Z \rangle = 1$ along the curve α is calculated with respect to T , it has been obtained the equations $\langle D_T T, T \rangle + \langle T, D_T T \rangle = 0 \Rightarrow 2\langle D_T T, T \rangle = 0 \Rightarrow \langle D_T T, T \rangle = 0$ and similarly $\langle D_T X, X \rangle = 0$ and $\langle D_T Z, Z \rangle = 0$. Here, if $a = \langle D_T T, X \rangle$, $b = \langle D_T T, Z \rangle$, $c = \langle D_T X, Z \rangle$, so it is achieved following matrix [\[4\]](#)

$$\begin{bmatrix} D_T T \\ D_T X \\ D_T Z \end{bmatrix} = \begin{bmatrix} 0 & a & b \\ -a & 0 & c \\ -b & -c & 0 \end{bmatrix} \begin{bmatrix} T \\ X \\ Z \end{bmatrix}. \tag{12}$$

If these equations are substituted in equation [\[12\]](#), parametric expression of parallel-like surface of ruled surface is as follows

$$\begin{aligned} \psi(u, v) &= \alpha(u) + vX + \lambda_1(T + v(-aT + cZ)) + \lambda_2X + \lambda_3\left(\frac{-cvT + (1 - av)Z}{\sqrt{c^2v^2 + (1 - av)^2}}\right) \\ &= \alpha(u) + \left((1 - av)\lambda_1 - \frac{cv\lambda_3}{\sqrt{c^2v^2 + (1 - av)^2}}\right)T \\ &\quad + (v + \lambda_2)X + \left(cv\lambda_1 + \frac{\lambda_3(1 - av)}{\sqrt{c^2v^2 + (1 - av)^2}}\right)Z \end{aligned}$$

and in other words

$$\begin{aligned} \psi(u, v) = & \alpha(u) + \left(X - a\lambda_1 T + c\lambda_1 Z - \frac{c\lambda_3 T + a\lambda_3 Z}{\sqrt{c^2 v^2 + (1 - av)^2}} \right) v \\ & + \lambda_1 T + \lambda_2 X + \frac{\lambda_3}{\sqrt{c^2 v^2 + (1 - av)^2}} Z \end{aligned} \quad (13)$$

is obtained. Is equation [13](#) also a ruled surface? It will now be investigated whether the parallel-like surface of the ruled surface is also a ruled surface or can be under certain conditions.

Consider the ruled surface given by equation $\phi(u, v) = \alpha(u) + vX(u)$. If the directrix curve α of the ruled surface M is chosen as the first parameter curve, then it is obtained that (see chapter 5)

$$\phi_u = \alpha'(u) = T. \quad (14)$$

Moreover, when the partial derivative of the general equation of the ruled surface given by eq. [10](#) is calculated with respect to u , following expressions are found

$$\begin{aligned} \phi_u &= \alpha'(u) + vX'(u) \\ &= T + v(-aT + cZ) \\ &= (1 - av)T + cvZ. \end{aligned} \quad (15)$$

Here, if equations [14](#) and [15](#) are compared, it is concluded that $a = 0$, $c = 0$. Substituting these results in the equation [13](#), then the parallel-like surface of the ruled surface will be

$$\psi(u, v) = \alpha(u) + \lambda_1 T + \lambda_2 X + \lambda_3 Z + vX(u). \quad (16)$$

Considering that the image of a curve on a parallel-like surface is

$$\alpha^f(u) = \beta(u) = \alpha(u) + \lambda_1 T + \lambda_2 X + \lambda_3 Z \quad (17)$$

and substituting eq. [17](#) in eq. [16](#), so we get

$$\psi(u, v) = \beta(u) + vX(u). \quad (18)$$

From here, it is clear that the equation [18](#) also denotes a ruled surface. Thus, the following result can be written.

Corollary 1. *If the directrix curve α of the ruled surface M is chosen as the first parameter curve, then the parallel-like surface of this ruled surface is also ruled surface.*

Now, in case the vector E_P in the definition of the parallel-like surface is chosen more specifically, it will be investigated the change in the parametric expression of the parallel-like surface of the ruled surface and in which cases the obtained surface will also be the ruled surface.

Proposition 1. *In case $\lambda_1 = 0$ in the definition of parallel-like surface, that is, if the vector E_P is lying in the plane $Sp\{\phi_v, Z\}$, then parametric expression of parallel-like surface of the ruled surface is*

$$\psi(u, v) = \alpha(u) - \frac{cv\lambda_3}{\sqrt{c^2v^2 + (1 - av)^2}}T + (v + \lambda_2)X + \frac{\lambda_3(1 - av)}{\sqrt{c^2v^2 + (1 - av)^2}}Z.$$

Proposition 2. *In case $\lambda_2 = 0$ in the definition of parallel-like surface, that is, if the vector E_P is lying in the plane $Sp\{\phi_u, Z\}$, then parametric expression of parallel-like surface of the ruled surface is*

$$\begin{aligned} \psi(u, v) = & \alpha(u) + \left((1 - av)\lambda_1 - \frac{cv\lambda_3}{\sqrt{c^2v^2 + (1 - av)^2}} \right) T \\ & + vX + \left(cv\lambda_1 + \frac{\lambda_3(1 - av)}{\sqrt{c^2v^2 + (1 - av)^2}} \right) Z. \end{aligned}$$

Proposition 3. *In case $\lambda_3 = 0$ in the definition of parallel-like surface, that is, if the vector E_P is lying in the plane $Sp\{\phi_u, \phi_v\}$, then parametric expression of parallel-like surface of the ruled surface is*

$$\psi(u, v) = \alpha(u) + \lambda_1(1 - av)T + (v + \lambda_2)X + cv\lambda_1Z.$$

Proposition 4. *In case $\lambda_1 = \lambda_2 = 0$ in the definition of parallel-like surface, that is, if the vector E_P is in the direction of the normal vector Z , then parametric expression of parallel-like surface of the ruled surface is*

$$\psi(u, v) = \alpha(u) - \frac{cv\lambda_3}{\sqrt{c^2v^2 + (1 - av)^2}}T + vX + \frac{\lambda_3(1 - av)}{\sqrt{c^2v^2 + (1 - av)^2}}Z.$$

Proposition 5. *In case $\lambda_2 = \lambda_3 = 0$ in the definition of parallel-like surface, that is, if the vector E_P is in the direction of the vector ϕ_u , then parametric expression of parallel-like surface of the ruled surface is*

$$\psi(u, v) = \alpha(u) + \lambda_1(1 - av)T + vX + cv\lambda_1Z.$$

Proposition 6. *In case $\lambda_1 = \lambda_3 = 0$ in the definition of parallel-like surface, that is, if the vector E_P is in the direction of the vector ϕ_v , then parametric expression of parallel-like surface of the ruled surface is*

$$\psi(u, v) = \alpha(u) + (v + \lambda_2)X.$$

5. DARBOUX FRAME OF CURVES LYING ON PARALLEL-LIKE SURFACES OF THE RULED SURFACES

Assuming that the directrix curve α of the ruled surface M given by the equation $\phi(u, v) = \alpha(u) + vX(u)$ is the first parameter curve, then

$$\phi_u = (1 - av)T + cvZ$$

and since u and v are arc parameters of the parameter curves on the ruled surface, $\phi_u = \alpha'(u) = T$ and so, $1 - av = 1$, $cv = 0$. As a result from here, $a = c = 0$, that is, in case the directrix curve α of the ruled surface M is chosen as the first parameter curve, it is seen that the directrix curve α is both the principal curvature line and the geodesic curve. Thus, $\kappa_g = 0$ and $t_r = 0$ for the directrix curve α . Principal directions relating to different curvature lines of the ruled surface M are orthogonal, thus we can take as $\phi_u = \alpha'(u) = T$ and $\phi_v = X$. Under these conditions, we can use Darboux frame $\{T, X, Z\}$ in place of orthonormal frame $\{\phi_u, \phi_v, Z\}$. If we consider definition of parallel-like surface of the ruled surface M , parametric representation of the curve β which is image of the curve α is

$$\beta(u) = \alpha(u) + \lambda_1 T + \lambda_2 X + \lambda_3 Z. \quad (19)$$

Now, we calculate Darboux frame $\{T^f, X^f, Z^f\}$ for partner of curve-surface (β, M^f) . It is clear that

$$T^f = \frac{\beta'(u)}{\|\beta'(u)\|}$$

If we take derivative according to u of eq. (19), we find

$$\beta'(u) = \alpha'(u) + \lambda_1 T' + \lambda_2 X' + \lambda_3 Z'$$

and if considering that $\alpha(u)$ is a principal line and so $t_r = 0$ equations (4) are substituted in this equation, we obtain

$$\beta'(u) = (1 - \kappa_n \lambda_3) T + \kappa_n \lambda_1 Z \quad (20)$$

where $\|\beta'(u)\| = C = \sqrt{(1 - \kappa_n \lambda_3)^2 + \lambda_1^2 \kappa_n^2}$. Thus, we find

$$T^f = \frac{(1 - \kappa_n \lambda_3)}{C} T + \frac{\kappa_n \lambda_1}{C} Z. \quad (21)$$

Moreover, we know already that

$$Z^f = \frac{\lambda_1 \kappa_1 (1 + \lambda_3 \kappa_2)}{A} T + \frac{\lambda_2 \kappa_2 (1 + \lambda_3 \kappa_1)}{A} X + \frac{(1 + \lambda_3 \kappa_1)(1 + \lambda_3 \kappa_2)}{A} Z. \quad (22)$$

For orthonormal frame $\{T^f, X^f, Z^f\}$, if we consider that $X^f = Z^f \times T^f$, we get

$$\begin{aligned} X^f &= \left[\frac{\kappa_n \lambda_1 \lambda_2 (\kappa_2 + \lambda_3 K)}{AC} \right] T \\ &+ \left[\frac{(1 + \lambda_3 H + \lambda_3^2 K)(1 - \kappa_n \lambda_3) - \kappa_n \lambda_1^2 (\kappa_1 + \lambda_3 K)}{AC} \right] X \\ &- \left[\frac{\lambda_2 (\kappa_1 + \lambda_3 K)(1 - \kappa_n \lambda_3)}{AC} \right] Z \end{aligned} \quad (23)$$

where $K = \kappa_1 \kappa_2$, $H = \kappa_1 + \kappa_2$ are Gauss curvature and mean curvature of the surface M , respectively.

Now, we calculate the geodesic curvature κ_g^f , the normal curvature κ_n^f , the geodesic torsion t_r^f of the curve $\beta(u)$. We will use to calculate these curvatures following equations [11](#)

$$\kappa_g^f = \frac{1}{C^2} \langle \beta''(u), X^f \rangle \tag{24}$$

$$\kappa_n^f = \frac{1}{C^2} \langle \beta''(u), Z^f \rangle \tag{25}$$

$$t_r^f = -\frac{1}{C} \langle (Z^f)', X^f \rangle. \tag{26}$$

Firstly we find vector $\beta''(u)$. If we take derivative of eq.[20](#) according to u and use equations [4](#), we obtain

$$\beta''(u) = -(\lambda_3 \kappa_n' + \lambda_1 \kappa_n^2) T + (\lambda_1 \kappa_n' + \kappa_n (1 - \kappa_n \lambda_3)) Z. \tag{27}$$

Furthermore we find vector $(Z^f)'$. If we take derivative of eq.[22](#) according to u and use equations [4](#), we obtain

$$(Z^f)' = \frac{1}{A} \left\{ \begin{array}{l} (\lambda_1 (\kappa_1' + \lambda_3 K') - A^{-1} B \lambda_1 (\kappa_1 + \lambda_3 K) - \kappa_n (1 + \lambda_3 H + \lambda_3^2 K)) T \\ + (\lambda_2 (\kappa_2' + \lambda_3 K') - A^{-1} B \lambda_2 (\kappa_2 + \lambda_3 K)) X \\ + (\lambda_3 H' + \lambda_3^2 K' - A^{-1} B (1 + \lambda_3 H + \lambda_3^2 K) + \kappa_n \lambda_1 (\kappa_1 + \lambda_3 K)) Z \end{array} \right\} \tag{28}$$

where

$$B = A' = \frac{1}{A} [\lambda_1^2 \kappa_1 \kappa_1' + \lambda_2^2 \kappa_2 \kappa_2' + \lambda_3 (\lambda_1^2 \kappa_1' + \lambda_2^2 \kappa_2') K + \lambda_3 (\lambda_1^2 \kappa_1 + \lambda_2^2 \kappa_2) K' + (\lambda_1^2 + \lambda_2^2) \lambda_3^2 K K' + (1 + \lambda_3 H + \lambda_3^2 K) (\lambda_3 H' + \lambda_3^2 K')].$$

So, if we substitute equations [23](#) and [27](#) into eq.[24](#), we obtain

$$\kappa_g^f = -\frac{1}{AC^3} \{ \kappa_n \lambda_2 (\kappa_2 + \lambda_3 K) ((1 - \kappa_n \lambda_3)^2 + \lambda_1 \lambda_3 \kappa_n') + \lambda_1^2 \lambda_2 \kappa_n^3 (\kappa_2 + \lambda_3 K) + \kappa_n' \lambda_1 \lambda_2 (\kappa_2 + \lambda_3 K) (1 - \kappa_n \lambda_3) \}. \tag{29}$$

Also, if we substitute equations [22](#) and [27](#) into eq.[25](#), we obtain

$$\kappa_n^f = \frac{1}{AC^2} \{ \lambda_1 (\kappa_1 + \lambda_3 K) (-\lambda_3 \kappa_n' - \lambda_1 \kappa_n^2) + (\lambda_1 \kappa_n' + \kappa_n (1 - \kappa_n \lambda_3)) (1 + \lambda_3 H + \lambda_3^2 K) \}. \tag{30}$$

And finally, if we substitute equations [23](#) and [28](#) into eq.[26](#), we obtain

$$t_r^f = \frac{1}{A^2 C^2} \{ \lambda_2 (\kappa_2 + \lambda_3 K) (1 - \kappa_n \lambda_3) (\kappa_n \lambda_1 (\kappa_1 + \lambda_3 K) + \lambda_3 H' + \lambda_3^2 K') \}$$

$$\begin{aligned}
& -\lambda_1^2 (\kappa_1' + \lambda_3 K') (\kappa_n \lambda_2 (\kappa_2 + \lambda_3 K)) \\
& -\lambda_2 (\kappa_2' + \lambda_3 K') (1 + \lambda_3 H + \lambda_3^2 K) (1 - \kappa_n \lambda_3) \\
& + \lambda_1 \lambda_2 \kappa_n^2 (\kappa_2 + \lambda_3 K) (1 + \lambda_3 H + \lambda_3^2 K) \\
& + \kappa_n \lambda_1^2 \lambda_2 (\kappa_1 + \lambda_3 K) (\kappa_2' + \lambda_3 K') \}.
\end{aligned} \tag{31}$$

Theorem 1. Let M be a ruled surface in E^3 and M^f be parallel-like surface of the ruled surface M that formed along directions of E_P lying in plane $Sp\{X, Z\}$, i.e. $\lambda_1 = 0$. Recall that the curve β on the surface M^f is image curve of the curve α lying on M , then curvatures of κ_g^f , κ_n^f , t_r^f for partner of curve-surface (β, M^f) are as follows

$$\kappa_g^f = -\frac{\lambda_2 \kappa_n (\kappa_2 + \lambda_3 K)}{AC} \tag{32}$$

$$\kappa_n^f = \frac{\kappa_n (1 + \lambda_3 H + \lambda_3^2 K)}{AC} \tag{33}$$

$$\begin{aligned}
t_r^f &= -\frac{\lambda_2}{A^2 C} \{ (\kappa_2' + \lambda_3 K') (1 + \lambda_3 H + \lambda_3^2 K) \\
& - (\kappa_2 + \lambda_3 K) (\lambda_3 H' + \lambda_3^2 K') \}.
\end{aligned} \tag{34}$$

Proof. If we substitute $\lambda_1 = 0$ in equations [29], [30], [31], we can easily hold equations [32], [33], [34] \square

Corollary 2. Providing $\lambda_1 = 0$, the curve β which is image curve of the directrix curve α is an asymptotic curve if and only if α is an asymptotic curve.

Corollary 3. Providing $\lambda_1 = 0$, the curve β which is image curve of the directrix curve α is a geodesic curve if and only if α is a asymptotic curve.

Theorem 2. Let M be a ruled surface in E^3 and M^f be parallel-like surface of the ruled surface M that formed along directions of E_P lying in plane $Sp\{T, Z\}$, i.e. $\lambda_2 = 0$. Then curvatures of κ_g^f , κ_n^f , t_r^f for partner of curve-surface (β, M^f) are as follows

$$\kappa_g^f = 0 \tag{35}$$

$$\begin{aligned}
\kappa_n^f &= \frac{1}{AC^2} \{ \lambda_1 (\kappa_1 + \lambda_3 K) (-\lambda_3 \kappa_n' - \lambda_1 \kappa_n^2) \\
& + (1 + \lambda_3 H + \lambda_3^2 K) (\lambda_1 \kappa_n' + \kappa_n (1 - \kappa_n \lambda_3)) \}
\end{aligned} \tag{36}$$

$$t_r^f = 0. \tag{37}$$

Proof. If we substitute $\lambda_2 = 0$ in equations [29], [30], [31], we can easily hold equations [35], [36], [37] \square

Corollary 4. *Providing $\lambda_2 = 0$, the curve β lying on M^f is both a geodesic curve and a principal line.*

Corollary 5. *Providing $\lambda_2 = 0$, the curve β which is image curve of the directrix curve α is an asymptotic curve if and only if α is an asymptotic curve.*

Theorem 3. *Let M be a ruled surface in E^3 and M^f be parallel-like surface of the ruled surface M that formed along directions of E_P lying in plane $Sp\{T, X\}$, i.e. $\lambda_3 = 0$. Then curvatures of $\kappa_g^f, \kappa_n^f, t_r^f$ for partner of curve-surface (β, M^f) are as follows*

$$\kappa_g^f = \frac{1}{AC^3} \{-\lambda_1^2 \lambda_2 \kappa_2 \kappa_n^3 - \lambda_2 \kappa_2 (\lambda_1 \kappa_n' + \kappa_n)\} \tag{38}$$

$$\kappa_n^f = \frac{1}{AC^2} \{-\lambda_1^2 \kappa_1 \kappa_n^2 + \lambda_1 \kappa_n' + \kappa_n\} \tag{39}$$

$$\begin{aligned} t_r^f = & -\frac{1}{A^3 C^2} \{ \lambda_1 \lambda_2 \kappa_n \kappa_2 (A \lambda_1 \kappa_1' - B \lambda_1 \kappa_1 - A \kappa_n) \\ & + (A \kappa_2' \lambda_2 - B \kappa_2 \lambda_2) (1 - \kappa_n \kappa_1 \lambda_1^2) \\ & - \lambda_2 \kappa_2 (A \kappa_n \kappa_1 \lambda_1 - B) \}. \end{aligned} \tag{40}$$

Proof. If we substitute $\lambda_3 = 0$ in equations [29](#), [30](#), [31](#), we can easily hold equations [38](#), [39](#), [40](#). □

Corollary 6. *Providing $\lambda_3 = 0$, the curve β which is image curve of the directrix curve α is a geodesic curve if and only if α is an asymptotic curve.*

Corollary 7. *Providing $\lambda_3 = 0$, the curve β which is image curve of the directrix curve α is an asymptotic curve if and only if α is an asymptotic curve.*

Theorem 4. *Let M be a ruled surface in E^3 and M^f be parallel-like surface of the ruled surface M that formed along vector field Z , i.e. $\lambda_1 = \lambda_2 = 0$. Then curvatures of $\kappa_g^f, \kappa_n^f, t_r^f$ for partner of curve-surface (β, M^f) are as follows*

$$\kappa_g^f = 0 \tag{41}$$

$$\kappa_n^f = \frac{\kappa_n}{1 - \kappa_n \lambda_3} \tag{42}$$

$$t_r^f = 0. \tag{43}$$

Proof. If we substitute $\lambda_1 = \lambda_2 = 0$ in equations [29](#), [30](#), [31](#), we can easily hold equations [41](#), [42](#), [43](#). □

Corollary 8. *Providing $\lambda_1 = \lambda_2 = 0$, the curve β lying on M^f is both a geodesic curve and principal line.*

Corollary 9. *Providing $\lambda_1 = \lambda_2 = 0$, the curve β lying on M^f is an asymptotic curve if and only if α lying on M is an asymptotic curve.*

Theorem 5. Let M be a ruled surface in E^3 and M^f be parallel-like surface of the ruled surface M that formed along vector field X , i.e. $\lambda_1 = \lambda_3 = 0$. Then curvatures of κ_g^f , κ_n^f , t_r^f for partner of curve-surface (β, M^f) are as follows

$$\kappa_g^f = \frac{-\lambda_2 \kappa_n \kappa_2}{\sqrt{\lambda_2^2 \kappa_2^2 + 1}} \quad (44)$$

$$\kappa_n^f = \frac{\kappa_n}{\sqrt{\lambda_2^2 \kappa_2^2 + 1}} \quad (45)$$

$$t_r^f = -\frac{\kappa_2' \lambda_2}{(\lambda_2^2 \kappa_2^2 + 1)}. \quad (46)$$

Proof. If we substitute $\lambda_1 = \lambda_3 = 0$ in equations [29], [30], [31], we can easily hold equations [44], [45], [46]. \square

Corollary 10. Providing $\lambda_1 = \lambda_3 = 0$, the curve β which is image curve of the directrix curve α is a geodesic curve if and only if α is an asymptotic curve.

Corollary 11. Providing $\lambda_1 = \lambda_3 = 0$, the curve β which is image curve of the directrix curve α is an asymptotic curve if and only if α is an asymptotic curve.

Theorem 6. Let M be a ruled surface in E^3 and M^f be parallel-like surface of the ruled surface M that formed along vector field T , i.e. $\lambda_2 = \lambda_3 = 0$. Then curvatures of κ_g^f , κ_n^f , t_r^f for partner of curve-surface (β, M^f) are as follows

$$\kappa_g^f = 0 \quad (47)$$

$$\kappa_n^f = \frac{1}{AC^2} \left\{ \kappa_n + \lambda_1 \kappa_n' - \lambda_1^2 \kappa_1 \kappa_n^2 \right\} \quad (48)$$

$$t_r^f = 0. \quad (49)$$

Proof. If we substitute $\lambda_2 = \lambda_3 = 0$ in equations [29], [30], [31], we can easily hold equations [47], [48], [49]. \square

Corollary 12. Providing $\lambda_2 = \lambda_3 = 0$, the curve β which is image curve of the directrix curve α is both a geodesic curve and a principal line.

Corollary 13. Providing $\lambda_2 = \lambda_3 = 0$, the curve β which is image curve of the directrix curve α is an asymptotic curve if and only if α is an asymptotic curve.

Declaration of Competing Interests The author declares that she has no competing interest.

Acknowledgements The author thanks the referees for their valuable suggestions which made this paper much improved.

REFERENCES

- [1] Ali, A.T., Non-lightlike constant angle ruled surfaces in Minkowski 3-space, *Journal of Geometry and Physics*, 157 (2020), 1-10. <https://doi.org/10.1016/j.geomphys.2020.103833>
- [2] Gray, A., Abbena, E., Salamon, S., *Modern Differential Geometry of Curves and Surfaces with Mathematica (Third Edition)*, Studies in Advanced Mathematics, 2006.
- [3] Güler, F., An approach for designing a developable and minimal ruled surfaces using the curvature theory, *Int. J. Geom. Methods Mod. Phys.*, 18(1) (2021), 2150015. <https://doi.org/10.1142/S0219887821500158>
- [4] Hacısalıhoğlu, H.H., *Differential Geometry*, İnönü University Faculty of Arts and Sciences Publications, Ankara, 1983.
- [5] Hagen, H., Pottmann, H., Divivier, A., Visualization functions on a surface, *Journal of Visualization and Animation*, 2 (1991), 52-58. <https://doi.org/10.1002/vis.4340020205>
- [6] Hagen, H., Stefanie, H., Schreiber, T., Visualization and computation of curvature behaviour of freeform curves and surfaces, *Comput.-Aided Des.*, 27 (1995), 545-552. [https://doi.org/10.1016/0010-4485\(95\)93587-P](https://doi.org/10.1016/0010-4485(95)93587-P)
- [7] Hashemian, A., Bo, P., Barton, M., Reparameterization of ruled surfaces: toward generating smooth jerk-minimized toolpaths for multi-axis flank CNC milling, *Comput.-Aided Des.*, 127 (2020), 102868. <https://doi.org/10.1016/j.cad.2020.102868>
- [8] Körpınar, T., Ünlütürk, Y., A new approach to the bienergy and biangle of a moving particle lying in a surface of lorentzian space, *Int. J. Nonlinear Sci. Numer. Simul.*, 22(7-8) (2021), 917-926. <https://doi.org/10.1515/ijnsns-2019-0306>
- [9] Kuhnel, W., *Differential Geometry Curves-Surfaces-Manifolds*, Wiesbaden Braunchweig, 1999.
- [10] Lee, W., Park, E., On curves lying on a rational normal surface scroll, *J. Pure Appl. Algebra*, 223(10) (2019), 4458-4476. <https://doi.org/10.1016/j.jpaa.2019.01.016>
- [11] Sabuncuoğlu, A., *Differential Geometry*, Nobel Publications, 2006.
- [12] Sağlam, D., Kalkan, Ö., Surfaces at a constant distance from the edge of regression on a surface in E_1^3 , *Differential Geometry-Dynamical Systems*, 12 (2010), 187-200.
- [13] Kızıltuğ, S., Tarakcı, Ö., Yaylı, Y., On the curves lying on parallel surfaces in the Euclidean 3-space E^3 , *Journal of Advanced Research in Dynamical and Control Systems*, 5 (2013), 26-35.
- [14] Kızıltuğ, S., Yaylı, Y., Timelike curves on timelike parallel surfaces in Minkowski 3-space E_1^3 , *Math. Aeterna*, 2 (2012), 689-700.
- [15] Sun, S., Yan, S., Jiang, S., Sun, Y., A high-accuracy tool path generation (HATPG) method for 5-axis flank milling of ruled surfaces with a conical cutter based on instantaneous envelope surface modelling, *Comput.-Aided Des.*, 151 (2022), 103354. <https://doi.org/10.1016/j.cad.2022.103354>
- [16] Tarakcı, Ö., Hacısalıhoğlu, H.H., Surfaces at a constant distance from the edge of regression on a surface, *Applied Mathematics and Computation*, 155 (2004), 81-93. [https://doi.org/10.1016/S0096-3003\(03\)00761-6](https://doi.org/10.1016/S0096-3003(03)00761-6)
- [17] Tarakcı, Ö., *Surfaces at a Constant Distance from the Edge of Regression on a Surface*, PhD thesis, Ankara University Institute of Science, 2002.
- [18] Yurttaçıkmaz, S., Tarakcı, Ö., The relationship between focal surfaces and surfaces at a constant distance from the edge of regression on a surface, *Adv. Math. Phys.*, 2015 (2015), Article ID 397126, 1-6. <https://doi.org/10.1155/2015/397126>
- [19] Yurttaçıkmaz, S., Tarakcı, Ö., Image curves on the parallel-like surfaces in E^3 , *Int. Electron. J. Geom.*, 16(1) (2023), 122-131. doi:10.36890/iejg.1178434



ANOTHER APPLICATION OF SMARANDACHE BASED RULED SURFACES WITH THE DARBOUX VECTOR ACCORDING TO FRENET FRAME IN E^3

Süleyman ŞENYURT¹, Davut CANLI², Elif ÇAN³ and Sümeyye GÜR MAZLUM⁴

^{1,2,3}Department of Mathematics, Ordu University, Ordu, TÜRKİYE

⁴Department of Computer Technology, Gümüşhane University, Gümüşhane, TÜRKİYE

ABSTRACT. In this study, we first define the Smarandache curves derived from the Frenet vectors and the Darboux vector of any curve. Then, we construct new ruled surfaces along these Smarandache curves with the direction vectors obtained from the Frenet vectors and the Darboux vector, and give the equations of these surfaces. In addition, we calculate the Gaussian and mean curvatures of these surfaces separately and present the conditions to be minimal and developable for these surfaces. Finally, as an example, we obtain ruled surfaces whose base curves are Viviani's curves and plot the graphics of these surfaces.

1. INTRODUCTION

A surface is defined to be the image of a function with two real variables in three-dimensional space. Surfaces can be characterized by their curvatures and engaged accordingly to many fields, especially in architecture and engineering. Research on the surface curvature went through various stages starting from Ancient Greece. After the studies of Descartes, Kepler, Fermat and Huygens, it gained momentum with the calculations developed by Newton and Leibniz in the 17th century. The curvature of curves and surfaces is an important topic in differential geometry, today. The method of calculating the curvature of a surface was defined by Gauss in the 19th century and therefore named Gaussian curvature. Gaussian curvature is related to the dimension of the surface. The developability of a surface depends

2020 *Mathematics Subject Classification.* 53A04, 53A05.

Keywords. Smarandache curve, ruled surfaces, mean curvature, Gaussian curvature, Viviani's curve.

¹ ✉ ssenyurt@odu.edu.tr; 0000-0003-1097-5541

² ✉ davutcanli@odu.edu.tr; 0000-0003-0405-9969

³ ✉ elif.cann@hotmail.com; 0000-0001-5870-114X

⁴ ✉ sumeyyegur@gumushane.edu.tr-Corresponding author; 0000-0003-2471-1627.

on its Gaussian curvature. A surface with zero Gaussian curvature at every point is known to be a developable surface. Since the average curvature of the surface is a ratio, it is independent of the size of the surface. Surfaces with a mean curvature of zero at every point are minimal surfaces. Therefore, it is one of the most used surfaces in architectural designs. There are numerous studies on surfaces, [5, 16, 17, 22, 24]. In surface theory, there are special surfaces of which one is named the ruled surface. A ruled surface is formed by infinitely many lines that move along a given curve. The basics related to this type of surfaces are given in [7, 23, 25]. And there are various other studies on ruled surfaces, [2, 3, 10, 12, 13, 27, 33, 36]. On the other hand, the theory of curves also occupies an important place in differential geometry. There are many studies on various special curves, [7, 9, 11, 14, 15, 21]. In addition, studies with Smarandache curves are available in [1, 4, 6, 24, 26, 31, 34, 35]. Recently, in [18-20], generating the way of new ruled surfaces have been given by exploiting the idea of Smarandache geometry and using the Frenet, the Darboux or the alternative frame. In the light of all these informations in this study, we obtain the ruled surfaces from the direction vector obtained from the Frenet and Darboux vectors of any curve and from the Smarandache base curve obtained in the same way. And we study some properties of these surfaces. Finally, we show all these results on an example and plot the graphs of the surfaces. This study is another application of our previous paper: Smarandache based ruled surfaces with the Darboux vector according to Frenet frame in E^3 , [32].

2. PRELIMINARIES

$\alpha : I \rightarrow E^3$ be a unit speed regular curve. The Frenet frame $\{T, N, B\}$, the curvature κ , the torsion τ and the Frenet derivative formulae of the curve α are given by

$$T = \alpha', N = \frac{\alpha''}{\|\alpha''\|}, B = T \wedge N, \kappa = \|\alpha''\|, \tau = \langle N', B \rangle,$$

and

$$T' = \kappa N, N' = -\kappa T + \tau B, B' = -\tau N.$$

here T, N and B are the tangent, normal and binormal vectors of α , respectively, [7]. Also $\langle \cdot, \cdot \rangle$ is the inner product, $\| \cdot \|$ is the norm and \wedge is the vectorial product functions in E^3 , [7]. The Darboux vector corresponding to the Frenet frame $\{T, N, B\}$ is defined by $W = \tau T + \kappa B$. Thus, we write the unit form of Darboux vector as

$$C = \sin \omega T + \cos \omega B,$$

where $\angle(B, W) = \omega$ and

$$\cos \omega = \frac{\kappa}{\sqrt{\kappa^2 + \tau^2}}, \quad \sin \omega = \frac{\tau}{\sqrt{\kappa^2 + \tau^2}},$$

$$\omega' = \left(\frac{\tau}{\kappa}\right)' \left(1 + \frac{\tau^2}{\kappa^2}\right),$$
(1)

[6]. On the other hand, a unit vector based on the Frenet frame elements can be defined by

$$\gamma = \frac{aT + bN + cB}{\sqrt{a^2 + b^2 + c^2}},$$
(2)

where a, b, c are some real valued functions. For $\forall s \in I$, the locus of the endpoints of the vector γ defines a differentiable curve. If γ is taken to be the position vector then the generated curve is called as Smarandache curve, [25]. A ruled surface is defined as a one parameter family of lines and it has the form

$$X(s, v) = \alpha(s) + vr(s),$$
(3)

here $\alpha(s)$ is the base curve, $r(s)$ is the direction vector of the ruled surface $X(s, v)$ and v is any real number, [9]. The normal vector field, the Gaussian and the mean curvatures of $X(s, v)$ are given by the relations [7]

$$N_X = \frac{X_s \wedge X_v}{\|X_s \wedge X_v\|},$$
(4)

$$K = \frac{eg - f^2}{EG - F^2}, \quad H = \frac{Eg - 2fF + eG}{2(EG - F^2)},$$
(5)

respectively. Here, the coefficients of the first and the second fundamental forms are defined by [7]

$$E = \langle X_s, X_s \rangle, \quad F = \langle X_s, X_v \rangle, \quad G = \langle X_v, X_v \rangle,$$
(6)

$$e = \langle X_{ss}, N_X \rangle, \quad f = \langle X_{sv}, N_X \rangle, \quad g = \langle X_{vv}, N_X \rangle.$$
(7)

3. ANOTHER APPLICATION OF SMARANDACHE BASED RULED SURFACES WITH THE DARBOUX VECTOR ACCORDING TO FRENET FRAME IN E^3

Let us remind the given expression [2]. We consider some special cases to generate new kind of Smarandache curves by choosing appropriate a, b, c functions:

- For $a = 1 + \sin \omega$, $b = 0$, $c = \cos \omega$, we define TC -Smarandache curve $\gamma_1 = \frac{T + C}{\sqrt{2 + 2 \sin \omega}}$, whose position vector is $\gamma = \frac{T + C}{\sqrt{2 + 2 \sin \omega}}$,

- For $a = \sin\omega$, $b = 1$, $c = \cos\omega$, we define NC - Smarandache curve $\gamma_2 = \frac{N+C}{\sqrt{2}}$, whose position vector is $\gamma = \frac{N+C}{\sqrt{2}}$,
- For $a = \sin\omega$, $b = 0$, $c = 1 + \cos\omega$, we define BC - Smarandache curve $\gamma_3 = \frac{B+C}{\sqrt{2+2\cos\omega}}$, whose position vector is $\gamma = \frac{B+C}{\sqrt{2+2\cos\omega}}$.

By this study, we define and consider the ruled surfaces where the base curve is one of these Smarandache curves and the generator line is one of the given position vectors. For each surface, we calculate the corresponding the Gaussian and mean curvatures.

Definition 1. *Let's define a ruled surface generated by continuously moving the vector $T + C$ along the TC - Smarandache curve. Thus, we provide its parametric form as*

$$\begin{aligned} \Sigma(s, v) &= \frac{T+C}{\sqrt{2+2\sin\omega}} + v \frac{T+C}{\sqrt{2+2\sin\omega}}, \\ \Sigma(s, v) &= \frac{1+v}{\sqrt{2}} \left(\sqrt{1+\sin\omega}T + \sqrt{1-\sin\omega}B \right). \end{aligned}$$

The first and the second partial differentials of $\Sigma(s, v)$ are

$$\begin{aligned} \Sigma_s &= \frac{1+v}{2\sqrt{2}} \begin{pmatrix} \omega' \sqrt{1-\sin\omega}T + 2(\kappa \sqrt{1+\sin\omega} - \tau \sqrt{1-\sin\omega})N \\ -\omega' \sqrt{1+\sin\omega}B \end{pmatrix}, \\ \Sigma_v &= \frac{1}{\sqrt{2}} \left(\sqrt{1+\sin\omega}T + \sqrt{1-\sin\omega}B \right), \\ \Sigma_{vv} &= 0, \\ \Sigma_{sv} &= \frac{1}{2\sqrt{2}} \begin{pmatrix} \omega' \sqrt{1-\sin\omega}T + 2(\kappa \sqrt{1+\sin\omega} - \tau \sqrt{1-\sin\omega})N \\ -\omega' \sqrt{1+\sin\omega}B \end{pmatrix}, \\ \Sigma_{ss} &= \frac{1+v}{4\sqrt{2}} \begin{bmatrix} \left((2\omega'' + 4\tau\kappa) \sqrt{1-\sin\omega} - (\omega'^2 + 4\kappa^2) \sqrt{1+\sin\omega} \right) T \\ + \left((2\kappa\omega' - 2\tau') \sqrt{1-\sin\omega} + (2\kappa' + 2\tau\omega') \sqrt{1+\sin\omega} \right) N \\ + \left((-2\omega'' + 4\tau\kappa) \sqrt{1-\sin\omega} - (\omega'^2 + 4\tau^2) \sqrt{1+\sin\omega} \right) B \end{bmatrix}. \end{aligned}$$

And the vectorial product of the vectors Σ_s , Σ_v and its norm are

$$\Sigma_s \wedge \Sigma_v = \frac{1+v}{2} \left((\sqrt{\kappa^2 + \tau^2} - \tau) T - \omega' N - \kappa B \right),$$

$$\|\Sigma_s \wedge \Sigma_v\| = \frac{1+v}{2} \sqrt{2\kappa^2 + 2\tau^2 + \omega'^2 - 2\tau\sqrt{\kappa^2 + \tau^2}}.$$

If we denote the normal vector field of the surface by N_Σ , then from the expression (4), we have

$$N_\Sigma = \frac{(\sqrt{\kappa^2 + \tau^2} - \tau) T - \omega' N - \kappa B}{(\omega'^2 + 2\kappa^2 + 2\tau^2 - 2\tau\sqrt{\kappa^2 + \tau^2})^{\frac{1}{2}}}.$$

From the expressions (6) and (7), we compute the coefficients of the first and the second fundamental forms as

$$E_\Sigma = \frac{(1+v)^2}{4} (\omega'^2 + 2\kappa^2 + 2\tau^2 - 2\tau\sqrt{\kappa^2 + \tau^2}),$$

$$F_\Sigma = 0, \quad G_\Sigma = 1$$

and

$$e_\Sigma = \frac{\begin{bmatrix} ((2\omega'' + 4\tau\kappa)(\sqrt{\kappa^2 + \tau^2} - \tau) - \omega'(2\kappa\omega' - 2\tau') - \kappa(-2\omega'' + 4\tau\kappa)) \\ \cdot \sqrt{1 - \sin \omega} \\ - ((\omega'^2 + 4\kappa^2)(\sqrt{\kappa^2 + \tau^2} - \tau) + \omega'(2\kappa' + 2\tau\omega') - \kappa(\omega'^2 + 4\tau^2)) \\ \cdot \sqrt{1 + \sin \omega} \end{bmatrix}}{4(1+v)^{-1}(\omega'^2 + 2\kappa^2 + 2\tau^2 - 2\tau\sqrt{\kappa^2 + \tau^2})^{\frac{1}{2}}},$$

$$f_\Sigma = \frac{\omega'(\sqrt{\kappa^2 + \tau^2} + \tau)\sqrt{1 - \sin \omega} - \kappa\omega'\sqrt{1 + \sin \omega}}{4(1+v)^{-1}(\omega'^2 + 2\kappa^2 + 2\tau^2 - 2\tau\sqrt{\kappa^2 + \tau^2})^{\frac{1}{2}}},$$

$$g_\Sigma = 0,$$

respectively. Finally, by using the expression (5), we get the Gaussian and the mean curvatures

$$K_{\Sigma} = - \left[\frac{\omega' (\sqrt{\kappa^2 + \tau^2} + \tau) \sqrt{1 - \sin \omega} - \kappa \omega' \sqrt{1 + \sin \omega}}{2 (\omega'^2 + 2\kappa^2 + 2\tau^2 - 2\tau\sqrt{\kappa^2 + \tau^2})} \right]^2,$$

$$H_{\Sigma} = \frac{\left[\begin{array}{l} ((2\omega'' + 4\tau\kappa) (\sqrt{\kappa^2 + \tau^2} - \tau) - \omega' (2\kappa\omega' - 2\tau') - \kappa (-2\omega'' + 4\tau\kappa)) \\ \cdot \sqrt{1 - \sin \omega} \\ - \left((\omega'^2 + 4\kappa^2) (\sqrt{\kappa^2 + \tau^2} - \tau) + \omega' (2\kappa' + 2\tau\omega') - \kappa (\omega'^2 + 4\tau^2) \right) \\ \cdot \sqrt{1 + \sin \omega} \end{array} \right]}{2 (\omega'^2 + 2\kappa^2 + 2\tau^2 - 2\tau\sqrt{\kappa^2 + \tau^2})^{\frac{3}{2}}},$$

respectively.

Corollary 1. *If $\alpha(s)$ is a general helix, then Σ is a developable surface.*

Definition 2. *Let's define a ruled surface generated by continuously moving the vector $N + C$ along the TC-Smarandache curve. Thus, we provide its parametric form as*

$$\Delta(s, v) = \frac{1}{\sqrt{2 + 2\sin \omega}} (T + C) + \frac{v}{\sqrt{2}} (N + C),$$

$$\Delta(s, v) = \frac{1}{\sqrt{2}} \left[\left(\sqrt{1 + \sin \omega} + v \sin \omega \right) T + vN + \left(\sqrt{1 - \sin \omega} + v \cos \omega \right) B \right].$$

The first and the second partial differentials of $\Delta(s, v)$ are

$$\Delta_s = \frac{1}{2\sqrt{2}} (xT + yN + zB),$$

$$\Delta_v = \frac{1}{\sqrt{2}} (\sin \omega T + N + \cos \omega B),$$

$$\Delta_{vv} = 0,$$

$$\Delta_{sv} = \frac{1}{\sqrt{2}} \left((-\kappa + \cos \omega) T + \left(\kappa\sqrt{1 + \sin \omega} - \tau\sqrt{1 - \sin \omega} \right) N + (\tau - \sin \omega) B \right),$$

$$\Delta_{ss} = \frac{1}{2\sqrt{2}} \left((x' - y\kappa) T + (x\kappa - z\tau + y') N + (y\tau + z') B \right).$$

And the vectorial product of the vectors Δ_s , Δ_v and its norm are

$$\Delta_s \wedge \Delta_v = \frac{1}{4} ((-z + y \cos \omega) T - (x \cos \omega - z \sin \omega) N + (x - y \sin \omega) B),$$

$$\|\Delta_s \wedge \Delta_v\| = \frac{1}{4} \left((-z + y \cos \omega)^2 + (x \cos \omega - z \sin \omega)^2 + (x - y \sin \omega)^2 \right)^{\frac{1}{2}},$$

where the coefficients x, y, z are

$$x = \omega' \sqrt{1 - \sin \omega} + 2v(-\kappa + \cos \omega),$$

$$y = 2\kappa \sqrt{1 + \sin \omega} - 2\tau \sqrt{1 - \sin \omega},$$

$$z = -\omega' \sqrt{1 + \sin \omega} + 2v(\tau - \sin \omega).$$

Thus, from the expression (4), the normal of the surface N_Δ is given as

$$N_\Delta = \frac{(-z + y \cos \omega) T - (x \cos \omega - z \sin \omega) N + (x - y \sin \omega) B}{\left((-z + y \cos \omega)^2 + (x \cos \omega - z \sin \omega)^2 + (x - y \sin \omega)^2 \right)^{\frac{1}{2}}}.$$

By following the expressions (6) and (7), the coefficients of the first and the second fundamental forms are

$$E_\Delta = \frac{1}{8} (x^2 + y^2 + z^2),$$

$$F_\Delta = \frac{1}{4} (x \sin \omega + y + z \cos \omega),$$

$$G_\Delta = 1$$

and

$$e_\Delta = \frac{\begin{pmatrix} (x' - y\kappa)(-z + y \cos \omega) - (x\kappa - z\tau + y')(x \cos \omega - z \sin \omega) \\ + (y\tau + z')(x - y \sin \omega) \end{pmatrix}}{2\sqrt{2} \left((-z + y \cos \omega)^2 + (x \cos \omega - z \sin \omega)^2 + (x - y \sin \omega)^2 \right)^{\frac{1}{2}}},$$

$$f_\Delta = \frac{\begin{pmatrix} z\kappa + x\tau - z \cos \omega - x \sin \omega + y(1 - \sqrt{\kappa^2 + \tau^2}) \\ - (x \cos \omega - z \sin \omega)(\kappa \sqrt{1 + \sin \omega} - \tau \sqrt{1 - \sin \omega}) \end{pmatrix}}{\sqrt{2} \left((-z + y \cos \omega)^2 + (x \cos \omega - z \sin \omega)^2 + (x - y \sin \omega)^2 \right)^{\frac{1}{2}}},$$

$$g_\Delta = 0,$$

respectively. Finally, from the expression (5), the Gaussian and mean curvatures are obtained as

$$K_{\Delta} = -\frac{8 \left[\begin{array}{l} z\kappa + x\tau + y(1 - \sqrt{\kappa^2 + \tau^2}) - (z \cos \omega + x \sin \omega) \\ - (x \cos \omega - z \sin \omega) (\kappa\sqrt{1 + \sin \omega} - \tau\sqrt{1 - \sin \omega}) \end{array} \right]^2}{\left((-z + y \cos \omega)^2 + (x \cos \omega - z \sin \omega)^2 + (x - y \sin \omega)^2 \right)^2},$$

$$H_{\Delta} = \frac{\left[\begin{array}{l} (x' - y\kappa)(-z + y \cos \omega) - (x\kappa - z\tau + y')(x \cos \omega - z \sin \omega) \\ + (y\tau + z')(x - y \sin \omega) - z\kappa + x\tau - z \cos \omega - x \sin \omega \\ + y(1 - \sqrt{\kappa^2 + \tau^2})(x \sin \omega + y + z \cos \omega) \\ + (x \cos \omega - z \sin \omega)(x \sin \omega + y + z \cos \omega)(\kappa\sqrt{1 + \sin \omega} - \tau\sqrt{1 - \sin \omega}) \end{array} \right]}{\left((-z + y \cos \omega)^2 + (x \cos \omega - z \sin \omega)^2 + (x - y \sin \omega)^2 \right)^{\frac{3}{2}}},$$

respectively.

Definition 3. Let's define a ruled surface generated by continuously moving the vector $B + C$ along the TC-Smarandache curve. Thus, we provide its parametric form as

$$\Upsilon(s, v) = \frac{1}{\sqrt{2 + 2 \sin \omega}}(T + C) + \frac{v}{\sqrt{2 + 2 \cos \omega}}(B + C),$$

$$\Upsilon(s, v) = \frac{1}{\sqrt{2}} \left[\left(\sqrt{1 + \sin \omega} + v\sqrt{1 - \cos \omega} \right) T + \left(\sqrt{1 - \sin \omega} + v\sqrt{1 + \cos \omega} \right) B \right].$$

If we assign $p(s, v) = \sqrt{1 + \sin \omega} + v\sqrt{1 - \cos \omega}$ and $q(s, v) = \sqrt{1 - \sin \omega} + v\sqrt{1 + \cos \omega}$, then we can rewrite the surface in a simple form as

$$\Upsilon(s, v) = \frac{1}{\sqrt{2}} (pT + qB).$$

Next, the first and the second partial differentials of $\Upsilon(s, v)$ are

$$\Upsilon_s = \frac{1}{\sqrt{2}} (p_s T + (\kappa p - \tau q) N + q_s B),$$

$$\Upsilon_v = \frac{1}{\sqrt{2}} (p_v T + q_v B),$$

$$\Upsilon_{vv} = 0,$$

$$\Upsilon_{ss} = \frac{1}{\sqrt{2}} \begin{bmatrix} (p_{ss} - \kappa^2 p + \tau \kappa q) T + (p_s \kappa - q_s \tau + (\kappa p - \tau q)_s) N \\ + (q_{ss} + \kappa \tau p - \tau^2 q) B \end{bmatrix},$$

$$\Upsilon_{sv} = \frac{1}{\sqrt{2}} (p_{sv} T + (\kappa p_v - \tau q_v) N + q_{sv} B).$$

And the vectorial product of the vectors Υ_s , Υ_v and its norm are

$$\Upsilon_s \wedge \Upsilon_v = \frac{1}{2} ((\kappa p q_v - \tau q q_v) T + (q_s p_v - p_s q_v) N - (\kappa p p_v - \tau q p_v) B),$$

$$\|\Upsilon_s \wedge \Upsilon_v\| = \frac{1}{2} \sqrt{(\kappa p - \tau q)^2 (p_v^2 + q_v^2) + (p_v q_s - p_s q_v)^2}.$$

From the expression (4), the normal of the surface N_Υ is

$$N_\Upsilon = \frac{q_v (\kappa p - \tau q) T + (p_v q_s - p_s q_v) N - p_v (\kappa p - \tau q) B}{\sqrt{(\kappa p - \tau q)^2 (p_v^2 + q_v^2) + (p_v q_s - p_s q_v)^2}}$$

From the expressions (6) and (7) to compute the coefficients of fundamental forms, we get

$$E_\Upsilon = \frac{1}{2} \left((p_s)^2 + (\kappa p - \tau q)^2 + (q_s)^2 \right),$$

$$F_\Upsilon = \frac{1}{2} (p_s p_v + q_s q_v),$$

$$G_\Upsilon = 1$$

and

$$e_{\Upsilon} = \frac{\left[(\kappa p - \tau q) (q_v (p_{ss} - \kappa^2 p + \tau \kappa q) - p_v (q_{ss} + \kappa \tau p - \tau^2 q)) + (p_v q_s - p_s q_v) (p_s \kappa - q_s \tau + (\kappa p - \tau q)_s) \right]}{\sqrt{(\kappa p - \tau q)^2 (p_v^2 + q_v^2) + (p_v q_s - p_s q_v)^2}},$$

$$f_{\Upsilon} = \frac{(\kappa p - \tau q) (q_v p_{sv} - p_v q_{sv}) + (p_v q_s - p_s q_v) (\kappa p_v - \tau q_v)}{\sqrt{2} \sqrt{(\kappa p - \tau q)^2 (p_v^2 + q_v^2) + (p_v q_s - p_s q_v)^2}},$$

$$g_{\Upsilon} = 0,$$

respectively. Finally, from the expression (5), we obtain the Gaussian and mean curvatures as

$$K_{\Upsilon} = - \left[\frac{(\kappa p - \tau q) (q_v p_{sv} - p_v q_{sv}) + (p_v q_s - p_s q_v) (\kappa p_v - \tau q_v)}{(\kappa p - \tau q)^2 (p_v^2 + q_v^2) + (p_v q_s - p_s q_v)^2} \right]^2,$$

$$H_{\Upsilon} = \frac{\left[(\kappa p - \tau q) (q_v p_{ss} - p_v q_{ss} - (\kappa p - \tau q) (\kappa q_v + \tau p_v)) + (p_v q_s - p_s q_v) (2p_s \kappa - 2q_s \tau + \kappa' p - \tau' q) - (\kappa p - \tau q) (p_s p_v + q_s q_v) (p_{sv} q_v - q_{sv} p_v + p_v q_s - p_s q_v) \right]}{\sqrt{2} \left((\kappa p - \tau q)^2 (p_v^2 + q_v^2) + (p_v q_s - p_s q_v)^2 \right)^{\frac{3}{2}}}.$$

Definition 4. Let's define a ruled surface generated by continuously moving the vector $T + C$ along the NC- Smarandache curve. Thus, we provide its parametric form as

$$\chi(s, v) = \frac{1}{\sqrt{2}} (N + C) + \frac{v}{\sqrt{2 + 2 \sin \omega}} (T + C),$$

$$\chi(s, v) = \frac{1}{\sqrt{2}} \left[(\sin \omega + v \sqrt{1 + \sin \omega}) T + N + (\cos \omega + v \sqrt{1 - \sin \omega}) B \right].$$

If we assign $m(s, v) = \sin \omega + v \sqrt{1 + \sin \omega}$ and $r(s, v) = \cos \omega + v \sqrt{1 - \sin \omega}$, then we can rewrite the surface in a simple form as

$$\chi(s, v) = \frac{1}{\sqrt{2}} (mT + N + rB).$$

Next, the first and second partial differentials of $\chi(s, v)$ are

$$\chi_s = \frac{1}{\sqrt{2}} ((m_s - \kappa)T + (m\kappa - r\tau)N + (r_s + \tau)B),$$

$$\chi_v = \frac{1}{\sqrt{2}} (m_v T + r_v B),$$

$$\chi_{vv} = 0,$$

$$\chi_{sv} = \frac{1}{\sqrt{2}} (m_{sv}T + (m_v\kappa - r_v\tau)N + r_{sv}B),$$

$$\chi_{ss} = \frac{1}{\sqrt{2}} \begin{bmatrix} (m_{ss} - m\kappa^2 - \kappa' + r\kappa\tau)T \\ + (2\kappa m_s - 2\tau r_s - \kappa^2 - \tau^2 + m\kappa' - r\tau')N \\ + (r_{ss} + m\tau\kappa + \tau' - r\tau^2)B \end{bmatrix}.$$

And the vectorial product of the vectors χ_s , χ_v and its norm are

$$\chi_s \wedge \chi_v = \frac{1}{2} (r_v (m\kappa - r\tau)T + (m_v (r_s + \tau) - r_v (m_s - \kappa))N - m_v (m\kappa - r\tau)B),$$

$$\|\chi_s \wedge \chi_v\| = \frac{1}{2} \left((m_v (r_s + \tau) - r_v (m_s - \kappa))^2 + 2(m\kappa - r\tau)^2 \right)^{\frac{1}{2}}.$$

From the expression (4), the normal of the ruled surface $\chi(s, v)$ is

$$N_\chi = \frac{r_v (m\kappa - r\tau)T + (m_v (r_s + \tau) - r_v (m_s - \kappa))N - m_v (m\kappa - r\tau)B}{\left((m_v (r_s + \tau) - r_v (m_s - \kappa))^2 + 2(m\kappa - r\tau)^2 \right)^{\frac{1}{2}}}.$$

From the expression (6) and (7) the coefficients of the first and the second fundamental forms are

$$E_\chi = \frac{1}{2} \left((m_s - \kappa)^2 + (m\kappa - r\tau)^2 + (r_s + \tau)^2 \right),$$

$$F_\chi = \frac{1}{2} (m_v (m_s - \kappa) + r_v (r_s + \tau)),$$

$$G_\chi = 1$$

and

$$e_\chi = \frac{\left[\begin{aligned} &(m\kappa - r\tau) (r_v (m_{ss} - m\kappa^2 - \kappa' + r\kappa\tau) - m_v (r_{ss} + m\tau\kappa + \tau' - r\tau^2)) \\ &+ (m_v (r_s + \tau) - r_v (m_s - \kappa)) (2\kappa m_s - 2\tau r_s - \kappa^2 - \tau^2 + m\kappa' - r\tau') \end{aligned} \right]}{\sqrt{2} \left((m_v (r_s + \tau) - r_v (m_s - \kappa))^2 + 2(m\kappa - r\tau)^2 \right)^{\frac{1}{2}}},$$

$$f_\chi = \frac{(m\kappa - r\tau) (r_v m_{sv} - m_v r_{sv}) + (m_v (r_s + \tau) - r_v (m_s - \kappa)) (m_v \kappa - r_v \tau)}{\sqrt{2} \left((m_v (r_s + \tau) - r_v (m_s - \kappa))^2 + 2(m\kappa - r\tau)^2 \right)^{\frac{1}{2}}},$$

$$g_\chi = 0,$$

respectively. Finally, from the expression (5), we compute the Gaussian and mean curvatures as

$$K_\chi = - \left[\frac{(m\kappa - r\tau) (r_v m_{sv} - m_v r_{sv}) + (m_v (r_s + \tau) - r_v (m_s - \kappa)) (m_v \kappa - r_v \tau)}{(m_v (r_s + \tau) - r_v (m_s - \kappa))^2 + 2(m\kappa - r\tau)^2} \right]^2,$$

$$H_\chi = \frac{\left[\begin{aligned} &(m\kappa - r\tau) \begin{pmatrix} r_v m_{ss} - r_v m\kappa^2 - r_v \kappa' + r_v r\kappa\tau - m_v r_{ss} \\ -m_v m\tau\kappa - m_v \tau' + m_v r\tau^2 \end{pmatrix} \\ &- (m\kappa - r\tau) (r_v m_{sv} - m_v r_{sv}) (m_v m_s - \kappa m_v + r_v r_s + r_v \tau) \\ &+ (m_v r_s + m_v \tau - r_v m_s + r_v \kappa) (2\kappa m_s - 2\tau r_s - \kappa^2 - \tau^2 + m\kappa' - r\tau') \\ &- (m_v r_s + m_v \tau - r_v m_s + r_v \kappa) (m_v m_s - m_v \kappa + r_v r_s + r_v \tau) \\ &\cdot (m_v \kappa - r_v \tau) \end{aligned} \right]}{\sqrt{2} \left((m_v (r_s + \tau) - r_v (m_s - \kappa))^2 + 2(m\kappa - r\tau)^2 \right)^{\frac{3}{2}}}.$$

Definition 5. Let's define a ruled surface generated by continuously moving the vector $N + C$ along the NC -Smarandache curve. Thus, we provide its parametric form as

$$P(s, v) = \frac{N + C}{\sqrt{2}} + v \frac{N + C}{\sqrt{2}},$$

$$P(s, v) = \frac{1 + v}{\sqrt{2}} (\sin \omega T + N + \cos \omega B).$$

Next, the first and the second partial differentials of $P(s, v)$ are

$$P_s = \frac{1+v}{\sqrt{2}} ((-\kappa + \omega' \cos \omega) T + (\tau - \omega' \sin \omega) B),$$

$$P_v = \frac{1}{\sqrt{2}} (\sin \omega T + N + \cos \omega B),$$

$$P_{ss} = \frac{1}{\sqrt{2}} (1+v) \left[\begin{array}{l} (-\kappa + \omega' \cos \omega)' T - (\kappa^2 + \tau^2 - \omega' (\kappa \cos \omega + \tau \sin \omega)) N \\ + (\tau - \omega' \sin \omega)' B \end{array} \right],$$

$$P_{sv} = \frac{1}{\sqrt{2}} ((-\kappa + \omega' \cos \omega) T + (\tau - \omega' \sin \omega) B),$$

$$P_{vv} = 0.$$

And the vectorial product of the vectors P_s , P_v and its norm are

$$P_s \wedge P_v = \frac{(1+v)}{2} [(\omega' \sin \omega - \tau) T + (\kappa \cos \omega + \tau \sin \omega - \omega') N + (\omega' \cos \omega - \kappa) B],$$

$$\|P_s \wedge P_v\| = \frac{(1+v)}{2} \sqrt{(\omega' \sin \omega - \tau)^2 + (\omega' \cos \omega - \kappa)^2 + (\kappa \cos \omega + \tau \sin \omega - \omega')^2}.$$

If we denote the normal vector of the surface by N_P , then from the expression (4), we get

$$N_P = \frac{(\omega' \sin \omega - \tau) T + (\kappa \cos \omega + \tau \sin \omega - \omega') N + (\omega' \cos \omega - \kappa) B}{\sqrt{(\omega' \sin \omega - \tau)^2 + (\omega' \cos \omega - \kappa)^2 + (\kappa \cos \omega + \tau \sin \omega - \omega')^2}}.$$

By using the expressions (6) and (7), the coefficients of the first and the second fundamental forms are given as

$$E_P = \frac{1}{2} \left((1+v)^2 \left((-\kappa + \omega' \cos \omega)^2 + (\tau - \omega' \sin \omega)^2 \right) \right),$$

$$F_P = 0,$$

$$G_P = 1$$

and

$$e_P = \frac{(1+v) \left[\begin{aligned} &(\omega' \cos \omega - \kappa)' (\omega' \sin \omega - \tau) + (\tau - \omega' \sin \omega)' (\omega' \cos \omega - \kappa) \\ &+ (\kappa \cos \omega + \tau \sin \omega - \omega')^2 \end{aligned} \right]}{\sqrt{2} \left((\omega' \sin \omega - \tau)^2 + (\omega' \cos \omega - \kappa)^2 + (\kappa \cos \omega + \tau \sin \omega - \omega')^2 \right)^{\frac{1}{2}}},$$

$$f_P = 0,$$

$$g_P = 0,$$

respectively. Finally, from the expression (5), the Gaussian and mean curvatures are obtained as:

$$K_P = 0,$$

$$H_P = \frac{\left[\begin{aligned} &(\sqrt{2}(1+v))^{-1} (-\kappa + \omega' \cos \omega)' (\omega' \sin \omega - \tau) \\ &+ (\tau - \omega' \sin \omega)' (-\kappa + \omega' \cos \omega) + (\kappa \cos \omega + \tau \sin \omega - \omega')^2 \end{aligned} \right]}{\left[\begin{aligned} &(\kappa^2 + \tau^2 + \omega'^2 - 2\omega' (\kappa \cos \omega + \tau \sin \omega)) \\ &\cdot \sqrt{(\omega' \sin \omega - \tau)^2 + (\omega' \cos \omega - \kappa)^2 + (\kappa \cos \omega + \tau \sin \omega - \omega')^2} \end{aligned} \right]}.$$

Corollary 2. *The ruled surface P (s, v) is always developable.*

Definition 6. *Let's define a ruled surface generated by continuously moving the vector B + C along the NC- Smarandache curve. Thus, we provide its parametric form as*

$$\delta(s, v) = \frac{1}{\sqrt{2}} (N + C) + \frac{v}{\sqrt{2 + 2 \cos \omega}} (B + C),$$

$$\delta(s, v) = \frac{1}{\sqrt{2}} \left[(\sin \omega + v\sqrt{1 + \cos \omega}) T + N + (\cos \omega + v\sqrt{1 - \cos \omega}) B \right].$$

If we assign $p^*(s, v) = \sin \omega + v\sqrt{1 + \cos \omega}$ and $q^*(s, v) = \cos \omega + v\sqrt{1 - \cos \omega}$, then we can rewrite the surface in a simple form as

$$\delta(s, v) = \frac{1}{\sqrt{2}} (p^*T + N + q^*B).$$

Next, the first and second partial differentials of $\delta(s, v)$ are

$$\begin{aligned}\delta_s &= \frac{1}{\sqrt{2}} ((-\kappa + p_s^*)T + (\kappa p^* - \tau q^*)N + (\tau + q_s^*)B), \\ \delta_v &= \frac{1}{\sqrt{2}} (p_v^*T + q_v^*B), \\ \delta_{vv} &= 0, \\ \delta_{sv} &= \frac{1}{\sqrt{2}} (p_{sv}^*T + (\kappa p_v^* - \tau q_v^*)N + q_{sv}^*B), \\ \delta_{ss} &= \frac{1}{\sqrt{2}} \left[\begin{aligned} &(-\kappa' + p_{ss}^* - \kappa^2 p^* + \tau \kappa q^*)T + (\tau' + q_{ss}^* + \kappa \tau p^* - \tau^2 q^*)B \\ &+ (2\kappa p_s^* - 2\tau q_s^* - \tau^2 - \kappa^2 + \kappa' p^* - \tau' q^*)N \end{aligned} \right].\end{aligned}$$

And the vectorial product of the vectors δ_s , δ_v and its norm are

$$\begin{aligned}\delta_s \wedge \delta_v &= \frac{1}{2} \begin{bmatrix} q_v^* (\kappa p^* - \tau q^*)T + (p_v^* (\tau + q_s^*) - q_v^* (-\kappa + p_s^*))N \\ -p_v^* (\kappa p^* - \tau q^*)B \end{bmatrix}, \\ \|\delta_s \wedge \delta_v\| &= \frac{1}{2} \left[(q_v^{*2} + p_v^{*2}) (\kappa p^* - \tau q^*)^2 + (p_v^* (\tau + q_s^*) - q_v^* (-\kappa + p_s^*))^2 \right]^{\frac{1}{2}}.\end{aligned}$$

From the expression (4), we compute the normal of the surface denoted by N_δ as

$$N_\delta = \frac{q_v^* (\kappa p^* - \tau q^*)T + (p_v^* (\tau + q_s^*) - q_v^* (-\kappa + p_s^*))N - p_v^* (\kappa p^* - \tau q^*)B}{\left[(q_v^{*2} + p_v^{*2}) (\kappa p^* - \tau q^*)^2 + (p_v^* (\tau + q_s^*) - q_v^* (-\kappa + p_s^*))^2 \right]^{\frac{1}{2}}}.$$

By the expressions (6) and (7), the coefficients of fundamental forms are given as

$$\begin{aligned}E_\delta &= \frac{1}{2} \left[(-\kappa + p_s^*)^2 + (\kappa p^* - \tau q^*)^2 + (\tau + q_s^*)^2 \right], \\ F_\delta &= \frac{1}{2} [(-\kappa + p_s^*)p_v^* + (\tau + q_s^*)q_v^*], \\ G_\delta &= 1\end{aligned}$$

and

$$e_\delta = \frac{\left[(\kappa p^* - \tau q^*) \left[q_v^* (-\kappa' + p_{ss}^* - \kappa^2 p^* + \tau \kappa q^*) - p_v^* (\tau' + q_{ss}^* + \kappa \tau p^* - \tau^2 q^*) \right] + (p_v^* (\tau + q_s^*) - q_v^* (-\kappa + p_s^*)) (2\kappa p_s^* - 2\tau q_s^* - \tau^2 - \kappa^2 + \kappa' p^* - \tau' q^*) \right]}{\sqrt{2} \left((q_v^{*2} + p_v^{*2}) (\kappa p^* - \tau q^*)^2 + (p_v^* (\tau + q_s^*) - q_v^* (-\kappa + p_s^*))^2 \right)^{\frac{1}{2}}},$$

$$f_\delta = \frac{(q_v^* p_{sv}^* - p_v^* q_{sv}^*) (\kappa p^* - \tau q^*) + (p_v^* (\tau + q_s^*) - q_v^* (-\kappa + p_s^*)) (\kappa p_v^* - \tau q_v^*)}{\sqrt{2} \left((q_v^{*2} + p_v^{*2}) (\kappa p^* - \tau q^*)^2 + (p_v^* (\tau + q_s^*) - q_v^* (-\kappa + p_s^*))^2 \right)^{\frac{1}{2}}},$$

$g_\delta = 0,$

respectively. Finally, from the expression (5), we compute the Gaussian and mean curvatures as

$$K_\delta = -2 \left[\frac{(q_v^* p_{sv}^* - p_v^* q_{sv}^*) (\kappa p^* - \tau q^*) + (p_v^* (\tau + q_s^*) - q_v^* (-\kappa + p_s^*)) (\kappa p_v^* - \tau q_v^*)}{(q_v^{*2} + p_v^{*2}) (\kappa p^* - \tau q^*)^2 + (p_v^* (\tau + q_s^*) - q_v^* (-\kappa + p_s^*))^2} \right]^2,$$

$$H_\delta = \frac{\left[(\kappa p^* - \tau q^*) \left[q_v^* (-\kappa' + p_{ss}^* - \kappa^2 p^* + \tau \kappa q^*) - p_v^* (\tau' + q_{ss}^* + \kappa \tau p^* - \tau^2 q^*) \right] + (p_v^* (\tau + q_s^*) - q_v^* (-\kappa + p_s^*)) (2\kappa p_s^* - 2\tau q_s^* - \tau^2 - \kappa^2 + \kappa' p^* - \tau' q^*) - (q_v^* p_{sv}^* - p_v^* q_{sv}^*) (\kappa p^* - \tau q^*) ((-\kappa + p_s^*) p_v^* + (\tau + q_s^*) q_v^*) - (p_v^* (\tau + q_s^*) - q_v^* (-\kappa + p_s^*)) (p_v^* (-\kappa + p_s^*) + q_v^* (\tau + q_s^*)) (\kappa p_v^* - \tau q_v^*) \right]}{2^{-\frac{1}{2}} \left[(q_v^{*2} + p_v^{*2}) (\kappa p^* - \tau q^*)^2 + (p_v^* (\tau + q_s^*) - q_v^* (-\kappa + p_s^*))^2 \right]^{\frac{3}{2}}}.$$

Definition 7. *Let's define a ruled surface generated by continuously moving the vector $T + C$ along the BC - Smarandache curve. Thus, we provide its parametric form as*

$$\begin{aligned} \eta(s, v) &= \frac{1}{\sqrt{2 + 2 \cos \omega}} (B + C) + \frac{v}{\sqrt{2 + 2 \sin \omega}} (T + C), \\ \eta(s, v) &= \frac{1}{\sqrt{2}} \left[\left((\sqrt{1 - \cos \omega}) + v (\sqrt{1 + \sin \omega}) \right) T \right. \\ &\quad \left. + \left((\sqrt{1 + \cos \omega}) + v (\sqrt{1 - \sin \omega}) \right) B \right]. \end{aligned}$$

If we assign $m^*(s, v) = (\sqrt{1 - \cos \omega} + v \sqrt{1 + \sin \omega})$ and $n^*(s, v) = (\sqrt{1 + \cos \omega} + v \sqrt{1 - \sin \omega})$, then we can rewrite the surface in a simple

form as

$$\eta(s, v) = \frac{1}{\sqrt{2}} (m^*(s, v)T(s) + n^*(s, v)B(s)).$$

Next, the first and the second partial differentials of $\eta(s, v)$ are

$$\eta_s = \frac{1}{\sqrt{2}} (m_s^*T + (\kappa m^* - \tau n^*)N + n_s^*B),$$

$$\eta_v = \frac{1}{\sqrt{2}} (m_v^*T + n_v^*B),$$

$$\eta_{vv} = 0,$$

$$\eta_{ss} = \frac{1}{\sqrt{2}} \left[\begin{array}{l} (m_{ss}^* - \kappa^2 m^* + \tau \kappa n_s^*)T + (\kappa' m^* - \tau' n_s^* + 2\kappa m_s^* - 2\tau n_s^*)N \\ + (n_{ss}^* + \kappa \tau m^* - \tau^2 n_s^*)B \end{array} \right],$$

$$\eta_{sv} = \frac{1}{\sqrt{2}} (m_{sv}^*T + (\kappa m_v^* - \tau n_v^*)N + n_{sv}^*B).$$

And the vectorial product of the vectors η_s , η_v and its norm are

$$\eta_s \wedge \eta_v = \frac{1}{2} (n_v^* (\kappa m^* - \tau n^*)T + (n_s^* m_v^* - m_s^* n_v^*)N - m_v^* (\kappa m^* - \tau n^*)B),$$

$$\|\eta_s \wedge \eta_v\| = \frac{1}{2} \left((\kappa m^* - \tau n^*)^2 (m_v^{*2} + n_v^{*2}) + (n_s^* m_v^* - m_s^* n_v^*)^2 \right)^{\frac{1}{2}}.$$

By using the expression (4), the normal vector field denoted by N_η can be computed as:

$$N_\eta = \frac{n_v^* (\kappa m^* - \tau n^*)T + (n_s^* m_v^* - m_s^* n_v^*)N - m_v^* (\kappa m^* - \tau n^*)B}{\left((\kappa m^* - \tau n^*)^2 (m_v^{*2} + n_v^{*2}) + (n_s^* m_v^* - m_s^* n_v^*)^2 \right)^{\frac{1}{2}}}.$$

From the expressions (6) and (7), the coefficients of fundamental forms can be given as:

$$E_\eta = \frac{1}{2} (m_s^{*2} + n_s^{*2} + (\kappa m^* - \tau n^*)^2),$$

$$F_\eta = \frac{1}{2} (m_s^* m_v^* + n_s^* n_v^*),$$

$$G_\eta = 1$$

and

$$e_\eta = \frac{\left[(\kappa m^* - \tau n^*) (n_v^* (m_{ss}^* - \kappa^2 m^* + \tau \kappa n_s^*) - m_v^* (n_{ss}^* + \kappa \tau m^* - \tau^2 n_s^*)) + (n_s^* m_v^* - m_s^* n_v^*) (\kappa' m^* - \tau' n_s^* + 2\kappa m_s^* - 2\tau n_s^*) \right]}{\sqrt{2} \left((\kappa m^* - \tau n^*)^2 (m_v^{*2} + n_v^{*2}) + (n_s^* m_v^* - m_s^* n_v^*)^2 \right)^{\frac{1}{2}}},$$

$$f_\eta = \frac{(\kappa m^* - \tau n^*) (n_v^* m_v^* - m_v^* n_v^*)}{\sqrt{2} \left((\kappa m^* - \tau n^*)^2 (m_v^{*2} + n_v^{*2}) + (n_s^* m_v^* - m_s^* n_v^*)^2 \right)^{\frac{1}{2}}},$$

$$g_\eta = 0,$$

respectively. Finally, from the expression (5), the Gaussian and mean curvatures are obtained as

$$K_\eta = -\frac{2(\kappa m^* - \tau n^*)^2 (n_v^* m_v^* - m_v^* n_v^*)^2}{\left((\kappa m^* - \tau n^*)^2 (m_v^{*2} + n_v^{*2}) + (n_s^* m_v^* - m_s^* n_v^*)^2 \right)^2},$$

$$H_\eta = \frac{\left[(\kappa m^* - \tau n^*) [n_v^* (m_{ss}^* - \kappa^2 m^* + \tau \kappa n_s^*) - m_v^* (n_{ss}^* + \kappa \tau m^* - \tau^2 n_s^*)] + (n_s^* m_v^* - m_s^* n_v^*) (\kappa' m^* - \tau' n_s^* + 2\kappa m_s^* - 2\tau n_s^*) - (\kappa m^* - \tau n^*) (n_v^* m_v^* - m_v^* n_v^*) (m_s^* m_v^* + n_s^* n_v^*) \right]}{2^{-\frac{1}{2}} \left((\kappa m^* - \tau n^*)^2 (m_v^{*2} + n_v^{*2}) + (n_s^* m_v^* - m_s^* n_v^*)^2 \right)^{\frac{3}{2}}}.$$

Definition 8. Let's define a ruled surface generated by continuously moving the vector $N + C$ along the BC -Smarandache curve. Thus, we provide its parametric form as

$$\varphi(s, v) = \frac{1}{\sqrt{2 + 2 \cos \omega}} (B + C) + \frac{v}{\sqrt{2}} (N + C),$$

$$\varphi(s, v) = \frac{1}{\sqrt{2}} \left((\sqrt{1 - \cos \omega} + v \sin \omega) T + vN + (\sqrt{1 + \cos \omega} + v \cos \omega) B \right).$$

If we assign $\mu(s, v) = (\sqrt{1 - \cos \omega} + v \sin \omega)$ and $\rho(s, v) = (\sqrt{1 + \cos \omega} + v \cos \omega)$, then we can rewrite the surface in a simple form as

$$\varphi(s, v) = \frac{1}{\sqrt{2}} (\mu T + vN + \rho B).$$

Next, the first and second partial differentials of $\varphi(s, v)$ are

$$\begin{aligned}\varphi_s &= \frac{1}{\sqrt{2}} ((\mu_s - v\kappa)T + (\kappa\mu - \tau\rho)N + (\rho_s + v\tau)B), \\ \varphi_v &= \frac{1}{\sqrt{2}} (\mu_v T + N + \rho_v B), \\ \varphi_{vv} &= 0, \\ \varphi_{sv} &= \frac{1}{\sqrt{2}} ((\mu_{sv} - \kappa)T + (\kappa\mu_v - \tau\rho_v)N + (\rho_{sv} + \tau)B), \\ \varphi_{ss} &= \frac{1}{\sqrt{2}} \begin{bmatrix} (\mu_{ss} - v\kappa' - \kappa^2\mu + \tau\kappa\rho)T \\ + (2\kappa\mu_s - 2\tau\rho_s + \kappa'\mu - \tau'\rho - v\kappa^2 - v\tau^2)N \\ + (\rho_{ss} + v\tau' + \tau\kappa\mu - \tau^2\rho)B \end{bmatrix}.\end{aligned}$$

And the vectorial product of the vectors φ_s , φ_v and its norm are

$$\begin{aligned}\varphi_s \wedge \varphi_v &= \frac{1}{2} \begin{bmatrix} (\rho_v(\kappa\mu - \tau\rho) - (\rho_s + v\tau))T + (\mu_v(\rho_s + v\tau) - \rho_v(\mu_s - v\kappa))N \\ + ((\mu_s - v\kappa) - \mu_v(\kappa\mu - \tau\rho))B \end{bmatrix}, \\ \|\varphi_s \wedge \varphi_v\| &= \frac{1}{2} \left[\begin{aligned} &(\rho_v(\kappa\mu - \tau\rho) - (\rho_s + v\tau))^2 + ((\mu_s - v\kappa) - \mu_v(\kappa\mu - \tau\rho))^2 \\ &+ (\mu_v(\rho_s + v\tau) - \rho_v(\mu_s - v\kappa))^2 \end{aligned} \right]^{\frac{1}{2}}.\end{aligned}$$

From the expression (4), the normal of the surface $\varphi(s, v)$ denoted by N_φ can then be given as:

$$N_\varphi = \frac{\begin{bmatrix} (\rho_v(\kappa\mu - \tau\rho) - (\rho_s + v\tau))T + (\mu_v(\rho_s + v\tau) - \rho_v(\mu_s - v\kappa))N \\ + ((\mu_s - v\kappa) - \mu_v(\kappa\mu - \tau\rho))B \end{bmatrix}}{\left[\begin{aligned} &(\rho_v(\kappa\mu - \tau\rho) - (\rho_s + v\tau))^2 + ((\mu_s - v\kappa) - \mu_v(\kappa\mu - \tau\rho))^2 \\ &+ (\mu_v(\rho_s + v\tau) - \rho_v(\mu_s - v\kappa))^2 \end{aligned} \right]^{\frac{1}{2}}}.$$

The coefficients of first and second fundamental form are calculated by using the expressions (6) and (7) as:

$$\begin{aligned}
 E_\varphi &= \frac{1}{2} \left((\mu_s - v\kappa)^2 + (\kappa\mu - \tau\rho)^2 + (\rho_s + v\tau)^2 \right), \\
 F_\varphi &= \frac{1}{2} (\mu_v (\mu_s - v\kappa) + (\kappa\mu - \tau\rho) + \rho_v (\rho_s + v\tau)), \\
 G_\varphi &= 1
 \end{aligned}$$

and

$$\begin{aligned}
 e_\varphi &= \frac{\left[\begin{aligned} &(\rho_v (\kappa\mu - \tau\rho) - (\rho_s + v\tau)) (\mu_{ss} - v\kappa' - \kappa^2\mu + \tau\kappa\rho) \\ &+ ((\mu_s - v\kappa) - \mu_v (\kappa\mu - \tau\rho)) (\rho_{ss} + v\tau' + \tau\kappa\mu - \tau^2\rho) \\ &+ (\mu_v (\rho_s + v\tau) - \rho_v (\mu_s - v\kappa)) (2\kappa\mu_s - 2\tau\rho_s + \kappa'\mu - \tau'\rho - v\kappa^2 - v\tau^2) \end{aligned} \right]}{\sqrt{2} \left[\begin{aligned} &(\rho_v (\kappa\mu - \tau\rho) - (\rho_s + v\tau))^2 + ((\mu_s - v\kappa) - \mu_v (\kappa\mu - \tau\rho))^2 \\ &+ (\mu_v (\rho_s + v\tau) - \rho_v (\mu_s - v\kappa))^2 \end{aligned} \right]^{\frac{1}{2}}}, \\
 f_\varphi &= \frac{\left[\begin{aligned} &(\rho_v (\kappa\mu - \tau\rho) - (\rho_s + v\tau)) (\mu_{sv} - \kappa) \\ &+ ((\mu_s - v\kappa) - \mu_v (\kappa\mu - \tau\rho)) (\rho_{sv} + \tau) \\ &+ (\mu_v (\rho_s + v\tau) - \rho_v (\mu_s - v\kappa)) (\kappa\mu_v - \tau\rho_v) \end{aligned} \right]}{\sqrt{2} \left[\begin{aligned} &(\rho_v (\kappa\mu - \tau\rho) - (\rho_s + v\tau))^2 + ((\mu_s - v\kappa) - \mu_v (\kappa\mu - \tau\rho))^2 \\ &+ (\mu_v (\rho_s + v\tau) - \rho_v (\mu_s - v\kappa))^2 \end{aligned} \right]^{\frac{1}{2}}}, \\
 g_\varphi &= 0,
 \end{aligned}$$

respectively. Finally, from the expression (5), we have the Gaussian and mean curvatures as in the following:

$$K_\varphi = - \frac{\left[\begin{aligned} &(\rho_v (\kappa\mu - \tau\rho) - (\rho_s + v\tau)) (\mu_{sv} - \kappa) \\ &+ ((\mu_s - v\kappa) - \mu_v (\kappa\mu - \tau\rho)) (\rho_{sv} + \tau) \\ &+ (\mu_v (\rho_s + v\tau) - \rho_v (\mu_s - v\kappa)) (\kappa\mu_v - \tau\rho_v) \end{aligned} \right]^2}{\left[\begin{aligned} &(\rho_v (\kappa\mu - \tau\rho) - (\rho_s + v\tau))^2 + ((\mu_s - v\kappa) - \mu_v (\kappa\mu - \tau\rho))^2 \\ &+ (\mu_v (\rho_s + v\tau) - \rho_v (\mu_s - v\kappa))^2 \end{aligned} \right]^2},$$

$$H_\varphi = \frac{\left[\begin{aligned} &(\rho_v (\kappa\mu - \tau\rho) - (\rho_s + v\tau)) (\mu_{ss} - v\kappa' - \kappa^2\mu + \tau\kappa\rho) \\ &+ ((\mu_s - v\kappa) - \mu_v (\kappa\mu - \tau\rho)) (\rho_{ss} + v\tau' + \tau\kappa\mu - \tau^2\rho) \\ &+ (\mu_v (\rho_s + v\tau) - \rho_v (\mu_s - v\kappa)) (2\kappa\mu_s - 2\tau\rho_s + \kappa'\mu - \tau'\rho - v\kappa^2 - v\tau^2) \\ &- (\rho_v (\kappa\mu - \tau\rho) - (\rho_s + v\tau)) \\ &\cdot (\mu_{sv} - \kappa) (\mu_v (\mu_s - v\kappa) + (\kappa\mu - \tau\rho) + \rho_v (\rho_s + v\tau)) \\ &- ((\mu_s - v\kappa) - \mu_v (\kappa\mu - \tau\rho)) (\rho_{sv} + \tau) \\ &\cdot (\mu_v (\mu_s - v\kappa) + (\kappa\mu - \tau\rho) + \rho_v (\rho_s + v\tau)) \\ &- (\mu_v (\rho_s + v\tau) - \rho_v (\mu_s - v\kappa)) (\kappa\mu_v - \tau\rho_v) \\ &\cdot (\mu_v (\mu_s - v\kappa) + (\kappa\mu - \tau\rho) + \rho_v (\rho_s + v\tau)) \end{aligned} \right]}{\sqrt{2} \left[\begin{aligned} &(\rho_v (\kappa\mu - \tau\rho) - (\rho_s + v\tau))^2 + ((\mu_s - v\kappa) - \mu_v (\kappa\mu - \tau\rho))^2 \\ &+ (\mu_v (\rho_s + v\tau) - \rho_v (\mu_s - v\kappa))^2 \end{aligned} \right]^{\frac{3}{2}}}.$$

Definition 9. *Let's define a ruled surface generated by continuously moving the vector $B + C$ along the BC - Smarandache curve. Thus, we provide its parametric form as*

$$\lambda(s, v) = \frac{B + C}{\sqrt{2 + 2 \cos \omega}} + v \frac{B + C}{\sqrt{2 + 2 \cos \omega}},$$

$$\lambda(s, v) = \frac{1 + v}{\sqrt{2}} ((\sqrt{1 - \cos \omega}) T + (\sqrt{1 + \cos \omega}) B).$$

Next, the first and second partial differentials of $\lambda(s, v)$ are

$$\lambda_s = \frac{1+v}{\sqrt{2}} (\omega' \cos \omega T - \tau N - \omega' \sin \omega B),$$

$$\lambda_v = \frac{1}{\sqrt{2}} (\sin \omega T + (1 + \cos \omega) B),$$

$$\lambda_{vv} = 0,$$

$$\lambda_{sv} = \frac{1}{\sqrt{2}} (\omega' \cos \omega T - \tau N - \omega' \sin \omega B),$$

$$\lambda_{ss} = \frac{1+v}{\sqrt{2}} \left((\kappa\tau + \omega' \cos \omega) T + (\omega' \sqrt{\kappa^2 + \tau^2} - \tau') N - (\tau^2 + \omega' \sin \omega) B \right),$$

And the vectorial product of the vectors λ_s , λ_v and its norm are

$$\lambda_s \wedge \lambda_v = \frac{1+v}{2} (-\tau(1 + \cos \omega) T - \omega'(1 + \cos \omega) N + \tau \sin \omega B)$$

$$\|\lambda_s \wedge \lambda_v\| = \frac{1+v}{2} \sqrt{(\tau^2 + \omega'^2)(1 + \cos \omega)^2 + \tau^2 \sin^2 \omega}.$$

From the expression (4), the normal of this surface shown by N_λ is given

$$N_\lambda = \frac{-\tau(1 + \cos \omega) T - \omega'(1 + \cos \omega) N + \tau \sin \omega B}{\sqrt{(\tau^2 + \omega'^2)(1 + \cos \omega)^2 + \tau^2 \sin^2 \omega}}.$$

Next, from the expressions (6) and (7), the coefficients of the first and the second fundamental forms can be calculated as

$$E_\lambda = \frac{1}{2} \left((1+v)^2 (\omega'^2 + \tau^2) \right),$$

$$F_\lambda = -\frac{1}{\sqrt{2}} (\omega' (1+v) \sin \omega),$$

$$G_\lambda = (1 + \cos \omega)$$

and

$$e_\lambda = -\frac{\tau^2 (\kappa + \sqrt{\kappa^2 + \tau^2}) + (\tau\omega' + \omega') (1 + \cos \omega) (\omega' \sqrt{\kappa^2 + \tau^2} - \tau')}{(1+v)^{-1} \sqrt{2} \sqrt{(\tau^2 + \omega'^2)(1 + \cos \omega)^2 + \tau^2 \sin^2 \omega}},$$

$$f_\lambda = 0,$$

$$g_\lambda = 0,$$

respectively. Finally, from the expression (5), we have the Gaussian and mean curvatures as

$$K_\lambda = 0,$$

$$H_\lambda = \frac{(-\kappa\tau^2 - \tau^2\sqrt{\kappa^2 + \tau^2})(1 + \cos\omega) - (\tau\omega' + \omega')(1 + \cos\omega)^2(\omega'\sqrt{\kappa^2 + \tau^2} - \tau')}{\left[\begin{array}{l} \sqrt{2}(1+v)\left((\omega'^2 + \tau^2)(1 + \cos\omega) - \omega'^2\sin^2\omega\right) \\ \cdot \sqrt{(\tau^2 + \omega'^2)(1 + \cos\omega)^2 + \tau^2\sin^2\omega} \end{array} \right]}.$$

Corollary 3. *The ruled surface $\lambda(s, v)$ is always developable.*

Example 1. *Let us consider the famous Viviani's curve whose parametric form is given by $\alpha(s) = (\cos^2(s), \cos(s)\sin(s), \sin(s))$. The Frenet vectors $T(s), N(s), B(s)$ and the unit Darboux vector $C(s)$ are given in respective order as*

$$T(s) = \left(-\frac{2\cos(s)\sin(s)}{\sqrt{\cos(s)^2 + 1}}, \frac{2\cos(s)^2 - 1}{\sqrt{\cos(s)^2 + 1}}, \frac{\cos(s)}{\sqrt{\cos(s)^2 + 1}} \right),$$

$$N(s) = \left(\begin{array}{l} -\frac{2(\cos(s)^4 + 2\cos(s)^2 - 1)}{\sqrt{3\cos(s)^2 + 5}\sqrt{\cos(s)^2 + 1}}, -\frac{\cos(s)\sin(s)(2\cos(s)^2 + 5)}{\sqrt{\cos(s)^2 + 1}\sqrt{3\cos(s)^2 + 5}}, \\ -\frac{\sin(s)}{\sqrt{\cos(s)^2 + 1}\sqrt{3\cos(s)^2 + 5}} \end{array} \right)$$

$$B(s) = \left(\frac{(2\cos(s)^2 + 1)\sin(s)}{\sqrt{3\cos(s)^2 + 5}}, -\frac{2\cos(s)^3}{\sqrt{3\cos(s)^2 + 5}}, \frac{2}{\sqrt{3\cos(s)^2 + 5}} \right),$$

$$C(s) = \begin{pmatrix} \frac{(-6 \cos(s)^4 + \cos(s)^2 + 5) \sin(s) \sqrt{\cos(s)^2 + 1}}{\sqrt{(36 \cos(s)^8 + 135 \cos(s)^6 + 243 \cos(s)^4 + 261 \cos(s)^2 + 125)}}, \\ \sqrt{\cdot (\cos(s)^2 + 1)} \\ \frac{2(3 \cos(s)^4 - 2 \cos(s)^2 - 3) \cos(s) \sqrt{\cos(s)^2 + 1}}{\sqrt{(36 \cos(s)^8 + 135 \cos(s)^6 + 243 \cos(s)^4 + 261 \cos(s)^2 + 125)}}, \\ \sqrt{\cdot (\cos(s)^2 + 1)} \\ \frac{2(3 \cos(s)^4 + 6 \cos(s)^2 + 5) \sqrt{\cos(s)^2 + 1}}{\sqrt{(36 \cos(s)^8 + 135 \cos(s)^6 + 243 \cos(s)^4 + 261 \cos(s)^2 + 125)}}. \\ \sqrt{\cdot (\cos(s)^2 + 1)} \end{pmatrix}$$

The graphs of ruled surfaces, obtained using these vectors and definitions and given the parametric equations below, are presented in FIGURE 1, 2 and 3, respectively.

$$\Sigma(s, v) = \frac{1}{\sqrt{2}}(T + C) + \frac{v}{\sqrt{2}}(T + C), \quad \Delta(s, v) = \frac{1}{\sqrt{2}}(T + C) + \frac{v}{\sqrt{2}}(N + C),$$

$$\Upsilon(s, v) = \frac{1}{\sqrt{2}}(T + C) + \frac{v}{\sqrt{2}}(B + C), \quad \chi(s, v) = \frac{1}{\sqrt{2}}(N + C) + \frac{v}{\sqrt{2}}(T + C),$$

$$P(s, v) = \frac{1}{\sqrt{2}}(N + C) + \frac{v}{\sqrt{2}}(N + C), \quad \delta(s, v) = \frac{1}{\sqrt{2}}(N + C) + \frac{v}{\sqrt{2}}(B + C),$$

$$\eta(s, v) = \frac{1}{\sqrt{2}}(B + C) + \frac{v}{\sqrt{2}}(T + C), \quad \varphi(s, v) = \frac{1}{\sqrt{2}}(B + C) + \frac{v}{\sqrt{2}}(N + C),$$

$$\lambda(s, v) = \frac{1}{\sqrt{2}}(B + C) + \frac{v}{\sqrt{2}}(B + C).$$

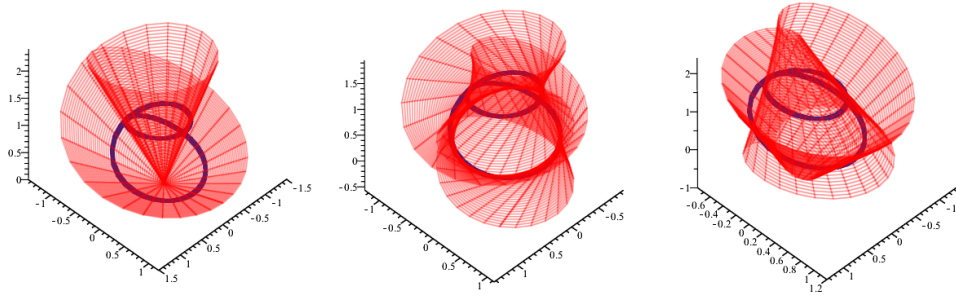


FIGURE 1. The ruled surfaces whose the base curve TC – Smarandache curve and the direction vector TC, NC, BC , respectively.

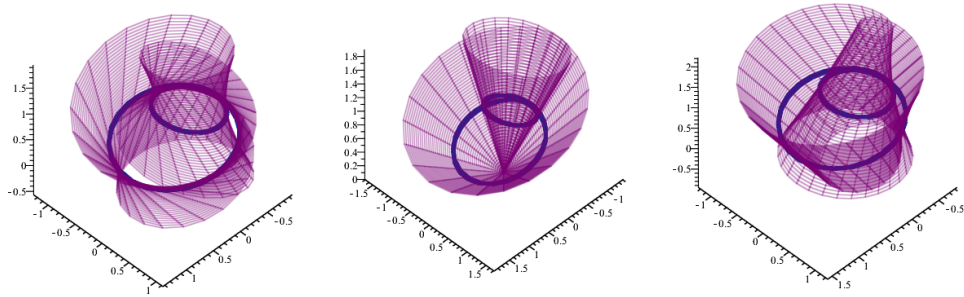


FIGURE 2. The ruled surfaces whose the base curve NC – Smarandache curve and the direction vector TC, NC, BC , respectively.

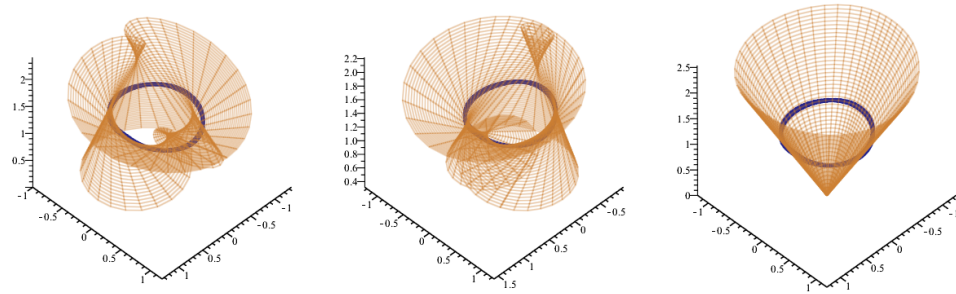


FIGURE 3. The ruled surfaces whose the base curve BC – Smarandache curve and the direction vector TC, NC, BC , respectively.

4. CONCLUSION

In this paper, Smarandache curves derived from Frenet vectors and Darboux vector of any curve are described. Then, by considering the direction vectors obtained from Frenet vectors and Darboux vectors, new ruled surfaces are obtained along these curves. Finally, the Gaussian and mean curvatures of these surfaces are given. This paper can also be studied by considering other frames defined on the curve, additionally it can be examined in the spaces other than Euclidean space.

Author Contribution Statements All authors contributed equally and significantly in writing this article. All authors read and approved the final manuscript.

Declaration of Competing Interests On behalf of all authors, the corresponding author states that there is no conflict of interest.

Acknowledgements The authors would like to thank the reviewers for their valuable suggestions that lead to a better presentation of the article, as well as the journal editors who took care of the article.

REFERENCES

- [1] Ali, A. T., Special Smarandache curves in the Euclidean space, *Int. J. Math. Comb.*, 2 (2010), 30–36.
- [2] Aslan, S., Bekar, M., Yaylı, Y., Ruled surfaces constructed by quaternions, *J. Geom. Phys.*, 161 (2021), 1–9. <https://doi.org/10.1016/j.geomphys.2020.104048>
- [3] Bektaş, M., On characterizations of general helices for ruled surfaces in the pseudo-Galilean space G_3^1 -(Part-I), *J. Math. of Kyoto Univ.*, 44(3) (2004), 523–528. <https://doi.org/10.1215/kjm/1250283082>
- [4] Bektaş, Ö., Yüce, S., Special Smarandache curves according to Darboux frame in E^3 , *Romanian J. Math. Comp. Sci.*, 3 (2013), 48–59.
- [5] Berk, A., A Structural Basis for Surface Discretization of Free Form Structures: Integration of Geometry, Materials and Fabrication, Ph.D Thesis, Michigan University, ABD, 2012.
- [6] Çetin, M., Kocayığıt, H., On the quaternionic Smarandache curves in Euclidean 3-space, *Int. J. Contemp. Math. Sci.*, 8(3) (2013), 139–150.
- [7] Do-Carmo, P. M., *Differential Geometry of Curves and Surfaces*, IMPA, 1976.
- [8] Fenchel, W., On the differential geometry of closed space curves, *Bull. Am. Math. Soc.*, 57 (1951), 44–54.
- [9] Gray, A., Abbena, E., Salamon, S., *Modern Differential Geometry of Curves and Surfaces with Mathematica*, Chapman and Hall/CRC, 2017.
- [10] Gür Mazlum, S., Şenyurt S., Grilli, L., The dual expression of parallel equidistant ruled surfaces in Euclidean 3-space, *Symmetry*, 14 (2022), 1062. <https://doi.org/10.3390/sym14051062>
- [11] Gür Mazlum, S., Bektaş, M., On the modified orthogonal frames of the non-unit speed curves in Euclidean 3-Space E^3 , *Turk. J. Sci.*, 7(2) 2022, 58–74.
- [12] Hathout, F., Bekar, M., Yaylı, Y., Ruled surfaces and tangent bundle of unit 2-sphere, *Int. J. Geom. Meth. Mod. Phys.*, 2 (2017). <https://doi.org/10.1142/S0219887817501456>
- [13] Karaca, E., Singularities of the ruled surfaces according to RM frame and natural lift curves, *Cumhur. Sci. J.*, 43(2) (2022), 308–315. <https://doi.org/10.17776/cs.j.1057212>

- [14] Kılıçoğlu, Ş., Hacısalihoglu, H., On the b-scrolls with time-like generating vector in 3-dimensional Minkowski space E_1^3 , *Beykent Univ. J. Sci. and Tech.*, 3(2) (2008), 55–67.
- [15] Li, Y., Liu, S., Wang, Z., Tangent developables and Darboux developables of framed curves, *Topol. Appl.* 301, (2021) 107526. <https://doi.org/10.1016/j.topol.2020.107526>
- [16] Li, Y., Şenyurt, S., Özdura, A., Canlı, D., The characterizations of parallel q-equidistant ruled surfaces, *Symmetry*, 14 (2022), 1879. <https://doi.org/10.3390/sym14091879>
- [17] Li, Y., Eren, K., Ayvaci, H., Ersoy, S., The developable surfaces with pointwise 1-type Gauss map of Frenet type framed base curves in Euclidean 3-space, *AIMS Math.*, 8(1) 2022, 2226–2239. <https://doi.org/10.3934/math.2023115>
- [18] Ouarab, S., Smarandache ruled surfaces according to Frenet-Serret frame of a regular curve in E^3 , *Hindawi Abst. Appl. Analy.*, Article ID 5526536 (2021), 8 pages.
- [19] Ouarab, S., Smarandache ruled surfaces according to Darboux Frame in E^3 , *Hindawi J. Math.*, Article ID 9912624 (2021), 10 pages. <https://doi.org/10.1155/2021/9912624>
- [20] Ouarab, S., NC-Smarandache ruled surface and NW-Smarandache ruled surface according to alternative moving frame in E^3 , *Hindawi J. Math.*, Article ID 9951434 (2021), 6 pages. <https://doi.org/10.1155/2021/9951434>
- [21] Öğrenmiş, A. O., Bektaş, M., Ergüt, M., On the helices in the Galilean space G^3 , *Iran J. Sci. Tech.*, 31(A2) (2007), 177–181.
- [22] Pottmann, H., Eigensatz, M., Vaxman, A., Wallner, J., Architectural geometry, *Comp. Graph.* 47 (2015), 145–164. <https://doi.org/10.1016/j.cag.2014.11.002>
- [23] Pressley, A., *Elementary Differential Geometry*, Springer Science & Business Media, 2010. <https://doi.org/10.1007/978-1-84882-891-9>
- [24] Stillwell, J., *Mathematics and Its History*, (Vol. 3) New York, Springer, 2010.
- [25] Struik, D. J., *Lectures on Classical Differential Geometry*, Addison-Wesley Publishing Company, 1961.
- [26] Şenyurt, S., Sivas, S., An application of Smarandache curve, *Ordu Univ. J. Sci. Tech.*, 3(1) (2013), 46–60.
- [27] Şenyurt, S., Canlı, D., Some special Smarandache ruled surfaces by Frenet frame in E^3 -I, *Turk. J. Sci.*, 7(1) (2020), 31–42. <https://doi.org/10.5831/HMJ.2022.44.4.594>
- [28] Şenyurt, S., Eren, K., Smarandache curves of spacelike anti-Salkowski curve with a spacelike principal normal according to Frenet frame, *Gümüşhane Üniv. Fen Bil. Derg.*, 10(1) (2020), 251–260. <https://doi.org/10.17714/gumusfenbil.621363>
- [29] Şenyurt, S., Eren, K., Smarandache curves of spacelike anti-Salkowski curve with a timelike principal normal according to Frenet frame, *Erzincan Univ. J. Sci. Tech.*, 13(2) (2020), 404–416. <https://doi.org/10.18185/erzifbed.621344>
- [30] Şenyurt, S., Eren, K., Smarandache curves of spacelike Salkowski curve with a spacelike principal normal according to Frenet frame, *Erzincan Univ. J. Sci. Tech.*, 13(special issue -I) (2020), 7–17. <https://doi.org/10.18185/erzifbed.590950>
- [31] Şenyurt, S., Eren, K., Some Smarandache curves constructed from a spacelike Salkowski curve with timelike principal normal, *Punjab Univ. J. Math.*, 53(9) (2021), 679–690.
- [32] Şenyurt, S., Canlı, D., Çan, E., Smarandache-based ruled surfaces with the Darboux vector according to Frenet frame in E^3 , *J. New Theory*, 39 (2022), 8–18. <https://doi.org/10.53570/jnt.1106331>
- [33] Şenyurt, S., Gür, S., Grilli, L., Gaussian curvatures of parallel ruled surfaces, *Appl. Math. Sci.*, 14(4) (2020), 173–184, <https://doi.org/10.12988/ams.2020.912175>.
- [34] Taşköprü, K., Tosun, M., Smarandache curves on S^2 , *Bol. Soc. Paran. Mat.*, 32(1) (2014), 51–59.
- [35] Turgut, M., Yılmaz, S., Smarandache curves in Minkowski space-time, *Int.l J. Math. Comb.*, 3 (2008), 51–55.
- [36] Yaylı, Y., Saracoglu, S., On developable ruled surfaces in Minkowski space, *Adv. Appl. Clifford Algebr.*, 22 (2012), 499–510. <https://doi.org/10.1007/s00006-011-0305-5>



MODULO PERIODIC POISSON STABLE SOLUTIONS OF DYNAMIC EQUATIONS ON A TIME SCALE

Fatma TOKMAK FEN¹ and Mehmet Onur FEN²

¹Department of Mathematics, Gazi University, Ankara, TÜRKİYE

²Department of Mathematics, TED University, Ankara, TÜRKİYE

ABSTRACT. Existence, uniqueness, and asymptotic stability of modulo periodic Poisson stable solutions of dynamic equations on a periodic time scale are investigated. The model under investigation involves a term which is constructed via a Poisson stable sequence. Novel definitions for Poisson stable as well as modulo periodic Poisson stable functions on time scales are given, and the reduction technique to systems of impulsive differential equations is utilized to achieve the main result. An example which confirms the theoretical results is provided.

1. INTRODUCTION AND PRELIMINARIES

Poisson stable motions, which were first introduced by Poincaré [29], include the cases of oscillations such as periodic, quasi-periodic, almost periodic, almost automorphic, recurrent, and pseudo-recurrent ones [8,9,14,21,37]. Results on Poisson stable solutions for stochastic differential equations and a class of fourth-order dynamical systems can be found in the studies [13,27,28]. Recently, a new type of flow called modulo periodic Poisson stable (MPPS) was introduced in paper [5], where the authors also considered the presence of MPPS trajectories in quasilinear systems of ordinary differential equations. In the interest of brevity, MPPS trajectories are the ones which can be decomposed as the sum of periodic and Poisson stable functions. Motivated by the importance of oscillations in real world processes [12,15,18,31,36] and various application fields of dynamic equations on time scales [23,26,32,34,35], in this study, we investigate the existence, uniqueness, and asymptotic stability of MPPS solutions in such equations. To the best of our

2020 *Mathematics Subject Classification.* 34N05, 34A37.

Keywords. Modulo periodic Poisson stability, dynamic equations, impulsive differential equations, periodic time scale.

¹ ✉ fatmatokmak@gazi.edu.tr; 0000-0002-4051-7798

² ✉ onur.fen@tedu.edu.tr-Corresponding author; 0000-0002-7787-7236.

knowledge this is the first time in the literature that Poisson stable as well as MPPS solutions are introduced and investigated for dynamic equations on time scales.

In the literature, the concept of dynamic equations on time scales has started with Hilger [19]. This concept, in general, unifies the studies of differential and difference equations. The basic definitions concerning dynamic equations on time scales are as follows [1, 11, 22]. A time scale is a nonempty closed subset of \mathbb{R} . On a time scale \mathbb{T} , the forward jump operator is defined by $\sigma(t) = \inf \{s \in \mathbb{T} : s > t\}$, whereas $\rho(t) = \sup \{s \in \mathbb{T} : s < t\}$ is the backward jump operator. A point $t \in \mathbb{T}$ is called right-dense if $\sigma(t) = t$ and it is called right-scattered if $\sigma(t) > t$. Similarly, $t \in \mathbb{T}$ is said to be left-dense, left-scattered if $\rho(t) = t$, $\rho(t) < t$, respectively. We say that a function $u : \mathbb{T} \rightarrow \mathbb{R}^m$ is rd-continuous if it is continuous at each right-dense point and its left-sided limit exists in each left-dense point. If t is a right-scattered point of \mathbb{T} , then the delta derivative u^Δ of a continuous function u is defined to be

$$u^\Delta(t) = \frac{u(\sigma(t)) - u(t)}{\sigma(t) - t}. \quad (1)$$

Additionally, we have

$$u^\Delta(t) = \lim_{r \rightarrow t, r \in \mathbb{T}} \frac{u(t) - u(r)}{t - r} \quad (2)$$

at a right-dense point t , provided that the limit exists.

It was shown by Akhmet and Turan [6] that dynamic equations on time scales which are union of disjoint closed intervals with positive length can be transformed to systems of impulsive differential equations. In the present study we make use of the technique introduced in [6] to investigate MPPS solutions of dynamic equations on a periodic time scale. More precisely, we take into account the time scale

$$\mathbb{T}_0 = \bigcup_{k=-\infty}^{\infty} [\theta_{2k-1}, \theta_{2k}], \quad (3)$$

where for each integer k the terms of the sequence $\{\theta_k\}_{k \in \mathbb{Z}}$ are defined by the equations

$$\theta_{2k-1} = \theta + \delta + (k-1)\omega, \quad \theta_{2k} = \theta + k\omega, \quad (4)$$

in which θ is a fixed real number and ω, δ are positive numbers such that $\omega > \delta$. The time scale \mathbb{T}_0 is periodic with period ω since $t \pm \omega \in \mathbb{T}_0$ whenever $t \in \mathbb{T}_0$, and

$$\theta_{2k+1} - \theta_{2k} = \delta, \quad k \in \mathbb{Z}.$$

For details of periodic time scales the reader is referred to [20], and some applications of dynamic equations on such time scales can be found in [10, 16, 17]. It is worth noting that for each $k \in \mathbb{Z}$, the points θ_{2k} are right-scattered and left-dense, the points θ_{2k-1} are left-scattered and right-dense, and $\sigma(\theta_{2k}) = \theta_{2k+1}$, $\rho(\theta_{2k+1}) = \theta_{2k}$.

Our main object of investigation is the equation

$$y^\Delta(t) = Ay(t) + f(t) + g(t), \tag{5}$$

where $t \in \mathbb{T}_0$, $A \in \mathbb{R}^{m \times m}$ is a constant matrix, $f : \mathbb{T}_0 \rightarrow \mathbb{R}^m$ is an rd-continuous function such that

$$f(t + \omega) = f(t) \tag{6}$$

for each $t \in \mathbb{T}_0$, the function $g : \mathbb{T}_0 \rightarrow \mathbb{R}^m$ is defined by

$$g(t) = \gamma_k \tag{7}$$

for $t \in [\theta_{2k-1}, \theta_{2k}]$, $k \in \mathbb{Z}$, and $\{\gamma_k\}_{k \in \mathbb{Z}}$ is a bounded sequence in \mathbb{R}^m . In this paper we rigorously prove that if the sequence $\{\gamma_k\}_{k \in \mathbb{Z}}$ is positively Poisson stable [33], then system (5) possesses a unique asymptotically stable MPPS solution.

It was shown in [5] that an MPPS function is Poisson stable if the corresponding Poisson number is zero. However, in this study, the structure of the function $g(t)$ in (5), which is defined by means of the sequence $\{\gamma_k\}_{k \in \mathbb{Z}}$, allows us to make discussion for the Poisson stability of the MPPS solution without taking into account the Poisson number.

The rest of the paper is organized as follows. In Section 2, we utilize the technique introduced in [6] to reduce (5) to an impulsive system. We investigate the presence of bounded solutions of the reduced impulsive system and hereby the ones for (5) in Section 3. The new definitions of positively Poisson stable and MPPS functions defined on time scales are provided in Section 4. Moreover, in that section we rigorously prove the existence and uniqueness of an asymptotically stable MPPS solution of system (5). Section 5, on the other hand, is devoted to an example, which confirms the theoretical results. Finally, some concluding remarks are provided in Section 6.

2. REDUCTION TO IMPULSIVE SYSTEMS

In this section we make use of the ψ -substitution method introduced by Akhmet and Turan [6,7] to reduce dynamic equation (5) to a system of impulsive differential equations.

We assume without loss of generality that $\theta_{-1} < 0 \leq \theta_0$. On the set

$$\mathbb{T}'_0 = \mathbb{T}_0 \setminus \{\theta_{2k-1} : k \in \mathbb{Z}\},$$

let us consider the ψ -substitution defined through the equation

$$\psi(t) = t - k\delta, \quad \theta_{2k-1} < t \leq \theta_{2k} \tag{8}$$

for each integer k [6]. The function $\psi : \mathbb{T}'_0 \rightarrow \mathbb{R}$ is one-to-one and onto, $\psi(0) = 0$, $\lim_{t \rightarrow \infty, t \in \mathbb{T}'_0} \psi(t) = \infty$, and

$$\psi^{-1}(s) = s + k\delta, \quad s_{k-1} < s \leq s_k \tag{9}$$

for each integer k , where $s_k = \psi(\theta_{2k})$. Equation (8) yields

$$s_k = \theta + k(\omega - \delta), \tag{10}$$

and accordingly, we have $s_{k+1} = s_k + \omega - \delta$ for $k \in \mathbb{Z}$.

The function $\psi^{-1} : \mathbb{R} \rightarrow \mathbb{T}'_0$ defined by (9) is piecewise continuous, and it has discontinuities of the first kind at the points s_k , $k \in \mathbb{Z}$, such that $\psi^{-1}(s_k+) - \psi^{-1}(s_k) = \delta$ with $\psi^{-1}(s_k+) = \lim_{s \rightarrow s_k^+} \psi^{-1}(s)$. Moreover, $d\psi(t)/dt = 1$ for $t \in \mathbb{T}'_0$ and $d\psi^{-1}(s)/ds = 1$ for $s \in \mathbb{R} \setminus \{s_k : k \in \mathbb{Z}\}$ (6). Since $\psi(\omega) = \omega - \delta$, one can attain by means of Corollary 12 (6) that the equality

$$\psi(t + \omega) = \psi(t) + \omega - \delta \tag{11}$$

is fulfilled for each $t \in \mathbb{T}'_0$.

In what follows $C_{rd}(\mathbb{T})$ stands for the set of all functions $\varphi(t) : \mathbb{T} \rightarrow \mathbb{R}^m$ which are rd-continuous on a time scale \mathbb{T} .

As a consequence of Lemma 13 and Lemma 14 mentioned in paper (6), we have the following assertion.

Lemma 1. *A function $\varphi(t) \in C_{rd}(\mathbb{T}_0)$ is periodic with period ω if and only if the function $\varphi(\psi^{-1}(s))$ is periodic on \mathbb{R} with period $\omega - \delta$.*

Utilizing the descriptions of the delta derivative at right-scattered and right-dense points given respectively by (1) and (2), one can express system (5) in the form

$$\begin{aligned} y'(t) &= Ay(t) + f(t) + g(t), \quad t \in \mathbb{T}'_0, \\ y(\theta_{2k+1}) &= y(\theta_{2k}) + \delta (Ay(\theta_{2k}) + f(\theta_{2k}) + \gamma_k). \end{aligned} \tag{12}$$

The substitution $s = \psi(t)$, where $\psi(t)$ is defined by (8), transforms (12) to the impulsive system

$$\begin{aligned} x'(s) &= Ax(s) + f(\psi^{-1}(s)) + g(\psi^{-1}(s)), \quad s \neq s_k, \\ \Delta x|_{s=s_k} &= \delta (Ax(s_k) + f(\psi^{-1}(s_k)) + \gamma_k), \end{aligned} \tag{13}$$

where $x(s) = y(\psi^{-1}(s))$, $\Delta x|_{s=s_k} = x(s_k+) - x(s_k)$, $x(s_k+) = \lim_{s \rightarrow s_k^+} x(s)$, and the sequence $\{s_k\}_{k \in \mathbb{Z}}$ of impulse moments is defined by (10).

It is worth noting that if a function $\tilde{x}(s) : \mathbb{R} \rightarrow \mathbb{R}^m$ is a solution of the impulsive system (13), then the function $\tilde{y}(t) : \mathbb{T}_0 \rightarrow \mathbb{R}^m$ defined by $\tilde{y}(t) = \tilde{x}(\psi(t))$ for $t \in \mathbb{T}'_0$ with $\tilde{y}(\theta_{2k+1}) = \tilde{x}(s_k+)$, $k \in \mathbb{Z}$, is a solution of (5), and vice versa.

Existence, uniqueness, and asymptotic stability of the bounded solution for system (5) is investigated in the next section.

3. BOUNDED SOLUTIONS

In the remaining parts of the paper we will denote by $i(J)$ the number of the terms of the sequence $\{s_k\}_{k \in \mathbb{Z}}$ which take place in an interval J . One can confirm using (10) that

$$i([r + \omega - \delta, s + \omega - \delta]) = i([r, s]) \tag{14}$$

for every $s, r \in \mathbb{R}$ with $s > r$.

Let us denote by $U(s, r)$ the matriciant [2, 30] of the linear homogeneous impulsive system

$$\begin{aligned} x'(s) &= Ax(s), \quad s \neq s_k, \\ \Delta x|_{s=s_k} &= \delta Ax(s_k) \end{aligned}$$

such that $U(s, s) = I$. The equation

$$U(s, r) = e^{A(s-r)}(I + \delta A)^{i([r, s])} \tag{15}$$

is fulfilled for $s > r$.

The following assumptions are required.

- (A1) $\det(I + \delta A) \neq 0$, where I is the $m \times m$ identity matrix;
- (A2) All eigenvalues of the matrix $e^{(\omega-\delta)A}(I + \delta A)$ lie inside the unit circle.

In the sequel we use the Euclidean norm for vectors and the spectral norm for square matrices. Under the assumptions (A1) and (A2) there exist real numbers $N \geq 1$ and $\lambda > 0$ such that

$$\|U(s, r)\| \leq N e^{-\lambda(s-r)} \tag{16}$$

for $s \geq r$ [30].

It is demonstrated in Theorem 87 [30] that the impulsive system (13) possesses a unique solution $\phi(s)$ which is bounded on the real axis and satisfies the equation

$$\begin{aligned} \phi(s) &= \int_{-\infty}^s U(s, r) (f(\psi^{-1}(r)) + g(\psi^{-1}(r))) dr \\ &+ \delta \sum_{-\infty < s_k < s} U(s, s_k+) (f(\psi^{-1}(s_k)) + \gamma_k), \end{aligned} \tag{17}$$

provided that (A1) and (A2) hold. It can be verified that

$$\left\| \int_{-\infty}^s U(s, r) (f(\psi^{-1}(r)) + g(\psi^{-1}(r))) dr \right\| \leq \frac{N(M_f + M_g)}{\lambda} \tag{18}$$

and

$$\left\| \sum_{-\infty < s_k < s} U(s, s_k+) (f(\psi^{-1}(s_k)) + \gamma_k) \right\| \leq \frac{N(M_f + M_\gamma)}{1 - e^{-\lambda(\omega-\delta)}}, \tag{19}$$

where

$$M_f = \sup_{t \in \mathbb{T}_0} \|f(t)\| \tag{20}$$

and

$$M_\gamma = \sup_{k \in \mathbb{Z}} \|\gamma_k\|. \quad (21)$$

The inequalities (18) and (19) imply that

$$\sup_{s \in \mathbb{R}} \|\phi(s)\| \leq N(M_f + M_\gamma) \left(\frac{1}{\lambda} + \frac{\delta}{1 - e^{-\lambda(\omega - \delta)}} \right).$$

Therefore, the function $\vartheta(t) : \mathbb{T}_0 \rightarrow \mathbb{R}^m$ defined by

$$\vartheta(t) = \phi(\psi(t)), \quad t \in \mathbb{T}'_0, \quad (22)$$

and satisfying

$$\vartheta(\theta_{2k+1}) = \phi(s_k+), \quad k \in \mathbb{Z}, \quad (23)$$

is the unique solution of system (5) which is bounded on \mathbb{T}_0 such that

$$\sup_{t \in \mathbb{T}_0} \|\vartheta(t)\| \leq N(M_f + M_\gamma) \left(\frac{1}{\lambda} + \frac{\delta}{1 - e^{-\lambda(\omega - \delta)}} \right).$$

The asymptotic stability of the bounded solution $\vartheta(t)$ is discussed in the following assertion.

Lemma 2. *If the assumptions (A1) and (A2) are valid, then the bounded solution $\vartheta(t)$ of system (5) is asymptotically stable.*

Proof. Let us consider a solution $\tilde{\vartheta}(t)$ of system (5) satisfying $\tilde{\vartheta}(t_0) = \vartheta_0$ for some $t_0 \in \mathbb{T}'_0$ and $\vartheta_0 \in \mathbb{R}^m$. We denote $\tilde{\phi}(s) = \tilde{\vartheta}(\psi^{-1}(s))$ and define $\phi_0 = \phi(\psi(t_0))$. For $s > \psi(t_0)$, using the equations

$$\begin{aligned} \phi(s) &= U(s, \psi(t_0)) \phi_0 + \int_{\psi(t_0)}^s U(s, r) (f(\psi^{-1}(r)) + g(\psi^{-1}(r))) dr \\ &+ \delta \sum_{\psi(t_0) < s_k < s} U(s, s_k+) (f(\psi^{-1}(s_k)) + \gamma_k) \end{aligned}$$

and

$$\begin{aligned} \tilde{\phi}(s) &= U(s, \psi(t_0)) \vartheta_0 + \int_{\psi(t_0)}^s U(s, r) (f(\psi^{-1}(r)) + g(\psi^{-1}(r))) dr \\ &+ \delta \sum_{\psi(t_0) < s_k < s} U(s, s_k+) (f(\psi^{-1}(s_k)) + \gamma_k), \end{aligned}$$

we obtain

$$\|\phi(s) - \tilde{\phi}(s)\| \leq N \|\phi_0 - \vartheta_0\| e^{-\lambda(s - \psi(t_0))}.$$

Thus,

$$\|\vartheta(t) - \tilde{\vartheta}(t)\| \leq N \|\phi_0 - \vartheta_0\| e^{-\lambda(\psi(t) - \psi(t_0))}, \quad t > t_0.$$

The last inequality implies that the bounded solution $\vartheta(t)$ of (5) is asymptotically stable. \square

The main result of the present paper is provided in the next section.

4. MODULO PERIODIC POISSON STABLE SOLUTIONS

The following definition is concerned with positively Poisson stable sequences [33].

Definition 1. ([33]) *A bounded sequence $\{\gamma_k\}_{k \in \mathbb{Z}}$ in \mathbb{R}^m is called positively Poisson stable if there exists a sequence $\{\zeta_n\}_{n \in \mathbb{N}}$ of positive integers which diverges to infinity such that $\|\gamma_{k+\zeta_n} - \gamma_k\| \rightarrow 0$ as $n \rightarrow \infty$ for each k in bounded intervals of integers.*

The definitions of positively Poisson stable and MPPS functions on time scales are as follows.

Definition 2. *Let \mathbb{T} be a time scale such that $\sup \mathbb{T} = \infty$. A bounded function $\varphi(t) \in C_{rd}(\mathbb{T})$ is called positively Poisson stable if there exists a sequence $\{\eta_n\}_{n \in \mathbb{N}}$ which diverges to infinity such that $\|\varphi(t + \eta_n) - \varphi(t)\| \rightarrow 0$ as $n \rightarrow \infty$ uniformly on compact subsets of \mathbb{T} .*

Definition 3. *Let \mathbb{T} be a time scale such that there exists a positive number ω with $t \pm \omega \in \mathbb{T}$ whenever $t \in \mathbb{T}$. A function $\varphi(t) \in C_{rd}(\mathbb{T})$ is called a modulo periodic Poisson stable function if $\varphi(t) = \varphi_1(t) + \varphi_2(t)$ for every $t \in \mathbb{T}$ in which the function $\varphi_1 \in C_{rd}(\mathbb{T})$ is periodic and $\varphi_2 \in C_{rd}(\mathbb{T})$ is positively Poisson stable.*

The main result of the present study is mentioned in the following theorem.

Theorem 1. *Suppose that the assumptions (A1) and (A2) are fulfilled. If the sequence $\{\gamma_k\}_{k \in \mathbb{Z}}$ is positively Poisson stable, then system (5) possesses a unique asymptotically stable MPPS solution.*

Proof. The bounded solution $\phi(s)$ of system (13), which is defined by (17), can be expressed in the form

$$\phi(s) = \phi_1(s) + \phi_2(s), \quad s \in \mathbb{R},$$

where

$$\phi_1(s) = \int_{-\infty}^s U(s, r) f(\psi^{-1}(r)) dr + \delta \sum_{-\infty < s_k < s} U(s, s_k+) f(\psi^{-1}(s_k)) \quad (24)$$

and

$$\phi_2(s) = \int_{-\infty}^s U(s, r) g(\psi^{-1}(r)) dr + \delta \sum_{-\infty < s_k < s} U(s, s_k+) \gamma_k. \quad (25)$$

The bounded solution $\vartheta(t)$ of system (5), given by (22) and (23), satisfies the equation

$$\vartheta(t) = \vartheta_1(t) + \vartheta_2(t), \quad (26)$$

in which the functions $\vartheta_1(t) : \mathbb{T}_0 \rightarrow \mathbb{R}^m$ and $\vartheta_2(t) : \mathbb{T}_0 \rightarrow \mathbb{R}^m$ are respectively defined by

$$\vartheta_1(t) = \phi_1(\psi(t))$$

and

$$\vartheta_2(t) = \phi_2(\psi(t))$$

such that the equations $\vartheta_1(\theta_{2k+1}) = \phi_1(s_k+)$ and $\vartheta_2(\theta_{2k+1}) = \phi_2(s_k+)$ are fulfilled for each $k \in \mathbb{Z}$.

The function $\vartheta(t)$ is an asymptotically stable solution of (5) by Lemma 2. In the rest of the proof, we will show that $\vartheta(t)$ is an MPPS function by respectively demonstrating the periodicity and Poisson stability of $\vartheta_1(t)$ and $\vartheta_2(t)$ in accordance with Definition 3.

Firstly, let us discuss the periodicity of $\vartheta_1(t)$. We attain by means of (24) that

$$\begin{aligned} \phi_1(s + \omega - \delta) &= \int_{-\infty}^{s+\omega-\delta} U(s + \omega - \delta, r) f(\psi^{-1}(r)) dr \\ &+ \delta \sum_{-\infty < s_k < s+\omega-\delta} U(s + \omega - \delta, s_k+) f(\psi^{-1}(s_k)) \\ &= \int_{-\infty}^s U(s + \omega - \delta, r + \omega - \delta) f(\psi^{-1}(r + \omega - \delta)) dr \\ &+ \delta \sum_{-\infty < s_k < s} U(s + \omega - \delta, s_{k+1}+) f(\psi^{-1}(s_{k+1})). \end{aligned} \tag{27}$$

Equations (14) and (15) yield $U(s + \omega - \delta, r + \omega - \delta) = U(s, r)$ for $s > r$. In accordance with (6), Lemma 1 implies that $f(\psi^{-1}(r + \omega - \delta)) = f(\psi^{-1}(r))$ for $r \in \mathbb{R}$ and $f(\psi^{-1}(s_{k+1})) = f(\psi^{-1}(s_k))$ for $k \in \mathbb{Z}$. Therefore, $\phi_1(s)$ is $(\omega - \delta)$ -periodic on \mathbb{R} by (27). Utilizing Lemma 1 one more time we obtain that the function $\vartheta_1(t)$ is ω -periodic on \mathbb{T}_0 .

Next, we will prove that $\vartheta_2(s)$ is positively Poisson stable. For that purpose, let us consider a fixed compact subset \mathcal{C} of the time scale \mathbb{T}_0 . There exist integers α and β with $\beta > \alpha$ such that $\mathcal{C} \subseteq [\theta_{2\alpha}, \theta_{2\beta}] \cap \mathbb{T}_0$. Accordingly we have $\psi(\mathcal{C}) \subseteq [s_\alpha, s_\beta]$.

Take an arbitrary positive number ε and a positive number τ_0 with

$$\tau_0 \leq \frac{1}{2N(1 + 2M_\gamma)} \left(\frac{1}{\lambda} + \frac{\delta}{1 - e^{-\lambda(\omega-\delta)}} \right)^{-1}. \tag{28}$$

Moreover, suppose that j is a sufficiently large positive integer satisfying

$$j \geq \frac{1}{\lambda(\omega - \delta)} \ln \left(\frac{1}{\tau_0 \varepsilon} \right). \tag{29}$$

Because $\{\gamma_k\}_{k \in \mathbb{Z}}$ is positively Poisson stable, there is a sequence $\{\zeta_n\}_{n \in \mathbb{N}}$ of positive integers which diverges to infinity such that $\|\gamma_{k+\zeta_n} - \gamma_k\| \rightarrow 0$ as $n \rightarrow \infty$ for each

k in bounded intervals of integers. Thus, there exists a natural number n_0 such that for $n \geq n_0$ the inequality

$$\left\| \gamma_{k+\zeta_n} - \gamma_k \right\| < \tau_0 \varepsilon \tag{30}$$

holds for each $k = \alpha - j + 1, \alpha - j + 2, \dots, \beta$. Accordingly, if $n \geq n_0$, then the inequality

$$\left\| g(\psi^{-1}(s + \mu_n)) - g(\psi^{-1}(s)) \right\| < \tau_0 \varepsilon \tag{31}$$

is satisfied for $s_{\alpha-j} < s \leq s_\beta$, where $\mu_n = (\omega - \delta)\zeta_n, n \in \mathbb{N}$.

Let us fix a natural number n such that $n \geq n_0$. Making benefit of (25) one can obtain

$$\begin{aligned} \phi_2(s + \mu_n) - \phi_2(s) &= \int_{-\infty}^s U(s, r) (g(\psi^{-1}(r + \mu_n)) - g(\psi^{-1}(r))) dr \\ &+ \delta \sum_{-\infty < s_k < s} U(s, s_k+) (\gamma_{k+\zeta_n} - \gamma_k). \end{aligned}$$

Therefore, for $s_{\alpha-j} \leq s \leq s_\beta$, we have

$$\begin{aligned} \|\phi_2(s + \mu_n) - \phi_2(s)\| &\leq \int_{-\infty}^{s_{\alpha-j}} N e^{-\lambda(s-r)} \|g(\psi^{-1}(r + \mu_n)) - g(\psi^{-1}(r))\| dr \\ &+ \int_{s_{\alpha-j}}^s N e^{-\lambda(s-r)} \|g(\psi^{-1}(r + \mu_n)) - g(\psi^{-1}(r))\| dr \\ &+ \delta \sum_{-\infty < s_k \leq s_{\alpha-j}} N e^{-\lambda(s-s_k)} \|\gamma_{k+\zeta_n} - \gamma_k\| \\ &+ \delta \sum_{s_{\alpha-j} < s_k < s} N e^{-\lambda(s-s_k)} \|\gamma_{k+\zeta_n} - \gamma_k\|. \end{aligned}$$

In compliance with (30) and (31), it can be verified that

$$\begin{aligned} \|\phi_2(s + \mu_n) - \phi_2(s)\| &\leq 2NM_\gamma \int_{-\infty}^{s_{\alpha-j}} e^{-\lambda(s-r)} dr + N\tau_0\varepsilon \int_{s_{\alpha-j}}^s e^{-\lambda(s-r)} dr \\ &+ 2\delta NM_\gamma \sum_{-\infty < s_k \leq s_{\alpha-j}} e^{-\lambda(s-s_k)} \\ &+ \delta N\tau_0\varepsilon \sum_{s_{\alpha-j} < s_k < s} e^{-\lambda(s-s_k)} \\ &< 2NM_\gamma \left(\frac{1}{\lambda} + \frac{\delta}{1 - e^{-\lambda(\omega-\delta)}} \right) e^{-\lambda(s-s_{\alpha-j})} \\ &+ N\tau_0\varepsilon \left(\frac{1}{\lambda} + \frac{\delta}{1 - e^{-\lambda(\omega-\delta)}} \right) (1 - e^{-\lambda(s-s_{\alpha-j})}). \end{aligned}$$

For $s \geq s_\alpha$, the inequality $e^{-\lambda(s-s_{\alpha-j})} \leq \tau_0\varepsilon$ is fulfilled since (29) is valid. Hence, if $s_\alpha \leq s \leq s_\beta$, then

$$\|\phi_2(s + \mu_n) - \phi_2(s)\| < (1 + 2M_\gamma) \left(\frac{1}{\lambda} + \frac{\delta}{1 - e^{-\lambda(\omega-\delta)}} \right) N\tau_0\varepsilon.$$

One can confirm using (28) that

$$\|\phi_2(s + \mu_n) - \phi_2(s)\| < \frac{\varepsilon}{2}, \quad s \in \psi(\mathcal{C}). \tag{32}$$

Now, let us denote

$$\eta_n = \omega\zeta_n \tag{33}$$

for each $n \in \mathbb{N}$. The sequence $\{\eta_n\}_{n \in \mathbb{N}}$ diverges to infinity since the same is true for $\{\zeta_n\}_{n \in \mathbb{N}}$. Equation (11) yields $\psi(t) + \mu_n = \psi(t + \eta_n)$, $n \in \mathbb{N}$. Hence, according to (32) we have

$$\|\vartheta_2(t + \eta_n) - \vartheta_2(t)\| < \frac{\varepsilon}{2}, \quad t \in \mathcal{C} \cap \mathbb{T}'_0$$

and

$$\|\vartheta_2(\theta_{2k+1} + \eta_n) - \vartheta_2(\theta_{2k+1})\| \leq \frac{\varepsilon}{2}, \quad k \in \mathbb{Z}.$$

Therefore,

$$\sup_{t \in \mathcal{C}} \|\vartheta_2(t + \eta_n) - \vartheta_2(t)\| < \varepsilon. \tag{34}$$

The last inequality ensures that $\|\vartheta_2(t + \eta_n) - \vartheta_2(t)\| \rightarrow 0$ as $n \rightarrow \infty$ uniformly on compact subsets of \mathbb{T}_0 . In other words, the function $\vartheta_2(t)$ is positively Poisson stable. Thus, the bounded solution $\vartheta(t)$ of (5) is an MPPS function. \square

In conformity with Theorem 1 we have the following remark.

Remark 1. *Suppose that the conditions of Theorem 1 are valid. Using the equation*

$$\|\vartheta_1(t + \eta_n) - \vartheta_1(t)\| = 0, \quad t \in \mathbb{T}_0,$$

together with (34), one can obtain for an arbitrary compact subset \mathcal{C} of \mathbb{T}_0 and an arbitrary positive number ε that

$$\sup_{t \in \mathcal{C}} \|\vartheta(t + \eta_n) - \vartheta(t)\| = \sup_{t \in \mathcal{C}} \|\vartheta_2(t + \eta_n) - \vartheta_2(t)\| < \varepsilon, \quad n \geq n_0$$

for some natural number n_0 , where $\{\eta_n\}_{n \in \mathbb{N}}$ is the sequence defined by (33) and $\vartheta(t)$ is the bounded solution of (5), which satisfies (26). For that reason $\vartheta(t)$ is positively Poisson stable. In other words, system (5) admits a positively Poisson stable solution, which is asymptotically stable.

In the next section, an example possessing an MPPS solution is provided.

5. AN EXAMPLE

According to the result of Theorem 4.1 [3], the logistic map

$$z_{k+1} = 3.9z_k(1 - z_k), \tag{35}$$

where $k \in \mathbb{Z}$, admits an orbit $\{z_k^*\}_{k \in \mathbb{Z}}$ inside the unit interval $[0, 1]$ which is positively Poisson stable in the sense of Definition 1 [1].

Let us take into account the time scale $\mathbb{T}_0 = \bigcup_{k=-\infty}^{\infty} [\theta_{2k-1}, \theta_{2k}]$, where $\theta_{2k-1} = 8k - 4$ and $\theta_{2k} = 8k + 1$ for $k \in \mathbb{Z}$. The equations (4) are satisfied for the time scale \mathbb{T}_0 with $\omega = 8$, $\delta = 3$, and $\theta = 1$.

We consider the system

$$\begin{aligned} y_1^\Delta(t) &= -\frac{2}{5}y_1(t) + \frac{1}{5}y_2(t) + \cos\left(\frac{\pi t}{4}\right) + g_1(t), \\ y_2^\Delta(t) &= -\frac{1}{5}y_1(t) - \frac{2}{5}y_2(t) + \sin\left(\frac{\pi t}{2}\right) + g_2(t), \end{aligned} \tag{36}$$

where $t \in \mathbb{T}_0$, and the functions $g_1(t) : \mathbb{T}_0 \rightarrow \mathbb{R}$ and $g_2(t) : \mathbb{T}_0 \rightarrow \mathbb{R}$ are respectively defined by $g_1(t) = z_k^*$ and $g_2(t) = 2z_k^*$ for $t \in [\theta_{2k-1}, \theta_{2k}]$, $k \in \mathbb{Z}$. It is worth noting that the sequence $\{\gamma_k\}_{k \in \mathbb{Z}}$ given by $\gamma_k = (z_k^*, 2z_k^*)^T$ is positively Poisson stable according to Theorem 3.2 [4]. System (36) is in the form of (5) with

$$y(t) = (y_1(t), y_2(t))^T, \quad A = \begin{pmatrix} -2/5 & 1/5 \\ -1/5 & -2/5 \end{pmatrix},$$

$$f(t) = \left(\cos\left(\frac{\pi t}{4}\right), \sin\left(\frac{\pi t}{2}\right) \right)^T, \quad g(t) = (g_1(t), g_2(t))^T.$$

The matrix $e^{5A}(I + 3A)$, where I is the 2×2 identity matrix, admits a pair of complex conjugate eigenvalues both of which are inside the unit circle, and $\det(I + 3A) = 2/5$. The assumptions (A1) and (A2) are satisfied for system (36), and therefore, it possesses a unique asymptotically stable MPPS solution by Theorem 1 [1]. Moreover, the MPPS solution is at the same time positively Poisson stable according to Remark 1 [1].

6. CONCLUSION

We take into account a periodic time scale which is the union of infinitely many disjoint compact intervals with a positive length, and investigate the existence, uniqueness as well as asymptotic stability of MPPS solutions for dynamic equation on such time scales. In our discussions we make use of the reduction technique to impulsive systems introduced in [6]. The Poisson stability in (5) is inherited from the sequence $\{\gamma_k\}_{k \in \mathbb{Z}}$. The descriptions of positively Poisson stable and MPPS functions on time scales are newly introduced in the present study. Moreover, it is shown that the obtained MPPS solutions are at the same time positively Poisson

stable. Even though in general MPPS functions are not necessarily positively Poisson stable [5], this is true in our case owing to the commensurability of the periods of the time scale \mathbb{T}_0 and the function $f(t)$ used in [5]. In the future, our results can be developed for differential equations on variable time scales [7].

Author Contribution Statements The authors contributed equally to this work. All authors read and approved the final copy of this paper.

Declaration of Competing Interests The authors declare that they have no known competing financial interest or personal relationships that could have appeared to influence the work reported in this paper.

Acknowledgements The authors wish to express their sincere gratitude to the anonymous reviewers for the helpful criticism and valuable suggestions, which helped to improve the paper.

REFERENCES

- [1] Agarwal, R., Bohner, M., O'Regan, D., Peterson, A., Dynamic equations on time scales: a survey, *J. Comput. Appl. Math.*, 141(1-2) (2002), 1–26. [https://doi.org/10.1016/S0377-0427\(01\)00432-0](https://doi.org/10.1016/S0377-0427(01)00432-0)
- [2] Akhmet, M., Principles of Discontinuous Dynamical Systems, Springer, New York, 2010.
- [3] Akhmet, M., Fen, M. O., Poincaré chaos and unpredictable functions, *Commun. Nonlinear Sci. Numer. Simulat.*, 48 (2017), 85–94. <https://doi.org/10.1016/j.cnsns.2016.12.015>
- [4] Akhmet, M., Fen, M. O., Non-autonomous equations with unpredictable solutions, *Commun. Nonlinear Sci. Numer. Simulat.*, 59 (2018), 657–670. <https://doi.org/10.1016/j.cnsns.2017.12.011>
- [5] Akhmet, M., Tleubergenova, M., Zhamanshin, A., Modulo periodic Poisson stable solutions of quasilinear differential equations, *Entropy*, 23 (2021), 1535. <https://doi.org/10.3390/e23111535>
- [6] Akhmet, M. U., Turan, M., The differential equations on time scales through impulsive differential equations, *Nonlinear Anal.*, 65(11) (2006), 2043–2060. <https://doi.org/10.1016/j.na.2005.12.042>
- [7] Akhmet, M. U., Turan, M., Differential equations on variable time scales, *Nonlinear Anal.*, 70(3) (2009), 1175–1192. <https://doi.org/10.1016/j.na.2008.02.020>
- [8] Birkhoff, G., Dynamical Systems, Amer. Math. Soc. Colloq. Publ., vol. 9, Amer. Math. Soc., Providence, R. I., 1966.
- [9] Bochner, S., Continuous mappings of almost automorphic and almost automorphic functions, *Proc. Natl. Acad. Sci. U.S.A.*, 52(4) (1964), 907–910. <https://doi.org/10.1073/pnas.52.4.907>
- [10] Bohner, M., Fan, M., Zhang, J., Periodicity of scalar dynamic equations and applications to population models, *J. Math. Anal. Appl.*, 330(1) (2007), 1–9. <https://doi.org/10.1016/j.jmaa.2006.04.084>
- [11] Bohner, M., Peterson, A., Dynamic Equations on Time Scales: An Introduction with Applications, Birkhäuser, Boston, 2001.
- [12] del R. Cantero, M., Perez, P. L., Smoler, M., Etchegoyen, C. V., Cantiello, H. F., Electrical oscillations in two-dimensional microtubular structures, *Sci. Rep.*, 6 (2016), 27143. <https://doi.org/10.1038/srep27143>

- [13] Cheban, D., Liu, Z., Periodic, quasi-periodic, almost periodic, almost automorphic, Birkhoff recurrent and Poisson stable solutions for stochastic differential equations, *J. Differ. Equ.*, 269(4) (2020), 3652–3685. <https://doi.org/10.1016/j.jde.2020.03.014>
- [14] Corduneanu, C., *Almost Periodic Oscillations and Waves*, Springer, New York, 2009.
- [15] Doelling, K. B., Assaneo, M. F., Neural oscillations are a start toward understanding brain activity rather than the end, *PLoS Biol.*, 19 (2021), e3001234. <https://doi.org/10.1371/journal.pbio.3001234>
- [16] Du, B., Hu, X., Ge, W., Periodic solution of a neutral delay model of single-species population growth on time scales, *Commun. Nonlinear Sci. Numer. Simulat.*, 15(2) (2010), 394–400. <https://doi.org/10.1016/j.cnsns.2009.03.014>
- [17] Fen, M. O., Tokmak Fen, F., SICNNs with Li-Yorke chaotic outputs on a time scale, *Neurocomputing*, 237 (2017), 158–165. <https://doi.org/10.1016/j.neucom.2016.09.073>
- [18] Gulev, S. K., Latif, M., The origins of a climate oscillation, *Nature*, 521 (2015), 428–430. <https://doi.org/10.1038/521428a>
- [19] Hilger, S., *Ein Maßkettenkalkül mit Anwendung auf Zentrumsmannigfaltigkeiten*, PhD thesis, Universität Würzburg, 1988.
- [20] Kaufmann, E. R., Raffoul, Y. N., Periodic solutions for a neutral nonlinear dynamical equation on a time scale, *J. Math. Anal. Appl.*, 319(1) (2006), 315–325. <https://doi.org/10.1016/j.jmaa.2006.01.063>
- [21] Knight, R. A., Recurrent and Poisson stable flows, *Proc. Am. Math. Soc.*, 83(1) (1981), 49–53. <https://doi.org/10.2307/2043889>
- [22] Lakshmikantham, V., Sivasundaram, S., Kaymakçalan, B., *Dynamic Systems on Measure Chains*, Kluwer Academic Publishers, Netherlands, 1996.
- [23] Li, Y., Periodic solutions of non-autonomous cellular neural networks with impulses and delays on time scales, *IMA J. Math. Control Inf.*, 31(2) (2014), 273–293. <https://doi.org/10.1093/imamci/dnt012>
- [24] Li, Y, Shen, S., Compact almost automorphic function on time scales and its application, *Qual. Theory Dyn. Syst.*, 20 (2021), Article number: 86. <https://doi.org/10.1007/s12346-021-00522-5>
- [25] Li, Z., Zhang, T., Permanence for Leslie-Gower predator-prey system with feedback controls on time scales, *Quaest. Math.*, 44(10) (2021), 1393–1407. <https://doi.org/10.2989/16073606.2020.1799256>
- [26] Liao, Q., Li, B., Li, Y., Permanence and almost periodic solutions for an n-species Lotka-Volterra food chain system on time scales, *Asian-Eur. J. Math.*, 8(2) (2015), 1550027. <https://doi.org/10.1142/S1793557115500278>
- [27] Liu, X., Liu, Z. X., Poisson stable solutions for stochastic differential equations with Lévy noise, *Acta Math. Sin. Engl.*, 38 (2022), 22–54. <https://doi.org/10.1007/s10114-021-0107-1>
- [28] Pchelintsev, A. N., On the Poisson stability to study a fourth-order dynamical system with quadratic nonlinearities, *Mathematics*, 9 (2021), 2057. <https://doi.org/10.3390/math9172057>
- [29] Poincaré, H., *Les Méthodes Nouvelles de la Mécanique Céleste*, Volume 1, Gauthier-Villars, Paris, 1892.
- [30] Samoilenko, A. M., Perestyuk, N. A., *Impulsive Differential Equations*, World Scientific, Singapore, 1995.
- [31] Samuelson, P. A., Generalized predator-prey oscillations in ecological and economic equilibrium, *Proc. Natl. Acad. Sci. U.S.A.*, 68(5) (1971), 980–983. <https://doi.org/10.1073/pnas.68.5.980>
- [32] Seiffertt, J., Adaptive resonance theory in the time scales calculus, *Neural Netw.*, 120 (2019), 32–39. <https://doi.org/10.1016/j.neunet.2019.08.010>
- [33] Sell, G. R., *Topological Dynamics and Ordinary Differential Equations*, Van Nostrand Reinhold Company, London, 1971.

- [34] Thomas, D., Weederann, M., Billings, L., Hoffacker, J., Washington-Allen, R. A., When to spray: a time-scale calculus approach to controlling the impact of West Nile virus, *Ecol. Soc.*, 14(2) (2009), 21. <https://doi.org/10.5751/ES-03006-140221>
- [35] Tisdell, C. C., Zaidi, A., Basic qualitative and quantitative results for solutions to nonlinear, dynamic equations on time scales with an application to economic modelling, *Nonlinear Anal. Theory Methods Appl.*, 68(11) (2008), 3504–3524. <https://doi.org/10.1016/j.na.2007.03.043>
- [36] Vance, W., Ross, J., Entrainment, phase resetting, and quenching of chemical oscillations, *J. Chem. Phys.*, 103(7) (1995), 2472. <https://doi.org/10.1063/1.469669>
- [37] Veech, W. A., Almost automorphic functions, *Proc. Natl. Acad. Sci. U.S.A.* 49(4) (1963), 462–464. <https://doi.org/10.1073/pnas.49.4.462>



THE TYPE I HEAVY-TAILED ODD POWER GENERALIZED WEIBULL-G FAMILY OF DISTRIBUTIONS WITH APPLICATIONS

Thatayaone MOAKOFI¹ and Broderick OLUYEDE²

^{1,2}Department of Mathematics and Statistical Sciences, Botswana International University of Science and Technology, Palapye, BOTSWANA

ABSTRACT. In this study, we propose a new heavy-tailed distribution, namely, the type I heavy-tailed odd power generalized Weibull-G family of distributions. Several statistical properties including hazard rate function, quantile function, moments, distribution of the order statistics and Rényi entropy are presented. Actuarial measures such as value at risk, tail value at risk, tail variance and tail variance premium are also derived. To obtain the estimates of the parameters of the new family of distributions, we adopt the maximum likelihood estimation method and assess the consistency property via a Monte Carlo simulation. Finally, we illustrate the usefulness of the new family of distributions by analyzing four real life data sets from different fields such as insurance, engineering, bio-medical and environmental sciences.

1. INTRODUCTION

Several researchers have developed probability models by adding one or more parameter(s) to well known classical distributions in order to improve their fitting power (flexibility). However, these extended distributions cannot model all real life data sets. Thus, serious efforts are still needed to propose and develop new flexible distributions. Several new generated distributions available in the literature include: Topp-Leone odd Burr III-G family of distributions by [23], the Marshall-Olkin exponentiated odd exponential half logistic-G family of distributions by [27], exponentiated odd Lomax exponential distribution by [16], the Marshall-Olkin odd

2020 *Mathematics Subject Classification.* 62E99, 60E05.

Keywords. Heavy-tailed, generalized distribution, actuarial measures, maximum likelihood estimation.

¹✉ thatayaone.moakofi@studentmail.biust.ac.bw-Corresponding author; 0000-0002-2676-7694

²✉ oluyedeo@biust.ac.bw; 0000-0002-9945-2255.

exponential half logistic-G family of distributions by [26], the shifted Gompertz-G family of distributions by [17], type II half-logistic odd Fréchet class of distributions by [7], generalized modified exponential-G family of distributions by [19], truncated Cauchy power Weibull-G class of distributions by [6], modified alpha power family of distributions by [20] and type II general exponential class of distributions by [18] to mention a few.

Data sets in different fields, such as actuarial sciences, reliability, engineering, bio-medical sciences, economic, risk management are usually positive, right-skewed, unimodal with heavier tails. These data sets need to be modelled by heavy-tailed distributions. Thus, there is need for development of heavy-tailed distributions. Some heavy-tailed distributions available in the literature include among others; the type-I heavy-tailed Weibull distribution by [30], heavy-tailed beta-power transformed Weibull distribution by [31], heavy-tailed log-logistic distribution by [29], heavy-tailed exponential distribution by [1], the logit slash distribution by [21], and the LogPH class of distributions by [2].

The type-I heavy-tailed (TI-HT) family of distributions introduced by [30] have the cumulative distribution function (cdf) and probability density function (pdf) given by

$$G(x; \theta, \xi) = 1 - \left(\frac{1 - F(x; \xi)}{1 - (1 - \theta)F(x; \xi)} \right)^\theta, \quad (1)$$

and

$$g(x; \theta, \xi) = \frac{\theta^2 f(x; \xi) (1 - F(x; \xi))^{\theta-1}}{(1 - (1 - \theta)F(x; \xi))^{\theta+1}}, \quad (2)$$

for $\theta > 0, x \in \mathbb{R}$. [24] introduced the odd power generalized Weibull-G family of distributions with the cdf and pdf given as

$$F(x; \alpha, \beta, \xi) = 1 - \exp \left(1 - \left[1 + \left(\frac{G(x; \xi)}{1 - G(x; \xi)} \right)^\alpha \right]^\beta \right), \quad (3)$$

and

$$\begin{aligned} f(x; \alpha, \beta, \xi) &= \alpha\beta \left[1 + \left(\frac{G(x; \xi)}{1 - G(x; \xi)} \right)^\alpha \right]^{\beta-1} \left(\frac{G(x; \xi)}{1 - G(x; \xi)} \right)^{\alpha-1} \\ &\times \exp \left(1 - \left[1 + \left(\frac{G(x; \xi)}{1 - G(x; \xi)} \right)^\alpha \right]^\beta \right) \frac{g(x; \xi)}{(1 - G(x; \xi))^2}, \end{aligned} \quad (4)$$

respectively, for $\alpha, \beta > 0$ and parameter vector ξ .

The aim of this paper is to develop a new family of heavy-tailed distributions namely, type I heavy-tailed odd power generalized Weibull-G (TI-HT-OPGW-G) family of distributions by combining equations (1), (2), (3) and (4).

The general objectives of constructing this new family of distributions include the following:

- to generate distributions which are skewed, symmetric, J-shaped or reversed-J shaped;
- to define new family of distributions that possesses various types of hazard rate functions including monotonic as well as non-monotonic shapes;
- to construct new statistical distributions with better fits and properties than other competitive distributions;
- to construct heavy-tailed distributions for modeling various real data sets.

The rest of the work is organized in the following manner. Section 2 present the new TI-HT-OPGW-G family of distributions, reliability and hazard rate functions, sub-families, linear representation and quantile function. In Section 3 moments, moment generating function, the distribution of order statistics, and Rényi entropy are presented. In Section 4, some special models from the TI-HT-OPGW-G family of distributions are presented. Section 5 contains the estimation of the unknown parameters of the TI-HT-OPGW-G family of distributions via the method of maximum likelihood and a Monte Carlo simulation study to examine the bias and mean square error of the maximum likelihood estimators is given in Section 6. The results verified that the estimates are consistent as the mean tend to the true parameters, the root mean square error and average bias decreases when the sample size (n) increases. Section 7 contains actuarial measures. Four real data applications are given in Section 8, followed by some concluding remarks in Section 9.

2. THE NEW FAMILY OF DISTRIBUTIONS

This section present the type I heavy-tailed odd power generalized Weibull-G (TI-HT-OPGW-G) family of distributions. The cdf and pdf of the TI-HT-OPGW-G family of distributions are

$$F(x; \theta, \alpha, \beta, \xi) = 1 - \left(\frac{\exp\left(1 - \left[1 + \left(\frac{G(x; \xi)}{1 - G(x; \xi)}\right)^\alpha\right]^\beta\right)}{1 - \bar{\theta} \left[1 - \exp\left(1 - \left[1 + \left(\frac{G(x; \xi)}{1 - G(x; \xi)}\right)^\alpha\right]^\beta\right)\right]} \right)^\theta, \quad (5)$$

and

$$\begin{aligned} f(x; \theta, \alpha, \beta, \xi) &= \theta^2 \alpha \beta \left[1 + \left(\frac{G(x; \xi)}{1 - G(x; \xi)}\right)^\alpha\right]^{\beta-1} \left(\frac{G(x; \xi)}{1 - G(x; \xi)}\right)^{\alpha-1} \\ &\times \exp\left(\theta \left(1 - \left[1 + \left(\frac{G(x; \xi)}{1 - G(x; \xi)}\right)^\alpha\right]^\beta\right)\right) \frac{g(x; \xi)}{(1 - G(x; \xi))^2} \\ &\times \left(1 - \bar{\theta} \left[1 - \exp\left(1 - \left[1 + \left(\frac{G(x; \xi)}{1 - G(x; \xi)}\right)^\alpha\right]^\beta\right)\right]\right)^{-(\theta+1)}, \end{aligned} \quad (6)$$

respectively, for $\alpha, \beta, \theta > 0$ and parameter vector ξ . Note that $\bar{\theta} = 1 - \theta$.

2.1. Reliability and Failure Rate Functions. The survival function, and hazard rate function (hrf) of the TI-HT-OPGW-G family of distributions are given respectively by

$$S(x; \theta, \alpha, \beta, \xi) = \left(\frac{\exp\left(1 - \left[1 + \left(\frac{G(x; \xi)}{1 - G(x; \xi)}\right)^\alpha\right]^\beta\right)}{1 - \bar{\theta} \left[1 - \exp\left(1 - \left[1 + \left(\frac{G(x; \xi)}{1 - G(x; \xi)}\right)^\alpha\right]^\beta\right)\right]} \right)^\theta, \quad (7)$$

and

$$\begin{aligned} h(x; \theta, \alpha, \beta, \xi) &= \theta^2 \alpha \beta \left[1 + \left(\frac{G(x; \xi)}{1 - G(x; \xi)}\right)^\alpha\right]^{\beta-1} \left(\frac{G(x; \xi)}{1 - G(x; \xi)}\right)^{\alpha-1} \\ &\times \exp\left(\theta \left(1 - \left[1 + \left(\frac{G(x; \xi)}{1 - G(x; \xi)}\right)^\alpha\right]^\beta\right)\right) \frac{g(x; \xi)}{(1 - G(x; \xi))^2} \\ &\times \left(1 - \bar{\theta} \left[1 - \exp\left(1 - \left[1 + \left(\frac{G(x; \xi)}{1 - G(x; \xi)}\right)^\alpha\right]^\beta\right)\right]\right)^{-(\theta+1)} \\ &\times \left[\left(\frac{\exp\left(1 - \left[1 + \left(\frac{G(x; \xi)}{1 - G(x; \xi)}\right)^\alpha\right]^\beta\right)}{1 - \bar{\theta} \left[1 - \exp\left(1 - \left[1 + \left(\frac{G(x; \xi)}{1 - G(x; \xi)}\right)^\alpha\right]^\beta\right)\right]}\right)^\theta\right]^{-1}, \quad (8) \end{aligned}$$

for $\alpha, \beta, \theta > 0$, $\bar{\theta} = 1 - \theta$, and parameter vector ξ .

2.2. Sub-Families of TI-HT-OPGW-G Family of Distributions.

- When $\theta = 1$, we obtain the odd power generalized Weibull-G (OPGW-G) family of distributions (see [24]) with the cdf

$$F(x; \alpha, \beta, \xi) = 1 - \exp\left(1 - \left[1 + \left(\frac{G(x; \xi)}{1 - G(x; \xi)}\right)^\alpha\right]^\beta\right),$$

for $\alpha, \beta > 0$ and parameter vector ξ .

- When $\beta = 1$, we obtain the new type I heavy-tailed Weibull-G (TI-HT-W-G) family of distributions with the cdf

$$F(x; \theta, \alpha, \xi) = 1 - \left(\frac{\exp\left(-\left(\frac{G(x; \xi)}{1 - G(x; \xi)}\right)^\alpha\right)}{1 - \bar{\theta} \left[1 - \exp\left(-\left(\frac{G(x; \xi)}{1 - G(x; \xi)}\right)^\alpha\right)\right]}\right)^\theta,$$

for $\theta, \alpha > 0$ and parameter vector ξ . This is a new family of distributions.

- When $\alpha = 1$, we obtain the new type I heavy-tailed odd Nadarajah Haghghi-G (TI-HT-ONH-G) family of distributions with the cdf

$$F(x; \theta, \beta, \xi) = 1 - \left(\frac{\exp \left(1 - \left[1 + \left(\frac{G(x; \xi)}{1 - G(x; \xi)} \right) \right]^\beta \right)}{1 - \bar{\theta} \left[1 - \exp \left(1 - \left[1 + \left(\frac{G(x; \xi)}{1 - G(x; \xi)} \right) \right]^\beta \right) \right]} \right)^\theta,$$

for $\theta, \beta > 0$, $\bar{\theta} = (1 - \theta)$, and parameter vector ξ . This is a new family of distributions.

- When $\theta = \beta = 1$, we obtain the Weibull-G (W-G) family of distributions (see [10]) with the cdf

$$F(x; \alpha, \xi) = 1 - \exp \left(- \left(\frac{G(x; \xi)}{1 - G(x; \xi)} \right)^\alpha \right),$$

for $\alpha > 0$, and parameter vector ξ .

- If $\theta = \alpha = 1$, we obtain the odd Nadarajah Haghghi-G (ONH-G) (see [25]) family of distributions with the cdf

$$F(x; \beta, \xi) = 1 - \exp \left(1 - \left[1 + \left(\frac{G(x; \xi)}{1 - G(x; \xi)} \right) \right]^\beta \right),$$

for $\beta > 0$, and parameter vector ξ .

- If $\theta = \alpha = \beta = 1$, we obtain the odd exponential-G (OE-G) family of distributions with the cdf

$$F(x; \xi) = 1 - \exp \left(- \left(\frac{G(x; \xi)}{1 - G(x; \xi)} \right) \right),$$

for parameter vector ξ . This is a new family of distributions.

- If $\theta = \beta = 1, \alpha = 2$ we obtain the odd Rayleigh-G (OR-G) family of distributions with the cdf

$$F(x; \xi) = 1 - \exp \left(- \left(\frac{G(x; \xi)}{1 - G(x; \xi)} \right)^2 \right),$$

for parameter vector ξ . This is a new family of distributions.

2.3. Linear Representation. Here, in this sub-section, we express the pdf of TI-HT-OPGW-G family of distributions as an infinite linear combination of exponentiated-G (Exp-G) family of distributions. Using the following generalized binomial and Taylor series expansions

$$(1 + z)^{-a} = \sum_{k=0}^{\infty} (-1)^k \binom{a + k - 1}{k} z^k \quad \text{for } |z| < 1, \quad \text{and} \quad e^z = \sum_{i=0}^{\infty} \frac{z^i}{i!},$$

respectively, we can write

$$f(x; \theta, \alpha, \beta, \xi) = \sum_{p=0}^{\infty} \varphi_{p+1} g_{p+1}(x; \xi), \quad (9)$$

where $g_{p+1}(x; \xi) = (p+1)[G(x; \xi)]^p g(x; \xi)$ is the Exp-G pdf with the power parameter $(p+1)$ and parameter vector ξ , and

$$\begin{aligned} \varphi_{p+1} &= \theta^2 \alpha \beta \sum_{h,i,j,k,l,m=0}^{\infty} \bar{\theta}^h \binom{\theta+h}{h} \binom{h}{i} \binom{j}{k} \binom{\beta(k+1)-1}{l} \binom{\alpha(l+1)-1}{m} \\ &\times \binom{\alpha(l+1)-m+p}{p} \frac{(\theta+i)^j (-1)^{i+k+m}}{j! (p+1)}. \end{aligned} \quad (10)$$

Consequently, the mathematical and statistical properties of the TI-HT-OPGW-G family of distributions follow directly from those of the Exp-G family of distributions. (**See the Appendix for derivations**).

2.4. Quantile Function. The quantile function is used in Monte Carlo simulations to generate random numbers for a specified probability distribution. It is obtained by inverting the cdf of a distribution. If the random variable X is from the TI-HT-OPGW-G family of distributions, then the quantile function of X can be obtained as follows:

$$F(x; \theta, \alpha, \beta, \xi) = 1 - \left(\frac{\exp \left(1 - \left[1 + \left(\frac{G(x; \xi)}{1-G(x; \xi)} \right)^\alpha \right]^\beta \right)}{1 - \bar{\theta} \left[1 - \exp \left(1 - \left[1 + \left(\frac{G(x; \xi)}{1-G(x; \xi)} \right)^\alpha \right]^\beta \right) \right]} \right)^\theta = u, \quad (11)$$

for $0 \leq u \leq 1$, that is,

$$G(x; \xi) = \left(\left[\left(1 - \log \left(\theta \left[(1-u)^{\frac{-1}{\theta}} - \bar{\theta} \right]^{-1} \right) \right)^{\frac{1}{\beta}} - 1 \right]^{\frac{-1}{\alpha}} + 1 \right)^{-1}. \quad (12)$$

Therefore, the quantile function of the TI-HT-OPGW-G family of distributions is given by

$$Q_x(u) = G^{-1} \left[\left(\left[\left(1 - \log \left(\theta \left[(1-u)^{\frac{-1}{\theta}} - \bar{\theta} \right]^{-1} \right) \right)^{\frac{1}{\beta}} - 1 \right]^{\frac{-1}{\alpha}} + 1 \right)^{-1} \right]. \quad (13)$$

Consequently, variates of the TI-HT-OPGW-G family of distributions can be obtained using equation (13) for specified baseline cdf G .

3. STATISTICAL PROPERTIES

In this section, we derived some statistical features of the TI-HT-OPGW-G family of distributions, specifically the moments, moment generating function, distribution of order statistics and Rényi entropy. Let the pdf of the TI-HT-OPGW-G family of distributions be denoted by $f(x)$.

3.1. Moments and Generating Function. Let $Y_{p+1} \sim Exponentiated - G(p + 1, \xi)$, then the n^{th} raw moment, μ'_n of the TI-HT-OPGW-G family of distributions is given by

$$\mu'_n = E(X^n) = \int_{-\infty}^{\infty} x^n f(x) dx = \sum_{p=0}^{\infty} \varphi_{p+1} E(Y_{p+1}^n),$$

where $E(Y_{p+1}^n)$ is the n^{th} moment of Y_{p+1} and φ_{p+1} is given by equation (10). The moment generating function (MGF), for $|t| < 1$, is given by:

$$M_X(t) = \sum_{p=0}^{\infty} \varphi_{p+1} M_{p+1}(t),$$

where $M_{p+1}(t)$ is the mgf of Y_{p+1} and φ_{p+1} is given by equation (10).

3.2. Order Statistics. Order statistics have many applications in survival, reliability, failure analysis, and it is a natural way to perform a reliability analysis of a system. Suppose X_1, X_2, \dots, X_n are independent and identically distributed random variables from the TI-HT-OPGW-G family of distributions. The pdf of the r^{th} order statistic from the TI-HT-OPGW-G pdf $f(x)$ can be written as

$$f_{r:n}(x) = \frac{n!f(x)}{(r-1)!(n-r)!} \sum_{z=0}^{n-r} (-1)^z \binom{n-r}{z} [F(x)]^{z+r-1}. \tag{14}$$

Using equations (5) and (6), we have

$$\begin{aligned} f(x)[F(x)]^{z+r-1} &= \theta^2 \alpha \beta \left[1 + \left(\frac{G(x; \xi)}{1 - G(x; \xi)} \right)^\alpha \right]^{\beta-1} \left(\frac{G(x; \xi)}{1 - G(x; \xi)} \right)^{\alpha-1} \\ &\times \exp \left(\theta \left(1 - \left[1 + \left(\frac{G(x; \xi)}{1 - G(x; \xi)} \right)^\alpha \right]^\beta \right) \right) \frac{g(x; \xi)}{(1 - G(x; \xi))^2} \\ &\times \left(1 - \bar{\theta} \left[1 - \exp \left(1 - \left[1 + \left(\frac{G(x; \xi)}{1 - G(x; \xi)} \right)^\alpha \right]^\beta \right) \right] \right)^{-(\theta+1)} \\ &\times \left[1 - \left(\frac{\exp \left(1 - \left[1 + \left(\frac{G(x; \xi)}{1 - G(x; \xi)} \right)^\alpha \right]^\beta \right)}{1 - \bar{\theta} \left[1 - \exp \left(1 - \left[1 + \left(\frac{G(x; \xi)}{1 - G(x; \xi)} \right)^\alpha \right]^\beta \right) \right]} \right)^\theta \right]^{z+r-1} \end{aligned}$$

$$\begin{aligned}
 &= \theta^2 \alpha \beta \sum_{q=0}^{\infty} \binom{z+r-1}{q} (-1)^q \left[1 + \left(\frac{G(x; \xi)}{1-G(x; \xi)} \right)^\alpha \right]^{\beta-1} \left(\frac{G(x; \xi)}{1-G(x; \xi)} \right)^{\alpha-1} \\
 &\times \exp \left(\theta(q+1) \left(1 - \left[1 + \left(\frac{G(x; \xi)}{1-G(x; \xi)} \right)^\alpha \right]^\beta \right) \right) \frac{g(x; \xi)}{(1-G(x; \xi))^2} \\
 &\times \left(1 - \bar{\theta} \left[1 - \exp \left(1 - \left[1 + \left(\frac{G(x; \xi)}{1-G(x; \xi)} \right)^\alpha \right]^\beta \right) \right] \right)^{-(\theta(q+1)+1)}.
 \end{aligned}$$

Now following the same steps leading to equation (9), we obtain

$$f(x)[F(x)]^{z+r-1} = \sum_{p=0}^{\infty} \rho_{p+1} g_{p+1}(x; \xi), \tag{15}$$

where $g_{p+1}(x; \xi) = (p+1)[G(x; \xi)]^p g(x; \xi)$ is the Exp-G pdf with the power parameter $(p+1)$ and parameter vector ξ , and

$$\begin{aligned}
 \rho_{p+1} &= \theta^2 \alpha \beta \sum_{h,i,j,k,l,m,q=0}^{\infty} \bar{\theta}^h \binom{z+r-1}{q} \binom{\theta(q+1)+h}{h} \binom{h}{i} \binom{j}{k} \binom{\beta(k+1)-1}{l} \\
 &\times \binom{\alpha(l+1)-1}{m} \binom{\alpha(l+1)-m+p}{p} \frac{(\theta(q+1)+i)^j (-1)^{q+i+k+m}}{j! (p+1)}.
 \end{aligned}$$

Thus, by substituting (15) into (14), the pdf of the r^{th} order statistic from the TI-HT-OPGW-G family of distributions can be written as

$$f_{r:n}(x) = \frac{n!}{(r-1)!(n-r)!} \sum_{p=0}^{\infty} \sum_{z=0}^{n-r} (-1)^z \binom{n-r}{z} \rho_{p+1} g_{p+1}(x; \xi).$$

3.3. Rényi Entropy. Rényi entropy is a very important tool in information theory, as a measure of randomness or uncertainty in the system. Rényi entropy is defined to be

$$I_R(v) = \frac{1}{1-v} \log \left(\int_0^\infty [f(x; \theta, \alpha, \beta, \xi)]^v dx \right), v \neq 1, v > 0. \tag{16}$$

Rényi entropy for the TI-HT-OPGW-G family of distributions is given by

$$\begin{aligned}
 I_R(v) &= \frac{1}{1-v} \log \left[\sum_{h,i,j,k,l,m,p=0}^{\infty} \bar{\theta}^h \binom{v(\theta+1)+h-1}{h} \binom{h}{i} \frac{(v\theta+i)^j (-1)^{i+k+m}}{j!} \binom{j}{k} \right. \\
 &\times \binom{\beta(k+v)-v}{l} \binom{\alpha(l+v)-v}{m} \binom{\alpha(l+v)+v-m+p-1}{p} \left. \frac{(\theta^2 \alpha \beta)^v}{\left[1 + \frac{p}{v}\right]^v} \right. \\
 &\times \left. \int_0^\infty \left(\left[1 + \frac{p}{v}\right] (G(x; \xi))^{\frac{p}{v}} (g(x; \xi))^v dx \right) \right]
 \end{aligned}$$

$$= \frac{1}{1-v} \log \left[\sum_{p=0}^{\infty} \tau_p \exp((1-v)I_{REG}) \right], \quad (17)$$

for $v > 0$, $v \neq 1$, where $I_{REG} = \frac{1}{1-v} \log \left[\int_0^{\infty} \left(\left[1 + \frac{p}{v} \right] (G(x; \xi))^{\frac{p}{v}} (g(x; \xi)) \right)^v dx \right]$ is the Rényi entropy of Exp-G distribution with power parameter $(\frac{p}{v} + 1)$ and

$$\begin{aligned} \tau_p &= \sum_{h,i,j,k,l,m=0}^{\infty} \bar{\theta}^h \binom{v(\theta+1)+h-1}{h} \binom{h}{i} \frac{(v\theta+i)^j (-1)^{i+k+m}}{j!} \binom{j}{k} \\ &\times \binom{\beta(k+v)-v}{l} \binom{\alpha(l+v)-v}{m} \binom{\alpha(l+v)+v-m+p-1}{p} \frac{(\theta^2 \alpha \beta)^v}{\left[1 + \frac{p}{v} \right]^v}. \end{aligned}$$

Therefore, Rényi entropy of the TI-HT-OPGW-G family of distributions can be obtained from those of the Exp-G family of distributions. (**See the Appendix for derivations**).

3.4. Moment of Residual and Reversed Residual Life. Moments of the residual life distribution are used to obtain the mean, variance and coefficient of variation of residual life which are extensively used in reliability analysis.

The s^{th} moment of the residual life, say $\kappa_s(t)$ of a random variable X is

$$\kappa_s(t) = E[(X-t)^s | X > t] = \frac{1}{\bar{F}(t)} \int_t^{\infty} (x-t)^s f(x) dx.$$

Consequently, $\kappa_s(t)$ for the TI-HT-OPGW-G family of distributions is given as follows:

$$\kappa_s(t) = \frac{1}{\bar{F}(t)} \sum_{p,u=0}^{\infty} \binom{s}{u} (-t)^{s-u} \varphi_{p+1} \int_t^{\infty} x^u g_{p+1}(x; \xi) dx, \quad (18)$$

where φ_{p+1} is as defined in equation (10) and $g_{p+1}(x; \xi)$ denotes the Exp-G distribution with power parameter $(p+1)$. The mean excess function of the TI-HT-OPGW-G family of distributions is obtained from the above formula with $s=1$. The s^{th} moment of the reversed residual life, say $\vartheta_s(t)$ of a random variable X is

$$\vartheta_s(t) = E[(t-X)^s | X \leq t] = \frac{1}{F(t)} \int_0^t (t-x)^s f(x) dx.$$

Subsequently, $\vartheta_s(t)$ for the TI-HT-OPGW-G family of distributions is given as follows:

$$\vartheta_s(t) = \frac{1}{F(t)} \sum_{p,u=0}^{\infty} \binom{s}{u} (-t)^{s-u} \varphi_{p+1} \int_0^t x^u g_{p+1}(x; \xi) dx,$$

where φ_{p+1} is as defined in equation (10) and $g_{p+1}(x; \xi)$ denotes the Exp-G distribution with power parameter $(p + 1)$. The mean inactivity time of the TI-HT-OPGW-G family of distributions is obtained from the above formula with $s = 1$.

4. SOME SPECIAL CASES

In this section, we present some special cases of the TI-HT-OPGW-G family of distributions. We considered cases when the baseline distributions are log-logistic, Weibull, Rayleigh and standard half logistic distributions.

4.1. TI-HT-OPGW-Log-Logistic (TI-HT-OPGW-LLoG) Distribution. Given the cdf and pdf of the log-logistic distribution as $G(x; c) = 1 - (1 + x^c)^{-1}$ and $g(x; c) = cx^{c-1}(1 + x^c)^{-2}$ for $c > 0$ and $x > 0$, we define the cdf and pdf of the TI-HT-OPGW-LLoG distribution as follows

$$F(x; \theta, \alpha, \beta, c) = 1 - \left(\frac{\exp \left(1 - \left[1 + \left(\frac{1 - (1 + x^c)^{-1}}{(1 + x^c)^{-1}} \right)^\alpha \right]^\beta \right)}{1 - \bar{\theta} \left[1 - \exp \left(1 - \left[1 + \left(\frac{1 - (1 + x^c)^{-1}}{(1 + x^c)^{-1}} \right)^\alpha \right]^\beta \right) \right]} \right)^\theta,$$

and

$$\begin{aligned} f(x; \theta, \alpha, \beta, c) &= \theta^2 \alpha \beta \left[1 + \left(\frac{1 - (1 + x^c)^{-1}}{(1 + x^c)^{-1}} \right)^\alpha \right]^{\beta-1} \left(\frac{1 - (1 + x^c)^{-1}}{(1 + x^c)^{-1}} \right)^{\alpha-1} \\ &\times \exp \left(\theta \left(1 - \left[1 + \left(\frac{1 - (1 + x^c)^{-1}}{(1 + x^c)^{-1}} \right)^\alpha \right]^\beta \right) \right) \frac{cx^{c-1}(1 + x^c)^{-2}}{((1 + x^c)^{-1})^2} \\ &\times \left(1 - \bar{\theta} \left[1 - \exp \left(1 - \left[1 + \left(\frac{1 - (1 + x^c)^{-1}}{(1 + x^c)^{-1}} \right)^\alpha \right]^\beta \right) \right] \right)^{-(\theta+1)}, \end{aligned}$$

respectively, for $\theta, \alpha, \beta, c > 0$, and $\bar{\theta} = 1 - \theta$. The hrf for the TI-HT-OPGW-LLoG distribution is given by

$$\begin{aligned} h(x; \theta, \alpha, \beta, c) &= \theta^2 \alpha \beta \left[1 + \left(\frac{1 - (1 + x^c)^{-1}}{(1 + x^c)^{-1}} \right)^\alpha \right]^{\beta-1} (1 - (1 + x^c)^{-1})^{\alpha-1} \\ &\times \left(1 - \bar{\theta} \left[1 - \exp \left(1 - \left[1 + \left(\frac{1 - (1 + x^c)^{-1}}{(1 + x^c)^{-1}} \right)^\alpha \right]^\beta \right) \right] \right)^{-1} \\ &\times \frac{cx^{c-1}(1 + x^c)^{-2}}{((1 + x^c)^{-1})^{\alpha+1}}, \end{aligned}$$

for $\theta, \alpha, \beta, c > 0$, and $\bar{\theta} = 1 - \theta$. Figure 1 shows the 3D plots of skewness and kurtosis of the TI-HT-OPGW-LLoG distribution. We observe that

- When we fix the parameters θ and β , the skewness and kurtosis of the TI-HT-OPGW-LLoG distribution changes from decreasing to increasing as α and c increases.
- When we fix the parameters α and β , the skewness and kurtosis of the TI-HT-OPGW-LLoG distribution increases as θ and c increases.

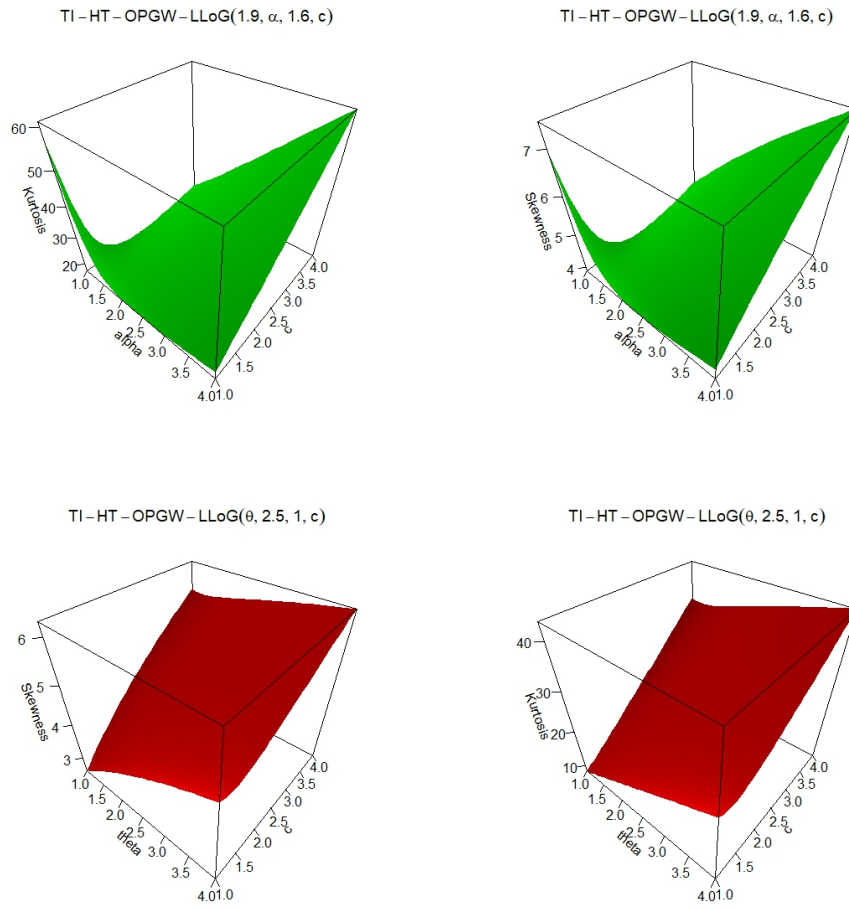


FIGURE 1. Plots of skewness and kurtosis for the TI-HT-OPGW-LLoG distribution

Figure 2 shows the plots of pdf and hazard functions of TI-HT-OPGW-LLoG distribution, respectively. The pdf can take several shapes including right-skewed, left-skewed, unimodal, J and reverse-J shapes. The TI-HT-OPGW-LLoG hrf displays increasing, decreasing, bathtub, upside-down bathtub and bathtub followed by upside-down bathtub shapes.

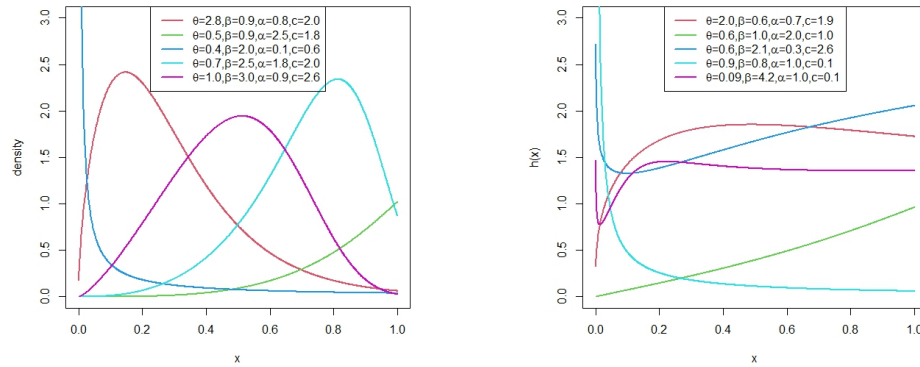


FIGURE 2. Plots of density and hazard rate function for TI-HT-OPGW-LLoG distribution

4.2. **TI-HT-OPGW-Weibull (TI-HT-OPGW-W) Distribution.** Suppose the cdf and pdf of the baseline distribution are given by $G(x; \lambda) = 1 - e^{-x^\lambda}$, and $g(x; \lambda) = \lambda x^{\lambda-1} e^{-x^\lambda}$, $x > 0, \lambda > 0$, then, the cdf and pdf of the TI-HT-OPGW-W distribution are given by

$$F(x; \theta, \alpha, \beta, \lambda) = 1 - \left(\frac{\exp \left(1 - \left[1 + \left(\frac{1 - e^{-x^\lambda}}{e^{-x^\lambda}} \right)^\alpha \right]^\beta \right)}{1 - \bar{\theta} \left[1 - \exp \left(1 - \left[1 + \left(\frac{1 - e^{-x^\lambda}}{e^{-x^\lambda}} \right)^\alpha \right]^\beta \right) \right]} \right)^\theta,$$

and

$$\begin{aligned} f(x; \theta, \alpha, \beta, \lambda) &= \theta^2 \alpha \beta \left[1 + \left(\frac{1 - e^{-x^\lambda}}{e^{-x^\lambda}} \right)^\alpha \right]^{\beta-1} \left(\frac{1 - e^{-x^\lambda}}{e^{-x^\lambda}} \right)^{\alpha-1} \\ &\times \exp \left(\theta \left(1 - \left[1 + \left(\frac{1 - e^{-x^\lambda}}{e^{-x^\lambda}} \right)^\alpha \right]^\beta \right) \right) \frac{\lambda x^{\lambda-1} e^{-x^\lambda}}{(e^{-x^\lambda})^2} \end{aligned}$$

$$\times \left(1 - \bar{\theta} \left[1 - \exp \left(1 - \left[1 + \left(\frac{1 - e^{-x^\lambda}}{e^{-x^\lambda}} \right)^\alpha \right]^\beta \right) \right] \right)^{-(\theta+1)},$$

respectively, for $\theta, \alpha, \beta, \lambda > 0$, and $\bar{\theta} = 1 - \theta$. The hrf for TI-HT-OPGW-W distribution is given by

$$\begin{aligned} h(x; \theta, \alpha, \beta, \lambda) &= \theta^2 \alpha \beta \left[1 + \left(\frac{1 - e^{-x^\lambda}}{e^{-x^\lambda}} \right)^\alpha \right]^{\beta-1} (1 - e^{-x^\lambda})^{\alpha-1} \\ &\times \left(1 - \bar{\theta} \left[1 - \exp \left(1 - \left[1 + \left(\frac{1 - e^{-x^\lambda}}{e^{-x^\lambda}} \right)^\alpha \right]^\beta \right) \right] \right)^{-1} \\ &\times \frac{\lambda x^{\lambda-1} e^{-x^\lambda}}{(e^{-x^\lambda})^{\alpha+1}}, \end{aligned}$$

for $\theta, \alpha, \beta, \lambda > 0$, and $\bar{\theta} = 1 - \theta$.

Figure 3 shows the 3D plots of skewness and kurtosis of the TI-HT-OPGW-W distribution. We observe that

- When we fix the parameters θ and λ , the skewness and kurtosis of the TI-HT-OPGW-W distribution decrease as α and β increases.
- When we fix the parameters β and λ , the skewness and kurtosis of the TI-HT-OPGW-W distribution increases as θ and α increases.

Figure 4 shows the plots of pdf and hrf of TI-HT-OPGW-W distribution, respectively. The pdf can take several shapes including right-skewed, left-skewed, unimodal, J and reverse-J shapes. The TI-HT-OPGW-W hrf displays increasing, decreasing, bathtub, upside-down bathtub and bathtub followed by upside-down bathtub shapes.

4.3. TI-HT-OPGW-Rayleigh (TI-HT-OPGW-R) Distribution. If the baseline cdf and pdf are given by $G(x; \lambda) = 1 - \exp\left(-\frac{x^2}{2\lambda^2}\right)$ and $g(x; \lambda) = \frac{x}{\lambda^2} \exp\left(-\frac{x^2}{2\lambda^2}\right)$ for $x > 0$, and $\lambda > 0$, then, the cdf and pdf of the TI-HT-OPGW-R distribution are given by

$$F(x; \theta, \alpha, \beta, \lambda) = 1 - \left(\frac{\exp \left(1 - \left[1 + \left(\frac{1 - \exp\left(-\frac{x^2}{2\lambda^2}\right)}{\exp\left(-\frac{x^2}{2\lambda^2}\right)} \right)^\alpha \right]^\beta \right)}{1 - \bar{\theta} \left[1 - \exp \left(1 - \left[1 + \left(\frac{1 - \exp\left(-\frac{x^2}{2\lambda^2}\right)}{\exp\left(-\frac{x^2}{2\lambda^2}\right)} \right)^\alpha \right]^\beta \right) \right]} \right)^\theta,$$

and

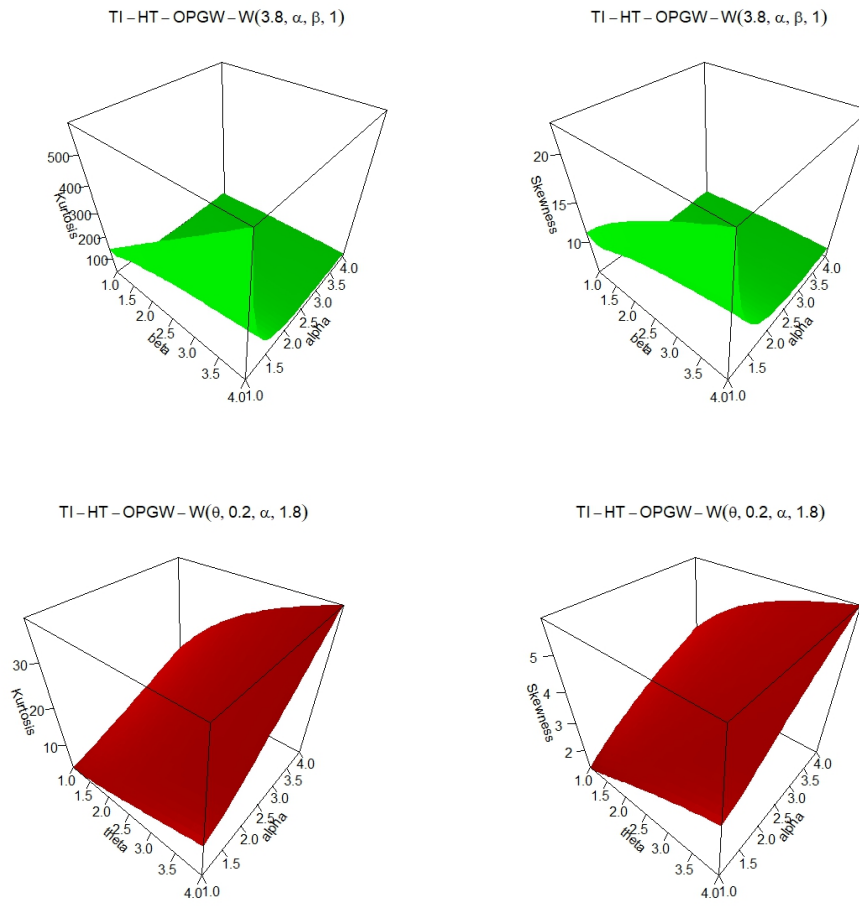


FIGURE 3. Plots of skewness and kurtosis for the TI-HT-OPGW-W distribution

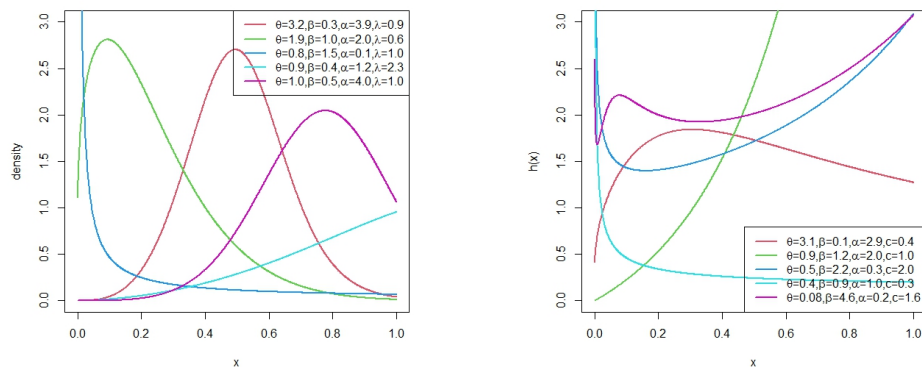


FIGURE 4. Plots of Density and Hazard Rate Function for TI-HT-OPGW-W Distribution

$$\begin{aligned}
 f(x; \theta, \alpha, \beta, \lambda) &= \theta^2 \alpha \beta \left[1 + \left(\frac{1 - \exp\left(-\frac{x^2}{2\lambda^2}\right)}{\exp\left(-\frac{x^2}{2\lambda^2}\right)} \right)^\alpha \right]^{\beta-1} \left(\frac{1 - \exp\left(-\frac{x^2}{2\lambda^2}\right)}{\exp\left(-\frac{x^2}{2\lambda^2}\right)} \right)^{\alpha-1} \\
 &\times \exp\left(\theta \left(1 - \left[1 + \left(\frac{1 - \exp\left(-\frac{x^2}{2\lambda^2}\right)}{\exp\left(-\frac{x^2}{2\lambda^2}\right)} \right)^\alpha \right]^\beta \right) \right) \frac{x^2 \exp\left(-\frac{x^2}{2\lambda^2}\right)}{\left(\exp\left(-\frac{x^2}{2\lambda^2}\right)\right)^2} \\
 &\times \left(1 - \bar{\theta} \left[1 - \exp\left(1 - \left[1 + \left(\frac{1 - \exp\left(-\frac{x^2}{2\lambda^2}\right)}{\exp\left(-\frac{x^2}{2\lambda^2}\right)} \right)^\alpha \right]^\beta \right) \right] \right)^{-(\theta+1)},
 \end{aligned}$$

respectively, for $\theta, \alpha, \beta, \lambda > 0$, and $\bar{\theta} = 1 - \theta$. The hrf for TI-HT-OPGW-R distribution is given by

$$\begin{aligned}
 h(x; \theta, \alpha, \beta, \lambda) &= \theta^2 \alpha \beta \left[1 + \left(\frac{1 - \exp\left(-\frac{x^2}{2\lambda^2}\right)}{\exp\left(-\frac{x^2}{2\lambda^2}\right)} \right)^\alpha \right]^{\beta-1} \left(1 - \exp\left(-\frac{x^2}{2\lambda^2}\right) \right)^{\alpha-1} \\
 &\times \left(1 - \bar{\theta} \left[1 - \exp\left(1 - \left[1 + \left(\frac{1 - \exp\left(-\frac{x^2}{2\lambda^2}\right)}{\exp\left(-\frac{x^2}{2\lambda^2}\right)} \right)^\alpha \right]^\beta \right) \right] \right)^{-1}
 \end{aligned}$$

$$\times \frac{\frac{x}{\lambda^2} \exp\left(-\frac{x^2}{2\lambda^2}\right)}{\left(\exp\left(-\frac{x^2}{2\lambda^2}\right)\right)^{\alpha+1}},$$

for $\theta, \alpha, \beta, \lambda > 0$, and $\bar{\theta} = 1 - \theta$. Figure 5 shows the 3D plots of skewness and kurtosis of the TI-HT-OPGW-R distribution.

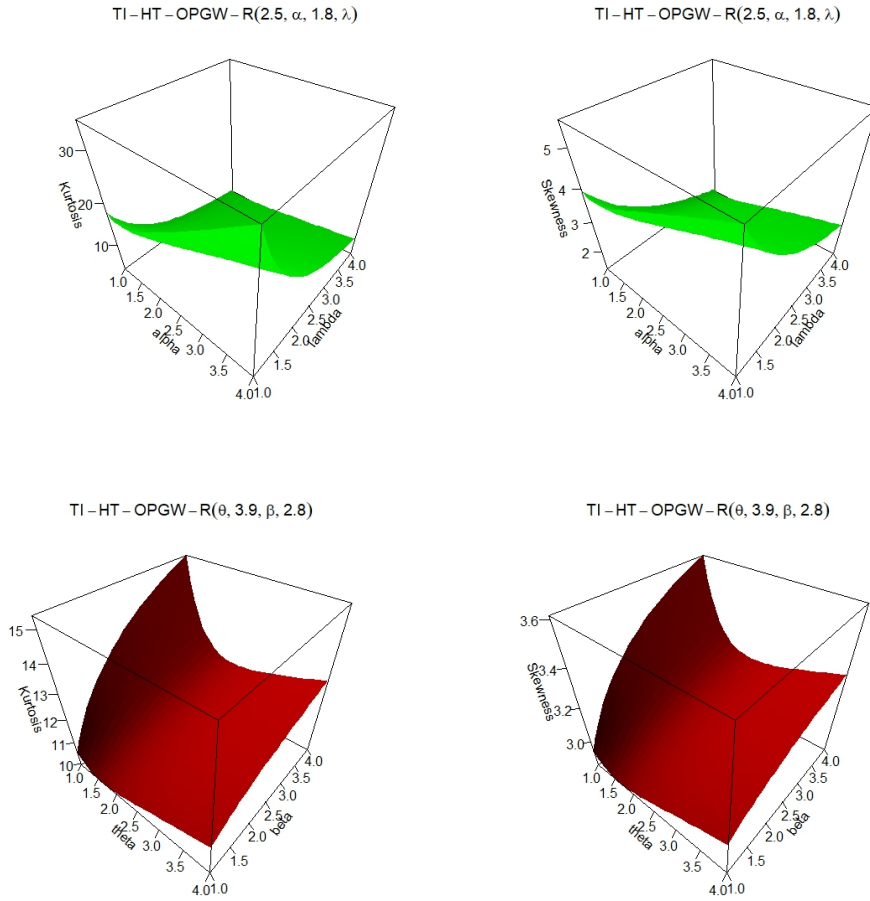


FIGURE 5. Plots of skewness and kurtosis for the TI-HT-OPGW-R distribution

We observe that

- When we fix the parameters θ and β , the skewness and kurtosis of the TI-HT-OPGW-R distribution decreases as α and λ increases.
- When we fix the parameters α and λ , the skewness and kurtosis of the TI-HT-OPGW-R distribution decreases and increases as θ and β increases.

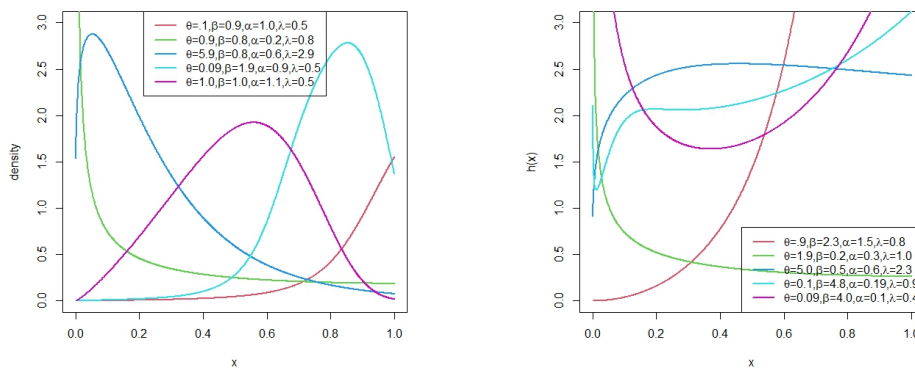


FIGURE 6. Plots of Density and Hazard Rate Function for TI-HT-OPGW-R Distribution

Figure 6 shows the plots of pdf and hrf of TI-HT-OPGW-R distribution, respectively. The pdf can take several shapes including right-skewed, left-skewed, uni-modal, J and reverse-J shapes. The TI-HT-OPGW-R hrf displays increasing, decreasing, bathtub and upside-down bathtub shapes.

4.4. TI-HT-OPGW-Standard Half Logistic (TI-HT-OPGW-SHL) Distribution. Suppose the cdf and pdf of the baseline distribution are given by $G(x) = \frac{1-e^{-x}}{1+e^{-x}}$, and $g(x) = \frac{2e^{-x}}{(1+e^{-x})^2}$, $x > 0$, then, the cdf and pdf of the TI-HT-OPGW-SHL distribution are given by

$$F(x; \theta, \alpha, \beta) = 1 - \left(\frac{\exp \left(1 - \left[1 + \left(\frac{1-e^{-x}}{1+e^{-x}} \right)^\alpha \right]^\beta \right)}{1 - \bar{\theta} \left[1 - \exp \left(1 - \left[1 + \left(\frac{1-e^{-x}}{1+e^{-x}} \right)^\alpha \right]^\beta \right) \right]} \right)^\theta,$$

and

$$f(x; \theta, \alpha, \beta) = \theta^2 \alpha \beta \left[1 + \left(\frac{1-e^{-x}}{1+e^{-x}} \right)^\alpha \right]^{\beta-1} \left(\frac{1-e^{-x}}{1+e^{-x}} \right)^{\alpha-1}$$

$$\begin{aligned} & \times \left(1 - \bar{\theta} \left[1 - \exp \left(1 - \left[1 + \left(\frac{1-e^{-x}}{1+e^{-x}} \right)^\alpha \right]^\beta \right) \right] \right)^{-(\theta+1)} \\ & \times \exp \left(\theta \left(1 - \left[1 + \left(\frac{1-e^{-x}}{1+e^{-x}} \right)^\alpha \right]^\beta \right) \right) \frac{2e^{-x}}{(1+e^{-x})^2} \left(1 - \frac{1-e^{-x}}{1+e^{-x}} \right)^2, \end{aligned}$$

respectively, for $\alpha, \beta, \theta > 0$, and $\bar{\theta} = 1 - \theta$. The hrf for TI-HT-OPGW-SHL distribution is given by

$$\begin{aligned} h(x; \theta, \alpha, \beta) &= \theta^2 \alpha \beta \left[1 + \left(\frac{1-e^{-x}}{1+e^{-x}} \right)^\alpha \right]^{\beta-1} \left(\frac{1-e^{-x}}{1+e^{-x}} \right)^{\alpha-1} \\ &\times \left(1 - \bar{\theta} \left[1 - \exp \left(1 - \left[1 + \left(\frac{1-e^{-x}}{1+e^{-x}} \right)^\alpha \right]^\beta \right) \right] \right)^{-1} \\ &\times \frac{\frac{2e^{-x}}{(1+e^{-x})^2}}{\left(1 - \frac{1-e^{-x}}{1+e^{-x}} \right)^{\alpha+1}}, \end{aligned}$$

for $\theta, \alpha, \beta > 0$, and $\bar{\theta} = 1 - \theta$.

Figure 7 shows the 3D plots of skewness and kurtosis of the TI-HT-OPGW-SHL distribution. We observe that

- When we fix the parameters β , the skewness and kurtosis of the TI-HT-OPGW-SHL distribution decreases as θ and α increases.
- When we fix the parameters α , the skewness and kurtosis of the TI-HT-OPGW-SHL distribution increases as θ and β increases.

Figure 8 shows the plots of pdf and hrf of TI-HT-OPGW-SHL distribution, respectively. The pdf can take several shapes including right-skewed, left-skewed, unimodal, J and reverse-J shapes. The TI-HT-OPGW-SHL hrf displays increasing, decreasing, bathtub, and upside-down bathtub followed by bathtub shapes.

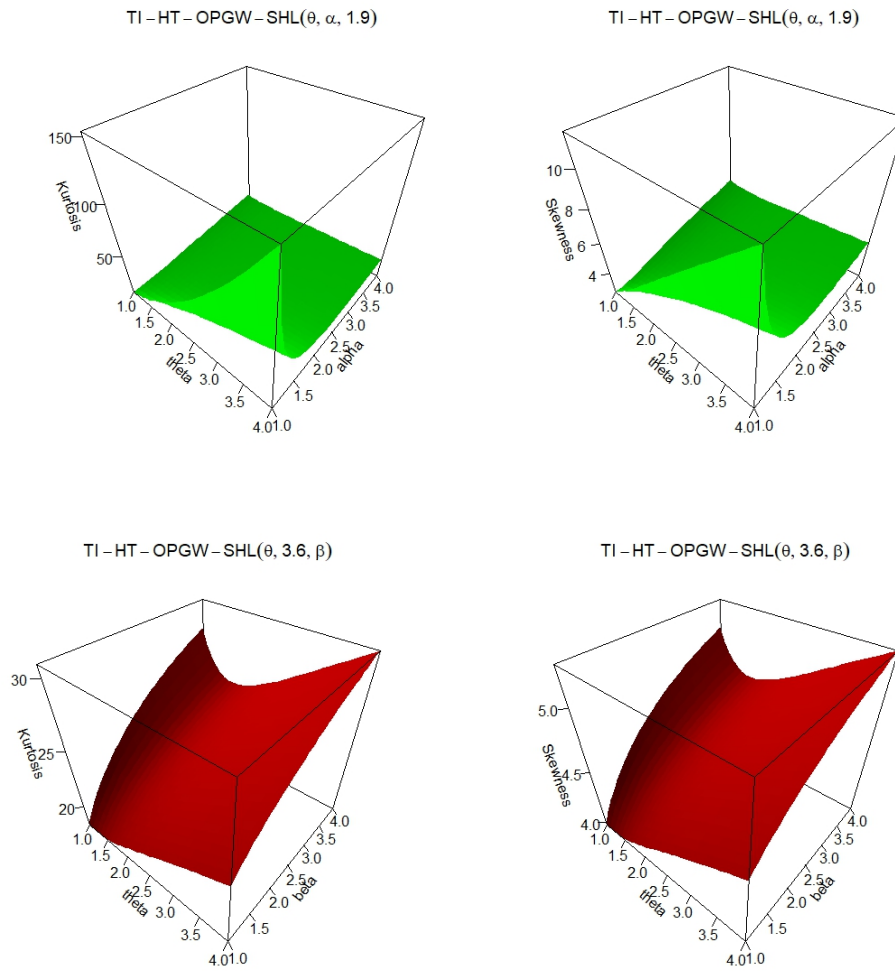


FIGURE 7. Plots for the skewness and kurtosis for the TI-HT-OPGW-SHL distribution

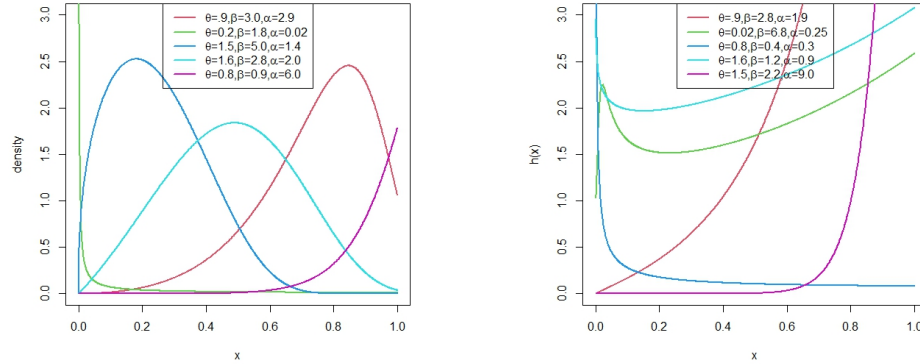


FIGURE 8. Plots of Density and Hazard Rate Functions for TI-HT-OPGW-SHL Distribution

5. PARAMETER ESTIMATION

In this section, we adopt the maximum likelihood estimation technique for estimating the parameters of the TI-HT-OPGW-G family of distributions. Let x_1, x_2, \dots, x_n be the realization from the TI-HT-OPGW-G family of distributions with the vector of model parameters $\Delta = (\theta, \alpha, \beta, \xi)^T$. Then, the corresponding log-likelihood function $\ell_n = \ell_n(\Delta)$ of this sample has the form

$$\begin{aligned}
 \ell_n(\Delta) &= n \ln(\theta^2 \alpha \beta) + (\beta - 1) \sum_{i=1}^n \log \left[1 + \left(\frac{G(x_i; \xi)}{1 - G(x_i; \xi)} \right)^\alpha \right] \\
 &+ (\alpha - 1) \sum_{i=1}^n \log \left(\frac{G(x_i; \xi)}{1 - G(x_i; \xi)} \right) + \sum_{i=1}^n \log(g(x_i; \xi)) \\
 &+ \sum_{i=1}^n \left(\theta \left(1 - \left[1 + \left(\frac{G(x_i; \xi)}{1 - G(x_i; \xi)} \right)^\alpha \right]^\beta \right) \right) - 2 \sum_{i=1}^n \log(1 - G(x_i; \xi)) \\
 &- (\theta + 1) \sum_{i=1}^n \log \left(1 - \bar{\theta} \left[1 - \exp \left(1 - \left[1 + \left(\frac{G(x_i; \xi)}{1 - G(x_i; \xi)} \right)^\alpha \right]^\beta \right) \right] \right).
 \end{aligned}
 \tag{19}$$

To obtain the maximum likelihood estimates of the unknown parameters, denoted by $\hat{\Delta}$, we set the nonlinear system of equations $(\frac{\partial \ell_n}{\partial \theta}, \frac{\partial \ell_n}{\partial \alpha}, \frac{\partial \ell_n}{\partial \beta}, \frac{\partial \ell_n}{\partial \xi})^T = \mathbf{0}$, and solve them simultaneously. However, since these equations are not in closed form, the MLEs can be found by maximizing $\ell_n(\Delta)$ numerically with respect to the parameters, using a numerical method such as Newton-Raphson procedure. We

maximized the likelihood function using the function `nlm` in R. The partial derivatives of the log-likelihood function with respect to each component of the parameter vector are given in the appendix. The observed Fisher information matrix is given by

$$J(\hat{\Delta}) = \begin{pmatrix} J_{\theta,\theta}(\hat{\Delta}) & J_{\theta,\alpha}(\hat{\Delta}) & J_{\theta,\beta}(\hat{\Delta}) & J_{\theta,\xi}(\hat{\Delta}) \\ J_{\alpha,\theta}(\hat{\Delta}) & J_{\alpha,\alpha}(\hat{\Delta}) & J_{\alpha,\beta}(\hat{\Delta}) & J_{\alpha,\xi}(\hat{\Delta}) \\ J_{\beta,\theta}(\hat{\Delta}) & J_{\beta,\alpha}(\hat{\Delta}) & J_{\beta,\beta}(\hat{\Delta}) & J_{\beta,\xi}(\hat{\Delta}) \\ J_{\xi,\theta}(\hat{\Delta}) & J_{\xi,\alpha}(\hat{\Delta}) & J_{\xi,\beta}(\hat{\Delta}) & J_{\xi,\xi}(\hat{\Delta}) \end{pmatrix}, \quad (20)$$

where $J_{i,j} = -\frac{\partial^2 \ell_n(\hat{\Delta})}{\partial_i \partial_j}$ for $i, j = \theta, \alpha, \beta, \xi$.

5.1. Standard error computation. The standard error of the estimate is a way to measure the accuracy of the predictions made by a model. It is also useful when calculating the confidence interval. It is given by

$$SE(\hat{\Delta}) = \sqrt{\left(J(\hat{\Delta})\right)^{-1}}, \quad (21)$$

where $\left(J(\hat{\Delta})\right)^{-1}$ is the inverse of the observed Fisher information matrix.

6. MONTE CARLO SIMULATION STUDY

In this section, we evaluate the efficiency and consistency property of the MLEs of TI-HT-OPGW-W distribution via a Monte Carlo simulation based on the following: $N=3000$ samples of size $n=50, 100, 200, 400, 800, 1600$ generated from the TI-HT-OPGW-W distribution for different parameter values. The process is carried out as follows:

- 3000 random samples of size $n=50, 100, 200, 400, 800, 1600$ was generated from the TI-HT-OPGW-W distribution.
- Different combinations for the true parameters are selected such as for Table 1: $\theta = 0.3, \alpha = 1.8, \beta = 0.3, \lambda = 1.5$; $\theta = 0.3, \alpha = 1.8, \beta = 0.3, \lambda = 0.6$, and for $\theta = 1.5, \alpha = 0.6, \beta = 0.3, \lambda = 0.3$. For Table 2: $\theta = 1.8, \alpha = 0.8, \beta = 1.0, \lambda = 1.0$; $\theta = 0.5, \alpha = 0.8, \beta = 1.0, \lambda = 1.0$, and $\theta = 1.0, \alpha = 0.8, \beta = 1.0, \lambda = 2.5$. These values are unknown, hence chosen arbitrary and then estimated using the TI-HT-OPGW-W distribution.
- Two statistical quantities (ABIAS and RMSE) are calculated to evaluate the consistency of the MLEs.

The simulation results from the TI-HT-OPGW-W distribution are presented in Tables 1 and 2. These tables report the average estimates (Mean), average bias (ABIAS) and root mean squared errors (RMSEs). The ABIAS and RMSE for the

TABLE 1. Monte Carlo Simulation Results 1

parameter	Sample Size	(0.3, 1.8, 0.3, 1.5)			(0.3, 1.8, 0.3, 0.6)			(1.5, 0.6, 0.3, 0.3)		
		Mean	RMSE	ABIAS	Mean	RMSE	ABIAS	Mean	RMSE	ABIAS
θ	50	0.4131	0.3320	0.1131	0.4025	0.3280	0.1025	1.9393	1.2849	0.4393
	100	0.3709	0.2615	0.0709	0.3627	0.2634	0.0627	1.8984	1.2093	0.3984
	200	0.3329	0.1659	0.0329	0.3323	0.1811	0.0323	1.8523	1.1403	0.3523
	400	0.3138	0.1020	0.0138	0.3130	0.1066	0.0130	1.7255	0.8857	0.2255
	800	0.3054	0.0655	0.0054	0.3038	0.0654	0.0038	1.7153	0.6723	0.2153
	1600	0.3033	0.0413	0.0033	0.3010	0.0421	0.0010	1.5500	0.4883	0.0500
α	50	2.8345	4.2902	1.0345	2.7212	3.9147	0.9212	0.8534	0.5010	0.2534
	100	2.1531	1.6306	0.3531	2.1017	1.6751	0.3017	0.7606	0.3709	0.1606
	200	1.9319	0.8064	0.1319	1.9023	0.8054	0.1023	0.6981	0.2622	0.0981
	400	1.8671	0.3683	0.0671	1.8506	0.3632	0.0506	0.6492	0.1579	0.0492
	800	1.8460	0.2244	0.0460	1.8195	0.2293	0.0195	0.6227	0.0930	0.0227
	1600	1.8287	0.1493	0.0287	1.8035	0.1513	0.0035	0.6227	0.0930	0.0227
β	50	0.2388	0.2563	-0.0611	0.3370	0.3062	0.0370	0.2218	0.1673	-0.0781
	100	0.2858	0.2929	-0.0141	0.3244	0.2383	0.0244	0.2387	0.1480	-0.0612
	200	0.3140	0.2744	0.0140	0.3152	0.1753	0.0152	0.2433	0.1306	-0.0566
	400	0.3065	0.2098	0.0065	0.3064	0.1087	0.0064	0.2606	0.1106	-0.0393
	800	0.3043	0.1543	0.0043	0.3034	0.0677	0.0034	0.2637	0.1009	-0.0362
	1600	0.2963	0.0612	-0.0036	0.3006	0.0408	0.0006	0.2858	0.0782	-0.0141
λ	50	2.2032	1.2778	0.7032	0.7148	0.3051	0.1148	0.4404	0.3475	0.1404
	100	1.9400	0.9330	0.4400	0.6682	0.2302	0.0682	0.3811	0.2420	0.0811
	200	1.7680	0.6684	0.2680	0.6349	0.1569	0.0349	0.3441	0.1859	0.0441
	400	1.6370	0.3791	0.1370	0.6156	0.0933	0.0156	0.3261	0.1673	0.0261
	800	1.5583	0.2246	0.0583	0.6034	0.0581	0.0034	0.3166	0.1470	0.0166
	1600	1.5143	0.0984	0.0143	0.6004	0.0386	0.0004	0.3035	0.1027	0.0035

estimated parameter, say, $\hat{\theta}$, are given by:

$$ABIAS(\hat{\theta}) = \frac{\sum_{i=1}^N \hat{\theta}_i}{N} - \theta, \quad \text{and} \quad RMSE(\hat{\theta}) = \sqrt{\frac{\sum_{i=1}^N (\hat{\theta}_i - \theta)^2}{N}},$$

respectively.

From Tables 1 and 2, it can be verified that the mean tend to the true parameters, the RMSEs and average bias decreases when n increases, thus showing that the estimates are consistent.

7. ACTUARIAL MEASURES

In actuarial sciences, actuaries need to evaluate the exposure of market risk in a portfolio of instruments. This section introduces some important risk measures for the TI-HT-OPGW-G family of distributions such as value-at-risk (VaR), tail-value-at-risk (TVaR), tail variance (TV) and tail variance premium (TVP).

7.1. Value-at-Risk (VaR). Value-at-risk (VaR) is an important and well known risk measure. It is also known as the quantile risk measure. The VaR of a random variable X is the q^{th} quantile of its cdf. If X is a random variable from TI-HT-OPGW-G family of distributions, then

TABLE 2. Monte Carlo Simulation Results 2

parameter	Sample Size	(1.0,0.8, 1.0, 1.0)			(0.5, 0.8, 1.0, 1.0)			(1.0, 0.8,1.0, 2.5)		
		Mean	RMSE	ABIAS	Mean	RMSE	ABIAS	Mean	RMSE	ABIAS
θ	50	1.4765	1.2119	0.4765	0.9008	0.8341	0.4008	1.4641	1.1880	0.4641
	100	1.3266	1.0090	0.3266	0.7723	0.6818	0.2723	1.2951	0.9814	0.2951
	200	1.1939	0.6730	0.1939	0.6529	0.4772	0.1529	1.1603	0.7228	0.1603
	400	1.0873	0.3151	0.0873	0.5586	0.2767	0.0586	1.0603	0.3698	0.0603
	800	1.0480	0.2065	0.0480	0.5255	0.1497	0.0255	1.0305	0.1995	0.0305
	1600	1.0343	0.1418	0.0343	0.5160	0.1074	0.0160	1.0176	0.1385	0.0176
α	50	0.6694	0.4028	-0.1305	0.7109	0.2963	-0.0890	0.6270	0.4801	-0.1729
	100	0.7054	0.2882	-0.0945	0.7314	0.2234	-0.0685	0.6734	0.3882	-0.1265
	200	0.7451	0.2180	-0.0548	0.7490	0.1776	-0.0509	0.7296	0.3072	-0.0703
	400	0.7697	0.1535	-0.0302	0.7791	0.1314	-0.0208	0.7621	0.2162	-0.0378
	800	0.7810	0.1067	-0.0189	0.7929	0.0878	-0.0070	0.7853	0.1568	-0.0146
	1600	0.7890	0.0757	-0.0109	0.7955	0.0575	-0.0044	0.7915	0.1107	-0.0084
β	50	1.3852	0.9164	0.3852	0.7714	0.6878	-0.2285	1.3469	0.8878	0.3469
	100	1.2787	0.7790	0.2787	0.8657	0.6477	-0.1342	1.2998	0.8349	0.2998
	200	1.2316	0.5893	0.2316	0.9453	0.5986	-0.0546	1.2538	0.6952	0.2538
	400	1.1744	0.4825	0.1744	1.0284	0.4209	0.0284	1.1921	0.5701	0.1921
	800	1.1190	0.3480	0.1190	1.0134	0.3097	0.0134	1.1502	0.4588	0.1502
	1600	1.0720	0.2444	0.0720	0.9976	0.1883	-0.0023	1.0938	0.3273	0.0938
λ	50	1.5395	0.9209	0.5395	1.4667	0.7605	0.4667	3.7769	2.2398	1.2769
	100	1.3303	0.6322	0.3303	1.3161	0.5817	0.3161	3.2118	1.5261	0.7118
	200	1.1754	0.4109	0.1754	1.1890	0.4010	0.1890	2.8540	0.9718	0.3540
	400	1.0872	0.2718	0.0872	1.0970	0.2440	0.0970	2.6753	0.6612	0.1753
	800	1.0468	0.1834	0.0468	1.0400	0.1368	0.0400	2.5916	0.4537	0.0916
	1600	1.0246	0.1229	0.0246	1.0157	0.0936	0.0157	2.5420	0.3094	0.0420

$$VaR_q = x_q = G^{-1} \left[\left(\left(\left(1 - \log \left(\theta \left[(1-q)^{\frac{-1}{\theta}} - \bar{\theta} \right]^{-1} \right) \right)^{\frac{1}{\beta}} - 1 \right)^{\frac{-1}{\alpha}} + 1 \right)^{-1} \right], \tag{22}$$

where $q \in (0, 1)$ is a specified level of significance.

7.2. Tail-Value-at-Risk (TVaR). TVaR is used to measure the expected loss given that an event outside a given probability level has occurred. Let X follows from TI-HT-OPGW-G family of distributions, then TVaR of X is defined as

$$\begin{aligned} TVaR_q &= \frac{1}{1-q} \int_{VaR_q}^{\infty} x f(x) dx \\ &= \frac{1}{1-q} \sum_{p=0}^{\infty} \int_{VaR_q}^{\infty} x \varphi_{p+1} g_{p+1}(x; \xi) dx, \end{aligned} \tag{23}$$

where $g_{p+1}(x; \xi) = (p+1)[G(x; \xi)]^p g(x; \xi)$ is the Exp-G pdf with the power parameter $(p+1)$ and parameter vector ξ , and φ_{p+1} is given by equation (10). Thus, TVaR of TI-HT-OPGW-G family of distributions can be obtained from those of Exp-G distribution.

7.3. Tail Variance (TV). The tail variance is one of the most important actuarial measures which looks at the variance beyond the VaR. The TV of the TI-HT-OPGW-G family of distributions can be defined as

$$\begin{aligned} TV_q &= E(X^2 | X > x_q) - (TVaR_q)^2 \\ &= \frac{1}{1-q} \int_{VaR_q}^{\infty} x^2 f(x) dx - (TVaR_q)^2 \\ &= \frac{1}{1-q} \sum_{p=0}^{\infty} \int_{VaR_q}^{\infty} x^2 \varphi_{p+1} g_{p+1}(x; \xi) dx - (TVaR_q)^2, \end{aligned} \quad (24)$$

where $g_{p+1}(x; \xi) = (p+1)[G(x; \xi)]^p g(x; \xi)$ is the Exp-G pdf with the power parameter $(p+1)$ and parameter vector ξ , and φ_{p+1} is given by equation (10). Thus, TV of TI-HT-OPGW-G family of distributions can be obtained from those of Exp-G distribution.

7.4. Tail Variance Premium (TVP). The TVP is an important actuarial measure that plays an essential role in insurance sciences. The TVP of the TI-HT-OPGW-G family of distributions takes the form

$$TVP_q = TVaR_q + \delta TV_q, \quad (25)$$

where $0 < \delta < 1$. The TVP of the TI-HT-OPGW-G family of distributions can be obtained by substituting the equations (23) and (24) into equation (25).

7.5. Numerical Study for the Risk Measures. This sub-section deals with the the numerical study of VaR, TVaR, TV and TVP for the TI-HT-OPGW-W distribution for different sets of parameters. The VaR, TVaR, TV and TVP of the TI-HT-OPGW-W distribution are compared with the type-I heavy-tailed Weibull (TI-HT-W) distribution, the half logistic generalized Weibull (HLGW) and Weibull distribution.

The process of obtaining the results is described as follows:

1. Random samples of size $n = 100$ are generated from each one of used distributions and parameters have been estimated via maximum likelihood method.
2. 1000 repetitions are made to calculate the VaR, TVaR, TV and TVP for these distributions.

Tables 3 and 4 present the simulated results of VaR, TVaR, TV and TVP of the compared distributions. A model with higher values of VaR, TVaR, TV and TVP is said to have a heavier tail. The simulated results provided in Tables 3 and 4 shows that the proposed TI-HT-OPGW-W distribution has higher values of the risk measures than the TI-HT-W, HLGW, and Weibull distributions.

TABLE 3. Simulation results 1 of VaR, TVaR, TV and TVP

Significance level		0.7	0.75	0.8	0.85	0.9	0.95	0.99
TI-HT-OPGW-W($\theta = 0.9, \alpha = 1.0, \beta = 1.0, \lambda = 0.5$)	VaR	1.9926	2.6118	3.4848	4.8008	7.0294	11.8902	
	TVaR	7.6930	8.7744	10.2127	12.2525	15.4771	21.8847	
	TV	73.5835	80.9009	90.1785	102.5321	120.3521	150.9723	
	TVP	59.2015	69.4501	82.3555	99.4047	123.7940	165.3084	
TI-HT-W($\theta = 0.9, \alpha = 1.0, \beta = 1.0$)	VaR	1.3277	1.6403	2.0526	2.6306	3.5303	5.2882	
	TVaR	3.5823	4.0032	4.5450	5.2855	6.4073	8.5284	
	TV	8.1989	8.7637	9.4695	10.4026	11.7593	14.1829	
	TVP	9.3215	10.5760	12.1206	14.1278	16.9907	22.0022	
HLGW($w = 0.9, \lambda = 1.0, \gamma = 1.0$)	VaR	1.8490	2.0965	2.3944	2.7727	3.2999	4.1968	
	TVaR	3.1698	3.4099	3.7023	4.0781	4.6077	5.5185	
	TV	1.8390	1.8495	1.8675	1.8971	1.9480	2.0518	
	TVP	4.4571	4.7971	5.1964	5.6907	6.3609	7.4678	
W($\lambda = 0.5$)	VaR	1.4484	1.9202	2.5892	3.6011	5.3150	9.0315	
	TVaR	5.9073	6.7544	7.8846	9.4938	12.0546	17.2314	
	TV	51.1712	56.9057	64.4260	74.9502	91.3972	124.0315	
	TVP	41.7272	49.4338	59.4254	73.2015	94.3121	135.0614	

TABLE 4. Simulation results 2 of VaR, TVaR, TV and TVP

Significance level		0.7	0.75	0.8	0.85	0.9	0.95	0.99
TI-HT-OPGW-W($\theta = 1.1, \alpha = 1.0, \beta = 0.7, \lambda = 0.85$)	VaR	1.9364	2.3451	2.8822	3.6337	4.8049	7.1085	
	TVaR	4.8986	5.4519	6.1648	7.1416	8.6279	11.4624	
	TV	16.0559	17.3282	18.9573	21.1721	24.5035	30.7003	
	TVP	16.1378	18.4481	21.3306	25.1379	30.6811	40.6277	
TI-HT-W($\theta = 1.1, \alpha = 1.0, \beta = 0.7$)	VaR	1.3891	1.7162	2.1476	2.7523	3.6937	5.5329	
	TVaR	3.7480	4.1884	4.7553	5.5301	6.7037	8.9230	
	TV	8.9912	9.6105	10.3845	11.4077	12.8957	15.5534	
	TVP	10.0419	11.3964	13.0630	15.2267	18.3099	23.6987	
HLGW($w = 1.0, \lambda = 1.0, \gamma = 1.7$)	VaR	1.0243	1.1469	1.2926	1.4750	1.7249	2.1408	
	TVaR	1.6523	1.7659	1.9030	2.0774	2.3201	2.7303	
	TV	0.3841	0.3812	0.3790	0.3781	0.3792	0.3856	
	TVP	1.9212	2.0518	2.2062	2.3988	2.6614	3.0967	
W($\lambda = 0.85$)	VaR	1.2421	1.4647	1.7443	2.1149	2.6543	3.6157	
	TVaR	2.5691	2.8131	3.1167	3.5156	4.0910	5.1058	
	TV	2.0797	2.1306	2.1905	2.2641	2.3622	2.5175	
	TVP	4.0249	4.4111	4.8691	5.4401	6.2170	7.4974	

8. APPLICATIONS

In this section, we illustrate the fitting power of the new TI-HT-OPGW-W distribution by analyzing four real life data sets from different fields. The choice of this special case is motivated by the applicability of the Weibull distribution in different fields as compared to other baseline distributions considered in defining other presented special cases. The goodness-of-fit of the TI-HT-OPGW-W distribution was compared to those of other well-known heavy-tailed distributions and some generalizations of the Weibull distribution. These distributions are: alpha power Topp-Leone Weibull (APTLW) distribution by [9], the type-I heavy-tailed Weibull (TI-HT-W) distribution by [30], the heavy-tailed beta-power transformed Weibull (HTBPT-W) distribution by [31], the half logistic generalized Weibull (HLGW) distribution by [8], odd generalized half-logistic Weibull (OGHLW-W) by [14], the Kumaraswamy-Weibull (KW) distribution by [15], and type II exponentiated

half logistic Weibull (TIIEHLW) distribution by [4]. The pdf's of these competing models are given in the appendix.

For comparison purposes, we used well-known goodness-of-fit statistics such as $-2\log$ -likelihood statistic ($-2\ln(L)$), Akaike Information Criterion ($AIC = 2p - 2\ln(L)$) by [3], Consistent Akaike Information Criterion ($CAIC = AIC + 2\frac{p(p+1)}{n-p-1}$) by [11], Bayesian Information Criterion ($BIC = p\ln(n) - 2\ln(L)$) by [28], (n is the number of observations, and p is the number of estimated parameters), Cramér-von Mises (W^*) statistic, and Anderson-Darling statistic (A^*) described by [13], Kolmogorov-Smirnov (K-S) statistic by [12], and its p -value. It is known that the smaller the values of all the goodness-of-fit statistics, except for the p -value of K-S statistic, the better the model for fitting the data set.

For the probability plot, we plotted $F(x_{(j)}) = F(x_{(j)}; \hat{\theta}, \hat{\alpha}, \hat{\beta}, \hat{\lambda})$ against $\frac{j - 0.375}{n + 0.25}$, $j = 1, 2, \dots, n$, where $x_{(j)}$ are the ordered values of the observed data. The measures of closeness are given by the sum of squares

$$SS = \sum_{j=1}^n \left[F(x_{(j)}) - \left(\frac{j - 0.375}{n + 0.25} \right) \right]^2.$$

8.1. Biomedical Sciences Data. The data set is on remission times (months) of 128 bladder cancer patients by [22]. (See the data in the Appendix).

Table 5 gives the MLEs of the fitted distributions together with the standard errors (in parenthesis). Table 6 gives the values of all considered goodness-of-fit statistics. It is evident that the TI-HT-OPGW-W distribution provides the best fit among the competitors since it has the lowest value of $-2\ln(L)$, AIC , $CAIC$, BIC , W^* , A^* , K-S statistic, and larger p -value. From the plots in Figure 9 we can see that the TI-HT-OPGW-W distribution follows the fitted histogram closely and has the smallest sum of squares (SS) value from the probability plots. This supports the conclusion made from Table 6.

The total test time (TTT) scaled plots, observed and the fitted Kaplan-Meier survival curves, theoretical and empirical cumulative distribution function (ECDF) and hazard rate function (HRF) plots of the TI-HT-OPGW-W distribution are shown in Figure 10. From the Kaplan-Meier and ECDF plots, it is clear that the TI-HT-OPGW-W distribution is a good candidate for modeling the biomedical data. The TTT scaled plot demonstrates that the data follow an upside-down bathtub hazard rate shape. Furthermore, the hazard rate function exhibit a non-monotonic shape for the remission times data.

8.2. Insurance Data. This data set from the insurance field represents monthly metrics on unemployment insurance from July 2008 to April 2013 from the department of labor, licensing and regulation. It consists of 58 observations and 21 variables, we studied the variable number 6.

TABLE 5. Estimates of models for remission times data

Model	Estimates			
	θ	α	β	λ
TI-HT-OPGW-W	0.1575 (0.0633)	4.6733 (2.6563)	0.3432 (0.2056)	0.2149 (0.0368)
APTLW	θ 0.3632 (0.1239)	α 2.6272×10^{02} (4.8767×10^{-05})	β 0.8610 (0.1241)	λ 0.1120 (0.0540)
TI-HT-W	α 1.1030 (0.6049)	θ 1.2551 (3.5043)	β 0.0564 (0.3501)	
HTBPT-W	α 1.0478 (0.0675)	γ 0.0938 (0.0190)	β 0.9999 (0.7280)	
HLGW	w 6.2967 (9.9402)	λ 0.5000 (0.0776)	γ 0.0516 (0.0804)	
KW	a 8.8278 (4.6441)	b 206.7178 (0.0352)	c 0.1835 (0.0580)	λ 0.0301 (0.0679)
TIIEHLW	a 1.0297×10^{03} (1.8761×10^{-06})	λ 1.0759×10^{02} (1.9066×10^{-04})	δ 2.4004 (2.1528×10^{-02})	γ 0.0500 (3.2111×10^{-03})
OGHLW-W	α 2.1269×10^{-05} (3.4793×10^{-06})	β 0.6471 (4.2738×10^{-04})	λ 14.4550 (1.9132×10^{-05})	γ 0.0774 (4.3136×10^{-03})

TABLE 6. Goodness-of-fit statistics for remission times data

Model	Statistics							
	$-2 \log L$	AIC	$AICC$	BIC	W^*	A^*	$K - S$	P-value
TI-HT-OPGW-W	822.0841	830.0841	830.4093	841.4922	0.0507	0.3255	0.0488	0.9196
APTLW	827.4507	835.4507	835.7759	846.8588	0.1275	0.7620	0.0727	0.5065
TI-HT-W	826.9924	832.9924	833.1859	841.5485	0.1150	0.6940	0.0684	0.5863
HTBPT-W	828.1738	834.1738	834.3673	842.7298	0.1313	0.7864	0.0700	0.5570
HLGW	851.9690	857.9690	858.1626	866.5251	0.2699	1.5921	0.1647	0.0019
KW	823.5203	831.5204	831.8456	842.9285	0.0776	0.4738	0.0567	0.8036
TIIEHLW	823.0934	831.0934	831.4186	842.5015	0.0710	0.4392	0.0549	0.8351
OGHLW-W	838.0349	846.0347	846.3599	857.4428	0.2477	1.4603	0.0952	0.1962

It is available at: <https://catalog.data.gov/dataset/unemployment-insurance-data-july-2008-to-april-2013>. (See the data in the Appendix).

For these data, the MLEs, standard errors (in parenthesis) are given in Table 7. From the goodness-of-fit statistics given in Table 8, we observe that the proposed

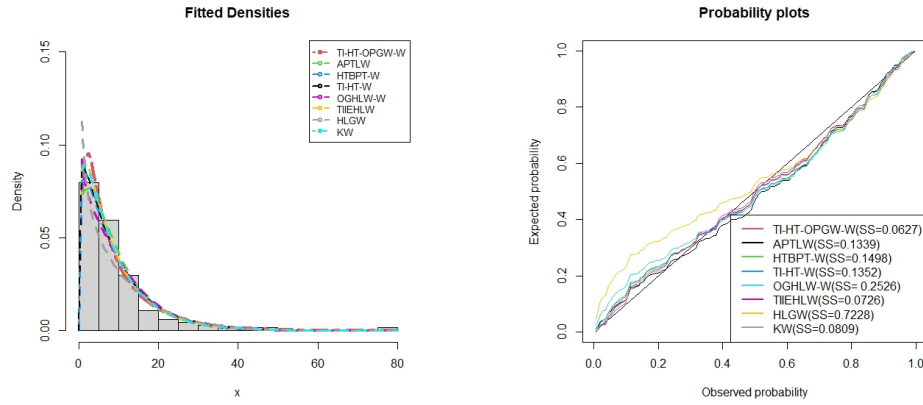


FIGURE 9. Fitted densities and probability plots for remission times data

TABLE 7. Estimates of models for insurance data

Model	Estimates			
	θ	α	β	λ
TI-HT-OPGW-W	0.3099 (0.1775)	2.0529 (1.8481×10^{-05})	0.0078 (0.0109)	1.1668 (0.2846)
APTLW	θ 1.3112 (2.3870×10^{-10})	α 2.3022 (5.1581×10^{-11})	β 2.3222 (2.4955×10^{-09})	λ 7.6494×10^{-05} (8.0428×10^{-06})
TI-HT-W	α 1.1963 (0.1374)	θ 0.1221 (0.0537)	β 0.0916 (0.0567)	
HTBPT-W	α 1.2034 (0.1125)	γ 0.0262 (0.01207)	β 7.1487×10^{-05} (6.8034×10^{-05})	
HLGW	w 545.6400 (1.2046×10^{-13})	λ 1.0121 (2.7123×10^{-10})	γ 3.2890×10^{-05} (2.0129×10^{-06})	
KW	a 1.2341×10^{02} (2.0464×10^{-07})	b 9.4224×10^{03} (3.0326×10^{-10})	c 0.1119 (6.1342×10^{-04})	λ 1.1220×10^{02} (6.9732×10^{-08})
TIEHLW	a 1.4145×10^{04} (9.5420×10^{-08})	λ 2.3843×10^{03} (3.7577×10^{-05})	δ 4.4752 (9.1240×10^{-02})	γ 0.0500 (5.0324×10^{-03})
OGHLW-W	α 0.0008 (0.0004)	β 1.2387 (0.2632)	λ 1.7631 (0.1435)	γ 0.3265 (0.0490)

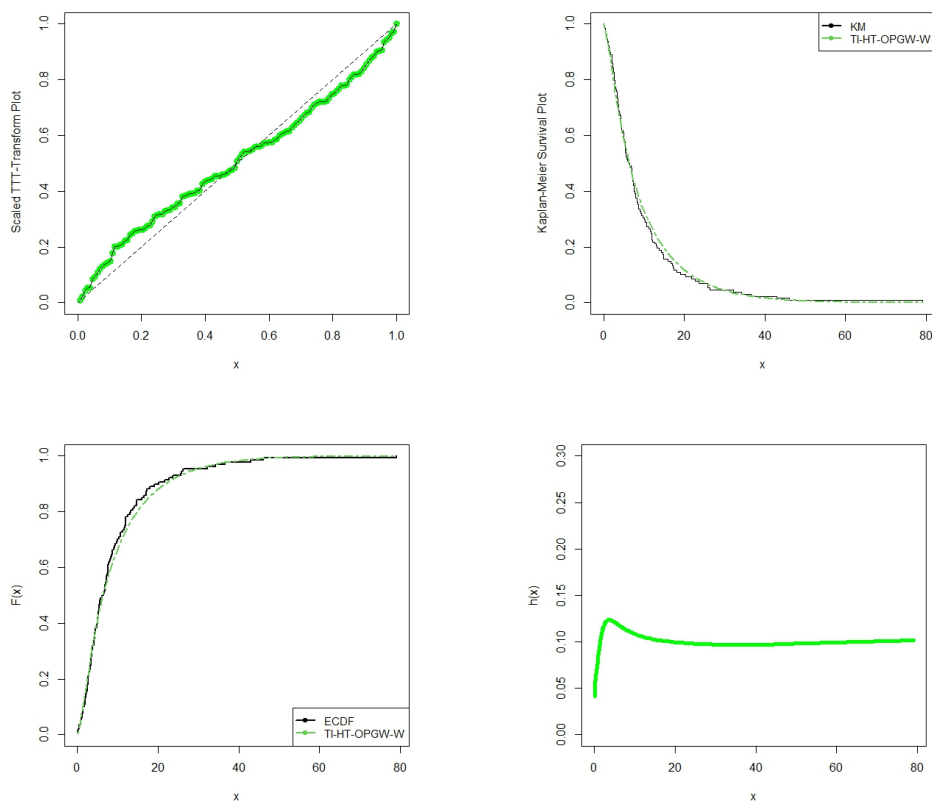


FIGURE 10. Fitted TTT, Kaplan-Meier Survival, ECDF and HRF plots for remission times data

TABLE 8. Goodness-of-fit statistics for insurance data

Model	Statistics							
	$-2 \log L$	AIC	$AICC$	BIC	W^*	A^*	$K - S$	P-value
TI-HT-OPGW-W	495.8290	503.8290	504.5838	512.0708	0.0578	0.3621	0.0719	0.9249
APTLW	496.5398	504.5398	505.2945	512.7816	0.1102	0.5583	0.1054	0.5394
TI-HT-W	525.6656	531.6656	532.1100	537.8469	0.3263	1.7175	0.2036	0.0162
HTBPT-W	505.3288	511.3291	511.7735	517.5104	0.2356	1.2313	0.1188	0.3853
HLGW	512.5666	518.5643	519.0087	524.7456	0.0841	0.4385	0.2242	0.0058
KW	498.6628	506.6629	507.4176	514.9047	0.1545	0.7836	0.1241	0.3328
TIIEHLW	498.9921	506.9921	507.7468	515.2338	0.1601	0.8126	0.1261	0.3145
OGHLW-W	496.0044	504.0044	504.7591	512.2462	0.0599	0.3634	0.0741	0.9069

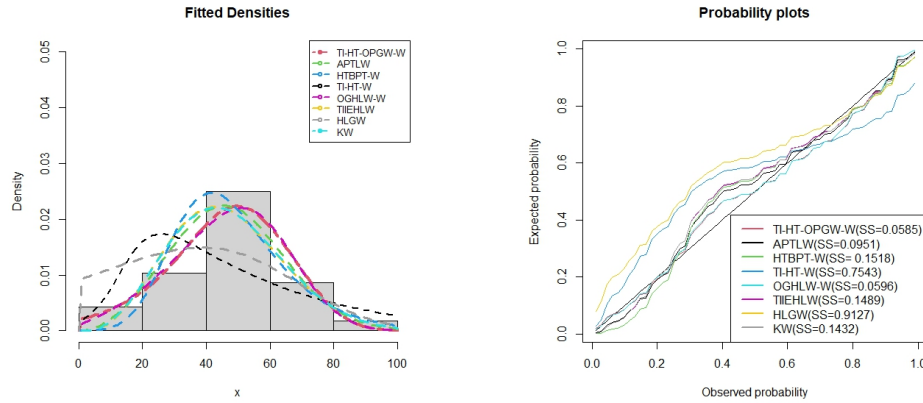


FIGURE 11. Fitted densities and probability plots for insurance data

TI-HT-OPGW-W distribution is the best choice to implement for fitting the insurance data since it has the smallest values of goodness-of-fit statistics and larger p-value compared to other fitted distributions. To support the results in Table 8 a visual illustrations is provided in Figure 11

Figure 12 shows the TTT scaled plots, observed and the fitted Kaplan-Meier survival curves, ECDF and HRF plots. We can see that the TI-HT-OPGW-W distribution follows the empirical cdf, and Kaplan-Meier survival curves very closely. The TTT scaled plot shows an increasing hrf, allowing us to fit the heavy-tailed insurance data using TI-HT-OPGW-W distribution. Furthermore, the estimated hazard rate function for insurance data is an increasing shape.

8.3. Agriculture Data. This dataset represents the total factor productivity (TFP) growth agricultural production for thirty-seven African countries from 2001-2010, see <https://dataverse.harvard.edu/dataset.xhtml?persistentId=doi:10.7910/DVN/9I0AKR>, accessed on 30 June 2022. (See the data in the Appendix).

The parameter estimates, standard error (in parentheses) are given in Table 9. The goodness-of-fit statistics: AIC, BIC, CAIC, W^* , A^* , K-S statistic, and its p-value are given in Table 10. The values in Table 10 shows that the TI-HT-OPGW-W distribution gives the smallest values for the goodness-of-fit statistics and the largest p-value of K-S statistic. Thus, the TI-HT-OPGW-W distribution provides better fit than the rest of the distributions for the TFP growth data. Plots of the fitted densities and the histogram, observed probability vs predicted probability are given in Figure 13.

Figure 14 presents the TTT scaled plots, empirical and theoretical Kaplan-Meier survival plots, cumulative frequency curve of the observed data with the fitted cdf

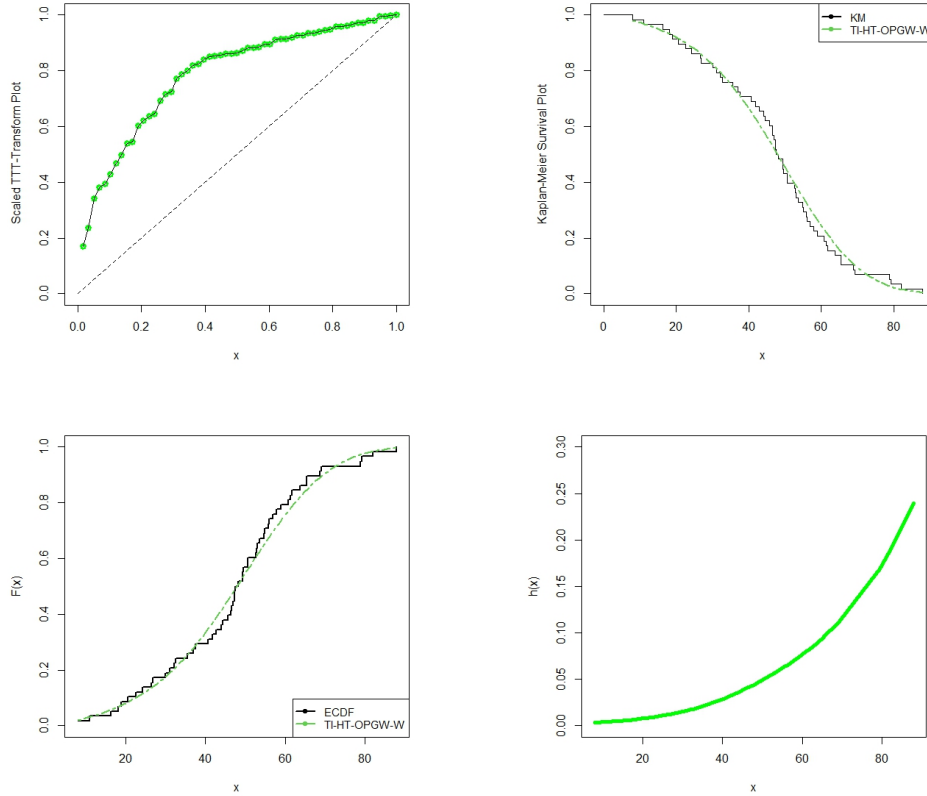


FIGURE 12. Fitted TTT, Kaplan-Meier survival, ECDF and HRF plots for insurance data

of the TI-HT-OPGW-W distribution and also, the HRF plot. It is visible that, the fitted empirical and theoretical plots are close to each other, hence we conclude that our model provide the better fit for the data. The TTT scaled plot clearly demonstrates that the data fit the increasing hazard rate structure. Furthermore, the estimated hazard rate function for TFP growth data is an increasing shape.

8.4. Failure Times Data. These data represent the failure time of a machine from Babel tyres factory (Iraq) in hours. The data was obtained from [5]. (See the data in the Appendix).

Table [11] and [12] presents numerical values of the MLEs with standard errors (in parenthesis), $-2 \ln(L)$, AIC , $CAIC$, BIC , W^* , A^* , K-S statistic, and its p -value for the failure times data. It can be seen that the TI-HT-OPGW-W distribution has

TABLE 9. Estimates of models for TFP growth data

Model	Estimates			
	θ	α	β	λ
TI-HT-OPGW-W	73.8740 (2.6403×10^{-11})	0.9815 (8.2976×10^{-10})	7.6304×10^{-05} (1.2706×10^{-05})	1.4386 (8.8095×10^{-10})
APTLW	3.1266 (5.8242)	12.1322 (29.4512)	0.6406 (0.5086)	1.0002 (1.0759)
TI-HT-W	0.8309 (0.1212)	0.2991 (0.1187)	2.7494 (1.1363)	
HTBPT-W	0.6588 (0.1140)	1.1740 (0.2605)	0.0286 (0.0330)	
HLGW	797.4800 (1.1333×10^{-07})	0.5000 (7.3374×10^{-02})	9.0808×10^{-04} (9.6790×10^{-05})	
KW	0.1293 (0.0446)	1.8134 (1.0046)	7.4198 (2.5729)	0.2015 (0.0385)
TIIEHLW	1.6908 (1.5011)	3.9314 (4.8099)	0.9271 (0.8245)	0.6168 (0.4828)
OGHLW-W	1.0774×10^{-04} (1.2797×10^{-04})	0.6420 (8.7916×10^{-02})	13.6300 (3.5390×10^{-03})	0.1275 (2.3757×10^{-02})

TABLE 10. Goodness-of-fit statistics for TFP growth data

Model	Statistics							
	$-2 \log L$	AIC	$AICC$	BIC	W^*	A^*	$K - S$	P-value
TI-HT-OPGW-W	107.0129	115.0129	116.2629	121.4566	0.0293	0.1812	0.0798	0.9722
APTLW	107.9218	115.9218	117.1718	122.3655	0.0368	0.2264	0.1049	0.8098
TI-HT-W	111.3917	117.3918	118.1191	122.2246	0.0368	0.2240	0.1197	0.6635
HTBPT-W	115.7192	121.7192	122.4464	126.5519	0.0311	0.1928	0.1807	0.1781
HLGW	117.7719	123.7719	124.4991	128.6046	0.0325	0.2050	0.2142	0.0670
KW	109.6151	117.6158	118.8658	124.0595	0.0745	0.4569	0.1043	0.8151
TIIEHLW	109.7821	117.7821	119.0321	124.2258	0.0643	0.4020	0.1255	0.6043
OGHLW-W	108.3969	116.3967	117.6467	122.8403	0.0428	0.2752	0.0889	0.9316

the lowest value for all goodness-of-fit statistics and a larger $p - value$ between all fitted distributions which gives it the superiority for fitting the failure times data. To support the best fitting power of the TI-HT-OPGW-W distribution, plots of the fitted densities and the histogram, observed probability vs predicted probability are given in Figure 15.

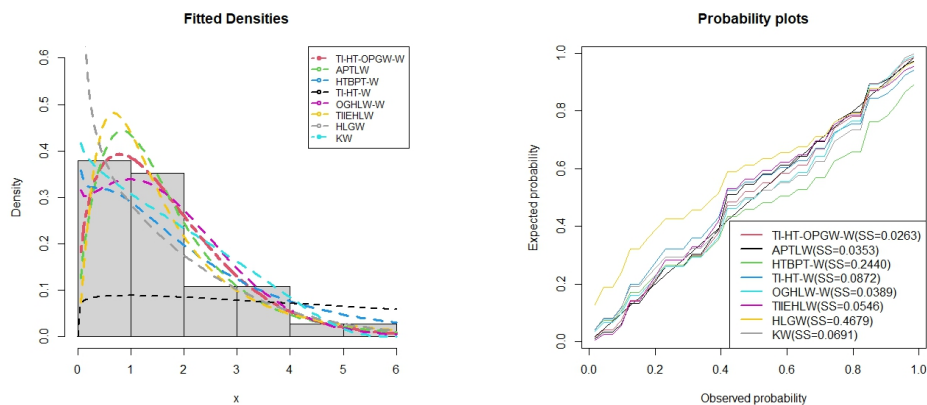


FIGURE 13. Fitted densities and probability plots for TFP growth data

TABLE 11. Estimates of models for failure times data

Model	Estimates			
	θ	α	β	λ
TI-HT-OPGW-W	0.1548 (0.1132)	24.2130 (4.5574×10^{-05})	0.0461 (0.0239)	0.1683 (0.0168)
APTLW	θ 0.5500 (0.0748)	α 0.0173 (0.0675)	β 1.3216 (0.0378)	λ 0.0001 (0.0001)
TI-HT-W	α 0.6980 (0.0756)	θ 0.1196 (0.0486)	β 0.4071 (0.1391)	
HTBPT-W	α 0.8987 (0.0783)	γ 0.0125 (0.0052)	β 1.0002 (0.4193)	
HLGW	w 0.2370 (0.0500)	λ 0.9780 (0.1847)	γ 0.5827 (0.4439)	
KW	a 15.4546 (4.7782)	b 62.0537 (0.1384)	c 0.0990 (0.0165)	λ 0.4869 (1.1236)
TIEHLW	a 27.4140 (3.2565×10^{-04})	λ 109.6900 (7.7848×10^{-04})	δ 2.6706 (8.9301×10^{-02})	γ 0.0500 (6.7886×10^{-03})
OGHLW-W	α 2.1083×10^{-05} (8.5735×10^{-06})	β 0.4143 (6.8140×10^{-04})	λ 21.2990 (1.3243×10^{-05})	γ 0.0510 (5.8370×10^{-03})

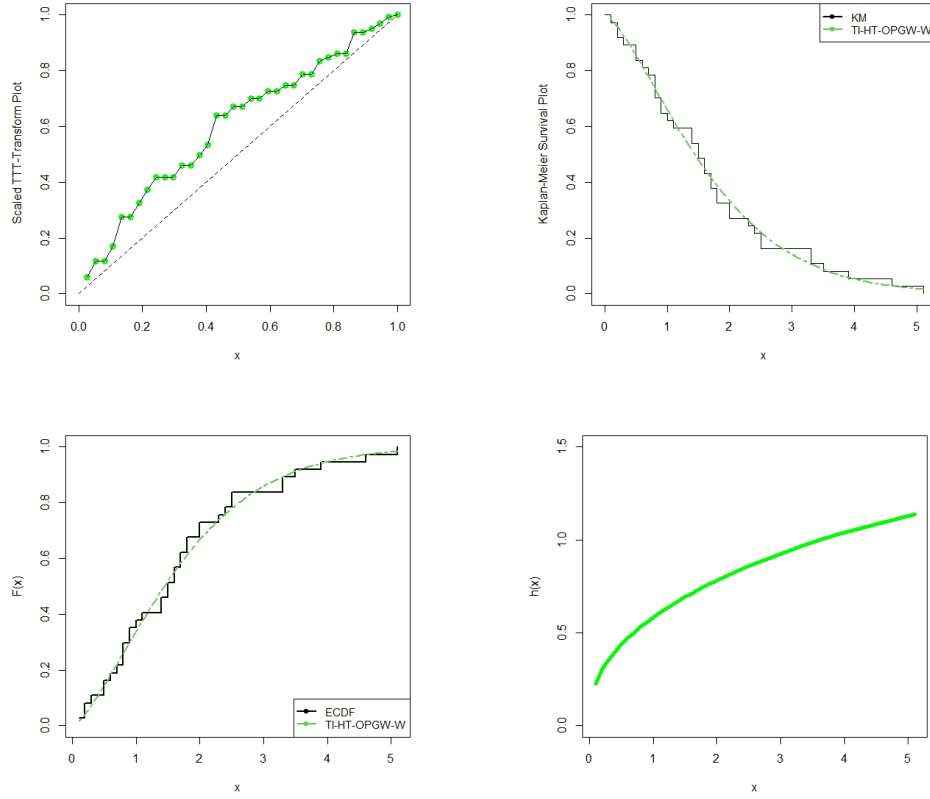


FIGURE 14. Fitted TTT, Kaplan-Meier survival, ECDF and HRF plots for TFP growth data

TABLE 12. Goodness-of-fit statistics for failure times data

Model	Statistics							
	$-2 \log L$	AIC	$AICC$	BIC	W^*	A^*	$K - S$	P-value
TI-HT-OPGW-W	327.3327	335.3327	336.9994	340.8019	0.0660	0.3691	0.1344	0.6705
APTLW	328.3628	336.3628	338.0295	341.8320	0.0845	0.4480	0.1495	0.5353
TI-HT-W	332.8800	338.8801	339.8401	342.9819	0.0687	0.3736	0.2413	0.0682
HTBPT-W	333.4933	339.4933	340.4533	343.5952	0.1034	0.5659	0.2861	0.0173
HLGW	333.0898	339.0899	340.0499	343.1918	0.0598	0.3901	0.1786	0.3132
KW	327.7001	335.7001	337.3668	341.1693	0.0696	0.3815	0.1365	0.6518
TIIEHLW	327.5437	335.8219	337.4885	341.2911	0.0731	0.3973	0.1377	0.6409
OGHLW-W	331.0865	339.0866	340.7532	344.5557	0.1181	0.6422	0.1616	0.4348

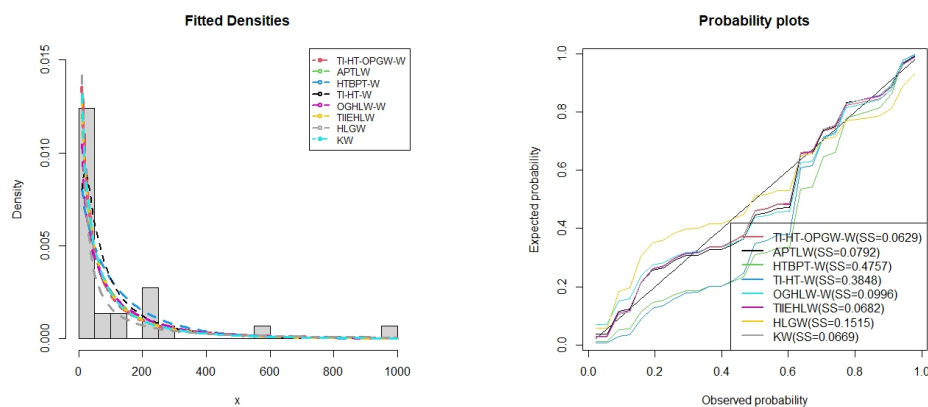


FIGURE 15. Fitted densities and probability plots for failure times data

Figure 16 depicts the TTT scaled plots, observed and the fitted Kaplan-Meier survival curves, theoretical and ECDF and HRF plots. The green line in the Kaplan-Meier and ECDF plots illustrates the good fit to the data. The TTT scaled plot demonstrates that the data follow a decreasing hazard rate shape. Furthermore, the hazard rate function exhibit a decreasing shape for the failure times data.

9. CONCLUDING REMARKS

We propose and study a new heavy-tailed family of distributions called type I heavy-tailed odd power generalized Weibull-G (TI-HT-OPGW-G) distribution. Many of its statistical properties such as quantile function, linear representation, moments, moment generating function, distribution of order statistics and Rényi entropy were derived. The maximum likelihood estimation method was derived and evaluated via a simulation study. Actuarial measures for the proposed distribution were also derived. Numerical comparisons of the actuarial measures with other distributions was conducted. Finally, the superiority and importance of the TI-HT-OPGW-G family of distributions was illustrated by using four real data sets from different fields. The TI-HT-OPGW-W model as a special case to this new family of distributions was applied to four datasets and from the results it is evident that the new proposed model performs better than several heavy tailed distributions.

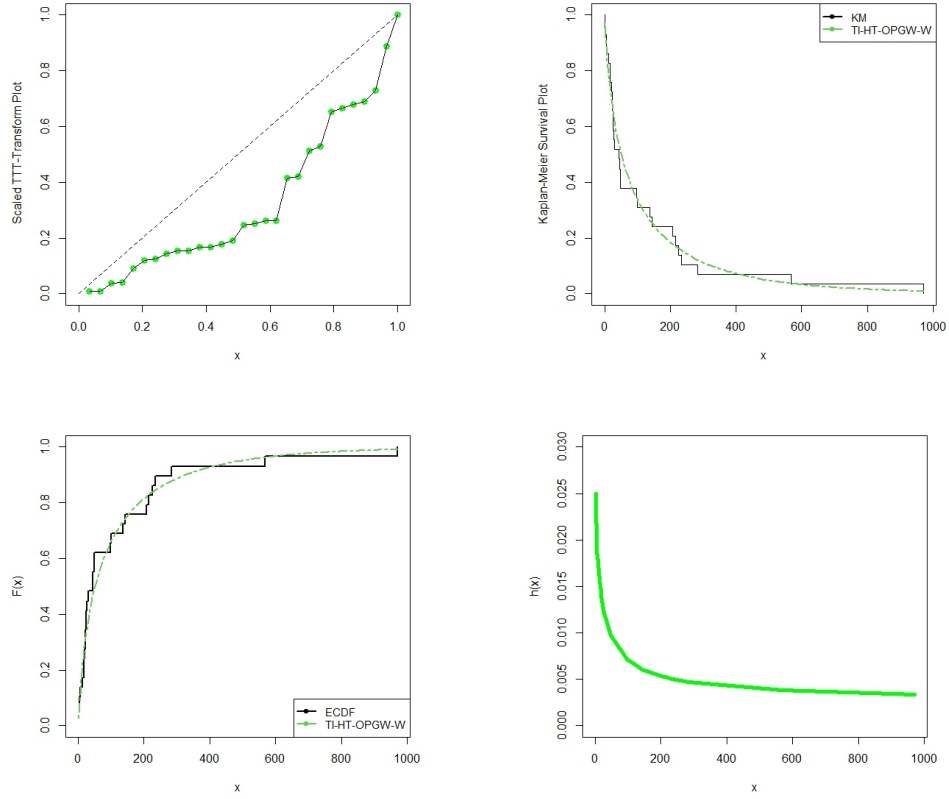


FIGURE 16. Fitted TTT, Kaplan-Meier survival, ECDF and HRF plots for failure times data

APPENDIX

Click the link below to access the appendix.

https://drive.google.com/file/d/124z_Bzokbw716cQ-kycxDC-yF_D_mRLn/view?usp=sharing

Author Contribution Statements Conceptualization, Broderick Oluyede; Methodology, Broderick Oluyede; Software, Thatayaone Moakofi; Formal analysis, Thatayaone Moakofi; Writing – review & editing, Broderick Oluyede and Thatayaone Moakofi. All authors have read and agreed to the published version of the manuscript.

Declaration of Competing Interests The authors declare no conflict of interest.

REFERENCES

- [1] Affify, A.Z., Gemeay, A.M., Ibrahim, N.A., The heavy-tailed exponential distribution: risk measures, estimation, and application to actuarial data, *Mathematics*, 8(8) (2020), 1276. <https://doi.org/10.3390/math8081276>
- [2] Ahn, S., Kim, J.H., Ramaswami, V., A new class of models for heavy-tailed distributions in finance and insurance risk, *Insurance: Mathematics and Economics*, 51(1) (2012), 43-52. <https://doi.org/10.1016/j.insmatheco.2012.02.002>
- [3] Akaike, H., A new look at the statistical model identification, *IEEE Transactions on Automatic Control*, 19(6) (1974), 716–723. DOI:[10.1109/TAC.1974.1100705](https://doi.org/10.1109/TAC.1974.1100705)
- [4] Al-Mofteh, H., Elgarhy, M., Afify, A., Zannon, M., Type II exponentiated half logistic generated family of distributions with applications, *Electronic Journal of Applied Statistical Analysis*, 13(2) (2020), 536-561. DOI:[10.1285/i20705948v13n2p536](https://doi.org/10.1285/i20705948v13n2p536)
- [5] AL-Kazrajy, A.A., Comparative study of estimation methods of reliability with complete data using simulation (With Application), *MSc thesis*(2001), Mosul University, Iraq.
- [6] Alotaibi, N., Elbatal, I., Almetwally, E.M., Alyami, S.A., Al-Moisheer, A.S., Elgarhy, M., Truncated Cauchy power Weibull-G class of distributions: Bayesian and non-Bayesian inference modelling for COVID-19 and carbon fiber data, *Mathematics*, 10(9) (2022), 1565. <https://doi.org/10.3390/math10091565>
- [7] Alyami, S.A., Babu, M.G., Elbatal, I., Alotaibi, N., Elgarhy, M., Type II half-logistic odd Fréchet class of distributions: Statistical theory and applications, *Symmetry*, 14(6) (2022), 1222. <https://doi.org/10.3390/sym14061222>
- [8] Anwar, A., Bibi, A., The half-logistic generalized Weibull distribution, *Journal of Probability and Statistics*, 2018 (2018), Article ID 8767826, 12 pages. <https://doi.org/10.1155/2018/8767826>
- [9] Benkhelifa, L., Alpha power Topp-Leone Weibull distribution: properties, characterizations, Regression modeling and applications, *Journal of Statistics and Management Systems*, 25(8) (2022), 1945-1970. <https://doi.org/10.1080/09720510.2021.1995217>
- [10] Bourguignon, M., Silva R. B., Cordeiro G. M., The Weibull-G family of probability distributions, *Journal of Data Science*, 12 (2014), 53-68.
- [11] Bozdogan, H., Model selection and Akaike's information criterion (AIC): The general theory and its analytical extensions, *Psychometrika*, 52(3) (1987), 345-370. <https://doi.org/10.1007/BF02294361>
- [12] Chakravarti, I.M., Laha, R.G., Roy, J., Handbook of methods of applied statistics, *Wiley Series in Probability and Mathematical Statistics*, 1 (1967), 392-394. DOI: [1130000794121857024](https://doi.org/10.1130000794121857024)
- [13] Chen, G., Balakrishnan, N., A general purpose approximate goodness-of-fit test, *Journal of Quality Technology*, 27(2) (1995), 154-161. <https://doi.org/10.1080/00224065.1995.11979578>
- [14] Chipepa, F., Oluyede, B., Makubate, B., The odd generalized half-logistic Weibull-G family of distributions: Properties and applications, *Journal of Statistical Modeling: Theory and Applications*, 1(1) (2020), 65-89. DOI: [10.22034/JSMTA.2020.1904](https://doi.org/10.22034/JSMTA.2020.1904)
- [15] Cordeiro, G. M. Ortega, E. M. M. & Nadarajaah, S., The Kumaraswamy Weibull distribution with application to failure data, *Journal of the Franklin Institute*, 347(8) (2010), 1399-1429. <https://doi.org/10.1016/j.jfranklin.2010.06.010>
- [16] Dhungana, G.P. and Kumar, V., Exponentiated odd Lomax exponential distribution with application to COVID-19 death cases of Nepal, *PloS One*, 17(6) (2022), <https://doi.org/10.1371/journal.pone.0269450>
- [17] Eghwerido, J.T., Agu, F.I., The shifted Gompertz-G family of distributions: properties and applications, *Mathematica Slovaca*, 71(5) (2021), 1291-1308. <https://doi.org/10.1515/ms-2021-0053>

- [18] Hamedani, G.G., Rasekhi, M., Najibi, S., Yousof, H.M., Alizadeh, M., Type II general exponential class of distributions, *Pakistan Journal of Statistics and Operation Research*, 15(2) (2019), 503-523. <https://doi.org/10.18187/pjsor.v15i2.1699>
- [19] Handique, L., Ahsan, A.L., Chakraborty, S., Generalized modified exponential-G family of distributions: its properties and applications, *International Journal of Mathematics and Statistics*, 21(1) (2020), 1-17.
- [20] Hussein, M., Elsayed, H., Cordeiro, G.M., A new family of continuous distributions: properties and estimation, *Symmetry*, 14(2) (2022), 276. <https://doi.org/10.3390/sym14020276>
- [21] Korkmaz, M.Ç., A new heavy-tailed distribution defined on the bounded interval: the logit slash distribution and its application, *Journal of Applied Statistics*, 47(12) (2020), 2097-2119. <https://doi.org/10.1080/02664763.2019.1704701>
- [22] Lee, E. T., & Wang, J., *Statistical Methods for Survival Data Analysis*, John Wiley & Sons, 2003.
- [23] Moakofi, T., Oluyede, B., Gabanakgosi, M., The Topp-Leone odd Burr III-G family of distributions: Model, properties and applications, *Statistics, Optimization & Information Computing*, 10(1) (2022), 236-262. <https://doi.org/10.19139/soic-2310-5070-1135>
- [24] Moakofi, T., Oluyede, B., Chipepa, F., Makubate, B., Odd power generalized Weibull-G family of distributions: Model, properties and applications, *Journal of Statistical Modelling: Theory and Applications*, 2(1) (2021), 121-142. DOI: [10.22034/JSMTA.2021.2333](https://doi.org/10.22034/JSMTA.2021.2333)
- [25] Nascimento, A.D., Silva, K.F., Cordeiro, G.M., Alizadeh, M., Yousof, H.M., Hamedani, G.G., The odd Nadarajah-Haghighi family of distributions: properties and applications, *Studia Scientiarum Mathematicarum Hungarica*, 56(2) (2019), 185-210. <https://doi.org/10.1556/012.2019.56.2.1416>
- [26] Oluyede, B., Chipepa, F., The Marshall-Olkin odd exponential half logistic-G family of distributions: Properties and applications, *Statistics, Optimization & Information Computing*, 11(2) (2021), 479-503. <https://doi.org/10.19139/soic-2310-5070-938>
- [27] Rannona, K., Oluyede, B., Chipepa, F., Makubate, B., The Marshall-Olkin-exponentiated odd exponential half logistic-G family of distributions with applications, *Eurasian Bulletin of Mathematics*, 4(3) (2022), 134-161.
- [28] Schwarz, Gideon E., Estimating the dimension of a model, *Annals of Statistics*, 6(2) (1978), 461-464. <https://www.jstor.org/stable/2958889>
- [29] Teamah, A.E.A., Elbanna, A.A., Gemeay, A.M., Heavy-tailed log-logistic distribution: Properties, risk measures and applications, *Statistics, Optimization & Information Computing*, 9(4) (2021), 910-941. <https://doi.org/10.19139/soic-2310-5070-1220>
- [30] Zhao, W., Khosa, S.K., Ahmad, Z., Aslam, M., Afify, A.Z., Type-I heavy-tailed family with applications in medicine, engineering and insurance, *PloS One*, 15(8) (2020). <https://doi.org/10.1371/journal.pone.0237462>
- [31] Zhao, J., Ahmad, Z., Mahmoudi, E., Hafez, E.H., Mohie El-Din, M.M., A new class of heavy-tailed distributions: Modeling and simulating actuarial measures, *Complexity*, 2021 (2021), <https://doi.org/10.1155/2021/5580228>

QUASI HEMI-SLANT PSEUDO-RIEMANNIAN SUBMERSIONS IN PARA-COMPLEX GEOMETRY

Esra BAŞARIR NOYAN¹ and Yılmaz GÜNDÜZALP²

^{1,2}Department of Mathematics, Dicle University, 21280, Sur, Diyarbakır, TÜRKİYE

ABSTRACT. We introduce a new class of pseudo-Riemannian submersions which are called quasi hemi-slant pseudo-Riemannian submersions from para-Kaehler manifolds to pseudo-Riemannian manifolds as a natural generalization of slant submersions, semi-invariant submersions, semi-slant submersions and hemi-slant Riemannian submersions in our study. Also, we give non-trivial examples of such submersions. Further, some geometric properties with two types of quasi hemi-slant pseudo-Riemannian submersions are investigated.

1. INTRODUCTION

A C^∞ -submersion ψ can be defined according to the following conditions. A pseudo-Riemannian submersion ([12], [16], [13], [17], [26]), an almost Hermitian submersion ([27], [29]), bi-slant submanifold ([3], [5]), a slant submersion ([7], [11], [1], [19], [23]), bi-slant submersion ([21]), an anti-invariant submersion ([8], [9], [10], [24]), a hemi-slant submersion ([28], [22]), a quasi-bi-slant Submersion ([20]), a semi-invariant submersion ([18], [25]), etc. As we know, Riemannian submersions were severally introduced by B. O'Neill ([17]) and A. Gray ([12]) in 1960s. In particular, by using the concept of almost Hermitian submersions, B. Watson ([30]) gave some differential geometric properties among fibers, base manifolds, and total manifolds. Some interesting results concerning para-Kaehler-like statistical submersions were obtained by G.E. Vilcu ([29]).

Motivated by the above studies, we presented quasi hemi-slant pseudo-Riemannian submersions in para-complex geometry from para-Kaehler manifolds onto pseudo-Riemannian manifolds. We organized our work in three sections. In section 2, we gather basic concepts and definitions needed in the following parts. In section 3,

2020 *Mathematics Subject Classification.* 53C43, 53B20, 53C40.

Keywords. Quasi hemi-slant submersion, hemi-slant submersion, para-Kaehler manifold, pseudo-Riemannian submersions.

¹✉ bsrrnoyan@gmail.com; 0000-0001-6535-7498

²✉ ygunduzalp@dicle.edu.tr-Corresponding author; 0000-0002-0932-949X.

We examined quasi hemi-slant pseudo-Riemannian submersions in para-complex geometry that satisfies certain conditions. We give some non-trivial examples of these submersions which satisfy the conditions of two types, while in we study the decomposition theorem of two types of the distributions.

2. PRELIMINARIES

By a para-Hermitian manifold we mean a triple $(\mathcal{B}, \mathcal{P}, g_{\mathcal{B}})$, where \mathcal{B} is connected differentiable manifold of $2n$ - dimensional , \mathcal{P} is a tensor field of type $(1,1)$ and a pseudo-Riemannian metric $g_{\mathcal{B}}$ on \mathcal{B} , satisfying

$$\mathcal{P}^2 E_1 = E_1, \quad g_{\mathcal{B}}(\mathcal{P}E_1, \mathcal{P}E_2) = -g_{\mathcal{B}}(E_1, E_2) \tag{1}$$

where E_1, E_2 are vector fields on \mathcal{B} . Then we can say that \mathcal{B} is a para-Kaehler manifold such that

$$\nabla \mathcal{P} = 0; \tag{2}$$

where ∇ denotes the Levi-Civita connection on \mathcal{B} ([15]).

Let $(\mathcal{B}, g_{\mathcal{B}})$ and $(\tilde{\mathcal{B}}, g_{\tilde{\mathcal{B}}})$ be two pseudo-Riemannian manifolds. Being a pseudo-Riemannian submersion $\psi : \mathcal{B} \rightarrow \tilde{\mathcal{B}}$ provides the following three properties;

- (i) $\psi_{*|p}$ is onto for all $p \in \mathcal{B}$,
- (ii) the fibres $\psi^{-1}(q)$, $q \in \tilde{\mathcal{B}}$, are r - dimensional pseudo-Riemannian submanifolds of \mathcal{B} , where $r = \dim(\mathcal{B}) - \dim(\tilde{\mathcal{B}})$,
- (iii) ψ_* preserves scalar products of vectors normal to fibres.

The vectors tangent to the fibres are called vertical and those normal to the fibres are called horizontal. A vector field U on \mathcal{B} is called basic if U is horizontal and ψ - related to a vector field U_* on $\tilde{\mathcal{B}}$, i.e., $\psi_* U_p = U_{*\psi_p}$ for all $p \in \mathcal{B}$. We indicate by \mathcal{V} the vertical distribution, by \mathcal{H} the horizontal distribution and by v and h the vertical and horizontal projection. We know that $(\mathcal{B}, g_{\mathcal{B}})$ is called total manifold and $(\tilde{\mathcal{B}}, g_{\tilde{\mathcal{B}}})$ is called base manifold of the submersion $\psi : (\mathcal{B}, g_{\mathcal{B}}) \rightarrow (\tilde{\mathcal{B}}, g_{\tilde{\mathcal{B}}})$.

Now, let's denote O'Neill's tensors \mathcal{T} and \mathcal{A} :

$$\mathcal{T}_U \mathcal{W} = h \nabla_{vU} v \mathcal{W} + v \nabla_{vU} h \mathcal{W} \tag{3}$$

and

$$\mathcal{A}_U \mathcal{W} = v \nabla_{hU} h \mathcal{W} + h \nabla_{hU} v \mathcal{W} \tag{4}$$

for every $U, \mathcal{W} \in \chi(\mathcal{B})$, on \mathcal{B} where ∇ is the Levi-Civita connection of $g_{\mathcal{B}}$.

Further, a pseudo-Riemannian submersion $\psi : \mathcal{B} \rightarrow \tilde{\mathcal{B}}$ has totally geodesic fibers if and only if $\mathcal{T} \equiv 0$. Also, if \mathcal{A} vanishes then the horizontal distribution is integrable(see [4], [6]). Using [3] and [4], we get

$$\nabla_U \mathcal{W} = \mathcal{T}_U \mathcal{W} + \hat{\nabla}_U \mathcal{W}; \tag{5}$$

$$\nabla_U \zeta = \mathcal{T}_U \zeta + h \nabla_U \zeta; \tag{6}$$

$$\nabla_{\zeta} U = \mathcal{A}_{\zeta} U + v \nabla_{\zeta} U; \tag{7}$$

$$\nabla_\zeta \eta = \mathcal{A}_\zeta \eta + h\nabla_\zeta \eta, \tag{8}$$

for any $\zeta, \eta \in \Gamma((ker\psi_*)^\perp)$, $U, W \in \Gamma(ker\psi_*)$. Also, if ζ is basic then $h\nabla_U \zeta = h\nabla_\zeta U = \mathcal{A}_\zeta U$.

We can easily see that \mathcal{T} is symmetric on the vertical distribution and \mathcal{A} is alternating on the horizontal distribution such that

$$\mathcal{T}_W U = \mathcal{T}_U W, \quad W, U \in \Gamma(ker\psi_*); \tag{9}$$

$$\mathcal{A}_Y V = -\mathcal{A}_V Y = \frac{1}{2}v[Y, V], \quad Y, V \in \Gamma((ker\psi_*)^\perp). \tag{10}$$

Also, it is easily seen that for any $\wp \in \Gamma(T\mathcal{B})$, \mathcal{T}_\wp and \mathcal{A}_\wp are skew-symmetric operators on $\Gamma(T\mathcal{B})$, such that

$$g_{\mathcal{B}}(\mathcal{T}_W U, \mathcal{X}) = -g_{\mathcal{B}}(\mathcal{T}_W \mathcal{X}, U) \tag{11}$$

$$g_{\mathcal{B}}(\mathcal{A}_W U, \mathcal{X}) = -g_{\mathcal{B}}(\mathcal{A}_W \mathcal{X}, U) \tag{12}$$

Definition 1. Let $\psi : (\mathcal{B}, g_{\mathcal{B}}, \mathcal{P}) \rightarrow (\tilde{\mathcal{B}}, g_{\tilde{\mathcal{B}}})$ be a pseudo-Riemannian submersion. Let us assume that the total manifold as an almost para-Hermitian manifold and base manifold as a pseudo-Riemannian manifold. Then, there exists a pseudo-Riemannian submersion ψ is an invariant pseudo-Riemannian submersion if the vertical distribution is invariant with respect to \mathcal{P} , i.e., $\mathcal{P}(ker\psi_*) = (ker\psi_*)$ [10].

Definition 2. Let $\psi : (\mathcal{B}, g_{\mathcal{B}}, \mathcal{P}) \rightarrow (\tilde{\mathcal{B}}, g_{\tilde{\mathcal{B}}})$ be a pseudo-Riemannian submersion. Let us assume that the total manifold as an almost para-Hermitian manifold and base manifold as a pseudo-Riemannian manifold. Then, there exists a pseudo-Riemannian submersion ψ such that $ker\psi_*$ is anti-invariant with respect to \mathcal{P} , i.e., $\mathcal{P}(ker\psi_*) \subseteq (ker\psi_*)^\perp$. So, we can say ψ is an anti-invariant pseudo-Riemannian submersion [8].

Definition 3. Let $\psi : (\mathcal{B}, g_{\mathcal{B}}, \mathcal{P}) \rightarrow (\tilde{\mathcal{B}}, g_{\tilde{\mathcal{B}}})$ be a pseudo-Riemannian submersion. Let us assume that the total manifold as an almost para-Hermitian manifold and base manifold as a pseudo-Riemannian manifold. Then, there exists a pseudo-Riemannian submersion ψ is a semi-invariant pseudo-Riemannian submersion if there is a distribution $\mathcal{D}_1 \subseteq ker\psi_*$, such that

$$ker\psi_* = \mathcal{D}_1 \oplus \mathcal{D}_2,$$

and

$$\mathcal{P}\mathcal{D}_1 = \mathcal{D}_1, \mathcal{P}\mathcal{D}_2 \subseteq (ker\psi_*)^\perp$$

where \mathcal{D}_2 is orthogonal complementary to \mathcal{D}_1 in $ker\psi_*$ [2].

We know that μ is the complementary orthogonal subbundle to $\mathcal{P}(ker\psi_*)$ in $(ker\psi_*)^\perp$.

Also we have;

$$(ker\psi_*)^\perp = \mathcal{P}\mathcal{D}_2 \oplus \mu.$$

From here we can say that μ is an invariant subbundle of $(ker\psi_*)^\perp$ with respect to the para-complex structure \mathcal{P} .

For any non-null vector field $U_2 \in (ker\psi_*)$, we get

$$\mathcal{P}U_2 = qU_2 + rU_2,$$

where qU_2 is vertical part and rU_2 is horizontal part.

If for non-null vector field $U_2 \in ker\psi_*$, the quotient $\frac{g_{\mathcal{B}}(qU_2, qU_2)}{g_{\mathcal{B}}(\mathcal{P}U_2, \mathcal{P}U_2)}$ is constant, i.e., it is independent of the choice of the point $\bar{q} \in \mathcal{B}$ and choice of the non-null vector field $U_2 \in \Gamma(ker\psi_*)$, we can say that ψ is a slant submersion. So, the angle is called the slant angle of the slant submersion ([10]).

Let $\psi : (\mathcal{B}, g_{\mathcal{B}}, \mathcal{P}) \rightarrow (\tilde{\mathcal{B}}, g_{\tilde{\mathcal{B}}})$ be a proper slant submersion. Let us assume that the total manifold as an almost para-Hermitian manifold and base manifold as a pseudo-Riemannian manifold. Then, we have;

type ~ 1 if for every space-like (time-like) vector field $U_2 \in \Gamma(ker\psi_*)$, qU_2 is time-like (space-like), and $\frac{\|qU_2\|}{\|\mathcal{P}U_2\|} > 1$,

type ~ 2 if for every space-like (time-like) vector field $U_2 \in \Gamma(ker\psi_*)$, qU_2 is time-like (space-like), and $\frac{\|qU_2\|}{\|\mathcal{P}U_2\|} < 1$ ([10]).

Theorem 1. ([10]) *Let $\psi : (\mathcal{B}, g_{\mathcal{B}}, \mathcal{P}) \rightarrow (\tilde{\mathcal{B}}, g_{\tilde{\mathcal{B}}})$ be a proper slant submersion. Let us assume that the total manifold as an almost para-Hermitian manifold and base manifold as a pseudo-Riemannian manifold. Then,*

(a) *ψ is slant submersion of type-1 if and only if for any space-like (time-like) vector field $U_1 \in ker\psi_*$, qU_1 is time-like (space-like) and there exists a constant $\mu \in (1, +\infty)$ such that*

$$q^2 = \mu Id.$$

where Id is the identity operator. If ψ is a proper slant submersion of type-1, then $\mu = \cosh^2 \varphi$, with $\varphi > 0$.

(b) *ψ is slant submersion of type-1 if and only if for any space-like (time-like) vector field $U_1 \in ker\psi_*$, qU_1 is time-like (space-like) and there exists a constant $\mu \in (0, 1)$ such that*

$$q^2 = \mu Id.$$

where Id is identity operator. If ψ is a proper slant submersion of type-1, then $\mu = \cos^2 \varphi$, with $0 < \varphi < \frac{\pi}{2}$.

Definition 4. *Let $(\mathcal{B}, g_{\mathcal{B}}, \mathcal{P})$ be an almost para-Hermitian manifold and $(\tilde{\mathcal{B}}, g_{\tilde{\mathcal{B}}})$ be a pseudo-Riemannian manifold. A pseudo-Riemannian submersion $\psi : (\mathcal{B}, g_{\mathcal{B}}, \mathcal{P}) \rightarrow (\tilde{\mathcal{B}}, g_{\tilde{\mathcal{B}}})$ is known a semi-slant submersion if there is a distribution $\mathcal{D}_1 \in ker\psi_*$ such*

that

$$\ker\psi_* = D_1 \oplus D_2, \quad \mathcal{P}(D_1) = D_1$$

and the angle φ is known the semi-slant angle of the submersion where D_2 is the orthogonal complement of D_1 in $\ker\psi_*$.

Definition 5. Let $(\mathcal{B}, g_{\mathcal{B}}, \mathcal{P})$ be an almost para-Hermitian manifold and $(\tilde{\mathcal{B}}, g_{\tilde{\mathcal{B}}})$ be a pseudo-Riemannian manifold. A pseudo-Riemannian submersion $\psi : (\mathcal{B}, g_{\mathcal{B}}, \mathcal{P}) \rightarrow (\tilde{\mathcal{B}}, g_{\tilde{\mathcal{B}}})$ is known a hemi-slant submersion if the vertical distribution $\ker\psi_*$ of ψ accepts two orthogonal complementary distribution D^φ and D^\perp , such that D^φ is slant and D^\perp is anti-invariant, i.e., we can show

$$\ker\psi_* = D^\varphi \oplus D^\perp$$

Therefore, the angle φ is known the hemi-slant angle of the submersion.

$\psi : \mathcal{B} \rightarrow \tilde{\mathcal{B}}$ is a differentiable map and $(\mathcal{B}, g_{\mathcal{B}})$ and $(\tilde{\mathcal{B}}, g_{\tilde{\mathcal{B}}})$ be pseudo-Riemannian manifolds. Then, the second fundamental form of ψ is described by

$$(\nabla\psi_*)(\zeta, V) = \nabla_\zeta^\psi \psi_* V - \psi_*(\nabla_\zeta V) \tag{13}$$

for $\zeta, V \in \Gamma(\mathcal{B})$. When $\text{trace}(\nabla\psi_*) = 0$, we can say that ψ is harmonic and ψ is a totally geodesic map when $(\nabla\psi_*)(\zeta, V) = 0$ for $\zeta, V \in \Gamma(T\mathcal{B})$ (14). Recall that ∇^ψ is the pullback connection.

3. QUASI HEMI-SLANT SUBMERSIONS

Definition 6. Let $(\mathcal{B}, g_{\mathcal{B}}, \mathcal{P})$ be an almost para-Hermitian manifold and $(\tilde{\mathcal{B}}, g_{\tilde{\mathcal{B}}})$ be a pseudo-Riemannian manifold. A pseudo-Riemannian submersion $\psi : (\mathcal{B}, g_{\mathcal{B}}, \mathcal{P}) \rightarrow (\tilde{\mathcal{B}}, g_{\tilde{\mathcal{B}}})$ is known a quasi hemi-slant submersion if there are three orthogonal distributions D , D^φ and D^\perp , such that

- $\ker\psi_* = D \oplus D^\varphi \oplus D^\perp$,
- $\mathcal{P}(D) = D$ i.e., D is invariant,
- the angle φ between $\mathcal{P}U$ and D^φ is constant. Also, the angle φ is known slant angle.
- D^\perp is anti-invariant, $\mathcal{P}D^\perp \subseteq (\ker\psi_*)^\perp$.

We can say that φ is quasi hemi-slant angle of \mathcal{B} .

Now, if we show the dimension of D , D^φ and D^\perp , by n_1, n_2 and n_3 , respectively, we can easily notice the following situations:

- (1) If $n_1 = 0$, then \mathcal{B} is a hemi-slant submersion
- (2) If $n_2 = 0$, then \mathcal{B} is a semi-invariant submersion
- (3) If $n_3 = 0$, then \mathcal{B} is a semi-slant submersion

If we observe the three items above , we can say that also they are all examples of quasi hemi-slant submersion.

Let $\psi : (\mathcal{B}, g_{\mathcal{B}}, \mathcal{P}) \rightarrow (\tilde{\mathcal{B}}, g_{\tilde{\mathcal{B}}})$ be a quasi hemi-slant submersion with type-1 or 2. Then, we obtain;

$$TB = \ker\psi_* \oplus (\ker\psi_*)^\perp \tag{14}$$

For any non-null vector field $U \in (\ker\psi_*)$, we get

$$U = KU + LU + RU, \tag{15}$$

where KU, LU and RU are projection morphisms of $\ker\psi_*$ onto D, D^φ and D^\perp , respectively.

We denote endomorphisms ϕ , the projection morphisms f on \mathcal{B} . For non-null vector field $U \in (\ker\psi_*)$, we have

$$\mathcal{P}U = \phi U + fU, \tag{16}$$

where $\phi U \in \ker\psi_*$ and $fU \in (\ker\psi_*)^\perp$.

From (15) and (16) we get:

$$\begin{aligned} \mathcal{P}U &= \mathcal{P}(KU) + \mathcal{P}(LU) + \mathcal{P}(RU), \\ &= \phi(KU) + f(KU) + \phi(LU) + f(LU) + \phi(RU) + f(RU). \end{aligned}$$

Since $\mathcal{P}(D) = (D)$ and $\mathcal{P}D^\perp \subseteq (\ker\psi_*)^\perp$ we obtain $f(KU) = 0$ and $\phi(RU) = 0$. Now, let us arrange the above equation

$$\mathcal{P}U = \phi(KU) + \phi(LU) + f(LU) + f(RU). \tag{17}$$

So, we have the following decomposition:

$$\mathcal{P}(\ker\psi_*) = D \oplus \phi D^\varphi \oplus fD^\varphi \oplus \mathcal{P}D^\perp. \tag{18}$$

Since, $fD^\varphi \subseteq (\ker\psi_*)^\perp$ and $\mathcal{P}D^\perp \subseteq (\ker\psi_*)^\perp$, we have;

$$(\ker\psi_*)^\perp = fD^\varphi \oplus \mathcal{P}D^\perp \oplus \mu$$

where μ is the orthogonal complementary distribution of $fD^\varphi \oplus \mathcal{P}D^\perp$ in $(\ker\psi_*)^\perp$.

In addition, for any non-null vector field $W \in (\ker\psi_*)^\perp$ is decomposed as

$$\mathcal{P}W = BW + CW \tag{19}$$

where $BW \in \Gamma(D^\varphi \oplus D^\perp)$ and $CW \in \Gamma(\mu)$.

Lemma 1. *Let $\psi : (\mathcal{B}, g_{\mathcal{B}}, \mathcal{P}) \rightarrow (\tilde{\mathcal{B}}, g_{\tilde{\mathcal{B}}})$ is a quasi hemi-slant submersion with type ~ 1 or 2 . Let us suppose the total manifold as an almost para-Hermitian manifold and base manifold as a pseudo-Riemannian manifold. Then, we obtain the following equations:*

- (a) $\phi D^\varphi = D^\varphi$ (b) $\phi D^\perp = \{0\}$
- (c) $BfD^\varphi = D^\varphi$ (d) $BfD^\perp = D^\perp$.

Proof. For any non-null vector field $W \in \Gamma(\mathcal{D}^\varphi)$, by (16), we have $\mathcal{P}W = \phi W + fW$. On the other hand, with the help of (18), $\mathcal{P}W \in \Gamma(\mathcal{D}^\varphi)$, i.e., $fW = 0$. Thus, we obtain $\phi\mathcal{D}^\varphi = \mathcal{D}^\varphi$. For any non-null vector field $U \in \Gamma(\mathcal{D}^\perp)$, by (16), we have $\mathcal{P}U = \phi U + fU$. Beside this, by using (18), $\mathcal{P}W \in (\ker\psi_*)^\perp$, i.e., $\phi U = 0$. Thus, we obtain $\phi\mathcal{D}^\perp = \{0\}$. To prove (c) and (d), the same method above can be used. \square

Lemma 2. *Let $\psi : (\mathcal{B}, g_{\mathcal{B}}, \mathcal{P}) \rightarrow (\tilde{\mathcal{B}}, g_{\tilde{\mathcal{B}}})$ is a quasi hemi-slant submersion with type ~ 1 or 2 . Let us suppose the total manifold as an almost para-Hermitian manifold and base manifold as a pseudo-Riemannian manifold. Then, we obtain the following equations:*

- (a) $\phi^2\mathcal{Z} + Bf\mathcal{Z} = \mathcal{Z}$ (b) $C^2U + fBU = U$
- (c) $\phi BU + BCU = \{0\}$ (d) $f\phi\mathcal{Z} + Cf\mathcal{Z} = \{0\}$ for all non-null vectors $\mathcal{Z} \in \Gamma(\ker\psi_*)$ and $U \in \Gamma(\ker\psi_*)^\perp$.

Proof. For any non-null vector field $\mathcal{Z} \in \Gamma(\ker\psi_*)$, by (1), we have $\mathcal{P}^2\mathcal{Z} = \mathcal{Z}$. Using (16) and (19), we have $\mathcal{Z} = \phi^2\mathcal{Z} + f\phi\mathcal{Z} + Bf\mathcal{Z} + Cf\mathcal{Z}$. If this equation is considered as decomposed into the vertical and horizontal parts, we obtain (a) and (d). (b) and (c) can be proved with the same method above. \square

Theorem 2. *Let $\psi : (\mathcal{B}, g_{\mathcal{B}}, \mathcal{P}) \rightarrow (\tilde{\mathcal{B}}, g_{\tilde{\mathcal{B}}})$ be a quasi hemi-slant submersion with type ~ 1 . Let us suppose the total manifold as an almost para-Hermitian manifold and base manifold as a pseudo-Riemannian manifold. In this case, ψ is quasi-hemi-slant submersion such that:*

- (a) $\phi^2\mathcal{Z} = \cosh^2\varphi\mathcal{Z}$
- (b) $g_{\mathcal{B}}(\phi\mathcal{Z}, \phi Y) = -\cosh^2\varphi g_{\mathcal{B}}(\mathcal{Z}, Y)$
- (c) $g_{\mathcal{B}}(f\mathcal{Z}, fY) = \sinh^2\varphi g_{\mathcal{B}}(\mathcal{Z}, Y)$

for any space-like(time-like) vector field $\mathcal{Z}, Y \in \Gamma(\mathcal{D}^\varphi)$.

Proof. (a) If ψ is a quasi hemi-slant submersion of type 1, for any space-like vector field $\mathcal{Z} \in \Gamma(\mathcal{D}^\varphi)$, $\phi\mathcal{Z}$ is timelike and by virtue of (1), $\mathcal{P}\mathcal{Z}$ is time-like. Then, there exists $\varphi > 0$ such that

$$\cosh\varphi = \frac{\|\phi\mathcal{Z}\|}{\|\mathcal{P}\mathcal{Z}\|} = \frac{\sqrt{-g_{\mathcal{B}}(\phi\mathcal{Z}, \phi\mathcal{Z})}}{\sqrt{-g_{\mathcal{B}}(\mathcal{P}\mathcal{Z}, \mathcal{P}\mathcal{Z})}}$$

Using the above equation, (1) and (16), we get:

$$g_{\mathcal{B}}(\phi^2\mathcal{Z}, \mathcal{Z}) = -g_{\mathcal{B}}(\phi\mathcal{Z}, \phi\mathcal{Z}) = -\cosh^2\varphi g_{\mathcal{B}}(\mathcal{P}\mathcal{Z}, \mathcal{P}\mathcal{Z}) = \cosh^2\varphi g_{\mathcal{B}}(\mathcal{P}^2\mathcal{Z}, \mathcal{Z}).$$

From the above equation and (1), we obtain $\phi^2\mathcal{Z} = \cosh^2\varphi\mathcal{Z}$.

Everything works in a similar way for any time-like vector field $\mathcal{Z} \in \Gamma(\mathcal{D}^\varphi)$.

(b) For any space-like(time-like) vector field $\mathcal{Z}, Y \in \Gamma(\mathcal{D}^\varphi)$, by virtue of (1), we get $g_{\mathcal{B}}(\mathcal{P}\mathcal{Z}, Y) = -g_{\mathcal{B}}(\mathcal{Z}, \mathcal{P}Y)$. On the other hand, with the help of (16), we get $g_{\mathcal{B}}(\phi\mathcal{Z} + f\mathcal{Z}, Y) = -g_{\mathcal{B}}(\mathcal{Z}, \phi Y + fY)$. If we arrange the last equation, we

obtain $g_{\mathcal{B}}(\phi Z, Y) = -g_{\mathcal{B}}(Z, \phi Y)$. Beside this, if $Y = \phi Y$ is accepted, we obtain $g_{\mathcal{B}}(\phi Z, \phi Y) = -g_{\mathcal{B}}(Z, \phi^2 Y)$. Using Theorem 2(a), we get $g_{\mathcal{B}}(\phi Z, \phi Y) = -\cosh^2 \varphi g_{\mathcal{B}}(Z, Y)$

To prove (c), the same method above can be used. □

Theorem 3. *Let $\psi : (\mathcal{B}, g_{\mathcal{B}}, \mathcal{P}) \rightarrow (\tilde{\mathcal{B}}, g_{\tilde{\mathcal{B}}})$ be a quasi hemi-slant submersion with type~2. Let us suppose the total manifold as an almost para-Hermitian manifold and base manifold as a pseudo-Riemannian manifold. In this case, ψ is quasi hemi-slant submersion such that:*

- (a) $\phi^2 Z = \cos^2 \varphi Z$
- (b) $g_{\mathcal{B}}(\phi Z, \phi Y) = -\cos^2 \varphi g_{\mathcal{B}}(Z, Y)$
- (c) $g_{\mathcal{B}}(f Z, f Y) = -\sin^2 \varphi g_{\mathcal{B}}(Z, Y)$

for any space-like(time-like) vector field $Z, Y \in \Gamma(\mathcal{D}^{\varphi})$.

Proof. This proof can be done using the techniques of the proof of Theorem 2.

Let's consider para-complex structure on R_n^{2n} :

$$P\left(\frac{\partial}{\partial y_{2i}}\right) = \frac{\partial}{\partial y_{2i-1}}, \quad P\left(\frac{\partial}{\partial y_{2i-1}}\right) = \frac{\partial}{\partial y_{2i}}, \quad g = (dy^1)^2 - (dy^2)^2 + (dy^3)^2 - \dots - (dy^{2n})^2$$

here $i \in \{1, \dots, n\}$. Also, $(y_1, y_2, \dots, y_{2n})$ denotes the cartesian coordinates over R_n^{2n} . □

We can easily present non-trivial examples of proper quasi hemi-slant pseudo-Riemannian submersions of type~1 and 2.

Example 1. *Let's determine map $\psi : R_5^{10} \rightarrow R_2^5$*

$$\psi(y_1, \dots, y_{10}) = (y_2 \sinh \beta + y_3 \cosh \beta, y_4, y_6, y_9, y_{10}),$$

So, ψ is a proper quasi hemi-slant pseudo-Riemannian submersion with type ~ 1 . By direct calculations, we have

$$D = \left\langle \frac{\partial}{\partial y_7}, \frac{\partial}{\partial y_8} \right\rangle$$

$$D^{\varphi} = \left\langle \cosh \beta \frac{\partial}{\partial y_2} - \sinh \beta \frac{\partial}{\partial y_3}, \frac{\partial}{\partial y_1} \right\rangle$$

$$D^{\perp} = \left\langle \frac{\partial}{\partial y_5} \right\rangle$$

with hemi-slant angle φ with $\phi^2 = \cosh^2 \beta I$.

Example 2. *Let's determine map $\psi : R_5^{10} \rightarrow R_2^5$*

$$\psi(y_1, \dots, y_{10}) = (y_1 \sin \alpha + y_3 \cos \alpha, y_2 \sin \beta + y_4 \cos \beta, y_6, y_9, y_{10})$$

So, ψ is a proper quasi hemi-slant pseudo-Riemannian submersion with type ~ 2 . By direct calculations, we get

$$D = \langle \frac{\partial}{\partial y_7}, \frac{\partial}{\partial y_8} \rangle$$

$$D^\varphi = \langle -\cos \alpha \frac{\partial}{\partial y_1} + \sin \alpha \frac{\partial}{\partial y_3}, -\cos \beta \frac{\partial}{\partial y_2} + \sin \beta \frac{\partial}{\partial y_4} \rangle$$

$$D^\perp = \langle \frac{\partial}{\partial y_5} \rangle \text{ with hemi-slant angle } \varphi \text{ with } \phi^2 = \cos^2(\alpha - \beta)I.$$

Lemma 3. Let $\psi : (\mathcal{B}, g_{\mathcal{B}}, \mathcal{P}) \rightarrow (\tilde{\mathcal{B}}, g_{\tilde{\mathcal{B}}})$ be a quasi hemi-slant pseudo-Riemannian submersion with type ~ 1 or 2 . Let us suppose the total manifold as a para-Kaehler manifold and base manifold as a pseudo-Riemannian manifold. So, we obtain the following equations.

$$\hat{\nabla}_U \phi W + \mathcal{T}_U fW = \phi \hat{\nabla}_U W + \mathcal{B} \mathcal{T}_U W \tag{20}$$

$$\mathcal{T}_U \phi W + \mathcal{H} \nabla_U fW = f \hat{\nabla}_U W + \mathcal{C} \mathcal{T}_U W \tag{21}$$

$$\mathcal{V} \nabla_{\mathcal{X}} \mathcal{B} \mathcal{Y} + \mathcal{A}_{\mathcal{X}} \mathcal{C} \mathcal{Y} = \phi \mathcal{A}_{\mathcal{X}} \mathcal{Y} + \mathcal{B} \mathcal{H} \nabla_{\mathcal{X}} \mathcal{Y} \tag{22}$$

$$\mathcal{A}_{\mathcal{X}} \mathcal{B} \mathcal{Y} + \mathcal{H} \nabla_{\mathcal{X}} \mathcal{C} \mathcal{Y} = f \mathcal{A}_{\mathcal{X}} \mathcal{Y} + \mathcal{C} \mathcal{H} \nabla_{\mathcal{X}} \mathcal{Y} \tag{23}$$

$$\hat{\nabla}_U \mathcal{B} \mathcal{X} + \mathcal{T}_U \mathcal{C} \mathcal{X} = \phi \mathcal{T}_U \mathcal{X} + \mathcal{B} \mathcal{H} \nabla_U \mathcal{X} \tag{24}$$

$$\mathcal{T}_U \mathcal{B} \mathcal{X} + \mathcal{H} \nabla_U \mathcal{C} \mathcal{X} = f \mathcal{T}_U \mathcal{X} + \mathcal{C} \mathcal{H} \nabla_U \mathcal{X}, \tag{25}$$

for any non-null vector fields $U, W \in \Gamma(\ker \psi_*)$ and $\mathcal{X}, \mathcal{Y} \in \Gamma(\ker \psi_*)^\perp$.

Proof. For any non-null vector fields $U, W \in \Gamma(\ker \psi_*)$, using (2), we get

$$\mathcal{P} \nabla_U W = \nabla_U \mathcal{P} W$$

Hence, using (5)~(6)~(16) and (19), we get

$$\mathcal{B} \mathcal{T}_U W + \mathcal{C} \mathcal{T}_U W + \phi \hat{\nabla}_U W + f \hat{\nabla}_U W = \mathcal{T}_U \phi W + \hat{\nabla}_U \phi W + \mathcal{T}_U fW + \mathcal{H} \nabla_U fW$$

Taking the vertical and horizontal parts of this equation, we get (20) and (21). The other assertions can be obtained by using (7)~(8)~(16) and (19).

Now we can show

$$(\nabla_U \phi)W = \hat{\nabla}_U \phi W - \phi \hat{\nabla}_U W$$

$$(\nabla_U f)W = \mathcal{H} \nabla_U fW - f \hat{\nabla}_U W,$$

$$(\nabla_X \mathcal{B})\zeta = \hat{\nabla}_X \mathcal{B} \zeta - \mathcal{B} \mathcal{H} \nabla_X \zeta$$

$$(\nabla_X \mathcal{C})\zeta = \mathcal{H} \nabla_X \mathcal{C} \zeta - \mathcal{C} \mathcal{H} \nabla_X \zeta$$

for any non-null vector fields $U, W \in \ker \psi_*$ and $X, \zeta \in (\ker \psi_*)^\perp$.

The above assertions can be obtained by using (20)~(21)~(22) and (23), respectively. \square

Lemma 4. *Let $\psi : (\mathcal{B}, g_{\mathcal{B}}, \mathcal{P}) \rightarrow (\tilde{\mathcal{B}}, g_{\tilde{\mathcal{B}}})$ be a quasi-hemi-slant pseudo-Riemannian submersion with type ~ 1 and type ~ 2 . Let us suppose the total manifold as a para-Kaehler manifold and base manifold as a pseudo-Riemannian manifold. So, we obtain the following equations.*

$$(\nabla_U \phi)W = \mathcal{B}\mathcal{T}_U W - \mathcal{T}_U fW \tag{26}$$

$$(\nabla_U f)W = \mathcal{C}\mathcal{T}_U W - \mathcal{T}_U \phi W \tag{27}$$

$$(\nabla_X B)\zeta = \phi \mathcal{A}_X \zeta - \mathcal{A}_X \mathcal{B}\zeta \tag{28}$$

$$(\nabla_X C)\zeta = f \mathcal{A}_X \zeta - \mathcal{A}_X \mathcal{C}\zeta \tag{29}$$

for any non-null vector fields $U, W \in \ker \psi_*$ and $X, \zeta \in (\ker \psi_*)^\perp$.

Proof. The proof is simple.

If ϕ and f are parallel with respect to ∇ on \mathcal{B} , from (26) and (27), we have

$$\mathcal{B}\mathcal{T}_U W = \mathcal{T}_U fW \text{ and } \mathcal{C}\mathcal{T}_U W = \mathcal{T}_U \phi W \text{ for any } U, W \in \Gamma(T\mathcal{B}). \quad \square$$

Theorem 4. *Let $\psi : (\mathcal{B}, g_{\mathcal{B}}, \mathcal{P}) \rightarrow (\tilde{\mathcal{B}}, g_{\tilde{\mathcal{B}}})$ be a proper quasi hemi-slant pseudo-Riemannian submersion with type ~ 1 or 2 from a para-Kaehler manifold to a pseudo-Riemannian manifold. The invariant distribution \mathcal{D} is integrable if and only if*

$$g_{\mathcal{B}}(\mathcal{T}_W \phi U - \mathcal{T}_U \phi W, fL\zeta + fR\zeta) = g_{\mathcal{B}}(\mathcal{V}\nabla_U \phi W - \mathcal{V}\nabla_W \phi U, \phi L\zeta) \tag{30}$$

for any non-null vector fields $U, W \in \Gamma(\mathcal{D})$ and $\zeta \in \Gamma(\mathcal{D}^\varphi \oplus \mathcal{D}^\perp)$.

Proof. For any non-null vector fields $U, W \in \Gamma(\mathcal{D})$ and $\zeta \in \Gamma(\mathcal{D}^\varphi \oplus \mathcal{D}^\perp)$. Then using (1), (2), (5) and (16) obtained:

$$\begin{aligned} g_{\mathcal{B}}([U, W], \zeta) &= -g_{\mathcal{B}}(\nabla_U \mathcal{P}W, \mathcal{P}\zeta) + g_{\mathcal{B}}(\nabla_W \mathcal{P}U, \mathcal{P}\zeta) \\ &= -g_{\mathcal{B}}(\nabla_U \phi W, \mathcal{P}\zeta) + g_{\mathcal{B}}(\nabla_W \phi U, \mathcal{P}\zeta) \\ &= g_{\mathcal{B}}(\mathcal{T}_W \phi U - \mathcal{T}_U \phi W, fL\zeta + fR\zeta) \\ &+ g_{\mathcal{B}}(\mathcal{V}\nabla_W \phi U - \mathcal{V}\nabla_U \phi W, \phi L\zeta). \end{aligned} \tag{31}$$

So, the proof is complete. □

Theorem 5. *Let $\psi : (\mathcal{B}, g_{\mathcal{B}}, \mathcal{P}) \rightarrow (\tilde{\mathcal{B}}, g_{\tilde{\mathcal{B}}})$ be a proper quasi hemi-slant pseudo-Riemannian submersion with type ~ 1 or 2 from a para-Kaehler manifold to a pseudo-Riemannian manifold. The slant distribution \mathcal{D}^φ is integrable if and only if*

$$\begin{aligned} g_{\mathcal{B}}(\mathcal{T}_U f\phi W - \mathcal{T}_W f\phi U, \mathcal{X}) &= g_{\mathcal{B}}(\mathcal{T}_U fW - \mathcal{T}_W fU, \phi K\mathcal{X}) \\ &+ g_{\mathcal{B}}(\mathcal{H}\nabla_U fW - \mathcal{H}\nabla_W fU, fR\mathcal{X}) \end{aligned} \tag{32}$$

for any non-null vector fields $U, W \in \Gamma(\mathcal{D}^\varphi)$ and $\mathcal{X} \in \Gamma(\mathcal{D} \oplus \mathcal{D}^\perp)$.

Proof. We only give its proof ψ is type~1. For any non-null vector fields $U, W \in \Gamma(\mathcal{D}^\varphi)$ and $\mathcal{X} \in \Gamma(\mathcal{D} \oplus \mathcal{D}^\perp)$. Then using (1), (2), (6), (16) and Theorem 2(a), we get:

$$\begin{aligned} g_{\mathcal{B}}([U, W], \mathcal{X}) &= -g_{\mathcal{B}}(\nabla_U \mathcal{P}W, \mathcal{P}\mathcal{X}) + g_{\mathcal{B}}(\nabla_W \mathcal{P}U, \mathcal{P}\mathcal{X}) \\ &= -g_{\mathcal{B}}(\nabla_U \phi W, \mathcal{P}\mathcal{X}) - g_{\mathcal{B}}(\nabla_U fW, \mathcal{P}\mathcal{X}) \\ &+ g_{\mathcal{B}}(\nabla_W \phi U, \mathcal{P}\mathcal{X}) + g_{\mathcal{B}}(\nabla_W fU, \mathcal{P}\mathcal{X}) \\ &= -\cosh^2 \varphi g_{\mathcal{B}}([U, W], \mathcal{X}) \\ &- g_{\mathcal{B}}(\mathcal{T}_U f\phi W - \mathcal{T}_W f\phi U, \mathcal{X}) \\ &+ g_{\mathcal{B}}(\mathcal{T}_U fW + \mathcal{H}\nabla_U fW, \phi K\mathcal{X} + fR\mathcal{X}) \\ &- g_{\mathcal{B}}(\mathcal{T}_W fU + \mathcal{H}\nabla_W fU, \phi K\mathcal{X} + fR\mathcal{X}). \end{aligned}$$

Then, we have;

$$\begin{aligned} (1 + \cosh^2 \varphi)g_{\mathcal{B}}([U, W], \mathcal{X}) &= g_{\mathcal{B}}(\mathcal{T}_U fW - \mathcal{T}_W fU, \phi K\mathcal{X}) \\ &+ g_{\mathcal{B}}(\mathcal{H}\nabla_U fW - \mathcal{H}\nabla_W fU, fR\mathcal{X}) \\ &- g_{\mathcal{B}}(\mathcal{T}_U f\phi W - \mathcal{T}_W f\phi U, \mathcal{X}) \end{aligned}$$

which completes proof. □

Corollary 1. *Let $\psi : (\mathcal{B}, g_{\mathcal{B}}, \mathcal{P}) \rightarrow (\tilde{\mathcal{B}}, g_{\tilde{\mathcal{B}}})$ be a proper quasi hemi-slant pseudo-Riemannian submersion with type~1 or 2 from a para-Kaehler manifold to a pseudo-Riemannian manifold. If for any non-null vector fields $U, W \in \Gamma(\mathcal{D}^\varphi)$ and $\mathcal{X} \in \Gamma(\mathcal{D} \oplus \mathcal{D}^\perp)$*

$$\begin{aligned} \mathcal{H}\nabla_U fW - \mathcal{H}\nabla_W fU &\in \Gamma(f\mathcal{D}^\varphi \oplus \mu) \\ \mathcal{T}_U f\phi W - \mathcal{T}_W f\phi U &\in \Gamma(\mathcal{D}^\varphi) \\ \mathcal{T}_U fW - \mathcal{T}_W fU &\in \Gamma(\mathcal{D}^\perp \oplus \mathcal{D}^\varphi) \end{aligned}$$

Theorem 6. *Let $\psi : (\mathcal{B}, g_{\mathcal{B}}, \mathcal{P}) \rightarrow (\tilde{\mathcal{B}}, g_{\tilde{\mathcal{B}}})$ be a proper quasi hemi-slant pseudo-Riemannian submersion with type~1 or 2 from a para-Kaehler manifold to a pseudo-Riemannian manifold. The slant distribution \mathcal{D}^\perp is integrable.*

Proof. The proof of Theorem 6 is similar to those given in (28). Therefore we skip its proof. □

Corollary 2. *Let $\psi : (\mathcal{B}, g_{\mathcal{B}}, \mathcal{P}) \rightarrow (\tilde{\mathcal{B}}, g_{\tilde{\mathcal{B}}})$ be a proper quasi hemi-slant pseudo-Riemannian submersion with type~1 or 2 from a para-Kaehler manifold to a pseudo-Riemannian manifold. In this case, for any non-null vector fields $U, W \in \Gamma(\mathcal{D}^\perp)$ we get*

$$\mathcal{T}_U \mathcal{P}W = \mathcal{T}_W \mathcal{P}U. \tag{33}$$

Proof. Using Lemma 1(b), from (20), we obtain

$$\mathcal{T}_U fW = \phi(\hat{\nabla}_U W) + \mathcal{B}\mathcal{T}_W U \tag{34}$$

If we take $U = W$ in (34) and subtracting it from (34), we get

$$\mathcal{T}_U fW - \mathcal{T}_W fU = \phi[U, W] \tag{35}$$

By Theorem 6 and Lemma 1(b), we get $\phi[U, W] = 0$ from (35). This gives (33), since $fU = PU$ for every non-null vector field $U \in \mathcal{D}^\perp$. \square

Theorem 7. *Let $\psi : (\mathcal{B}, g_{\mathcal{B}}, \mathcal{P}) \rightarrow (\tilde{\mathcal{B}}, g_{\tilde{\mathcal{B}}})$ be a proper quasi hemi-slant pseudo-Riemannian submersion with type~1 from a para-Kaehler manifold to a pseudo-Riemannian manifold. In this case, the horizontal distribution $(\ker\psi_*)^\perp$ describes a totally geodesic foliation on \mathcal{B} if and only if*

$$g_{\mathcal{B}}(\mathcal{A}_{\mathcal{W}}\mathcal{Z}, K\zeta + \cosh^2 \varphi L\zeta) = -g_{\mathcal{B}}(\mathcal{H}\nabla_{\mathcal{W}}\mathcal{Z}, f\phi K\zeta + f\phi L\zeta) + g_{\mathcal{B}}(\mathcal{A}_{\mathcal{W}}B\mathcal{Z} + \mathcal{H}\nabla_{\mathcal{W}}C\mathcal{Z}, f\zeta) \tag{36}$$

for any non-null vector fields $\mathcal{W}, \mathcal{Z} \in (\ker\psi_*)^\perp$ and $\zeta \in (\ker\psi_*)$.

Proof. For any non-null vectors $\mathcal{W}, \mathcal{Z} \in (\ker\psi_*)^\perp$ and $\zeta \in (\ker\psi_*)$, we get:

$$g_{\mathcal{B}}(\nabla_{\mathcal{W}}\mathcal{Z}, \zeta) = g_{\mathcal{B}}(\nabla_{\mathcal{W}}\mathcal{Z}, K\zeta + L\zeta + R\zeta)$$

Then using (1), (2), (7), (8), (16), (17) and Theorem 2(a), we get

$$\begin{aligned} g_{\mathcal{B}}(\nabla_{\mathcal{W}}\mathcal{Z}, \zeta) &= -g_{\mathcal{B}}(\nabla_{\mathcal{W}}\mathcal{P}\mathcal{Z}, \mathcal{P}K\zeta) - g_{\mathcal{B}}(\nabla_{\mathcal{W}}\mathcal{P}\mathcal{Z}, \mathcal{P}L\zeta) \\ &\quad - g_{\mathcal{B}}(\nabla_{\mathcal{W}}\mathcal{P}\mathcal{Z}, \mathcal{P}R\zeta) \\ &= g_{\mathcal{B}}(\mathcal{A}_{\mathcal{W}}\mathcal{Z}, K\zeta + BfK\zeta + \cosh^2 \varphi L\zeta) \\ &\quad + g_{\mathcal{B}}(\mathcal{H}\nabla_{\mathcal{W}}\mathcal{Z}, f\phi K\zeta + f\phi L\zeta) \\ &\quad - g_{\mathcal{B}}(\mathcal{A}_{\mathcal{W}}B\mathcal{Z} + \mathcal{H}\nabla_{\mathcal{W}}C\mathcal{Z}, fK\zeta + fL\zeta + fR\zeta). \end{aligned}$$

Since $fK\zeta = 0$ and $fK\zeta + fL\zeta + fR\zeta = f\zeta$, we obtain;

$$\begin{aligned} g_{\mathcal{B}}(\nabla_{\mathcal{W}}\mathcal{Z}, \zeta) &= g_{\mathcal{B}}(\mathcal{A}_{\mathcal{W}}\mathcal{Z}, K\zeta + \cosh^2 \varphi L\zeta) \\ &\quad + g_{\mathcal{B}}(\mathcal{H}\nabla_{\mathcal{W}}\mathcal{Z}, f\phi K\zeta + f\phi L\zeta) \\ &\quad - g_{\mathcal{B}}(\mathcal{A}_{\mathcal{W}}B\mathcal{Z} + \mathcal{H}\nabla_{\mathcal{W}}C\mathcal{Z}, f\zeta) \end{aligned}$$

which gives proof. \square

Similarly, the following conclusion is obtained.

Theorem 8. *Let $\psi : (\mathcal{B}, g_{\mathcal{B}}, \mathcal{P}) \rightarrow (\tilde{\mathcal{B}}, g_{\tilde{\mathcal{B}}})$ be a proper quasi hemi-slant pseudo-Riemannian submersion with type~1 from a para-Kaehler manifold to a pseudo-Riemannian manifold. In this case, the vertical distribution $(\ker\psi_*)$ describes a totally geodesic foliation on \mathcal{B} if and only if*

$$g_{\mathcal{B}}(\mathcal{T}_U\zeta + \cosh^2 \varphi \mathcal{T}_U L\zeta, \mathcal{W}) = g_{\mathcal{B}}(\mathcal{H}\nabla_U f\phi K\zeta + \mathcal{H}\nabla_U f\phi L\zeta, \mathcal{W}) + g_{\mathcal{B}}(\mathcal{T}_U f\zeta, B\mathcal{W}) + g_{\mathcal{B}}(\mathcal{H}\nabla_U f\zeta, C\mathcal{W}). \tag{37}$$

for any non-null vector fields $U, \zeta \in \Gamma(\ker\psi_*)$ and $\mathcal{W} \in \Gamma(\ker\psi_*)^\perp$.

Using Theorem 7 and Theorem 8, we get the Theorem 9.

Theorem 9. Let $\psi : (\mathcal{B}, g_{\mathcal{B}}, \mathcal{P}) \rightarrow (\tilde{\mathcal{B}}, g_{\tilde{\mathcal{B}}})$ be a proper quasi hemi-slant pseudo-Riemannian submersion with type~1 from a para-Kaehler manifold to a pseudo-Riemannian manifold. In this case, the total space is a locally product $\mathcal{B}_{ker\psi_*} \times \mathcal{B}_{ker\psi_*^\perp}$ where $\mathcal{B}_{ker\psi_*}$ and $\mathcal{B}_{ker\psi_*^\perp}$ are leaves of $(ker\psi_*)$ and $(ker\psi_*)^\perp$, respectively, if and only if (36) and (37) are satisfied.

Theorem 10. Let $\psi : (\mathcal{B}, g_{\mathcal{B}}, \mathcal{P}) \rightarrow (\tilde{\mathcal{B}}, g_{\tilde{\mathcal{B}}})$ be a proper quasi hemi-slant pseudo-Riemannian submersion with type~1 or 2 from a para-Kaehler manifold to a pseudo-Riemannian manifold. In this case, the invariant distribution \mathcal{D} describes a totally geodesic foliation on \mathcal{B} if and only if

$$g_{\mathcal{B}}(\mathcal{T}_{\mathcal{W}}\phi\mathcal{Z}, fLY + fRY) = -g_{\mathcal{B}}(\mathcal{V}\nabla_{\mathcal{W}}\phi\mathcal{Z}, \phi LY) \tag{38}$$

and

$$g_{\mathcal{B}}(\mathcal{T}_{\mathcal{W}}\phi\mathcal{Z}, C\xi) = -g_{\mathcal{B}}(\mathcal{V}\nabla_{\mathcal{W}}\phi\mathcal{Z}, B\xi) \tag{39}$$

Proof. For all non-null vectors $\mathcal{W}, \mathcal{Z} \in \Gamma(\mathcal{D})$ and $Y \in \Gamma(\mathcal{D}^{\varphi_1} \oplus \mathcal{D}^{\varphi_2})$ and $\xi \in \Gamma(ker\psi_*)^\perp$. Then using (1), (2), (5), (16) and $f\mathcal{Z} = 0$, we get:

$$\begin{aligned} g_{\mathcal{B}}(\nabla_{\mathcal{W}}\mathcal{Z}, Y) &= -g_{\mathcal{B}}(\nabla_{\mathcal{W}}\mathcal{P}\mathcal{Z}, \mathcal{P}Y) \\ &= -g_{\mathcal{B}}(\nabla_{\mathcal{W}}\mathcal{P}\mathcal{Z}, \mathcal{P}LY + \mathcal{P}RY) \\ &= -g_{\mathcal{B}}(\mathcal{T}_{\mathcal{W}}\phi\mathcal{Z}, fLY + fRY) - g_{\mathcal{B}}(\mathcal{V}\nabla_{\mathcal{W}}\phi\mathcal{Z}, \phi LY) \end{aligned}$$

Then, again using (1), (2), (5), (16), (19) and $f\mathcal{Z} = 0$, we get:

$$\begin{aligned} g_{\mathcal{B}}(\nabla_{\mathcal{W}}\mathcal{Z}, \xi) &= -g_{\mathcal{B}}(\nabla_{\mathcal{W}}\mathcal{P}\mathcal{Z}, \mathcal{P}\xi) \\ &= -g_{\mathcal{B}}(\nabla_{\mathcal{W}}\phi\mathcal{Z}, B\xi + C\xi) \\ &= -g_{\mathcal{B}}(\mathcal{T}_{\mathcal{W}}\phi\mathcal{Z}, C\xi) - g_{\mathcal{B}}(\mathcal{V}\nabla_{\mathcal{W}}\phi\mathcal{Z}, B\xi). \end{aligned}$$

So, the proof is complete. □

Theorem 11. Let $\psi : (\mathcal{B}, g_{\mathcal{B}}, \mathcal{P}) \rightarrow (\tilde{\mathcal{B}}, g_{\tilde{\mathcal{B}}})$ be a proper quasi hemi-slant pseudo-Riemannian submersion with type~1 or 2 from a para-Kaehler manifold to a pseudo-Riemannian manifold. In this case, the slant distribution \mathcal{D}^φ describes a totally geodesic foliation on \mathcal{B} if and only if

$$g_{\mathcal{B}}(\mathcal{T}_U f\phi V, Y) = g_{\mathcal{B}}(\mathcal{T}_U fV, \phi KY) + g_{\mathcal{B}}(\mathcal{H}\nabla_U fV, fRY) \tag{40}$$

and

$$g_{\mathcal{B}}(\mathcal{H}\nabla_U f\phi V, \xi) = g_{\mathcal{B}}(\mathcal{H}\nabla_U fV, C\xi) + g_{\mathcal{B}}(\mathcal{T}_U fV, B\xi) \tag{41}$$

for any non-null vector fields $U, V \in \Gamma(\mathcal{D}^\varphi)$ and $Y \in \Gamma(\mathcal{D} \oplus \mathcal{D}^\perp)$ and $\xi \in \Gamma(ker\psi_*)^\perp$.

Proof. We will show it when ψ is type~1. For all non-null vectors $U, V \in \Gamma(\mathcal{D}^\varphi)$ and $Y \in \Gamma(\mathcal{D} \oplus \mathcal{D}^\perp)$ and $\xi \in \Gamma(ker\psi_*)^\perp$. Then using (1), (2), (6), (16) and Theorem 2(a), we get:

$$\begin{aligned} g_{\mathcal{B}}(\nabla_U V, Y) &= -g_{\mathcal{B}}(\nabla_U \phi V, \mathcal{P}Y) - g_{\mathcal{B}}(\nabla_U fV, \mathcal{P}Y) \\ &= \cosh^2 \varphi g_{\mathcal{B}}(\nabla_U V, Y) + g_{\mathcal{B}}(\mathcal{T}_U f\phi V, Y) \end{aligned}$$

$$- g_{\mathcal{B}}(\mathcal{T}_U fV, \phi KY) - g_{\mathcal{B}}(\mathcal{H}\nabla_U fV, fRY).$$

Hence we obtain;

$$\begin{aligned} -\sinh^2 \varphi_1 g_{\mathcal{B}}(\nabla_U V, Y) &= g_{\mathcal{B}}(\mathcal{T}_U f\phi V, Y) - g_{\mathcal{B}}(\mathcal{T}_U fV, \phi KY) \\ &\quad - g_{\mathcal{B}}(\mathcal{H}\nabla_U fV, fRY). \end{aligned}$$

Similarly, using (1), (2), (6), (16), (19) and Theorem 3.4(a), we get:

$$\begin{aligned} g_{\mathcal{B}}(\nabla_U V, \xi) &= -g_{\mathcal{B}}(\nabla_U \phi V, \mathcal{P}\xi) - g_{\mathcal{B}}(\nabla_U fV, \mathcal{P}\xi) \\ &= \cosh^2 \varphi_1 g_{\mathcal{B}}(\nabla_U V, \xi) + g_{\mathcal{B}}(\mathcal{H}\nabla_U f\phi V, \xi) \\ &\quad - g_{\mathcal{B}}(\mathcal{H}\nabla_U fV, C\xi) - g_{\mathcal{B}}(\mathcal{T}_U fV, B\xi). \end{aligned}$$

Hence, arrive at

$$\begin{aligned} -\sinh^2 \varphi_1 g_{\mathcal{B}}(\nabla_U V, \xi) &= g_{\mathcal{B}}(\mathcal{H}\nabla_U f\phi V, \xi) - g_{\mathcal{B}}(\mathcal{H}\nabla_U fV, C\xi) \\ &\quad - g_{\mathcal{B}}(\mathcal{T}_U fV, B\xi) \end{aligned}$$

which gives proof. □

Theorem 12. *Let $\psi : (\mathcal{B}, g_{\mathcal{B}}, \mathcal{P}) \rightarrow (\tilde{\mathcal{B}}, g_{\tilde{\mathcal{B}}})$ be a proper quasi-hemi-slant pseudo-Riemannian submersion with type~1 or 2 from a para-Kaehler manifold to a pseudo-Riemannian manifold. In this case, the anti-invariant distribution \mathcal{D}^\perp describes a totally geodesic foliation on \mathcal{B} if and only if*

$$g_{\mathcal{B}}(\mathcal{A}_U \zeta, f\phi KV + f\phi LV) = -g_{\mathcal{B}}(\mathcal{H}\nabla_U f\zeta, fV) \tag{42}$$

and

$$g_{\mathcal{B}}(\mathcal{A}_U \mathcal{P}\zeta, B\xi) = -g_{\mathcal{B}}(\mathcal{H}\nabla_U \mathcal{P}\zeta, C\xi) \tag{43}$$

for any non-null vector fields $U, \zeta \in \Gamma(\mathcal{D}^\perp)$ and $V \in \Gamma(\mathcal{D} \oplus \mathcal{D}^\varphi)$ and $\xi \in \Gamma(\ker \psi_*)^\perp$.

Proof. We will show it when ψ is type~1. For all non-null vectors $U, \zeta \in \Gamma(\mathcal{D}^\perp)$ and $KV + LV \in \Gamma(\mathcal{D} \oplus \mathcal{D}^\varphi)$ and $\xi \in \Gamma(\ker \psi_*)^\perp$. Then using (1), (16), (19) and Theorem 2(a), we get:

$$\begin{aligned} g_{\mathcal{B}}(\nabla_U \zeta, V) &= -g_{\mathcal{B}}(\nabla_U \mathcal{P}\zeta, \mathcal{P}V) = -g_{\mathcal{B}}(\nabla_U \mathcal{P}\zeta, \phi V) - g_{\mathcal{B}}(\nabla_U \mathcal{P}\zeta, fV) \\ &= \cosh^2 \varphi g_{\mathcal{B}}(\nabla_U \zeta, LV) - g_{\mathcal{B}}(\nabla_U \zeta, KV) + g_{\mathcal{B}}(\nabla_U \zeta, BfKV) \\ &\quad - g_{\mathcal{B}}(\nabla_U \zeta, f\phi KV) - g_{\mathcal{B}}(\nabla_U \zeta, f\phi LV) \\ &\quad - g_{\mathcal{B}}(\nabla_U \mathcal{P}\zeta, fV). \end{aligned} \tag{44}$$

We know that $g_{\mathcal{B}}(\nabla_U \zeta, V) = g_{\mathcal{B}}(\nabla_U \zeta, KV) + g_{\mathcal{B}}(\nabla_U \zeta, LV)$ and using (8) and (16) from equation (44), we arrive at;

$$\begin{aligned} g_{\mathcal{B}}(\nabla_U \zeta, -\sinh^2 \varphi LV - BfKV) &= -g_{\mathcal{B}}(\mathcal{A}_U \zeta, f\phi KV + f\phi LV) \\ &\quad - g_{\mathcal{B}}(\mathcal{H}\nabla_U f\zeta, fV) \end{aligned} \tag{45}$$

which gives (42). Similarly, using (8) and (19), we get:

$$g_{\mathcal{B}}(\nabla_U \zeta, \xi) = -g_{\mathcal{B}}(\nabla_U \mathcal{P}\zeta, \mathcal{P}\xi) = -g_{\mathcal{B}}(\mathcal{A}_U \mathcal{P}\zeta, B\xi) - g_{\mathcal{B}}(\mathcal{H}\nabla_U \mathcal{P}\zeta, C\xi) \tag{46}$$

which gives (43). □

Now, from Theorem 10, Theorem 11 and Theorem 12 we arrive at the Theorem 13. This is decomposition theorem for the fiber:

Theorem 13. *Let $\psi : (\mathcal{B}, g_{\mathcal{B}}, \mathcal{P}) \rightarrow (\tilde{\mathcal{B}}, g_{\tilde{\mathcal{B}}})$ be a proper quasi-hemi-slant pseudo-Riemannian submersion with type ~ 1 or 2 from a para-Kaehler manifold to a pseudo-Riemannian manifold. In this case, the fibers of ψ are locally product $\mathcal{B}_{\mathcal{D}} \times \mathcal{B}_{\mathcal{D}^{\varphi}} \times \mathcal{B}_{\mathcal{D}^{\perp}}$ are leaves of \mathcal{D} , \mathcal{D}^{φ} and \mathcal{D}^{\perp} , respectively, if and only if the conditions (38), (39), (40), (41), (42) and (43) hold.*

Theorem 14. *Let $\psi : (\mathcal{B}, g_{\mathcal{B}}, \mathcal{P}) \rightarrow (\tilde{\mathcal{B}}, g_{\tilde{\mathcal{B}}})$ be a proper quasi hemi-slant pseudo-Riemannian submersion with type ~ 1 from a para-Kaehler manifold to a pseudo-Riemannian manifold. In this case, ψ is a totally geodesic map on \mathcal{B} if and only if*

$$\begin{aligned} &g_{\mathcal{B}}(\cosh^2 \varphi \nabla_U LW + \mathcal{H} \nabla_U f \phi LW, Y) \\ &= g_{\mathcal{B}}(\mathcal{V} \nabla_U \mathcal{P}KW + \mathcal{T}_U f LW + \mathcal{T}_U f RW, \mathcal{P}Y) \\ &+ g_{\mathcal{B}}(\mathcal{T}_U \mathcal{P}KW + \mathcal{H} \nabla_U f LW + \mathcal{H} \nabla_U f RW, CY) \end{aligned} \tag{47}$$

and

$$\begin{aligned} &g_{\mathcal{B}}(\cosh^2 \varphi \nabla_Y LU + \mathcal{H} \nabla_Y f \phi LU, Z) \\ &= g_{\mathcal{B}}(\mathcal{V} \nabla_Y \mathcal{P}KU + \mathcal{A}_Y f LU + \mathcal{A}_Y \mathcal{P}RU, BZ) \\ &g_{\mathcal{B}}(\mathcal{A}_Y \mathcal{P}KU + \mathcal{H} \nabla_Y f LU + \mathcal{H} \nabla_Y f RU, CZ) \end{aligned} \tag{48}$$

For any non-null vector fields $U, W \in \Gamma(\ker \psi_*)$ and $Y, Z \in \Gamma(\ker \psi_*)^{\perp}$.

Proof. For any non-null vector fields $U, W \in \Gamma(\ker \psi_*)$ and $Y, Z \in \Gamma(\ker \psi_*)^{\perp}$. Then, using (1), (2), (5), (16), (19) and Theorem 2(a) we get:

$$\begin{aligned} g_{\mathcal{B}}(\nabla_U W, Y) &= -g_{\mathcal{B}}(\nabla_U \mathcal{P}W, \mathcal{P}Y) \\ &= -g_{\mathcal{B}}(\nabla_U \mathcal{P}KW, \mathcal{P}Y) - g_{\mathcal{B}}(\nabla_U \mathcal{P}LW, \mathcal{P}Y) \\ &\quad - g_{\mathcal{B}}(\nabla_U \mathcal{P}RW, \mathcal{P}Y) \\ &= -g_{\mathcal{B}}(\mathcal{V} \nabla_U \mathcal{P}KW + \mathcal{T}_U f LW + \mathcal{T}_U f RW, \mathcal{P}Y) \\ &\quad + g_{\mathcal{B}}(\cosh^2 \varphi \nabla_U LW + \mathcal{H} \nabla_U f \phi LW, Y) \\ &\quad - g_{\mathcal{B}}(\mathcal{T}_U \mathcal{P}KW + \mathcal{H} \nabla_U f LW + \mathcal{H} \nabla_U f RW, CY) \end{aligned}$$

Then, again using (1), (7), (8), (16), (19) and Theorem 2(a), we get:

$$\begin{aligned} g_{\mathcal{B}}(\nabla_Y U, Z) &= -g_{\mathcal{B}}(\nabla_Y \mathcal{P}U, \mathcal{P}Z) \\ &= -g_{\mathcal{B}}(\nabla_Y \mathcal{P}KU, \mathcal{P}Z) - g_{\mathcal{B}}(\nabla_Y \mathcal{P}LU, \mathcal{P}Z) \\ &\quad - g_{\mathcal{B}}(\nabla_Y \mathcal{P}RU, \mathcal{P}Z) \\ &= -g_{\mathcal{B}}(\mathcal{V} \nabla_Y \mathcal{P}KU + \mathcal{A}_Y f LU + \mathcal{A}_Y f RU, BZ) \\ &\quad - g_{\mathcal{B}}(\cosh^2 \varphi \nabla_Y LU + \mathcal{H} \nabla_Y f \phi LU, Z) \end{aligned}$$

$$- g_{\mathcal{B}}(\mathcal{A}_Y \mathcal{P} K U + \mathcal{H} \nabla_Y f L U + \mathcal{H} \nabla_Y f R U, C Z).$$

Therefore, a pseudo-Riemannian submersion ψ is said to be totally umbilical if

$$\mathcal{T}_{U_1} U_2 = g(U_1, U_2) H, \quad (49)$$

here H is the mean curvature vector field of the fibre in \mathcal{B} for all non-null vector fields $U_1, U_2 \in \Gamma(\ker \psi_*)$. The fibre is said to be minimal if $H = 0$ ([4]). \square

Theorem 15. *Let $\psi : (\mathcal{B}, g_{\mathcal{B}}, \mathcal{P}) \rightarrow (\tilde{\mathcal{B}}, g_{\tilde{\mathcal{B}}})$ be a proper quasi-hemi-slant pseudo-Riemannian submersion from a para-Kaehler manifold to a pseudo-Riemannian manifold with totally umbilical fibers. In that case, either the anti-invariant distribution $\dim(D^{\perp}) = 1$ or the mean curvature vector field H of any fiber $\psi^{-1}(\bar{q})$, $\bar{q} \in \mathcal{B}$ is perpendicular to PD^{\perp} . Eventually, if ϕ is parallel, then $H \in \Gamma(\mu)$. Moreover, if f is parallel, then $\mathcal{T} \equiv 0$.*

Proof. The proof is obtained by simple calculations. \square

Author Contribution Statements The authors jointly worked on the results and they read and approved the final manuscript.

Declaration of Competing Interests The authors declare no potential conflict of interests.

REFERENCES

- [1] Akyol, M. A., Şahin, B., Conformal slant submersions, *Hacettepe Journal of Mathematics and Statistics*, 48(1) (2019), 28-44. <https://doi.org/10.15672/HJMS.2017.506>
- [2] Akyol, M. A., Gündüzalp, Y., Semi-invariant semi-Riemannian submersions, *Communications Faculty of Sciences University of Ankara Series A1 Mathematics and Statistics*, 67(1) (2018), 80-92. <https://doi.org/10.1501/Commua1\0000000832>
- [3] Alegre, P., Carriazo, A., Bi-slant submanifolds of para-Hermitian manifolds, *Mathematics*, 7(7) (2019), 618. <https://doi.org/10.3390/math7070618>
- [4] Baditoiu, G., Ianus, S., Semi-Riemannian submersions from real and complex pseudo-hyperbolic spaces, *Diff. Geom. and Appl.*, 16(1) (2002), 79-94. [https://doi.org/10.1016/S0926-2245\(01\)00070-5](https://doi.org/10.1016/S0926-2245(01)00070-5)
- [5] Carriazo, A., Bi-slant immersions, *Proc. ICRAMS 2000*, (2000), 88-97.
- [6] Falcitelli, M., Ianus, S., Pastore, A. M., *Riemannian Submersions and Related Topics*, World Scientific, 2004.
- [7] Gündüzalp, Y., Slant submersions in paracontact geometry, *Hacettepe Journal of Mathematics and Statistics*, 49(2) (2020), 822-834. <https://doi.org/10.15672/hujms.458085>
- [8] Gündüzalp, Y., Anti-invariant semi-Riemannian submersions from almost para-Hermitian manifolds, *Journal of Function Spaces and Applications*, 2013 (2013). <https://doi.org/10.1155/2013/720623>
- [9] Gündüzalp, Y., Anti-invariant Pseudo-Riemannian submersions and Clairaut submersions from Paracosymplectic manifolds, *Mediterr. J. Math.*, 16 (2019), 1-18. <https://doi.org/10.1007/s00009-019-1359-1>
- [10] Gündüzalp, Y., Neutral slant submersions in paracomplex geometry, *Afrika Matematika*, 32 (2021), 1095-1110. <https://doi.org/10.1007/s13370-021-00884-8>
- [11] Gündüzalp, Y., Slant submersions from almost product Riemannian manifolds, *Turkish Journal of Mathematics*, 37(5) (2013), 863-873. <https://doi.org/10.3906/mat-1205-64>

- [12] Gray, A., Pseudo-Riemannian almost product manifolds and submersions, *J. Math. Mech.*, 16 (1967), 715-737.
- [13] Ianus, S., Mazzocco, R., Vilcu, G. E., Riemannian submersions from quaternionic manifolds, *Acta Appl. Math.*, 104 (2008), 83-89. <https://doi.org/10.1007/s10440-008-9241-3>
- [14] Ianus, S., Vilcu, G. E., Voicu, R. C., Harmonic maps and Riemannian submersions between manifolds endowed with special structures, *Banach Center Publications*, 93 (2011), 277-288.
- [15] Ivanov, S., Zamkovoy, S., Para-Hermitian and para-quaternionic manifolds, *Diff. Geom. and Its Appl.*, 23 (2005), 205-234. <https://doi.org/10.1016/j.difgeo.2005.06.002>
- [16] Lee, C. W., Lee, J. W., Şahin, B., Vilcu, G-E., Optimal inequalities for Riemannian maps and Riemannian submersions involving Casorati curvatures, *Annali di Matematica*, 200 (2021), 1277-1295. <https://doi.org/10.1007/s10231-020-01037-7>
- [17] O'Neill, B., The fundamental equations of a submersion, *Michigan Math. J.*, 13 (1966), 459-469. <https://doi.org/10.1307/mmj/1028999604>
- [18] Özdemir, F., Sayar, C., Taştan, H. M., Semi-invariant submersions whose total manifolds are locally product Riemannian, *Quaestiones Mathematicae*, 40(7) (2017), 909-926. <https://doi.org/10.2989/16073606.2017.1335657>
- [19] Sepet, S. A., Ergüt, M., Pointwise slant submersions from cosymplectic manifolds, *Turkish Journal of Mathematics*, 40(3) (2016), 582-593. <https://doi.org/10.3906/mat-1503-98>
- [20] Prasad, R., Shukla, S. S., Kumar, S., On Quasi-bi-slant submersions, *Mediterr. J. Math.*, 16 (2019), 1-18. <https://doi.org/10.1007/s00009-019-1434-7>
- [21] Sayar, C., Akyol, M. A., Prasad, R., Bi-slant submersions in complex geometry, *International Journal of Geometric Methods in Modern Physics*, 17(04) (2020), 2050055. <https://doi.org/10.1142/S0219887820500553>
- [22] Sari, R., Akyol, M. A., Hemi-slant ξ -Riemannian submersions in contact geometry, *Filomat*, 34(11) (2020), 3747-3758. <https://doi.org/10.2298/FIL2011747S>
- [23] Şahin, B., Slant submersions from almost Hermitian manifolds, *Bull. Math. Soc.Sci. Math. Roumanie Tome.*, 54(102) (2011), 93-105.
- [24] Şahin, B., Anti-invariant Riemannian submersions from almost Hermitian manifolds, *Central European J.Math.*, 8(3) (2010), 437-447. <https://doi.org/10.2478/s11533-010-0023-6>
- [25] Şahin, B., Semi-invariant submersions from almost Hermitian manifold, *Canadian Mathematical Bulletin*, 56(1) (2013), 173-183. <https://doi.org/10.4153/CMB-2011-144-8>
- [26] Şahin, B., Riemannian Submersions, Riemannian Maps in Hermitian Geometry, and Their Applications, Academic Press, 2017.
- [27] Şahin, B., Riemannian submersions from almost Hermitian manifolds, *Taiwanese J. Math.*, 17(2) (2013), 629-659. <https://doi.org/10.11650/tjm.17.2013.2191>
- [28] Taştan, H. M., Şahin, B., Yanan, Ş., Hemi-slant submersions, *Mediterr. J. Math.*, 13 (2016), 2171-2184. <https://doi.org/10.1007/s00009-015-0602-7>
- [29] Vilcu, G. E., Almost product structures on statistical manifolds and para-Kähler-like statistical submersions, *Bulletin des Sciences Mathématiques*, 171 (2021), 103018. <https://doi.org/10.1016/j.bulsci.2021.103018>
- [30] Watson, B., Almost Hermitian submersions, *J. Differential Geom.*, 11 (1976), 147-165. <https://doi.org/10.4310/jdg/1214433303>



SUSTAINABLE METHOD FOR TENDER SELECTION USING LINEAR DIOPHANTINE MULTI-FUZZY SOFT SET

Jeevitha KANNAN¹ and Vimala JAYAKUMAR²

^{1,2}Department of Mathematics, Alagappa University, Karaikudi, INDIA

ABSTRACT. Tender selection is a fundamental issue for the success of construction projects since it contributes to the overall outline's performance. In real-life problems, the decision-makers cannot express certain crisp data, so there is uncertainty and vagueness in the values. In this paper, a sustainable technique is proposed to find desirable tenderers coherently and fairly under the needed circumstances. This paper presents three methods of an algorithmic approach to evaluate the tendering process and rank the tenderers. The attributes are expressed as Linear Diophantine Multi-Fuzzy Soft numbers (LDMFSN) since the existence of reference parameters makes the DM freely choose their grade values. Some of the rudimentary properties of LDMFSN are presented. An illustrative example is demonstrated to validate our proposed method. The uniqueness of the result in all three algorithms shows the effectiveness of our proposed approach.

1. INTRODUCTION

The tender selection process is one of the most vital processes in the construction industry. Many of the selection processes are associated with the lowest bid price method. But, the lower price bid does not assure the best outcomes. Hence, many researchers have recognised the prominent criteria for the selection process. The selection of an appropriate tenderer is directly correlated with the success of the project. So, it is essential to explore a suitable tender for a successful outcome. Many researchers studied the tender selection process using fuzzy theory.

The focus of research has been on bid evaluation models and indication systems. Researchers concentrate on various indicators in their studies of bid evaluation systems [9, 16, 17]. In decision-making problems, there are a large number of

2020 *Mathematics Subject Classification.* 03E72, 08A72, 94D05, 90B50.

Keywords. Linear Diophantine fuzzy, tender selection, threshold fuzzy, comparison matrix, score value.

¹ ✉ kjeevitha991@gmail.com; 0000-0001-7846-9173

² ✉ vimaljey@alagappauniveristy.ac.in-Corresponding author; 0000-0003-3138-9365.

uncertainties in the information. To solve such ambiguity, Zadeh [33] introduced the idea of a fuzzy set. For the purpose of scoring contractors in the study of bid assessment models, AHP [4], Fuzzy-AHP [8] and Fuzzy AHP-SMART [20] were employed. Jamili [13] proposed a novel fuzzy approach for the tender selection problem. Later, another fuzzy support decision model [1] was constructed for selection of contractors. Membership grades are not sufficient to handle some problems resulting in the origination of an intuitionistic fuzzy set [2]. Using Intuitionistic fuzzy information, many decision model [18,29] were established for bid selection. Later, some generalizations like Pythagorean fuzzy set [32], q-rung orthopair fuzzy set [31] are introduced. These fuzzy sets have immense applications in the tender selection process. But, it has some limitations on their membership grades.

In order to relax these deficiencies, Riaz and Hashmi [24] introduced a Linear Diophantine Fuzzy Set (LDFS) with the inclusion of reference parameters. The existence of reference parameters extends the space of grade values. The practical advantages of LDFS attracted the attention of several researchers in various scientific fields, and a number of icon works were written as a result. A. Iampam [12] addressed using LDFS with a variety of Einstein aggregation approaches for MCDM issues. Later, S. Ayub [3] used decision-making to create LDF relations and related algebraic characteristics. Kamac [14] created the intricate LDFS and provided a description of the cosine similarity metric and its intended uses. By incorporating the concept of soft rough sets for use in material handling equipment, Riaz et al. [25] extended the LDFS. The use of spherical linear Diophantine fuzzy sets with modelling uncertainty in MCDM was addressed by Hashmi et al. Riaz et al. [23] built prioritised AOs for linear Diophantine fuzzy numbers (LDFNs) and used them to choose third-party logistic service providers.

Maji [19] investigated the fuzzy soft set theory, which got the boom in recent times. Later, it was extended to the formulation of the hybrid models named Fuzzy soft group [22], Intuitionistic Fuzzy soft group [26] Intuitionistic Fuzzy Soft Set (IFSS) [7], Pythagorean Fuzzy Soft Set (PFSS) [21]. Hussain [10] investigated q-Rung Orthopair Fuzzy Soft Set (q-ROFSS) with aggregation operators. Further, the multi-fuzzy soft set [30] is a fusion of multi-fuzzy set [27] and fuzzy soft set, which has a extensive application in many fields. The mixture of the multi-valued approach and the parametric approach helps to express the problems that are not able to be expressed in other existing fuzzy models. Begam [5,6] introduced a novel approach to lattice ordered multi-fuzzy soft set based decision-making. In this paper, the implementation of a multi-fuzzy set in the LDFS is presented. The hybrid concept of LDMFSS was initiated along with the LDMFSN and some of its properties are discussed.

1.1. Motivation and Inspiration. The following is an explanation of the intended objectives of this research:

- (1) A superior mathematical model beyond membership and non-membership grades is LDFS, which does deal with these limitations. It helps the DM select the grade values at their discretion. A general method for coping with uncertainty is a soft set. Based on these benefits, this study introduces the novel hybrid concept of linear Diophantine multi-fuzzy soft set(LDMFSS) in order to fill the research gap.
- (2) This theory was found to be more useful for dealing with uncertain values in decision analysis. Our analysis of the literature revealed that there is no research investigating tender selection employing LDF data. Hence, the main intent of this paper is to apply the LDMFSS decision model to the selection of tenders.
- (3) This paper presents three different algorithms to solve the LDMFSS model using a comparison matrix, score function, and threshold fuzzy. The illustrative example is presented, and the result is analysed using three different algorithms to show the validity of our proposed method.

The outline that follows is the organisational structure of the manuscript: Section 2 focuses on several fundamental concepts, such as FS, IFS, PFS, and LDFS. In Section 3, the new hybrid concepts of LDMFS and LDMFSS were established. LDMFSN and some of its properties are discussed. Section 4 comprises a case study for tender selection and three different algorithms. A comparative study of the results of three proposed algorithms was initiated. In the end, Section 5 summarised the conclusion of this study.

2. PRELIMINARIES

Throughout this paper \mathfrak{U} is used as a universal set and Π is a parameter set.

Definition 1. [33] *The fuzzy set \mathcal{F} on \mathfrak{U} is a mapping $\mu: \mathfrak{U} \rightarrow [0, 1]$ where $\mu(x)$ represents the degrees of elements in \mathfrak{U} and it is represented in the form*

$$\mathcal{F} = \{(x, \mu(x)) / x \in \mathfrak{U}\}$$

Definition 2. [27] *Let $K = \{1, 2, \dots, k\}$ be the set of indices. The multi-fuzzy set \mathcal{M} with dimension k on \mathfrak{U} is symbolized as follow:*

$$\mathcal{M} = \{(x, \mu^K(x)) / x \in \mathfrak{U}\}$$

where $\mu^K = (\mu_1, \mu_2, \mu_3, \dots, \mu_k)$, $\mu_l: \mathfrak{U} \rightarrow [0, 1]$ for every $l \in K = \{1, 2, \dots, k\}$ and the collection of all multi-fuzzy set of dimension k over \mathfrak{U} is represented by $M_kFS(\mathfrak{U})$.

Definition 3. [19] *A pair (\mathcal{F}, Π) is called a multi-fuzzy soft set of dimension k over \mathfrak{U} , where \mathcal{F} is a mapping given by $\mathcal{F}: \Pi \rightarrow M_kFS(\mathfrak{U})$, where Π is a parameter set.*

Definition 4. [2] *The intuitionistic fuzzy set (IFS) on \mathfrak{U} is represented as*

$$\mathcal{J} = \{x, \langle \mu_{\mathcal{J}}(x), \nu_{\mathcal{J}}(x) \rangle : x \in \mathfrak{U}\}$$

where $\mu_{\mathcal{J}}(x), \nu_{\mathcal{J}}(x)$ are degrees of membership and non-membership which belongs to $[0, 1]$ subject to the condition $0 \leq \mu_{\mathcal{J}}(x) + \nu_{\mathcal{J}}(x) \leq 1$.

Definition 5. [32] The Pythagorean fuzzy set (PFS) on \sqsupset is in the mathematical form

$$\mathcal{P} = \{x, \langle \mu_{\mathcal{P}}(x), \nu_{\mathcal{P}}(x) \rangle : x \in \sqsupset\}$$

where $\mu_{\mathcal{P}}(x), \nu_{\mathcal{P}}(x)$ are degrees of membership and non-membership which belongs to $[0,1]$ subject to the condition $0 \leq \mu_{\mathcal{P}}^2(x) + \nu_{\mathcal{P}}^2(x) \leq 1$.

Definition 6. [31] The q -rung orthopair fuzzy set (q -ROFS) on \sqsupset is in the mathematical form

$$\mathcal{R} = \{x, \langle \mu_{\mathcal{R}}(x), \nu_{\mathcal{R}}(x) \rangle : x \in \sqsupset\}$$

where $\mu_{\mathcal{R}}(x), \nu_{\mathcal{R}}(x)$ are degrees of membership and non-membership which belongs to $[0,1]$ subject to the condition $0 \leq \mu_{\mathcal{R}}^q(x) + \nu_{\mathcal{R}}^q(x) \leq 1$.

Definition 7. [24] A linear Diophantine fuzzy set \mathcal{L} on \sqsupset is a structure symbolized as:

$$\mathcal{L} = \{(x, \langle \mu_{\mathcal{L}}(x), \nu_{\mathcal{L}}(x) \rangle, \langle \tau_{\mathcal{L}}(x), \eta_{\mathcal{L}}(x) \rangle) : x \in \sqsupset\}$$

where, $\mu_{\mathcal{L}}(x), \nu_{\mathcal{L}}(x), \tau_{\mathcal{L}}(x), \eta_{\mathcal{L}}(x) \in [0, 1]$ are degrees of membership, non-membership and their reference parameters respectively. These grades satisfy the condition $0 \leq \tau_{\mathcal{L}}(x)\mu_{\mathcal{L}}(x) + \eta_{\mathcal{L}}(x)\nu_{\mathcal{L}}(x) \leq 1$ for all $x \in \sqsupset$ with $0 \leq \tau_{\mathcal{L}}(x) + \eta_{\mathcal{L}}(x) \leq 1$.

3. LINEAR DIOPHANTINE MULTI-FUZZY SOFT SET

Definition 8. [15, 28] Let K be the set of indices. A linear Diophantine multi-fuzzy set \mathcal{J} on \sqsupset with dimension k is the set of ordered sequences in the form

$$\mathcal{J} = \{(x, \langle \mu_{\mathcal{J}}^K(x), \nu_{\mathcal{J}}^K(x) \rangle, \langle \tau_{\mathcal{J}}^K(x), \eta_{\mathcal{J}}^K(x) \rangle) : x \in \sqsupset\}$$

where,

$$\mu_{\mathcal{J}}^K(x) = (\mu_{\mathcal{J}}^1(x), \mu_{\mathcal{J}}^2(x), \mu_{\mathcal{J}}^3(x), \dots, \mu_{\mathcal{J}}^k(x))$$

$$\nu_{\mathcal{J}}^K(x) = (\nu_{\mathcal{J}}^1(x), \nu_{\mathcal{J}}^2(x), \nu_{\mathcal{J}}^3(x), \dots, \nu_{\mathcal{J}}^k(x))$$

$$\tau_{\mathcal{J}}^K(x) = (\tau_{\mathcal{J}}^1(x), \tau_{\mathcal{J}}^2(x), \tau_{\mathcal{J}}^3(x), \dots, \tau_{\mathcal{J}}^k(x))$$

$$\eta_{\mathcal{J}}^K(x) = (\eta_{\mathcal{J}}^1(x), \eta_{\mathcal{J}}^2(x), \eta_{\mathcal{J}}^3(x), \dots, \eta_{\mathcal{J}}^k(x))$$

and $\mu_{\mathcal{J}}^K(x), \nu_{\mathcal{J}}^K(x), \tau_{\mathcal{J}}^K(x), \eta_{\mathcal{J}}^K(x)$ are collection of multi membership, multi non-membership and multi reference parameters values respectively. Along that, it satisfies the condition

$$\begin{aligned} 0 \leq \mu_{\mathcal{J}}^l(x)\tau_{\mathcal{J}}^l(x) + \nu_{\mathcal{J}}^l(x)\eta_{\mathcal{J}}^l(x) &\leq 1 \\ 0 \leq \tau_{\mathcal{J}}^l(x) + \eta_{\mathcal{J}}^l(x) &\leq 1 \end{aligned}$$

for every $l \in K = \{1, 2, 3, \dots, k\}$.

The collection of all linear Diophantine multi-fuzzy set of dimension k over \sqsupset is denoted by $LDM_kF(\sqsupset)$.

Remark 1. The term $\mu^K(x)$ represents collection of memberships of k dimension whereas $\mu^l(x)$ is the element of $\mu^K(x)$ and it represents the membership value of x for the l^{th} dimensional parameter.

Definition 9. Let Π be the set of parameters. Define a map $\mathfrak{J} : \Pi \rightarrow LDM_kFS(\mathfrak{Q})$. Then the ordered pair (\mathfrak{J}, ω) is claimed to be linear Diophantine multi-fuzzy soft set of dimension k and it is of the structure

$$\{(\omega_i, \mathfrak{J}(\omega_i)) : \omega_i \in \Pi\}$$

where $\mathfrak{J}(\omega_i)$ is a $LDM_kFS(\mathfrak{Q})$.

Definition 10. The linear Diophantine multi-fuzzy soft set

$$\mathfrak{J} = \{(\omega_i, (x, \langle \mu_{\mathfrak{J}(\omega_i)}^K(x), \nu_{\mathfrak{J}(\omega_i)}^K(x) \rangle, \langle \tau_{\mathfrak{J}(\omega_i)}^K(x), \eta_{\mathfrak{J}(\omega_i)}^K(x) \rangle)) : \forall x \in \mathfrak{Q}, \omega_i \in \Pi\}$$

is claimed to be absolute linear Diophantine multi-fuzzy soft set if $\mu_{\mathfrak{J}(\omega_i)}^K(x) = 1, \nu_{\mathfrak{J}(\omega_i)}^K(x) = 0, \tau_{\mathfrak{J}(\omega_i)}^K(x) = 1, \eta_{\mathfrak{J}(\omega_i)}^K(x) = 0$.

i.e., $\mu_{\mathfrak{J}(\omega_i)}^l(x) = 1, \nu_{\mathfrak{J}(\omega_i)}^l(x) = 0, \tau_{\mathfrak{J}(\omega_i)}^l(x) = 1, \eta_{\mathfrak{J}(\omega_i)}^l(x) = 0$, for every $l \in K, \omega_i \in \Pi$.

Definition 11. The linear Diophantine multi-fuzzy soft set

$$\mathfrak{J} = \{(\omega_i, (x, \langle \mu_{\mathfrak{J}(\omega_i)}^K(x), \nu_{\mathfrak{J}(\omega_i)}^K(x) \rangle, \langle \tau_{\mathfrak{J}(\omega_i)}^K(x), \eta_{\mathfrak{J}(\omega_i)}^K(x) \rangle)) : \forall x \in \mathfrak{Q}, \omega_i \in \Pi\}$$

is said to be null linear Diophantine multi-fuzzy soft set if $\mu_{\mathfrak{J}(\omega_i)}^K(x) = 0, \nu_{\mathfrak{J}(\omega_i)}^K(x) = 1, \tau_{\mathfrak{J}(\omega_i)}^K(x) = 0, \eta_{\mathfrak{J}(\omega_i)}^K(x) = 1$.

i.e., $\mu_{\mathfrak{J}(\omega_i)}^l(x) = 0, \nu_{\mathfrak{J}(\omega_i)}^l(x) = 1, \tau_{\mathfrak{J}(\omega_i)}^l(x) = 0, \eta_{\mathfrak{J}(\omega_i)}^l(x) = 1$, for every $l \in K, \omega_i \in \Pi$.

Definition 12. The linear Diophantine multi-fuzzy soft number(LDM_kFSN) is expressed as $\mathfrak{J}(\omega_i) = \langle \mu_{\mathfrak{J}(\omega_i)}^K(x), \nu_{\mathfrak{J}(\omega_i)}^K(x) \rangle, \langle \tau_{\mathfrak{J}(\omega_i)}^K(x), \eta_{\mathfrak{J}(\omega_i)}^K(x) \rangle$ and it satisfies the following conditions:

- (i) $0 \leq \mu_{\mathfrak{J}(\omega_i)}^l(x) \tau_{\mathfrak{J}(\omega_i)}^l(x) + \nu_{\mathfrak{J}(\omega_i)}^l(x) \eta_{\mathfrak{J}(\omega_i)}^l(x) \leq 1$ and
- (ii) $0 \leq \tau_{\mathfrak{J}(\omega_i)}^l(x) + \eta_{\mathfrak{J}(\omega_i)}^l(x) \leq 1$, where $l = 1, 2, 3, \dots, k$

Definition 13. Considering two $LDMFSN$

$$\mathfrak{J}(\omega_1) = \langle \mu_{\mathfrak{J}(\omega_1)}^K(x), \nu_{\mathfrak{J}(\omega_1)}^K(x) \rangle, \langle \tau_{\mathfrak{J}(\omega_1)}^K(x), \eta_{\mathfrak{J}(\omega_1)}^K(x) \rangle$$

$$\mathfrak{J}(\omega_2) = \langle \mu_{\mathfrak{J}(\omega_2)}^K(x), \nu_{\mathfrak{J}(\omega_2)}^K(x) \rangle, \langle \tau_{\mathfrak{J}(\omega_2)}^K(x), \eta_{\mathfrak{J}(\omega_2)}^K(x) \rangle$$

and defined some operations as follows:

$$(i) \mathfrak{J}(\omega_1) \cup \mathfrak{J}(\omega_2) = \langle \max\{\mu_{\mathfrak{J}(\omega_1)}^l, \mu_{\mathfrak{J}(\omega_2)}^l\}, \min\{\nu_{\mathfrak{J}(\omega_1)}^l, \nu_{\mathfrak{J}(\omega_2)}^l\} \rangle, \langle \max\{\tau_{\mathfrak{J}(\omega_1)}^l, \tau_{\mathfrak{J}(\omega_2)}^l\}, \min\{\eta_{\mathfrak{J}(\omega_1)}^l, \eta_{\mathfrak{J}(\omega_2)}^l\} \rangle, \text{ for every } l \in K$$

$$(ii) \mathfrak{J}(\omega_1) \cap \mathfrak{J}(\omega_2) = \langle \min\{\mu_{\mathfrak{J}(\omega_1)}^l, \mu_{\mathfrak{J}(\omega_2)}^l\}, \max\{\nu_{\mathfrak{J}(\omega_1)}^l, \nu_{\mathfrak{J}(\omega_2)}^l\} \rangle, \langle \min\{\tau_{\mathfrak{J}(\omega_1)}^l, \tau_{\mathfrak{J}(\omega_2)}^l\}, \max\{\eta_{\mathfrak{J}(\omega_1)}^l, \eta_{\mathfrak{J}(\omega_2)}^l\} \rangle \text{ for every } l \in K$$

$$\begin{aligned}
(iii) \mathfrak{J}(\omega_1) \oplus \mathfrak{J}(\omega_2) &= \langle \mu_{\mathfrak{J}(\omega_1)}^l + \mu_{\mathfrak{J}(\omega_2)}^l - \mu_{\mathfrak{J}(\omega_1)}^l \mu_{\mathfrak{J}(\omega_2)}^l, \nu_{\mathfrak{J}(\omega_1)}^l \nu_{\mathfrak{J}(\omega_2)}^l \rangle, \\
&\quad \langle \tau_{\mathfrak{J}(\omega_1)}^l + \tau_{\mathfrak{J}(\omega_2)}^l - \tau_{\mathfrak{J}(\omega_1)}^l \tau_{\mathfrak{J}(\omega_2)}^l, \eta_{\mathfrak{J}(\omega_1)}^l \eta_{\mathfrak{J}(\omega_2)}^l \rangle \text{ for every } l \in K \\
(iv) \mathfrak{J}(\omega_1) \otimes \mathfrak{J}(\omega_2) &= \langle \mu_{\mathfrak{J}(\omega_1)}^l \mu_{\mathfrak{J}(\omega_2)}^l, \nu_{\mathfrak{J}(\omega_1)}^l + \nu_{\mathfrak{J}(\omega_2)}^l - \nu_{\mathfrak{J}(\omega_1)}^l \nu_{\mathfrak{J}(\omega_2)}^l \rangle, \\
&\quad \langle \tau_{\mathfrak{J}(\omega_1)}^l \tau_{\mathfrak{J}(\omega_2)}^l, \eta_{\mathfrak{J}(\omega_1)}^l + \eta_{\mathfrak{J}(\omega_2)}^l - \eta_{\mathfrak{J}(\omega_1)}^l \eta_{\mathfrak{J}(\omega_2)}^l \rangle \text{ for every } l \in K \\
(v) \mathfrak{J}(\omega_1) \leq \mathfrak{J}(\omega_2) \text{ iff } &\mu_{\mathfrak{J}(\omega_1)}^l \leq \mu_{\mathfrak{J}(\omega_2)}^l, \nu_{\mathfrak{J}(\omega_1)}^l \geq \nu_{\mathfrak{J}(\omega_2)}^l, \\
&\tau_{\mathfrak{J}(\omega_1)}^l \leq \tau_{\mathfrak{J}(\omega_2)}^l, \eta_{\mathfrak{J}(\omega_1)}^l \geq \eta_{\mathfrak{J}(\omega_2)}^l \text{ for every } l \in K \\
(vi) \mathfrak{J}(\omega_1)^c &= \langle \nu_{\mathfrak{J}(\omega_1)}^l(x), \mu_{\mathfrak{J}(\omega_1)}^l(x), \langle \eta_{\mathfrak{J}(\omega_1)}^l(x), \tau_{\mathfrak{J}(\omega_1)}^l(x) \rangle \rangle \text{ for every } l \in K \\
(vii) \alpha \mathfrak{J}(\omega_1) &= \langle 1 - (1 - \mu_{\mathfrak{J}(\omega_1)}^l)^\alpha, (\nu_{\mathfrak{J}(\omega_1)}^l)^\alpha \rangle, \\
&\quad \langle 1 - (1 - \tau_{\mathfrak{J}(\omega_1)}^l)^\alpha, (\eta_{\mathfrak{J}(\omega_1)}^l)^\alpha \rangle \text{ for every } l \in K \\
(viii) \mathfrak{J}(\omega_1)^\alpha &= \langle (\mu_{\mathfrak{J}(\omega_1)}^l)^\alpha, 1 - (1 - \nu_{\mathfrak{J}(\omega_1)}^l)^\alpha \rangle, \\
&\quad \langle (\tau_{\mathfrak{J}(\omega_1)}^l)^\alpha, 1 - (1 - \eta_{\mathfrak{J}(\omega_1)}^l)^\alpha \rangle \text{ for every } l \in K
\end{aligned}$$

Example 1. Let $\mathfrak{J}(\omega_1) = \langle (0.7, 0.6), (0.3, 0.5) \rangle, \langle (0.8, 0.7), (0.1, 0.2) \rangle$ and $\mathfrak{J}(\omega_2) = \langle (0.8, 0.5), (0.1, 0.5) \rangle, \langle (0.8, 0.9), (0.1, 0.1) \rangle$ Then

- (1) $\mathfrak{J}(\omega_1) \cup \mathfrak{J}(\omega_2) = \langle (0.8, 0.6), (0.1, 0.5) \rangle, \langle (0.8, 0.9), (0.1, 0.1) \rangle$
- (2) $\mathfrak{J}(\omega_1) \cap \mathfrak{J}(\omega_2) = \langle (0.7, 0.5), (0.3, 0.5) \rangle, \langle (0.8, 0.7), (0.1, 0.2) \rangle$
- (3) $\mathfrak{J}(\omega_1) \oplus \mathfrak{J}(\omega_2) = \langle (0.94, 0.8), (0.03, 0.25) \rangle, \langle (0.96, 0.97), (0.01, 0.08) \rangle$
- (4) $\mathfrak{J}(\omega_1) \otimes \mathfrak{J}(\omega_2) = \langle (0.56, 0.30), (0.37, 0.75) \rangle, \langle (0.64, 0.63), (0.19, 0.28) \rangle$
- (5) $(0.2)\mathfrak{J}(\omega_1) = \langle (0.21, 0.17), (0.79, 0.87) \rangle, \langle (0.30, 0.21), (0.63, 0.72) \rangle$
- (6) $\mathfrak{J}(\omega_1)^{0.1} = \langle (0.96, 0.95), (0.09, 0.07) \rangle, \langle (0.98, 0.96), (0.01, 0.02) \rangle$

Proposition 1. Let $\mathfrak{J}(\omega_1), \mathfrak{J}(\omega_2)$ be two LDMFSNs. Then the following operations holds.

- (1) $\mathfrak{J}(\omega_1) \oplus \mathfrak{J}(\omega_2) = \mathfrak{J}(\omega_2) \oplus \mathfrak{J}(\omega_1)$
- (2) $\mathfrak{J}(\omega_1) \otimes \mathfrak{J}(\omega_2) = \mathfrak{J}(\omega_2) \otimes \mathfrak{J}(\omega_1)$
- (3) $\mathfrak{J}(\omega_1) \oplus (\mathfrak{J}(\omega_2) \oplus \mathfrak{J}(\omega_3)) = (\mathfrak{J}(\omega_1) \oplus \mathfrak{J}(\omega_2)) \oplus \mathfrak{J}(\omega_3)$
- (4) $\mathfrak{J}(\omega_1) \otimes (\mathfrak{J}(\omega_2) \otimes \mathfrak{J}(\omega_3)) = (\mathfrak{J}(\omega_1) \otimes \mathfrak{J}(\omega_2)) \otimes \mathfrak{J}(\omega_3)$
- (5) $\alpha(\mathfrak{J}(\omega_1) \oplus \mathfrak{J}(\omega_2)) = (\alpha \mathfrak{J}(\omega_1) \oplus \alpha \mathfrak{J}(\omega_2))$
- (6) $(\mathfrak{J}(\omega_1) \otimes \mathfrak{J}(\omega_2))^\alpha = \mathfrak{J}(\omega_1)^\alpha \otimes \mathfrak{J}(\omega_2)^\alpha$
- (7) $\alpha \mathfrak{J}(\omega_1) \oplus \beta \mathfrak{J}(\omega_1) = (\alpha + \beta) \mathfrak{J}(\omega_1)$

Proof. The proof follows from above definition. \square

Definition 14. Comparison Matrix: The Comparison Matrix is a matrix having the columns as a elements in universe and rows as a set of parameters. The elements

in the matrix (α_{ij}) corresponding the element x_i and the parameter ω_j is defined by the number

$$\alpha_{ij} = \frac{1}{2}[(\Gamma_{ij} - \sigma_{ij}) + (\gamma_{ij} - \phi_{ij})]$$

where,

$$\Gamma_{ij} = \sum_{l=1}^k \{\text{how many times } \mu_{\mathcal{K}(\omega_j)}^l(x_i) \text{ exceeds } \mu_{\mathcal{K}(\omega_j)}^l(x_j)\}$$

$$\sigma_{ij} = \sum_{l=1}^k \{\text{how many times } \nu_{\mathcal{K}(\omega_j)}^l(x_i) \text{ exceeds } \nu_{\mathcal{K}(\omega_j)}^l(x_j)\}$$

$$\gamma_{ij} = \sum_{l=1}^k \{\text{how many times } \tau_{\mathcal{K}(\omega_j)}^l(x_i) \text{ exceeds } \tau_{\mathcal{K}(\omega_j)}^l(x_j)\}$$

$$\phi_{ij} = \sum_{l=1}^k \{\text{how many times } \eta_{\mathcal{K}(\omega_j)}^l(x_i) \text{ exceeds } \eta_{\mathcal{K}(\omega_j)}^l(x_j)\}$$

Definition 15. Total Score of an Object:

The Score of an attribute x_i is given by

$$S_i = \sum_j \alpha_{ij}$$

where α_{ij} is computed from the comparison matrix.

Definition 16. Score function for LDMFSN:

Let $\mathfrak{J}(\omega_j) = (\langle \mu_{\mathfrak{J}\omega_j}^K, \nu_{\mathfrak{J}\omega_j}^K \rangle, \langle \tau_{\mathfrak{J}\omega_j}^K, \eta_{\mathfrak{J}\omega_j}^K \rangle)$ be a LDMFSN over \mathfrak{J} . Then the score function of LDMFSN $\mathfrak{J}\omega_j$ is characterized as

$$\Omega(\mathfrak{J}\omega_j) = \sum_{l=1}^k \frac{1}{2} [(\mu_{\mathfrak{J}\omega_j}^l - \nu_{\mathfrak{J}\omega_j}^l) + (\tau_{\mathfrak{J}\omega_j}^l - \eta_{\mathfrak{J}\omega_j}^l)]$$

where $l \in K = \{1, 2, \dots, k\}$.

4. OVERVIEW OF PROPOSED APPROACH

The proposed approach is a fuzzy-based bid evaluation of tenders in order to evaluate tenderers and obtain the optimal tenderer promptly under some instances. The attributes of the tenderers are expressed as LDMFSNs. After analyzing the literature, it was found that there are many criteria affecting the pre-evaluation for selecting an appropriate tenderer. Those factors may vary in their importance and strength of the effect in selecting process. Some may have a high effect and some may have a low effect depending on the project and place. With the help of some expertise, five important factors are identified which have high effects on our selection process. The factors are listed below in the Figure 1.

4.1. Case study. A government tendering sector wants to select the most appropriate tender for the building project. After pre-evaluation, four companies $\{x_1, x_2, x_3, x_4\}$ are remained as alternatives for further evaluation. Based on above discussion, five criteria $\{\omega_1, \omega_2, \omega_3, \omega_4, \omega_5\}$ were identified as the main factors affecting tender selection.

- $\omega_1 = \text{Professional Activity}$
- $\omega_2 = \text{Resource Availability}$
- $\omega_3 = \text{Organizational Availability}$
- $\omega_4 = \text{Quality}$
- $\omega_5 = \text{Management capacity}$

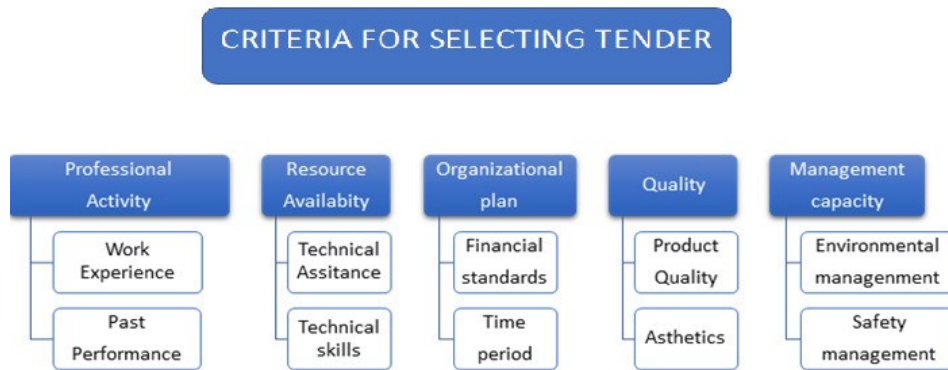


FIGURE 1. Selection criteria

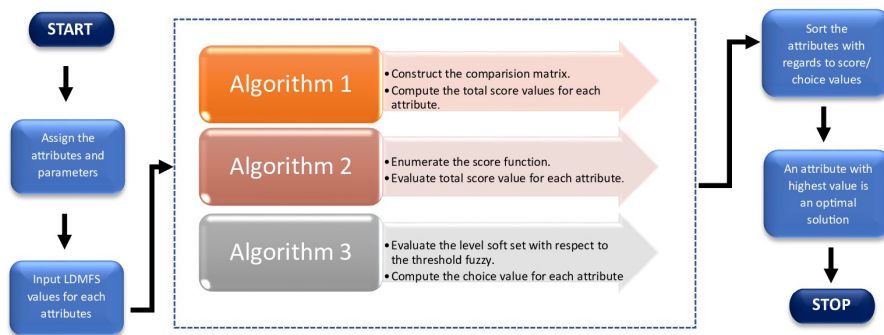


FIGURE 2. Flow chart diagram of algorithms 1, 2 and 3

We proposed three new algorithms for LDMFSS for selecting best tender. The graphical view of the algorithms are given in the Figure 2.

Algorithm 1: Algorithm based on comparison table

This novel and hybrid approach contains following steps:

Input:

(i) Define linear Diophantine multi-fuzzy soft values for each attributes $\{x_1, x_2, \dots, x_n\}$ with respect to the parameters $\{\omega_1, \omega_2, \dots, \omega_k\}$.

(ii) Input the above defined values (\mathfrak{J}, ω) in the table.

Calculations:

(iii) Construct the comparison matrix for (\mathfrak{J}, ω) with the knowledge of the given definition.

(iv) Evaluate the total score value of an object as defined in the previous section.

(v) Find the maximum score and rank the attributes.

Final decision:

(vi) An attribute with a high score is the required optimal solution.

Algorithm:2 Algorithm based on Score function:

Input:

(i) Define linear Diophantine multi-fuzzy soft values for each attributes $\{x_1, x_2, \dots, x_n\}$ with respect to the parameters $\{\omega_1, \omega_2, \dots, \omega_k\}$.

(ii) Input LDMFSN for each attributes $\{x_1, x_2, \dots, x_n\}$.

Calculations:

(iii) Evaluate the score function value Ω_{ij} for each x_i by using the definition.

(iv) Enumerate the total score value of each attribute.

(v) Rank the attributes based on score values and find the maximum.

Final decision:

(vi) An attribute with a high score is the required optimal solution.

Algorithm:3 Algorithm-based threshold fuzzy:

Input:

(i) Define linear Diophantine multi-fuzzy soft values for each attributes $\{x_1, x_2, \dots, x_n\}$ with respect to the parameters $\{\omega_1, \omega_2, \dots, \omega_k\}$.

(ii) LDMFSS (\mathfrak{J}, ω) and parameter weights $\phi(\omega_i)$ are taken as input.

Calculations:

(iii) Induced fuzzy soft set $\Delta_{\mathfrak{J}}$ [7,19] is computed.

(iv) A threshold fuzzy set $\lambda : A \rightarrow [0, 1]$ which is the mid-level decision rule is chosen for decision making.

(v) Evaluate the level soft set $L(\Delta_{\mathfrak{J}}, \lambda)$ with respect to threshold fuzzy.

- (vi) Enumerate the choice value c_i for x_i
- (vii) Sort the attributes in regards to the choice value.

Final decision:

- (viii) An attribute with a high score is the required optimal solution.

4.2. **Solution for algorithm 1:** According to the company and selection criteria given in Figure ??, our expert team provides their preference for the attributes. It can be converted in the form of LDMFSN. Defined values for each attributes $\{x_1, x_2, x_3, x_4\}$ are given in the Table 1.

TABLE 1. Linear Diophantine multi-Fuzzy soft set

(\mathfrak{J}, ω)	ω_1	ω_2	ω_3	ω_4	ω_5
x_1	$\langle(0.71,0.68)\rangle$ $\langle(0.30,0.39)\rangle$ $\langle(0.80,0.92)\rangle$ $\langle(0.17,0.04)\rangle$	$\langle(0.41,0.32)\rangle$ $\langle(0.69,0.54)\rangle$ $\langle(0.76,0.83)\rangle$ $\langle(0.18,0.12)\rangle$	$\langle(0.52,0.73)\rangle$ $\langle(0.41,0.29)\rangle$ $\langle(0.96,0.92)\rangle$ $\langle(0.01,0.02)\rangle$	$\langle(0.39,0.59)\rangle$ $\langle(0.62,0.45)\rangle$ $\langle(0.84,0.94)\rangle$ $\langle(0.15,0.03)\rangle$	$\langle(0.56,0.67)\rangle$ $\langle(0.45,0.35)\rangle$ $\langle(0.79,0.80)\rangle$
x_2	$\langle(0.82,0.73)\rangle$ $\langle(0.24,0.31)\rangle$ $\langle(0.82,0.90)\rangle$ $\langle(0.14,0.08)\rangle$	$\langle(0.59,0.72)\rangle$ $\langle(0.45,0.33)\rangle$ $\langle(0.76,0.80)\rangle$ $\langle(0.22,0.13)\rangle$	$\langle(0.73,0.82)\rangle$ $\langle(0.30,0.24)\rangle$ $\langle(0.85,0.88)\rangle$ $\langle(0.12,0.09)\rangle$	$\langle(0.49,0.52)\rangle$ $\langle(0.53,0.51)\rangle$ $\langle(0.91,0.94)\rangle$ $\langle(0.07,0.04)\rangle$	$\langle(0.72,0.64)\rangle$ $\langle(0.29,0.37)\rangle$ $\langle(0.68,0.84)\rangle$ $\langle(0.30,0.12)\rangle$
x_3	$\langle(0.32,0.42)\rangle$ $\langle(0.69,0.59)\rangle$ $\langle(0.89,0.72)\rangle$ $\langle(0.10,0.26)\rangle$	$\langle(0.92,0.84)\rangle$ $\langle(0.11,0.20)\rangle$ $\langle(0.96,0.82)\rangle$ $\langle(0.03,0.14)\rangle$	$\langle(0.76,0.54)\rangle$ $\langle(0.30,0.46)\rangle$ $\langle(0.82,0.87)\rangle$ $\langle(0.17,0.11)\rangle$	$\langle(0.41,0.22)\rangle$ $\langle(0.52,0.73)\rangle$ $\langle(0.79,0.85)\rangle$ $\langle(0.20,0.17)\rangle$	$\langle(0.57,0.68)\rangle$ $\langle(0.50,0.40)\rangle$ $\langle(0.90,0.85)\rangle$ $\langle(0.07,0.11)\rangle$
x_4	$\langle(0.35,0.75)\rangle$ $\langle(0.60,0.27)\rangle$ $\langle(0.85,0.82)\rangle$ $\langle(0.14,0.15)\rangle$	$\langle(0.60,0.75)\rangle$ $\langle(0.40,0.30)\rangle$ $\langle(0.80,0.72)\rangle$ $\langle(0.19,0.26)\rangle$	$\langle(0.80,0.75)\rangle$ $\langle(0.35,0.30)\rangle$ $\langle(0.90,0.91)\rangle$ $\langle(0.09,0.08)\rangle$	$\langle(0.32,0.67)\rangle$ $\langle(0.70,0.39)\rangle$ $\langle(0.91,0.87)\rangle$ $\langle(0.07,0.11)\rangle$	$\langle(0.72,0.83)\rangle$ $\langle(0.29,0.19)\rangle$ $\langle(0.87,0.82)\rangle$ $\langle(0.11,0.15)\rangle$

The comparison matrix is computed in the Table 2. Then, the score values for each attributes are calculated. Ranking of the attributes are as follows: $x_2 > x_3 >$

TABLE 2. Comparison matrix

(\mathfrak{J}, ω)	ω_1	ω_2	ω_3	ω_4	ω_5	Score values
x_1	$\frac{5}{2}$	$\frac{-3}{2}$	$\frac{3}{2}$	1	-3	$\frac{1}{2}$
x_2	4	1	3	$\frac{5}{2}$	-1	$\frac{19}{2}$
x_3	-1	5	0	$\frac{-7}{2}$	$\frac{3}{2}$	2
x_4	$\frac{-9}{2}$	$\frac{-9}{2}$	-5	$\frac{1}{2}$	$\frac{3}{2}$	-12

$x_1 > x_4$. Clearly, it shows that the company x_2 is most suitable for the selection.

The graphical representation of the outcomes shown in the Figure 3

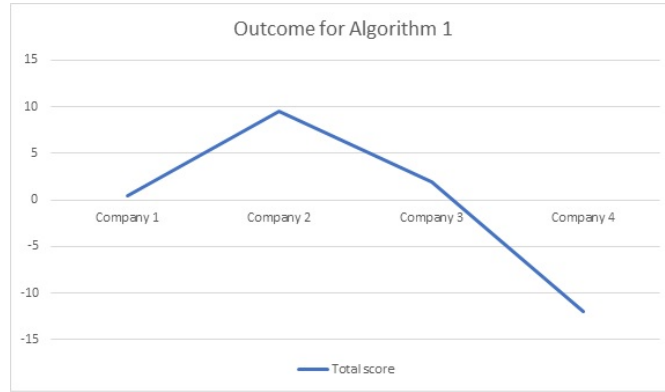


FIGURE 3. Graph of total score values using algorithm 1

4.3. **Solution for algorithm 2:** LDMFSN are taken as a input from the Table 1. The score function values of all attributes are enumerated in the Table 3

The total score values of each attributes are $S(x_1)= 4.252$, $S(x_2)= 5.12$, $S(x_3) =$

TABLE 3. Score function value

Ω_{ij}	ω_1	ω_2	ω_3	ω_4	ω_5
x_1	1.105	0.36	1.2	0.762	0.825
x_2	1.25	0.85	1.265	0.855	0.9
x_3	0.355	1.53	0.975	0.345	0.96
x_4	0.175	0.21	0.545	0.75	1.25

4.165, $S(x_4)= 2.93$. Ranking of the attributes are as follows: $x_2 > x_1 > x_3 > x_4$. It is shown that the company x_2 is the best company for our selection. The final outcome of algorithm 2 is shown in the Figure 4

4.4. **Solution of algorithm 3:** Taking the values from the Table 1 as a input. The induced soft set is given in the Table 4. The mid values are obtained as follows: $mid_{\Delta} = \{(\omega_1, 1.9905), (\omega_2, 1.9825), (\omega_3, 1.987), (\omega_4, 1.987), (\omega_5, 2.002)\}$. The mid-level soft set with choice values is given in the Table 5

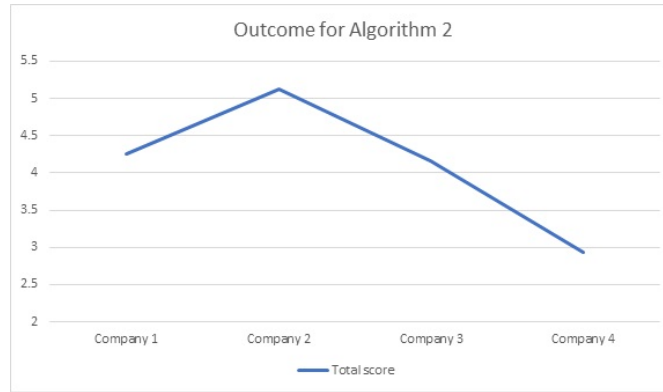


FIGURE 4. Graph of total score values using algorithm 2

TABLE 4. Induced fuzzy soft set

Δ	ω_1	ω_2	ω_3	ω_4	ω_5
	$\phi(\omega_1)=(0.6,0.4)$	$\phi(\omega_2)=(0.5,0.5)$	$\phi(\omega_3)=(0.3,0.7)$	$\phi(\omega_4)=(0.6,0.4)$	$\phi(\omega_5)=(0.6,0.4)$
x_1	2	1.96	1.942	2.004	1.996
x_2	2.02	2.02	2.021	2.004	1.982
x_3	1.996	2.01	2.001	1.924	2.04
x_4	1.946	1.94	1.983	2.016	1.99

TABLE 5. mid-level soft set with choice values

Δ	ω_1	ω_2	ω_3	ω_4	ω_5	choice value
x_1	1	0	0	1	0	2
x_2	1	1	1	1	0	4
x_3	1	1	1	0	1	3
x_4	0	0	0	1	0	1

Ranking of the attributes are as follows: $x_2 > x_3 > x_1 > x_4$. Likewise, x_2 is the required optimal solution. The Figure 5 shows the final outcomes for algorithm 3.

4.5. Discussion. The previously mentioned three findings demonstrate that the bid x_2 is the one that is economically most advantageous. The innovation and robustness of our suggested methods are demonstrated by the distinctiveness of the results of the three algorithms. The picture 6 displays a comparison of our three suggested algorithm outcomes.

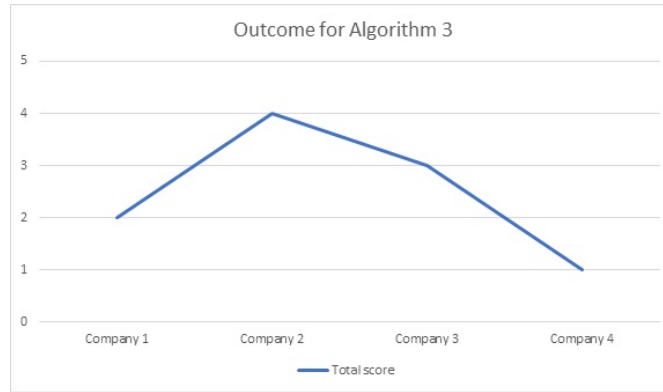


FIGURE 5. Graph of total score values using algorithm 3

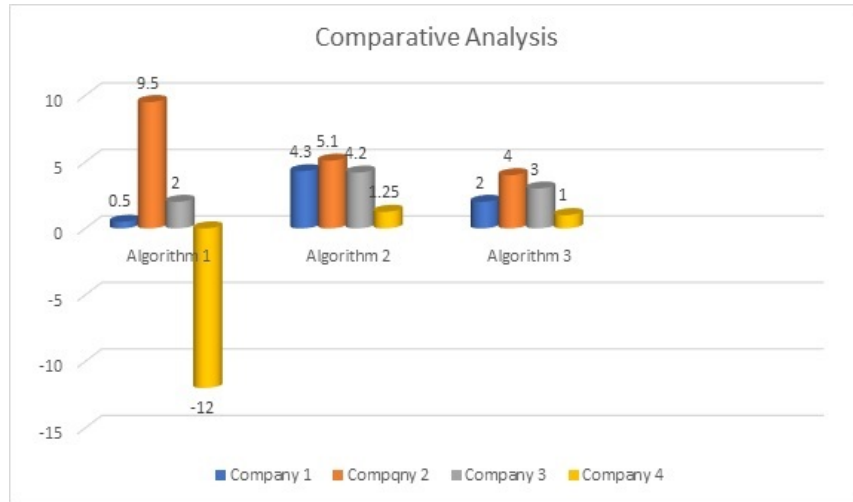


FIGURE 6. Comparison between Algorithm 1, 2 and 3

5. CONCLUSION

In this paper, the concept of LDMFSN is introduced. Some of the properties are discussed. The main motive of this paper is to find the most suitable tender for the government based on the same selection criteria. There are three different algorithms, like those based on comparison matrix, score function, and threshold

fuzzy, that are initiated. Our proposed methods are used to sort the tenderers and select the optimal one among them. The illustrative example and the obtained results show the effectiveness of our proposed algorithms. In the future, the work will be extended to similarity measures and entropy measures between two LDMFSS.

Author Contribution Statements Jeevitha Kannan: Conceptualization and design of the study, writing, methodology. Vimala Jayakumar: Reviewing, editing, and validation.

Declaration of Competing Interests All authors declare no conflicts of interest in this paper.

Acknowledgements This paper is presented in the Conference ICAMM-2023. The article has been written with the joint financial support of RUSA-Phase 2.0 grant sanctioned vide letter No.F 24-51/2014-U, Policy (TN Multi-Gen), Dept. of Edn. Govt. of India, Dt. 09.10.2018, DST-PURSE 2nd Phase programme vide letter No. SR/PURSE Phase 2/38 (G) Dt. 21.02.2017 and DST (FIST - level I) 657876570 vide letter No.SR/FIST/MS-I/2018/17 Dt. 20.12.2018.

REFERENCES

- [1] Akcay, C., Manisali, E., Fuzzy decision support model for the selection of contractor in construction works, *Revista de la Construction*, 17 (2018), 258–266. DOI: 10.7764/RDLC.17.2.258
- [2] Atanassov K.T, Intuitionistic fuzzy sets, *Fuzzy Set System*, 20 (1986), 87–96. [https://doi.org/10.1016/S0165-0114\(86\)80034-3](https://doi.org/10.1016/S0165-0114(86)80034-3)
- [3] Ayub, S., Shabir, M., Riaz, M., Aslam, M., Chinram, R., Linear Diophantine fuzzy relations and their algebraic properties with decision making, *Symmetry*, 13(6) (2021), 945. <https://doi.org/10.3390/sym13060945>
- [4] Al-Harbi, K.M.A.S., Application of the AHP in project management, *International Journal of Project Management*, 19(1) (2001), 19–27. [https://doi.org/10.1016/S0263-7863\(99\)00038-1](https://doi.org/10.1016/S0263-7863(99)00038-1)
- [5] Begam, S.S., Vimala, J., Application of lattice ordered multi-fuzzy soft set in forecasting process, *Journal of Intelligent & Fuzzy Systems*, 36(3) (2019), 2323–2331. 10.3233/JIFS-169943
- [6] Begam, S.S., Vimala, J., Preethi, D., A novel study on the algebraic applications of special class of lattice ordered multi-fuzzy soft sets, *Journal of Discrete Mathematical Sciences and Cryptography*, 22(5) (2019), 883–899. DOI: 10.1080/09720529.2019.1685239
- [7] Das, S., Kar, S., Intuitionistic Multi Fuzzy Soft Set and Its Application in Decision Making, *International Conference on Pattern Recognition and Machine Intelligence, Lecture Notes in Computer Science*, Springer, Berlin, Heidelberg, 2013, 587–592. <https://doi.org/10.1007/978-3-642-45062-4-82>
- [8] Deng, H., Multi-criteria analysis with fuzzy pairwise comparison, *International Journal of Approximate Reasoning*, 21(3) (1999), 215–231. [https://doi.org/10.1016/S0888-613X\(99\)00025-0](https://doi.org/10.1016/S0888-613X(99)00025-0)
- [9] Hatush, Z., Skitmore, M., Contractor selection using multi-criteria utility theory: An additive model, *Building and Environment*, 33(23) (1998), 105–115. [https://doi.org/10.1016/S0360-1323\(97\)00016-4](https://doi.org/10.1016/S0360-1323(97)00016-4)

- [10] Hussain, A., Ali, M.I., Mahmood, T., Munir, M., q-Rung orthopair fuzzy soft average aggregation operators and their application in multi-criteria decision-making, *International Journal of Intelligent Systems*, 35(4) (2020), 571–599. <https://doi.org/10.1002/int.22217>
- [11] Hashmi, M.R., Tehrim, S.T., Riaz, M., Pamucar, D., Cirovic G, Spherical linear Diophantine fuzzy soft rough sets with multi-criteria decision making, *Axioms*, 10(185) (2021). <https://doi.org/10.3390/axioms10030185>
- [12] Iampan, A., Garcia, G.S., Riaz, M., Athar Farid, H.M., Chinram, R., Linear Diophantine fuzzy Einstein aggregation operators for multi-criteria decision-making problems, *Journal of Mathematics*, 2021 (2021), 1–31. <https://doi.org/10.1155/2021/5548033>
- [13] Jamili, A., Tender participation selection problem with fuzzy approach, *Advances in Industrial Engineering*, 54(4) (2020), 355–364. 10.22059/JIENG.2021.325197.1772
- [14] Kamaci, H., Linear Diophantine fuzzy algebraic structures, *J Ambient Intell Human Comput*, 12 (2021), 10353–10373. <https://doi.org/10.1007/s12652-020-02826-x>
- [15] Kannan, J., Garg, H., Jayakumar, V., Hananf, A., Aty, A., Haleem, A., Linear Diophantine multi-fuzzy aggregation operators and its application in digital transformation, *Journal of Intelligent & Fuzzy Systems*, 45(2) (2023), 3097–3107. DOI: 10.3233/JIFS-223844
- [16] Lambropoulos, S., The use of time and cost utility for construction contract award under European Union Legislation, *Building and Environment*, 42(1) (2007), 452–463. <https://doi.org/10.1016/j.buildenv.2005.08.002>
- [17] Lai, K.K., Liu, S.L., Wang, S.Y., A method used for evaluating bids in the Chinese construction industry, *International Journal of Project Management*, 22 (2004), 193–201. [https://doi.org/10.1016/S0263-7863\(03\)00009-7](https://doi.org/10.1016/S0263-7863(03)00009-7)
- [18] Liu, B., Huo, T., Wang, X., Shen, G.Q., Chen, Y., The decision model of the intuitionistic fuzzy group bid evaluation for urban infrastructure projects considering social costs, *Canadian Journal of Civil Engineering*, 40(3) (2013), 263–273. 10.1139/cjce-2012-0283
- [19] Maji, P.K., Biswas, R., Roy, A.R., Fuzzy soft sets, *J. Fuzzy Math.*, 9(3) (2001), 589–602.
- [20] Padhi, S.S., Mohapatra, P.K.J., Contractor selection in government procurement auctions: A case study, *European Journal of Industrial Engineering*, 3(2) (2009), 170–186. DOI: 10.1504/EJIE.2009.023604
- [21] Peng X.A., Yang, Y., Song, J., Pythagoren fuzzy soft set and its application, *Computer Engineering*, 41 (2015), 224–229. <https://doi.org/10.1016/j.jksuci.2021.08.010>
- [22] Reeta, A.J., Vimala, J., A study on distributive and modular lattice ordered fuzzy soft group and its duality, *Appl. Math. J. Chin. Univ.*, 31 (2016), 491–502.
- [23] Riaz, M., Farid, H.M.A., Aslam, M., Pamucar, D., Bozanic, D., Novel approach for third-party reverse logistic provider selection process under linear Diophantine fuzzy prioritized aggregation operators, *Symmetry*, 13 (2021), 1152. <https://doi.org/10.3390/sym13071152>
- [24] Riaz, M., Hashmi, M.R., Masooma, R., Linear Diophantine fuzzy set and its applications towards multi-attribute decision-making problems, *Journal of Intelligent and Fuzzy Systems*, 37 (2019), 5417–5439. <https://doi.org/10.3233/JIFS-190550>
- [25] Riaz, M., Hashmi, M.R., Kalsoom, H., Pamucar, D., Chu, M., Linear Diophantine fuzzy soft rough sets for the selection of sustainable material handling equipment, *Symmetry*, 12 (2020), 1215. <https://doi.org/10.3390/sym12081215>
- [26] Rajareega, S., Vimala, J., Operations on complex intuitionistic fuzzy soft lattice ordered group and CIFS-COPRAS method for equipment selection process, *Journal of Intelligent & Fuzzy Systems*, 41(5) (2021), 5709–5718. DOI: 10.3233/JIFS-189890
- [27] Sebastian, S., Multi-fuzzy sets, *International Mathematical Forum*, 5 (2010), 2471–2476.
- [28] Vimala, J., Garg, H., Jeevitha, K., Prognostication of myocardial infarction using lattice ordered linear Diophantine multi-fuzzy soft set, *Intelligent Journal of Fuzzy System*, (2023). <https://doi.org/10.1007/s40815-023-01574-2>

- [29] Wang, Y., Xi, C., Zhang, S., Zhang, W., Yu, D., Combined approach for government e-tendering using GA and TOPSIS with intuitionistic fuzzy information, *PloS One*, 10 (2015), e0130767. [10.1371/journal.pone.0130767](https://doi.org/10.1371/journal.pone.0130767)
- [30] Yang, Y., Tan, X., Meng, C., The multi-fuzzy soft set and its application in decision making, *Applied Mathematical Modelling*, 37 (2013), 4915–4923. <https://doi.org/10.1016/j.apm.2012.10.015>
- [31] Yager, R.R., Generalized orthopair fuzzy sets, *IEEE Transactions on Fuzzy Systems*, 25(5) (2017), 1222–1230. <https://doi.org/10.1109/TFUZZ.2016.2604005>
- [32] Yager, R.R., Pythagorean membership grades in multicriteria decision making, *IEEE Transactions on Fuzzy Systems*, 22(4) (2014), 958–965. <https://doi.org/10.1109/TFUZZ.2013.2278989>
- [33] Zadeh, L.A., Fuzzy sets, *Information Controls*, 8 (1965), 338–353. [https://doi.org/10.1016/S0019-9958\(65\)90241-X](https://doi.org/10.1016/S0019-9958(65)90241-X)



A DIOPHANTINE EQUATION INCLUDING FIBONACCI AND FIBONOMIAL COEFFICIENTS

Nurettin IRMAK

Konya Technical University, Engineering and Natural Science Faculty, Department of Engineering Basic Science, Konya, TÜRKİYE

ABSTRACT. In this paper, we solve the equation

$$\sum_{k=0}^m \begin{bmatrix} 2m+1 \\ k \end{bmatrix}_F \pm F_k = F_n,$$

under weak assumptions. Here, F_n is n^{th} Fibonacci number and $\begin{bmatrix} \cdot \\ \cdot \end{bmatrix}_F$ denotes Fibonomial coefficient.

1. INTRODUCTION

For $n \geq 2$, the Fibonacci sequence $\{F_n\}$ is defined by recurrence relation

$$F_n = F_{n-1} + F_{n-2}$$

with $F_0 = 0$ and $F_1 = 1$. A few terms of Fibonacci sequence are 0, 1, 1, 2, 3, 5, 8, 13, Its Binet formula is known as

$$F_n = \frac{\alpha^n - \beta^n}{\alpha - \beta}$$

where α and β are the roots of the characteristic equation $x^2 - x - 1 = 0$.

The Fibonacci companion sequence $\{L_n\}$ is known as the Lucas sequence which satisfies the same recurrence relations with Fibonacci sequence and the initials $L_0 = 2$, $L_1 = 1$. A few terms of Lucas sequence are 2, 1, 3, 4, 7, 11, 18, 29, The Binet formula of n^{th} Lucas number is

$$L_n = \alpha^n + \beta^n.$$

2020 *Mathematics Subject Classification.* 11B39, 11D72.

Keywords. Fibonomial coefficient, Fibonacci number, Diophantine equation.

✉ irmaknurettin@gmail.com; 0000-0003-0409-4342.

Another concept of the paper is Fibonomial coefficient. For $n \geq k > 0$, the number

$$\frac{F_n F_{n-1} \dots F_{n-k+1}}{F_1 F_2 \dots F_k}$$

is known as Fibonomial coefficient inspired by the binomial coefficient and denoted by $\begin{bmatrix} n \\ k \end{bmatrix}_F$. Also, for $k = 0$, it is defined by $\begin{bmatrix} n \\ 0 \end{bmatrix}_F = 1$. It is interesting that this coefficient always gets integer values for $n, k \in \mathbb{Z}^+$.

The Diophantine equation

$$n! + 1 = m^2 \tag{1}$$

is known as Brocard-Ramanujan Diophantine equation. It is known that $m = 4, 5$ and 7 are the solutions of the this equation. These are not full solutions of the equation [1]. Berndt and Galway [1] showed that there are no further solutions with $m \leq 10^9$. The Brocard-Ramanujan equation is still open problem. A number of mathematicians have contributed several generalizations and results regarding this Diophantine equation. For example, Grossman and Luca [4] proved that the equation

$$F_n = m_1! + m_2! + \dots + m_k!$$

has finitely many positive integers n for fixed k . Moreover, the case $k \leq 2$ was determined. The case $k = 3$ was solved by Bollman, Hernandez and Luca in [2]. Luca and Siksek [9] found all factorials expressible as the sum of at least three Fibonacci numbers. Marques handled the different versions of the Brocard-Ramanujan equation including Fibonacci and Fibonomial coefficient (for the details see [10], [11], [12]). In what follows, Szalay [13] solved the equation

$$G_{n_1} G_{n_2} \dots G_{n_k} + 1 = G_m^2$$

where the sequence $\{G_n\}$ is either Fibonacci sequence or the Lucas sequence or the sequence of balancing numbers, respectively. Recently, the author [5] proved that the solutions of the equation

$$\sum_{k=0}^m \begin{bmatrix} 2m+1 \\ k \end{bmatrix}_F \pm 1 = F_n \tag{2}$$

are $(m, n) = (1, 3), (3, 14)$ according to the sign $-$. If the sign is $+$, then there is no solution.

In this paper we focus on the generalization of the equation [2]. Our result is following,

Theorem 1. *Let n and t are positive integers such that $n \equiv t \pmod{2}$ or $n - t = 1, 3$. The solutions of the equations*

$$\sum_{k=0}^m \begin{bmatrix} 2m+1 \\ k \end{bmatrix}_F \pm F_t = F_n \tag{3}$$

are

m	1	1	2	2
n	5	6	9	10
t	3	5	7	9

according to the sign $+$. If the sign is $-$, then the solutions are

m	1	1	2	2	4	4
n	3	1, 2	7	6	22	10
t	1, 2	3	6	7	10	22

2. PRELIMINARY

Before going further, we give several lemmas to prove our theorem.

Definition 1. A primitive divisor p of F_n is a prime factor of F_n which does not divide $\prod_{j=1}^{n-1} F_j$.

For example, we know that $29 \mid F_{14}$, but $29 \nmid \prod_{j=1}^{13} F_j$. Here, 29 is a primitive divisor of F_{14} . The following lemma guarantees the existence of a primitive divisor for the Fibonacci sequence.

Lemma 1. A primitive divisor p of F_n exists whenever $n \geq 13$ (see [3]).

We present several identities regarding Fibonacci and Lucas numbers that we will use them later.

Lemma 2. We have the following

- i. For any $k \geq 0$, then $F_k L_k = F_{2k}$.
- ii. For any $k \geq 0$, then $F_{k+3} - F_k = 2F_{k+1}$ and $F_{k+3} + F_k = 2F_{k+2}$.
- iii. Let n and t are positive integers such that $n \equiv t \pmod{2}$. Then

$$F_n \mp F_t = \begin{cases} F_{\frac{n \mp t}{2}} L_{\frac{n \pm t}{2}}, & \text{if } n \equiv t \pmod{4} \\ F_{\frac{n \pm t}{2}} L_{\frac{n \mp t}{2}} & \text{if } n \not\equiv t \pmod{4} \end{cases}$$

holds.

- iv. For any $k \geq 0$, then $3 \mid F_{4k}$.

Proof. (i) can be proven easily by using Binet formulas of the sequence Fibonacci and Lucas. By the recurrence of Fibonacci sequence, we have $F_{n+3} - F_n = F_{n+2} + F_{n+1} - F_n = 2F_{n+1}$. This proves (ii).

iii. Assume that $n \equiv t \pmod{4}$, then we have followings,

$$\begin{aligned} F_{\frac{n+t}{2}} L_{\frac{n-t}{2}} &= \frac{\alpha^{(n+t)/2} - \beta^{(n+t)/2}}{\alpha - \beta} (\alpha^{(n-t)/2} + \beta^{(n-t)/2}) \\ &= \frac{1}{\alpha - \beta} (\alpha^n - \beta^n + (\alpha\beta)^{(n-t)/2} (\alpha^t - \beta^t)) \\ &= F_n + F_t. \end{aligned}$$

iv. We refer the book of Koshy [8] (Theorem 16.1, p. 196). □

Lemma 3. *Let m be a positive integer, then the identity*

$$\sum_{k=0}^m \begin{bmatrix} 2m+1 \\ k \end{bmatrix}_F = \prod_{k=1}^m L_{2k}$$

holds (see [7]).

The proof of the following lemma is given in [6] as Lemma 2.3.

Lemma 4. *For integers $s > t > 1$, the equation*

$$F_r = F_s + F_t$$

is satisfied only for $r - 1 = s = t + 1$.

3. PROOF

Now, we will investigate the solutions of the equation (3) in two different cases $n \equiv t \pmod{2}$ and $n \not\equiv t \pmod{2}$.

3.1. The case $n \equiv t \pmod{2}$. In this case, Lemma 2 (iii) yields the following equations

$$\sum_{k=0}^m \begin{bmatrix} 2m+1 \\ k \end{bmatrix}_F = F_{\frac{n-t}{2}} L_{\frac{n+t}{2}} \tag{4}$$

or

$$\sum_{k=0}^m \begin{bmatrix} 2m+1 \\ k \end{bmatrix}_F = F_{\frac{n+t}{2}} L_{\frac{n-t}{2}}. \tag{5}$$

We will consider the equation (4). Lemma 3 yields that

$$L_2 L_4 \dots L_{2m} = F_{\frac{n-t}{2}} L_{\frac{n+t}{2}}.$$

If we multiply both sides with $F_2 F_4 \dots F_{2m}$ and $F_{\frac{n+t}{2}}$, then we have

$$\begin{aligned} (L_2 L_4 \dots L_{2m})(F_2 F_4 \dots F_{2m}) F_{\frac{n+t}{2}} &= (F_2 L_2)(F_4 L_4) \dots (F_{2m} L_{2m}) F_{\frac{n+t}{2}} \\ &= F_4 F_8 \dots F_{4m} F_{\frac{n+t}{2}} \\ &= (F_2 F_4 \dots F_{2m}) F_{\frac{n-t}{2}} (F_{\frac{n+t}{2}} L_{\frac{n+t}{2}}) \\ &= (F_2 F_4 \dots F_{2m}) F_{\frac{n-t}{2}} F_{n+t} \end{aligned}$$

where we use the fact $F_n L_n = F_{2n}$ that given in Lemma 2 (i). That is to say, we get

$$F_4 F_8 \dots F_{4m} F_{\frac{n+t}{2}} = (F_2 F_4 \dots F_{2m}) F_{\frac{n-t}{2}} F_{n+t}. \tag{6}$$

Assume that $m \geq 5$. Since $4m \geq 20$, we can use the Primitive Divisor Theorem (PDT). If $4m > n + t$, then there exists a prime p dividing F_{4m} does not divide $F_2, F_4, \dots, F_{2m}, F_{\frac{n-t}{2}}, F_{n+t}$. So, the equation (6) does not hold. Similarly, if

$4m < n + t$, then there exist a prime p such that $p \mid F_{n+t}$, but $p \nmid F_i$ where $i = 4, 8, \dots, 4m, \frac{n+t}{2}$. Since the inequalities $4m > n + t$ and $4m < n + t$ are not true, then we get $4m = n + t$. After simplifying the equation (6), then the equation

$$F_4 F_8 \dots F_{4m-4} = F_2 F_4 \dots F_{2m-2} F_{2m-t}$$

follows where we use $(n - t)/2 = 2m - t$ (because $4m = n + t$).

If m is even integer, then we have

$$F_{2m} F_{2m+4} \dots F_{4m-4} = F_{2m-t} F_2 F_6 \dots F_{2m-6} F_{2m-2}. \tag{7}$$

If m is odd integer, then

$$F_{2m+2} F_{2m+6} \dots F_{4m-4} = F_{2m-t} F_2 F_6 \dots F_{2m-8} F_{2m-4} \tag{8}$$

follows. Since $4m - 4 \geq 16$, then we apply PDT again. If $2m - t \geq 4m - 4$, then we have $4 - t \geq 2m$ which is not possible as $m \geq 5$ and t is positive integer. If $4m - 4 > 2m - t$, then there exists a prime p dividing F_{4m-4} . But $p \nmid F_j$ where $j = 2, 6, \dots, 2m - 6, 2m - 2, 2m - t$ for the equation (7). Since we arrive at a similar contradiction for the equation (8), we omit it. We get the similar calculations for the equation (5).

Therefore, $m \leq 4$. So, we have

$$\sum_{k=0}^1 \binom{3}{k}_F = 3 = F_n \mp F_t, \quad \sum_{k=0}^4 \binom{9}{k}_F = 17766 = F_n \mp F_t$$

$$\sum_{k=0}^2 \binom{5}{k}_F = 21 = F_n \mp F_t, \quad \sum_{k=0}^5 \binom{11}{k}_F = 2185218 = F_n \mp F_t.$$

Namely, we investigate the solutions of the equations

$$F_n \mp F_t = 3 \tag{9}$$

$$F_n \mp F_t = 21 \tag{10}$$

$$F_n \mp F_t = 17766 \tag{11}$$

and

$$F_n \mp F_t = 2185218 \tag{12}$$

Assume that the sign is $-$. We focus on the equations (9) and (10). Since $F_4 = 3$ and $F_8 = 21$, by Lemma 4 there is one solution of the equation $F_n - F_t = F_4 = 3$ which is $(n, t) = (5, 3)$. Similarly, the only solution of the equation $F_n - F_t = F_8 = 21$ is $(n, t) = (9, 7)$. Consider the equation (11). By Lemma 2 (iii), we have

$$F_n - F_t = F_{\frac{n+t}{2}} L_{\frac{n-t}{2}} = 17766 = 2 \cdot 3^3 \cdot 7 \cdot 47.$$

Since 17766 is not the product of two Fibonacci and Lucas number, the equation (11) has no solution. Similarly, there is no solution of the equation (12).

If the sign is $+$ for the equations (9), (10), (11) and (12), then we obtain the solutions given in the Table 1 below.

TABLE 1. Solutions of the equations $F_n + F_t = F_j$

	(n, t)
$F_n + F_t = 3$	$(3, 2), (2, 3), (3, 1), (1, 3)$
$F_n + F_t = 21$	$(6, 7), (7, 6)$
$F_n + F_t = 17766$	$(22, 10), (10, 22)$
$F_n + F_t = 2185218$	no solution

3.2. **The case $n \not\equiv t \pmod{2}$.** In this case, we will solve the equation (6) under the conditions $n - t = 1$ or $n - t = 3$.

Firstly, we will deal with the case $n - t = 1$. This yields $F_n \mp F_t$ is a Fibonacci number. Then the equation (3) turns to

$$\sum_{k=0}^m \begin{bmatrix} 2m+1 \\ k \end{bmatrix}_F = F_x \tag{13}$$

where $F_n \mp F_t = F_x$ and $x \in \mathbb{Z}^+$. After multiplying both sides with $F_2F_4 \dots F_{2m}$, we have

$$F_4F_8 \dots F_{4m} = F_2F_4 \dots F_{2m}F_x.$$

Assume that $m \geq 4$. Since $4m \geq 16$, we can use PDT which yields $4m = x$. Then,

$$F_4F_8 \dots F_{4m-4} = F_2F_4 \dots F_{2m}$$

follows which is a contradiction. Because left hand side of the equation is obviously bigger than right hand side. Now, assume $m \leq 3$.

If $m = 1$, then we have the equation $F_x = F_n \mp F_t = 3 = F_4$. We obtain $x = 4$. So, the pairs $(n, t) = (3, 2), (2, 3), (3, 1), (1, 3)$ are the solutions of the equation $F_n + F_t = 3$. The pair $(n, t) = (6, 5)$ is the only solution of the equation $F_n - F_t = 3$ by Lemma 4.

If $m = 2$, then we get $F_x = F_n \mp F_t = 21 = F_8$. We get $x = 8$. The solutions of $F_n + F_t = 21$ are $(n, t) = (6, 7), (7, 6)$. The pair $(n, t) = (10, 9)$ is the only solution of the equation $F_n - F_t = 21$.

If $m = 3$, then we obtain $L_2L_4L_6 = 378$ which is not a Fibonacci number. That is, the equation (3.2) is not satisfied.

Now, assume that $n - t = 3$. Firstly, we handle the equation

$$\sum_{k=0}^m \begin{bmatrix} 2m+1 \\ k \end{bmatrix}_F + F_t = F_n.$$

By Lemma 2 (ii), we have

$$\sum_{k=0}^m \begin{bmatrix} 2m+1 \\ k \end{bmatrix}_F = L_2L_4 \dots L_{2m} = F_n - F_t = 2F_{n-2}.$$

After multiplying both sides with $F_2F_4 \dots F_{2m}$, we get

$$F_4F_8 \dots F_{4m} = F_2F_4 \dots F_{2m}2F_{n-2}. \quad (14)$$

Assume that $m \geq 4$. By PDT, there exists a primitive divisor p such that $p \mid F_{4m}$. If $p = 2$, then p can not be a primitive divisor since, at least, $2 \mid F_6$. This yields that $p \neq 2$. If $4m > n - 2$, then $p \nmid F_2F_4 \dots F_{2m}2F_{n-2}$ which is not possible. We get the similar contradiction if $n - 2 > 4m$. So, we deduce $4m = n - 2$. Then the equation (14) reduces to

$$L_2L_4 \dots L_{2m-2} = 2F_{2m}. \quad (15)$$

where we use the fact $F_{2n} = F_nL_n$. This is not possible for $m \geq 4$. Because left hand side of the equation (15) is greater than right hand side. Now, we assume $m \leq 3$. So, we have to solve the following equation

$$2F_{n-2} = q$$

where $q \in \{L_2 = 3, L_2L_4 = 21, L_2L_4L_6 = 378\}$. Obviously, there is no solution. We arrive at similar contradictions for the equation

$$\sum_{k=0}^m \left[\begin{matrix} 2m+1 \\ k \end{matrix} \right]_F = L_2L_4 \dots L_{2m} = F_n + F_t = 2F_{n-1}.$$

We do not give its details.

Finally, we complete the proof.

Declaration of Competing Interests The author declares that he has no competing interest.

Acknowledgements The author expresses his gratitude to the anonymous reviewers for the instructive suggestions and remarks.

REFERENCES

- [1] Berndt, B. C., Galway, W., The Brocard–Ramanujan diophantine equation $n! + 1 = m^2$, *Ramanujan J.*, 4 (2000), 41–42. <https://doi.org/10.1023/A:1009873805276>
- [2] Bollman, M., Hernandez, H. S., Luca, F., Fibonacci numbers which are sums of three factorials, *Publ. Math. Debrecen*, 77 (2010), 211–224.
- [3] Carmichael, R. D., On the numerical factors of the arithmetics forms $\alpha^n \pm \beta^n$, *Annals Math.*, 2(15) (1913), 30–70.
- [4] Grossman, G., Luca, F., Sums of factorials in binary recurrence sequences, *J. Number Theory*, 93 (2002), 87–107. <https://doi.org/10.1006/jnth.2001.2718>
- [5] Irmak, N., Sum of the Fibonomial coefficients at most one away from Fibonacci numbers, *Math. Reports*, 18(68)(4) (2016), 567–571.
- [6] Irmak, N., Şiar, Z., Keskin, R., On the sum of the three arbitrary Fibonacci and Lucas numbers, *Notes Numbers Theory Discrete Math.*, 25(4) (2019), 96–101. <https://doi.org/10.7546/nntdm.2019.25.4.96-101>
- [7] Kilic, E., Akkuş, I., Ohtsuka, H., Some generalized Fibonomial sums related with the Gaussian q -Binomial sum, *Bull. Math. Soc. Sci. Math. Roumanie Tome*, 55(103)(1) (2012), 51–61.

- [8] Koshy, T., *Fibonacci and Lucas Numbers with Applications*, John Wiley and Sons, Proc., New York-Toronto, 2001.
- [9] Luca, F., Siksek, S., Factorials expressible as sums of at most three Fibonacci numbers, *Proc. of the Edinburgh Math. Soc.*, 53 (2010), 679–729. <https://doi.org/10.1017/S0013091508000874>
- [10] Marques, D., Fibonomial coefficients at most one away from Fibonacci Numbers, *Demonstratio Math.*, 45(1) (2012), 25–28. <https://doi.org/10.1515/dema-2013-0360>
- [11] Marques, D., The Fibonacci version of a variant the Brocard-Ramanujan Diophantine equation, *Far East J. Math. Sci.*, 56(2) (2011), 219–224.
- [12] Marques, D., The Fibonacci version of the Brocard-Ramanujan Diophantine equation, *Portugal. Math.*, 68(2) (2011), 185–189. <https://doi.org/10.4171/PM/1887>
- [13] Szalay, L., Diophantine equations with binary recurrences associated to Brocard-Ramanujan problem, *Portugal. Math.*, 69 (2012), 213–220. <https://doi.org/10.4171/PM/1914>



BMO ESTIMATE FOR THE HIGHER ORDER COMMUTATORS OF MARCINKIEWICZ INTEGRAL OPERATOR ON GRAND VARIABLE HERZ-MORREY SPACES

Babar SULTAN¹, Mehvish SULTAN² and Ferit GÜRBÜZ³

¹Department of Mathematics, Quaid-I-Azam University 45320, Islamabad 44000, PAKISTAN

²Department of Mathematics, Capital University Of Science and Technology,
Islamabad, PAKISTAN

³Department of Mathematics, Kırklareli University, Kırklareli 39100, TÜRKİYE

ABSTRACT. Let \mathbb{S}^{n-1} denote the unit sphere in \mathbb{R}^n with the normalized Lebesgue measure. Let $\Phi \in L^r(\mathbb{S}^{n-1})$ is a homogeneous function of degree zero and b is a locally integrable function on \mathbb{R}^n . In this paper we define the higher order commutators of Marcinkiewicz integral $[b, \mu_\Phi]^m$ and prove the boundedness of $[b, \mu_\Phi]^m$ under some proper assumptions on grand variable Herz-Morrey spaces $M\dot{K}_{u,v(\cdot)}^{\alpha(\cdot),\beta}(\mathbb{R}^n)$.

1. INTRODUCTION

Function spaces with variable exponents are an essential tools in harmonic analysis, operator theory and have gained significant attention in recent years, some instances of these works are in [3, 23]. The study of variable exponent function spaces is closely related to operator theory, which deals with linear operators acting on function spaces. In particular, the boundedness and compactness properties of operators in variable exponent spaces are of great interest. Understanding these properties is crucial for solving partial differential equations and analyzing various problems in applied mathematics.

The first generalization of Herz spaces with variable exponents, along with the proof of boundedness for sublinear operators in these spaces, was presented in [7].

2020 *Mathematics Subject Classification.* 46E30,47B38.

Keywords. BMO spaces, Marcinkiewicz integral operator, grand Herz-Morrey spaces, grand Herz spaces.

¹✉ babarsultan40@yahoo.com; 0000-0003-2833-4101

²✉ mehvishsultanbaz@gmail.com; 0009-0005-2379-0476

³✉ feritgurbuz@klu.edu.tr-Corresponding author; 0000-0003-3049-688X.

Herz-Morrey spaces, on the other hand, are further generalization of Herz spaces with variable exponents. The author in [6] introduced this class of function spaces. Continual Herz spaces with variable exponents were defined and studied in [14]. Understanding the boundedness of sublinear operators is of particular interest, its boundedness on continual Herz spaces can be seen in [14].

The concept of grand Morrey spaces, along with the boundedness of a class of integral operators in these spaces, were introduced in [10]. The author established the boundedness results for a specific class of integral operators, in newly defined grand Morrey spaces.

The idea of grand Herz spaces was introduced in [12]. This work expanded upon the classical Herz spaces by incorporating additional parameters. To explore the boundedness properties of other operators in grand variable Herz spaces, [2, 13, 18, 21, 22] can be consulted. These works likely provide insights into the boundedness of specific operators in the context of grand variable Herz spaces, enriching our understanding of the behavior of operators in this framework.

Subsequently, in the context of Herz-Morrey spaces with variable exponents, the concept of grand variable Herz-Morrey spaces were introduced in [17, 19]. These function spaces further extended the framework of Herz-Morrey spaces by incorporating the variable exponent setting. The authors demonstrated the boundedness of the Riesz potential operator in the newly defined grand variable Herz-Morrey spaces. Finally, in the article mentioned, the authors demonstrated the boundedness of higher-order commutators of the Marcinkiewicz integral operator in grand variable Herz-Morrey spaces. This result further explores the behavior of commutators in the context of grand variable Herz-Morrey spaces and contributes to the broader understanding of these function spaces.

Dividing the article into different sections helps to organize and present the material in a structured manner. Introduction provides an overview of the topic. A section presents the necessary mathematical background, definitions and relevant lemmas. Last section is dedicated to the main results of the article. It discusses the boundedness of the higher order commutators of the Marcinkiewicz integral operator in the context of grand variable Herz-Morrey spaces.

2. PRELIMINARIES

It is worth noting that the Lebesgue space with variable exponent $L^{p(\cdot)}(H)$ inherits many properties from the classical Lebesgue spaces with constant exponents. We can define the Lebesgue space with variable exponent $L^{p(\cdot)}(H)$ as the set of all measurable functions f defined on a measurable set H such that the norm is finite. Consider a measurable set H in \mathbb{R}^n and a measurable function $p(\cdot) : H \rightarrow [1, \infty)$.

Definition 1. *If H be a measurable set in \mathbb{R}^n and $p(\cdot) : H \rightarrow [1, \infty)$ be a measurable function. We suppose that*

$$1 \leq p_-(H) \leq p(h) \leq p_+(H) < \infty, \quad (1)$$

where $p_- := \operatorname{ess\,inf}_{h \in H} p(h)$, $p_+ := \operatorname{ess\,sup}_{h \in H} p(h)$.

(a) Lebesgue space with variable exponent $L^{p(\cdot)}(H)$ is defined as

$$L^{p(\cdot)}(H) = \left\{ f \text{ measurable} : \int_H \left(\frac{|f(y)|}{\gamma} \right)^{p(y)} dy < \infty, \text{ where } \gamma \text{ is a constant} \right\}.$$

Norm in $L^{p(\cdot)}(H)$ is defined as

$$\|f\|_{L^{p(\cdot)}(H)} = \inf \left\{ \gamma > 0 : \int_H \left(\frac{|f(y)|}{\gamma} \right)^{p(y)} dy \leq 1 \right\}.$$

(b) The space $L_{\text{loc}}^{p(\cdot)}(H)$ is defined as

$$L_{\text{loc}}^{p(\cdot)}(H) := \left\{ f : f \in L^{p(\cdot)}(K) \text{ for all compact subsets } K \subset H \right\}.$$

In the sequel we use the well known log-condition

$$|p(x) - p(y)| \leq \frac{C(p)}{-\ln|x-y|}, \quad |x-y| \leq \frac{1}{2}, \quad x, y \in H, \quad (2)$$

where $C(p) > 0$. And the decay condition: there exists a number $p_\infty \in (1, \infty)$, such that

$$|p(h) - p_\infty| \leq \frac{C}{\ln(e+|h|)}, \quad (3)$$

and also decay condition

$$|p(h) - p_0| \leq \frac{C}{-\ln|h|}, \quad |h| \leq \frac{1}{2}, \quad (4)$$

holds for some $p_0 \in (1, \infty)$. (Note that: $C > 0$ & $|h| \leq \frac{1}{2} \Rightarrow \frac{C}{\ln|h|} < 0$).

We use these notations in this article:

- (i) The set $\mathcal{P}(H)$ consists of all measurable functions $p(\cdot)$ satisfying (1).
- (ii) $\mathcal{P}^{\log} = \mathcal{P}^{\log}(H)$ consists of all functions $p \in \mathcal{P}(H)$ satisfying (1) and (2).
- (iii) $\mathcal{P}_\infty(H)$ and $\mathcal{P}_{0,\infty}(H)$ are the subsets of $\mathcal{P}(H)$ and values of these subsets lies in $[1, \infty)$ which satisfy the condition (3) and both conditions (3) and (4) respectively.
- (iv)

$$\chi_l = \chi_{R_l}, \quad R_l = B_l \setminus B_{l-1}, \quad B_l = B(0, 2^l) = \{x \in \mathbb{R}^n : |x| < 2^l\}$$

for all $l \in \mathbb{Z}$.

C is a positive constant, its value can change from line to line and is independent of main parameters involved.

Now we will define variable exponent Herz spaces.

Definition 2. Let $u, v \in [1, \infty)$, $\alpha \in \mathbb{R}$, the norms of classical versions of non-homogeneous and homogeneous Herz spaces are given below,

$$\|g\|_{K_{u,v}^\alpha(\mathbb{R}^n)} := \|g\|_{L^u(B(0,1))} + \left\{ \sum_{l \in \mathbb{N}} 2^{l\alpha v} \left(\int_{R_{2^{l-1}, 2^l}} |g(y)|^u dy \right)^{\frac{v}{u}} \right\}^{\frac{1}{v}}, \quad (5)$$

where

$$\|g\|_{\dot{K}_{u,v}^\alpha(\mathbb{R}^n)} := \left\{ \sum_{l \in \mathbb{Z}} 2^{l\alpha v} \left(\int_{R_{2^{l-1}, 2^l}} |g(y)|^u dy \right)^{\frac{v}{u}} \right\}^{\frac{1}{v}}, \quad (6)$$

respectively.

Definition 3. Let $u \in [1, \infty)$, $v(\cdot) \in \mathcal{P}(\mathbb{R}^n)$ and $\alpha \in \mathbb{R}$. The homogeneous version of variable exponent Herz space $\dot{K}_{v(\cdot)}^{\alpha,u}(\mathbb{R}^n)$ can be defined as

$$\dot{K}_{v(\cdot)}^{\alpha,u}(\mathbb{R}^n) = \left\{ g \in L_{\text{loc}}^{v(\cdot)}(\mathbb{R}^n \setminus \{0\}) : \|g\|_{\dot{K}_{v(\cdot)}^{\alpha,u}(\mathbb{R}^n)} < \infty \right\}, \quad (7)$$

where

$$\|g\|_{\dot{K}_{v(\cdot)}^{\alpha,u}(\mathbb{R}^n)} = \left(\sum_{l=-\infty}^{\infty} \|2^{l\alpha} g \chi_l\|_{L^{v(\cdot)}}^u \right)^{\frac{1}{u}}.$$

Definition 4. Let $u \in [1, \infty)$, $\alpha \in \mathbb{R}$ and $v(\cdot) \in \mathcal{P}(\mathbb{R}^n)$. The non-homogeneous version of variable exponent Herz space $K_{v(\cdot)}^{\alpha,u}(\mathbb{R}^n)$ can be defined as

$$K_{v(\cdot)}^{\alpha,u}(\mathbb{R}^n) = \left\{ g \in L_{\text{loc}}^{v(\cdot)}(\mathbb{R}^n \setminus \{0\}) : \|g\|_{K_{v(\cdot)}^{\alpha,u}(\mathbb{R}^n)} < \infty \right\}, \quad (8)$$

where

$$\|g\|_{K_{v(\cdot)}^{\alpha,u}(\mathbb{R}^n)} = \|g\|_{L^{v(\cdot)}(B(0,1))} + \left(\sum_{k=-\infty}^{\infty} \|2^{k\alpha} g \chi_k\|_{L^{v(\cdot)}}^u \right)^{\frac{1}{u}}.$$

Definition 5. Let $\alpha(\cdot) \in L^\infty(\mathbb{R}^n)$, $u \in [1, \infty)$, $q : \mathbb{R}^n \rightarrow [1, \infty)$, $\theta > 0$. A grand variable Herz spaces $\dot{K}_{q(\cdot)}^{\alpha(\cdot),u,\theta}$ are defined by,

$$\dot{K}_{q(\cdot)}^{\alpha(\cdot),u,\theta} = \left\{ g \in L_{\text{loc}}^{q(\cdot)}(\mathbb{R}^n \setminus \{0\}) : \|g\|_{\dot{K}_{q(\cdot)}^{\alpha(\cdot),u,\theta}} < \infty \right\},$$

where

$$\|g\|_{\dot{K}_{q(\cdot)}^{\alpha(\cdot),u,\theta}} = \sup_{\epsilon > 0} \left(\epsilon^\theta \sum_{k \in \mathbb{Z}} 2^{k\alpha(\cdot)u(1+\epsilon)} \|g \chi_k\|_{L^{q(\cdot)}}^{u(1+\epsilon)} \right)^{\frac{1}{u(1+\epsilon)}}.$$

Now we will define variable Herz-Morrey spaces.

Definition 6. For $\alpha(\cdot) : \mathbb{R}^n \rightarrow \mathbb{R}$, $0 < u < \infty$, $v(\cdot) \in \mathcal{P}(\mathbb{R}^n)$ and $0 \leq \beta < \infty$. A variable Herz-Morrey spaces $M\dot{K}_{u,v(\cdot)}^{\alpha(\cdot),\beta}(\mathbb{R}^n)$ are defined by,

$$M\dot{K}_{u,v(\cdot)}^{\alpha(\cdot),\beta}(\mathbb{R}^n) = \left\{ g \in L_{loc}^{v(\cdot)}(\mathbb{R}^n \setminus \{0\}) : \|g\|_{M\dot{K}_{u,v(\cdot)}^{\alpha(\cdot),\beta}(\mathbb{R}^n)} < \infty \right\},$$

where

$$\|g\|_{M\dot{K}_{u,v(\cdot)}^{\alpha(\cdot),\beta}(\mathbb{R}^n)} = \sup_{k_0 \in \mathbb{Z}} 2^{-k_0\beta} \left(\sum_{t=-\infty}^{k_0} 2^{k\alpha(\cdot)u} \|g\chi_k\|_{L^{v(\cdot)}(\mathbb{R}^n)}^u \right)^{\frac{1}{u}}.$$

Definition 7. To define homogeneous version of GVHM spaces, let $s : \mathbb{R}^n \rightarrow [1, \infty)$, $u \in [1, \infty)$, $\theta > 0$, $0 \leq \lambda < \infty$, and $\alpha(\cdot) \in L^\infty(\mathbb{R}^n)$. The GVHM spaces are given by:

$$M\dot{K}_{\lambda,s(\cdot)}^{\alpha(\cdot),u,\theta}(\mathbb{R}^n) = \left\{ g \in L_{loc}^{s(\cdot)}(\mathbb{R}^n \setminus \{0\}) : \|g\|_{M\dot{K}_{\lambda,s(\cdot)}^{\alpha(\cdot),u,\theta}(\mathbb{R}^n)} < \infty \right\},$$

where

$$\|g\|_{M\dot{K}_{\lambda,s(\cdot)}^{\alpha(\cdot),u,\theta}(\mathbb{R}^n)} = \sup_{\epsilon > 0} \sup_{l_0 \in \mathbb{Z}} 2^{-l_0\lambda} \left(\epsilon^\theta \sum_{k=-\infty}^{l_0} 2^{k\alpha(\cdot)u(1+\epsilon)} \|g\chi_k\|_{L^{s(\cdot)}(\mathbb{R}^n)}^{u(1+\epsilon)} \right)^{\frac{1}{u(1+\epsilon)}}.$$

Non-homogeneous version of GVHM spaces can be defined in the similar way. As grand variable Herz-Morrey spaces is the generalization of grand variable Herz spaces, $\lambda = 0$, grand variable Herz-Morrey spaces become grand variable Herz spaces.

Definition 8 (BMO space). A BMO function is a locally integrable function u whose mean oscillation given by $\frac{1}{|B|} \int_B |u(y) - u_B| dy$ is bounded, i.e.

$$\|u\|_{BMO} = \sup_B \frac{1}{|B|} \int_B |u(y) - u_B| dy < \infty.$$

Lemma 1. [14] Let $B > 1$ and $p \in \mathcal{P}_{0,\infty}(\mathbb{R}^n)$. Then

$$\frac{1}{t_0} s^{\frac{n}{p(0)}} \leq \|\chi_{R_{s,B_s}}\|_{p(\cdot)} \leq t_0 s^{\frac{n}{p(0)}}, \text{ for } 0 < s \leq 1 \tag{9}$$

and

$$\frac{1}{t_\infty} s^{\frac{n}{p_\infty}} \leq \|\chi_{R_{s,B_s}}\|_{p(\cdot)} \leq t_\infty s^{\frac{n}{p_\infty}}, \text{ for } s \geq 1, \tag{10}$$

respectively, where $t_0 \geq 1$ and $t_\infty \geq 1$ and depending on B but independent of s .

Lemma 2. [23][Generalized Hölder's inequality] Consider a measurable subset H such that $H \subseteq \mathbb{R}^n$, and $1 \leq p_-(H) \leq p_+(H) \leq \infty$. Then

$$\|fg\|_{L^{r(\cdot)}(H)} \leq \|f\|_{L^{p(\cdot)}(H)} \|g\|_{L^{q(\cdot)}(H)}$$

holds, where $f \in L^{p(\cdot)}(H)$, $g \in L^{q(\cdot)}(H)$ and $\frac{1}{r(x)} = \frac{1}{p(x)} + \frac{1}{q(x)}$ for every $x \in H$.

Lemma 3. [8] *Let k be a positive integer. Let $b \in BMO(\mathbb{R}^n)$ and choose $w, l \in \mathbb{Z}$ with $l < w$,*

$$\frac{1}{C} \|b\|_{BMO}^k \leq \sup_{B:ball} \frac{1}{\|\chi_B\|_{p(\cdot)}} \|(b - b_B)^k \chi_B\|_{p(\cdot)} \tag{11}$$

$$\leq C \|b\|_{BMO}^k, \tag{12}$$

$$\|(b - b_{B_t})^k \chi_{B_w}\|_{p(\cdot)} \leq C(w - t)^k \|b\|_{BMO}^k \|\chi_{B_w}\|_{p(\cdot)}. \tag{13}$$

Let \mathbb{S}^{n-1} denote the unit sphere in \mathbb{R}^n with the normalized Lebesgue measure. Let $\Phi \in L^r(\mathbb{S}^{n-1})$ is a homogeneous function of degree zero such that

$$\int_{\mathbb{S}^{n-1}} \Phi(y') d\sigma(y') = 0, \tag{14}$$

where $y' = y/|y|$ and y is not zero. The Marcinkiewicz fractional operator is introduced with Littlewood-Paley g -function as:

$$\mu_\Phi(f)(x) = \left(\int_0^\infty |F_{\Phi,s}(f)(x)|^2 \frac{ds}{s^3} \right)^{\frac{1}{2}},$$

where

$$F_{\Phi,s}(f)(x) = \int_{|x-y| \leq s} \frac{\Phi(x-y)}{|x-y|^{n-1}} f(y) dy.$$

Consider a locally integrable function b on \mathbb{R}^n , now we can define higher order commutators of Marcinkiewicz integral $[b, \mu_\Phi]^m$ by using μ_Φ and b

$$[b, \mu_\Phi]^m(f)(x) = \left(\int_0^\infty \left| \int_{|x-y| \leq s} \frac{\Phi(x-y)}{|x-y|^{n-1}} [b(x) - b(y)]^m f(y) dy \right|^2 \frac{ds}{s^3} \right)^{\frac{1}{2}}.$$

Lemma 4. [11] *Let $a > 0$, $s \in [1, \infty]$, $0 < d \leq s$ and $-n + (n-1)\frac{d}{s} < u < \infty$, then*

$$\left(\int_{|y| \leq a|x|} |y|^u |\Phi(x-y)|^d dy \right)^{1/d} \leq |x|^{(u+n)/d} \|\Phi\|_{L^s(\mathbb{S}^{n-1})}.$$

It is easy to see that for $m = 1$, we get $[b, \mu_\Phi]^m(f)(x) = [b, \mu_\Phi](f)(x)$ (commutator of Marcinkiewicz integral operator defined in [25]). When $m = 0$, the higher order commutators of Marcinkiewicz integral operator will be simply Marcinkiewicz integrals operator.

It's worth noting that the specific details and advancements in these works can only be fully explored by referring to the papers [\[1, 4, 5, 9, 15, 16, 20, 24\]](#).

3. BMO ESTIMATE FOR THE HIGHER ORDER COMMUTATORS OF MARCINKIEWICZ INTEGRALS OPERATOR

The main purpose of this paper is to establish the boundedness of higher order commutators of Marcinkiewicz fractional operator on grand variable Herz-Morrey spaces by using some properties of the variable exponent and BMO function. It is easy to see that our results generalize the main results of [\[13\]](#). Now, we will show the boundedness of higher order commutators of Marcinkiewicz integrals operator on grand variable Herz-Morrey spaces.

Theorem 1. *Let $0 < v \leq 1$, $\alpha(\cdot), q(\cdot) \in \mathcal{P}_{0,\infty}(\mathbb{R}^n)$ with $1 < q^- \leq q^+ < \infty$, $m \in \mathbb{Z}$, $1 \leq u < \infty$, $0 \leq \beta < \infty$ and $b \in BMO(\mathbb{R}^n)$. Let Φ be a homogeneous of degree zero and $\Phi \in L^s(\mathbb{S}^{n-1})$, $s > q'^-$. Let α be such that :*

- (i) $-\frac{n}{q(0)} - v - \frac{n}{s} < \alpha(0) < \frac{n}{q'(0)} - v - \frac{n}{s}$
- (ii) $-\frac{n}{q_\infty} - v - \frac{n}{s} < \alpha_\infty < \frac{n}{q'_\infty} - v - \frac{n}{s}$,

then operator $[b, \mu_\Phi]^m$ will be bounded on $M\dot{K}_{\beta, q(\cdot)}^{\alpha(\cdot), u, \theta}(\mathbb{R}^n)$.

Proof. Let $g \in M\dot{K}_{\beta, q(\cdot)}^{\alpha(\cdot), u, \theta}(\mathbb{R}^n)$, and $g(x) = \sum_{l=-\infty}^{\infty} g(x)\chi_l(x) = \sum_{l=-\infty}^{\infty} g_l(x)$, for $k_0 > 0$ we have,

$$\begin{aligned} & \| [b, \mu_\Phi]^m g \|_{M\dot{K}_{\beta, q(\cdot)}^{\alpha(\cdot), u, \theta}(\mathbb{R}^n)} = \sup_{\epsilon > 0} \sup_{k_0 \in \mathbb{Z}} 2^{-k_0 \beta} \\ & \quad \times \left(\epsilon^\theta \sum_{t=-\infty}^{k_0} 2^{t\alpha(\cdot)u(1+\epsilon)} \| \chi_t [b, \mu_\Phi]^m g \|_{L^{q(\cdot)}}^{u(1+\epsilon)} \right)^{\frac{1}{u(1+\epsilon)}} \\ & \leq \sup_{\epsilon > 0} \sup_{k_0 \in \mathbb{Z}} 2^{-k_0 \beta} \left(\epsilon^\theta \sum_{t=-\infty}^{k_0} 2^{t\alpha(\cdot)u(1+\epsilon)} \left(\sum_{l=-\infty}^{\infty} \| \chi_t [b, \mu_\Phi]^m g_l \|_{L^{q(\cdot)}}^{u(1+\epsilon)} \right) \right)^{\frac{1}{u(1+\epsilon)}} \\ & \leq \sup_{\epsilon > 0} \sup_{k_0 \in \mathbb{Z}} 2^{-k_0 \beta} \left(\epsilon^\theta \sum_{t=-\infty}^{k_0} 2^{t\alpha(\cdot)u(1+\epsilon)} \left(\sum_{l=-\infty}^t \| \chi_t [b, \mu_\Phi]^m g_l \|_{L^{q(\cdot)}} \right)^{u(1+\epsilon)} \right)^{\frac{1}{u(1+\epsilon)}} \\ & + \sup_{\epsilon > 0} \sup_{k_0 \in \mathbb{Z}} 2^{-k_0 \beta} \left(\epsilon^\theta \sum_{t=-\infty}^{k_0} 2^{t\alpha(\cdot)u(1+\epsilon)} \left(\sum_{l=t+1}^{\infty} \| \chi_t [b, \mu_\Phi]^m g_l \|_{L^{q(\cdot)}} \right)^{u(1+\epsilon)} \right)^{\frac{1}{u(1+\epsilon)}} \\ & =: E_1 + E_2. \end{aligned}$$

Apply Minkowski's inequality to split E_1 .

$$\begin{aligned}
 E_1 &\leq \sup_{\epsilon > 0} \sup_{k_0 \in \mathbb{Z}} 2^{-k_0\beta} \left(\epsilon^\theta \sum_{t=-\infty}^{-1} 2^{t\alpha(\cdot)u(1+\epsilon)} \left(\sum_{l=-\infty}^t \|\chi_t[b, \mu_\Phi]^m g_l\|_{L^{q(\cdot)}} \right)^{u(1+\epsilon)} \right)^{\frac{1}{u(1+\epsilon)}} \\
 &+ \sup_{\epsilon > 0} \sup_{k_0 \in \mathbb{Z}} 2^{-k_0\beta} \left(\epsilon^\theta \sum_{t=0}^{k_0} 2^{t\alpha(\cdot)u(1+\epsilon)} \left(\sum_{l=-\infty}^t \|\chi_t[b, \mu_\Phi]^m g_l\|_{L^{q(\cdot)}} \right)^{u(1+\epsilon)} \right)^{\frac{1}{u(1+\epsilon)}} \\
 &:= E_{11} + E_{12}.
 \end{aligned}$$

We use the facts that, for each $t \in \mathbb{Z}$ and $l \leq t$ and a.e. $x \in R_t, y \in R_l$, we know that $|x - y| \approx |x| \approx 2^t$.

$$\begin{aligned}
 |\mu_\Phi(g\chi_l)(x)| &\leq \left(\int_0^{|x|} \int_{|x-y|\leq t} \frac{\Phi(x-y)}{|x-y|^{n-1}} [b(x-b(y))]^m g_l(y) dy \left| \frac{dt}{t^3} \right|^2 \right)^{1/2} \\
 &+ \left(\int_{|x|}^\infty \int_{|x-y|\leq t} \frac{\Phi(x-y)}{|x-y|^{n-1}} [b(x-b(y))]^m g_l(y) dy \left| \frac{dt}{t^3} \right|^2 \right)^{1/2} \\
 &=: I_{11} + I_{12}.
 \end{aligned}$$

By the virtue of mean value theorem we obtain,

$$\left| \frac{1}{|x-y|^2} - \frac{1}{|x|^2} \right| \leq \frac{|y|}{|x-y|^3}. \tag{15}$$

For I_{11} , by using Minkowski's inequality, generalized Hölder's inequality, and inequality [15](#) we have

$$\begin{aligned}
 I_{11} &\leq \int_{\mathbb{R}^n} \frac{|\Phi(x-y)|}{|x-y|^{n-1}} |b(x-b(y))^m g_l(y)| \left(\int_{|x-y|}^{|x|} \frac{dt}{t^3} \right)^{1/2} dy \\
 &\leq \int_{\mathbb{R}^n} \frac{|\Phi(x-y)|}{|x-y|^{n-1}} |b(x-b(y))^m g_l(y)| \left| \frac{1}{|x-y|^2} - \frac{1}{|x|^2} \right|^{1/2} dy \\
 &\leq \int_{\mathbb{R}^n} \frac{|\Phi(x-y)|}{|x-y|^{n-1}} |b(x-b(y))^m g_l(y)| \left| \frac{|y|}{|x-y|^3} \right|^{1/2} dy \\
 &\leq \frac{2^{l/2}}{|x|^{n+1/2}} \int_{R_l} |\Phi(x-y)| |b(x-b(y))^m g_l(y)| dy
 \end{aligned}$$

$$\begin{aligned} &\leq 2^{(l-t)/2} 2^{-tn} \left\{ |b(x) - b_{B_l}|^m \int_{R_l} |\Phi(x - y)| |g_l(y)| dy \right. \\ &+ \int_{R_l} |b(y) - b_{B_l}|^m |\Phi(x - y)| |g_l(y)| dy \\ &\leq 2^{(l-t)/2} 2^{-tn} \|g_l\|_{L^q(\cdot)} \left\{ |b(x) - b_{B_l}|^m \|\Phi(x - \cdot)\chi_l(\cdot)\|_{L^{q'}(\cdot)} \right. \\ &\left. + \|(b(\cdot) - b_{B_l})^m (\Phi(x - \cdot)\chi_l(\cdot))\|_{L^{q'}(\cdot)} \right\}. \end{aligned}$$

Similarly, we can consider I_{12} , we have

$$\begin{aligned} I_{12} &\leq \int_{\mathbb{R}^n} \frac{|\Phi(z - 1 - y)|}{|x - y|^{n-1}} |b(x - b(y))^m| |g_l(y)| \left(\int_{|x|}^{\infty} \frac{dt}{t^3} \right)^{1/2} dy \\ &\leq \int_{\mathbb{R}^n} \frac{|\Phi(x - y)|}{|x - y|^n} |b(x) - b(y)|^m |g_l(y)| dy \\ &\leq |x|^{-n} \int_{R_l} |\Phi(x - y)| |b(x) - b(y)|^m |g_l(y)| dy \\ &\leq 2^{-tn} \|g_l\|_{L^q(\cdot)} \left\{ |b(x) - b_{B_l}|^m \|\Phi(x - \cdot)\chi_l(\cdot)\|_{L^{q'}(\cdot)} \right. \\ &\left. + \|(b(\cdot) - b_{B_l})^m (\Phi(x - \cdot)\chi_l(\cdot))\|_{L^{q'}(\cdot)} \right\}. \end{aligned}$$

So we have,

$$\begin{aligned} &|\mu_{\Phi}(g\chi_l)(x)| \\ &\leq 2^{-tn} \|g_l\|_{L^q(\cdot)} \left\{ |b(x) - b_{B_l}|^m \|\Phi(x - \cdot)\chi_l(\cdot)\|_{L^{q'}(\cdot)} \right. \\ &\left. + \|(b(\cdot) - b_{B_l})^m (\Phi(x - \cdot)\chi_l(\cdot))\|_{L^{q'}(\cdot)} \right\}. \end{aligned}$$

We define $q(\cdot)$ by the relation $\frac{1}{q'(\cdot)} = \frac{1}{q(\cdot)} + \frac{1}{s}$. By using Lemma (4) and generalized Hölder's inequality we have

$$\begin{aligned} \|\Phi(x - \cdot)\chi_l(\cdot)\|_{L^{q'}(\cdot)} &\leq \|\Phi(x - \cdot)\chi_l(\cdot)\|_{L^s(\mathbb{R}^n)} \|\chi_l(\cdot)\|_{L^q(\cdot)} \\ &\leq 2^{-lv} \left(\int_{2^{l-1} < |y| < 2^l} |\Phi(x - y)|^s |y|^{sv} dy \right)^{1/s} \|\chi_{B_l}\|_{L^q(\cdot)} \\ &\leq 2^{-lv} 2^{t(v + \frac{n}{s})} \|\Phi\|_{L^s(\mathbb{S}^{n-1})} \|\chi_{B_l}\|_{L^q(\cdot)}. \end{aligned}$$

Similarly, by using Lemma [3](#) we have

$$\begin{aligned} & \| (b(\cdot) - b_{B_l})^m (\Phi(x - \cdot) \chi_l(\cdot)) \|_{L^{q'(\cdot)}} \\ & \leq \| \Phi(x - \cdot) \chi_l(\cdot) \|_{L^s(\mathbb{R}^n)} \| (b(\cdot) - b_{B_l})^m \chi_l(\cdot) \|_{L^{q(\cdot)}} \\ & \leq C \| b \|_{BMO(\mathbb{R}^n)}^m \| \chi_{B_l} \|_{L^{q(\cdot)}} \| \Phi(x - \cdot) \chi_l(\cdot) \|_{L^s(\mathbb{R}^n)} \\ & \leq C \| b \|_{BMO(\mathbb{R}^n)}^m 2^{-lv} 2^{t(v + \frac{n}{s})} \| \Phi \|_{L^s(\mathbb{S}^{n-1})} \| \chi_{B_l} \|_{L^{q(\cdot)}}. \end{aligned}$$

As a result we get

$$\begin{aligned} & \| [b, \mu_\Phi(g_l)] \chi_t \|_{L^{q(\cdot)}} \\ & \leq C 2^{-tn} \| g_l \|_{L^{q(\cdot)}} \left\{ \| (b(\cdot) - b_{B_l})^m \chi_t(\cdot) \|_{L^{q(\cdot)}} 2^{-lv} 2^{t(v + \frac{n}{s})} \| \Phi \|_{L^s(\mathbb{S}^{n-1})} \| \chi_{B_l} \|_{L^{q(\cdot)}} \right. \\ & \quad \left. + \| b \|_{BMO(\mathbb{R}^n)}^m 2^{-lv} 2^{t(v + \frac{n}{s})} \| \Phi \|_{L^s(\mathbb{S}^{n-1})} \| \chi_{B_l} \|_{L^{q(\cdot)}} \| \chi_t \|_{L^{q(\cdot)}} \right\} \\ & \leq C 2^{-tn} \| g_l \|_{L^{q(\cdot)}} \left\{ (t - l)^m \| b \|_{BMO(\mathbb{R}^n)}^m \| \chi_{B_t} \|_{L^{q(\cdot)}} 2^{-lv} 2^{t(v + \frac{n}{s})} \| \Phi \|_{L^s(\mathbb{S}^{n-1})} \| \chi_{B_l} \|_{L^{q(\cdot)}} \right. \\ & \quad \left. + \| b \|_{BMO(\mathbb{R}^n)}^m 2^{-lv} 2^{t(v + \frac{n}{s})} \| \Phi \|_{L^s(\mathbb{S}^{n-1})} \| \chi_{B_l} \|_{L^{q(\cdot)}} \| \chi_{B_t} \|_{L^{q(\cdot)}} \right\} \\ & \leq C 2^{-tn} \| g_l \|_{L^{q(\cdot)}} (t - l)^m \| b \|_{BMO(\mathbb{R}^n)}^m \| \chi_{B_t} \|_{L^{q(\cdot)}} 2^{-lv} 2^{t(v + \frac{n}{s})} \| \Phi \|_{L^s(\mathbb{S}^{n-1})} \| \chi_{B_l} \|_{L^{q(\cdot)}} \\ & \leq C (t - l)^m \| \Phi \|_{L^s(\mathbb{S}^{n-1})} \| b \|_{BMO(\mathbb{R}^n)}^m 2^{-tn} 2^{-lv} 2^{t(v + \frac{n}{s})} \| \chi_{B_t} \|_{L^{q(\cdot)}} \| \chi_{B_l} \|_{L^{q(\cdot)}} \| g_l \|_{L^{q(\cdot)}}. \end{aligned}$$

Applying results to E_{11} we can get

$$\begin{aligned} E_{11} & \leq C \sup_{\epsilon > 0} \sup_{k_0 \in \mathbb{Z}} 2^{-k_0 \beta} \left[\epsilon^\theta \sum_{t=-\infty}^{-1} 2^{t\alpha(0)u(1+\epsilon)} \left(\sum_{l=-\infty}^t (t - l)^m \| \Phi \|_{L^s(\mathbb{S}^{n-1})} \| b \|_{BMO(\mathbb{R}^n)}^m \right. \right. \\ & \quad \left. \left. \times 2^{(l-t)(n/q'(0) - v - \frac{n}{s})} \| g_l \|_{L^{q(\cdot)}} \right)^{u(1+\epsilon)} \right]^{\frac{1}{u(1+\epsilon)}} \\ & \leq C \| \Phi \|_{L^s(\mathbb{S}^{n-1})} \| b \|_{BMO(\mathbb{R}^n)}^m \sup_{\epsilon > 0} \sup_{k_0 \in \mathbb{Z}} 2^{-k_0 \beta} \\ & \quad \times \left[\epsilon^\theta \sum_{t=-\infty}^{-1} \left(\sum_{l=-\infty}^t 2^{\alpha(0)l} \| g_l \|_{L^{q(\cdot)}} 2^{b(l-t)} (t - l)^m \right)^{u(1+\epsilon)} \right]^{\frac{1}{u(1+\epsilon)}}. \end{aligned}$$

Let $b = \frac{n}{q_1'(0)} - v - \frac{n}{s} - \alpha(0) > 0$, applying Hölder's inequality, Fubini's theorem for series and $2^{-u(1+\epsilon)} < 2^{-u}$ we get,

$$E_{11} \leq C \| \Phi \|_{L^s(\mathbb{S}^{n-1})} \| b \|_{BMO(\mathbb{R}^n)}^m \sup_{\epsilon > 0} \sup_{k_0 \in \mathbb{Z}} 2^{-k_0 \beta} \left[\epsilon^\theta \sum_{t=-\infty}^{-1} \left(\sum_{l=-\infty}^t 2^{\alpha(0)u(1+\epsilon)l} \| g_l \|_{L^{q(\cdot)}}^{u(1+\epsilon)} \right) \right]$$

$$\begin{aligned}
& \times \left. 2^{bu(1+\epsilon)(l-t)/2} \sum_{l=-\infty}^t 2^{b(u(1+\epsilon))'(l-t)/2} (t-l)^{m(u(1+\epsilon))'} \right)^{\frac{u(1+\epsilon)}{(u(1+\epsilon))'}} \Bigg]^{\frac{1}{u(1+\epsilon)}} \\
& \leq C \|\Phi\|_{L^s(\mathbb{S}^{n-1})} \|b\|_{BMO(\mathbb{R}^n)}^m \sup_{\epsilon>0} \sup_{k_0 \in \mathbb{Z}} 2^{-k_0\beta} \\
& \times \left(\epsilon^\theta \sum_{t=-\infty}^{-1} \sum_{l=-\infty}^t 2^{\alpha(0)u(1+\epsilon)l} \|g_l\|_{L^{q(\cdot)}}^{u(1+\epsilon)} 2^{bu(1+\epsilon)(l-t)/2} \right)^{\frac{1}{u(1+\epsilon)}} \\
& \leq C \|b\|_{BMO(\mathbb{R}^n)}^m \sup_{\epsilon>0} \sup_{k_0 \in \mathbb{Z}} 2^{-k_0\beta} \\
& \times \left(\epsilon^\theta \sum_{l=-\infty}^{-1} 2^{\alpha(0)u(1+\epsilon)l} \|g_l\|_{L^{q(\cdot)}}^{u(1+\epsilon)} \sum_{t=l+2}^{-1} 2^{bu(1+\epsilon)(l-t)/2} \right)^{\frac{1}{u(1+\epsilon)}} \\
& \leq C \|b\|_{BMO(\mathbb{R}^n)}^m \sup_{\epsilon>0} \sup_{k_0 \in \mathbb{Z}} 2^{-k_0\beta} \\
& \times \left(\epsilon^\theta \sum_{l=-\infty}^{-1} 2^{\alpha(0)u(1+\epsilon)l} \|g_l\|_{L^{q(\cdot)}}^{u(1+\epsilon)} \sum_{t=l+2}^{-1} 2^{bu(1+\epsilon)(l-t)/2} \right)^{\frac{1}{u(1+\epsilon)}} \\
& \leq C \|b\|_{BMO(\mathbb{R}^n)}^m \sup_{\epsilon>0} \sup_{k_0 \in \mathbb{Z}} 2^{-k_0\beta} \left(\epsilon^\theta \sum_{l=-\infty}^{-1} 2^{\alpha(0)u(1+\epsilon)l} \|g_l\|_{L^{q(\cdot)}}^{u(1+\epsilon)} \right)^{\frac{1}{u(1+\epsilon)}} \\
& \leq C \|b\|_{BMO(\mathbb{R}^n)}^m \sup_{\epsilon>0} \sup_{k_0 \in \mathbb{Z}} 2^{-k_0\beta} \left(\epsilon^\theta \sum_{l=-\infty}^{k_0} 2^{\alpha(\cdot)u(1+\epsilon)l} \|g_l\|_{L^{q(\cdot)}}^{u(1+\epsilon)} \right)^{\frac{1}{u(1+\epsilon)}} \\
& \leq C \|b\|_{BMO(\mathbb{R}^n)}^m \|g\|_{MK_{\beta, q(\cdot)}^{\alpha(\cdot), u, \theta}(\mathbb{R}^n)}.
\end{aligned}$$

Now apply Minkowski's inequality to split E_{12} , we have

$$\begin{aligned}
E_{12} & \leq \sup_{\epsilon>0} \sup_{k_0 \in \mathbb{Z}} 2^{-k_0\beta} \left(\epsilon^\theta \sum_{t=0}^{k_0} 2^{t\alpha(\cdot)u(1+\epsilon)} \left(\sum_{l=-\infty}^{-1} \|\chi_t[b, \mu_\Phi]^m g_l\|_{L^{q(\cdot)}} \right)^{u(1+\epsilon)} \right)^{\frac{1}{u(1+\epsilon)}} \\
& \quad + \sup_{\epsilon>0} \sup_{k_0 \in \mathbb{Z}} 2^{-k_0\beta} \left(\epsilon^\theta \sum_{t=0}^{k_0} 2^{t\alpha(\cdot)u(1+\epsilon)} \left(\sum_{l=0}^{t-2} \|\chi_t[b, \mu_\Phi]^m g_l\|_{L^{q(\cdot)}} \right)^{u(1+\epsilon)} \right)^{\frac{1}{u(1+\epsilon)}} \\
& := A_1 + A_2.
\end{aligned}$$

To obtain the estimate for A_2 , we can follow a similar approach as for E_{11} , but with some modifications. We will replace $q'(0)$ with q'_∞ and use the fact that $b = \frac{n}{q'_\infty} - v - \frac{n}{s} - \alpha_\infty > 0$.

For A_1 we have

$$\begin{aligned} & \| [b, \mu_\Phi]_\beta (g\chi_l)\chi_t \|_{L^{q(\cdot)}} \\ & \leq C(t-l)^m \|\Phi\|_{L^s(\mathbb{S}^{n-1})} \|b\|_{BMO(\mathbb{R}^n)}^m 2^{-tn} 2^{-lv} 2^{t(v+\frac{n}{s})} \|\chi_{B_t}\|_{L^{q(\cdot)}} \|\chi_{B_l}\|_{L^{q(\cdot)}} \|g_l\|_{L^{q(\cdot)}} \\ & \leq C(t-l)^m \|\Phi\|_{L^s(\mathbb{S}^{n-1})} \|b\|_{BMO(\mathbb{R}^n)}^m 2^{l(\frac{n}{q(0)}-v)} 2^{t(v+\frac{n}{s}-\frac{n}{q'_\infty})} \|g_l\|_{L^{q(\cdot)}}. \end{aligned}$$

Now by using the fact $-\frac{n}{q'_\infty} + v + \frac{n}{s} + \alpha_\infty < 0$ we have,

$$\begin{aligned} A_1 & \leq \sup_{\epsilon > 0} \sup_{k_0 \in \mathbb{Z}} 2^{-k_0\beta} \left(\epsilon^\theta \sum_{t=0}^{k_0} 2^{t\alpha_\infty u(1+\epsilon)} \left(\sum_{l=-\infty}^{-1} \|\chi_t [b, \mu_\Phi]^m g_l\|_{L^{q(\cdot)}} \right)^{u(1+\epsilon)} \right)^{\frac{1}{u(1+\epsilon)}} \\ & \leq C \|\Phi\|_{L^s(\mathbb{S}^{n-1})} \|b\|_{BMO(\mathbb{R}^n)}^m \sup_{\epsilon > 0} \sup_{k_0 \in \mathbb{Z}} 2^{-k_0\beta} \\ & \quad \times \left[\epsilon^\theta \sum_{t=0}^{k_0} 2^{t\alpha_\infty u(1+\epsilon)} \left(\sum_{l=-\infty}^{-1} 2^{l(\frac{n}{q(0)}-v)} 2^{t(v+\frac{n}{s}-\frac{n}{q'_\infty})} (t-l)^m \|g_l\|_{L^{q(\cdot)}} \right)^{u(1+\epsilon)} \right]^{\frac{1}{u(1+\epsilon)}} \\ & \leq C \|\Phi\|_{L^s(\mathbb{S}^{n-1})} \|b\|_{BMO(\mathbb{R}^n)}^m \sup_{\epsilon > 0} \sup_{k_0 \in \mathbb{Z}} 2^{-k_0\beta} \left[\epsilon^\theta \sum_{t=0}^{k_0} 2^{t(\alpha_\infty + v + \frac{n}{s} - \frac{n}{q'_\infty}) u(1+\epsilon)} \right. \\ & \quad \left. \times (t-l)^{m u(1+\epsilon)} \left(\sum_{l=-\infty}^{-1} 2^{l(\frac{n}{q(0)}-v)} \|g_l\|_{L^{q(\cdot)}} \right)^{u(1+\epsilon)} \right]^{\frac{1}{u(1+\epsilon)}} \\ & \leq C \|\Phi\|_{L^s(\mathbb{S}^{n-1})} \|b\|_{BMO(\mathbb{R}^n)}^m \sup_{\epsilon > 0} \sup_{k_0 \in \mathbb{Z}} 2^{-k_0\beta} \\ & \quad \times \left(\epsilon^\theta \left(\sum_{l=-\infty}^{-1} 2^{l(\frac{n}{q(0)}-v)} \|g_l\|_{L^{q(\cdot)}} \right)^{u(1+\epsilon)} \right)^{\frac{1}{u(1+\epsilon)}} \\ & \leq C \|b\|_{BMO(\mathbb{R}^n)}^m \sup_{\epsilon > 0} \sup_{k_0 \in \mathbb{Z}} 2^{-k_0\beta} \\ & \quad \times \left(\epsilon^\theta \left(\sum_{l=-\infty}^{-1} 2^{l\alpha(0)} \|g\chi_l\|_{L^{q(\cdot)}} 2^{l(\frac{n}{q(0)}-v-\alpha(0))} \right)^{u(1+\epsilon)} \right)^{\frac{1}{u(1+\epsilon)}}. \end{aligned}$$

Now we can apply the Hölder's inequality and we can also use the fact that $\frac{n}{q'} - \frac{n}{s} - v - \alpha(0) > 0$. Here is

$$\begin{aligned} &\leq C \|b\|_{BMO(\mathbb{R}^n)}^m \sup_{\epsilon > 0} \sup_{k_0 \in \mathbb{Z}} 2^{-k_0 \beta} \left[e^\theta \sum_{l=-\infty}^{-1} 2^{\alpha(0)lu(1+\epsilon)} \|g_l\|_{L^{q(\cdot)}}^{u(1+\epsilon)} \right. \\ &\quad \left. \times \left(\sum_{l=-\infty}^{-1} 2^{l(\frac{n}{q'} - v - \alpha(0))(u(1+\epsilon))'} \right)^{\frac{u(1+\epsilon)}{(u(1+\epsilon))'}} \right]^{\frac{1}{u(1+\epsilon)}} \\ &\leq C \|b\|_{BMO(\mathbb{R}^n)}^m \sup_{\epsilon > 0} \sup_{k_0 \in \mathbb{Z}} 2^{-k_0 \beta} \left(\epsilon^\theta \left(\sum_{l=-\infty}^{k_0} 2^{\alpha(\cdot)lu(1+\epsilon)} \|g_l\|_{L^{q(\cdot)}}^{u(1+\epsilon)} \right) \right)^{\frac{1}{u(1+\epsilon)}} \\ &\leq C \|b\|_{BMO(\mathbb{R}^n)}^m \|g\|_{MK_{\beta, q(\cdot)}^{\alpha(\cdot), u, \theta}(\mathbb{R}^n)}. \end{aligned}$$

Now we will find the estimate for E_2 . For each $t \in \mathbb{Z}$ and $l \geq t+1$ and a.e. $x \in R_t$, $y \in R_l$, we know that $|x-y| \approx |y| \approx 2^l$, we consider

$$\begin{aligned} |\mu_\Phi(g\chi_l)(x)| &\leq \left(\int_0^{|y|} \left| \int_{|x-y| \leq t} \frac{\Phi(x-y)}{|x-y|^{n-1}} g_l(y) dy \right|^2 \frac{dt}{t^3} \right)^{1/2} \\ &\quad + \left(\int_{|y|}^\infty \left| \int_{|x-y| \leq t} \frac{\Phi(x-y)}{|x-y|^{n-1}} f_l(y) dy \right|^2 \frac{dt}{t^3} \right)^{1/2} \\ &=: I_{21} + I_{22}. \end{aligned}$$

By using similar arguments as used in estimating I_{11} , we obtain

$$I_{21} \leq 2^{(t-l)/2} 2^{-\ln} \|g_l\|_{L^{q(\cdot)}} \left\{ |b(x) - b_{B_l}|^m \|\Phi(x-\cdot)\chi_l(\cdot)\|_{L^{q'(\cdot)}} \|b(\cdot) - (b_{B_l})^m (\Phi(x-\cdot)\chi_l(\cdot))\|_{L^{q'(\cdot)}} \right\}.$$

Similar to the arguments of I_{12} , we have

$$I_{22} \leq 2^{-\ln} \|g_l\|_{L^{q(\cdot)}} \left\{ |b(x) - b_{B_l}|^m \|\Phi(x-\cdot)\chi_l(\cdot)\|_{L^{q'(\cdot)}} + \|b(\cdot) - (b_{B_l})^m (\Phi(x-\cdot)\chi_l(\cdot))\|_{L^{q'(\cdot)}} \right\}.$$

So, we have

$$|[b, \mu_\Phi] - (f_l)(x)| \leq 2^{-\ln} \|g_l\|_{L^{q(\cdot)}}$$

$$\left\{ \|b(x) - b_{B_l}\|^m \|\Phi(x - \cdot)\chi_l(\cdot)\|_{L^{q'(\cdot)}} + \|b(\cdot) - (b_{B_l})^m (\Phi(x - \cdot)\chi_l(\cdot))\|_{L^{q'(\cdot)}} \right\}.$$

Consequently we will get

$$\begin{aligned} & \| [b, \mu_\Phi(g_l)] \chi_t \|_{L^{q(\cdot)}} \\ & \leq C 2^{-ln} \|g_l\|_{L^{q(\cdot)}} \left\{ \| (b(\cdot) - b_{B_l})^m \chi_t(\cdot) \|_{L^{q(\cdot)}} 2^{-lv} 2^{t(v+\frac{n}{s})} \|\Phi\|_{L^s(\mathbb{S}^{n-1})} \|\chi_{B_l}\|_{L^{q(\cdot)}} \right. \\ & \quad \left. + \|b\|_{BMO(\mathbb{R}^n)}^m 2^{-lv} 2^{t(v+\frac{n}{s})} \|\Phi\|_{L^s(\mathbb{S}^{n-1})} \|\chi_{B_l}\|_{L^{q(\cdot)}} \|\chi_t\|_{L^{q(\cdot)}} \right\} \\ & \leq C 2^{-ln} \|g_l\|_{L^{q(\cdot)}} \left\{ (t-l)^m \|b\|_{BMO(\mathbb{R}^n)}^m \|\chi_{B_t}\|_{L^{q(\cdot)}} 2^{-lv} 2^{t(v+\frac{n}{s})} \|\Phi\|_{L^s(\mathbb{S}^{n-1})} \|\chi_{B_l}\|_{L^{q(\cdot)}} \right. \\ & \quad \left. + \|b\|_{BMO(\mathbb{R}^n)}^m 2^{-lv} 2^{t(v+\frac{n}{s})} \|\Phi\|_{L^s(\mathbb{S}^{n-1})} \|\chi_{B_l}\|_{L^{q(\cdot)}} \|\chi_{B_t}\|_{L^{q(\cdot)}} \right\} \\ & \leq C 2^{-ln} \|g_l\|_{L^{q(\cdot)}} (t-l)^m \|b\|_{BMO(\mathbb{R}^n)}^m \|\chi_{B_t}\|_{L^{q(\cdot)}} 2^{-lv} 2^{t(v+\frac{n}{s})} \|\Phi\|_{L^s(\mathbb{S}^{n-1})} \|\chi_{B_l}\|_{L^{q(\cdot)}} \\ & \leq C (t-l)^m \|\Phi\|_{L^s(\mathbb{S}^{n-1})} \|b\|_{BMO(\mathbb{R}^n)}^m 2^{-ln} 2^{-lv} 2^{t(v+\frac{n}{s})} \|\chi_{B_t}\|_{L^{q(\cdot)}} \|\chi_{B_l}\|_{L^{q(\cdot)}} \|g_l\|_{L^{q(\cdot)}} \\ & \leq C (t-l)^m \|\Phi\|_{L^s(\mathbb{S}^{n-1})} \|b\|_{BMO(\mathbb{R}^n)}^m 2^{-ln} 2^{-lv} 2^{t(v+\frac{n}{s})} 2^{ln/q_\infty} 2^{tn/q_\infty} \|g_l\|_{L^{q(\cdot)}} \\ & \leq C (t-l)^m \|\Phi\|_{L^s(\mathbb{S}^{n-1})} \|b\|_{BMO(\mathbb{R}^n)}^m 2^{(t-l)m(v+\frac{n}{s}+\frac{n}{q_\infty})} \|g_l\|_{L^{q(\cdot)}}. \end{aligned}$$

Now splitting E_2 we have

$$\begin{aligned} E_2 & \leq \sup_{\epsilon > 0} \sup_{k_0 \in \mathbb{Z}} 2^{-k_0\beta} \left(\epsilon^\theta \sum_{t=-\infty}^{k_0} 2^{t\alpha(\cdot)u(1+\epsilon)} \left(\sum_{l=t+2}^{\infty} \|\chi_t[b, \mu_\Phi]^m g_l\|_{L^{q(\cdot)}} \right)^{u(1+\epsilon)} \right)^{\frac{1}{u(1+\epsilon)}} \\ & \leq \sup_{\epsilon > 0} \sup_{k_0 \in \mathbb{Z}} 2^{-k_0\beta} \left(\epsilon^\theta \sum_{t=-\infty}^{-1} 2^{t\alpha(\cdot)u(1+\epsilon)} \left(\sum_{l=t+2}^{\infty} \|\chi_t[b, \mu_\Phi]^m g_l\|_{L^{q(\cdot)}} \right)^{u(1+\epsilon)} \right)^{\frac{1}{u(1+\epsilon)}} \\ & \quad + \sup_{\epsilon > 0} \sup_{k_0 \in \mathbb{Z}} 2^{-k_0\beta} \left(\epsilon^\theta \sum_{t=0}^{k_0} 2^{t\alpha(\cdot)u(1+\epsilon)} \left(\sum_{l=t+2}^{\infty} \|\chi_t[b, \mu_\Phi]^m g_l\|_{L^{q(\cdot)}} \right)^{u(1+\epsilon)} \right)^{\frac{1}{u(1+\epsilon)}} \\ & := E_{21} + E_{22}. \end{aligned}$$

For E_{22} we have

$$\begin{aligned} E_{22} & \leq C \|b\|_{BMO(\mathbb{R}^n)}^m \sup_{\epsilon > 0} \sup_{k_0 \in \mathbb{Z}} 2^{-k_0\beta} \\ & \quad \times \left(\epsilon^\theta \sum_{t=0}^{k_0} 2^{t\alpha_\infty u(1+\epsilon)} \left(\sum_{l=t+2}^{\infty} 2^{(t-l)(v+\frac{n}{s}+\frac{n}{q_\infty})} (t-l)^m \|g_l\|_{L^{q(\cdot)}} \right)^{u(1+\epsilon)} \right)^{\frac{1}{u(1+\epsilon)}} \end{aligned}$$

$$\leq C \|b\|_{BMO(\mathbb{R}^n)}^m \sup_{\epsilon > 0} \sup_{k_0 \in \mathbb{Z}} 2^{-k_0 \beta} \times \left(\epsilon^\theta \sum_{t=0}^{k_0} \left(\sum_{l=t+2}^{\infty} 2^{l\alpha_\infty} \|g_l\|_{L^{q(\cdot)}} 2^{(t-l)(v+\frac{n}{s}+\frac{n}{q_\infty})} (t-l)^m \right)^{u(1+\epsilon)} \right)^{\frac{1}{u(1+\epsilon)}},$$

for $d = \frac{n}{q_\infty} + v + \frac{n}{s} > 0$. Then we can apply the Hölder's inequality for series and $2^{-u(1+\epsilon)} < 2^{-u}$ to get

$$\begin{aligned} E_{22} &\leq C \|b\|_{BMO(\mathbb{R}^n)}^m \sup_{\epsilon > 0} \sup_{k_0 \in \mathbb{Z}} 2^{-k_0 \beta} \left[\epsilon^\theta \sum_{t=0}^{k_0} \left(\sum_{l=t+2}^{\infty} 2^{l\alpha_\infty u(1+\epsilon)} \|g_l\|_{L^{q(\cdot)}}^{u(1+\epsilon)} 2^{du(1+\epsilon)(t-l)/2} \right) \right. \\ &\quad \left. \times \left(\sum_{l=t+2}^{\infty} 2^{d(u(1+\epsilon))'(t-l)/2} (t-l)^{m(u(1+\epsilon))'} \right)^{\frac{u(1+\epsilon)}{(u(1+\epsilon))'}} \right]^{\frac{1}{u(1+\epsilon)}} \\ &\leq C \|b\|_{BMO(\mathbb{R}^n)}^m \sup_{\epsilon > 0} \sup_{k_0 \in \mathbb{Z}} 2^{-k_0 \beta} \\ &\quad \times \left(\epsilon^\theta \sum_{t=0}^{k_0} \sum_{l=t+2}^{\infty} 2^{l\alpha_\infty u(1+\epsilon)} \|g_l\|_{L^{q(\cdot)}}^{u(1+\epsilon)} 2^{du(1+\epsilon)(t-l)/2} \right)^{\frac{1}{u(1+\epsilon)}} \\ &\leq C \|b\|_{BMO(\mathbb{R}^n)}^m \sup_{\epsilon > 0} \sup_{k_0 \in \mathbb{Z}} 2^{-k_0 \beta} \\ &\quad \times \left(\epsilon^\theta \sum_{t=0}^{k_0} \sum_{l=t+2}^{\infty} \sum_{j=-\infty}^l 2^{j\alpha_\infty u(1+\epsilon)} \|g_j\|_{L^{q(\cdot)}}^{u(1+\epsilon)} 2^{du(1+\epsilon)(t-l)/2} \right)^{\frac{1}{u(1+\epsilon)}} \\ &\leq C \|b\|_{BMO(\mathbb{R}^n)}^m \sup_{\epsilon > 0} \sup_{k_0 \in \mathbb{Z}} 2^{-k_0 \beta} \left(\epsilon^\theta \sum_{t=0}^{k_0} \sum_{l=t+2}^{\infty} 2^{du(1+\epsilon)(t-l)/2} \right)^{\frac{1}{u(1+\epsilon)}} \\ &\quad \times \|g\|_{MK_{\beta, q(\cdot)}^{\alpha(\cdot), u, \theta}(\mathbb{R}^n)} \\ &\leq C \|b\|_{BMO(\mathbb{R}^n)}^m \|g\|_{MK_{\beta, q(\cdot)}^{\alpha(\cdot), u, \theta}(\mathbb{R}^n)}. \end{aligned}$$

Now for E_{21} using Minkowski's inequality we have

$$E_{21} \leq \sup_{\epsilon > 0} \sup_{k_0 \in \mathbb{Z}} 2^{-k_0 \beta} \left(\epsilon^\theta \sum_{t=-\infty}^{-1} 2^{t\alpha(\cdot)u(1+\epsilon)} \left(\sum_{l=t+2}^{-1} \|\chi_t[b, \mu_\Phi]^m g_l\|_{L^{q(\cdot)}} \right)^{u(1+\epsilon)} \right)^{\frac{1}{u(1+\epsilon)}}$$

$$\begin{aligned}
 & + \sup_{\epsilon > 0} \sup_{k_0 \in \mathbb{Z}} 2^{-k_0\beta} \left(\epsilon^\theta \sum_{t=-\infty}^{-1} 2^{t\alpha(\cdot)u(1+\epsilon)} \left(\sum_{l=0}^{\infty} \|\chi_t[b, \mu_\Phi]^m g_l\|_{L^{q(\cdot)}} \right)^{u(1+\epsilon)} \right)^{\frac{1}{u(1+\epsilon)}} \\
 & := B_1 + B_2.
 \end{aligned}$$

The estimate for B_1 follows in a similar manner to E_{22} with q_∞ replaced by $q(0)$ and using the fact that $\frac{n}{q(0)} + v + \frac{n}{s} + \alpha(0) > 0$. For B_2 we have

$$\begin{aligned}
 & \| [b, \mu_\Phi](g_l)\chi_t \|_{L^{q(\cdot)}} \\
 & \leq C 2^{-ln} \|g_l\|_{L^{q(\cdot)}} \left\{ \|(b(\cdot) - b_{B_t})^m \chi_t(\cdot)\|_{L^{q(\cdot)}} 2^{-lv} 2^{t(v+\frac{n}{s})} \|\Phi\|_{L^s(\mathbb{S}^{n-1})} \|\chi_{B_t}\|_{L^{q(\cdot)}} \right. \\
 & \left. + \|b\|_{BMO(\mathbb{R}^n)}^m 2^{-lv} 2^{t(v+\frac{n}{s})} \|\Phi\|_{L^s(\mathbb{S}^{n-1})} \|\chi_{B_t}\|_{L^{q(\cdot)}} \|\chi_t\|_{L^{q(\cdot)}} \right\} \\
 & \leq C 2^{-ln} \|g_l\|_{L^{q(\cdot)}} \left\{ (t-l)^m \|b\|_{BMO(\mathbb{R}^n)}^m \|\chi_{B_t}\|_{L^{q(\cdot)}} 2^{-lv} 2^{t(v+\frac{n}{s})} \|\Phi\|_{L^s(\mathbb{S}^{n-1})} \|\chi_{B_t}\|_{L^{q(\cdot)}} \right. \\
 & \left. + \|b\|_{BMO(\mathbb{R}^n)}^m 2^{-lv} 2^{t(v+\frac{n}{s})} \|\Phi\|_{L^s(\mathbb{S}^{n-1})} \|\chi_{B_t}\|_{L^{q(\cdot)}} \|\chi_{B_t}\|_{L^{q(\cdot)}} \right\} \\
 & \leq C 2^{-ln} \|g_l\|_{L^{q(\cdot)}} (t-l)^m \|b\|_{BMO(\mathbb{R}^n)}^m \|\chi_{B_t}\|_{L^{q(\cdot)}} 2^{-lv} 2^{t(v+\frac{n}{s})} \|\Phi\|_{L^s(\mathbb{S}^{n-1})} \|\chi_{B_t}\|_{L^{q(\cdot)}} \\
 & \leq C (t-l)^m \|\Phi\|_{L^s(\mathbb{S}^{n-1})} \|b\|_{BMO(\mathbb{R}^n)}^m 2^{-ln} 2^{-lv} 2^{t(v+\frac{n}{s})} \|\chi_{B_t}\|_{L^{q(\cdot)}} \|\chi_{B_t}\|_{L^{q(\cdot)}} \|g_l\|_{L^{q(\cdot)}} \\
 & \leq C (t-l)^m \|\Phi\|_{L^s(\mathbb{S}^{n-1})} \|b\|_{BMO(\mathbb{R}^n)}^m 2^{-ln} 2^{-lv} 2^{t(v+\frac{n}{s})} \|g_l\|_{L^{q(\cdot)}} 2^{ln/q_\infty} 2^{tn/q(0)} \\
 & \leq C (t-l)^m \|\Phi\|_{L^s(\mathbb{S}^{n-1})} \|b\|_{BMO(\mathbb{R}^n)}^m 2^{-l(v+\frac{n}{s}+\frac{n}{q_\infty})} 2^{t(v+\frac{n}{q(0)}+\frac{n}{s})} \|g_l\|_{L^{q(\cdot)}}.
 \end{aligned}$$

$$\begin{aligned}
 B_2 & \leq \sup_{\epsilon > 0} \sup_{k_0 \in \mathbb{Z}} 2^{-k_0\beta} \left(\epsilon^\theta \sum_{k=-\infty}^{-1} 2^{t\alpha(0)u(1+\epsilon)} \left(\sum_{l=0}^{\infty} \|\chi_t[b, \mu_\Phi]^m g_l\|_{L^{q(\cdot)}} \right)^{u(1+\epsilon)} \right)^{\frac{1}{u(1+\epsilon)}} \\
 & \leq C \|b\|_{BMO(\mathbb{R}^n)}^m \sup_{\epsilon > 0} \sup_{k_0 \in \mathbb{Z}} 2^{-k_0\beta} \left(\epsilon^\theta \sum_{k=-\infty}^{-1} 2^{t\alpha(0)u(1+\epsilon)} \right. \\
 & \quad \left. \times \left(\sum_{l=0}^{\infty} 2^{-l(v+\frac{n}{s}+\frac{n}{q_\infty})} 2^{t(v+\frac{n}{q(0)}+\frac{n}{s})} \|g_l\|_{L^{q(\cdot)}} (t-l)^m \right)^{u(1+\epsilon)} \right)^{\frac{1}{u(1+\epsilon)}} \\
 & \leq C \|b\|_{BMO(\mathbb{R}^n)}^m \sup_{\epsilon > 0} \sup_{k_0 \in \mathbb{Z}} 2^{-k_0\beta} \left(\epsilon^\theta \sum_{k=-\infty}^{-1} 2^{t(v+\frac{n}{q(0)}+\frac{n}{s}+\alpha(0))u(1+\epsilon)} (t-l)^m \right)
 \end{aligned}$$

$$\begin{aligned}
 & \times \left(\sum_{l=0}^{\infty} 2^{-l(v+\frac{n}{s}+\frac{n}{q_{\infty}})} \|g_l\|_{L^{q(\cdot)}} \right)^{u(1+\epsilon)} \frac{1}{u(1+\epsilon)} \\
 \leq & C \|b\|_{BMO(\mathbb{R}^n)}^m \sup_{\epsilon>0} \sup_{k_0 \in \mathbb{Z}} 2^{-k_0\beta} \\
 & \times \left(\epsilon^{\theta} \left(\sum_{l=0}^{\infty} 2^{-l(v+\frac{n}{s}+\frac{n}{q_{\infty}})} \|g_l\|_{L^{q(\cdot)}} \right)^{u(1+\epsilon)} \right)^{\frac{1}{u(1+\epsilon)}} \\
 \leq & C \|b\|_{BMO(\mathbb{R}^n)}^m \sup_{\epsilon>0} \sup_{k_0 \in \mathbb{Z}} 2^{-k_0\beta} \\
 & \times \left(\epsilon^{\theta} \left(\sum_{l=0}^{\infty} 2^{\alpha_{\infty}l} \|g_l\|_{L^{q(\cdot)}} 2^{-l(v+\frac{n}{s}+\frac{n}{q_{\infty}}+\alpha_{\infty})} \right)^{u(1+\epsilon)} \right)^{\frac{1}{u(1+\epsilon)}} \\
 \leq & C \|b\|_{BMO(\mathbb{R}^n)}^m \sup_{\epsilon>0} \sup_{k_0 \in \mathbb{Z}} 2^{-k_0\beta} \\
 & \times \left(\epsilon^{\theta} \left(\sum_{l=0}^{\infty} \sum_{j=-\infty}^l 2^{\alpha_{\infty}j} \|g_j\|_{L^{q(\cdot)}} 2^{-l(v+\frac{n}{s}+\frac{n}{q_{\infty}}+\alpha_{\infty})} \right)^{u(1+\epsilon)} \right)^{\frac{1}{u(1+\epsilon)}}.
 \end{aligned}$$

Now by applying Hölder’s inequality and using the fact that $\frac{n}{q(\infty)} + v + \frac{n}{s} + \alpha(\infty) > 0$ we have

$$\begin{aligned}
 B_2 \leq & C \|b\|_{BMO(\mathbb{R}^n)}^m \sup_{\epsilon>0} \sup_{k_0 \in \mathbb{Z}} 2^{-k_0\beta} \left(\epsilon^{\theta} \left(\sum_{l=0}^{\infty} 2^{-l(v+\frac{n}{s}+\frac{n}{q_{\infty}}+\alpha_{\infty})} \right)^{u(1+\epsilon)} \right)^{\frac{1}{u(1+\epsilon)}} \\
 & \times \|g\|_{MK_{\beta,q(\cdot)}^{\alpha(\cdot),u,\theta}(\mathbb{R}^n)} \\
 \leq & \|b\|_{BMO(\mathbb{R}^n)}^m \|g\|_{MK_{\beta,q(\cdot)}^{\alpha(\cdot),u,\theta}(\mathbb{R}^n)}.
 \end{aligned}$$

Combining the estimates for E_1 and E_2 yields

$$\|[b, \mu_{\Phi}]^m(g)\|_{MK_{\beta,q(\cdot)}^{\alpha(\cdot),u,\theta}(\mathbb{R}^n)} \leq \|b\|_{BMO(\mathbb{R}^n)}^m \|g\|_{MK_{\beta,q(\cdot)}^{\alpha(\cdot),u,\theta}(\mathbb{R}^n)},$$

which completes the proof. □

Author Contribution Statements The authors contributed equally to this work. All authors read and approved the final copy of this paper.

Declaration of Competing Interests The authors declare that they have no known competing financial interest or personal relationships that could have appeared to influence the work reported in this paper.

Acknowledgement The authors are thankful to the referees for making valuable suggestions leading to the better presentations of this paper.

REFERENCES

- [1] Asim, M., Hussain, A., Weighted variable Morrey-Herz estimates for fractional Hardy operators, *J. Inequal. Appl.*, 2(2022) (2022) 12pp. <https://doi.org/10.1186/s13660-021-02739-z>
- [2] Bashir, S., Sultan, B., Hussain, A., Khan, A., Abdeljawad, T., A note on the boundedness of Hardy operators in grand Herz spaces with variable exponent, *AIMS Mathematics*, 8(9) (2023), 22178–22191. <https://doi.org/10.3934/math.20231130>
- [3] Diening, L., Harjuletho, P., Hastö, P., Ruzicka, M., Lebesgue and Sobolev Spaces with Variable Exponents, Springer, 2011. <https://doi.org/10.1007/978-3-642-18363-8>
- [4] Hussain, A., Asim, M., Aslam, M., Jarad, F., Commutators of the fractional Hardy operator on weighted variable Herz-Morrey spaces, *J. Funct. Spaces.*, ID 9705250 (2021), 10 pages. <https://doi.org/10.1155/2021/9705250>
- [5] Hussain, A., Asim, M., Jarad, F., Variable λ -Central Morrey space estimates for the fractional Hardy operators and commutators, *Journal of Mathematics*, ID 5855068 (2022), 12 pp. <https://doi.org/10.1155/2022/5855068>
- [6] Izuki, M., Boundedness of vector-valued sublinear operators on Herz-Morrey spaces with variable exponents, *Math. Sci. J.*, 13(10) (2009), 243–253.
- [7] Izuki, M., Boundedness of sublinear operators on Herz spaces with variable exponent and application to wavelet characterization, *Anal. Math.*, 36(1) (2010), 33–50.
- [8] Izuki, M., Boundedness of commutators on Herz spaces with variable exponent, *Rendiconti del Circolo Matematico di Palermo.*, 59 (2010), 199–213. <https://doi.org/10.1007/s12215-010-0015-1>
- [9] Kováčik, O., Rákosník, J., On spaces $L^{p(x)}$ and $W^{k,p(x)}$, *Czechoslov. Math. J.*, 41(4) (1991), 592–618.
- [10] Meskhi, A., Maximal functions, potentials and singular integrals in grand Morrey spaces, *Complex Variables and Elliptic Equations*, 56(10-11) (2011), 1003-1019. <https://doi.org/10.1080/17476933.2010.534793>
- [11] Muckenhoupt, B., Wheeden, R. L., Weighted norm inequalities for singular and fractional integrals, *Trans. Am. Maths Soc.*, 161 (1971), 249–258.
- [12] Nafis, H., Rafeiro, H., Zaighum, M. A., A note on the boundedness of sublinear operators on grand variable Herz spaces, *J. Inequal Appl.*, 2020(1) (2020), 1–13. <https://doi.org/10.1186/s13660-019-2265-6>
- [13] Nafis, H., Rafeiro, H., Zaighum, M. A., Boundedness of the Marcinkiewicz integral on grand Herz spaces, *J. Math. Ineq.*, 15(2) (2021), 739–753. <https://doi.org/10.7153/jmi-2021-15-52>
- [14] Samko, S., Variable exponent Herz spaces, *Mediterr. J. Math.* 10(4) (2013), 2007–2025. <https://doi.org/10.1007/s00009-013-0335-4>
- [15] Sultan, B., Sultan, M., Mehmood, M., Azmi, F., Alghaffi, M.A., Mlaiki, N., Boundedness of fractional integrals on grand weighted Herz spaces with variable exponent, *AIMS Mathematics*, 8(1) (2023), 752–764. <https://doi.org/10.3934/math.2023036>
- [16] Sultan, B., Azmi, F.M., Sultan, M., Mahmood, T., Mlaiki, N., Souayah, N., Boundedness of fractional integrals on grand weighted Herz-Morrey spaces with variable exponent, *Fractal and Fractional*, 6(11) (2022), 660. <https://doi.org/10.3390/fractalfract6110660>
- [17] Sultan, B., Azmi, F., Sultan, M., Mehmood, M., Mlaiki, N., Boundedness of Riesz potential operator on grand Herz-Morrey spaces, *Axioms*, 11(11) (2022), 583. <https://doi.org/10.3390/axioms11110583>
- [18] Sultan, M., Sultan, B., Aloqaily, A., Mlaiki, N., Boundedness of some operators on grand Herz spaces with variable exponent, *AIMS Mathematics*, 8(6) (2023), 12964–12985. <https://doi.org/10.3934/math.2023653>

- [19] Sultan, B., Sultan, M., Khan, A., Abdeljawad, T., Boundedness of Marcinkiewicz integral operator of variable order in grand Herz-Morrey spaces, *AIMS Mathematics*, 8(9) (2023), 22338–22353. <https://doi.org/10.3934/math.20231139>
- [20] Sultan, B., Sultan, M., Zhang, Q. Q., Mlaiki, N., Boundedness of Hardy operators on grand variable weighted Herz spaces, *AIMS Mathematics*, 8(10) (2023), 24515–24527.
- [21] Sultan, B., Sultan, M., Khan, I., On Sobolev theorem for higher commutators of fractional integrals in grand variable Herz spaces, *Commun. Nonlinear Sci. Numer. Simul.*, 126 (2023). DOI 10.1016/j.cnsns.2023.107464
- [22] Sultan, B., Sultan, M., Boundedness of commutators of rough Hardy operators on grand variable Herz spaces, *Forum Mathematicum*, 2023. <https://doi.org/10.1515/forum-2023-0152>
- [23] Uribe, D. C., Fiorenza, A., Variable Lebesgue spaces, Foundations and Harmonic Analysis, Appl. Numer. Harmon. Anal., Birkhäuser, Heidelberg, 2013.
- [24] Uribe, D. C., et al., The boundedness of classical operators on variable L^p spaces, *Acad. Sci. Fenn. Math.*, 31(1) (2006), 239–264.
- [25] Wang, H., Commutators of Marcinkiewicz integrals on Herz spaces with variable exponent, *Czech Math J.*, 66 (2016), 251–269.



DEMONSTRATION OF THE STRENGTH OF STRONG CONVEXITY VIA JENSEN'S GAP

Asia¹ and Shahid KHAN²

^{1,2}Department of Mathematics, University of Peshawar, Peshawar 25000, PAKISTAN

ABSTRACT. This paper demonstrates through a numerical experiment that utilization of strongly convex functions strengthens the bound presented for the Jensen gap in [4]. Consequently the improved result enables to present improvements in the bounds obtained for the Hölder and Hermite-Hadamard gaps and proposes such improvements in the results obtained for various entropies and divergences in information theory.

1. INTRODUCTION

Being a part of analysis, the field of mathematical inequalities in the sense of convexity has seen exponential growth in numerous domains of science, art, and technology [1, 3, 5, 7-9, 14-16, 22-24, 26, 27, 29-31, 36, 37, 40, 41, 43, 45]. Among these inequalities, the Jensen inequality is the most important inequality. Many other well-known used inequalities such as Young's, Hölder's, the arithmetic-geometric, the Hermite-Hadamard, and Minkowski's inequality etc can be obtained from this inequality by manipulating suitable substitutions. Furthermore, this inequality is comprehensively used in distinct areas of science and technology for example statistics [33], qualitative theory of differential and integral equations [32], engineering [17], economics [34], finance [10], information theory and coding [6, 25] etc. In addition, there are countless papers dealing with counterparts, refinements, generalizations, improvements and converse results of Jensen's inequality, (see, for instance [11-13, 19, 20, 39]). In fact, this inequality generalizes the classical notion of convexity and states that [28]:

Theorem 1. *If $\varphi : [\sigma_1, \sigma_2] \rightarrow \mathbb{R}$ is a convex function and $\vartheta_i \in [\sigma_1, \sigma_2]$, $k_i \geq 0$ for each $i \in \{1, 2, \dots, n\}$ with $\sum_{i=1}^n k_i := K_n > 0$, then for $\frac{1}{K_n} \sum_{i=1}^n k_i \vartheta_i := \vartheta$, the*

2020 *Mathematics Subject Classification.* 26A51, 26D15, 68P30.

Keywords. Jensen inequality, strongly convex function, Hölder inequality, Hermite-Hadamard inequality, Taylor Formula.

¹ ✉ asiakhanuom356@gmail.com; 0000-0003-4012-5417;

² ✉ shahidmathematics@gmail.com-Corresponding Author; 0000-0003-1966-3130.

following inequality holds

$$\varphi(\bar{\vartheta}) \leq \frac{1}{K_n} \sum_{i=1}^n k_i \varphi(\vartheta_i).$$

In reference [2], the integral form of Theorem 1 can be seen, also here it is:

Theorem 2. Assume that $[\sigma_1, \sigma_2] \subset \mathbb{R}$ and $\xi_2, \xi_1 : [\rho_1, \rho_2] \rightarrow \mathbb{R}$ are two functions with the condition that $\xi_2(t) \in [\sigma_1, \sigma_2]$, $\forall t \in [\rho_1, \rho_2]$. Further, assume that the function $\varphi : [\sigma_1, \sigma_2] \rightarrow \mathbb{R}$ is convex and $\xi_1, \xi_2 \xi_1, (\varphi \circ \xi_2) \cdot \xi_1$ are integrable on $[\rho_1, \rho_2]$. Furthermore, suppose that $\xi_1(t) \geq 0$ for all $t \in [\rho_1, \rho_2]$ and $\int_{\rho_1}^{\rho_2} \xi_1(t) dt := D > 0$, $\frac{1}{D} \int_{\rho_1}^{\rho_2} \xi_2(t) \xi_1(t) dt := \bar{\xi}$, then

$$\varphi(\bar{\xi}) \leq \frac{1}{D} \int_{\rho_1}^{\rho_2} (\varphi \circ \xi_2)(t) \xi_1(t) dt.$$

Following is the definition of a strongly convex function while the next theorem gives a criteria for checking the strong convexity of twice differentiable functions [44]:

Definition 1. Let $\varphi : [\sigma_1, \sigma_2] \rightarrow \mathbb{R}$ be a function, then with modulus $\lambda > 0$, it is strongly convex, if the following inequality holds

$$\varphi(\gamma\vartheta_1 + (1-\gamma)\vartheta_2) \leq \gamma\varphi(\vartheta_1) + (1-\gamma)\varphi(\vartheta_2) - \lambda\gamma(1-\gamma)(\vartheta_1 - \vartheta_2)^2,$$

for all $\vartheta_1, \vartheta_2 \in [\sigma_1, \sigma_2]$ and $\gamma \in [0, 1]$.

It is significant that every strongly convex function is convex but the converse is not true generally.

Theorem 3. If the function φ is twice differentiable then it is strongly convex with modulus $\lambda > 0$, if and only if $\varphi''(\vartheta_1) \geq 2\lambda$ for all $\vartheta_1 \in [\sigma_1, \sigma_2]$.

In this manuscript, we make use of the well-known Taylor formula and the concept of strong convexity to improve an existing bound for the Jensen gap. Many results may be found in the literature regarding Jensen's inequality for strongly convex functions (see for instance [21, 35, 38, 42]).

Following is the Taylor Formula [4]:

Theorem 4. If $\vartheta_2 \in [\sigma_1, \sigma_2] \subseteq \mathbb{R}$ and $\varphi : [\sigma_1, \sigma_2] \rightarrow \mathbb{R}$ is a function, then for a point $\mu \in [\sigma_1, \sigma_2]$, the well-known Taylor's formula is given by

$$\varphi(\vartheta_2) = \sum_{i=0}^{n-1} \frac{\varphi^{(i)}(\mu)}{i!} (\vartheta_2 - \mu)^i + \frac{1}{(n-1)!} \int_{\mu}^{\vartheta_2} \varphi^{(n)}(t) (\vartheta_2 - t)^{n-1} dt, \quad (1)$$

provided that φ^{n-1} is absolutely continuous for natural number n .

Setting $n = 2$ in Equation (1), we get

$$\varphi(\vartheta_2) = \varphi(\mu) + \varphi'(\mu)(\vartheta_2 - \mu) + \int_{\mu}^{\vartheta_2} \varphi''(t)(\vartheta_2 - t) dt. \quad (2)$$

2. MAIN RESULTS

The following theorem actually gives the improvement in an existing bound for the classical Jensen gap through the concept of strong convexity:

Theorem 5. *Let $|\varphi''|$ be a strongly convex function with modulus λ for twice differentiable functions φ defined on $[\sigma_1, \sigma_2]$. Also, let $\mu, \vartheta_i \in [\sigma_1, \sigma_2]$, $k_i \geq 0$ for $i = 1, 2, \dots, n$ with $\sum_{i=1}^n k_i := K_n > 0$ and $\frac{1}{K_n} \sum_{i=1}^n k_i \vartheta_i := \bar{\vartheta}$, then*

$$\begin{aligned} & \left| \frac{1}{K_n} \sum_{i=1}^n k_i \varphi(\vartheta_i) - \varphi(\bar{\vartheta}) \right| \\ & \leq \frac{1}{K_n} \sum_{i=1}^n k_i (\vartheta_i - \mu)^2 \left[\frac{|\varphi''(\mu)|}{3} + \frac{|\varphi''(\vartheta_i)|}{6} + \frac{\mu\lambda}{12}(\vartheta_i - \mu) - \frac{\vartheta_i\lambda}{12}(\vartheta_i - \mu) \right] \\ & \quad + (\bar{\vartheta} - \mu)^2 \left[\frac{|\varphi''(\mu)|}{3} + \frac{|\varphi''(\bar{\vartheta})|}{6} + \frac{\mu\lambda}{12}(\bar{\vartheta} - \mu) - \frac{\bar{\vartheta}\lambda}{12}(\bar{\vartheta} - \mu) \right]. \end{aligned} \tag{3}$$

Proof. Using (2) in $\frac{1}{K_n} \sum_{i=1}^n k_i \varphi(\vartheta_i)$ and $\varphi(\bar{\vartheta})$, then some calculations lead towards the following identity

$$\frac{1}{K_n} \sum_{i=1}^n k_i \varphi(\vartheta_i) - \varphi(\bar{\vartheta}) = \frac{1}{K_n} \sum_{i=1}^n k_i \int_{\mu}^{\vartheta_i} (\vartheta_i - t) \varphi''(t) dt - \int_{\mu}^{\bar{\vartheta}} (\bar{\vartheta} - t) \varphi''(t) dt. \tag{4}$$

Inequality (5) can be acquired by taking absolute value of both sides of (4) and then applying triangle inequality

$$\begin{aligned} & \left| \frac{1}{K_n} \sum_{i=1}^n k_i \varphi(\vartheta_i) - \varphi(\bar{\vartheta}) \right| \\ & = \left| \frac{1}{K_n} \sum_{i=1}^n k_i \int_{\mu}^{\vartheta_i} (\vartheta_i - t) \varphi''(t) dt - \int_{\mu}^{\bar{\vartheta}} (\bar{\vartheta} - t) \varphi''(t) dt \right| \\ & \leq \frac{1}{K_n} \sum_{i=1}^n k_i \int_{\mu}^{\vartheta_i} (\vartheta_i - t) |\varphi''(t)| dt + \int_{\mu}^{\bar{\vartheta}} (\bar{\vartheta} - t) |\varphi''(t)| dt. \end{aligned} \tag{5}$$

Change of the variable $t = \theta\mu + (1 - \theta)\vartheta_i$ for $\theta \in [0, 1]$ will give the following result

$$\int_{\mu}^{\vartheta_i} (\vartheta_i - t) |\varphi''(t)| dt = (\vartheta_i - \mu) \int_0^1 (\vartheta_i\theta - \mu\theta) |\varphi''(\theta\mu + (1 - \theta)\vartheta_i)| d\theta. \tag{6}$$

Using the strong convexity of $|\varphi''|$ in (6), the following result acquires

$$\begin{aligned} & \int_{\mu}^{\vartheta_i} (\vartheta_i - t) |\varphi''(t)| dt \\ & \leq (\vartheta_i - \mu) \int_0^1 (\vartheta_i\theta - \mu\theta) \times \left(\theta |\varphi''(\mu)| + (1 - \theta) |\varphi''(\vartheta_i)| - \mu\theta(1 - \theta)(\mu - \vartheta_i)^2 \right) d\theta \end{aligned}$$

$$\begin{aligned}
&= (\vartheta_i - \mu) \int_0^1 (\vartheta_i \theta - \mu \theta) \left[\theta |\varphi''(\mu)| + |\varphi''(\vartheta_i)| - \theta |\varphi''(\vartheta_i)| \right. \\
&\quad \left. - \lambda \theta (\mu - \vartheta_i)^2 + \lambda \theta^2 (\mu - \vartheta_i)^2 \right] d\theta \\
&= (\vartheta_i - \mu) \int_0^1 \left(\vartheta_i \theta^2 |\varphi''(\mu)| - \mu \theta^2 |\varphi''(\mu)| + \vartheta_i \theta |\varphi''(\vartheta_i)| - \mu \theta |\varphi''(\vartheta_i)| \right. \\
&\quad \left. - \vartheta_i \theta^2 |\varphi''(\vartheta_i)| + \mu \theta^2 |\varphi''(\vartheta_i)| - \vartheta_i \lambda \theta^2 (\mu - \vartheta_i)^2 + \mu \lambda \theta^2 (\mu - \vartheta_i)^2 \right. \\
&\quad \left. + \vartheta_i \lambda \theta^3 (\mu - \vartheta_i)^2 - \mu \lambda \theta^3 (\mu - \vartheta_i)^2 \right) d\theta. \\
&= (\vartheta_i - \mu) \left[(\vartheta_i - \mu) \left(\frac{|\varphi''(\mu)|}{3} + \frac{|\varphi''(\vartheta_i)|}{6} \right) + \frac{\mu \lambda}{12} (\vartheta_i - \mu)^2 - \frac{\vartheta_i \lambda}{12} (\vartheta_i - \mu)^2 \right] \\
&= (\vartheta_i - \mu)^2 \left[\frac{|\varphi''(\mu)|}{3} + \frac{|\varphi''(\vartheta_i)|}{6} + \frac{\mu \lambda}{12} (\vartheta_i - \mu) - \frac{\vartheta_i \lambda}{12} (\vartheta_i - \mu) \right]. \tag{7}
\end{aligned}$$

Substitution of ϑ_i by $\bar{\vartheta}$ in (7) gives the following inequality

$$\int_{\mu}^{\bar{\vartheta}} (\bar{\vartheta} - t) |\varphi''(t)| dt \leq (\bar{\vartheta} - \mu)^2 \left[\frac{|\varphi''(\mu)|}{3} + \frac{|\varphi''(\bar{\vartheta})|}{6} + \frac{\mu \lambda}{12} (\bar{\vartheta} - \mu) - \frac{\bar{\vartheta} \lambda}{12} (\bar{\vartheta} - \mu) \right]. \tag{8}$$

From (5), (7) and (8) we get (3). \square

Example 1. Let $\varphi(t) = t^4, t \in [0, 1]$, then $\varphi''(t) = 12t^2 > 0$, $|\varphi''|'(t) = 24 \geq 2(12)$ for all $t \in [0, 1]$. Which show that φ is convex and with modulus $\lambda = 12$ the function $|\varphi''|$ is strongly convex on $[0, 1]$. Now, let $k_1, k_2, k_3 = 0.2, 0.3, 0.5$ and $v_1, v_2, v_3 = 0.5, 0.25, 0.2$ respectively, then applying these values in (3), we get

$$0 < \sum_{i=1}^3 k_i \varphi(\vartheta_i) - \varphi \left(\sum_{i=1}^3 k_i \vartheta_i \right) \leq 6\mu^4 - 2.2\mu^3 + 0.0001\mu^2 + 0.0202 = T(\mu) \tag{9}$$

Here at $\mu = 0.275$, $T(\mu)$ will reach towards its minimum value, which is 0.0086 and hence from (9) we have

$$0 < \sum_{i=1}^3 k_i \varphi(\vartheta_i) - \varphi \left(\sum_{i=1}^3 k_i \vartheta_i \right) \leq 0.0086. \tag{10}$$

For $|\varphi''|$ as a convex function and for the above values of k_1, k_2, k_3 and v_1, v_2, v_3 , the following result has been obtained in (4).

$$0 < \sum_{i=1}^3 k_i \varphi(\vartheta_i) - \varphi \left(\sum_{i=1}^3 k_i \vartheta_i \right) \leq 0.0092. \tag{11}$$

It is easy to understand that inequality (10) gives better result than the results obtained in inequality (11) for the Jensen gap. Thus through this gap it is understandable that strongly convex functions actually strengthens the results.

Proposition 1. Let (a_1, \dots, a_n) , and (b_1, \dots, b_n) be two positive n – tuples and $[\sigma_1, \sigma_2]$ be a positive interval. Then

1. for $q > 1, p \in (1, 2) \cup (3, 4)$ such that $\frac{1}{p} + \frac{1}{q} = 1$ with $\mu, \frac{\sum_{i=1}^n a_i b_i}{\sum_{i=1}^n b_i^q}, a_i b_i^{-\frac{q}{p}} \in [\sigma_1, \sigma_2]$ for $i = 1, \dots, n$, the following inequality holds

$$\begin{aligned} & \left(\sum_{i=1}^n a_i^p\right)^{\frac{1}{p}} \left(\sum_{i=1}^n b_i^q\right)^{\frac{1}{q}} - \sum_{i=1}^n a_i b_i \\ & \leq \frac{p(p-1)}{24} \frac{1}{\sum_{i=1}^n b_i^q} \sum_{i=1}^n b_i^q \left(a_i b_i^{-\frac{q}{p}} - \mu\right)^2 \\ & \quad \times \left[8\mu^{p-2} + 4a_i^{p-2} b_i^{\frac{q}{p}-1} - (p-2)(p-3)\sigma_2^{p-4} \left(a_i b_i^{-\frac{q}{p}} - \mu\right)^2\right] \\ & \quad + \left(\frac{\sum_{i=1}^n a_i b_i^{-\frac{q}{p}}}{\sum_{i=1}^n b_i^q} - \mu\right)^2 \\ & \quad \times \left[8\mu^{p-2} + 4\left(\frac{\sum_{i=1}^n a_i b_i^{-\frac{q}{p}}}{\sum_{i=1}^n b_i^q}\right)^{p-2} - (p-2)(p-3)\sigma_2^{p-4} \left(\frac{\sum_{i=1}^n a_i b_i^{-\frac{q}{p}}}{\sum_{i=1}^n b_i^q} - \mu\right)^2\right] \end{aligned} \tag{12}$$

2. If the statement of part 1 satisfied, then the following inequality holds but this time keeping the condition that $p > 4$

$$\begin{aligned} & \left(\sum_{i=1}^n a_i^p\right)^{\frac{1}{p}} \left(\sum_{i=1}^n b_i^q\right)^{\frac{1}{q}} - \sum_{i=1}^n a_i b_i \\ & \leq \frac{p(p-1)}{24} \frac{1}{\sum_{i=1}^n b_i^q} \sum_{i=1}^n b_i^q \left(a_i b_i^{-\frac{q}{p}} - \mu\right)^2 \\ & \quad \times \left[8\mu^{p-2} + 4a_i^{p-2} b_i^{\frac{q}{p}-1} - (p-2)(p-3)\sigma_1^{p-4} (a_i b_i^{-\frac{q}{p}} - \mu)^2\right] \\ & \quad + \left(\frac{\sum_{i=1}^n a_i b_i^{-\frac{q}{p}}}{\sum_{i=1}^n b_i^q} - \mu\right)^2 \\ & \quad \times \left[8\mu^{p-2} + 4\left(\frac{\sum_{i=1}^n a_i b_i^{-\frac{q}{p}}}{\sum_{i=1}^n b_i^q}\right)^{p-2} - (p-2)(p-3)\sigma_1^{p-4} \left(\frac{\sum_{i=1}^n a_i b_i^{-\frac{q}{p}}}{\sum_{i=1}^n b_i^q} - \mu\right)^2\right] \end{aligned} \tag{13}$$

Proof. 1. Let $\varphi(t) = t^p, t \in [\sigma_1, \sigma_2]$ then $\varphi''(t) = p(p-1)t^{p-2} > 0, |\varphi''|'(t) = p(p-1)(p-2)(p-3)t^{p-4}$, which show that the function φ is convex, and for the given value of p , the function $|\varphi''|'(t)$ is decreasing while $|\varphi''|'(t) \geq 2\left(\frac{p(p-1)(p-2)(p-3)\sigma_2^{p-4}}{2}\right)$ for all $t \in [\sigma_1, \sigma_2]$. Therefore the function $|\varphi''|$ is strongly convex with $\lambda =$

$\frac{p(p-1)(p-2)(p-3)\sigma_2^{p-4}}{2}$, so using (3) for $\varphi(t) = t^p, k_i = b_i^q$ and $\vartheta_i = a_i b_i^{-\frac{q}{p}}$, we derive

$$\begin{aligned} & \left(\left(\sum_{i=1}^n a_i^p \right) \left(\sum_{i=1}^n b_i^q \right)^{p-1} - \left(\sum_{i=1}^n a_i b_i \right)^p \right)^{\frac{1}{p}} \\ & \leq \frac{p(p-1)}{24} \frac{1}{\sum_{i=1}^n b_i^q} \sum_{i=1}^n b_i^q \left(a_i b_i^{-\frac{q}{p}} - \mu \right)^2 \\ & \quad \times \left[8\mu^{p-2} + 4a_i^{p-2} b_i^{\frac{q}{p}-1} - (p-2)(p-3)\sigma_2^{p-4} \left(a_i b_i^{-\frac{q}{p}} - \mu \right)^2 \right] \\ & \quad + \left(\frac{\sum_{i=1}^n a_i b_i^{-\frac{q}{p}}}{\sum_{i=1}^n b_i^q} - \mu \right)^2 \\ & \quad \times \left[8\mu^{p-2} + 4 \left(\frac{\sum_{i=1}^n a_i b_i^{-\frac{q}{p}}}{\sum_{i=1}^n b_i^q} \right)^{p-2} - (p-2)(p-3)\sigma_2^{p-4} \left(\frac{\sum_{i=1}^n a_i b_i^{-\frac{q}{p}}}{\sum_{i=1}^n b_i^q} - \mu \right)^2 \right] \end{aligned} \tag{14}$$

By applying the inequality $\alpha^s - \beta^s \leq (\alpha - \beta)^s, \beta \in [0, \alpha], s \in [0, 1]$ for $\alpha = \left(\sum_{i=1}^n a_i^p \right) \left(\sum_{i=1}^n b_i^q \right)^{p-1}, \beta = \left(\sum_{i=1}^n a_i b_i \right)^p$ and $s = \frac{1}{p}$ we obtain

$$\left(\sum_{i=1}^n a_i^p \right)^{\frac{1}{p}} \left(\sum_{i=1}^n b_i^q \right)^{\frac{1}{q}} - \left(\sum_{i=1}^n a_i b_i \right) \leq \left(\left(\sum_{i=1}^n a_i^p \right) \left(\sum_{i=1}^n b_i^q \right)^{p-1} - \left(\sum_{i=1}^n a_i b_i \right)^p \right)^{\frac{1}{p}} \tag{15}$$

From (14) and (15), we get (12)

2. We get $\lambda = \frac{p(p-1)(p-2)(p-3)\sigma_1^{p-4}}{2}$, as by applying the same proposed value of p , the function $|\varphi''|$ become an increasing function. Now by applying the same method of part 1 the inequality (13) can be obtained. \square

Here in the following theorem, we present a generalized version of Theorem 5.

Theorem 6. Let $\varphi \in \mathbb{C}^2[\sigma_1, \sigma_2]$ such that $|\varphi''|$ is strongly convex function with modulus λ , and $\xi_1 \geq 0$ integrable function such that $\xi_1 : [\rho_1, \rho_2] \rightarrow \mathbb{R}$ with $\int_{\rho_1}^{\rho_2} \xi_1(t) dt = D > 0$. Also, assuming the integrable function ξ_2 such that $\xi_2 : [\rho_1, \rho_2] \rightarrow \mathbb{R}$ where $\xi_2(t) \in [\sigma_1, \sigma_2], \forall t \in [\rho_1, \rho_2]$. Then the following inequality holds for $\bar{\xi} = \frac{1}{D} \int_{\rho_1}^{\rho_2} \xi_2(t)\xi_1(t)dt$ and $\mu \in [\sigma_1, \sigma_2]$.

$$\begin{aligned} & \left| \frac{1}{D} \int_{\rho_1}^{\rho_2} \xi_1(t) (\varphi \circ \xi_2)(t) dt - \varphi(\bar{\xi}) \right| \\ & \leq \frac{1}{D} \int_{\rho_1}^{\rho_2} \xi_1(t) (\xi_2(t) - \mu)^2 \end{aligned}$$

$$\begin{aligned} & \times \left(\frac{\varphi''(\mu)}{3} + \frac{\varphi''(\xi_2(t))}{6} + \frac{\mu\lambda}{12} (\xi_2(t) - \mu) - \frac{\lambda\xi_2(t)}{12} (\xi_2(t) - \mu) \right) dt \\ & + (\bar{\xi} - \mu)^2 \left[\frac{\varphi''(\mu)}{3} + \frac{\varphi''(\bar{\xi})}{6} + \frac{\mu\lambda}{12} (\bar{\xi} - \mu) - \frac{\bar{\xi}\lambda}{12} (\bar{\xi} - \mu) \right]. \end{aligned} \tag{16}$$

Proof. Using (2) in $\frac{1}{D} \int_{\rho_1}^{\rho_2} \xi_1(t) (\varphi \circ \xi_2)(t) dt$ and $\varphi(\bar{\xi})$, then some calculations lead towards the following identity.

$$\begin{aligned} & \frac{1}{D} \int_{\rho_1}^{\rho_2} \xi_1(t) (\varphi \circ \xi_2)(t) dt - \varphi(\bar{\xi}) \\ & = \frac{1}{D} \int_{\rho_1}^{\rho_2} \left(\xi_1(t) \int_{\mu}^{\xi_2(t)} (\xi_2(t) - t) \varphi''(t) dt \right) dt - \int_{\mu}^{\bar{\xi}} (\bar{\xi} - t) \varphi''(t) dt. \end{aligned} \tag{17}$$

From here, adopting the procedure of the proof of Theorem 5 we get the result. \square

Remark 1. The integral form of Proposition 1 may be shown as an application of Theorem 6.

Corollary 1. Let $\Phi : [\rho_1, \rho_2] \rightarrow \mathbb{R}$ be such that $|\Phi''|$ is strongly convex function with modulus λ and $\mu \in [\rho_1, \rho_2]$, then the following inequality can be obtained:

$$\begin{aligned} & \left| \frac{1}{\rho_2 - \rho_1} \int_{\rho_1}^{\rho_2} \Phi(t) dt - \Phi\left(\frac{\rho_1 + \rho_2}{2}\right) \right| \\ & \leq \frac{1}{6(\rho_2 - \rho_1)} \int_{\rho_1}^{\rho_2} (t - \mu)^2 \Phi''(t) dt + \frac{1}{24} \left| \Phi''\left(\frac{\rho_1 + \rho_2}{2}\right) \right| (\rho_1 + \rho_2 - 2\mu)^2 \\ & \quad + \frac{\Phi''(\mu)}{36} (7\rho_1^2 + 7\rho_2^2 + 10\rho_1\rho_2 - 24\mu\rho_1 - 24\mu\rho_2 + 24\mu^2) \\ & \quad + \frac{\mu\lambda}{48 \times 96} (2(\rho_1 + \rho_2)(\rho_1^2 + \rho_2^2) - 4(\rho_1^2 + \rho_2^2 + \rho_1\rho_2) - 4\mu^3) + (\rho_1 + \rho_2 - 2\mu)^3 \\ & \quad - \frac{\lambda}{12(\rho_2 - \rho_1)} \left(\frac{\rho_2^5 - \rho_1^5}{5} - \frac{\mu^3(\rho_2^2 - \rho_1^2)}{2} - \frac{3\mu(\rho_2^4 - \rho_1^4)}{4} + \mu^2(\rho_2^3 - \rho_1^3) \right) \\ & \quad - \frac{\lambda(\rho_1 + \rho_2)}{192} (\rho_1 + \rho_2 - 2\mu)^3. \end{aligned} \tag{18}$$

Proof. By utilizing (16) for $\Phi = \varphi$, $[\sigma_1, \sigma_2] = [\rho_1, \rho_2]$ and $\xi_1(t) = 1, \xi_2(t) = t$ for all $t \in [\rho_1, \rho_2]$, we get (18). \square

3. APPLICATIONS IN INFORMATION THEORY

In information theory, we study about the storage, quantification and communication of information about certain events in different aspects. In this field, various such events may be practiced through different divergences, distances or entropies for example Kullback-Leibler and Rényi-divergences, Hellinger distance, Shannon and Zipf-Mandelbrot entropies etc, which are special cases of the Csiszár divergence. In analysis, the Jensen inequality is one of the most important inequalities which produces various results for Csiszár divergence by manipulating suitable substitutions. Such practices are made in this section. Following is the Csiszár divergence functional [18]:

Definition 2 (Csiszár divergence). *Let $[\sigma_1, \sigma_2] \subset \mathbb{R}$ and $T : [\sigma_1, \sigma_2] \rightarrow \mathbb{R}$ be a function, then for $\mathbf{h} = (h_1, \dots, h_n) \in \mathbb{R}^n$ and $\mathbf{z} = (z_1, \dots, z_n) \in \mathbb{R}_+^n$ such that $\frac{h_i}{z_i} \in [\sigma_1, \sigma_2]$, for $i = 1, \dots, n$, the Csiszár divergence is defined as:*

$$C(\mathbf{h}, \mathbf{z}) = \sum_{i=1}^n z_i T\left(\frac{h_i}{z_i}\right).$$

Theorem 7. *Let for the function $T \in C^2[\sigma_1, \sigma_2]$, such that with modulus λ , $|T''|$ is strongly convex function. Also, let $\mathbf{h} = (h_1, \dots, h_n) \in \mathbb{R}^n$ and $\mathbf{z} = (z_1, \dots, z_n) \in \mathbb{R}_+^n$, such that $\mu, \frac{\sum_{i=1}^n h_i}{\sum_{i=1}^n z_i}, \frac{h_i}{z_i} \in [\sigma_1, \sigma_2] \subset \mathbb{R}$, for $i = 1, 2, \dots, n$ then,*

$$\begin{aligned} & \left| \frac{1}{\sum_{i=1}^n z_i} C(\mathbf{h}, \mathbf{z}) - T\left(\frac{\sum_{i=1}^n h_i}{\sum_{i=1}^n z_i}\right) \right| \\ & \leq \frac{1}{\sum_{i=1}^n z_i} \sum_{i=1}^n z_i \left(\frac{h_i}{z_i} - \mu\right)^2 \\ & \quad \times \left[\frac{|T''(\mu)|}{3} + \frac{|T''\left(\frac{h_i}{z_i}\right)|}{6} + \frac{\mu\lambda}{12} \left(\frac{h_i}{z_i} - \mu\right) - \frac{\left(\frac{h_i}{z_i}\right)\lambda}{12} \left(\frac{h_i}{z_i} - \mu\right) \right] \\ & \quad + \left(\frac{\sum_{i=1}^n h_i}{\sum_{i=1}^n z_i} - \mu\right)^2 \left[\frac{|T''(\mu)|}{3} + \frac{|T''\left(\frac{\sum_{i=1}^n h_i}{\sum_{i=1}^n z_i}\right)|}{6} + \frac{\mu\lambda}{12} \left(\frac{\sum_{i=1}^n h_i}{\sum_{i=1}^n z_i} - \mu\right) \right. \\ & \quad \left. - \frac{\left(\frac{\sum_{i=1}^n h_i}{\sum_{i=1}^n z_i}\right)\lambda}{12} \left(\frac{\sum_{i=1}^n h_i}{\sum_{i=1}^n z_i} - \mu\right) \right]. \end{aligned} \tag{19}$$

Proof. Utilizing $\varphi = T, \vartheta_i = \frac{h_i}{z_i}$ and $k_i = \frac{z_i}{\sum_{i=1}^n z_i}$ in (3) we obtain (19). \square

Definition 3 (Rényi-divergence). *For two positive probability distributions $\mathbf{h} = (h_1, \dots, h_n), \mathbf{z} = (z_1, \dots, z_n)$ and $\eta \geq 0, \eta \neq 1$, the Rényi-divergence is defined as:*

$$R(\mathbf{h}, \mathbf{z}) = \frac{1}{\eta - 1} \log \left(\sum_{i=1}^n h_i^\eta z_i^{1-\eta} \right).$$

Corollary 2. Let $\mathbf{h} = (h_1, \dots, h_n), \mathbf{z} = (z_1, \dots, z_n)$ be two positive probability distributions and $\eta > 1$ such that $\mu, \sum_{i=1}^n z_i \left(\frac{h_i}{z_i}\right)^\eta, \left(\frac{h_i}{z_i}\right)^{\eta-1} \in [\sigma_1, \sigma_2] \subseteq \mathbb{R}$ for $i = 1, 2, \dots, n$ then

$$\begin{aligned} R(\mathbf{h}, \mathbf{z}) &= \frac{1}{\eta-1} \sum_{i=1}^n h_i \log \left(\frac{h_i}{z_i}\right)^{\eta-1} \\ &\leq \frac{1}{\eta-1} \sum_{i=1}^n h_i \left(\frac{h_i}{z_i} - \mu\right)^2 \left[\frac{1}{3\mu^2} + \frac{1}{6} \left(\frac{z_i}{h_i}\right)^{2(\eta-1)} - \frac{1}{4\sigma_2^4} \left(\left(\frac{h_i}{z_i}\right)^{\eta-1} - \mu \right)^2 \right] \\ &\quad + \left(\sum_{i=1}^n h_i^\eta z_i^{\eta-1} - \mu \right)^2 \left[\frac{1}{3\mu^2} + \frac{1}{6 \left(\sum_{i=1}^n h_i^\eta z_i^{1-\eta}\right)^2} - \frac{1}{4\sigma_2^4} \left(\sum_{i=1}^n h_i^\mu z_i^{1-\eta} - \mu \right)^2 \right]. \end{aligned} \quad (20)$$

Proof. Let $\varphi(t) = -\frac{1}{\eta-1} \log(t), t \in [\sigma_1, \sigma_2]$, then $\varphi''(t) = \frac{1}{(\eta-1)t^2}$ and $|\varphi''|'(t) = \frac{6}{(\eta-1)t^4} \geq 2 \left(\frac{3}{(\eta-1)\sigma_2^4}\right)$ which implies that φ is convex and with $\lambda = \frac{3}{(\eta-1)\sigma_2^4}$, $|\varphi''|$ is strongly convex. Thus we get (20) by applying (3) for $\varphi(t) = -\frac{1}{\eta-1} \log(t), k_i = h_i$ and $\vartheta_i = \left(\frac{h_i}{z_i}\right)^{\eta-1}$. \square

Definition 4 (Shannon entropy). Let $\mathbf{z} = (z_1, \dots, z_n)$ be a positive probability distribution, then the information divergence or Shannon entropy is defined as:

$$S(\mathbf{z}) = - \sum_{i=1}^n z_i \log(z_i).$$

Corollary 3. Suppose a positive probability distribution $\mathbf{z} = (z_1, \dots, z_n)$ and $\mu, \frac{1}{z_i} \in [\sigma_1, \sigma_2] \subseteq \mathbb{R}^+$ for $i = 1, \dots, n$. then

$$\begin{aligned} \log n - S(\mathbf{z}) &\leq \sum_{i=1}^n z_i \left(\frac{1}{z_i} - \mu\right)^2 \left[\frac{1}{3\mu^2} + \frac{z_i^2}{6} - \frac{1}{4\sigma_2^4} \left(\mu - \frac{1}{z_i}\right)^2 \right] \\ &\quad + (n - \mu)^2 \left[\frac{1}{3\mu^2} + \frac{1}{6n^2} - \frac{1}{4\sigma_2^4} (n - \mu)^2 \right]. \end{aligned} \quad (21)$$

Proof. Let $\varphi(t) = -\log t, t \in [\sigma_1, \sigma_2]$ then $\varphi''(t) = \frac{1}{t^2} > 0$ and $|\varphi''|'(t) = \frac{6}{t^4} \geq 2 \frac{3}{\sigma_2^4}$, which presented that the function φ is convex and with $\lambda = \frac{3}{\sigma_2^4}$, $|\varphi''|$ is strongly convex. Therefore applying (19) for $\varphi(t) = -\log(t), (h_1, \dots, h_n) = (1, \dots, 1)$, we get (21). \square

Definition 5 (Kullback-Leibler divergence). *For two positive probability distributions, $\mathbf{h} = (h_1, \dots, h_n)$ and $\mathbf{z} = (z_1, \dots, z_n)$, the Kullback-Leibler divergence is defined as:*

$$KL(\mathbf{h}, \mathbf{z}) = \sum_{i=1}^n h_i \log \left(\frac{h_i}{z_i} \right).$$

Corollary 4. *Consider that $[\sigma_1, \sigma_2] \subseteq \mathbb{R}^+$ and $\mathbf{h} = (h_1, \dots, h_n), \mathbf{z} = (z_1, \dots, z_n)$ are two positive probability distributions, with $\mu, \frac{h_i}{z_i} \in [\sigma_1, \sigma_2]$, then*

$$KL(\mathbf{h}, \mathbf{z}) \leq \sum_{i=1}^n z_i \left(\frac{h_i}{z_i} - \mu \right)^2 \left[\frac{1}{3\mu} + \frac{z_i}{6h_i} - \frac{1}{12\sigma_2^3} \left(\frac{h_i}{z_i} - \mu \right)^2 \right] + (\mu - 1)^2 \left[\frac{1}{3\mu} - \frac{1}{12\sigma_2^3} (\mu - 1)^2 \right]. \tag{22}$$

Proof. Let $\varphi(t) = t \log t, t \in [\sigma_1, \sigma_2]$, then $\varphi''(t) = \frac{1}{t} > 0$, which conclude that φ is convex function. Also, $|\varphi''|'(t) = \frac{2}{t^3} \geq 2 \left(\frac{1}{\sigma_2^3} \right)$, which implies, with $\lambda = \frac{1}{\sigma_2^3} > 0$ the function $|\varphi''|$ is strongly convex. Thus we get (22) by applying (19) for $\varphi(t) = t \log t$. \square

Definition 6 (Bhattacharyya coefficient). *If $\mathbf{z} = (z_1, \dots, z_n)$ and $\mathbf{h} = (h_1, \dots, h_n)$ are two positive probability distributions, then the mathematical form of Bhattacharyya coefficient is given by:*

$$B(\mathbf{h}, \mathbf{z}) = \sum_{i=1}^n \sqrt{h_i z_i}.$$

Corollary 5. *Consider that $\mathbf{h} = (h_1, \dots, h_n)$ and $\mathbf{z} = (z_1, \dots, z_n)$ are some positive probability distributions with the following conditions $\mu, \frac{h_i}{z_i} \in [\sigma_1, \sigma_2]$ where $[\sigma_1, \sigma_1] \subseteq \mathbb{R}^+$ and $i = 1, 2, \dots, n$ then*

$$1 - B(\mathbf{h}, \mathbf{z}) \leq \sum_{i=1}^n z_i \left(\frac{h_i}{z_i} - \mu \right)^2 \left[\frac{1}{12\mu^{\frac{3}{2}}} + \frac{1}{24} \left(\frac{z_i}{h_i} \right)^{\frac{3}{2}} - \frac{5}{128\sigma_2^{\frac{7}{2}}} \right] + (1 - \mu)^2 \left[\frac{1}{24} + \frac{1}{12\mu^{\frac{3}{2}}} - \frac{5}{128\sigma_2^{\frac{7}{2}}} (1 - \mu)^2 \right]. \tag{23}$$

Proof. Let $\varphi(t) = -\sqrt{t}, t \in [\sigma_1, \sigma_2]$ then $\varphi''(t) = \frac{1}{4t^{\frac{3}{2}}} > 0$ and $|\varphi''|'(t) = \frac{15}{16t^{\frac{7}{2}}} \geq 2 \left(\frac{15}{32\sigma_2^{\frac{7}{2}}} \right)$. Which show that the function φ is convex and with $\lambda = \frac{15}{32\sigma_2^{\frac{7}{2}}}, |\varphi''|$ is strongly convex. Therefore by putting $\varphi(t) = -\sqrt{t}$, in (19), we can get (23). \square

Definition 7 (Hellinger distance). For two positive probability distributions $\mathbf{z} = (z_1, \dots, z_n)$, $\mathbf{h} = (h_1, \dots, h_2)$, the Hellinger distance is define as:

$$H(\mathbf{h}, \mathbf{z}) = \frac{1}{2} \sum_{i=1}^n \left(\sqrt{h_i} - \sqrt{z_i} \right)^2.$$

Corollary 6. let $\mathbf{h} = (h_1, \dots, h_n)$ and $\mathbf{z} = (z_1, \dots, z_n)$ be two positive probability distributions, such that $\mu, \frac{h_i}{z_i} \in [\sigma_1, \sigma_2]$, where $[\sigma_1, \sigma_1] \subseteq \mathbb{R}^+$ and $i = 1, 2, \dots, n$ then

$$H(\mathbf{h}, \mathbf{z}) \leq \sum_{i=1}^n z_i \left(\frac{h_i}{z_i} - \mu \right)^2 \left[\frac{1}{12\mu^{\frac{3}{2}}} + \frac{1}{24 \left(\frac{h_i}{z_i} \right)^{\frac{3}{2}}} - \frac{5}{128\sigma_2^{\frac{7}{2}}} \right] + (1 - \mu)^2 \left[\frac{1}{24} + \frac{1}{12\mu^{\frac{3}{2}}} - \frac{5}{128\sigma_2^{\frac{7}{2}}} (1 - \mu)^2 \right]. \tag{24}$$

Proof. Let $\varphi(t) = \frac{1}{2}(1 - \sqrt{t})^2$, $t \in [\sigma_1, \sigma_2]$, then $\varphi''(t) = \frac{1}{4t^{\frac{3}{2}}} > 0$ and $|\varphi''|'(t) = \frac{15}{16t^{\frac{7}{2}}} \geq 2 \left(\frac{15}{32\sigma_2^{\frac{7}{2}}} \right)$. This shows that φ is convex and $|\varphi''|$ is strongly convex with modulus $\lambda = \frac{15}{32\sigma_2^{\frac{7}{2}}}$. Hence we can obtained (24) by utilizing (19) for $\varphi(t) = \frac{1}{2}(1 - \sqrt{t})^2$. □

Definition 8 (Triangular discrimination). Assume that $\mathbf{h} = (h_1, \dots, h_n)$ and $\mathbf{z} = (z_1, \dots, z_n)$ are two positive probability distributions then the mathematical formula for the Triangular discrimination is given by:

$$T_d(\mathbf{h}, \mathbf{z}) = \sum_{i=1}^n \frac{(h_i - z_i)^2}{(h_i + z_i)}.$$

Corollary 7. let $\mathbf{z} = (z_1, \dots, z_n)$ and $\mathbf{h} = (h_1, \dots, h_n)$ be two positive probability distributions. Further assume that $\mu, \frac{h_i}{z_i} \in [\sigma_1, \sigma_2]$ where $[\sigma_1, \sigma_1] \subseteq \mathbb{R}^+$ and $i = 1, 2, \dots, n$ then

$$T_d(\mathbf{h}, \mathbf{z}) \leq \sum_{i=1}^n z_i \left(\frac{h_i}{z_i} - \mu \right)^2 \left[\frac{8}{3(\mu + 1)^3} + \frac{4z_i^3}{3(h_i + z_i)^3} - \frac{4}{(\sigma_2 + 1)^5} \left(\frac{h_i}{z_i} - \mu \right)^2 \right] + (1 - \mu)^2 \left[\frac{8}{3(\mu + 1)^3} - \frac{4}{(\sigma_2 + 1)^5} (1 - \mu)^2 \right]. \tag{25}$$

Proof. Let $\varphi(t) = \frac{(t-1)^2}{(t+1)}$, $t \in [\sigma_1, \sigma_2]$, then $\varphi''(t) = \frac{8}{(t+1)^3} > 0$ and $|\varphi''|'(t) = \frac{96}{(t+1)^5} \geq 2 \left(\frac{48}{(\sigma_2+1)^5} \right)$. This presented that φ is a convex function and with $\lambda = \frac{48}{(\sigma_2+1)^5}$, $|\varphi''|$ is a strongly convex function. Therefore using (19) for such values we may deduce (25). □

4. CONCLUDING REMARKS

In fact, among the mathematical inequalities for convex functions, the Jensen inequality is the most powerful inequality whose gap can be utilized for various purposes specially in the approximation of certain parameters in optimization problems. In this regard, better estimates for its gap can be used to obtain better results. The strongly convex functions are some tools to strengthen such estimates. In this paper, it is demonstrated through a numerical experiment that replacing convex functions by strongly convex functions actually strengthens the bound presented for the Jensen gap in [4]. Similarly the improved result enabled us to present improvements in the bounds obtained for the Hölder and Hermite-Hadamard gaps and proposed such improvements in the results obtained for various entropies and divergences in information theory. The idea presented in the paper, further motivates the mathematicians to establish such results in future.

Author Contribution Statements Both the authors contributed equally and significantly in writing this article. The authors read and approved the final manuscript.

Declaration of Competing Interests The authors declare that they have no competing interest.

Acknowledgements We are thankful to the respected reviewers for their valuable suggestions

REFERENCES

- [1] Adamek, M., On a Jensen-type inequality for F-convex functions, *Math. Inequal. Appl.*, 22 (2019), 1355-1364. <https://doi.org/10.7153/mia-2019-22-93>
- [2] Adil Khan, M., Khan, S., Chu, Y.-M., A new bound for the Jensen gap with applications in information theory, *IEEE Access*, 8 (2020), 98001-98008. <https://doi.org/10.1109/ACCESS.2020.2997397>
- [3] Adil Khan, M., Khan, S., Chu, Y.-M., New estimates for the Jensen gap using s-convexity with applications, *Front. Phys.*, 8 (2020), Article ID 313. <https://doi.org/10.3389/fphy.2020.00313>
- [4] Adil Khan, M., Khan, S., Ullah, I., Khan, K. A., Chu, Y.-M., A novel approach to the Jensen gap through Taylor's theorem, *Math. Methods Appl. Sci.*, 44(5) (2020), 3324-3333. <https://doi.org/10.1002/mma.6944>
- [5] Adil Khan, M., Mohammad, N., Nwaeze, E. R., Chu, Y.-M., Quantum Hermite-Hadamard inequality by means of a Green function, *Adv. Difference Equ.*, 2020 (2020), Article ID 99. <https://doi.org/10.1186/s13662-020-02559-3>
- [6] Adil Khan, M., Pečarić, Đ. Pečarić, J., Bounds for Shannon and Zipf-Mandelbrot entropies, *Math. Methods Appl. Sci.*, 40 (2017), 7316-7322. <https://doi.org/10.1002/mma.4531>
- [7] Adil Khan, M., Zaheer Ullah, S., Chu, Y.-M., The concept of coordinate strongly convex functions and related inequalities, *Rev. R. Acad. Cienc. Exactas Fis. Nat. Ser. A Mat. RACSAM*, 113 (2019), 2235-2251. <https://doi.org/10.1007/s13398-018-0615-8>
- [8] Ahmad, K., Adil Khan, M., Khan, S., Ali, A., Chu, Y.-M., New estimates for generalized Shannon and Zipf-Mandelbrot entropies via convexity results, *Results Phys.*, 18 (2020), Article ID 103305. <https://doi.org/10.1016/j.rinp.2020.103305>

- [9] Ansari, Q. H., Lalitha, C. S., Mehta, M., Generalized Convexity, Nonsmooth Variational Inequalities and Nonsmooth Optimization, Chapman and Hall/CRC, 2019. <https://doi.org/10.1201/b15244>
- [10] Azar, S. A., Jensen's inequality in finance, *Int. Adv. Econ. Res.*, 14 (2008), 433-440. <https://doi.org/10.1007/s11294-008-9172-9>
- [11] Bakula, M. K., Pečarić, J., On the Jensen's inequality for convex functions on the coordinates in a rectangle from the plane, *Taiwanese J. Math.*, 10 (2006), 1271-1292. <https://doi.org/10.11650/twjm/1500557302>
- [12] Beesack, P. R., Pečarić, J., On Jensen's inequality for convex functions, *J. Math. Anal. Appl.*, 110(2) (1985), 536-552. [https://doi.org/10.1016/0022-247X\(85\)90315-4](https://doi.org/10.1016/0022-247X(85)90315-4)
- [13] Bibi, R., Nosheen, A., Bano, S., Pečarić, J., Generalizations of the Jensen functional involving diamond integrals via Abel-Gontscharoff interpolation, *J. Inequal. Appl.*, 2022 (2022), Article ID 15. <https://doi.org/10.1186/s13660-021-02748-y>
- [14] Bradanović, S. I., More accurate majorization inequalities obtained via superquadraticity and convexity with application to entropies, *Mediterr. J. Math.*, 18 (2021), Article ID 79. <https://doi.org/10.1007/s00009-021-01708-6>
- [15] Butt, S. I., Akdemir, A. O., Nasir, J., Jarad, F., Some Hermite-Jensen-Mercer like inequalities for convex functions through a certain generalized fractional integrals and related results, *Miskolc Math. Notes*, 21 (2020), 689-715. <https://doi.org/10.18514/MMN.2020.3339>
- [16] Butt, S. I., Yousaf, S., Ahmad, H., Nofal, T. A., Jensen-Mercer inequality and related results in the fractal sense with applications, *Fractals*, 30(1) (2021), Article ID 2240008. <https://doi.org/10.1142/S0218348X22400084>
- [17] Cloud, M. J., Drachman, B. C., Lebedev, L. P., Inequalities with Applications to Engineering, Springer: Cham Heidelberg New York Dordrecht London, 2014. <https://doi.org/10.1007/978-3-319-05311-0>
- [18] Deng, Y., Ullah, H., Adil Khan, M., Iqbal, S., Wu, S., Refinements of Jensen's inequality via majorization results with applications in the information theory, *J. Math.*, 2021 (2021), Article ID 1951799. <https://doi.org/10.1155/2021/1951799>
- [19] Dragomir, S. S., A new refinement of Jensen's inequality in linear spaces with applications, *Math. Comput. Modelling*, 52(9) (2010), 1497-1505. <https://doi.org/10.1016/j.mcm.2010.05.035>
- [20] Dragomir, S. S., A refinement of Jensen's inequality with applications for f -divergence measures, *Taiwanese J. Math.*, 14 (2010), 153-164. <https://doi.org/10.11650/twjm/1500405733>
- [21] Dragomir, S. S., Nikodem, K., Jensen's and Hermite-Hadamard's type inequalities for lower and strongly convex functions on normed spaces, *Bull. Iran. Math. Soc.*, 44 (2018), 1337-1349. <https://doi.org/10.1007/s41980-018-0095-9>
- [22] Erdem, Y., Ogunmez, H., Budak, H., Some generalized inequalities of Hermite-Hadamard type for strongly s -convex functions, *New Trend Math. Sci.*, 5(3) (2017), 22-32. <http://dx.doi.org/10.20852/ntmsci.2017.181>
- [23] Erdem, Y., Ogunmez, H., Budak, H., On some Hermite-Hadamard type inequalities for strongly s -convex functions, *New Trend Math. Sci.*, 5(3) (2017), 154-161. <https://doi.org/10.20852/ntmsci.2017.192>
- [24] Han, W., Numerical analysis of stationary variational-hemivariational inequalities with applications in contact mechanics, *Math. Mech. Solids*, 23 (2018), 279-293. <https://doi.org/10.1177/1081286517713342>
- [25] Horváth, L., Pečarić, Đ., Pečarić, J., Estimations of f -and Rényi divergences by using a cyclic refinement of the Jensen's inequality, *Bull. Malays. Math. Sci. Soc.*, 42(3) (2019), 933-946. <https://doi.org/10.1007/s40840-017-0526-4>
- [26] Iqbal, A., Adil Khan, M., Ullah, S., Chu, Y.-M., Some new Hermite-Hadamard-type inequalities associated with conformable fractional integrals and their applications, *J. Funct. Spaces*, 2020 (2020), Article ID 9845407. <https://doi.org/10.1155/2020/9845407>

- [27] Kashuri, A., Liko, R., Ali, M. A., Budak, H., New estimates of Gauss-Jacobi and trapezium type inequalities for strongly (h_1, h_2) -preinvex mappings via general fractional integrals, *Int. J. Nonlinear Anal. Appl.*, 12(1) (2021), 979-996. <https://doi.org/10.22075/IJNAA.2020.19718.2096>
- [28] Khan, S., Adil Khan, M., Butt, S. I., Chu, Y.-M., A new bound for the Jensen gap pertaining twice differentiable functions with applications, *Adv. Difference Equ.*, 2020 (2020), Article ID 333. <https://doi.org/10.1186/s13662-020-02794-8>
- [29] Khan, Z. A., Shah, K., Discrete fractional inequalities pertaining a fractional sum operator with some applications on time scales, *J. Funct. Spaces*, 2021 (2021), Article ID 8734535. <https://doi.org/10.1155/2021/8734535>
- [30] Khurshid, Y., Adil Khan, M., Chu, Y.-M., Conformable integral inequalities of the Hermite-Hadamard type in terms of GG- and GA-convexities, *J. Funct. Spaces*, 2019 (2019), Article ID 6926107. <https://doi.org/10.1155/2019/6926107>
- [31] Khurshid, Y., Adil Khan, M., Chu, Y.-M., Khan, Z. A., Hermite-Hadamard-Fejér inequalities for conformable fractional integrals via preinvex functions, *J. Funct. Spaces*, 2019 (2019), Article ID 3146210. <https://doi.org/10.1155/2019/3146210>
- [32] Lakshmikantham, V., Vatsala, A. S., Theory of Differential and Integral Inequalities with Initial Time Difference and Applications, Springer: Berlin, 1999. <https://doi.org/10.1007/978-94-011-4577-0-12>
- [33] Liao, J. G., Berg, A., Sharpening Jensen's inequality, *Amer. Statist.*, 4 (2018), 1-4. <https://doi.org/10.1080/00031305.2017.1419145>
- [34] Lin, Q., Jensen inequality for superlinear expectations, *Stat. Probabil. Lett.*, 151 (2019), 79-83. <https://doi.org/10.1016/j.spl.2019.03.006>
- [35] Merentes, N., Nikodem, K., Remarks on strongly convex functions, *Aequat. Math.*, 80 (2010), 193-199. <https://doi.org/10.1007/s00010-010-0043-0>
- [36] Moradi, H. R., Omidvar, M. E., Adil Khan, M., Nikodem, K., Around Jensen's inequality for strongly convex functions, *Aequat. Math.*, 92 (2018), 25-37. <https://doi.org/10.1007/s00010-017-0496-5>
- [37] Niezgoda, M., A Jensen-Sherman type inequality with a control map for G-invariant convex functions, *Positivity*, 25 (2021), 431-446. <https://doi.org/10.1007/s11117-020-00769-3>
- [38] Nikodem, K., On Strongly Convex Functions and Related Classes of Functions, Handbook of Functional Equations, Springer, New York, NY, USA, 2014, 365-405. <https://doi.org/10.1007/978-1-4939-1246-9-16>
- [39] Nikolova, L., Persson, L.-E., Varošanec, S., Continuous refinements of some Jensen-type inequalities via strong convexity with applications, *J. Inequal. Appl.*, 2022 (2022), Article ID 63. <https://doi.org/10.1186/s13660-022-02801-4>
- [40] Rubab, F., Nabi, H. Khan, A. R., Generalization and refinements of Jensen inequality, *J. Math. Anal.*, 12(5) (2021), 1-27. <https://doi.org/10.54379/jma-2021-5-1>
- [41] Sahoo, S. K., Tariq, M., Ahmad, H., Nasir, J., Aydi, H., Mukheimer, A., New Ostrowski-type fractional integral inequalities via generalized exponential-type convex functions and applications, *Symmetry*, 13(8) (2021), Article ID 1429. <https://doi.org/10.3390/sym13081429>
- [42] Song, Y.-Q., Adil Khan, M., Zaheer Ullah, S., Chu, Y.-M., Integral inequalities involving strongly convex functions, *J. Funct. Spaces*, 2018 (2018), Article ID 6595921. <https://doi.org/10.1155/2018/6595921>
- [43] Thompson, C. J., Inequality with applications in statistical mechanics, *J. Math. Phys.*, 6 (1965), 1812-1813. <https://doi.org/10.1063/1.1704727>
- [44] Zaheer Ullah, S., Adil Khan, M., Khan, Z. A. H., Chu, Y.-M., Integral majorization type inequalities for the functions in the sense of strong convexity, *J. Funct. Spaces*, 2019 (2019), Article ID 9487823. <https://doi.org/10.1155/2019/9487823>

- [45] Zhongyi, Z., Farid, G., Mahreen, K., Inequalities for unified integral operators via strongly $(\alpha, h - m)$ -convexity, *J. Funct. Spaces*, 2021 (2021), Article ID 6675826. <https://doi.org/10.1155/2021/6675826>

NUMERICAL APPROXIMATION WITH THE SPLITTING ALGORITHM TO A SOLUTION OF THE MODIFIED REGULARIZED LONG WAVE EQUATION

Melike KARTA

Department of Mathematics, Ağrı İbrahim Çeçen University, Ağrı, TÜRKİYE

ABSTRACT. In this article, a Lie-Totter splitting algorithm, which is highly reliable, flexible and convenient, is proposed along with the collocation finite element method to approximate solutions of the modified regular long wave equation. For this article, quintic B-spline approximation functions are used in the implementation of collocation methods. Four numerical examples including a single solitary wave, the interaction of two- three solitary waves, and a Maxwellian initial condition are presented to test the closeness of the solutions obtained by the proposed algorithm to the exact solutions. The solutions produced are compared with those in some studies with the same parameters that exist in the literature. The fact that the present algorithm produces results as intended is a proof of how useful, accurate and reliable it is. It can be stated that this fact will be very useful the application of the presented technique for other partial differential equations, with the thought that it may lead the reader to obtain superior results from this study.

1. INTRODUCTION

Nonlinear partial differential equations play an important role in the modeling of many disciplines. The generalized regularized long wave (GRLW), presented in the form below, is among these equations

$$U_t + U_x - \mu U_{xxt} + \epsilon U^p U_x = 0 \quad (1)$$

in which p is positive integer, μ and ϵ non-negative constants. The solutions of this equation, which have an important place in the propagation of nonlinear dispersion waves, are among the solitary wave types, which are packets or pulses propagating in a nonlinear dispersion medium. They have shapes that are not affected by

2020 *Mathematics Subject Classification.* 65N30, 65D07, 33F10, 97N40, 76B25.

Keywords. The modified regularized long wave equation, B-splines, collocation method, Lie-Trotter splitting.

✉ mkarta@agri.edu.tr,  0000-0003-3412-4370.

collisions. These waves preserve their stable wave form since the nonlinear and dispersive effects have dynamical balance. Sometimes it is not easy to obtain analytical solutions of all partial differential equations. In this case, various numerical methods have been developed to obtain approximate solutions to such problems. Some authors have proposed various approaches to solve Eq.(1) numerically. A few of them can be given as Petrov-Galerkin finite element method, Petrov-Galerkin scheme and lumped Galerkin method based on cubic B-splines, respectively, by Refs. [6,37,46], and a collocation method with cubic, septic and quintic B-splines, respectively, by Refs. [10,20,47], and also Chebyshev-spectral collocation scheme by Ref. [14], parabolic Monge-Ampere moving mesh and uniform by Ref. [2], an approximate quasilinearization approach by Ref. [33], basis of reproducing kernel space by Ref. [27], exponential B-spline collocation scheme by Ref. [28] and element-free kp-Ritz method by Ref. [12]. When $p = 1$ in Eq. (1), it becomes the regularized long wave (RLW) equation used to model a significant number of physical phenomena with weak nonlinearity and dispersion waves containing longitudinal dispersive waves in elastic rods, phonon packets in non-linear crystals, the transverse waves in shallow water, a pressure wave in liquid's gas bubbles, ion-acoustic waves and magnetohydrodynamic wave in plasma. This equation was first introduced by [32] then [5] worked. Many studies can be found in the literature for the approximate solution of the RLW equation. Some of those can be given, Refs. [3,8,15,23] with the finite difference method, Refs. [9,24,41] with the Galerkin and Petrov Galerkin methods and Refs. [7,36,39,40,44,45] with the collocation algorithm as the finite element method. Additionally, it were worked on methods explicit multistep by Ref. [25] and Haar wavelet by Ref. [30] for RLW equation. In the present studied, the modified regularized long wave equation will be discussed

$$U_t + U_x - \mu U_{xxt} + 6U^2U_x = 0 \tag{2}$$

given with initial condition

$$U(x, 0) = g(x), \quad x_L \leq x \leq x_R \tag{3}$$

and boundary conditions

$$\begin{aligned} U(x_L, t) &= U(x_R, t) = 0, \\ U_x(x_L, t) &= U_x(x_R, t) = 0, \\ U_{xx}(x_L, t) &= U_{xx}(x_R, t) = 0. \end{aligned} \tag{4}$$

It can be seen that the approximate solutions of the MRLW equation have been calculated by many methods in the literature. For example, as the finite element method, while the Galerkin and Petrov Galerkin approaches were studied by Refs. [16,18,37], the collocation algorithm with B-splines was studied by Refs. [11,13,16,19,21,22,34,36]. At the same time, [17] used finite difference scheme for the MRLW, [1] solved the equation with mesh free collocation method using radial basis function and [38] acquired the solutions of the equation with the help of Butcher's fifth-order Runge-Kutta (BFRK) scheme.

In this paper, the numerical algorithm of the MRLW equation has been obtained by obtaining two numerical schemes with the help of the Lie-Trotter splitting algorithm and the quintic B-spline collocation method has been applied to each scheme. Thanks to this algorithm, the motion of a single solitary wave, the interaction of two and three solitary waves and the Maxwell initial state have been examined and thus numerical solutions produced with a hybrid approach have been obtained as targeted. Furthermore, Linear stability analysis has been investigated with the help of Von Neumann method.

2. THE SPLITTING ALGORITHM

One of the developed methods to produce numerical solutions of partial differential equations is operator splitting methods. A time-dependent partial differential equation, which usually represents complex physical phenomena such as convection, diffusion, reaction in chemical phenomena, or diffusion, may consist of a combination of one or more operators. Although the computational power of computers has increased rapidly in recent years, good results may not be obtained even if a lot of time is spent in obtaining numerical solutions of a complex problem. Operator splitting methods can be a good approach to numerical solution of such problems. One of these methods is the first-order Lie-Trotter splitting method according to time. This method is the simplest splitting method that reduces the solution of the Cauchy problem given as below to the successive solution of two subproblems

$$\frac{dU(t)}{dt} = \Lambda U(t), \quad U(0) = U_0, t \geq 0, \quad (5)$$

where operator Λ can be written as the sum of operators \hat{A} and \hat{B} . In this case, equation (5) can be written in the following form

$$\frac{dU(t)}{dt} = \hat{A}U(t) + \hat{B}U(t), \quad U(0) = U_0, t \geq 0, \quad (6)$$

in which $U_0 \in X$ is the vector obtained from the initial condition, $u(x, t)$ is solution vector, the operators $\Lambda, \hat{A}, \hat{B}$ are bounded or unbounded operators in a finite or infinite Banach space X . To solve the equation (6) numerically, firstly splitting technique split the equation into as follows

$$\frac{dU(t)}{dt} = \hat{A}U(t), \quad \frac{dU(t)}{dt} = \hat{B}U(t). \quad (7)$$

Here, let $\rho_{\Delta t}^{[\hat{A}]}$ and $\rho_{\Delta t}^{[\hat{B}]}$ be the numerical solutions of the equations containing the expressions \hat{A} and \hat{B} in expression (7), and let the exact solution of (6) be given as $\psi_{\Delta t}$. The simplest splitting methods are introduced as follows

$$\rho_{\Delta t}^{[\hat{B}]} \circ \rho_{\Delta t}^{[\hat{A}]} = e^{\Delta t \hat{B}} e^{\Delta t \hat{A}} \quad \text{or} \quad \rho_{\Delta t}^{[\hat{A}]} \circ \rho_{\Delta t}^{[\hat{B}]} = e^{\Delta t \hat{A}} e^{\Delta t \hat{B}}.$$

and it is known as the Lie-Trotter splitting technique [42] in the literature. Using the Taylor series, It can be stated that the following approximation for an initial

value U_0 is a first-order approximation to the solution of equation (6)

$$\psi_{\Delta t}(U_0) = (\rho_{\Delta t}^{[\hat{A}]} \circ \rho_{\Delta t}^{[\hat{B}]})(U_0) + O(\Delta t^2).$$

Let the formal solution of (6) be given in the form

$$U(t_{n+1}) = e^{\Lambda \Delta t} U(t_n) = e^{(\hat{A} + \hat{B}) \Delta t} U(t_n). \tag{8}$$

Unfolding Taylor series for this solution can be given in the following form

$$U(t_{n+1}) = e^{\Delta t(\hat{A} + \hat{B})} U(t_n) = \sum_{k=0}^{\infty} \frac{t^k}{k!} (\hat{A}(u(t)) \frac{\partial}{\partial U} + \hat{B}(u(t)) \frac{\partial}{\partial U})^k U(t_n).$$

By calculating the sum of the operators \hat{A} and \hat{B} instead of Λ , a new approach to Equation (6) can be obtained, presented in the form below

$$U(t_{n+1}) = e^{\hat{A} \Delta t} e^{\hat{B} \Delta t} U(t_n). \tag{9}$$

An error occurs if (9) is used instead of the equation (8). This is a local splitting error given as follows

$$\begin{aligned} Te &= \frac{1}{\Delta t} (e^{\Delta t(\hat{A} + \hat{B})} - e^{\Delta t \hat{B}} e^{\Delta t \hat{A}}) U(t_n) \\ &= \frac{1}{\Delta t} \left[\frac{\Delta t^2}{2} (\hat{A} \hat{B} - \hat{B} \hat{A}) U(t_n) + O(\Delta t^3) \right] \\ &= \frac{1}{\Delta t} [\hat{A}, \hat{B}] U(t_n) + O(\Delta t^2) \end{aligned}$$

To explain in more detail: Splitting technique splits the given original problem into two parts according to the time. As a result, subproblems with a simpler structure are obtained. Thus, the solution of the original problem is obtained from the solution of the subproblems. In the Lie-Trotter schemes, the first subproblem with operator \hat{A} is solved using the original initial condition given with the problem. Then, the solutions generated with the operator \hat{A} are utilized as the initial condition for the solution of the second sub-problem given with the operator \hat{B} and presented as the solution of the main problem in the first time step. In this way, approximate solutions at the next time levels are obtained similarly to those in the first time step. Algorithm of the mentioned technique with $t_0 = 0$ and $t_N = T$,

$$\begin{aligned} \frac{dU^*(t)}{dt} &= \hat{A}U^*(t), \quad U^*(t_n) = U_n^0, \quad t \in [t_n, t_{n+1}], \\ \frac{dU^{**}(t)}{dt} &= \hat{B}U^{**}(t), \quad U^{**}(t_n) = U^*(t_{n+1}), \quad t \in [t_n, t_{n+1}]. \end{aligned}$$

where U_n^0 is the original initial condition given in (5), Δt is the time step, $\Delta t = t_{n+1} - t_n, n = 0, 1, \dots, N - 1$. Thus, the targeted solutions are obtained with $U(t_{n+1}) = u^{**}(t_{n+1})$. This scheme is called as $(\hat{A} - \hat{B})$ -shaped splitting scheme. It can be stated here that solving the sub-problems separately is more advantageous in terms of computational cost rather than solving the whole problem [26, 43].

3. THE QUINTIC B-SPLINES

In order to make approximate calculations of the MRLW equation, the solution region is limited to the interval $x_R \leq x \leq x_N$. This range is partitioned by nodes x_j into uniformly finite elements of length h such that $x_L = x_0 \leq x_1 \leq \dots \leq x_N = x_R$ and $h = x_{j+1} - x_j$. The set of quintic B-splines $\varphi_j(x)$ for $j = -2(1)N + 2$ forming a base on the interval $[x_L, x_R]$ at nodes x_j is presented as follows by [31]

$$\varphi_j(x) = \frac{1}{h^5} \begin{cases} p_0 = (x - x_{j-3})^5, & x \in [x_{j-3}, x_{j-2}] \\ p_1 = p_0 - 6(x - x_{j-2})^5, & x \in [x_{j-2}, x_{j-1}] \\ p_2 = p_1 - 6(x - x_{j-2})^5 + 15(x - x_{j-1})^5, & x \in [x_{j-1}, x_j] \\ p_3 = p_2 - 6(x - x_{j-2})^5 - 20(x - x_j)^5, & x \in [x_j, x_{j+1}] \\ p_4 = p_3 - 6(x - x_{j-2})^5 + 15(x - x_{j+1})^5, & x \in [x_{j+1}, x_{j+2}] \\ p_5 = p_4 - 6(x - x_{j-2})^5 - 6(x - x_{j+2})^5, & x \in [x_{j+2}, x_{m,j3}] \\ 0, & \text{otherwise.} \end{cases} \tag{10}$$

The numerical solution $U_N(x, t)$ corresponding to the exact solution $U(x, t)$ is searched in terms of quintic B-splines in the following form

$$U_N(x, t) = \sum_{j=-2}^{N+2} \varphi_j(x) \delta_j(t) \tag{11}$$

Here, $\delta_j(t)$ are the unknown time parameters determined with both boundary and collocation conditions. When the trial function (10) is substituted in the equation (11), The knot values U_j, U'_j, U''_j at nodes x_j are acquired in terms of the parameter $\delta_j(t)$ with form

$$\begin{aligned} U_j &= \delta_{m-2} + 26\delta_{j-1} + 66\delta_j + 26\delta_{j+1} + \delta_{j+2}, \\ U'_j &= \frac{5}{h}(-\delta_{j-2} - 10\delta_{j-1} + 10\delta_{j+1} + \delta_{j+2}), \\ U''_j &= \frac{20}{h^2}(\delta_{j-2} + 2\delta_{j-1} - 6\delta_j + 2\delta_{j+1} + \delta_{j+2}), \end{aligned} \tag{12}$$

Here, the first and second derivatives with respect to x are denoted by the symbols ' and ". The all of quintic B-spline base functions are zero outside of $\phi_{j-2}, \phi_{j-1}, \phi_j, \phi_{j+1}, \phi_{j+2}$ and ϕ_{j+3} .

4. THE IMPLEMENTATION OF COLLOCATION METHOD

In this section, firstly, the MRLW equation with the initial-boundary value problem is split. In an other saying, the main problem is divided into sub-equations as follows to obtain two partial differential equations, one linear and the other nonlinear, with respect to time

$$U_t - \mu U_{xxt} + U_x = 0 \tag{13}$$

$$U_t - \mu U_{xxt} + 6U^2 U_x = 0. \tag{14}$$

When U_j and its first derivatives U'_j and U''_j given in the (12) equation are substituted in equations (13) and (14), system of ordinary differential equations given in the following form are obtained for $j = 0(1)N$ in the entire solution region

$$\begin{aligned} & \dot{\delta}_{m-2} + 26\dot{\delta}_{m-1} + 66\dot{\delta}_m + 26\dot{\delta}_{m+1} + \dot{\delta}_{m+2} \\ & - \mu \frac{20}{h^2} (\dot{\delta}_{m-2} + 2\dot{\delta}_{m-1} - 6\dot{\delta}_m + 2\dot{\delta}_{m+1} + \dot{\delta}_{m+2}) \\ & + \frac{5}{h} (-\delta_{m-2} - 10\delta_{m-1} + 10\delta_{m+1} + \delta_{m+2}) = 0, \end{aligned} \tag{15}$$

$$\begin{aligned} & \dot{\delta}_{m-2} + 26\dot{\delta}_{m-1} + 66\dot{\delta}_m + 26\dot{\delta}_{m+1} + \dot{\delta}_{m+2} \\ & - \mu \frac{20}{h^2} (\dot{\delta}_{m-2} + 2\dot{\delta}_{m-1} - 6\dot{\delta}_m + 2\dot{\delta}_{m+1} + \dot{\delta}_{m+2}) \\ & + \frac{5z_j}{h} (-\delta_{m-2} - 10\delta_{m-1} + 10\delta_{m+1} + \delta_{m+2}) = 0 \end{aligned} \tag{16}$$

in which the first derivative according to time t is shown with symbol "." and z_j is gotten as

$$z_j = 6(\delta_{j-2} + 26\delta_{j-1} + 66\delta_j + 26\delta_{j+1} + \delta_{j+2})^2$$

to linearize the (16) system. Then, by applying $\frac{\delta_j^{n+1} + \delta_j^n}{2}$ for spatial discretization and $\frac{\delta_j^{n+1} - \delta_j^n}{\Delta t}$ for time discretization to these two systems, two numerical schemes are obtained with form

$$\begin{aligned} & k_1 \delta_{m-2}^{n+1} + k_2 \delta_{m-1}^{n+1} + k_3 \delta_m^{n+1} + k_4 \delta_{m+1}^{n+1} + k_5 \delta_{m+2}^{n+1} \\ & = k_6 \delta_{m-2}^n + k_7 \delta_{m-1}^n + k_8 \delta_m^n + k_9 \delta_{m+1}^n + k_{10} \delta_{m+2}^n, \end{aligned} \tag{17}$$

$$\begin{aligned} & l_1 \delta_{m-2}^{n+1} + l_2 \delta_{m-1}^{n+1} + l_3 \delta_m^{n+1} + l_4 \delta_{m+1}^{n+1} + l_5 \delta_{m+2}^{n+1} \\ & = l_6 \delta_{m-2}^n + l_7 \delta_{m-1}^n + l_8 \delta_m^n + l_9 \delta_{m+1}^n + l_{10} \delta_{m+2}^n \end{aligned} \tag{18}$$

in which $k_i, l_i (i = 1(1)10)$ and z_j are $z_j = 6U^2$

$$\begin{aligned} k_1 &= 1 - \frac{20\mu}{h^2} - \frac{5\Delta t}{2h}, k_2 = 26 - \frac{40\mu}{h^2} - \frac{25\Delta t}{h}, k_3 = 66 + \frac{120\mu}{h^2}, \\ k_4 &= 26 - \frac{40\mu}{h^2} + \frac{25\Delta t}{h}, k_5 = 1 - \frac{20\mu}{h^2} + \frac{5\Delta t}{h} \end{aligned}$$

$$\begin{aligned} k_6 &= 1 - \frac{20\mu}{h^2} + \frac{5\Delta t}{2h}, k_7 = 26 - \frac{40\mu}{h^2} - \frac{25\Delta t}{h}, k_8 = 66 + \frac{120\mu}{h^2}, \\ k_9 &= 26 - \frac{40\mu}{h^2} + \frac{25\Delta t}{h}, k_{10} = 1 - \frac{20\mu}{h^2} - \frac{5\Delta t}{h} \end{aligned}$$

$$l_1 = 1 - \frac{20\mu}{h^2} - \frac{5z_j\Delta t}{2h}, l_2 = 26 - \frac{40\mu}{h^2} - \frac{25z_j\Delta t}{h}, l_3 = 66 + \frac{120\mu}{h^2},$$

$$l_4 = 26 - \frac{40\mu}{h^2} + \frac{25z_j\Delta t}{h}, l_5 = 1 - \frac{20\mu}{h^2} + \frac{5z_j\Delta t}{2h}.$$

$$l_6 = 1 - \frac{20\mu}{h^2} + \frac{5z_j\Delta t}{2h}, l_7 = 26 - \frac{40\mu}{h^2} + \frac{25z_j\Delta t}{h}, l_8 = 66 + \frac{120\mu}{h^2},$$

$$l_9 = 26 - \frac{40\mu}{h^2} - \frac{25z_j\Delta t}{h}, l_{10} = 1 - \frac{20\mu}{h^2} - \frac{5z_j\Delta t}{2h}.$$

(17) and (18) are systems consisting of $(N + 1)$ equations with $(N + 5)$ unknowns. These systems contain four additional element parameters $\delta_{-2}, \delta_{-1}, \delta_{N+1}, \delta_{N+2}$ outside the solution region of the problem. To obtain the only solution of systems (17) and (18), the parameters that are not in the solution region must be eliminated from these systems. For this purpose, the nodal values of U_j and $(U_j)'$ in the equation (12) and the boundary conditions $U(x_L, t) = U(x_R, t) = 0$ and $U_x(x_L, t) = U_x(x_R, t) = 0$ are used. Thus, systems (17) and (18) are reduced to the $(N + 1) \times (N + 1)$ matrix system.

For approximate solutions of the (17) and (18) systems, it is necessary to find the initial vector δ_j^0 . This required initial vector is found by solving the system of algebraic equations given in the following form, using the initial condition $U(x_j, 0) = U_N(x_j, 0) = g_0(x_j)$, and the approach $U_N(x, 0) = \sum_{j=-2}^{N+2} \varphi_j(x)\delta_j^0(0)$

$$\begin{aligned} U_m &= \delta_{j-2}^0 + 26\delta_{j-1}^0 + 66\delta_j^0 + 26\delta_{j+1}^0 + \delta_{j+2}^0, j = 0(1)N, \\ U_0 &= \delta_{-2}^0 + 26\delta_{-1}^0 + 66\delta_0^0 + 26\delta_1^0 + \delta_2^0, \\ U_1 &= \delta_{-1}^0 + 26\delta_0^0 + 66\delta_1^0 + 26\delta_2^0 + \delta_3^0, \\ &\cdot \\ &\cdot \\ &\cdot \\ U_{N-1} &= \delta_{N-3}^0 + 26\delta_{N-2}^0 + 66\delta_{N-1}^0 + 26\delta_N^0 + \delta_{N+1}^0, \\ U_N &= \delta_{N-2}^0 + 26\delta_{N-1}^0 + 66\delta_N^0 + 26\delta_{N+1}^0 + \delta_{N+2}^0. \end{aligned} \tag{19}$$

with unknown element parameters δ_j^0 . By using the boundary conditions $U_x(x_L, t) = U_x(x_R, t) = 0$ and $U_{xx}(x_L, t) = U_{xx}(x_R, t) = 0$ for these systems, $\delta_{-2}, \delta_{-1}, \delta_{N+1}, \delta_{N+2}$ are eliminated so that the following matrix equation is obtained

$$\lambda b^0 = d$$

schemes for linear or linearized partial differential equations. Via the Euler formula $e^{i\Phi} = \cos\Phi + i\sin\Phi$, growth factors ϱ_1 and ϱ_2 submitted as follows are acquired

$$\varrho_1 = \frac{A_1 - iB_1}{A_1 + iB_1}, \quad \varrho_2 = \frac{A_1 - iC_1}{A_1 + iC_1}, \quad (22)$$

$$A_1 = \left(2 - \frac{40\mu}{h^2}\right)\cos(2\gamma h) + \left(52 - \frac{80\mu}{h^2}\right)\cos(\gamma h) + \left(66 + \frac{120\mu}{h^2}\right),$$

$$B = \frac{5\Delta t}{h}\sin(2\gamma h) + \frac{50\Delta t}{h}\sin(\gamma h),$$

and

$$C = \frac{5z_m\Delta t}{h}\sin(2\gamma h) + \frac{50z_m\Delta t}{h}\sin(\gamma h).$$

For $k_1, k_2, \dots, k_9, k_{10}$ and $l_1, l_2, \dots, l_9, l_{10}$ founded in section 3. $|\varrho_1| = |\varrho_2| = 1$ from Equation (22) and hence, for the whole system with Lie Trotter-Splitting algorithm can be written as $|\varrho_1| \cdot |\varrho_2| = 1$. Because the conditions $|\varrho_1| \leq 1$, and $|\varrho_2| \leq 1$ according to the von Neumann theory are satisfied, it can be clearly said that the systems (17) and (18) are unconditionally stable.

6. NUMERICAL EXPERIMENTS AND DISCUSSION

For numerical calculations of main problem are considered to the movement of single solitary wave, two and three solitary wave interactions and the Maxwellian initial condition. The difference between the exact and approximate solutions is calculated by choosing some specific times to match the studies in the literature. For this, the following error norms are used

$$L_2 = \|U - U_N\|_2 = \sqrt{h \sum_{j=0}^N (U - U_N)^2},$$

and

$$L_\infty = \|U - U_N\|_\infty = \max_j |U - U_N|.$$

To check the conservation of numerical schemes during the simulation of solitary wave motion, the invariants I_1, I_2 and I_3 are calculated, which correspond to the conservation of mass, momentum and energy proved by Olver [29] and presented as follows

$$I_1 = \int_{x_L}^{x_R} U(x, t) dx,$$

$$I_2 = \int_{x_L}^{x_R} [U^2(x, t) + \mu U_x^2(x, t)] dx,$$

$$I_3 = \int_{x_L}^{x_R} [U^4(x, t) - \mu U_x^2(x, t)] dx.$$

6.1. **Example I: The movement of a single solitary wave.** This example considers the MRLW equation by taking into accounting boundary condition $U \rightarrow 0$ when $x \rightarrow \pm\infty$ and initial condition

$$U(x, 0) = \sqrt{c} \operatorname{sech}[s(x - x_0)].$$

The exact solution for this problem is presented in the following form

$$U(x, t) = \sqrt{c} \operatorname{sech}[s(x - (c + 1)t - x_0)].$$

Here, c and x_0 are arbitrary constants and $s = \sqrt{\frac{c}{\mu(c+1)}}$. The exact values of the conservation quantities of a single solitary wave with width s and amplitude \sqrt{c} as in [11] are given as follows

$$\begin{aligned} I_1 &= \int_{x_L}^{x_R} U(x, t) dx = \frac{\pi\sqrt{c}}{s}, \\ I_2 &= \int_{x_L}^{x_R} [U^2(x, t) + \mu U_x^2(x, t)] dx = \frac{2c}{s} + \frac{2\mu sc}{3}, \\ I_3 &= \int_{x_L}^{x_R} [U^4(x, t) - \mu U_x^2(x, t)] dx = \frac{4c^2}{3s} - \frac{2\mu sc}{3}. \end{aligned} \tag{23}$$

For solitary wave motion with amplitude 1, All of calculations and comparisons in Table [1,2] are done with $\mu = 1, x_0 = 40, c = 1, \Delta t = 0.025$ and $h = 0.2$ over $[0, 100]$ to match those in [11, 16, 21, 22, 36, 37]. Table [1] reports the invariant and error norm amounts of the current approach from $t = 0$ to 10 with one increment value. This table shows that the calculated invariants are compatible with each other and gratifying because the error norms L_2 and L_∞ are quite small. Furthermore, it can be seen from Table [1] that the the changing of invariants I_1, I_2, I_3 are less than $0.8 \times 10^{-7}, 1.1 \times 10^{-7}, 1.26 \times 10^{-5}$, respectively. The comparison of the ones of the previously recorded methods with the results of the proposed technique is given in Table [2] at time $t = 10$. Looking at the table, it can be easily seen that the current approach produces the best results for error norms and the computed invariant values are in agreement with the analytical ones $I_1 = 4.4428829, I_2 = 3.2998316$ and $I_3 = 1.4142135$. The motion of a single solitary wave at various time levels with parameters $\Delta t = 0.025, h = 0.2, c = 1$ is plotted in Fig.[1] and this figure shows that the soliton shifts to the right at a constant velocity with an almost unchanged amplitude even as time increases, as hoped. At $t = 0$, the amplitude is 1 which is situated at $x = 40$ and $x = 60$.

For Table [3,4], the parameters $\mu = 1, x_0 = 40, c = 0.3, \Delta t = 0.01$ and $h = 0.1$ over $[0, 100]$ are selected as in n Refs. [21]. Thus, The amplitude of the solitary wave is 0.547723. Table [3] displays the invariant and error norm amounts of the present approach from $t = 0$ to 20 with two increment value. From this table, it can be observed that very small and pleasing solutions are obtained with the Lie-Trotter splitting technique. Invariants I_1, I_3 are compatible with each other and I_2 remains constant. Furthermore, it can be seen from Table [3] that the the

TABLE 1. The error norms and invariants of the single solitary wave with $\Delta t = 0.025, h = 0.2$, for $c = 1$ on the region $[0, 100]$

t	I_1	I_2	I_3	$L_2 \times 10^3$	$L_\infty \times 10^3$
0	4.44288294	3.29983161	1.41421360	0.00000000	0.00000000
1	4.44288293	3.29983161	1.41420559	1.56533150	1.02551887
2	4.44288292	3.29983159	1.41419884	2.41711399	1.40020924
3	4.44288292	3.29983158	1.41419842	2.67081261	1.22652109
4	4.44288291	3.29983157	1.41419926	2.68157587	1.04668636
5	4.44288290	3.29983156	1.41419995	2.62782252	1.10627938
6	4.44288289	3.29983155	1.41420040	2.56931532	1.11288942
7	4.44288289	3.29983153	1.41420067	2.52306335	1.07889684
8	4.44288288	3.29983152	1.41420084	2.49240521	1.02360259
9	4.44288287	3.29983151	1.41420094	2.47654106	0.95806880
10	4.44288286	3.29983150	1.41420100	2.47366508	0.89643465

TABLE 2. Comparisons of the error norms and invariants of the single solitary wave with $\Delta t = 0.025, h = 0.2$, for $c = 1$ on the region $[0, 100]$ at $t = 10$

method	I_1	I_2	I_3	$L_2 \times 10^3$	$L_\infty \times 10^3$
Exact	4.4428829	3.2998316	1.4142135	0	0
Present	4.4428829	3.2998315	1.4142010	2.47366508	0.89643465
21	4.4428661	3.2997108	1.4143165	2.58891	1.35164
22	4.44288	3.29983	1.41420	9.30196	5.43718
16	4.4431919	3.3003022	1.4146930	2.41750	1.08099
36	4.445176	3.302476	1.417411	0.8644	1.2475
11 1	4.442	9.299	1.413	19.39	9.24
11 2	4.440	3.296	1.411	20.3	11.2
37	4.44288	3.29981	1.41416	3.00533	1.68749

changing of invariants I_1, I_3 are less than 1.4×10^{-7} , 0.9×10^{-7} , respectively and 0 of I_2 during the execution of the program. Table 4 presents a comparison of the results of the proposed study and other registered ones by calculating error norms L_2 and L_∞ and invariant values I_1, I_2 and I_3 . All comparisons are made for time $t=20$. As a result of this comparison, it can easily be seen that the present technique produces more satisfactory results. Invariant values are consistent with those compared. The motion of a single solitary wave at various time levels with parameters $\Delta t = 0.01, h = 0.1, c = 0.3$ is plotted in Fig. 2. Fig. 3 shows the graphs of the error distributions of the solitary wave with amplitude of 1 and 0.3 respectively, at $t = 10$ and 20.

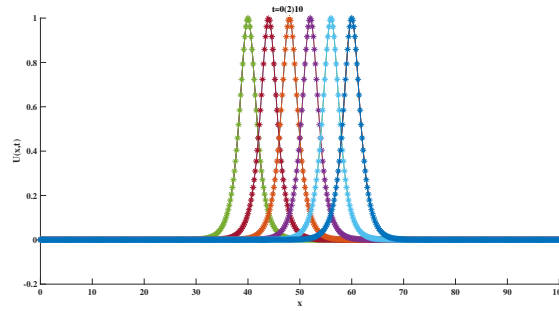


FIGURE 1. Movement of a single solitary wave at $t = 0(2)10$ for MRLW equation

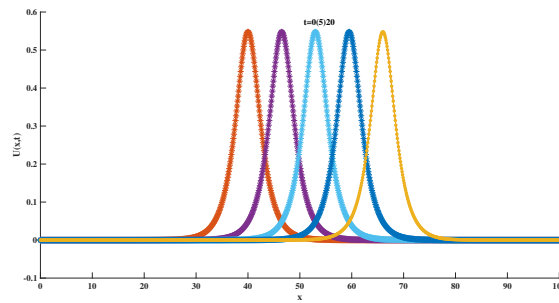


FIGURE 2. Movement of a single solitary wave at $t = 0(5)20$ for MRLW equation

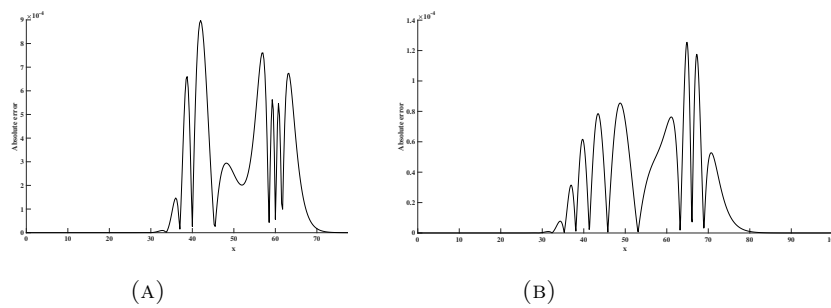


FIGURE 3. Error distribution graphs for a) $\Delta t = 0.025, h = 0.2, c = 1$ and b) $\Delta t = 0.01, h = 0.1, c = 0.3$ over $[0, 100]$.

TABLE 3. The error norms and invariants of the single solitary wave with $\Delta t = 0.01$, $h = 0.1$, for $c = 0.3$ on the region $[0, 100]$

t	I_1	I_2	I_3	$L_2 \times 10^3$	$L_\infty \times 10^3$
0	3.58196673	1.34507649	0.15372303	0.00000000	0.00000000
2	3.58196674	1.34507649	0.15372299	0.17472238	0.09673881
4	3.58196675	1.34507649	0.15372294	0.28047087	0.14367750
6	3.58196676	1.34507649	0.15372293	0.32725879	0.14066701
8	3.58196677	1.34507649	0.15372293	0.34590142	0.13215052
10	3.58196678	1.34507649	0.15372293	0.35279733	0.13158877
12	3.58196678	1.34507649	0.15372294	0.35465095	0.13057054
14	3.58196679	1.34507649	0.15372294	0.35426140	0.12926338
16	3.58196678	1.34507649	0.15372294	0.35288262	0.12791317
18	3.58196674	1.34507649	0.15372294	0.35110940	0.12661543
20	3.58196659	1.34507649	0.15372294	0.34923321	0.12540476

TABLE 4. Comparisons of the error norms and invariants of the single solitary wave with $\Delta t = 0.01$, $h = 0.1$, for $c = 0.3$ on the region $[0, 100]$ at $t = 20$

method	I_1	I_2	I_3	$L_2 \times 10^4$	$L_\infty \times 10^4$
Present	3.58196659	1.34507649	0.15372294	0.34923321	0.12540476
21	3.5820204	1.3450974	0.1537250	0.8112594	0.3569076
22	3.58197	1.34508	0.153723	6.06885	2.96650
16	3.5820206	1.3450944	0.1537284	1.2273638	0.4472294
36	3.582265	1.345182	0.1538901	3.379583	7.672911
1 MQ	3.5819665	1.3450764	0.153723	0.51498	0.22551
1 TPS	3.5819663	1.3450759	0.153723	0.51498	0.26605
13	3.581967	1.345076	0.153723	0.5089274	0.2222848

6.2. Example II: Interaction of two solitary waves. This example considers the problem of interaction of two solitary waves with various amplitudes and for Eq.(2), the following initial conditions are written as the linear sum of two well-separated solitary waves with different amplitudes

$$U(x, 0) = \sum_{i=1}^2 a_i \operatorname{sech}[s_i(x - x_i)],$$

in which c_i and x_i are arbitrary constants, $a_i = \sqrt{c_i}$, $s_i = \sqrt{\frac{c_i}{\mu(c_i+1)}}$, $i = 1(1)2$. The exact values of the conservation quantities are given as follows [11]

$$I_1 = \sum_{i=1}^2 \frac{\pi\sqrt{c_i}}{s_i},$$

$$I_2 = \sum_{i=1}^2 \frac{2c_i}{s_i} + \frac{2\mu s_i c_i}{3},$$

$$I_3 = \sum_{i=1}^2 \frac{4c_i^2}{3s_i} - \frac{2\mu s_i c_i}{3}.$$

Numerical simulation is done on the $[0, 250]$ region by selecting the parameters $\mu = 1, x_1 = 25, x_2 = 55, c_1 = 4, c_2 = 1, \Delta t = 0.025, h = 0.2$ as in Ref. [21]. The experimental results obtained by running the numerical experiments at $t=0(2)20$ times are shown in Table 5. The exact values of the invariants are $I_1 = 11.467698, I_2 = 14.629243$ and $I_3 = 22.880466$. Table 5 submits a comparison of the solutions in the proposed method with those in the references [1,16,19,21,22,34,37,38] and this table displays that the invariant quantities I_1, I_2 and I_3 are quite conservative and the values found are consistent with their exact values throughout the operation of the computer program. Fig.4 reports the interactions of two solitary waves at various time levels. It can be clearly seen from this figure that at $t = 0$, the wave with the smaller amplitude is to the right of the wave with the larger amplitude. Since the shorter wave moves slower than the longer one, the longer wave catches the short wave at $t = 12$ and collides. Later, it fars away from the shorter one with the advancing time. At $t = 20$, while the amplitude of the smaller wave becomes 1.014 at $x = 84.2$ the amplitude of the larger wave becomes 1.998 at $x = 97.4$.

6.3. Example III:Interaction of three solitary waves. This example deals with the problem of interaction of three solitary waves with different amplitudes and advancing in the same direction and for MRLW equation, the following initial conditions are written as the linear sum of three well-separated solitary waves with different amplitudes

$$U(x, 0) = \sum_{i=1}^3 a_i sech[s_i(x - x_i)],$$

in which c_i and x_i are arbitrary constants, $a_i = \sqrt{c_i}$, $s_i = \sqrt{\frac{c_i}{\mu(c_i+1)}}$, $i = 1(1)3$. The exact values of the conservation quantities obtained from Eq.(18) are given as follows

$$I_1 = \sum_{i=1}^3 \frac{\pi\sqrt{c_i}}{s_i},$$

TABLE 5. Comparison of invariants of two solitary waves with values $\Delta t = 0.025, h = 0.2$, for $x_1 = 25, x_2 = 55, c_1 = 4, c_2 = 1$ on the region $[0, 250]$ at $t = 0(2)20$ with those in [13]

t	method			[13]		
	I_1	I_2	I_3	I_1	I_2	I_3
0	11.46769804	14.62924273	22.88046615	11.467698	14.629277	22.880432
2	11.46769804	14.62924273	22.88046615	11.467698	14.624259	22.860365
4	11.46769804	14.62924273	22.88046615	11.467698	14.619226	22.840279
6	11.46769804	14.62924273	22.88046615	11.467699	14.614169	22.820069
8	11.46769804	14.62924273	22.88046615	11.467700	14.606821	22.787857
10	11.46769804	14.62924273	22.88046615	11.467700	14.603687	22.771773
12	11.46788404	14.62924273	22.88046615	11.467699	14.603056	22.775766
14	11.46769804	14.62924273	22.88046615	11.467699	14.598059	22.756029
16	11.46769804	14.62924273	22.88046615	11.467700	14.593048	22.736127
18	11.46769804	14.62924273	22.88046615	11.467700	14.588061	22.716289
20	11.46769804	14.62924273	22.88046615	11.467701	14.583089	22.696510
20 [19] 1	11.4676541	14.6292088	22.8803901			
20 [19] 2	11.4676452	14.6309639	22.8786025			
20 [34]	11.4677	14.6299	22.8806			
20 [38]	11.4676977	14.62927316	22.8804154			
20 [21]	11.4691886	14.6331334	22.8764330			
20 [16]	11.4662207	14.6253125	22.8650456			
20 [37]	11.4677	14.6299	22.8806			
20 [22]	11.4677	14.6292	22.8809			
20 [1] MQ	11.467698	14.583052	22.696539			
20 [1] TPS	11.467742	14.582424	22.694269			

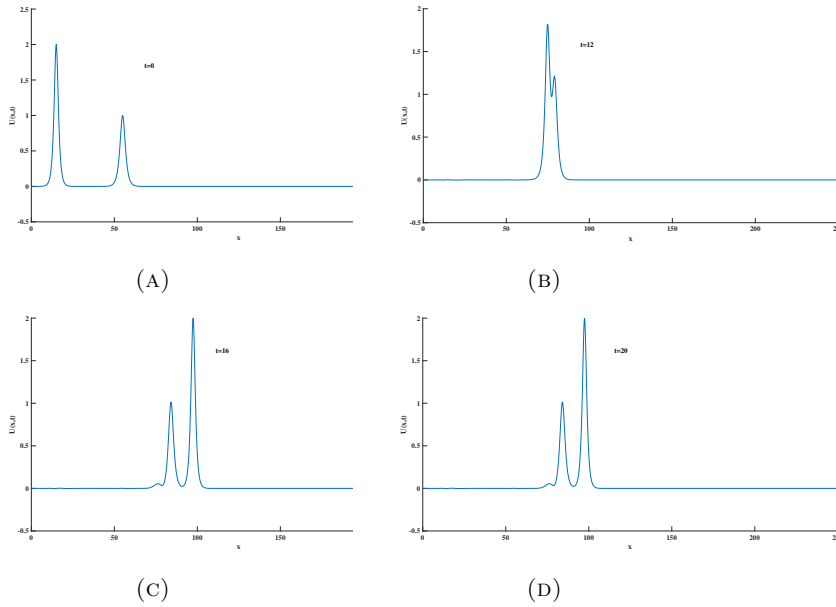


FIGURE 4. The interactions of two solitary waves at various time levels of MRLW equation

$$I_2 = \sum_{i=1}^3 \frac{2c_i}{s_i} + \frac{2\mu s_i c_i}{3},$$

$$I_3 = \sum_{i=1}^3 \frac{4c_i^2}{3s_i} - \frac{2\mu s_i c_i}{3}.$$

During the numerical simulation, the calculation process is performed by taking the parameters $\mu = 1, x_1 = 15, x_2 = 45, x_3 = 60, c_1 = 4, c_2 = 1, c_3 = 0.25, \Delta t = 0.025, h = 0.2$ on the region $[0, 250]$. This process is carried out at times $0(5)45$ and the exact values of the invariants here are $I_1 = 14.9801, I_2 = 15.8218$ and $I_3 = 22.9923$. Table 6 presents a comparison of the solutions in the suggested method with those in the references [1, 21, 22, 34] and this table displays that the invariant quantities I_1, I_2 and I_3 are quite conservative and the values found are consistent with their exact values throughout the operation of the computer program. Here, the interaction of solitary waves using various times is shown in Fig. 5. This figure indicates that the interaction started at approximately $t = 10$. there were overlaps at time $t = 40$, and then the waves returned to their original state at $t = 40$.

TABLE 6. Comparison of invariants of three solitary waves with values $\Delta t = 0.025, h = 0.2$, for $x_1 = 15, x_2 = 45, x_3 = 60, c_1 = 4, c_2 = 1, c_3 = 0.25$ on the region $[0, 250]$ at $t = 0(5)45$ with those in [13]

t	method			[13]		
	I_1	I_2	I_3	I_1	I_2	I_3
0	14.97251076	15.82181232	22.99226955	14.980099	15.837528	23.008136
5	14.97251076	15.82181232	22.99226955	14.980105	15.837528	22.957891
10	14.97251076	15.82181232	22.99226955	14.980109	15.807025	22.877972
15	14.97251076	15.82181232	22.99226955	14.980106	15.807032	22.885947
20	14.97251076	15.82181232	22.99226955	14.980106	15.795022	22.837454
25	14.97251076	15.82181232	22.99226955	14.980107	15.782840	22.788852
30	14.97251076	15.82181232	22.99226955	14.980107	15.770634	22.740419
35	14.97251076	15.82181232	22.99226955	14.980108	15.758480	22.692279
40	14.97251076	15.82181232	22.99226955	14.980108	15.746389	22.644448
45	14.97251076	15.82181232	22.99226955	14.968030	15.734374	22.596591
20 [34]	14.930390	15.822500	22.964190			
20 [21]	14.7145273	15.4927592	23.3529062			
20 [22]	13.7043	15.6563	22.9303			
20 [1] MQ	14.96814	15.73434	22.596625			
20 [1] TPS	14.96824	15.73376	22.594494			

6.4. **Example IV: The Maxwellian initial condition.** This last example examines the improvement of the following the Maxwell initial condition in the sequence of solitary waves

$$U(x, 0) = \exp(-(x - 40)^2).$$

Here, the solution behavior for the Maxwellian condition presented above is evaluated with the values of μ . Approximate values of invariants are shown in Table 7. All figures are depicted in Fig. 6 at time 14.5. At the end of the study for values

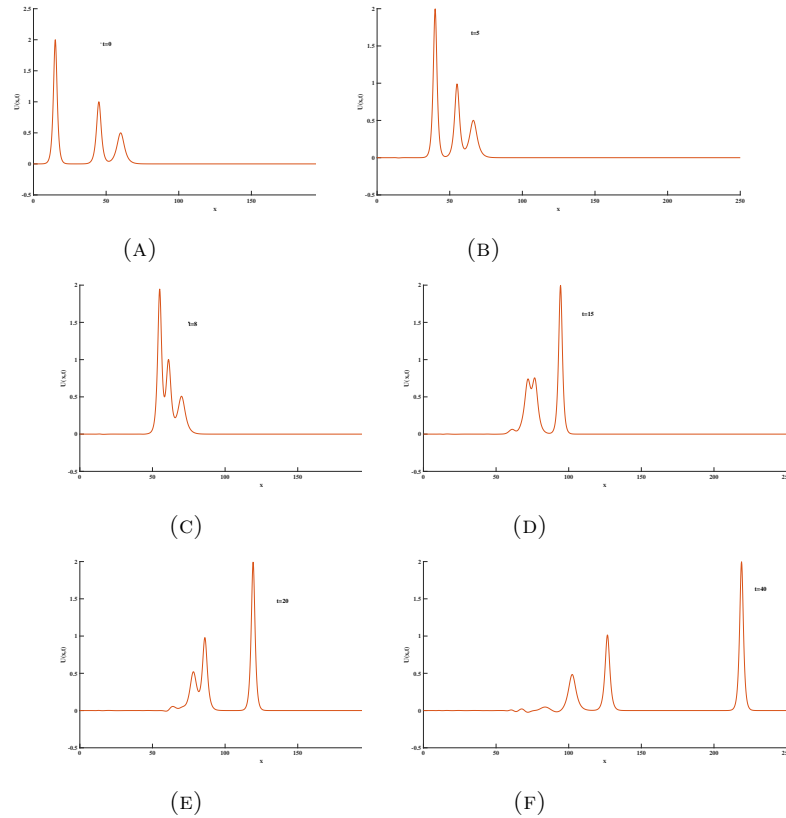


FIGURE 5. The interactions of three solitary waves at various time levels of MRLW equation

$\mu = 0.1, 0.04, 0.015$ and $\mu = 0.01$, it is observed that only a single soliton movement is followed for $\mu = 0.1$ and this is pictured with a). When $\mu = 0.04, 0.015$ are taken, it is shown with b) and c) that two and three stable solitons are occurred and when the value $\mu = 0.01$ is selected, the Maxwellian initial condition decomposes into four solitary waves and it is plotted with d). In all the figures in this example, the presence of a small oscillating tail formed behind the last wave is observed. The peaks of the well-developed wave whose speeds are linearly dependent on their amplitudes lie on a straight line.

7. CONCLUSION

In this article, Lie-trotter splitting algorithm with collocation finite element method has been presented. Four experimental examples are given to measure

TABLE 7. Values of the invariants of the MRLW equation for the Maxwellian initial condition

t	μ	I_1	I_2	I_3	μ	I_1	I_2	I_3
0	0.1	1.77245385	1.37864519	0.76089588	0.015	1.77245385	1.27211379	0.86742727
3		1.77242409	1.37853754	0.66726850		1.74470267	1.23369811	0.72548127
6		1.77237678	1.37846448	0.66768464		1.71890317	1.17440856	0.73866510
9		1.77232940	1.37839090	0.66787415		1.70124953	1.13869004	0.74633211
12		1.77228192	1.37831554	0.66798301		1.68830339	1.11560302	0.75073526
15		1.77223441	1.37823955	0.66805774		1.68128767	1.11897777	0.74641698
0	0.01	1.77245385	1.26584724	0.87369382	0.04	1.77245385	1.30344656	0.83609451
3		1.71307229	1.14513104	0.76148916		1.77091565	1.30148045	0.69106562
6		1.68854075	1.12482375	0.75995674		1.76851865	1.29612046	0.69320291
9		1.66818971	1.08010404	0.76885908		1.76632858	1.29227683	0.69439710
12		1.65804755	1.07686486	0.76703741		1.76426994	1.28925313	0.69497936
15		1.64143143	1.02666184	0.77926968		1.76221840	1.28586712	0.69570702

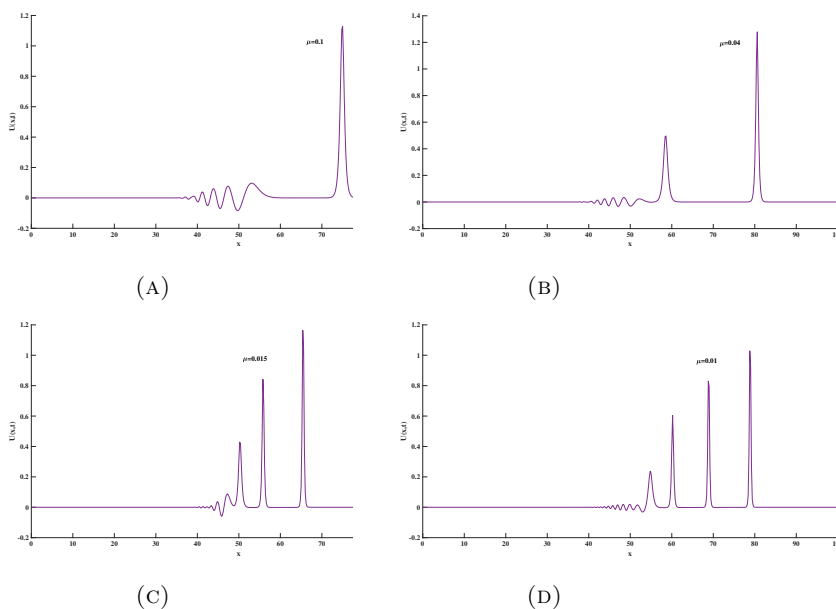


FIGURE 6. The interactions of two solitary waves at various time levels of MRLW equation

the reliability and performance of the method in this study. The error norms L_2 and L_∞ are calculated to show that results are superior to those of the methods in the literature and the results produced have been compared in tables and figures. The error norms are, as hoped, smaller than the results in the literature and thus closer to the analytic solution. The invariants I_1, I_2 and I_3 are satisfactorily well preserved throughout the entire computer run. The computed solutions displays it

can be easily said that the current algorithm will be beneficial in applying to other nonlinear equation types such as MRLW.

Declaration of Competing Interests The author declares that there is no competing interest regarding the publication of this paper.

REFERENCES

- [1] Ali, A., Mesh Free Collocation Method for Numerical Solution of Initial-Boundary Value Problems Using Radial Basis Functions, Dissertation, Ghulam Ishaq Khan Institute of Engineering Sciences and Technology, 2009.
- [2] Alharbi, A.R., Al-Munawarah, A.M., Arabia, S., Numerical investigation for the GRLW equation using parabolic Monge Ampere equation, *Comput. Sci.*, 15 (2020), 443–462.
- [3] Bhardwaj, D., Shankar, R., A computational method for regularized long wave equation, *Comput. Math. Appl.*, 40 (2000), 1397-1404. [https://doi.org/10.1016/S0898-1221\(00\)00248-0](https://doi.org/10.1016/S0898-1221(00)00248-0)
- [4] Başhan, A., Yağmurlu, N.M., A mixed method approach to the solitary wave, undular bore and boundary-forced solutions of the regularized long wave equation, *Comp. Appl. Math.*, 41(169) (2022). <https://doi.org/10.1007/s40314-022-01882-7>
- [5] Benjamin, T.B., Bona, J.L., Mahony, J.J., Model equations for long waves in nonlinear dispersive systems, *Philos. Trans. R. Soc. A Math. Phys. Eng. Sci.*, 272 (1972), 47–78. <https://doi.org/10.1098/rsta.1972.0032>
- [6] Bhowmik, S.K., Karakoc, S.B.G., Numerical approximation of the generalized regularized long wave equation using Petrov–Galerkin finite element method, *Numer. Methods Partial Differ. Equ.*, 35 (2019) 2236–2257. <https://doi.org/10.1002/num.22410>
- [7] Dağ, I., Saka, B., Irk, D., Application of cubic B-splines for numerical solution of the RLW equation, *Appl. Math. Comput.*, 159 (2004) 373–389. <https://doi.org/10.1016/j.amc.2003.10.020>
- [8] Danaf, T.S., Raslan, K.R., Ali, K.K., New numerical treatment for the generalized regularized long wave equation based on finite difference scheme, *Int. J. Soft Comput. Eng.*, 4(2014), 16–24.
- [9] Esen, A., Kutluay, S., Application of a lumped Galerkin method to the regularized long wave equation, *Appl. Math. Comput.*, 174 (2006), 833–845. <https://doi.org/10.1016/j.amc.2005.05.032>
- [10] El-Danaf, T.S., Raslan, K.R., Ali, K.K., Collocation method with cubic B-Splines for solving the GRLW equation, *Int. J. Numer. Methods Appl.*, 15(1) (2016), 39-59. <http://dx.doi.org/10.17654/NM015010039>
- [11] Gardner, L.R.T., Gardner, G.A., Ayoub F.A., Amein, N.K., Approximations of solitary waves of the MRLW equation by B-spline finite element, *Arab. J. Sci. Eng.*, 22 (1997), 183–193.
- [12] Guo, P.F., Zhang, L.W., Liew, K.M., Numerical analysis of generalized regularized long wave equation using the element free kp-Ritz method, *Appl. Math. Comput.*, 240 (2014) 91–101. <https://doi.org/10.1016/j.amc.2014.04.023>
- [13] Haq, F., Islam, S., Tirmizi, I.A., A numerical technique for solution of the MRLW equation using quartic B-splines, *Appl. Math. Model.*, 34(2010) 4151-4160. <https://doi.org/10.1016/j.apm.2010.04.012>
- [14] Hammad, D.A., El-Azab, M.S., Chebyshev–Chebyshev spectral collocation method for solving the generalized regularized long wave (GRLW) equation, *Appl. Math. Comput.*, 285 (2016), 228–240. <https://doi.org/10.1016/j.amc.2016.03.033>
- [15] Jain, P.C., Shankar, R., Singh, T.V., Numerical solution of regularized long-wave equation, *Commun. Numer. Methods Eng.*, 9(1993), 579-586. <https://doi.org/10.1002/cnm.1640090705>

- [16] Karakoc, S.B.G., Uçar, Y., Yağmurlu, N.M., Numerical solutions of the MRLW equation by cubic B-spline Galerkin finite element method, *Kuwait J. Sci.*, 42 (2) (2015) 141-159.
- [17] Khalifa, A.K., Raslan, K.R., Alzubaidi, H.M., A finite difference scheme for the MRLW and solitary wave interactions, *Appl. Math. Comput.*, 189 (2007) 346-354. <https://doi.org/10.1016/j.amc.2006.11.104>
- [18] Karakoc, S.B.G., Geyikli, T., Petrov-Galerkin finite element method for solving the MRLW equation, *Math. Sci.*, 7(25) (2013). <https://doi.org/10.1186/2251-7456-7-25>
- [19] Karakoc, S.B.G., Geyikli, T., Bashan, A., A numerical solution of the modified regularized long wave (MRLW) equation using quartic B-splines, *TWMS J. Appl. Eng. Math.*, 3 (231) (2013)
- [20] Karakoç, S.B.G., Zeybek, H., Solitary-wave solutions of the GRLW equation using septic B-spline collocation method, *Appl. Math. Comput.*, 289 (2016) 159-171. <https://doi.org/10.1016/j.amc.2016.05.021>
- [21] Karakoc, S.B.G., Yağmurlu, N.M., Uçar, Y., Numerical approximation to a solution of the modified regularized long wave equation using quintic B-splines, *Boundary Value Problems*, 27 (2013). <https://doi.org/10.1186/1687-2770-2013-27>
- [22] Khalifaa, A.K., Raslana, K.R., Alzubaidib, H.M., A collocation method with cubic B-splines for solving the MRLW equation, *Journal of Computational and Applied Mathematics*, 212 (2008) 406 - 418. <https://doi.org/10.1016/j.cam.2006.12.029>
- [23] Kutluay, S., Esen, A., A finite difference solution of the regularized long wave equation, *Mathematical Problems in Engineering*, (2006). <https://doi.org/10.1155/MPE/2006/85743>
- [24] Mei, L., Chen, Y., Numerical solutions of RLW equation using Galerkin method with extrapolation techniques, *Comput. Phys. Commun.*, 183 (2012), 1609-1616. <https://doi.org/10.1016/j.cpc.2012.02.029>
- [25] Mei, L., Chen, Y., Explicit multistep method for the numerical solution of RLW equation, *Appl. Math. Comput.*, 218 (2012), 9547-9554. <https://doi.org/10.1016/j.amc.2012.03.050>
- [26] MacNamara, S., Strang, G., Operator Splitting. In: Glowinski R., Osher S., Yin W. (eds) *Splitting Methods in Communication, Imaging, Science, and Engineering*, Springer, 2016.
- [27] Mohammadi, M., Mokhtari, R., Solving the generalized regularized long wave equation on the basis of a reproducing kernel space, *J. Comput. Appl. Math.*, 235 (2011). 4003-4014. <https://doi.org/10.1016/j.cam.2011.02.012>
- [28] Mohammadi, R., Exponential B-spline collocation method for numerical solution of the generalized regularized long wave equation, *Chin. Phys. B*, 24 (2015), 050206. <https://doi.org/10.1088/1674-1056/24/5/050206>
- [29] Olver, P.J., Euler operators and conservation laws of the BBM equation, *Mathematical Proceedings of the Cambridge Philosophical Society*, 85 (1979), 143-159. <https://doi.org/10.1017/S0305004100055572>
- [30] Oruç, O., Bulut, F., Esen, A., Numerical solutions of regularized long wave equation by Haar wavelet method, *Mediterr. J. Math.*, 13 (2016), 3235-3253. <https://doi.org/10.1007/s00009-016-0682-z>
- [31] Prenter, P.M., *Splines and Variational Methods*, Wiley, New York, 1975.
- [32] Peregrine, D.H., Calculations of the development of an undular bore, *J. Fluid Mech.*, 25(1966), 321-330. <https://doi.org/10.1017/S0022112066001678>
- [33] Ramos, J.I., Solitary wave interactions of the GRLW equation, *Chaos Solit. Fractals*, 33 (2007), 479-491. <https://doi.org/10.1016/j.chaos.2006.01.016>
- [34] Raslan, K.R., El-Danaf, T.S., Solitary waves solutions of the MRLW equation using quintic B-splines, *J. King Saud Univ. Sci.*, 22 (2010), 161-166. <https://doi.org/10.1016/j.jksus.2010.04.004>
- [35] Raslan, K.R., A computational method for the regularized long wave (RLW) equation, *Appl. Math. Comput.*, 167 (2005), 1101-1118. <https://doi.org/10.1016/j.amc.2004.06.130>

- [36] Raslan, K.R., Numerical study of the modified regularized long wave (MRLW) equation, *Chaos Soliton Fractals*, 42 (2009), 1845–1853. <https://doi.org/10.1016/j.chaos.2009.03.098>
- [37] Roshan, T., A Petrov-Galerkin method for solving the generalized regularized long wave (GRLW) equation, *Comput. Math. Appl.*, 63 (2012), 943–956. <https://doi.org/10.1016/j.camwa.2011.11.059>
- [38] Saumya Ranjan Jena, S.R., Senapati, A., Gebremedhin, G.S., Approximate solution of MRLW equation in B-spline environment, *Math. Sci.*, 14 (2020), 345–357. <https://doi.org/10.1007/s40096-020-00345-6>
- [39] Soliman, A.A., Hussien, M.H., Collocation solution for RLW equation with septic spline, *Appl. Math. Comput.* 161 (2005), 623–636. <https://doi.org/10.1016/j.amc.2003.12.053>
- [40] Soliman, A.A., Raslan, K.R., Collocation method using quadratic B-spline for the RLW equation, *Int. J. Comput. Math.*, 78 (2001), 399–412. <https://doi.org/10.1080/00207160108805119>
- [41] Saka, B., Dag, I., Dogan, A., Galerkin method for the numerical solution of the RLW equation using quadratic B-splines, *Int. J. Comput. Math.*, 81(6) (2004), 727–739. <https://doi.org/10.1016/j.cam.2005.04.026>
- [42] Trotter, H. F., On the product of semi-groups of operators, *Proc. American Math. Society*, 10 (1959) 545–551.
- [43] Xiao, X., Gui, D., Feng, X., A highly efficient operator-splitting finite element method for 2D/3D nonlinear Allen–Cahn equation, *International Journal of Numerical Methods for Heat and Fluid Flow*, 27 (2017), 530–542. <https://doi.org/10.1108/HFF-12-2015-0521>
- [44] Yagmurlu, N.M., Ucar, Y., Celikkaya, İ., Operator splitting for numerical solutions of the RLW equation, *Journal of Applied Analysis and Computation*, 8(5) 2018, 1494–1510. <http://jaac-online.com/DOI:10.11948/2018>
- [45] Zaki, S.I., Solitary waves of the splitted RLW equation, *Comput. Phys. Commun.*, 138 (2001), 80–91. [https://doi.org/10.1016/S0010-4655\(01\)00200-4](https://doi.org/10.1016/S0010-4655(01)00200-4)
- [46] Zeybek, H., Karakoç, S.B.G., A numerical investigation of the GRLW equation using lumped Galerkin approach with cubic B-spline, *Springer Plus*, 5(199) (2016). <https://doi.org/10.1186/s40064-016-1773-9>
- [47] Zeybek, H., Karakoç, S.B.G., A collocation algorithm based on quintic B-splines for the solitary wave simulation of the GRLW equation, *Scientia Iranica B*, 26(6) (2019), 3356–3368. <https://doi.org/10.24200/SCI.2018.20781>

RENEWED STRUCTURE OF NEUTROSOPHIC SOFT GRAPHS AND ITS APPLICATION IN DECISION-MAKING PROBLEM

Yıldray ÇELİK

Department of Mathematics, Ordu University, 52200 Ordu, TÜRKİYE

ABSTRACT. This study is designed with the renewed concept of neutrosophic soft graph (briefly ns-graph) which is a combination of graphs and neutrosophic soft sets. We re-define notions of ns-graphs and ns-subgraphs with the different perspective from the study in [4]. Also, we introduce some new operations on ns-graphs and detailed them with convenient examples. Moreover, we present an application of ns-graphs to determine of optimal object by using given data with the help of an algorithm. This algorithm we developed is new inventiveness domain for problems which are involving uncertainty, and effectively finds the optimal result between the states where vagueness exists. We also provide a comparative analysis with the existing method given in [4].

1. INTRODUCTION

It is clear that the uncertainty arising from different areas cannot be explained and expressed with precise definitions. Different types of uncertainty are common in many fields such as economics, biology, physics, engineering, medicine and social sciences. Since uncertainty is a complex and broad concept that is not clearly defined, many fields dealing with uncertainty have failed to model this situation successfully with classical mathematical methods. In valuing a phenomenon in real life, we use intermediate values, that is, fuzzy values. For example, when evaluating the temperature of the air, we make ratings such as cold, slightly cold, warm, slightly hot and hot. Therefore, classical set theory falls short of expressing intermediate state values. This inadequate situation in classical set theory was first tried to be overcome with fuzzy set theory [21]. A fuzzy set A is characterized with the help of a membership function $\mu_A(x)$, a mapping from the universal set X to the unit interval $[0,1]$, where x in the fuzzy set A has a certain degree of membership. Although a phenomenon can be represented with only one of 0 and 1 values in

2020 *Mathematics Subject Classification.* 03E72, 05C90.

Keywords. Neutrosophic soft set, graf, neutrosophic soft graph.

✉ ycelik61@gmail.com;  0000-0003-3373-3916.

classical set theory, it can take infinite values in fuzzy logic. Thus, a phenomenon can have uncertain values in the fuzzy approach. Fuzzy logic controllers have been applied many areas from electrical household appliances to auto electronics, from business machines we use daily to production engineering, from industrial control technologies to automation. Atanassov [5] put forward the intuitionistic fuzzy set theory which is a generalized type of the fuzzy set theory. In intuitionistic fuzzy sets, unlike fuzzy sets, the elements have degrees of non-membership. However, in these theories, the uncertainty of an element is not discussed, although the values of an element such as whether it is a member or not. Based on this, Smarandache [19] introduced the neutrosophic set theory which is an extended and special case of fuzzy set theory. The neutrosophic sets are stated by three functions. These are truth, indeterminacy and falsity membership function. The neutrosophic models produce more suitable solutions for the complex systems. In addition, an individual may not always be fully informed about a subject. In this case, the indeterminacy membership function comes into play and it provides a very large place for modeling events involving many uncertainties. Maji [14] defined the neutrosophic soft set concept and examined the properties of this concept. Broumi [7] worked on generalized neutrosophic soft sets. Deli [11] gave the notion of interval-valued neutrosophic soft set and also applied this concept to the a decision-making problem.

Some great scientific theories grew out of answers to simple questions. Graf theory is one of them. Graf theory was first put forward by Euler [12]. Graph theory which is an important mathematical tool for solving complicated problems in many different fields. Graphs are used to put forth a relevance between elements in a given set, where every element can be expressed with the help of vertices and their relation edges. Since graph theory provides conveniences in modeling complicated systems, it has many number of applications. A simple graph is showed by $G^* = (\nu, \varepsilon)$ where ν and ε represents sets of vertices and edges, respectively. After Euler's introduction of the graph concept, Rosenfeld [17] introduced the fuzzy graph theory. Bhattacharya [6] gave some properties of fuzzy graphs. Mordeson and Peng [16] have defined some operations on fuzzy graphs. Later, many researchers discussed the concept of fuzzy sets on the graph theory and defined different structures. Akram and Dudek [1] gave the concept of interval-valued fuzzy graphs and examined their related properties. Broumi et al. [9] gave the concept of interval valued pentapartitioned neutrosophic graphs. Broumi et al. [8] defined interval-valued fermatean neutrosophic graphs and presented some operations on this. Thumbakara and George [20] gave the concepts of soft graph and soft subgraph, and examined the properties of these structures. Akram and Nawaz [2] described some new algebraic operations on soft graphs. Mohinta and Samanta [15] defined the concept of fuzzy soft graph. Later, Akram and Nawaz [3] studied different types of fuzzy soft graphs. Zihni et al. [22] gave the concept of interval-valued fuzzy soft graph and examined its basic properties. Çelik [10] gave the concept of bipolar fuzzy soft graph and investigated some operations on this concept. Kandasamy et al. [13]

gave the concept of neutrosophic graph and made various applications of neutrosophic graphs. Akram et al. [4] combined neutrosophic soft set concept and graph theory, then define notion of neutrosophic soft graph (ns-graph). They also applied the ns-graphs to the a decision-making problem. Shah and Hussain [18] gave new features on ns-graphs.

In the current study, the renewed concept of ns-graphs is defined and some new operations not previously defined such us extended union, restricted union, extended intersection, restricted intersection and complement are presented. Also illustrative examples related these operations are given. Hence an application of ns-graphs for a decision-making problem is examined with the method we developed. Moreover a comparative analysis between proposed method and existing method given in [4] are revealed.

2. PRELIMINARIES

Definition 1. [19] Let $X \neq \emptyset$ be an universe. Then a neutrosophic set A on X is given by $A = \{(x, T_A(x), I_A(x), F_A(x)), x \in X\}$, where the functions T_A, I_A and F_A are fuzzy sets on X under the conditions $0 \leq T_A(x) + I_A(x) + F_A(x) \leq 3$ for all $x \in X$. The family of all neutrosophic sets on X is denoted by $\mathcal{N}(X)$.

Definition 2. [14] Let X be an initial universe. Let E be a set of parameters. Then, a pair (f, E) is called a neutrosophic soft set (briefly ns-set) over X representing a mapping by $f : E \rightarrow \mathcal{N}(X)$.

Definition 3. [14] Let $(f, E) \in \mathcal{N}(X)$. Then, for all $e \in E$ and $x \in X$,

- (a) (f, E) is called a null ns-set if $T_{f(e)}(x) = 0, I_{f(e)}(x) = 1$ and $F_{f(e)}(x) = 1$.
- (b) (f, E) is called a whole ns-set if $T_{f(e)}(x) = 1, I_{f(e)}(x) = 0$ and $F_{f(e)}(x) = 0$.

Definition 4. [14] Let (f, E_1) and (g, E_2) be two ns-sets over X , then (f, E_1) is said to be a ns-subset of (g, E_2) if

- i. $E_1 \subseteq E_2$
- ii. $T_{f(e)}(x) \leq T_{g(e)}(x), I_{f(e)}(x) \geq I_{g(e)}(x), F_{f(e)}(x) \geq F_{g(e)}(x)$ for all $e \in E_1$ and $x \in X$.

3. RENEWED STRUCTURE OF NS-GRAPHS WITH SOME NEW OPERATIONS

Definition 5. A ns-graph is an order 4-tuple $G_N = (G^*, f, g, E)$ such that

- i. $G^* = (\nu, \varepsilon)$ is a simple graph
- ii. $E \neq \emptyset$ is a set of parameters
- iii. (f, E) is a ns-set over ν
- iv. (g, E) is a ns-set over ε
- v. $h(e) = (f(e), g(e))$ is a neutrosophic graph for all $e \in E$. That is, for all $e \in E$ and $xy \in \varepsilon$,

$$T_{ge}(xy) \leq \min\{T_{fe}(x), T_{fe}(y)\}$$

$$I_{ge}(xy) \geq \max\{I_{fe}(x), I_{fe}(y)\}$$

$$F_{ge}(xy) \geq \max\{F_{fe}(x), F_{fe}(y)\}$$

Note that (f, E) is called a ns-vertex and (g, E) is called a ns-edge.

Example 1. Let $G^* = (\nu, \varepsilon)$ be a simple graph with $\nu = \{v_1, v_2, v_3\}$ and $\varepsilon = \{v_1v_2, v_1v_3, v_2v_3\}$. Let $E = \{e_1, e_2, e_3\}$ be a set of parameters. Let consider ns-sets f and g over ν and ε , respectively, as given in Table 1.

TABLE 1. Ns-sets (f, E) and (g, E)

f	v_1	v_2	v_3
e_1	$(0.2, 0.4, 0.5)$	$(0.4, 0.5, 0.6)$	$(0, 1, 1)$
e_2	$(0.2, 0.7, 0.8)$	$(0.3, 0.5, 0.6)$	$(0.5, 0.6, 0.7)$
e_3	$(0.3, 0.3, 0.5)$	$(0.2, 0.2, 0.3)$	$(0.3, 0.4, 0.9)$
g	v_1v_2	v_2v_3	v_1v_3
e_1	$(0.1, 0.6, 0.7)$	$(0, 1, 1)$	$(0, 1, 1)$
e_2	$(0.1, 0.7, 0.9)$	$(0, 1, 1)$	$(0.2, 0.8, 0.9)$
e_3	$(0.2, 0.4, 0.6)$	$(0.1, 0.5, 0.9)$	$(0.3, 0.5, 0.9)$

Clearly $G_N = (G^*, f, g, E)$ is a ns-graph over G^* .

Definition 6. Let $G^* = (\nu, \varepsilon)$ be a simple graph. A ns-graph $G'_N = (G^*, f^1, g^1, E_1)$ is called a ns-subgraph of $G_N = (G^*, f, g, E_2)$ if

- i. $E_1 \subseteq E_2$
 - ii. $f^1_e \subseteq f_e$, that is $T_{f^1_e}(x) \leq T_{f_e}(x)$, $I_{f^1_e}(x) \geq I_{f_e}(x)$, $F_{f^1_e}(x) \geq F_{f_e}(x)$
 - iii. $g^1_e \subseteq g_e$, that is, $T_{g^1_e}(x) \leq T_{g_e}(x)$, $I_{g^1_e}(x) \geq I_{g_e}(x)$, $F_{g^1_e}(x) \geq F_{g_e}(x)$
- for all $e \in E_1, x \in \nu$.

Example 2. Let consider a ns-graph $G_N = (G^*, f, g, E)$ as taken in Example 1. Let consider another ns-graph $G'_N = (G^*, f^1, g^1, E_1)$ as in the Table 2 with the parameter set $E_1 = \{e_1, e_2\}$.

TABLE 2. Ns-sets (f^1, E_1) and (g^1, E_1)

f^1	v_1	v_2	v_3
e_1	$(0.2, 0.5, 0.6)$	$(0.3, 0.6, 0.8)$	$(0, 1, 1)$
e_2	$(0.1, 0.7, 0.9)$	$(0.1, 0.5, 0.7)$	$(0.2, 0.8, 0.9)$
g^1	v_1v_2	v_2v_3	v_1v_3
e_1	$(0.1, 0.7, 0.8)$	$(0, 1, 1)$	$(0, 1, 1)$
e_2	$(0.1, 0.9, 0.9)$	$(0, 1, 1)$	$(0.1, 0.8, 0.9)$

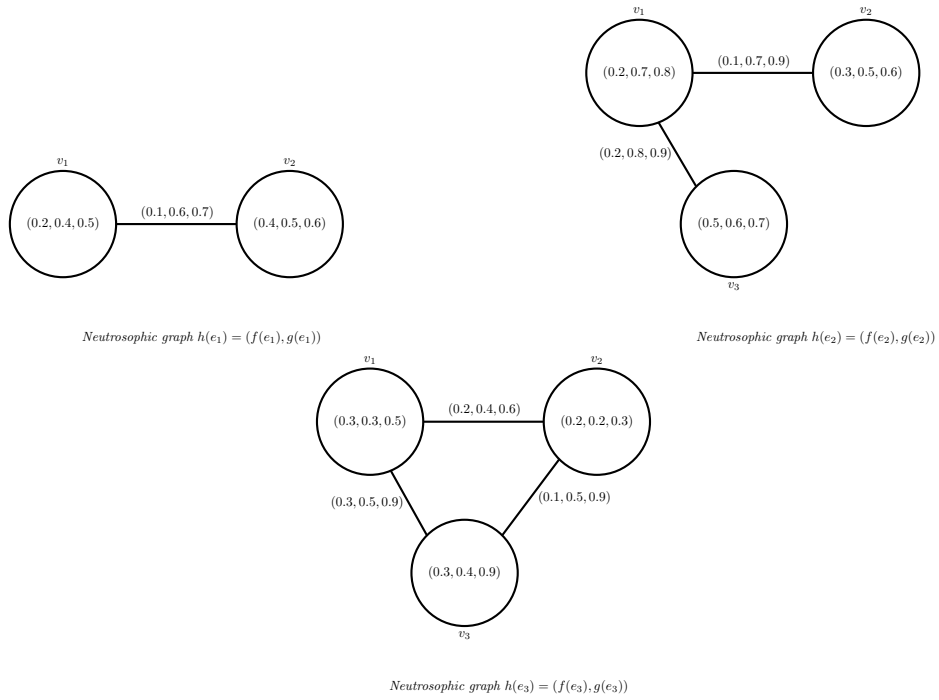


FIGURE 1. Ns-graph $G_N = (G^*, f, g, E)$

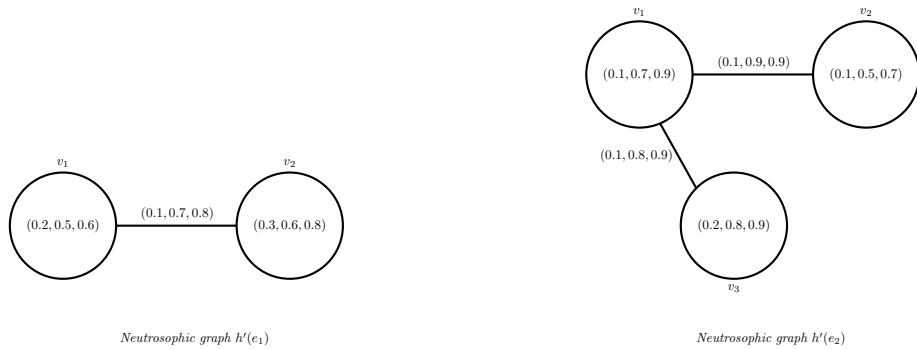


FIGURE 2. Ns-graph $G'_N = (G^*, f^1, g^1, E_1)$

It is evident that $G'_N = (G^*, f^1, g^1, E_1)$ is a ns-subgraph of $G_N = (G^*, f, g, E)$.

Definition 7. Let $G_N = (G^*, f, g, E)$ be a ns-graph over $G^* = (\nu, \varepsilon)$. Then G_N is called strong ns-graph iff

$$T_{g_e}(xy) = \min\{T_{f_e}(x), T_{f_e}(y)\}$$

$$I_{g_e}(xy) = \max\{I_{f_e}(x), I_{f_e}(y)\}$$

$$F_{g_e}(xy) = \max\{F_{f_e}(x), F_{f_e}(y)\}$$

for all $e \in E$ and $xy \in \varepsilon$.

Example 3. Let $G^* = (\nu, \varepsilon)$ be a simple graph with $\nu = \{v_1, v_2, v_3\}$ and $\varepsilon = \{v_1v_2, v_1v_3, v_2v_3\}$. Let $E = \{e_1, e_2, e_3\}$ be a set of parameters. Let consider ns-sets f and g over ν and ε , respectively, as given in Table 3.

TABLE 3. Ns-sets (f, E) and (g, E)

f	v_1	v_2	v_3
e_1	$(0.2, 0.4, 0.5)$	$(0.4, 0.5, 0.6)$	$(0, 1, 1)$
e_2	$(0.2, 0.7, 0.8)$	$(0.3, 0.5, 0.6)$	$(0.5, 0.6, 0.7)$
e_3	$(0.3, 0.3, 0.5)$	$(0.2, 0.2, 0.3)$	$(0.3, 0.4, 0.9)$
g	v_1v_2	v_2v_3	v_1v_3
e_1	$(0.2, 0.5, 0.6)$	$(0, 1, 1)$	$(0, 1, 1)$
e_2	$(0.2, 0.7, 0.8)$	$(0.3, 0.6, 0.7)$	$(0.2, 0.7, 0.8)$
e_3	$(0.2, 0.3, 0.5)$	$(0.2, 0.4, 0.9)$	$(0.3, 0.4, 0.9)$

Clearly $G_N = (G^*, f, g, E)$ is strong ns-graph.

Definition 8. Let $G_N = (G^*, f, g, E)$ be a ns-graph over $G^* = (\nu, \varepsilon)$. Then the complement of $G_N = (G^*, f, g, E)$ is denoted by $\overline{G_N} = (G^*, \bar{f}, \bar{g}, E)$ and is defined by

i. $T_{\bar{f}_e}(x) = T_{f_e}(x), I_{\bar{f}_e}(x) = I_{f_e}(x), F_{\bar{f}_e}(x) = F_{f_e}(x)$

ii. $T_{\bar{g}_e}(x, y) = \min\{T_{f_e}(x), T_{f_e}(y)\} - T_{g_e}(x, y)$

$$I_{\bar{g}_e}(x, y) = \max\{I_{f_e}(x), I_{f_e}(y)\} - I_{g_e}(x, y)$$

$$F_{\bar{g}_e}(x, y) = \max\{F_{f_e}(x), F_{f_e}(y)\} - F_{g_e}(x, y)$$

for all $e \in E$ and $xy \in \varepsilon$.

Definition 9. Let $G_N = (G^*, f^1, g^1, E_1)$ and $G'_N = (G^*, f^2, g^2, E_2)$ be two ns-graphs over the simple graph $G^* = (\nu, \varepsilon)$. The extended union of G_N and G'_N is denoted by $G_N \cup G'_N = (G^*, f, g, E)$, where $E = E_1 \cup E_2$. T, I and F membership values of vertices and edges of $G_N \cup G'_N$ are defined by as follow.

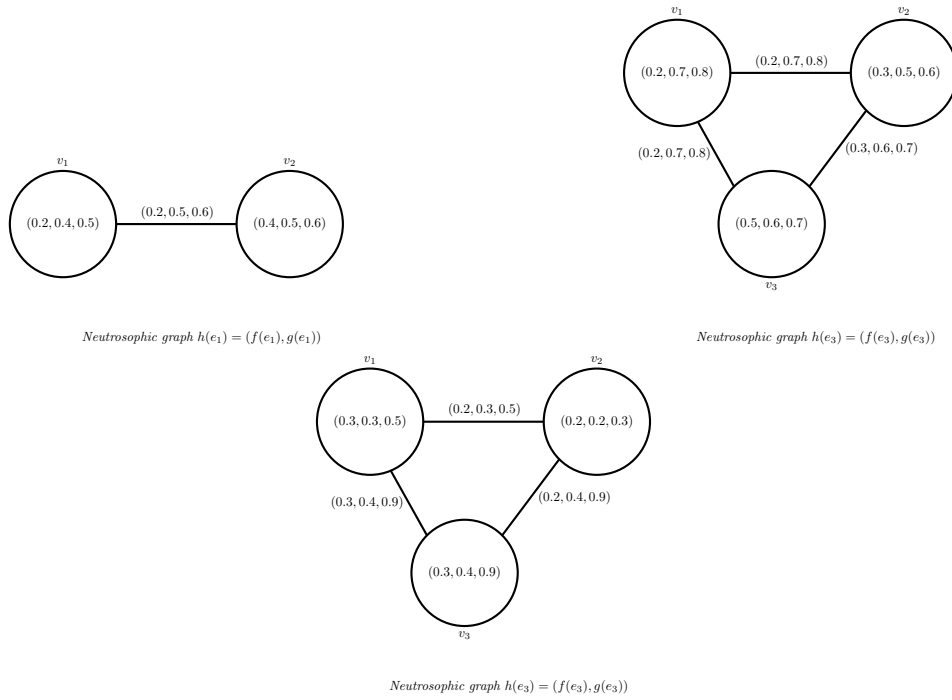


FIGURE 3. Strong ns-graph $G_N = (G^*, f, g, E)$

i. For all $e \in E$ and $x \in \nu$

$$T_{f_e}(x) = \begin{cases} T_{f_e^1}(x) & e \in E_1 \setminus E_2 \\ T_{f_e^2}(x) & e \in E_2 \setminus E_1 \\ \max\{T_{f_e^1}(x), T_{f_e^2}(x)\} & e \in E_1 \cap E_2 \end{cases}$$

$$I_{f_e}(x) = \begin{cases} I_{f_e^1}(x) & e \in E_1 \setminus E_2 \\ I_{f_e^2}(x) & e \in E_2 \setminus E_1 \\ \min\{I_{f_e^1}(x), I_{f_e^2}(x)\} & e \in E_1 \cap E_2 \end{cases}$$

$$F_{f_e}(x) = \begin{cases} F_{f_e^1}(x) & e \in E_1 \setminus E_2 \\ F_{f_e^2}(x) & e \in E_2 \setminus E_1 \\ \min\{F_{f_e^1}(x), F_{f_e^2}(x)\} & e \in E_1 \cap E_2 \end{cases}$$

ii. For all $e \in E$ and $xy \in \varepsilon$

$$\begin{aligned}
 T_{g_e}(xy) &= \begin{cases} T_{g_e^1}(xy) & e \in E_1 \setminus E_2 \\ T_{g_e^2}(xy) & e \in E_2 \setminus E_1 \\ \max\{T_{g_e^1}(xy), T_{g_e^2}(xy)\} & e \in E_1 \cap E_2 \end{cases} \\
 I_{g_e}(xy) &= \begin{cases} I_{g_e^1}(xy) & e \in E_1 \setminus E_2 \\ I_{g_e^2}(xy) & e \in E_2 \setminus E_1 \\ \min\{I_{g_e^1}(xy), I_{g_e^2}(xy)\} & e \in E_1 \cap E_2 \end{cases} \\
 F_{g_e}(xy) &= \begin{cases} F_{g_e^1}(xy) & e \in E_1 \setminus E_2 \\ F_{g_e^2}(xy) & e \in E_2 \setminus E_1 \\ \min\{F_{g_e^1}(xy), F_{g_e^2}(xy)\} & e \in E_1 \cap E_2 \end{cases}
 \end{aligned}$$

Example 4. Let $G^* = (\nu, \varepsilon)$ be a simple graph with $\nu = \{v_1, v_2, v_3, v_4, v_5\}$. Let consider a ns-graph $G_N = (G^*, f^1, g^1, E_1)$ with the parameter set $E_1 = \{e_1, e_2, e_3\}$ as in the Table 4.

TABLE 4. Ns-sets (f^1, E_1) and (g^1, E_1)

f^1	v_1	v_2	v_3	v_4	v_5
e_1	$(0,1,0.2,0.3)$	$(0,1,1)$	$(0.2,0.3,0.4)$	$(0.2,0.5,0.7)$	$(0,1,1)$
e_2	$(0.1,0.3,0.7)$	$(0,1,1)$	$(0.4,0.6,0.7)$	$(0.1,0.2,0.3)$	$(0,1,1)$
e_3	$(0.5,0.6,0.7)$	$(0,1,1)$	$(0.6,0.8,0.9)$	$(0.3,0.4,0.6)$	$(0,1,1)$

g^1	v_1v_2	v_1v_3	v_1v_4	v_1v_5	v_2v_3
e_1	$(0,1,1)$	$(0.1,0.4,0.5)$	$(0.1,0.6,0.7)$	$(0,1,1)$	$(0,1,1)$
e_2	$(0,1,1)$	$(0.1,0.7,0.8)$	$(0.1,0.4,0.8)$	$(0,1,1)$	$(0,1,1)$
e_3	$(0,1,1)$	$(0,1,1)$	$(0.2,0.7,0.9)$	$(0,1,1)$	$(0,1,1)$

g^1	v_2v_4	v_2v_5	v_3v_4	v_3v_5	v_4v_5
e_1	$(0,1,1)$	$(0,1,1)$	$(0.1,0.6,0.8)$	$(0,1,1)$	$(0,1,1)$
e_2	$(0,1,1)$	$(0,1,1)$	$(0.1,0.8,0.9)$	$(0,1,1)$	$(0,1,1)$
e_3	$(0,1,1)$	$(0,1,1)$	$(0.3,0.8,0.9)$	$(0,1,1)$	$(0,1,1)$

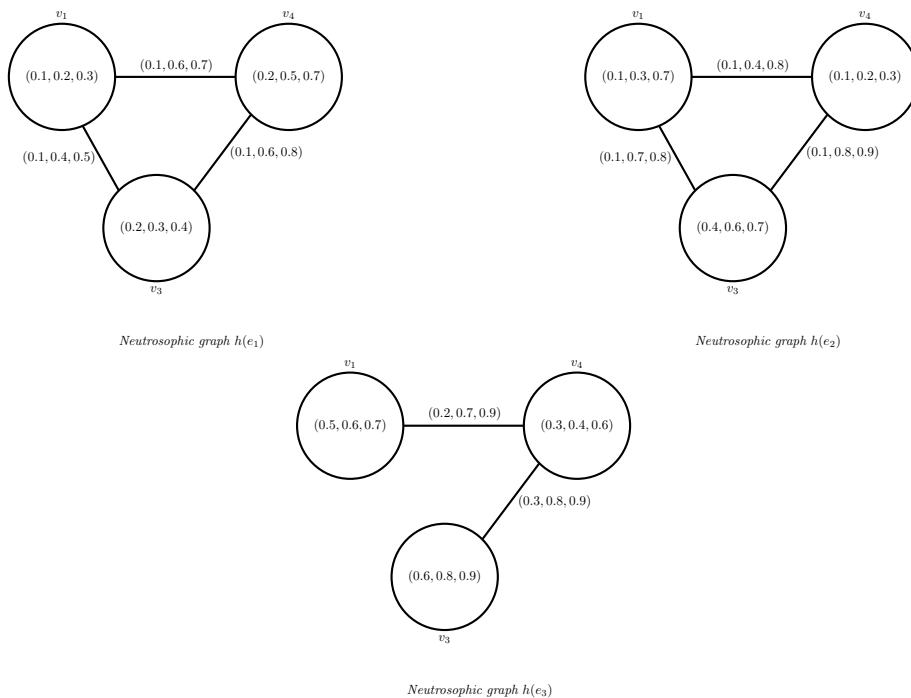


FIGURE 4. Ns -graph $G_N = (G^*, f^1, g^1, E_1)$

Now let consider another ns -graph $G'_N = (G^*, f^2, g^2, E_2)$ with the parameter set $E_2 = \{e_2, e_4\}$ as in the Table 5.

TABLE 5. Ns -sets (f^2, E_2) and (g^2, E_2)

f^2	v_1	v_2	v_3	v_4	v_5
e_2	$(0, 1, 1)$	$(0.1, 0.2, 0.4)$	$(0.2, 0.3, 0.4)$	$(0, 1, 1)$	$(0.4, 0.6, 0.7)$
e_4	$(0, 1, 1)$	$(0.3, 0.6, 0.8)$	$(0.5, 0.7, 0.9)$	$(0, 1, 1)$	$(0.3, 0.4, 0.5)$
g^2	v_1v_2	v_1v_3	v_1v_4	v_1v_5	v_2v_3
e_2	$(0, 1, 1)$	$(0, 1, 1)$	$(0, 1, 1)$	$(0, 1, 1)$	$(0.1, 0.4, 0.8)$
e_4	$(0, 1, 1)$	$(0, 1, 1)$	$(0, 1, 1)$	$(0, 1, 1)$	$(0.2, 0.7, 0.9)$
g^2	v_2v_4	v_2v_5	v_3v_4	v_3v_5	v_5v_6
e_2	$(0, 1, 1)$	$(0, 1, 1)$	$(0, 1, 1)$	$(0.2, 0.8, 0.9)$	$(0, 1, 1)$
e_4	$(0, 1, 1)$	$(0.2, 0.6, 0.8)$	$(0, 1, 1)$	$(0.3, 0.9, 0.9)$	$(0, 1, 1)$

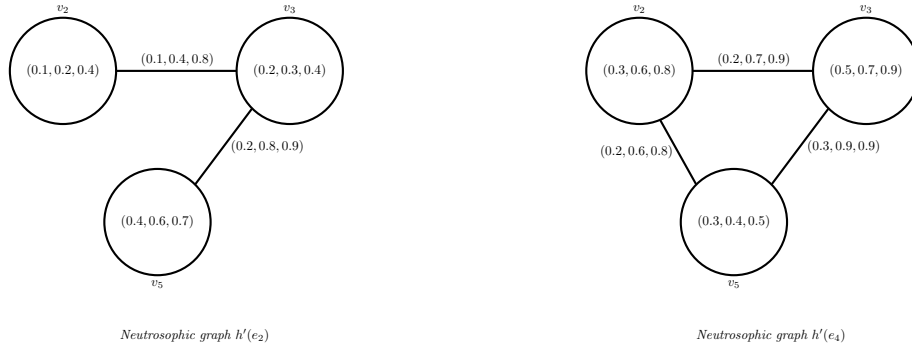


FIGURE 5. Ns-graph $G'_N = (G^*, f^2, g^2, E_2)$

The parameter set of $G_N \cup G'_N = (G^*, f, g, E)$ is $E = E_1 \cup E_2 = \{e_1, e_2, e_3, e_4\}$. Moreover the ns-graph $G_N \cup G'_N = (G^*, f, g, E)$ is obtained as in the Table 6 and Table 7.

TABLE 6. Ns-set (f, E)

f	v_1	v_2	v_3	v_4	v_5
e_1	$(0.1, 0.2, 0.3)$	$(0, 1, 1)$	$(0.2, 0.3, 0.4)$	$(0.2, 0.5, 0.7)$	$(0, 1, 1)$
e_2	$(0.1, 0.3, 0.7)$	$(0.1, 0.2, 0.4)$	$(0.2, 0.4, 0.4)$	$(0.1, 0.2, 0.3)$	$(0.4, 0.6, 0.7)$
e_3	$(0.5, 0.6, 0.7)$	$(0, 1, 1)$	$(0.6, 0.8, 0.9)$	$(0.3, 0.4, 0.6)$	$(0, 1, 1)$
e_4	$(0, 1, 1)$	$(0.3, 0.6, 0.8)$	$(0.5, 0.7, 0.9)$	$(0, 1, 1)$	$(0.3, 0.4, 0.5)$

TABLE 7. Ns-set (g, E)

g	v_1v_2	v_1v_3	v_1v_4	v_1v_5	v_2v_3
e_1	$(0, 1, 1)$	$(0.1, 0.4, 0.5)$	$(0.1, 0.6, 0.7)$	$(0, 1, 1)$	$(0, 1, 1)$
e_2	$(0, 1, 1)$	$(0.1, 0.7, 0.8)$	$(0.1, 0.4, 0.8)$	$(0, 1, 1)$	$(0.1, 0.4, 0.8)$
e_3	$(0, 1, 1)$	$(0, 1, 1)$	$(0.2, 0.7, 0.9)$	$(0, 1, 1)$	$(0, 1, 1)$
e_4	$(0, 1, 1)$	$(0, 1, 1)$	$(0, 1, 1)$	$(0, 1, 1)$	$(0.2, 0.7, 0.9)$
g	v_2v_4	v_2v_5	v_3v_4	v_3v_5	v_4v_5
e_1	$(0, 1, 1)$	$(0, 1, 1)$	$(0.1, 0.6, 0.8)$	$(0, 1, 1)$	$(0, 1, 1)$
e_2	$(0, 1, 1)$	$(0, 1, 1)$	$(0.1, 0.8, 0.9)$	$(0.2, 0.8, 0.9)$	$(0, 1, 1)$
e_3	$(0, 1, 1)$	$(0, 1, 1)$	$(0.2, 0.8, 0.9)$	$(0, 1, 1)$	$(0, 1, 1)$
e_4	$(0, 1, 1)$	$(0.2, 0.6, 0.8)$	$(0, 1, 1)$	$(0.3, 0.9, 0.9)$	$(0, 1, 1)$

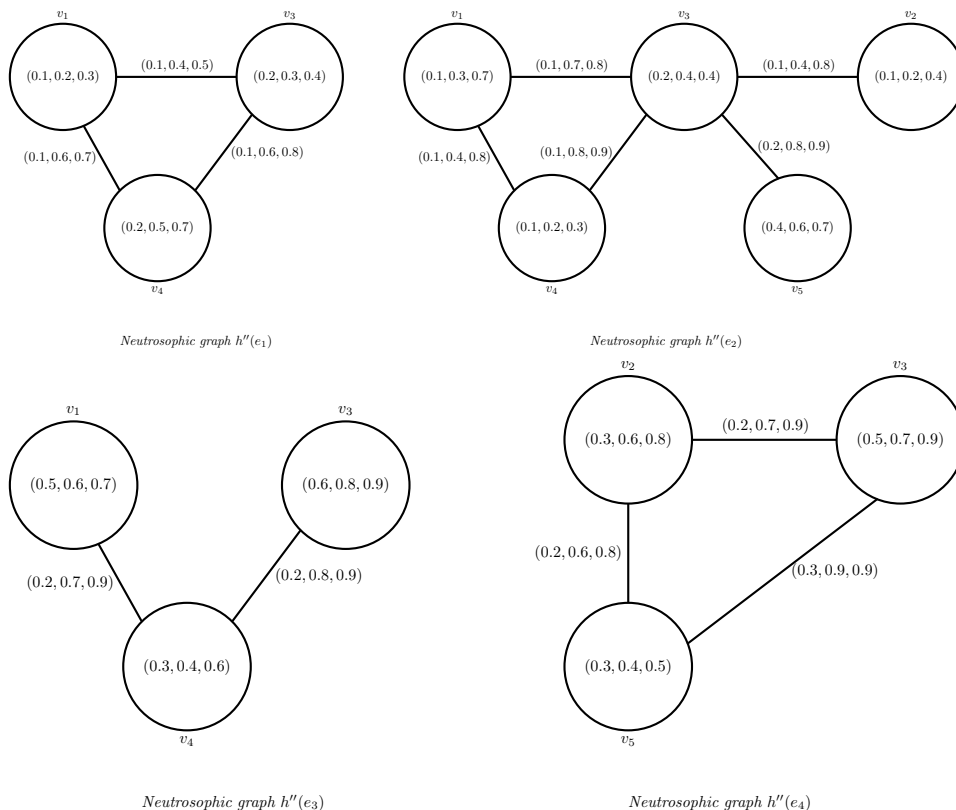


FIGURE 6. Ns-graph $G_N \cup G'_N = (G^*, f, g, E)$

Definition 10. Let $G_N = (G^*, f^1, g^1, E_1)$ and $G'_N = (G^*, f^2, g^2, E_2)$ be two ns-graph over $G^* = (\nu, \varepsilon)$. The restricted union of G_N and G'_N is denoted by $G_N \sqcup G'_N = (G^*, f, g, E)$, where $E = E_1 \cap E_2$. T, I and F membership values of vertices and edges of $G_N \sqcup G'_N$ are defined by as follow.

i. For all $e \in E$ and $x \in \nu$

$$T_{f_e}(x) = \max\{T_{f_e^1}(x), T_{f_e^2}(x)\}$$

$$I_{f_e}(x) = \min\{I_{f_e^1}(x), I_{f_e^2}(x)\}$$

$$F_{f_e}(x) = \min\{F_{f_e^1}(x), F_{f_e^2}(x)\}$$

ii. For all $e \in E$ and $xy \in \varepsilon$

$$T_{g_e}(xy) = \max\{T_{g_e^1}(xy), T_{g_e^2}(xy)\}$$

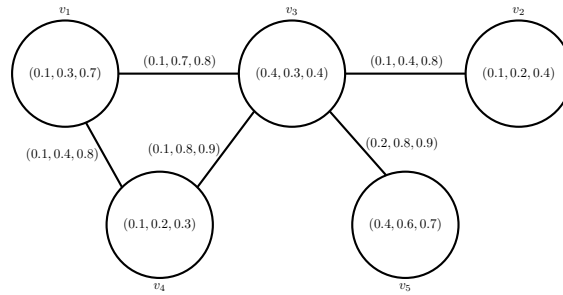
$$I_{g_e}(xy) = \min\{I_{g_e^1}(xy), I_{g_e^2}(xy)\}$$

$$F_{g_e}(xy) = \min\{F_{g_e^1}(xy), F_{g_e^2}(xy)\}$$

Example 5. Let consider ns-graphs $G_N = (G^*, f^1, g^1, E_1)$ and $G'_N = (G^*, f^2, g^2, E_2)$ as taken in Example 4. Clearly $E = E_1 \cap E_2 = \{e_2\}$. Also the restricted union of G_N and G'_N is obtained as follow.

TABLE 8. Ns-sets (f, E) and (g, E)

f	v_1	v_2	v_3	v_4	v_5
e_2	$(0.1, 0.3, 0.7)$	$(0.1, 0.2, 0.4)$	$(0.4, 0.3, 0.4)$	$(0.1, 0.2, 0.3)$	$(0.4, 0.6, 0.7)$
g	v_1v_4	v_3v_4	v_1v_3	v_2v_3	v_3v_5
e_2	$(0.1, 0.4, 0.8)$	$(0.1, 0.8, 0.9)$	$(0.1, 0.7, 0.8)$	$(0.1, 0.4, 0.8)$	$(0.2, 0.8, 0.9)$



Neutrosophic graph $h'(e_2)$

FIGURE 7. Ns-graph $G_N \sqcup G'_N = (G^*, f, g, E)$

Definition 11. Let $G_N = (G^*, f^1, g^1, E_1)$ and $G'_N = (G^*, f^2, g^2, E_2)$ be two ns-graph over $G^* = (\nu, \varepsilon)$. The extended intersection of G_N and G'_N is denoted by $G_N \cap G'_N = (G^*, f, g, E)$, where $E = E_1 \cup E_2$. T , I and F membership values of vertices and edges of $G_N \cap G'_N$ are defined by as follow.

i. For all $e \in E$ and $x \in \nu$

$$T_{f_e}(x) = \begin{cases} T_{f_e^1}(x), & e \in E_1 \setminus E_2 \\ T_{f_e^2}(x), & e \in E_2 \setminus E_1 \\ \min\{T_{f_e^1}(x), T_{f_e^2}(x)\}, & e \in E_1 \cap E_2 \end{cases}$$

$$I_{f_e}(x) = \begin{cases} I_{f_e^1}(x), & e \in E_1 \setminus E_2 \\ I_{f_e^2}(x), & e \in E_2 \setminus E_1 \\ \max\{I_{f_e^1}(x), I_{f_e^2}(x)\}, & e \in E_1 \cap E_2 \end{cases}$$

$$F_{f_e}(x) = \begin{cases} F_{f_e^1}(x), & e \in E_1 \setminus E_2 \\ F_{f_e^2}(x), & e \in E_2 \setminus E_1 \\ \max\{F_{f_e^1}(x), F_{f_e^2}(x)\}, & e \in E_1 \cap E_2 \end{cases}$$

ii. For all $e \in E$ and $xy \in \varepsilon$

$$T_{g_e}(xy) = \begin{cases} T_{g_e^1}(xy) & e \in E_1 \setminus E_2 \\ T_{g_e^2}(xy) & e \in E_2 \setminus E_1 \\ \min\{T_{g_e^1}(xy), T_{g_e^2}(xy)\}, & e \in E_1 \cap E_2 \end{cases}$$

$$I_{g_e}(x) = \begin{cases} I_{g_e^1}(xy) & e \in E_1 \setminus E_2 \\ I_{g_e^2}(xy) & e \in E_2 \setminus E_1 \\ \max\{I_{g_e^1}(xy), I_{g_e^2}(xy)\}, & e \in E_1 \cap E_2 \end{cases}$$

$$F_{g_e}(xy) = \begin{cases} F_{g_e^1}(xy) & e \in E_1 \setminus E_2 \\ F_{g_e^2}(xy) & e \in E_2 \setminus E_1 \\ \max\{F_{g_e^1}(xy), F_{g_e^2}(xy)\}, & e \in E_1 \cap E_2 \end{cases}$$

Example 6. Let $G^* = (\nu, \varepsilon)$ be a simple graph with $V = \{v_1, v_2, v_3, v_4\}$ and $E = \{v_1v_2, v_1v_4, v_2v_4\}$. Let $E_1 = \{e_1, e_2\}$ be a set of parameters. Consider a ns-graph $G_N = (G^*, f^1, g^1, E_1)$ over $G^* = (\nu, \varepsilon)$ as taken in the Table 9.

TABLE 9. Ns-sets (f^1, E_1) and (g^1, E_1)

f^1	v_1	v_2	v_3	v_4
e_1	$(0.1, 0.2, 0.3)$	$(0.2, 0.4, 0.5)$	$(0, 1, 1)$	$(0.1, 0.5, 0.7)$
e_2	$(0.2, 0.3, 0.7)$	$(0.4, 0.6, 0.7)$	$(0, 1, 1)$	$(0.3, 0.4, 0.6)$

g^1	v_1v_2	v_1v_3	v_1v_4	v_2v_3	v_2v_4	v_3v_4
e_1	$(0.1, 0.5, 0.6)$	$(0, 1, 1)$	$(0.1, 0.5, 0.7)$	$(0, 1, 1)$	$(0, 1, 1)$	$(0, 1, 1)$
e_2	$(0.2, 0.7, 0.8)$	$(0, 1, 1)$	$(0.1, 0.6, 0.7)$	$(0, 1, 1)$	$(0.2, 0.7, 0.9)$	$(0, 1, 1)$

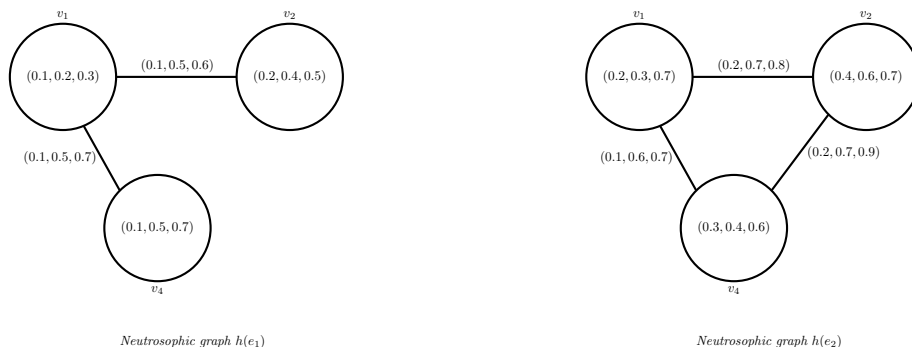


FIGURE 8. Ns-graph $G_N = (G^*, f^1, g^1, E_1)$

Now let consider another ns-graph $G'_N = (G^*, f^2, g^2, E_2)$ with the parameter set $E_2 = \{e_2, e_3\}$ as taken in the Table 10.

TABLE 10. Ns-sets (f^2, E_2) and (g^2, E_2)

f^2	v_1	v_2	v_3	v_4
e_2	$(0, 1, 1)$	$(0.3, 0.5, 0.6)$	$(0.2, 0.4, 0.5)$	$(0.4, 0.5, 0.9)$
e_3	$(0, 1, 1)$	$(0.2, 0.4, 0.5)$	$(0.1, 0.2, 0.6)$	$(0.1, 0.5, 0.7)$

g^2	v_1v_2	v_1v_3	v_1v_4	v_2v_3	v_2v_4	v_3v_4
e_2	$(0, 1, 1)$	$(0, 1, 1)$	$(0, 1, 1)$	$(0.1, 0.6, 0.7)$	$(0.2, 0.6, 0.9)$	$(0.2, 0.7, 0.9)$
e_3	$(0, 1, 1)$	$(0, 1, 1)$	$(0, 1, 1)$	$(0.1, 0.5, 0.8)$	$(0.1, 0.7, 0.8)$	$(0.1, 0.8, 0.9)$

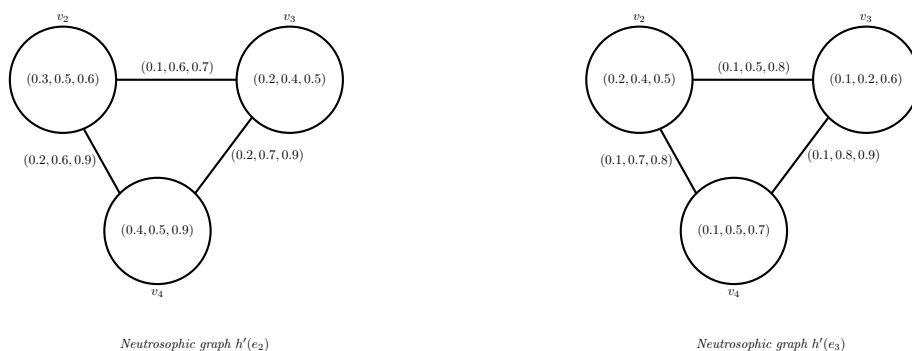


FIGURE 9. Ns-graph $G'_N = (G^*, f^2, g^2, E_2)$

Clearly the parameter set of $G_N \cap G'_N$ is $E = E_1 \cup E_2 = \{e_1, e_2, e_3\}$. If the membership values of vertices and edges of $G_N \cap G'_N$ are calculated, then the ns-graph $G_N \cap G'_N = (G^*, f, g, E)$ is obtained as in the Table 11.

TABLE 11. Ns-sets (f, E) and (g, E)

f	v_1	v_2	v_3	v_4
e_1	$(0.1, 0.2, 0.3)$	$(0.2, 0.4, 0.5)$	$(0, 1, 1)$	$(0.1, 0.5, 0.7)$
e_2	$(0, 1, 1)$	$(0.3, 0.6, 0.7)$	$(0, 1, 1)$	$(0.3, 0.5, 0.9)$
e_3	$(0, 1, 1)$	$(0.2, 0.4, 0.5)$	$(0.1, 0.2, 0.6)$	$(0.1, 0.5, 0.7)$

g	v_1v_2	v_1v_3	v_1v_4	v_2v_3	v_2v_4	v_3v_4
e_1	$(0.1, 0.5, 0.6)$	$(0, 1, 1)$	$(0.1, 0.5, 0.7)$	$(0, 1, 1)$	$(0, 1, 1)$	$(0, 1, 1)$
e_2	$(0, 1, 1)$	$(0, 1, 1)$	$(0, 1, 1)$	$(0, 1, 1)$	$(0.2, 0.7, 0.9)$	$(0, 1, 1)$
e_3	$(0, 1, 1)$	$(0, 1, 1)$	$(0, 1, 1)$	$(0.1, 0.5, 0.8)$	$(0.1, 0.7, 0.8)$	$(0.1, 0.8, 0.9)$

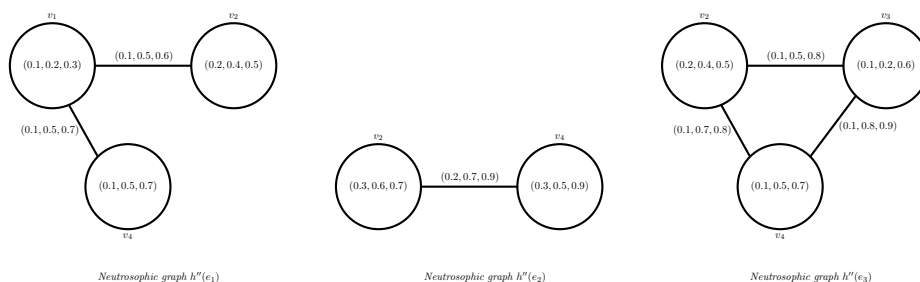


FIGURE 10. Ns-graph $G_N \cap G'_N = (G^*, f, g, E)$

Definition 12. Let $G_N = (G^*, f^1, g^1, E_1)$ and $G'_N = (G^*, f^2, g^2, E_2)$ be two ns-graph over $G^* = (\nu, \varepsilon)$. The restricted intersection of G_N and G'_N is denoted by $G_N \cap G'_N = (G^*, f, g, E)$, where $E = E_1 \cap E_2$. T, I and F membership values of vertices and edges of $G_N \cap G'_N$ are defined by as follow.

i. For all $e \in E$ and $x \in \nu$

$$T_{f_e}(x) = \min\{T_{f^1_e}(x), T_{f^2_e}(x)\}$$

$$I_{f_e}(x) = \max\{I_{f^1_e}(x), I_{f^2_e}(x)\}$$

$$F_{f_e}(x) = \max\{F_{f^1_e}(x), F_{f^2_e}(x)\}$$

ii. For all $e \in E$ and $xy \in \varepsilon$

$$T_{g_e}(xy) = \min\{T_{g^1_e}(xy), T_{g^2_e}(xy)\}$$

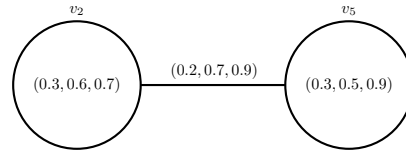
$$I_{g_e}(xy) = \max\{I_{g^1_e}(xy), I_{g^2_e}(xy)\}$$

$$F_{g_e}(xy) = \max\{F_{g_e^1}(xy), F_{g_e^2}(xy)\}$$

Example 7. Let consider ns-graphs $G_N = (G^*, f^1, g^1, E_1)$ and $G'_N = (G^*, f^2, g^2, E_2)$ as taken in Example 6. Clearly $E = E_1 \cap E_2 = \{e_2\}$. Also the restricted intersection of G_N and G'_N is obtained as follow.

TABLE 12. Ns-sets (f, E) and (g, E)

f	v_1	v_2	v_3	v_4		
e_2	$(0, 1, 1)$	$(0.3, 0.6, 0.7)$	$(0, 1, 1)$	$(0.3, 0.5, 0.9)$		
g	(v_1v_2)	(v_1v_3)	(v_1v_4)	(v_2v_3)	(v_2v_4)	(v_3v_4)
e_2	$(0, 1, 1)$	$(0, 1, 1)$	$(0, 1, 1)$	$(0, 1, 1)$	$(0.2, 0.7, 0.9)$	$(0, 1, 1)$



Neutrosophic graph $h''(e_2)$

FIGURE 11. Ns-graph $G_N G'_N = (G^*, f, g, E)$

Definition 13. Let $G_N = (G^*, f, g, E)$ be an neutrosophic soft graph of $G^* = (\nu, \varepsilon)$ and $E = \{e_1, e_2, \dots, e_n\}$ be a set of parameters. The \vee -union of subgraphs of G_N is denoted by $h(e) = h(e_1) \vee h(e_2) \vee \dots \vee h(e_n)$ and for all $xy \in \varepsilon$

$$T_{h(e)}(xy) = \max\{T_{g(e_1)}(xy), T_{g(e_2)}(xy), \dots, T_{g(e_n)}(xy)\}$$

$$I_{h(e)}(xy) = \min\{I_{g(e_1)}(xy), I_{g(e_2)}(xy), \dots, I_{g(e_n)}(xy)\}$$

$$F_{h(e)}(xy) = \min\{F_{g(e_1)}(xy), F_{g(e_2)}(xy), \dots, F_{g(e_n)}(xy)\}$$

Definition 14. Let $G_N = (G^*, f, g, E)$ be an neutrosophic soft graph of $G^* = (\nu, \varepsilon)$ and $E = \{e_1, e_2, \dots, e_n\}$ be a set of parameters. The \wedge -intersection of subgraphs of G_N is denoted by $h(e) = h(e_1) \wedge h(e_2) \wedge \dots \wedge h(e_n)$ and for all $xy \in \varepsilon$

$$T_{h(e)}(xy) = \min\{T_{g(e_1)}(xy), T_{g(e_2)}(xy), \dots, T_{g(e_n)}(xy)\}$$

$$I_{h(e)}(xy) = \max\{I_{g(e_1)}(xy), I_{g(e_2)}(xy), \dots, I_{g(e_n)}(xy)\}$$

$$F_{h(e)}(xy) = \max\{F_{g(e_1)}(xy), F_{g(e_2)}(xy), \dots, F_{g(e_n)}(xy)\}$$

4. AN APPLICATION OF NS-GRAPHS IN A DECISION-MAKING PROBLEM

Ns-graphs are important mathematical tool to cope with uncertainties occurs in real life problems. In this section, we have applied the concept of ns-graph to a decision-making problem and then we have gave an algorithm for optimal object selection by using given data. Suppose that $\nu = \{v_1, v_2, v_3, v_4, v_5\}$ be the set of five mobile phones under consideration. A customer is going to purchase a mobile phone on the basis certain parameters set $E = \{e_1 = \text{performance}, e_2 = \text{material quality}, e_3 = \text{price}\}$. Let (f, E) and (g, E) be two neutrosophic soft sets on ν and $\varepsilon = \{v_1v_2, v_1v_3, v_1v_4, v_1v_5, v_2v_3, v_2v_4, v_2v_5, v_3v_4, v_3v_5, v_4v_5\}$, respectively, as in the table 13. Where (f, E) describes the value of mobile phones according to given parameters, (g, E) describes the value obtained by comparing two mobile phones based upon each parameter.

TABLE 13. Ns-sets (f, E) and (g, E)

f	v_1	v_2	v_3	v_4	v_5
e_1	(0.1,0.5,0.3)	(0.2,0.4,0.5)	(0.5,0.6,0.1)	(0.3,0.2,0.1)	(0.5,0.7,0.1)
e_2	(0.3,0.5,0.1)	(0.3,0.2,0.1)	(0.7,0.5,0.4)	(0.2,0.1,0.8)	(0.4,0.3,0.6)
e_3	(0.2,0.3,0.2)	(0.4,0.3,0.5)	(0.6,0.4,0.3)	(0.3,0.2,0.6)	(0.1,0.4,0.5)

g	v_1v_2	v_1v_3	v_1v_4	v_1v_5	v_2v_3
e_1	(0.1,0.6,0.6)	(0,1,1)	(0,1,1)	(0.1,0.8,0.4)	(0.1,0.8,0.6)
e_2	(0.2,0.5,0.3)	(0,1,1)	(0,1,1)	(0.1,0.6,0.8)	(0.3,0.6,0.5)
e_3	(0.1,0.4,0.6)	(0,1,1)	(0,1,1)	(0.1,0.5,0.6)	(0.3,0.5,0.7)

g	v_2v_4	v_2v_5	v_3v_4	v_3v_5	v_4v_5
e_1	(0.2,0.7,0.7)	(0.1,0.8,0.5)	(0.2,0.7,0.2)	(0.3,0.7,0.5)	(0,1,1)
e_2	(0,1,1)	(0.3,0.4,0.7)	(0.2,0.6,0.8)	(0,1,1)	(0,1,1)
e_3	(0.2,0.4,0.8)	(0.1,0.7,0.8)	(0.1,0.6,0.6)	(0,1,1)	(0.1,0.5,0.7)

The matrice representations of neutrosophic graphs $h(e_1)$, $h(e_2)$ and $h(e_3)$ corresponding to the parameters e_1 , e_2 and e_3 , respectively, are represented by as follows.

$$h(e_1) = \begin{bmatrix} (0,1,1) & (0.1,0.6,0.6) & (0,1,1) & (0,1,1) & (0.1,0.8,0.4) \\ (0.1,0.6,0.6) & (0,1,1) & (0.1,0.8,0.6) & (0.2,0.7,0.7) & (0.1,0.8,0.5) \\ (0,1,1) & (0.1,0.8,0.6) & (0,1,1) & (0.2,0.7,0.2) & (0.3,0.7,0.5) \\ (0,1,1) & (0.2,0.7,0.7) & (0.2,0.7,0.2) & (0,1,1) & (0,1,1) \\ (0.1,0.8,0.4) & (0.1,0.8,0.5) & (0.3,0.7,0.5) & (0,1,1) & (0,1,1) \end{bmatrix}$$

$$h(e_2) = \begin{bmatrix} (0,1,1) & (0.2,0.5,0.3) & (0,1,1) & (0,1,1) & (0.1,0.6,0.8) \\ (0.1,0.6,0.6) & (0,1,1) & (0.3,0.6,0.5) & (0,1,1) & (0.3,0.4,0.7) \\ (0,1,1) & (0.3,0.6,0.5) & (0,1,1) & (0.2,0.6,0.8) & (0,1,1) \\ (0,1,1) & (0,1,1) & (0.2,0.6,0.8) & (0,1,1) & (0,1,1) \\ (0.1,0.6,0.8) & (0.3,0.4,0.7) & (0,1,1) & (0,1,1) & (0,1,1) \end{bmatrix}$$

$$h(e_3) = \begin{bmatrix} (0,1,1) & (0.1,0.4,0.6) & (0,1,1) & (0,1,1) & (0.1,0.5,0.6) \\ (0.1,0.4,0.6) & (0,1,1) & (0.3,0.5,0.7) & (0.2,0.4,0.8) & (0.1,0.7,0.8) \\ (0,1,1) & (0.3,0.5,0.7) & (0,1,1) & (0.1,0.6,0.6) & (0,1,1) \\ (0,1,1) & (0.2,0.4,0.8) & (0.1,0.6,0.6) & (0,1,1) & (0.1,0.5,0.7) \\ (0.1,0.5,0.6) & (0.1,0.7,0.8) & (0,1,1) & (0.1,0.5,0.7) & (0,1,1) \end{bmatrix}$$

If the operations \vee and \wedge are applied, we get resultant neutrosophic graphs $h(e)$ and $h'(e)$. Their incidence matrices are given by as follows.

$$h(e) = \begin{bmatrix} (0,1,1) & (0.2,0.4,0.3) & (0,1,1) & (0,1,1) & (0.1,0.5,0.4) \\ (0.1,0.4,0.6) & (0,1,1) & (0.3,0.5,0.5) & (0.2,0.4,0.7) & (0.3,0.4,0.5) \\ (0,1,1) & (0.3,0.5,0.5) & (0,1,1) & (0.2,0.6,0.2) & (0.3,0.7,0.5) \\ (0,1,1) & (0.2,0.4,0.7) & (0.2,0.6,0.2) & (0,1,1) & (0.1,0.5,0.7) \\ (0.1,0.5,0.4) & (0.3,0.4,0.5) & (0.3,0.7,0.5) & (0.1,0.5,0.7) & (0,1,1) \end{bmatrix}$$

$$h'(e) = \begin{bmatrix} (0,1,1) & (0.1,0.6,0.6) & (0,1,1) & (0,1,1) & (0.1,0.8,0.8) \\ (0.1,0.6,0.6) & (0,1,1) & (0.1,0.8,0.7) & (0,1,1) & (0.1,0.8,0.8) \\ (0,1,1) & (0.1,0.8,0.7) & (0,1,1) & (0.1,0.7,0.8) & (0,1,1) \\ (0,1,1) & (0,1,1) & (0.1,0.7,0.8) & (0,1,1) & (0,1,1) \\ (0.1,0.8,0.8) & (0.1,0.8,0.8) & (0,1,1) & (0,1,1) & (0,1,1) \end{bmatrix}$$

For a given neutrosophic set $A = \{ \langle x, T_A(x), I_A(x), F_A(x) \rangle \}$, the possible membership degree of an element x is calculated by $S(x) = \frac{1}{3} [T_A(x) + 1 - I_A(x) + 1 - F_A(x)]$.

Based on this formula, we construct the tabular representation of score value of incidence matrices and calculate choice value for each mobile phone v_k for $k = 1, 2, 3, 4, 5$ as follows.

If the arithmetic average of v'_k and v''_k are calculated, we find the average score values of $h(e)$ and $h'(e)$ as follow.

It is evident that the maximum score value is 1.150. Then the best choice for customer is mobile phone v_2 .

Algorithm

1. Input the set E which express choice of parameters.
2. Determine the ns-sets (f, E) and (g, E) .

TABLE 14. Score value of incidence matrix $h(e)$

	v_1	v_2	v_3	v_4	v_5	v'_k
v_1	0.0	0.500	0.0	0.0	0.400	0.900
v_2	0.367	0.0	0.434	0.366	0.467	1.634
v_3	0.0	0.434	0.0	0.467	0.366	1.267
v_4	0.0	0.366	0.467	0.0	0.300	1.500
v_5	0.400	0.467	0.366	0.300	0.0	1.533

TABLE 15. Score value of incidence matrix $h'(e)$

	v_1	v_2	v_3	v_4	v_5	v''_k
v_1	0.0	0.300	0.0	0.0	0.167	0.467
v_2	0.300	0.0	0.200	0.0	0.167	0.667
v_3	0.0	0.200	0.0	0.200	0.0	0.400
v_4	0.0	0.0	0.200	0.0	0.0	0.200
v_5	0.167	0.167	0.0	0.0	0.0	0.334

TABLE 16. Avarage score values of $h(e)$ and $h'(e)$

	v'_k	v''_k	v_k
v_1	0.900	0.467	0.683
v_2	1.634	0.667	1.150
v_3	1.267	0.400	0.833
v_4	1.500	0.200	0.850
v_5	1.533	0.334	0.933

3. Construct the ns-graph $G_N = (G^*, f, g, E)$.
4. Compute the resultant neutrosophic graphs $h(e)$ and $h'(e)$ with $h(e) = \bigvee_{k \in \Lambda} h(e_k)$ and $h'(e) = \bigwedge_{k \in \Lambda} h(e_k)$, respectively, for all $k \in \Lambda$.
5. Construct incidence matrix forms of $h(e)$ and $h'(e)$.
6. Calculate the score S_k of v_k for all $k \in \Lambda$.
7. Determine decision as v_k if $v'_k = \max v_k$.

5. COMPARATIVE STUDY AND DISCUSSION

In this section, for determining of optimal object, a comparative study based on the results of numerical computation is discussed. For this, based on the application discussed above, we present a comparative analysis between the our proposed method and the existing method in [4]. The method given in [4] just takes into

consideration “AND” or “OR” operations to obtain resultant ns-graph which is used determine of optimal object. However if these two operations are applied separately, different results occur in the selection of the optimal object. So this leads to uncertainty in determining the most appropriate choice. Our proposed approach just takes into consideration both of \wedge -intersection and \vee -union operations to obtain resultant ns-graphs, because we observe that these two operations should be interdependent in determining the possible choice. When the existing method given in [4] is compared with the current proposed method, ranking orders both of them are appeared as in Table 17.

TABLE 17. Comparison

Model	Ranking order
Existing method given in [4]	$v_1 > v_3 > v_2 > v_4 > v_5$ $v_5 > v_3 > v_2 > v_4 > v_1$
Proposed method	$v_2 > v_5 > v_4 > v_3 > v_1$

In existing method, the obtained ranking results are quite close where the first and fifth ranking order are changed but the second, third and fourth ranks are consistent. Nevertheless, obtaining two different rankings causes problems in decision-making process. In proposed method, the obtained ranking result is unique and more effective in determining the appropriate choice. Clearly, the proposed method consider the problem in all aspects and reveals a final result although existing method provides a set of alternatives as a final selection to consider the problem.

6. CONCLUSIONS

When compared with soft graph and fuzzy soft graph models, ns-graphs are more useful mathematical tools. Ns-graphs can be used in many areas with uncertainty. We have introduced the concept of ns-graphs of a simple graph with some new notions such as union and intersection, and gave illustrative examples related to these notions. Also we have applied the concept of ns-graph to a decision-making problem, and then a case study has been given to show the application of the technique. Hence a comparative analysis is conducted to show the applicability and validity of the proposed approach. The proposed method can be used in dealing with decision making process involving uncertainty especially in solving the real scientific and engineering problems. For future research, another algorithm can be developed by incorporate the complement of ns-graphs. Therefore we will work for the extension of the this method in different neutrosophic structures and decision-making applications. We plan to extend this research work to (i) Vague ns-graphs, (ii) Intuitionistic ns-graphs, and (iii) Bipolar ns-graphs.

Declaration of Competing Interests The author declares that he has no competing interest.

REFERENCES

- [1] Akram, M., Dudek, W.A., Interval-valued fuzzy graphs, *Computers and Mathematics with Applications*, 61(2) (2011), 289–299. <https://doi.org/10.1016/j.camwa.2010.11.004>
- [2] Akram, M., Nawaz, S., Operations on soft graphs, *Fuzzy Information and Engineering*, 7(4) (2015), 423–449. <https://doi.org/10.1016/j.fiae.2015.11.003>
- [3] Akram, M., Nawaz, S., Fuzzy soft graphs with applications, *Journal of Intelligent and Fuzzy Systems*, 30(6) (2016), 3619–3632. <https://doi.org/10.3233/IFS-162107>
- [4] Akram, M., Sundas, S., Neutrosophic soft graphs with application, *Journal of Intelligent and Fuzzy Systems*, 32(1) (2017), 841–858. <https://doi.org/10.3233/JIFS-16090>
- [5] Atanassov, K. T., Gargov, G., Intuitionistic Fuzzy Sets: Theory and Applications, Springer Physica-Verlag, Berlin, 1999.
- [6] Bhattacharya, P., Some remarks on fuzzy graphs, *Pattern Recognition Letters.*, 6(5) (1987), 297–302. [https://doi.org/10.1016/0167-8655\(87\)90012-2](https://doi.org/10.1016/0167-8655(87)90012-2)
- [7] Broumi, S., Generalized neutrosophic soft set, *International Journal of Computer Science, Engineering and Information Technology*, 3(2) (2013), 17–30. <https://doi.org/10.5121/ijcseit.2013.3202>
- [8] Broumi, S., Sundareswaran, R., Shanmugapriya, M., Nordo, G., Talea, M., Bakali, A., Smarandache, F., Interval-valued fermatean neutrosophic graphs, *Decision Making: Applications in Management and Engineering*, 5(2) (2022), 176–200. <https://doi.org/10.31181/dmame0311072022b>
- [9] Broumi, S., Ajay, D., Chellamani, P., Malayalan, L., Talea, M., Bakali, A., Schweizer, P., Jafari, S., Interval valued pentapartitioned neutrosophic graphs with an application to MCDM, *Operational Research in Engineering Sciences: Theory and Applications*, 5(3) (2022) 68–91.
- [10] Çelik, Y., On bipolar fuzzy soft graphs, *Creative Mathematics and Informatics*, 27(2) (2018), 123–132. <https://doi.org/10.37193/CMI.2018.02.04>
- [11] Deli, I., Interval-valued neutrosophic soft sets and its decision making, *International Journal of Machine Learning and Cybernetics*, 8 (2015), 1–12. <https://doi.org/10.1007/s13042-015-0461-3>
- [12] Euler, L., Solutio problematis ad geometriam situs pertinentis, *Commentarii Academiae Scientiarum Imperialis Petropolitanae*, 8 (1736), 128–140.
- [13] Kandasamy, W. B., Ilanthenral, K., Smarandache, F., Neutrosophic Graphs: A New Dimension to Graph Theory, EuropaNova, USA, 2015.
- [14] Maji, P. K., Neutrosophic soft set, *Annals of Fuzzy Mathematics and Informatics*, 5(1) (2013), 157–168.

- [15] Mohinta, S, Samanta, T., An introduction to fuzzy soft graphs, *Mathematica Moravica*, 19(2) (2015), 35–48.
- [16] Mordeson J. N., Peng, C. S., Operations on fuzzy graphs, *Information Sciences*, 79(3-4) (1994), 159–170. [https://doi.org/10.1016/0020-0255\(94\)90116-3](https://doi.org/10.1016/0020-0255(94)90116-3)
- [17] Rosenfeld, A., Fuzzy graphs, *Fuzzy Sets and Their Applications to Cognitive and Decision Processes*, Academic Press, New York, 1975.
- [18] Shah, N., Hussain, A., Neutrosophic soft graphs, *Neutrosophic Sets and Systems*, 11 (2016), 31–44.
- [19] Smarandache, F., Neutrosophic set-a generalization of the intuitionistic fuzzy set, *International Journal of Pure and Applied Mathematics*, 24(3) (2005), 287–297.
- [20] Thumbakara, R. K., George, B. Soft graphs, *General Mathematics Notes*, 21(2) (2014), 75–86.
- [21] Zadeh, L. A., Fuzzy sets, *Information and Control*, 8(3) (1965), 338–353. [https://doi.org/10.1016/S0019-9958\(65\)90241-X](https://doi.org/10.1016/S0019-9958(65)90241-X)
- [22] Zihni, O., Çelik, Y., Kara, G., Interval-valued fuzzy soft graphs, *Topological Algebra and its Applications*, 5(1) (2017), 17–29. <https://doi.org/10.1515/taa-2017-0004>



NUMERICAL ANALYSIS OF A TIME RELAXATION FINITE DIFFERENCE METHOD FOR THE HEAT EQUATION

Özgül İLHAN¹, Osman R. ISIK² and Simge BOZKURT³

¹Department of Mathematics, Faculty of Science, Muğla Sıtkı Koçman University, 48050 Muğla, TÜRKİYE

²Elementary Mathematics Education Program, Faculty of Education, Muğla Sıtkı Koçman University, 48050 Muğla, TÜRKİYE

³Marmaris Sınav Special Education Course, Marmaris, 48050 Muğla, TÜRKİYE

ABSTRACT. In this study, we first consider the time-relaxation model, which consists of adding the term $\kappa(u - \bar{u})$ to the heat equation. Then, an explicit discretization scheme for the model is introduced to find the finite difference solutions. We first obtain the solutions by using the scheme and then investigate the method's consistency, stability, and convergence properties. We prove that the method is consistent and unconditionally stable for any given value of r and appropriate values of κ and δ . As a result, the method obtained by adding the time relaxation term to the first-order finite-difference explicit method behaves like the second-order implicit method. Finally, we apply the method to some test examples.

1. INTRODUCTION

The heat equation has a fundamental importance in various scientific fields. Heat is a form of energy that exists in any material. For example, the temperature in an object changes with time and the position within the object. Furthermore, this equation can be applied to solve the heat flow related to science and engineering. The numerical and analytical methods can be used to solve the heat equation problem in science or engineering fields. The finite difference method is one of several techniques for numerical solutions to boundary value problems. Morton and Mayers [16], and Cooper [5] provide a modern introduction to partial differential equations theory by considering the development of finite difference methods and

2020 *Mathematics Subject Classification.* 35K05, 65B10, 65M06, 65M12.

Keywords. Heat equation, time-relaxation model, differential filter, finite difference method.

¹ ✉ oilhan@mu.edu.tr-Corresponding author; 0000-0003-2199-1301

² ✉ osmanrasit@mu.edu.tr; 0000-0003-1401-4553

³ ✉ simgebzkr9095@gmail.com; 0000-0002-6963-7136.

numerical methods in more detail. Fletcher [7] described the method to implement finite differences to solve boundary value problems.

The time relaxation (based on spatial averaging) regularizations considered by Rosenau [19], Schochet and Tadmor [20], Stolz et. al. [22] are often referred to as "secondary regularization" or "time relaxation" to regularize the flow. Stolz and Adams [1] studied the approximate deconvolution model (ADM) for the large-eddy simulation of incompressible flows and applied it to turbulent channel flow. Layton and Neda [13] developed a time relaxation regularization of flow problems suggested by Stolz and Adams. Ervin et al. [6] studied the numerical errors in finite elements discretization of a time relaxation model of fluid motion. They showed that the point of the relaxation term is to approach the unresolved fluctuations in a computational simulation to zero exponentially fast by an appropriate and depending on the problem choice of its coefficient; thus, they concluded that this relaxation term is intermediate between a tunable numerical stabilization and a continuum modeling term. Neda [17] investigated a high-order family of time relaxation models based on approximate deconvolution. This problem was also considered in [14] to regularize the flow. They studied the analogous approach based on time scales, time filtering, and damping of under-resolved temporal features and investigated theoretical and practical aspects of temporally damped fluid-flow simulations. Isik et al. [12] analysed the NSE time relaxation model which is obtained adding term " $\kappa(u - \bar{u})$ " where \bar{u} denotes the time filter of u introduced by Pruet et al [18]. An advantage of adding the term time-relaxation is that it provides a faster approach to steady-state solutions [12], [10] [11]. In some problems obtained by adding this term, the solutions can be achieved in some cases where the numerical solutions can not be obtained [12]. Cibik et al. [4] introduced the backward Euler method obtained by adding the time relaxation term to MHD flow. They proved that the method improves the accuracy of the solution without a significant change in the complexity of the system.

We know that leapfrog discretization time filter methods are applied to geophysical fluid dynamics. While these methods decrease spurious oscillations to improve estimations, they reduce numerical accuracy and excessively dampen the physical model [2]. Williams proposed a successfully tuned model which reduces undesired numerical damping of [2] with higher-order accuracy [23]. This model is also studied by others see; [15], [24]. Otherwise, it is often preferable to use the backward Euler method for a steady-state problem in practice. This method is stable, but the solutions are inefficient and time accurate transient [8]. Guzel and Layton stabilized the backward Euler discretization using time filter for the classical numerical ODE theory by improving solutions [9].

In this paper, we investigate the finite difference solution of the model, which is obtained by adding the time relaxation term " $\kappa\delta\bar{u}_t$ " to the heat equation,

$$u_t + \kappa\delta\bar{u}_t = u_{xx} \tag{1}$$

where, \bar{u} is the differential filter defined as [18],

$$\bar{u}_t = \frac{u - \bar{u}}{\delta}, \quad u(0) = \bar{u}(0).$$

Here, κ and δ are positive real constants. It is well known that the finite difference solution of Eqn (1) obtained by the explicit method is stable for $r \leq \frac{1}{2}$ whereas the implicit method is unconditionally stable for $\kappa = 0$. Also, the explicit method is consistent and the convergence order for this method is $O(k + h^2)$ for $\kappa = 0$. To obtain the finite difference solutions of eqn. (1) we will develop an algorithm by using the explicit method. We analyze the consistency and stability of the finite difference solution obtained by this algorithm. Thus, the proposed method is consistent on an unbounded domain subset of $\kappa\delta$ -plane. For any given value of r , the method will be stable for some particular values of κ and δ . Although this algorithm seems structurally explicit, the behavior of stability results is similar to the implicit method. We applied the method to some numerical examples. We found that the numerical results are consistent with the theoretical results. For each example, we show that the convergence order for the method is 1 and 2, and the method is stable for any given r . All computations are done using MATLAB R2020b.

The paper is organized as follows. An algorithm that depends on the finite difference method is introduced for Eqn (1) in Section 2. Then consistency and stability of the finite difference method obtained by the algorithm are investigated, and some properties are given in the same section. Some numerical examples are given to verify the theoretical results in Section 3. It is seen that the numerical results obtained by numerical examples are consistent with the theoretical results in this section. While the solutions blow-up for $\kappa = 0$ and $r = 5$, convergence results are obtained for appropriate values of κ and δ . Finally, the conclusions of this study are given in Section 4.

2. FINITE DIFFERENCE APPROXIMATION

The finite difference method is a numerical method in which the solution of a differential problem given on an interval at a point is approached with finite differences. The methods generally generate the solutions that are either as accurate as the data warrant or as accurate as is necessary for the technical purpose for which the solutions are required. One of the finite difference approximations to the "Heat equation",

$$\frac{\partial U}{\partial t} = \frac{\partial^2 U}{\partial x^2}, \tag{2}$$

is

$$u_{i,j+1} = ru_{i-1,j} + (1 - 2r)u_{i,j} + ru_{i+1,j}, \quad r = \frac{k}{h^2}. \tag{3}$$

where U is the exact solution of the heat equation and $u_{i,j+1}$ is the unknown temperature at the $(i, j + 1)$ th mesh point in terms of known "temperatures" along

the j th time-row. This method is referred as explicit method. The consistency and stability results for explicit method can be found in any book involves finite difference methods, i.e., [21].

Theorem 1. (*Lax's Equivalence Theorem*) *Given a properly posed linear initial-value problem and a linear finite-difference approximation to it that satisfies the consistency condition, then stability is the necessary and sufficient condition for convergence [21].*

We consider an explicit discretization of model (1):

Algorithm 1.

$$\frac{u_{i,j+1} - u_{i,j}}{k} + \kappa\delta \left(\frac{\bar{u}_{i,j+1} - \bar{u}_{i,j}}{k} \right) = \left(\frac{u_{i+1,j} - 2u_{i,j} + u_{i-1,j}}{h^2} \right) \quad (4)$$

$$\frac{\bar{u}_{i,j+1} - \bar{u}_{i,j}}{k} = \frac{u_{i,j+1} - \bar{u}_{i,j+1}}{\delta} \quad (5)$$

where $\kappa \geq 0$, $\delta > 0$ and $u_{i,j} := u(x_i, t_j)$ is the known value of temperature at the (i, j) th mesh point. Note that $u_{i,j+1}$ and $\bar{u}_{i,j+1}$ can be written as

$$u_{i,j+1} = \left(1 + \frac{\delta}{k} \right) \bar{u}_{i,j+1} - \frac{\delta}{k} \bar{u}_{i,j}. \quad (6)$$

and

$$\bar{u}_{i,j+1} = \left(1 + \frac{\delta}{k} \right)^{-1} u_{i,j+1} + \frac{\delta}{k} \left(1 + \frac{\delta}{k} \right)^{-1} \bar{u}_{i,j}, \quad (7)$$

respectively. Thus, by substituting Eqn (7) into Eqn (4), we obtain the following explicit scheme

$$u_{i,j+1} = \frac{1}{\left(1 + \frac{k\kappa\delta}{k+\delta} \right)} \left(ru_{i+1,j} + (1-2r)u_{i,j} + ru_{i-1,j} + \frac{k\kappa\delta}{k+\delta} \bar{u}_{i,j} \right) \quad (8)$$

$$\bar{u}_{i,j+1} = \left(1 + \frac{\delta}{k} \right)^{-1} u_{i,j+1} + \frac{\delta}{k} \left(1 + \frac{\delta}{k} \right)^{-1} \bar{u}_{i,j}$$

Now, we will show the von-Neumann stability of Eqn (8).

Lemma 1. *Let $u_{i,j}$ be the finite difference solution of model (1) obtained by Eqn (8). Then, the method is unconditionally stable on an unbounded region in the $\kappa\delta$ -plane.*

Proof. Substituting Eqn (6) into Eqn (8) yields

$$\begin{aligned} \left(1 + \frac{\delta}{k} \right) \bar{u}_{i,j+1} - \frac{\delta}{k} \bar{u}_{i,j} + \kappa\delta \bar{u}_{i,j+1} &= r \left(1 + \frac{\delta}{k} \right) \bar{u}_{i+1,j} - r \frac{\delta}{k} \bar{u}_{i+1,j-1} \\ &\quad + (1-2r) \left(1 + \frac{\delta}{k} \right) \bar{u}_{i,j} \end{aligned}$$

$$\begin{aligned}
 & - (1 - 2r) \frac{\delta}{k} \bar{u}_{i,j-1} + r \left(1 + \frac{\delta}{k} \right) \bar{u}_{i-1,j} \\
 & - r \frac{\delta}{k} \bar{u}_{i-1,j-1} + \kappa \delta \bar{u}_{i,j}
 \end{aligned}$$

or

$$\begin{aligned}
 \left(1 + \frac{\delta}{k} + \kappa \delta \right) \bar{u}_{i,j+1} &= r \left(1 + \frac{\delta}{k} \right) \bar{u}_{i+1,j} + \left((1 - 2r) \left(1 + \frac{\delta}{k} \right) + \frac{\delta}{k} + \kappa \delta \right) \bar{u}_{i,j} \\
 &+ r \left(1 + \frac{\delta}{k} \right) \bar{u}_{i-1,j} - r \frac{\delta}{k} \bar{u}_{i+1,j-1} - (1 - 2r) \frac{\delta}{k} \bar{u}_{i,j-1} \\
 &- r \frac{\delta}{k} \bar{u}_{i-1,j-1}.
 \end{aligned}$$

Then, putting $\bar{u}_{i,j} = e^{i\beta p h} \xi^q$ into the finite difference scheme yields

$$\begin{aligned}
 \left(1 + \frac{\delta}{k} + \kappa \delta \right) e^{i\beta p h} \xi^{q+1} &= r \left(1 + \frac{\delta}{k} \right) e^{i\beta(p+1)h} \xi^q \\
 &+ \left((1 - 2r) \left(1 + \frac{\delta}{k} \right) + \frac{\delta}{k} + \kappa \delta \right) e^{i\beta p h} \xi^q \\
 &+ r \left(1 + \frac{\delta}{k} \right) e^{i\beta(p-1)h} \xi^q - r \frac{\delta}{k} e^{i\beta(p+1)h} \xi^{q-1} \\
 &- (1 - 2r) \frac{\delta}{k} e^{i\beta p h} \xi^{q-1} - r \frac{\delta}{k} e^{i\beta(p-1)h} \xi^{q-1}.
 \end{aligned}$$

If we simplify " $e^{i\beta p h} \xi^q$ " term from both sides, we get

$$\begin{aligned}
 \left(1 + \frac{\delta}{k} + \kappa \delta \right) \xi &= 2r \left(1 + \frac{\delta}{k} \right) \cos \theta + \left((1 - 2r) \left(1 + \frac{\delta}{k} \right) + \frac{\delta}{k} + \kappa \delta \right) \\
 &- 2r \frac{\delta}{k} \xi^{-1} \cos \theta - (1 - 2r) \frac{\delta}{k} \xi^{-1}
 \end{aligned}$$

Multiplying both sides with " ξ " gives

$$\begin{aligned}
 \left(1 + \frac{\delta}{k} + \kappa \delta \right) \xi^2 - \left[2r \left(1 + \frac{\delta}{k} \right) \cos \theta - \left((1 - 2r) \left(1 + \frac{\delta}{k} \right) + \frac{\delta}{k} + \kappa \delta \right) \right] \xi \\
 + 2r \frac{\delta}{k} \cos \theta + (1 - 2r) \frac{\delta}{k} = 0. \tag{9}
 \end{aligned}$$

Then, we can find two solutions of Eqn (9):

$$\xi_1 = \frac{1}{2k + 2\delta + 2k\kappa\delta} \left(k + 2\delta - 2r\delta - \sqrt{\begin{matrix} 6r^2\delta^2 - 4k^2r + 6k^2r^2 + k^2 \\ -8k^2r^2 \cos \theta - 4kr\delta - 8r^2\delta^2 \cos \theta \\ +2k^2r^2 \cos 2\theta + 12kr^2\delta + 4k^2r \cos \theta \\ +2r^2\delta^2 \cos 2\theta + k^2\kappa^2\delta^2 + 2k^2\kappa\delta \\ +4kr^2\delta \cos 2\theta + 4kr\delta \cos \theta \\ +4kr\kappa\delta^2 - 4k^2r\kappa\delta - 16kr^2\delta \cos \theta \\ -4kr\kappa\delta^2 \cos \theta + 4k^2r\kappa\delta \cos \theta \end{matrix}} \right)$$

$$\xi_2 = \frac{1}{2k + 2\delta + 2k\kappa\delta} \left(k + 2\delta - 2r\delta + \sqrt{\begin{matrix} 6r^2\delta^2 - 4k^2r + 6k^2r^2 + k^2 \\ -8k^2r^2 \cos \theta - 4kr\delta - 8r^2\delta^2 \cos \theta \\ +2k^2r^2 \cos 2\theta + 12kr^2\delta + 4k^2r \cos \theta \\ +2r^2\delta^2 \cos 2\theta + k^2\kappa^2\delta^2 \\ +2k^2\kappa\delta + 4kr^2\delta \cos 2\theta \\ +4kr\delta \cos \theta + 4kr\kappa\delta^2 - 4k^2r\kappa\delta \\ -16kr^2\delta \cos \theta - 4kr\kappa\delta^2 \cos \theta \\ +4k^2r\kappa\delta \cos \theta \end{matrix}} \right)$$

Let us find the stability condition $|\xi| \leq 1$ for ξ_1 .

$$\begin{aligned} &6r^2\delta^2 - 4k^2r + 6k^2r^2 + k^2 - 8k^2r^2 \cos \theta - 4kr\delta - 8r^2\delta^2 \cos \theta + 2k^2r^2 \cos 2\theta + 12kr^2\delta \\ &+ 4k^2r \cos \theta + 2r^2\delta^2 \cos 2\theta + k^2\kappa^2\delta^2 + 2k^2\kappa\delta + 4kr^2\delta \cos 2\theta + 4kr\delta \cos \theta \\ &+ 4kr\kappa\delta^2 - 4k^2r\kappa\delta - 16kr^2\delta \cos \theta - 4kr\kappa\delta^2 \cos \theta + 4k^2r\kappa\delta \cos \theta \\ &\leq \left(k + k\kappa\delta + 4kr \sin^2 \frac{\theta}{2} + 4r\delta \sin^2 \frac{\theta}{2} \right)^2 \end{aligned}$$

If we simplify the above equation, we get

$$8kr (\cos \theta - 1) (k + \delta + k\kappa\delta) \leq 0$$

which is valid for all $\kappa \geq 0, \delta > 0$.

On the other hands, for the second root, we can use the same process:

$$\begin{aligned} &6r^2\delta^2 - 4k^2r + 6k^2r^2 + k^2 - 8k^2r^2 \cos \theta - 4kr\delta - 8r^2\delta^2 \cos \theta + 2k^2r^2 \cos 2\theta + 12kr^2\delta \\ &+ 4k^2r \cos \theta + 2r^2\delta^2 \cos 2\theta + k^2\kappa^2\delta^2 + 2k^2\kappa\delta + 4kr^2\delta \cos 2\theta + 4kr\delta \cos \theta + 4kr\kappa\delta^2 \\ &- 4k^2r\kappa\delta - 16kr^2\delta \cos \theta - 4kr\kappa\delta^2 \cos \theta + 4k^2r\kappa\delta \cos \theta \\ &\geq (-3k - 4\delta - 3k\kappa\delta + 4kr \sin^2 \frac{1}{2}\theta + 4r\delta \sin^2 \frac{1}{2}\theta)^2 \end{aligned}$$

or

$$8(k + \delta + k\kappa\delta) (k + 2\delta - 2r\delta - kr + kr \cos \theta + k\kappa\delta + 2r\delta \cos \theta) \geq 0.$$

Let us find κ and δ as

$$k + 2\delta - 2r\delta - kr + kr \cos \theta + k\kappa\delta + 2r\delta \cos \theta \geq 0.$$

Since

$$2r\delta + kr - kr \cos \theta - 2r\delta \cos \theta \leq 4r\delta + 2kr$$

and

$$k + 2\delta - 2r\delta - kr + kr \cos \theta + k\kappa\delta + 2r\delta \cos \theta \geq k + 2\delta + k\kappa\delta - 4r\delta - 2kr,$$

the term is $k + 2\delta + k\kappa\delta - 4r\delta - 2kr \geq 0$ for $k\kappa\delta - 4r\delta - 2kr \geq 0$. Hence, selecting

$$\kappa \geq \frac{4r}{k} + \frac{2r}{\delta} = \frac{4}{h^2} + \frac{2r}{\delta} \tag{10}$$

yields the stability of the scheme. It can be said that the increased δ will give stability for $k\kappa - 4r > 0$. \square

2.1. Consistency. In this subsection, we deal with the consistency of the method for various κ and δ . We will prove that the convergence order of the method is $O(\delta^{\frac{k}{2}} + \frac{k}{2} + \kappa\delta^{\frac{k}{2}} - 1)$. Specifically, we proved that for a constant δ and under the condition $\kappa\delta \leq \frac{2}{k}$, the method is consistent and the convergence order is 1.

Proposition 1. *Let k, h, κ and δ be fixed positive real numbers. If $u = u(x, t)$ is smooth enough, then the method is consistent and the convergence order of the method is $O(\delta^{\frac{k}{2}} + \frac{k}{2} + \kappa\delta^{\frac{k}{2}} - 1)$.*

Proof. Firstly, when $u(x, t)$ is expanded to Taylor polynomials at $(x, t) = (x_i, t_j)$ point and then these polynomials are substituted into Eqn (4), we can get following,

$$\begin{aligned} & \frac{u_{i,j} + ku_t(x_i, t_j) + \frac{k^2}{2}u_{tt} - u_{i,j}}{k} + \kappa\delta \left(\frac{\bar{u}_{i,j} + k\bar{u}_t + \frac{k^2}{2}\bar{u}_{tt} - \bar{u}_{i,j}}{k} \right) \\ &= \frac{u_{i,j} + hu_x + \frac{h^2}{2}u_{xx} + \frac{h^3}{6}u_{xxx} + \frac{h^4}{24}u_{xxxx}}{h^2} \\ &+ \frac{-2u_{i,j} + u_{i,j} - hu_x + \frac{h^2}{2}u_{xx} - \frac{h^3}{6}u_{xxx} + \frac{h^4}{24}u_{xxxx}}{h^2}. \end{aligned}$$

If necessary simplifications are done, we get

$$T(x_i, t_j) := u_t + \frac{k}{2}u_{tt} + \kappa\delta\bar{u}_t + \kappa\delta\frac{k}{2}\bar{u}_{tt} - u_{xx} - \frac{h^2}{12}u_{xxxx} + O(h^4)$$

or

$$T(x_i, t_j) = \frac{k}{2}\delta\bar{u}_{ttt} + \left(\frac{k}{2} + \kappa\delta\frac{k}{2} - 1 \right) \bar{u}_{tt} - \frac{h^2}{12}\delta\bar{u}_{ttt} + O(k^2 + h^4).$$

Hence, $T(x_i, t_j) \rightarrow 0$ is satisfied for $h, k \rightarrow 0$, so, the method is consistent with the convergence order $O(\delta^{\frac{k}{2}} + \frac{k}{2} + \kappa\delta^{\frac{k}{2}} - 1)$ in time. As a special case, we will prove

the consistency for a constant δ and under the condition $\kappa\delta \leq \frac{2}{k}$. To show the consistency, let us show the following inequality,

$$\frac{k}{2} + \kappa\delta\frac{k}{2} - 1 \leq k \quad (11)$$

Simplifying Eqn (11), we can get the following inequality

$$\left(\frac{k\delta}{2} - 1 + \frac{1}{2}\right)k \leq 1$$

or

$$k \leq \frac{1}{\frac{k\delta}{2} - \frac{1}{2}}. \quad (12)$$

Finally, we can obtain the following inequality

$$\kappa\delta \leq \frac{2}{k} \quad (13)$$

which satisfies Eqn (11). It can be easily seen that $\lim_{(h,k) \rightarrow (0,0)} T(x_j, t_j) = 0$ is satisfied for a constant δ and under the condition $\kappa\delta \leq \frac{2}{k}$. Therefore, for a constant δ and under the condition $\kappa\delta \leq \frac{2}{k}$, the method is consistent and the convergence order for the method is 1. \square

Note that it can come to the question to mind: Is it possible to get the convergence order from 1 to 2 in time? A way of doing this can order 2 be found in time for

$$\frac{k}{2} + \kappa\delta\frac{k}{2} - 1 \leq k^2. \quad (14)$$

If necessary operations are performed here, we obtain

$$\kappa \leq \frac{2k^2 - k + 2}{k\delta} = \frac{2k}{\delta} + \frac{2-k}{k\delta}.$$

By applying the stability condition (10) and (14), we get following inequality:

$$\frac{4r}{k} + \frac{2r}{k} \leq \kappa \leq \frac{2k}{\delta} + \frac{2-k}{k^2} \implies \frac{6r}{k} \leq \kappa \leq 2 + \frac{2-k}{k^2}. \quad (15)$$

It means that the method is order of 2 for values of κ in this interval. In addition, for any value of r and values of κ and δ satisfying the (15) condition under the stability condition, the method is stable and the convergence order is 2.

Corollary 1. *If the stability condition and the (15) condition are satisfied for a given r value, a method that is convergent to the second order is obtained.*

As an example, for $r = 5$, we obtain the following inequality

$$\frac{30}{k} \leq \kappa \leq 2 + \frac{2-k}{k^2}. \quad (16)$$

Then, there is a solution in κ if

$$\frac{30}{k} \leq 2 + \frac{2-k}{k^2} \text{ or } \implies 2k^2 - 31k + 2 \geq 0$$

which is valid for $k \in (0, 6.4787 \times 10^{-2}] \cup [15, \infty)$. Therefore, the method is consistent and is of order 2 for $k \leq 0.065$, $r = 5$, $\delta = k$ and κ satisfy (16).

3. NUMERICAL EXAMPLES

In this section, we give some numerical examples to illustrate the method. We use MATLAB R2020b program for all computation. For the term $\bar{u}_{i,j+1}$, the following relation can be used for each time step, so there is only one unknown term in time.

$$\bar{u}_{i,j+1} = \left(1 + \frac{\delta}{k}\right)^{-1} u_{i,j+1} + \frac{\delta}{k} \left(1 + \frac{\delta}{k}\right)^{-1} \bar{u}_{i,j}.$$

Example 1. Let us consider the heat equation, (3)

$$\frac{\partial U}{\partial t} = \frac{\partial^2 U}{\partial x^2}, \quad 0 \leq x \leq 1, \quad 0 \leq t \leq T,$$

where

$$U(0, t) = U(1, t) = 0, \quad U(x, 0) = \sin(\pi x).$$

The exact solution is

$$u(x, t) = e^{-\pi^2 t} \sin(\pi x).$$

The results are given in Tables 1, 2, 3 and 4 and Figure 1.

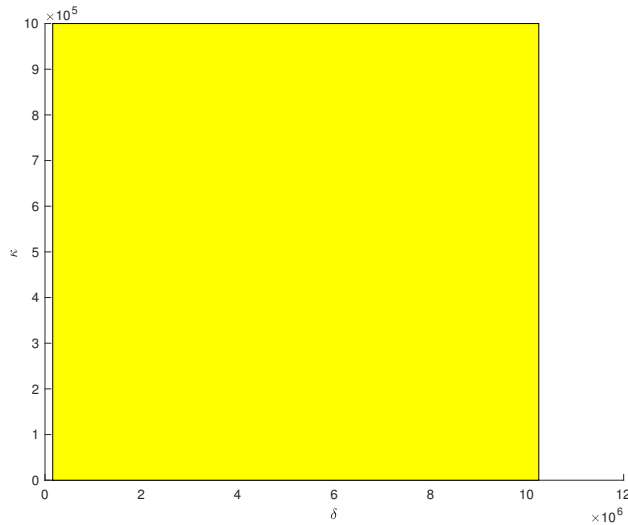


FIGURE 1. Stability region $\kappa\delta$ -plane

TABLE 1. Numerical results of Example 1, for $160010 \leq \kappa \leq 10240010$ in the domain satisfying the stability condition, $\delta = 0.0001$ and $r = 5$

t	k	$ e_{i,j} $	$order$
0.005	0.00125	<i>blowup</i>	–
0.005	0.00125	0.0506	–
0.0025	$3.1250e - 05$	0.0250	1.0172
0.00125	$7.8125e - 06$	0.0124	1.0116
0.000625	$1.9531e - 06$	0.0062	1

TABLE 2. Numerical results of Example 1, for $62521 \leq \kappa \leq 4000000$ in the domain satisfying the stability condition, $0.0001 \leq \delta$ and $r = 10.4167$

t	k	$ e_{i,j} $	$order$
0.01	$6.6667e - 04$	<i>blowup</i>	–
0.01	$6.6667e - 04$	0.1039	–
0.005	$1.6667e - 04$	0.0506	1.0380
0.0025	$4.1667e - 05$	0.0250	1.017
0.00125	$1.0417e - 05$	0.0124	1.0116

TABLE 3. Numerical results of Example 1, for $1590250 \leq \kappa \leq 12790000$ in the domain satisfying the stability condition, $\delta = 0.0001$

t	k	r	$ e_{i,j} $	$order$
0.025	0.0125	11.25	<i>blowup</i>	–
0.025	0.0125	11.25	1.8529	–
0.0125	0.0063	22.5	0.4722	1.9723
0.00625	0.0031	45	0.1218	1.9549
0.003125	0.0016	90	0.0322	1.9194

TABLE 4. Numerical results of Example 1, for $5850 \leq \kappa \leq 3881.2$ in the domain satisfying the stability condition, $\delta = 0.01$

t	k	r	$ e_{i,j} $	order
0.025	0.0125	11.25	blowup	–
0.025	0.0125	11.25	0.2881	–
0.0125	0.0063	5.6250	0.1366	1.0776
0.0063	0.0031	2.8125	0.0675	1.0170
0.0031	0.0016	1.4062	0.0471	0.5192

It can be seen from Table 1 that, for

$$\kappa = 0, \quad k = 0.00125, \quad r = \frac{k}{h^2} = 5, \quad T = 0.005,$$

the solution blows-up. However, for

$$r = \frac{k}{h^2} = 5, \quad 160010 \leq \kappa \leq 10240010, \quad 0.0001 \leq \delta, \quad T = 0.005,$$

the solutions do not blow-up. Moreover, we have obtained convergent solutions of order 1. Similarly, Table 2 shows that for

$$\kappa = 0, \quad k = 6.6667e - 04, \quad T = 0.01$$

the solution blows-up. But, the solutions do not blow-up for

$$160010 \leq \kappa \leq 10240010, \quad 0.0001 \leq \delta, \quad r = \frac{k}{h^2} = 10.4167, \quad T = 0.01.$$

Otherwise, the solutions are convergent with the order of 1. Figure 1 shows the $\kappa\delta$ -stability domain which is unbounded subset of R^2 . The solutions are stable in this domain. In other words, for $r = 6$ and any chosen $\kappa\delta$ -pairs which are in this region, the solutions do not blow-up.

It is seen in Table 3 that the solutions are convergent with the order of 2 in time for the $\delta = 0.0001$ and selected κ values. Although r increases, the solutions are convergent with the order of 2.

It is shown in Table 4 that for different κ values the solutions are convergent with the order of 1 in time. These κ values are satisfied to Eqn. 13.

Example 2. Consider the heat equation with boundary condition for $0 \leq x \leq 2\pi$ and in time interval $0 \leq t \leq T = 0.5$.

$$U(0, t) = e^{-t}, \quad U(\pi, t) = -e^{-t}, \quad 0 \leq t \leq T \quad U(x, 0) = \cos(x)$$

The exact solution is

$$u(x, t) = e^{-t} \cos(x).$$

The results are given in Tables 5-10 and Figures 2 and 3.

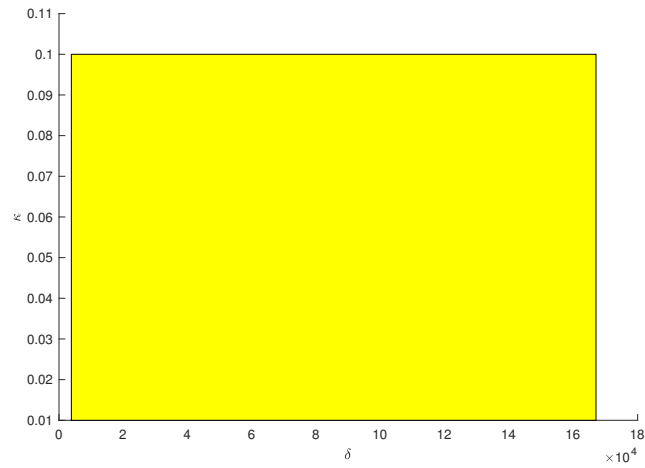


FIGURE 2. Stability region $\kappa\delta$ -plane

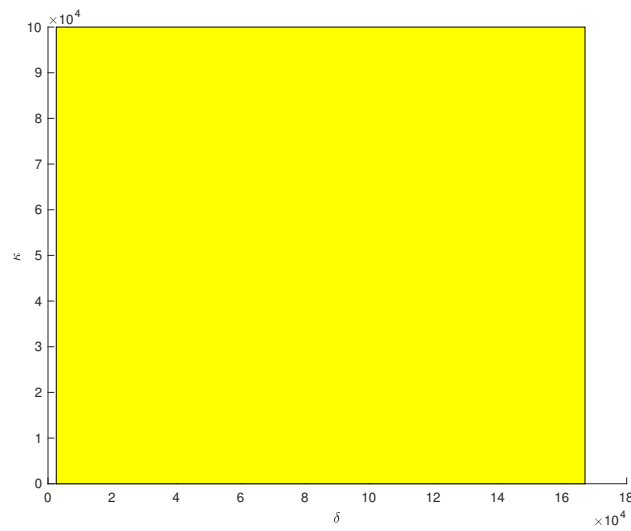


FIGURE 3. $\kappa\delta$ -plane-2

TABLE 5. Numerical results of Example 2, for $11599 \leq \kappa \leq 664800$ in the domain satisfying the stability condition, $\delta = 0.01$ and $r = 6.4038$

t	k	$ e_{i,j} $	$order$
0.5	0.0025	<i>blowup</i>	–
0.5	0.0025	0.3882	–
0.25	$6.2500e - 04$	0.2206	0.8154
0.125	$1.5625e - 04$	0.1174	0.9100
0.0625	$3.9063e - 05$	0.0606	0.9540

TABLE 6. Numerical results of Example 2, for $10439 \leq \kappa \leq 167040$ in the domain satisfying the stability condition, $0.1 \leq \delta$ and $r = 6.4441$

t	k	$ e_{i,j} $	$order$
0.5	0.0025	<i>blowup</i>	–
0.5	0.0025	0.3929	–
0.25	$6.2500e - 04$	0.2211	0.8295
0.125	$1.5625e - 04$	0.1175	0.9120
0.0625	$3.9063e - 05$	0.0606	0.9553

TABLE 7. Numerical results of Example 2, for $14185 \leq \kappa \leq 269510$ in the domain satisfying the stability condition, $\delta = 0.01$ and $r = 50.6606$

t	k	$ e_{i,j} $	$order$
0.5	0.05	<i>blowup</i>	–
0.5	0.05	0.4919	–
0.25	0.0125	0.2194	1.1648
0.125	0.0031	0.1173	0.9034
0.0625	$7.8125e - 04$	0.0606	0.9528

TABLE 8. Numerical results of Example 2, for $0.0079 \leq \kappa \leq 0.0639$ in the domain satisfying the stability condition, $\delta = 10000$

t	k	r	$ e_{i,j} $	$order$
0.05	0.025	25.0776	$5.8580e - 04$	—
0.025	0.0125	50.4076	$1.4576e - 04$	2.0068
0.0125	0.0063	101.0680	$3.4952e - 05$	2.0601
0.0063	0.0031	202.3891	$7.8493e - 06$	2.1547

TABLE 9. Numerical results of Example 2, for $0.0079 \leq \kappa \leq 0.0639$ in the domain satisfying the stability condition, $\delta = 10000$

t	k	r	$ e_{i,j} $	$order$
0.05	0.025	25.0776	$5.8580e - 04$	—
0.025	0.0125	12.5388	$1.4422e - 04$	2.0221
0.0125	0.0063	6.2694	$3.3985e - 05$	2.0853
0.0063	0.0031	3.1347	$7.3399e - 06$	2.2111

TABLE 10. Numerical results of Example 2, for $\kappa = 4012.4$ in the domain satisfying the stability condition, $\delta = 10000$

t	k	r	$ e_{i,j} $	$order$
0.05	0.025	25.0776	0.0485	—
0.025	0.0125	12.5388	0.0244	0.9911
0.0125	0.0063	6.2694	0.0122	1
0.0063	0.0031	3.1347	0.0060	1.0238

It can be concluded from Tables [5](#), [6](#), [7](#) that, for $\kappa = 0$, we get blow-up solutions for values of

$$k = 0.0025, \quad r = \frac{k}{h^2} = 6.4038 \quad \text{and} \quad k = 0.05, \quad r = \frac{k}{h^2} = 50.6606$$

respectively. Contrary to this, we can see in Tables 5 and 6 that the solutions do not blow-up for

$$r = \frac{k}{h^2} = 6.4038, \quad 3842 \leq \kappa \leq 167040, \quad \delta = 0.01 \quad \text{and} \quad 2574.3 \leq \kappa \leq 167040, \quad 0.1 \leq \delta,$$

respectively. Table 7 presents that for

$$r = \frac{k}{h^2} = 6.4038, \quad 14185 \leq \kappa \leq 269510, \quad \delta = 0.01$$

the solutions do not blow-up. Furthermore, these solutions are convergent of order close to 1. Figures 2 and 3 show the $\kappa\delta$ -stability domains which are unbounded subsets of R^2 . The solutions are stable in these domains. Namely, for $r = 6.4038$ and $r = 50.6606$ and any chosen $\kappa\delta$ -pairs which are in these domains, the solutions do not blow-up.

It is seen in Table 8 that the solutions are convergent with the order of 2 in time for the $\delta = 10000$ and selected κ values. Although r increases, the solutions are convergent with the order of 2. Table 9 shows that for a constant value of h the solutions are almost convergent with the order of 2 in time. It is shown in Table 10 that for different κ values the solutions are convergent with the order of 1 in time. These κ values are satisfied to Eqn. 13.

4. CONCLUSION

In this study, we present a model which is obtained by adding the time-relaxation term $\kappa(u - \bar{u})$ to the heat equation. We develop an algorithm using the explicit method to find the solutions of this model. We analyze the consistency, stability and convergence properties of the solution. We find that the method is consistent on an unbounded domain subset of $\kappa\delta$ -plane. Moreover, we see that for any given value of r , the method is stable for some particular values of κ and δ which are selected from an unbounded consistency region which is the subset of R^2 . The algorithm seems structurally explicit. Besides, for any value of r , the behavior of the stability results shows that this algorithm is similar to the implicit method, but this method is still explicit. On the other hand, we obtain the convergence order of convergence as 1 when stability condition holds. If the condition 15 is satisfied in addition to the stability condition, the convergence order of the method is increased from 1 to 2, which means that the convergence is accelerated. Consequently, the presented model is an efficient model that stabilizes an unstable method by specifying unbounded $\kappa - \delta$ region. Moreover adding the term time-relaxation to the heat equation in this presented model expands the stability range for the explicit method. We give two examples to validate theoretical results and how the method works. We observe that the blow-up solutions which is obtained by $\kappa = 0$ are stabilized by selecting suitable pair of κ and δ as given in examples. This shows that for any value of r , the convergence order for the method is 1 and 2 for the appropriate values of κ and δ . As a result, the numerical results obtained by using the algorithm are consistent with the theoretical results. As further works, the

time-relaxation term will be added to elliptic or hyperbolic equations.

Author Contribution Statements The authors contributed equally to this work. All authors read and approved the final copy of this paper.

Declaration of Competing Interests The authors declare that they have no known competing financial interest or personal relationships that could have appeared to influence the work reported in this paper.

REFERENCES

- [1] Adams, N. A., Stolz, S., Deconvolution methods for subgrid-scale approximation in LES, in *Modern Simulation Strategies for Turbulent Flow* (eds. B. Geurts and R.T. Edwards), (2001), pp. 21–41.
- [2] Asselin, R., Frequency filter for time integrations, *Mon. Weather Rev.*, 100 (1972), 487–490. [https://doi.org/10.1175/1520-0493\(1972\)100<0487:FFFTI>2.3.CO;2](https://doi.org/10.1175/1520-0493(1972)100<0487:FFFTI>2.3.CO;2)
- [3] Burden, R. L., Faires, J. D., Numerical Analysis, Brooks/Cole, Pacific Grove, 9th Edition, 2011.
- [4] Cibik, A., Eroglu, F. G., Kaya, S., Numerical analysis of an efficient second order time filtered backward Euler method for MHD equations, *Journal of Scientific Computing*, 82(2) (2020), 1–25. <https://doi.org/10.48550/arXiv.1906.07922>
- [5] Cooper, J., Introduction to Partial Differential Equations with Matlab, Birkhauser, Bosten, 1998.
- [6] Ervin, V. J., Layton, W., Neda, M., Numerical analysis of a higher order time relaxation model of fluids, *Int. J. Numer. Anal. Model.*, 4 (2007), 648–670.
- [7] Fletcher, C. A. J., Computational Techniques for Fluid Dynamics, Springer-Verlag, Berlin, 1998.
- [8] Gresho, P. M., Sani, R. L., Incompressible Flow and the Finite Element Method, John Wiley & Sons, Inc, 1998.
- [9] Guzel, A., Layton, W., Time filters increase accuracy of the fully implicit method, *BIT Numer. Math.*, 58(3) (2018), 301–315. DOI:10.1007/s10543-018-0695-z
- [10] Isik, O. R., Spin up problem and accelerating convergence to steady state, *Applied Mathematical Modelling*, 37(5) (2013), 3242–3253. <https://doi.org/10.1016/j.apm.2012.07.033>
- [11] Isik, O. R., Takhirov, A., Zheng, H., Second order time relaxation model for accelerating convergence to steady-state equilibrium for Navier-Stokes equations, *Applied Numerical Mathematics*, 119 (2017), 67–78. <https://doi.org/10.1016/j.apnum.2017.03.016>
- [12] Isik, O. R., Yuksel, G., Demir, B., Analysis of second order and unconditionally stable for BDF2-AB2 method for the Navier-Stokes Equations with nonlinear time relaxation, *Numerical Methods for Partial Differential Equations*, 34(6) (2018), 2060–2078. <https://doi.org/10.1002/num.22276>
- [13] Layton, W., Neda, M., Truncation of scales by time relaxation, *J. Math. Anal. Appl.*, 325 (2007), 788–807. <https://doi.org/10.1016/j.jmaa.2006.02.014>
- [14] Layton, W., Pruet, C. D., Rebholz, L. G. Temporally regularized direct numerical simulation, *Appl. Math. Comput.*, 216 (2010), 3728–3738. DOI:10.1016/j.amc.2010.05.031
- [15] Li, Y., Trenchea, C., A higher-order Robert-Asselin type time filter, *J. Comput. Phys.*, 259 (2014), 23–32. <https://doi.org/10.1016/j.jcp.2013.11.022>
- [16] Morton, K. W., Mayers, D. F., Numerical Solution of Partial Differential Equations: An Introduction, Cambridge University Press, 1994.

- [17] Neda, M., Discontinuous time relaxation method for the time-dependent Navier-Stokes equations, *Advance in Numerical Analysis*, 2010, Article ID 419021, 21 pages, (2010). <https://doi.org/10.1155/2010/419021>
- [18] Pruet, C. D., Gatski, T. B., Grosch, C. E., Thacker, W. D., The temporally filtered Navier-Stokes equations: properties of the residual-stress, *Phys. Fluids*, 15 (2003), 2127–2140. <https://doi.org/10.1063/1.1582858>
- [19] Rosenau, P., Extending hydrodynamics via the regularization of the Chapman-Enskog expansion, *Phys. Rev.*, A40(7193) (1989). <https://doi.org/10.1103/PhysRevA.40.7193>
- [20] Schochet, S., Tadmor, E., The regularized Chapman-Enskog expansion for scalar conservation laws, *Arch. Ration. Mech. Anal.*, 119(95) (1992). <https://doi.org/10.1007/BF00375117>
- [21] Smith, G. D., *Numerical Solution of Partial Differential Equations: Finite Difference Methods*, Oxford University Press, 1985.
- [22] Stolz, S., Adams, N. A., Kleiser, L., The approximate deconvolution model for LES of compressible flows and its application to shock-turbulent boundary layer interaction, *Phys. Fluids*, 13(2985) (2001). <https://doi.org/10.1063/1.1397277>
- [23] Williams, P. D., A proposed modification to the Robert-Asselin time filter, *Mon. Weather Rev.*, 137(8) (2009), 2538–2546. <https://doi.org/10.1175/2009MWR2724.1>
- [24] Williams, P. D., The RAW filter: An improvement to the Robert-Asselin filter in semi-implicit integrations, *Mon. Weather Rev.*, 139(6) (2011), 1996–2007. <https://doi.org/10.1175/2010MWR3601.1>



ANHOLONOMIC CO-ORDINATES AND ELECTROMAGNETIC CURVES WITH ALTERNATIVE MOVING FRAME VIA MAXWELL EVOLUTION

Hazal CEYHAN,¹ Ebru YANIK² and Zehra ÖZDEMİR³

^{1,2}Department of Mathematics, Ankara University, 06100 Ankara, TÜRKİYE

³Department of Mathematics, Amasya University, 05189 Amasya, TÜRKİYE

ABSTRACT. In this study, we examine the Berry's phase equation for E-M curves in the C - direction and W - direction throughout an optic fiber via alternative moving frame in three dimensional space. Moreover, electromagnetic curve's C - direction and W - direction Rytov parallel transportation laws are defined. Finally, we examine the electromagnetic curve with anholonomic co-ordinates for Maxwellian evolution by Maxwell's equation.

1. INTRODUCTION

Electromagnetic (E-M) theory and magnetic theory are very significant topics for the scientific world. Mathematically, at first, it started to be researched in terms of topology [20]. Then, it was noted that a geometric perspective could be presented with this approach and Berry made a the publication leading the way in this regard [16]. After that, Ross studied the rotational motion of the polarization state together with the optical fiber geometrically and gave a relationship with the most important branch of geometry, curves [11]. Haldane examined the geometric phase of a light wave in tangential vector space [5]. Dandoloﬀ, Zakrzewski and Frins, Dultz researched parallel transport with Berry's phase and correlated the space curve with the trajectories of the light wave along the optical fiber [4, 19]. On the other hand, there has been a very important paper that has led to the study of this subject for geometers recently. In that paper, the relationship between the magnetic field and Killing vector field and the connection with the classical elastic

2020 *Mathematics Subject Classification.* 53Z05, 78A25.

Keywords. Applications to physics, magnetic curves, vector fields, Maxwell equations, electromagnetic theory, anholonomic co-ordinates, alternative moving frame.

¹ ✉ hazalceyhan@gmail.com-Corresponding author; 0000-0001-6201-5134;

² ✉ ebruyanic@ankara.edu.tr; 0000-0003-0768-9931

³ ✉ zehra.ozdemir@amasya.edu.tr; 0000-0001-9750-507X.

theory and the Hall effect were given [12,13]. Then, the magnetic flow and field were studied in some geometric structures, thanks to the interest in the geometric phase and the important publications written on this subject [7,9,10]. With this, the geometrical phase shift of the angular momentum and their densities were researched analytically so that Frenet-Serret coordinate system and the special curve were associated [18]. Afterward, Özdemir [27] and Ceyhan [6] calculated magnetic and electromagnetic trajectories and they presented some motivated examples of motion of the polarization light wave. Finally, in [17,21], Körpınar and Gürbüz examined the connection between electromagnetic theory and Maxwell's equations from a geometric perspective.

Recently optical fiber is a very important field that come into prominence in physics and geometry. Polarized light is generally thought of as the transport of an electromagnetic wave and its appearances. When it is assumed to propagate within the optical fiber, it is well-defined, owing to the Maxwell's equations. The set of Maxwell's equations implicitly shows how electromagnetic field vectors propagate and explicitly tell sources of the field. In the optical fiber configuration of uniform, isotropic, nonconducting, free-from charge, magnetic flux, and non-dispersive etc. The evolution of the space curve is a very influential way to understand many physical processes such as vortex filaments, dynamics of Heisenberg spin chain, integrable systems, soliton equation theory, sigma models, relativity, water wave theory, fluid dynamics, field theories, linear and nonlinear optics. We give example publications of the applications mentioned above. Authors researched the relationship between non-linear Schrödinger equation rogue soliton equivalent in the spin system [2]. In [14], authors gave a sufficient conclusion by using Da Rios vortex filament equation and the evolution equation for the torsion is the Viscous Burger's equation. Then in comprehensive paper [26], Banica and Miot investigated evolution, interaction and collisions of vortex filaments. Moreover, Körpınar and et. al. studied Binormal Schrödinger system of Heisenberg ferromagnetic equation and flux surface by using normal direction equations [23-25]. In [22], author studied binormal direction with magnetic flows equations for Berry's phase applications.

In this study, we analyze the geometric phase equation for E-M curves in the C - direction and W - direction directions throughout an optic fiber via an alternative moving frame in three dimensional space. At the same time, we research the electromagnetic curve's via anholonomic co-ordinates for Maxwellian evolution by Maxwell's equation. The first section includes the historical background of the work and a description of what has been done in this paper. In the second section, equations of alternative moving frame studied in this study and anholonomic coordinate calculations to be used in other parts are given. The third section comprises evaluation of directional derivative expressions for the alternative moving frame and the S - direction, C - direction, W - direction derivatives of Serret-Frenet relations in matrix form. The fourth section we calculate \vec{E}_c and \vec{E}_w electric field, magnetic field, electromagnetic matrix form and \vec{E}_c , \vec{E}_w Rytov curves. Finally, in the last

section, we give mathematical approach of Maxwell equations for electromagnetic and magnetic waves via alternative moving frame.

2. FUNDAMENTAL BACKGROUND

Let $\gamma = \gamma(s)$ be an arbitrary curve in 3D Riemannian manifolds. If $\langle \vec{\gamma}'(s), \vec{\gamma}'(s) \rangle = 0$ for any $s \in I$, γ is called an arc-length parametrized curve where \langle , \rangle is defined as;

$$\langle , \rangle = du_1^2 + du_2^2 + du_3^2$$

that (u_1, u_2, u_3) is a coordinate of \mathbb{E}^3 .

Alternative frame's fields as $\{\vec{t}, \vec{n}, \vec{b}\}$ Frenet frame are given as below;

$$\vec{N}, \quad \vec{C} = \frac{\vec{N}'}{\|\vec{N}'\|}, \quad \vec{W} = \frac{\tau t + \kappa b}{\sqrt{\kappa^2 + \tau^2}}$$

where \vec{N} is a unit principal normal vector field and \vec{W} is a Darboux vector field.

The one-parameter derivative s , which is the arc-length parameter of the alternative moving frame's fields is as follows;

$$\begin{aligned} \vec{N}'(s) &= f(s)\vec{C}(s) \\ \vec{C}'(s) &= -f(s)\vec{N}(s) + g(s)\vec{W}(s) \\ \vec{W}'(s) &= -g(s)\vec{C}(s) \end{aligned}$$

which $f(s)$ and $g(s)$ are curvature of the curve γ (κ and τ are the curvature and the torsion of the curve γ in terms of Frenet's frame, respectively); are defined as;

$$f = \kappa\sqrt{1 + H^2} \quad g = \sigma f$$

where $H = \frac{\tau}{\kappa}$ is harmonic curvature and $\sigma = \frac{\kappa^2}{(\kappa^2 + \tau^2)^{\frac{3}{2}}} (\frac{\tau}{\kappa})'$, ([3]).

With \vec{A} being an arbitrary vector field, the gradient and the curl of this vector field are given respectively, as ([1])

$$\begin{aligned} grad \vec{A} &= \vec{N}\vec{N} \cdot grad \vec{A} + \vec{C}\vec{C} \cdot grad \vec{A} + \vec{W}\vec{W} \cdot grad \vec{A}, \\ curl \vec{A} &= \vec{N} \times \frac{\partial \vec{A}}{\partial s} + \vec{C} \times \frac{\partial \vec{A}}{\partial s} + \vec{W} \times \frac{\partial \vec{A}}{\partial s}. \end{aligned}$$

On the other hand, the directional derivatives of arbitrary scalar f , along the vector \vec{N} , vector \vec{C} and Darboux vector \vec{W} , are defined in the above expression as;

$$\begin{aligned} \frac{\partial f}{\partial s} &= \vec{N} \cdot \text{grad}f, \\ \frac{\partial f}{\partial c} &= \vec{C} \cdot \text{grad}f, \\ \frac{\partial f}{\partial w} &= \vec{W} \cdot \text{grad}f. \end{aligned}$$

Assume that a directional derivative of an arbitrary vector \vec{A} with respect to direction η where $\eta \in \{\vec{N}, \vec{C}, \vec{W}\}$ and considering the directional derivative $\frac{\partial \vec{A}}{\partial \eta}$ which calculated as follows; the divergence operator div acting on an arbitrary vector \vec{A} is written as;

$$div \vec{A} = \vec{N} \cdot \frac{\partial \vec{A}}{\partial \eta} + \vec{C} \cdot \frac{\partial \vec{A}}{\partial \eta} + \vec{W} \cdot \frac{\partial \vec{A}}{\partial \eta}.$$

The directional derivative of the vector \vec{N} can be written in a general form as follows;

$$\left. \begin{aligned} \frac{\partial \vec{N}}{\partial s} &= (\vec{N} \cdot \frac{\partial \vec{N}}{\partial s})\vec{N} + (\vec{C} \cdot \frac{\partial \vec{N}}{\partial s})\vec{C} + (\vec{W} \cdot \frac{\partial \vec{N}}{\partial s})\vec{W}, \\ \frac{\partial \vec{N}}{\partial c} &= (\vec{N} \cdot \frac{\partial \vec{N}}{\partial c})\vec{N} + (\vec{C} \cdot \frac{\partial \vec{N}}{\partial c})\vec{C} + (\vec{W} \cdot \frac{\partial \vec{N}}{\partial c})\vec{W}, \\ \frac{\partial \vec{N}}{\partial w} &= (\vec{N} \cdot \frac{\partial \vec{N}}{\partial w})\vec{N} + (\vec{C} \cdot \frac{\partial \vec{N}}{\partial w})\vec{C} + (\vec{W} \cdot \frac{\partial \vec{N}}{\partial w})\vec{W}. \end{aligned} \right\} \quad (1)$$

For the other directional derivatives of the vectors which are vector \vec{C} and Darboux vector \vec{W} , we can use the same method. Here we give various interrelationships between directional derivatives found by solving the following sets of equations;

$$\left. \begin{aligned} \frac{\partial}{\partial s}(\vec{N} \cdot \vec{N}) &= 2\vec{N} \frac{\partial \vec{N}}{\partial s} \\ &= 0 \\ \frac{\partial}{\partial s}(\vec{C} \cdot \vec{C}) &= 2\vec{C} \frac{\partial \vec{C}}{\partial s} \\ &= 0 \\ \frac{\partial}{\partial s}(\vec{W} \cdot \vec{W}) &= 2\vec{W} \frac{\partial \vec{W}}{\partial s} \\ &= 0 \end{aligned} \right\} \quad (2)$$

$$\left. \begin{aligned} \frac{\partial}{\partial s}(\vec{N} \cdot \vec{C}) &= \vec{N} \cdot \frac{\partial \vec{C}}{\partial s} + \vec{C} \cdot \frac{\partial \vec{N}}{\partial s} \\ &= 0 \\ \vec{N} \cdot \frac{\partial \vec{C}}{\partial s} &= -\vec{C} \cdot \frac{\partial \vec{N}}{\partial s} \\ &= f(s) \end{aligned} \right\} \quad (3)$$

$$\left. \begin{aligned} \frac{\partial}{\partial s}(\vec{N} \cdot \vec{W}) &= \vec{N} \cdot \frac{\partial \vec{W}}{\partial s} + \vec{W} \cdot \frac{\partial \vec{N}}{\partial s} \\ &= 0 \\ \vec{N} \cdot \frac{\partial \vec{W}}{\partial s} &= -\vec{W} \cdot \frac{\partial \vec{N}}{\partial s} \end{aligned} \right\} \quad (4)$$

$$\left. \begin{aligned} \frac{\partial}{\partial s}(\vec{C} \cdot \vec{W}) &= \vec{C} \cdot \frac{\partial \vec{W}}{\partial s} + \vec{W} \cdot \frac{\partial \vec{C}}{\partial s} \\ &= 0 \\ \vec{C} \cdot \frac{\partial \vec{W}}{\partial s} &= -\vec{W} \cdot \frac{\partial \vec{C}}{\partial s} \\ &= g(s) \end{aligned} \right\} \quad (5)$$

The equations obtained above for the $\frac{\partial}{\partial s}$ are also written in the same way for the directional derivatives $\frac{\partial}{\partial c}$ and $\frac{\partial}{\partial w}$.

And also in [15], defined four additional terms of the directional derivatives. These are as follows

$$\left. \begin{aligned} \vec{C} \cdot \frac{\partial \vec{N}}{\partial c} &= -\vec{N} \cdot \frac{\partial \vec{C}}{\partial c} \\ &= \Psi_{cs} \\ \vec{W} \cdot \frac{\partial \vec{N}}{\partial w} &= -\vec{N} \cdot \frac{\partial \vec{W}}{\partial w} \\ &= \Psi_{ws} \\ \vec{W} \cdot \frac{\partial \vec{N}}{\partial c} &= -\vec{N} \cdot \frac{\partial \vec{W}}{\partial c} \\ &= \frac{1}{2}(\Phi_s + \Lambda_s) \\ \vec{C} \cdot \frac{\partial \vec{N}}{\partial w} &= -\vec{N} \cdot \frac{\partial \vec{C}}{\partial w} \\ &= \frac{1}{2}(\Phi_s - \Lambda_s) \end{aligned} \right\} \quad (6)$$

The symbol Ψ_{cs} represents the normal deformation of the vector tube in the direction of the \vec{C} , Ψ_{ws} represents the normal deformation of the vector tube in the direction of the \vec{W} , Φ_s is called the abnormality parameter of the vector s -line, Λ_s is the shear deformation in the normal plane (i.e. plane containing the \vec{N} and \vec{W} vectors).

Note that the abnormality parameter of the vectors $\vec{N}, \vec{C}, \vec{W}$ are denoted by the symbols Λ_s, Λ_c and Λ_w and defined as

$$\left. \begin{aligned} \Lambda_c &= -g(s) - \frac{1}{2}(\Phi_s - \Lambda_s) \\ &= -g(s) + \vec{N} \cdot \frac{\delta \vec{C}}{\delta w}, \\ \Lambda_w &= -g(s) + \frac{1}{2}(\Phi_s + \Lambda_s) \\ &= -g(s) - \vec{N} \cdot \frac{\delta \vec{W}}{\delta c}, \\ \Lambda_s &= -\vec{W} \cdot \frac{\delta \vec{N}}{\delta c} + \vec{C} \cdot \frac{\delta \vec{N}}{\delta w}, \end{aligned} \right\} \tag{7}$$

respectively. The three abnormalities can be written as follows upon examining the above expression as follows

$$\left. \begin{aligned} \text{curl} \vec{N} \cdot \vec{N} &= \Lambda_s \\ \text{curl} \vec{C} \cdot \vec{C} &= \Lambda_c \\ \text{curl} \vec{W} \cdot \vec{W} &= \Lambda_w \end{aligned} \right\} \tag{8}$$

The abnormality parameter of the vector s - line is obtained by setting the torsion τ in (7) equal to each other, such that,

$$\Phi_s = \Lambda_w - \Lambda_c$$

3. EVALUATION OF DIRECTIONAL DERIVATIVE EXPRESSIONS FOR THE ALTERNATIVE MOVING FRAME

Here we consider that $\gamma(s, c, w)$ be a curve that exists in the 3D space. Via (1)-(8) we can write the other geometric equations in terms of anholonomic coordinates

respectively;

$$\begin{aligned} \operatorname{div} \vec{N} &= \vec{N} \cdot \frac{\partial \vec{N}}{\partial s} + \vec{C} \cdot \frac{\partial \vec{N}}{\partial c} + \vec{W} \cdot \frac{\partial \vec{N}}{\partial w} \\ &= \Psi_{cs} + \Psi_{ws}, \\ \operatorname{div} \vec{C} &= \vec{N} \cdot \frac{\partial \vec{C}}{\partial s} + \vec{C} \cdot \frac{\partial \vec{C}}{\partial c} + \vec{W} \cdot \frac{\partial \vec{C}}{\partial w} \\ &= -f(s) + \vec{W} \cdot \frac{\partial \vec{C}}{\partial w}, \\ \operatorname{div} \vec{W} &= \vec{N} \cdot \frac{\partial \vec{W}}{\partial s} + \vec{C} \cdot \frac{\partial \vec{W}}{\partial c} + \vec{W} \cdot \frac{\partial \vec{W}}{\partial w} \\ &= \vec{C} \cdot \frac{\partial \vec{W}}{\partial c}. \end{aligned}$$

Furthermore,

$$\begin{aligned} \operatorname{curl} \vec{N} &= \vec{N} \times \frac{\partial \vec{N}}{\partial s} + \vec{C} \times \frac{\partial \vec{N}}{\partial c} + \vec{W} \times \frac{\partial \vec{N}}{\partial w} \\ &= \Lambda_s + f(s) \vec{W}, \\ \operatorname{curl} \vec{C} &= \vec{N} \times \frac{\partial \vec{C}}{\partial s} + \vec{C} \times \frac{\partial \vec{C}}{\partial c} + \vec{W} \times \frac{\partial \vec{C}}{\partial w} \\ &= (-\operatorname{div} \vec{W}) \vec{N} + (-g(s) - \frac{1}{2}(\Phi_s - \Lambda_s)) \vec{C} + \Psi_{cs} \cdot \vec{W}, \\ \operatorname{curl} \vec{W} &= \vec{N} \times \frac{\partial \vec{W}}{\partial s} + \vec{C} \times \frac{\partial \vec{W}}{\partial c} + \vec{W} \times \frac{\partial \vec{W}}{\partial w} \\ &= (\operatorname{div} \vec{C} + f(s)) \vec{N} + (-\Psi_{ws}) \vec{C} + (-g(s) + \frac{1}{2}(\Phi_s + \Lambda_s)) \cdot \vec{W}. \end{aligned}$$

Thanks to the above equations, the Serret-Frenet formulas for each direction of the frame together with the anholonomic coordinates of the $\{N, C, W\}$ frame are obtained as the following matrix forms;

$$\begin{aligned} \frac{\partial}{\partial s} \begin{pmatrix} \vec{N} \\ \vec{C} \\ \vec{W} \end{pmatrix} &= \begin{pmatrix} 0 & f(s) & 0 \\ -f(s) & 0 & g(s) \\ 0 & -g(s) & 0 \end{pmatrix} \begin{pmatrix} \vec{N} \\ \vec{C} \\ \vec{W} \end{pmatrix}, \\ \frac{\partial}{\partial c} \begin{pmatrix} \vec{N} \\ \vec{C} \\ \vec{W} \end{pmatrix} &= \begin{pmatrix} 0 & \Psi_{cs} & \Lambda_w + g(s) \\ -\Psi_{cs} & 0 & -\operatorname{div} \vec{W} \\ -(\Lambda_w + g(s)) & \operatorname{div} \vec{W} & 0 \end{pmatrix} \begin{pmatrix} \vec{N} \\ \vec{C} \\ \vec{W} \end{pmatrix}, \\ \frac{\partial}{\partial w} \begin{pmatrix} \vec{N} \\ \vec{C} \\ \vec{W} \end{pmatrix} &= \begin{pmatrix} 0 & -(\Lambda_c + g(s)) & \Psi_{ws} \\ \Lambda_c + g(s) & 0 & f(s) + \operatorname{div} \vec{C} \\ -\Psi_{ws} & -(f(s) + \operatorname{div} \vec{C}) & 0 \end{pmatrix} \begin{pmatrix} \vec{N} \\ \vec{C} \\ \vec{W} \end{pmatrix}. \end{aligned} \tag{9}$$

4. RELATIONSHIP BETWEEN ANHOLONOMIC COORDINATES AND ELECTROMAGNETIC CURVES

Berry's (geometric) phase in the directions throughout C – *direction* and W – *direction* arises with the dissemination of an E-M wave along with the optical fiber for the alternative moving frame of curve γ . Optical fiber can be defined as a curve $\gamma(s, c, w)$ via alternative moving frame in three dimensional space. The E-M wave dissemination is in the direction of $\vec{N} = (s, c, w)$ the polarization of the E-M wave is mentioned by the direction of the electric field vector $\vec{E} = (s, c, w)$ and magnetic field is described as $\vec{V} = (s, c, w)$. Here basically the electric field will be shown perpendicular to the direction of W will be examined.

Case 1 : The derivation of the \vec{E} between any two points in the C – *direction* for the alternative moving frame $\{N, C, W\}$ of the curve $\gamma(s, c, w)$ can be defined as

$$\frac{\partial}{\partial c} \vec{E}(s, c, w) = \lambda_1 \vec{N} + \lambda_2 \vec{C} + \lambda_3 \vec{W} \quad (10)$$

where $\lambda_i(s, c, w)$, $i = 1, 2, 3$ are sufficiently smooth arbitrary functions along the γ . The electric field is right angle to \vec{N} and if we consider that because of the absorption, there is no mechanism loss in the optical fiber, we can write the following equations;

$$\langle \vec{N}, \vec{E} \rangle = 0, \quad \langle \vec{E}, \vec{E} \rangle = c. \quad (11)$$

Taking the derivative of (11) and using the Eqs. (9)-(11), we get

$$\left\langle \frac{\partial \vec{N}}{\partial c}, \vec{E} \right\rangle = -\lambda_1.$$

Using Eqs. (10) and (11) we can calculate,

$$\lambda_1 = -(\Psi_{cs} \mathbf{E}^C + (\Lambda_w + g(s)) \mathbf{E}^W) \quad (12)$$

where \mathbf{E}^C and \mathbf{E}^W are smooth components of the \vec{C} and \vec{W} . If we taking derivative of the second one in (11), we can get

$$\left\langle \frac{\partial \vec{E}}{\partial c}, \vec{E} \right\rangle = 0.$$

Therefore, using (9), (11) and (12), we obtain

$$\vec{E}_c = -(\Psi_{cs} \mathbf{E}^C + (\Lambda_w + g(s)) \mathbf{E}^W) \vec{N} + \lambda (\vec{E} \times \vec{N}) \quad (13)$$

that λ is a constant term.

The last equation allows us to find the rotation of the electric field in the C – *direction* around the \vec{n} . Moreover, we can assume that $\lambda = 0$, with that we can

finalize which $\vec{\mathbf{E}}$ is a Rytov parallel transport in the C -direction by the conditions given above

$$\vec{\mathbf{E}}_c = -(\vec{\mathbf{E}} \cdot N_c)N. \quad (14)$$

Furthermore, the Fermi-Walker transportation law is given as

$$\vec{B}_c^{FW} = \vec{B}_c \pm (\vec{B} \cdot \vec{N}_c)\vec{N} + (\vec{B} \cdot \vec{N})\vec{N}_c. \quad (15)$$

Generally, we can write

$$\vec{\mathbf{E}} = \mathbf{E}^C \vec{C} + \mathbf{E}^W \vec{W}. \quad (16)$$

Deriving (16) and combining with (9) we can write,

$$\frac{\partial}{\partial c} \vec{\mathbf{E}} = -(\Psi_{cs} \mathbf{E}^C + (\Lambda_w + g(s)) \mathbf{E}^W) \vec{N} + (\mathbf{E}_c^C + \text{div} \vec{W} \cdot \mathbf{E}^W) \vec{C} + (\mathbf{E}_c^W - \text{div} \vec{W} \cdot \mathbf{E}^C) \vec{W}. \quad (17)$$

If the electric field is assumed to be Rytov parallel transported in C -direction, then comparing (14) and (17) satisfies that;

$$\begin{pmatrix} \mathbf{E}_c^C \\ \mathbf{E}_c^W \end{pmatrix} = \begin{pmatrix} 0 & -\text{div} \vec{W} \\ \text{div} \vec{W} & 0 \end{pmatrix} \begin{pmatrix} \mathbf{E}^C \\ \mathbf{E}^W \end{pmatrix}. \quad (18)$$

Therefore, we can accomplish that (18) describes the motion of the polarization plane in the C -direction along the optical fiber thus a Berry's phase $\rho = (s, c, w)$ in the c direction is defined by;

$$\frac{\partial}{\partial c} \rho = \text{div} \vec{W}.$$

Using the information provided it is found the magnetic field vector in relation to the ingredient of the electric field as ;

$$\vec{V} = \mathbf{E}^C \vec{W} - \mathbf{E}^W \vec{C} \quad (19)$$

that provides the following conditions;

$$\vec{V} \perp \vec{\mathbf{E}} \quad \vec{V} \perp \vec{N} \quad (20)$$

where

$$V^C = -\mathbf{E}^W \quad V^W = \mathbf{E}^C.$$

Using (20) and (9), deriving (19), we get

$$\frac{\partial \vec{V}}{\partial c} = (\mathbf{E}^W \Psi_{cs} - \mathbf{E}^C (\Lambda_w + g(s))) \vec{N} + (\mathbf{E}^C \text{div} \vec{W} - \mathbf{E}_c^W) \vec{C} + (\mathbf{E}_c^C + \mathbf{E}^W \text{div} \vec{W}) \vec{W} \quad (21)$$

which satisfies

$$\left\langle \frac{\partial \vec{V}}{\partial c}, \vec{\mathbf{E}} \right\rangle + \left\langle \frac{\partial \vec{\mathbf{E}}}{\partial c}, \vec{V} \right\rangle = 0$$

and

$$\left\langle \frac{\partial \vec{V}}{\partial c}, \vec{N} \right\rangle + \left\langle \frac{\partial \vec{N}}{\partial c}, \vec{V} \right\rangle = 0.$$

Within the results obtained, we can make the following inference, magnetic field and electric field have alike Berry’s phase in the same conditions as follows

$$\vec{V}_c = -(\vec{V} \cdot \vec{N}_c)\vec{N}. \tag{22}$$

We show that if \vec{E} is the Rytov parallel transported the $C - direction$ if and only if it is Fermi-Walker parallel transported in the $C - direction$ throughout optical fiber via alternative moving frame of the curve γ .

The Lorentz force is the force acting on a charged particle moving in electromagnetic field in three dimensional space. At that time, the electromagnetic field in the $C - direction$ along with the curve γ via alternative moving frame with concerning anholonomic coordinates help of Lorentz equation $\phi(\vec{E}) = \vec{X} \times \vec{E}$ where \vec{X} is a Killing magnetic field in three dimensional space and (9) is given as follows;

$$\langle \phi_c(\vec{E}), \vec{N} \rangle = -\langle \phi(\vec{N}), \vec{E}_C \rangle = \langle \frac{\partial \vec{E}}{\partial c}, \vec{N} \rangle = -\Psi_{cs}\mathbf{E}^C - (\Lambda_w + g(s))\mathbf{E}^W.$$

When necessary arrangements are made, we can write;

$$\begin{aligned} \phi_c(\vec{N}) &= \Psi_{cs}\mathbf{E}^C + (\Lambda_w + g(s))\mathbf{E}^W + a_1\mathbf{E}^N \\ \phi_c(\vec{C}) &= -\lambda\mathbf{E}^W + a_2\mathbf{E}^N \\ \phi_c(\vec{W}) &= \lambda\mathbf{E}^C + a_3\mathbf{E}^N. \end{aligned} \tag{23}$$

Taking (23) and (9) into account, Lorentz force in the $C - direction$ throughout the optical fiber that is determined curve γ for the alternative moving frame implies the following matrix form;

$$\begin{pmatrix} \phi_c(\vec{N}) \\ \phi_c(\vec{C}) \\ \phi_c(\vec{W}) \end{pmatrix} = \begin{pmatrix} 0 & \Psi_{cs} & (\Lambda_w + g(s)) \\ -\Psi_{cs} & 0 & -\lambda \\ -(\Lambda_w + g(s)) & \lambda & 0 \end{pmatrix} \begin{pmatrix} \mathbf{E}^N \\ \mathbf{E}^C \\ \mathbf{E}^W \end{pmatrix}$$

Case 2 : The derivation of the electric field vector \vec{E} between any two points in the $W - direction$ for the alternative moving frame $\{N, C, W\}$ of the curve $\gamma(s, c, w)$ can be defined as

$$\frac{\partial}{\partial w} \vec{E}(s, c, w) = \lambda_1 \vec{N} + \lambda_2 \vec{C} + \lambda_3 \vec{W} \tag{24}$$

where $\lambda_i(s, c, w)$, $i = 1, 2, 3$ are sufficiently smooth arbitrary functions along the γ . The electric field is right angle to \vec{N} and if we consider that because of the absorption, there is no mechanism loss in the optical fiber, we can write the following equations;

$$\langle \vec{N}, \vec{E} \rangle = 0, \quad \langle \vec{E}, \vec{E} \rangle = c. \tag{25}$$

Taking derivative of (25) and using the Eqs. (9)-(25), we get

$$\left\langle \frac{\partial \vec{N}}{\partial w}, \vec{E} \right\rangle = \lambda_1$$

Using Eqs. (24) and (25) we can calculate,

$$\lambda_1 = ((\Lambda_c + g(s))\mathbf{E}^C - \Psi_{ws}\mathbf{E}^W)\vec{N}. \quad (26)$$

If we taking derivative of the second one in (25), we can get

$$\left\langle \frac{\partial \vec{E}}{\partial w}, \vec{E} \right\rangle = 0.$$

After that we collect (9), (25) and (25) we obtain

$$\vec{E}_w = ((\Lambda_c + g(s))\mathbf{E}^C - \Psi_{ws}\mathbf{E}^W)\vec{N} + \lambda(\vec{E} \times \vec{N}) \quad (27)$$

that λ is a constant.

Considering the last equation we get the rotation of the \vec{E} in the W - direction around the \vec{N} . Furthermore, we assume that $\lambda = 0$, in this manner we finalize that \vec{E} is a parallel transport in the W - direction with the above terms

$$\vec{E}_w = -(\vec{E}, \vec{N}_w)\vec{N}. \quad (28)$$

Additionally, this motion can be defined through the Fermi-Walker transportation law in three dimensional space is as follows;

$$\vec{B}_w^{FW} = \vec{B}_w \pm (\vec{B} \cdot \vec{N}_w)\vec{N} + (\vec{B} \cdot \vec{N})\vec{N}_w. \quad (29)$$

Generally, we get

$$\vec{E} = \mathbf{E}^C \vec{C} + \mathbf{E}^W \vec{W} \quad (30)$$

where \mathbf{E}^C and \mathbf{E}^W are smooth components of the \vec{C} and \vec{W} . Deriving (30) and combining with (9) we can write,

$$\begin{aligned} \frac{\partial}{\partial w} \vec{E} &= ((\Lambda_c + g(s))\mathbf{E}^C - \Psi_{ws}\mathbf{E}^W)\vec{N} + (\mathbf{E}_w^C - (div\vec{C} + f(s))\mathbf{E}^W)\vec{C} \\ &+ (\mathbf{E}_w^W + (f(s) + div\vec{C})\mathbf{E}^C)\vec{W}. \end{aligned} \quad (31)$$

If the electric field is presumed to be Rytov parallel transported in the direction W , then comparing (28) and (31) implies that

$$\begin{pmatrix} \mathbf{E}_w^C \\ \mathbf{E}_w^W \end{pmatrix} = \begin{pmatrix} 0 & div\vec{C} + f(s) \\ -(div\vec{C} + f(s)) & 0 \end{pmatrix} \begin{pmatrix} \mathbf{E}^C \\ \mathbf{E}^W \end{pmatrix}. \quad (32)$$

Therefore, (32) describes the rotation of the polarization plane in the W - direction along the optical fiber thus a Berry's phase $\rho = (s, c, w)$ in the W - direction described by;

$$\frac{\partial}{\partial w} \rho = div\vec{C} + f(s).$$

We can indicate the magnetic field vector in relation to the ingredient of the electric field as;

$$\vec{V} = \mathbf{E}^C \vec{W} - \mathbf{E}^W \vec{C} \tag{33}$$

that ensures the following conditions;

$$\vec{V} \perp \vec{\mathbf{E}} \quad \vec{V} \perp \vec{N} \tag{34}$$

where

$$V^C = \mathbf{E}^W \quad V^W = \mathbf{E}^C.$$

Using (9), (34) and deriving (33), we can get;

$$\begin{aligned} \frac{\partial \vec{V}}{\partial w} = & (-\mathbf{E}^C \Psi_{ws} - \mathbf{E}^W (\Lambda_C + g(s)) \vec{N} + (-\mathbf{E}^C (f(s) + \text{div} \vec{C}) - \mathbf{E}_w^W) \vec{C} \tag{35} \\ & + (\mathbf{E}_w^C + \mathbf{E}^W (f(s) + \text{div} \vec{C})) \vec{W} \end{aligned}$$

which satisfies

$$\langle \frac{\partial \vec{V}}{\partial w}, \vec{\mathbf{E}} \rangle + \langle \frac{\partial \vec{\mathbf{E}}}{\partial w}, \vec{V} \rangle = 0$$

and

$$\langle \frac{\partial \vec{V}}{\partial w}, \vec{N} \rangle + \langle \frac{\partial \vec{N}}{\partial w}, \vec{V} \rangle = 0.$$

Consequently, we can say that magnetic field and electric field have Berry's phase in the same conditions as follows;

$$\vec{V}_w = -(\vec{V} \cdot \vec{N}_w) \vec{N}$$

if $\vec{\mathbf{E}}$ is the Rytov parallel transported the $W - direction$ if and only if it is Fermi-Walker parallel transported in the $W - direction$ along with optical fiber via alternative moving frame of the curve γ .

The electromagnetic field in the $W - direction$ along with the curve γ via alternative moving frame with respect to anholonomic coordinates help of Lorentz equation and (9) is given as follows;

$$\langle \phi_w(\vec{\mathbf{E}}), \vec{N} \rangle = -\langle \phi(\vec{N}), \vec{\mathbf{E}}_W \rangle = \langle \frac{\partial \vec{\mathbf{E}}}{\partial w}, \vec{N} \rangle = (\Lambda_c + g(s) \mathbf{E}^C - \Psi_{ws} \mathbf{E}^W). \tag{36}$$

When necessary arrangements are made, we can write;

$$\begin{aligned} \phi_w(\vec{N}) &= \Psi_{ws} \mathbf{E}^W - (\Lambda_c + g(s) \mathbf{E}^C + a_1 \mathbf{E}^N \\ \phi_w(\vec{C}) &= -\lambda \mathbf{E}^W + a_2 \mathbf{E}^N \\ \phi_w(\vec{W}) &= \lambda \mathbf{E}^C + a_3 \mathbf{E}^N. \end{aligned} \tag{37}$$

Taking (37) and (9) into account, the Lorentz force in the direction W along with the optical fiber that is determined curve γ for the alternative moving frame implies the following matrix form;

$$\begin{pmatrix} \phi_w(\vec{N}) \\ \phi_w(\vec{C}) \\ \phi_w(\vec{W}) \end{pmatrix} = \begin{pmatrix} 0 & -(\Lambda_c + g(s)) & \Psi_{ws} \\ (\Lambda_c + g(s)) & 0 & -\lambda \\ -\Psi_{ws} & \lambda & 0 \end{pmatrix} \begin{pmatrix} \mathbf{E}^N \\ \mathbf{E}^C \\ \mathbf{E}^W \end{pmatrix} \quad (38)$$

5. MATHEMATICAL APPROACH OF MAXWELL EQUATIONS FOR ELECTROMAGNETIC AND MAGNETIC WAVES VIA ALTERNATIVE MOVING FRAME

Maxwell's equations consist of four main equations that are very important for understanding electromagnetic theory. Maxwell's equations, together with the Lorentz force law, are a set of partial differential equations that form the basis for the fields of classical electrodynamics and optics. These equations describe how magnetic and electric fields are exchanged and produced by each other, by charges and currents. Maxwell equations are given by,

$$\nabla \cdot \vec{\mathbf{E}} = 0 \quad (39)$$

$$\nabla \cdot \vec{\mathbf{V}} = 0 \quad (40)$$

$$\nabla \times \vec{\mathbf{V}} = \epsilon v \frac{\partial \mathbf{E}}{\partial u} \quad (41)$$

$$\nabla \times \vec{\mathbf{E}} = -\frac{\partial \mathbf{V}}{\partial u} \quad (42)$$

where ϵ and v have the same values at all points and (s, c, w) and u space, time variables. If we assume that the electric field is perpendicular to the tangent direction and (17), (31) and (39), we can obtain;

$$\begin{aligned} \nabla \cdot \vec{\mathbf{E}} &= (\vec{N} \cdot \frac{\partial}{\partial s} + \vec{C} \cdot \frac{\partial}{\partial c} + \vec{W} \cdot \frac{\partial}{\partial w}) \cdot \vec{\mathbf{E}} \\ &= \vec{N} \cdot \frac{\partial \vec{\mathbf{E}}}{\partial s} + \vec{C} \cdot \frac{\partial \vec{\mathbf{E}}}{\partial c} + \vec{W} \cdot \frac{\partial \vec{\mathbf{E}}}{\partial w} \\ &= 0 \end{aligned}$$

that satisfies;

$$\mathbf{E}_c^C - \mathbf{E}_w^W = -\mathbf{E}^C \operatorname{div} \vec{C} + \mathbf{E}^W \operatorname{div} \vec{W}. \quad (43)$$

In the same way, we are aware that \mathbf{E} is right angle to the tangent directional and using (17), (31) and (40), we can compute that;

$$\begin{aligned}\nabla \cdot \vec{V} &= (\vec{N} \cdot \frac{\partial}{\partial s} + \vec{C} \frac{\partial}{\partial c} + \vec{W} \frac{\partial}{\partial w}) \cdot \vec{V} \\ &= \vec{N} \cdot \frac{\partial \vec{V}}{\partial s} + \vec{C} \cdot \frac{\partial \vec{V}}{\partial c} - \vec{W} \cdot \frac{\partial \vec{V}}{\partial w} \\ &= 0\end{aligned}$$

which implies that,

$$\mathbf{E}_c^W - \mathbf{E}_w^C = \mathbf{E}^C \operatorname{div} \vec{W} - \mathbf{E}^W \operatorname{div} \vec{C}. \quad (44)$$

If we think comprehensively (43) and (44), then it is calculated that Laplacian-like equations through C - lines and W - lines of the electromagnetic waves are as follows;

$$\begin{aligned}\frac{\partial^2}{\partial c^2} \mathbf{E}^W - \frac{\partial^2}{\partial w^2} \mathbf{E}^W &= \mathbf{E}^C ((\operatorname{div} \vec{W})_c + (\operatorname{div} \vec{C})_w) + \mathbf{E}^W ((\operatorname{div} \vec{W})_w + (\operatorname{div} \vec{C})_c) \\ &\quad + \operatorname{div} \vec{W} (\mathbf{E}_c^C + \mathbf{E}_w^W) + \operatorname{div} \vec{C} (\mathbf{E}_c^W + \mathbf{E}_w^C) \\ \frac{\partial^2}{\partial c^2} \mathbf{E}^C - \frac{\partial^2}{\partial w^2} \mathbf{E}^C &= \mathbf{E}^C ((\operatorname{div} \vec{W})_w - (\operatorname{div} \vec{C})_c) + \mathbf{E}^W ((\operatorname{div} \vec{W})_w - (\operatorname{div} \vec{C})_c) \\ &\quad + \operatorname{div} \vec{W} (\mathbf{E}_w^C - \mathbf{E}_c^W) + \operatorname{div} \vec{C} (\mathbf{E}_w^W - \mathbf{E}_c^C).\end{aligned}$$

If we consider that the electric field is right angle to the tangential direction and (17), (31) and (41), we get;

$$\begin{aligned}\nabla \times \vec{V} &= \epsilon v \frac{\partial \vec{E}}{\partial u} = (\vec{N} \cdot \frac{\partial}{\partial s} + \vec{C} \frac{\partial}{\partial c} + \vec{W} \frac{\partial}{\partial w}) \times \vec{V} \\ &= (\vec{N} \times \frac{\partial}{\partial s} \vec{V} + \vec{C} \times \frac{\partial}{\partial c} \vec{V} + \vec{W} \times \frac{\partial}{\partial w} \vec{V})\end{aligned}$$

which satisfies that;

$$\begin{aligned}\epsilon v \frac{\partial \vec{E}}{\partial u} &= -(\mathbf{E}_c^C + \mathbf{E}^W \operatorname{div} \vec{W} + \mathbf{E}_w^W + \mathbf{E}^C (f(s) + \operatorname{div} \vec{C}) \vec{N} \\ &\quad + (\mathbf{E}_s^C + \Lambda_c \mathbf{E}^W + \Psi_{ws} E^W) \vec{C} + (-\mathbf{E}_s^W - \Lambda_w \mathbf{E}^C + \Psi_{cs} \mathbf{E}^W) \vec{W}.\end{aligned}$$

In the same sense, we attention to the \vec{E} is right angle to the tangent directional and (17), (31) and (42), we can write that;

$$\begin{aligned}-\frac{\partial}{\partial u} \vec{V} &= \nabla \times \vec{E} = (\vec{N} \cdot \frac{\partial}{\partial s} + \vec{C} \frac{\partial}{\partial c} + \vec{W} \frac{\partial}{\partial w}) \times \vec{E} \\ &= \vec{N} \times \frac{\partial}{\partial s} \vec{E} + \vec{C} \times \frac{\partial}{\partial c} \vec{E} + \vec{W} \times \frac{\partial}{\partial w} \vec{E}\end{aligned}$$

which implies that,

$$-\frac{\partial}{\partial u} \vec{V} = (-\mathbf{E}_c^W + \mathbf{E}^C \operatorname{div} \vec{W} + E_w^C - \mathbf{E}^W (f(s) + \operatorname{div} \vec{C})) \vec{N} \\ + (-\mathbf{E}_s^C - \Lambda_c \mathbf{E}^C + \Psi_{ws} \mathbf{E}^W) \vec{C} + (-\mathbf{E}_s^W - \Psi_{cs} \mathbf{E}^C - \Lambda_w \mathbf{E}^W) \vec{W}.$$

6. CONCLUSION

In this study, we found the movement of polarized light along the optical fiber by calculating the equations of the electric field and magnetic field in cases where the frame of the space is at a right angle with respect to the alternative frame's vector fields. Thus, we had the opportunity to examine the motion of light in the field of geometry. In this way, the relationship of the motion of light in space with special curves, which is an important subject of geometry, can be investigated. At the same time, we investigated the geometric phase issue and Maxwell's equations together. We have obtained two important cases. These situations gave us the chance to examine the motion of light in the C - *direction* and in the direction of the Darboux vector. We also give their connections with Fermi-Walker parallel transportation laws via alternative moving frame. For further research, we aim to study Maxwellian evolution equations relationship between spherical coordinates to better understand the solutions of the equations.

Author Contribution Statements The authors contributed equally to this work. All authors read and approved the final copy of this paper.

Declaration of Competing Interests The authors declare that they have no known competing financial interest or personal relationships that could have appeared to influence the work reported in this paper.

Acknowledgements We are grateful to the referees for their very helpful comments and suggestions.

REFERENCES

- [1] Marris, A., Passman, S., Vector fields and flows on developable surfaces, *Arch. Ration. Mech. Anal.*, 32(1) (1969), 29-86.
- [2] Mukhopadhyay, A., Vyas, V., Panigrahi, P., Rogue waves and breathers in Heisenberg spin chain, *Eur. Phys. J. B.*, 88 (2015), 188. <https://doi.org/10.1140/epjb/e2015-60229-8>
- [3] Uzunoglu, B., Gök, I., Yaylı, Y., A new approach on curves of constant precession, *Appl. Math. Comput.*, 27 (2016), 317-323.
- [4] Frins, E. M., Dultz, W., Rotation of the polarization plane in optical fibers, *J. Lightwave Tech.*, 15 (1997), 144-147.
- [5] Haldane, F. D. M., Path dependence of the geometric rotation of polarization in optical fibers, *Opt. Lett.*, 11 (1986), 730-732.
- [6] Ceyhan, H., Özdemir, Z., Gök I., Ekmekci, F. N., Electromagnetic curves and rotation of the polarization plane through alternative moving frame, *Eur. Phys. J. Plus.*, 135(867) (2020). <https://doi.org/10.1140/epjp/s13360-020-00881-z>

- [7] Satija, I. I., Balakrishnan, R., Geometric phases in twisted strips, *Arch. Phys. Lett. A.*, 373 (2009), 3582-3585. <https://doi.org/10.1016/j.physleta.2009.07.083>
- [8] Amor, J., Gimenez, A., Lucas, P., Integrability aspects of the vortex filaments equation for pseudo-null curves, *Int. J. Geom. Methods Mod. Phys.*, 14 (2017), 1750090. <https://doi.org/10.1142/S0219887817500906>
- [9] Cabrerizo, J. L., Fernandez, M., Gomez, J. S., The contact magnetic flow in 3D Sasakian manifolds, *J. Phys. A: Math. Theor.*, 42 (2009), 195201. doi 10.1088/1751-8113/42/19/195201
- [10] Cabrerizo, J. L., Magnetic fields in 2D and 3D sphere, *J. Nonlinear. Math. Phys.*, 20 (2013), 440-450. <https://doi.org/10.1080/14029251.2013.855052>
- [11] Ross, J. N., The rotation of the polarization in low birefringence monomode optical fibres due to geometric effects, *Opt. Quantum Electron.*, 16 (1984), 455-461.
- [12] Barros, M., Romero, A., Cabrerizo, J. L., Fernandez, M., The Gauss-Landau-Hall problem on Riemannian surfaces, *J. Math. Phys.*, 46 (2005), 112905. <https://doi.org/10.1063/1.2136215>
- [13] Barros, M., Cabrerizo, J. L., Fernandez, M., Romero, A., Magnetic vortex filament flows, *J. Math. Phys.*, 48 (2007), 082904. <https://doi.org/10.1063/1.2767535>
- [14] Grbovic, M., Nesovic, E., On Backlund transformation and vortex filament equation for pseudo-null curves in Minkowski 3-space, *Int. J. Geom. Methods Mod. Phys.*, 13 (2016), 1650077. doi 10.1142/S0219887816500778
- [15] Unger, M., Unger, L.P., Gizé, A., The Theory of Quantum Torus Knots: Its Foundation in Differential Geometry - Volume II, Lulu, USA, 2020.
- [16] Berry, M. V., Quantal phase factors accompanying adiabatic changes, *Proc. R. Soc. Lond. A.*, 392 (1984), 45-57.
- [17] Gürbüz, N., The pseudo-null geometric phase along optical fiber, *Int. J. Geom. Methods Mod. Phys.*, 18(14) (2021), 2150230. doi 10.1142/S0219887821502303
- [18] Yamashita, O., Geometrical phase shift of the extrinsic orbital momentum density of light propagating in a helically wound optical fiber, *Opt. Commun.*, 285 (2012), 3061-3065. <https://doi.org/10.1016/j.optcom.2012.02.041>
- [19] Dandoloff, R., Zakrzewski, W. J., Parallel transport along a space curve and related phases, *J. Phys. A: Math. Gen.*, 22 (1989), L461-L466.
- [20] Rytov, S. M., Dokl. Akad. Nauk. SSSR 18 (1938) 263; Topological Phases in Quantum Theory, eds. B. Markovski and S. I. Vinitzky (World Scientific, Singapore, 1989) (reprinted).
- [21] Körpınar, T., Demirkol, R. C., Körpınar, Z., Asil, V., Maxwellian evolution equations along the uniform optical fiber in Minkowski space, *Rev. Mex. de Fis.*, 66 (2020), 431-439. <https://doi.org/10.31349/RevMexFis.66.431>
- [22] Körpınar, T., Optical directional binormal magnetic flows with geometric phase: Heisenberg ferromagnetic model, *Optik* 219 (2020), 165134. <https://doi.org/10.1016/j.ijleo.2020.165134>
- [23] Körpınar, T., Körpınar, Z., Demirkol, R. C., Binormal schrodinger system of wave propagation field of light radiate in the normal direction with q-HATM approach, *Optik*, 235 (2021), 166444. <https://doi.org/10.1016/j.ijleo.2021.166444>
- [24] Körpınar, T., Demirkol, R. C., Körpınar, Z., Approximate solutions for the inextensible Heisenberg antiferromagnetic flow and solitonic magnetic flux surfaces in the normal direction in Minkowski space. *Optik*, 238 (2021), 166403. <https://doi.org/10.1016/j.ijleo.2021.166403>
- [25] Körpınar, T., Demirkol, R. C., Körpınar, Z., Binormal schrodinger system of Heisenberg ferromagnetic equation in the normal direction with Q-HATM approach, *Int. J. Geom. Methods Mod. Phys.*, 18(6) (2021), 2150082. doi 10.1142/S0219887821500821
- [26] Banica, V., Miot, E., Evolution, interaction and collisions of vortex filaments, *Differential Integral Equations*, 26(3/4) (2013), 355.
- [27] Özdemir, Z., A new calculus for the treatment of Rytov's law in the optical fiber, *Int. J. Light Electr. Opt.*, 216 (2020), 164892. <https://doi.org/10.1016/j.ijleo.2020.164892>



NEW PROOFS OF FEJER'S AND DISCRETE HERMITE-HADAMARD INEQUALITIES WITH APPLICATIONS

Cagla SEKIN¹, Mehmet Emin TAMAR² and Ilham A. ALIYEV³

^{1,3}Department of Mathematics, Akdeniz University, Antalya, TÜRKİYE
²Department of Mathematics, Abdullah Gul University, Kayseri, TÜRKİYE

ABSTRACT. New proofs of the classical Fejer inequality and discrete Hermite-Hadamard inequality (HH) are presented and several applications are given, including (HH)-type inequalities for the functions, whose derivatives have inflection points. Moreover, some estimates from below and above for the first moments of functions $f : [a, b] \rightarrow \mathbb{R}$ about the midpoint $c = (a+b)/2$ are obtained and the reverse Hardy inequality for convex functions $f : (0, \infty) \rightarrow (0, \infty)$ is established.

1. INTRODUCTION

The famous Hermite-Hadamard inequality (HH) asserts that the integral mean value of a convex function $f : [a, b] \rightarrow \mathbb{R}$ can be estimated above and below by its values at the points a, b and $(a+b)/2$. More precisely,

$$f\left(\frac{a+b}{2}\right) \leq \frac{1}{b-a} \int_a^b f(x)dx \leq \frac{f(a)+f(b)}{2}. \quad (\text{HH})$$

Equality holds only for functions of the form $f(x) = cx + d$. Following Niculescu and Persson [17], we denote the right and left sides of (HH) by (RHH) and (LHH), respectively.

(HH) has many generalizations, extensions and refinements. There is an extensive literature in this area, such as books by Niculescu and Persson [18]; Mitrinovic,

2020 *Mathematics Subject Classification*. Primary 26D10; Secondary 26D15, 26A51.

Keywords. Fejer inequality, convex functions, discrete Hermite-Hadamard inequality, Jensen inequality, Hardy inequality.

¹ ✉ caglasekin@akdeniz.edu.tr; 0000-0001-7176-5164;

² ✉ mehmetemin.tamar@agu.edu.tr; 0000-0001-8933-8769

³ ✉ ialiev@akdeniz.edu.tr-Corresponding author; 0000-0003-2353-7700.

Pecaric and Fink [16]; Dragomir and Pearce [6] and papers [1, 5, 7, 12, 15, 17, 19, 21, 22], which are a small part of the relevant references.

The content of this article is organized as follows.

In Section 2 we give two new proofs of (HH). We first present a short proof of Fejer's inequality, from which (HH) follows immediately. The second proof includes a discrete version of (HH), which, in our opinion, is of independent interest. As an application, we give an estimation from below and above of the integral of the convex function $f : [0, \infty) \rightarrow (0, \infty)$ via the series $\sum_1^{\infty} f(k)$ and $\sum_1^{\infty} f(k - \frac{1}{2})$.

In Section 3, we give some new inequalities arising as a combination of (HH) with Hardy's inequality and iterated Hölder's inequality. For example, as a consequence we prove that, if $f : (0, \infty) \rightarrow (0, \infty)$ is convex and $f \in L_p(0, \infty)$, $\forall p > 1$, then

$$\lim_{p \rightarrow \infty} \frac{\|\frac{1}{x} \int_0^x f\|_p}{\|f\|_p} = 1.$$

Moreover, we obtain a reverse Hardy inequality for some family of convex functions on $(0, \infty)$.

Section 4 is devoted to the (HH)-type inequalities for the functions whose first derivatives have an inflection point. As a particular case, we show that if f' is concave on $[a, \frac{a+b}{2}]$ and convex on $[\frac{a+b}{2}, b]$, then

$$\frac{f(a) + f(b)}{2} - \frac{1}{b-a} \int_a^b f(x) dx \leq \frac{b-a}{12} (f'(b) - f'(a)).$$

In the last section we prove various inequalities for functions having convex first or second order derivatives. According to the authors' knowledge, there are some inequalities for functions whose *absolute values* of the derivatives are convex, see, e.g. [2, 5, 19]. In Theorems [7, 8, and 9] the convexity condition is imposed on the derivatives themselves, not on their absolute values. One of the interesting particular results obtained in this section is as follows.

Given $f : [a, b] \rightarrow \mathbb{R}$, let f' be convex. Then

$$\int_{\frac{a+b}{2}}^b f(x) dx - \int_a^{\frac{a+b}{2}} f(x) dx \leq \frac{b-a}{4} (f(b) - f(a)).$$

Another new result in this section is the estimation from below and above of the first moment about the midpoint $c = (a+b)/2$ of a function $f : [a, b] \rightarrow \mathbb{R}$, i.e. the integral $M_f = \int_a^b (x - \frac{a+b}{2}) f(x) dx$, when f' is convex.

2. NEW PROOFS OF FEJER'S INEQUALITY AND DISCRETE (HH)

At first, we give an auxiliary inequality that is satisfied by convex functions.

Lemma 1. (cf. [11] and Lemma 1.3 in [15]) *Let f be a convex function on $[a, b]$. Then*

$$f(a) + f(b) \geq f(a+b-x) + f(x), \quad (\forall x \in [a, b]). \quad (1)$$

By making use of (1) we give here a short proof of the (HH) "without pulling the pen on the paper". More precisely, we give a short proof of a generalization of Hermite-Hadamard's inequality, which is named as the Fejer inequality and asserts that if f is convex on $[a, b]$ and the function $g : [a, b] \rightarrow [0, \infty)$ is integrable and symmetric with respect to the midpoint $\frac{a+b}{2}$, i.e. $g(a+b-x) = g(x)$, ($\forall x \in [a, b]$), then

$$f\left(\frac{a+b}{2}\right) \int_a^b g(x)dx \leq \int_a^b f(x)g(x)dx \leq \frac{f(a)+f(b)}{2} \int_a^b g(x)dx. \quad (2)$$

For $g = 1$, (2) turns into (HH).

To prove this inequality we will use of (1) and the following easily verifiable equality:

$$\int_a^b f(x)g(x)dx = \frac{1}{2} \int_a^b [f(x) + f(a+b-x)]g(x)dx. \quad (3)$$

Now, we give a short proof of (2):

We have

$$\begin{aligned} f\left(\frac{a+b}{2}\right) \int_a^b g(x)dx &= \int_a^b f\left(\frac{a+b}{2}\right) g(x)dx = \int_a^b f\left(\frac{x+a+b-x}{2}\right) g(x)dx \\ &\leq \frac{1}{2} \int_a^b [f(x) + f(a+b-x)]g(x)dx \stackrel{(3)}{=} \int_a^b f(x)g(x)dx \\ &\stackrel{(3)}{=} \frac{1}{2} \int_a^b [f(x) + f(a+b-x)]g(x)dx \\ &\stackrel{(1)}{\leq} \frac{f(a)+f(b)}{2} \int_a^b g(x)dx, \end{aligned}$$

which is nothing but Fejer's inequality (2).

Remark 1. Although the (HH) has several proofs, as far as we know the first simple proof was given by Azbetia [3]; (see, also Niculescu and Persson [17], p. 664). Another simple proof and refinement was given by El Farissi [8].

The inequality given in the following theorem is a discrete version of (HH), and classical (HH) can be obtained by passing to limit in this inequality.

Theorem 1. If $f : [a, b] \rightarrow \mathbb{R}$ is convex and $x_k = a + k\frac{b-a}{n}$, ($k = 1, 2, \dots, n$), then

$$f\left(\frac{\left(1 - \frac{1}{n}\right)a + \left(1 + \frac{1}{n}\right)b}{2}\right) \leq \frac{1}{n} \sum_{k=1}^n f(x_k) \leq \frac{1}{2} \left[f(a) \left(1 - \frac{1}{n}\right) + f(b) \left(1 + \frac{1}{n}\right) \right]. \quad (4)$$

Proof. Let $x_k = a + k\frac{b-a}{n}$, ($k = 1, 2, \dots, n$). Then writing x_k as

$$x_k = \frac{b-x_k}{b-a}a + \frac{x_k-a}{b-a}b$$

and using

$$f(x_k) \leq \frac{b-x_k}{b-a} f(a) + \frac{x_k-a}{b-a} f(b),$$

one has

$$\begin{aligned} \sum_{k=1}^n f(x_k) &\leq \frac{f(a)}{b-a} \sum_{k=1}^n (b-x_k) + \frac{f(b)}{b-a} \sum_{k=1}^n (x_k-a) \\ &= \frac{1}{2} [f(a)(n-1) + f(b)(n+1)], \end{aligned}$$

and therefore,

$$\frac{1}{n} \sum_{k=1}^n f(x_k) \leq \frac{1}{2} \left[f(a) \left(1 - \frac{1}{n}\right) + f(b) \left(1 + \frac{1}{n}\right) \right]. \tag{5}$$

On the other hand, the Jensen inequality yields

$$\frac{1}{n} \sum_{k=1}^n f(x_k) \geq f\left(\frac{1}{n} \sum_{k=1}^n x_k\right) = f\left(\frac{(1-\frac{1}{n})a + (1+\frac{1}{n})b}{2}\right). \tag{6}$$

By combining (5) and (6) we obtain (4). □

Corollary 1. *After taking limit as $n \rightarrow \infty$ in (4) and using the fact that the convex function is continuous (maybe except the end-points a and b), we obtain (HH).*

The following two theorems are the simple consequences of (HH).

Theorem 2 (a "refinement" of (RHH)). *Let $f : [a, b] \rightarrow \mathbb{R}$ be convex. Then*

$$\begin{aligned} \frac{1}{b-a} \int_a^b f(x) dx &\leq \frac{1}{b-a} \int_a^b f(x) \left[\ln \frac{(b-a)^2}{(b-x)(x-a)} - 1 \right] dx \\ &\leq \frac{f(a) + f(b)}{2} \end{aligned} \tag{7}$$

Proof. For any $x \in (a, b]$ one has

$$f\left(\frac{a+x}{2}\right) \leq \frac{1}{x-a} \int_a^x f(t) dt \leq \frac{f(a) + f(x)}{2}.$$

Integrating over (a, b) we have

$$\int_a^b f\left(\frac{a+x}{2}\right) dx \leq \int_a^b \frac{1}{x-a} \left(\int_a^x f(t) dt \right) dx \leq \int_a^b \frac{f(a) + f(x)}{2} dx. \tag{8}$$

After simple calculations, (8) leads to

$$2 \int_a^{\frac{a+b}{2}} f(x) dx \leq \int_a^b f(x) \ln \frac{b-a}{x-a} dx \leq \frac{1}{2} \left[f(a)(b-a) + \int_a^b f(x) dx \right]. \tag{9}$$

Similarly, integrating the inequality

$$f\left(\frac{x+b}{2}\right) \leq \frac{1}{b-x} \int_x^b f(t)dt \leq \frac{f(x)+f(b)}{2}$$

over (a, b) we get

$$\int_a^b f\left(\frac{x+b}{2}\right) dx \leq \int_a^b \frac{1}{b-x} \left(\int_x^b f(t)dt\right) dx \leq \int_a^b \frac{f(x)+f(b)}{2} dx$$

which leads to

$$2 \int_{\frac{a+b}{2}}^b f(x)dx \leq \int_a^b f(x) \ln \frac{b-a}{b-x} dx \leq \frac{1}{2} \left[f(b)(b-a) + \int_a^b f(x)dx \right]. \quad (10)$$

After summing up (9) and (10) we obtain (7). \square

Theorem 3. Let $f : [0, \infty) \rightarrow (0, \infty)$ be a strictly convex function and $\sum_{k=1}^{\infty} f(k) < \infty$. Then

$$\sum_{k=1}^{\infty} f\left(k - \frac{1}{2}\right) < \int_0^{\infty} f(x)dx < \frac{1}{2}f(0) + \sum_{k=1}^{\infty} f(k). \quad (11)$$

Proof. For, $0 \leq a < b < \infty$, denote $x_0 = a$ and $x_k = a + k\frac{b-a}{n}$, $(k = 1, 2, \dots, n)$. Since f is strictly convex, we have

$$f\left(\frac{x_{k-1} + x_k}{2}\right) < \frac{1}{x_k - x_{k-1}} \int_{x_{k-1}}^{x_k} f(x)dx < \frac{f(x_{k-1}) + f(x_k)}{2}, \quad (k = 1, 2, \dots, n).$$

Taking into account the formulas

$$x_k - x_{k-1} = \frac{b-a}{n} \quad \text{and} \quad \frac{x_{k-1} + x_k}{2} = a + \left(k - \frac{1}{2}\right) \frac{b-a}{n}$$

and summing the inequalities above we obtain

$$\begin{aligned} \sum_{k=1}^n \frac{1}{n} f\left(a + \left(k - \frac{1}{2}\right) \frac{b-a}{n}\right) &< \frac{1}{b-a} \int_a^b f(x)dx \\ &< \frac{1}{n} \left[\frac{f(a) + f(b)}{2} + \sum_{k=1}^{n-1} f\left(a + k \frac{b-a}{n}\right) \right]. \end{aligned}$$

Setting now $a = 0$, $b = n$ we have

$$\sum_{k=1}^n f\left(k - \frac{1}{2}\right) < \int_0^n f(x)dx < \frac{f(0) + f(n)}{2} + \sum_{k=1}^{n-1} f(k).$$

Taking limit as $n \rightarrow \infty$ and using $\lim_{n \rightarrow \infty} f(n) = 0$ we obtain the desired formula (11). \square

Remark 2. Since $f : [0, \infty) \rightarrow (0, \infty)$ is convex and $\lim_{n \rightarrow \infty} f(n)$ is finite (actually, zero), then f is monotonically decreasing and therefore the comparison of the areas under graphics gives the following well-known inequalities

$$\sum_{k=1}^{\infty} f(k) < \int_0^{\infty} f(x) dx < f(0) + \sum_{k=1}^{\infty} f(k). \tag{12}$$

It is clear that, the inequalities (11) are better than (12).

Example 1. If $f(x) = e^{-x}$ then from (11) we have

$$\frac{\sqrt{e}}{e-1} < 1 < \frac{1}{2} + \frac{1}{e-1} \text{ and therefore, } \sqrt{e} < e-1 < \frac{1}{2}(e+1),$$

whereas the formula (12) gives the rougher estimate $1 < e-1 < e$.

3. SOME INEQUALITIES ARISING AS A COMBINATION OF (HH) WITH THE OTHER INEQUALITIES

Theorem 4. Let $1 < p < \infty$ and $\alpha p > 1$. Let further, $f : (0, \infty) \rightarrow (0, \infty)$ be convex and such that

$$\|x^{1-\alpha} f(x)\|_p \equiv \left(\int_0^{\infty} (x^{1-\alpha} f(x))^p dx \right)^{1/p} < \infty.$$

Then

$$2^{1-\alpha+\frac{1}{p}} \leq \frac{\|x^{-\alpha} \int_0^x f\|_p}{\|x^{1-\alpha} f(x)\|_p} \leq \frac{1}{\alpha - 1/p}. \tag{13}$$

Corollary 2. (a) If $\alpha = 1$, then

$$2^{\frac{1}{p}} \leq \frac{\|\frac{1}{x} \int_0^x f\|_p}{\|f\|_p} \leq \frac{1}{1 - 1/p}. \tag{14}$$

(b) Let, in addition, $f \in L_p(0, \infty)$, ($\forall p > 1$). Then by taking the limit in (14) as $p \rightarrow \infty$ one has

$$\lim_{p \rightarrow \infty} \frac{\|\frac{1}{x} \int_0^x f\|_p}{\|f\|_p} = 1. \tag{15}$$

Proof of Theorem 4. We will use the classical weighted Hardy inequality, which asserts that

$$\left(\int_0^{\infty} \left| x^{-\alpha} \int_0^x f(t) dt \right|^p dx \right)^{1/p} \leq c \left(\int_0^{\infty} |x^{1-\alpha} f(x)|^p dx \right)^{1/p}, \tag{16}$$

where $c = \frac{p}{\alpha p - 1}$, $1 < p < \infty$, $\alpha p > 1$.

Now, by (LHH) we have

$$f\left(\frac{x}{2}\right) < \frac{1}{x} \int_0^x f(t) dt \Rightarrow x^{1-\alpha} f\left(\frac{x}{2}\right) < x^{-\alpha} \int_0^x f(t) dt,$$

and therefore

$$\int_0^\infty \left(x^{1-\alpha} f\left(\frac{x}{2}\right)\right)^p dx \leq \int_0^\infty \left(x^{-\alpha} \int_0^x f(t) dt\right)^p dx$$

$$\stackrel{(16)}{\leq} \left(\frac{p}{\alpha p - 1}\right)^p \int_0^\infty (x^{1-\alpha} f(x))^p dx. \tag{17}$$

Since

$$\int_0^\infty \left(x^{1-\alpha} f\left(\frac{x}{2}\right)\right)^p dx = 2^{p(1-\alpha)+1} \int_0^\infty (x^{1-\alpha} f(x))^p dx,$$

we have from (17) the desired result (13) and its consequences (14) and (15). \square

Remark 3. The left hand side of (13) shows that under the conditions of Theorem 4 the following reverse Hardy's inequality is valid:

$$\left\|x^{-\alpha} \int_0^x f\right\|_p \geq 2^{1-\alpha+\frac{1}{p}} \|x^{1-\alpha} f(x)\|_p.$$

Example 2. a) Let $k > 0$ and $f(x) = e^{-kx}$. Then (15) yields

$$\lim_{p \rightarrow \infty} \left(\int_0^\infty \left(\frac{1 - e^{-kx}}{x}\right)^p dx\right)^{1/p} = k.$$

b) If $f(x) = \frac{1}{x+1}$, ($0 < x < \infty$), then from (15) we have

$$\lim_{p \rightarrow \infty} \left(\int_0^\infty \frac{\ln^p(x+1)}{x^p} dx\right)^{1/p} = 1.$$

In the next theorem we will make use of a combination of (RHH)

$$\frac{1}{b-a} \int_a^b f(x) dx \leq \frac{f(a) + f(b)}{2}$$

and the inequality

$$\left(\int_a^b \left(\prod_{k=1}^n u_k(x)\right) dx\right)^n \leq \prod_{k=1}^n \left(\int_a^b u_k^n(x) dx\right), \tag{18}$$

where $u_1 \geq 0, \dots, u_n \geq 0$.

Recall that the inequality (18) is a special case of the iterated Hölder inequality.

We need also the following

Lemma 2. If $u : [a, b] \rightarrow (0, \infty)$ is convex, then u^n is convex as well for any $n \in \mathbb{N}$.

This Lemma is actually a special case of the following more general proposition:

If $u : [a, b] \rightarrow (0, \infty)$ is convex and $f : (0, \infty) \rightarrow (0, \infty)$ is increasing and convex, then the composition $f \circ u : [a, b] \rightarrow (0, \infty)$ is convex as well. Here, we get $f(t) = t^n$, ($0 < t < \infty$). Note that Lemma 2 can also be proved by induction.

Remark 4. The convexity of the functions $u_1 \geq 0, u_2 \geq 0, \dots, u_n \geq 0$ does not guarantee the convexity of their product $u_1 u_2 \cdots u_n$. Indeed, for example, although the functions $u_1(x) = x^2, u_2(x) = x^2, \dots, u_{n-1}(x) = x^2$ and $u_n(x) = (2-x)^{2n-2}$, ($n \geq 2$) are convex on $[0, 2]$, their product $u(x) = x^{2n-2}(2-x)^{2n-2}$ is not convex because of $u''(1) = 4(2n-2)(1-n) < 0$.

Theorem 5. For given $n \geq 2$, let the functions $u_1 \geq 0, u_2 \geq 0, \dots, u_n \geq 0$ be convex on $[a, b]$. Then

$$\frac{1}{b-a} \int_a^b \left(\prod_{k=1}^n u_k(x) \right) dx \leq \frac{1}{2} \prod_{k=1}^n (u_k^n(a) + u_k^n(b))^{\frac{1}{n}}. \tag{19}$$

Proof. Since u_k , ($k = 1, 2, \dots, n$) is convex on $[a, b]$, then u_k^n is also convex by Lemma 2. Then the (RHH) yields

$$\frac{1}{b-a} \int_a^b u_k^n(x) dx \leq \frac{1}{2} [u_k^n(a) + u_k^n(b)], \quad (k = 1, 2, \dots, n).$$

By multiplying these inequalities we have

$$\frac{1}{(b-a)^n} \prod_{k=1}^n \left(\int_a^b u_k^n(x) dx \right) \leq \frac{1}{2^n} \prod_{k=1}^n (u_k^n(a) + u_k^n(b)). \tag{20}$$

Here, by making use of the inequality (18), we get

$$\frac{1}{(b-a)^n} \left(\int_a^b \left(\prod_{k=1}^n u_k(x) \right) dx \right)^n \leq \frac{1}{2^n} \prod_{k=1}^n (u_k^n(a) + u_k^n(b)),$$

from which the inequality (19) follows. □

Remark 5. For $n = 2$, the inequality (19) was proved by Amrahov [1]. Another generalization of Amrahov's result for the product of two functions was noted by D. A. Ion [12]:

If $u \geq 0, v \geq 0$ are convex and $\frac{1}{p} + \frac{1}{q} = 1$, ($1 < p, q < \infty$), then

$$\frac{1}{b-a} \int_a^b u(t)v(t)dt \leq \frac{1}{2} (u^p(a) + u^p(b))^{1/p} (u^q(a) + u^q(b))^{1/q}.$$

It should also be mentioned that, in the same paper [12] Ion gives some generalization of Amrahov's result for the product of two functions in Orlicz spaces.

4. (RHH)-TYPE INEQUALITY FOR THE FUNCTIONS WHOSE DERIVATIVES HAVE AN INFLECTION POINT

Theorem 6. Given $c \in [a, b]$ and $f : [a, b] \rightarrow \mathbb{R}$, let the derivative f' be concave on $[a, c]$ and convex on $[c, b]$. Then

$$\left[\frac{c-a}{b-a} f(a) + \frac{b-c}{b-a} f(b) \right] - \frac{1}{b-a} \int_a^b f(x) dx$$

$$\leq \frac{1}{3} \left[\frac{(b-c)^2}{b-a} f'(b) - \frac{(c-a)^2}{b-a} f'(a) + \left(\frac{a+b}{2} - c \right) f'(c) \right]. \quad (21)$$

Corollary 3. In case of $c = \frac{a+b}{2}$ we have

$$\frac{f(a) + f(b)}{2} - \frac{1}{b-a} \int_a^b f(x) dx \leq \frac{b-a}{12} (f'(b) - f'(a))$$

Proof of Theorem 6. Integration by parts yields

$$\begin{aligned} \frac{c-a}{b-a} f(a) + \frac{b-c}{b-a} f(b) - \frac{1}{b-a} \int_a^b f(x) dx &= \frac{1}{b-a} \int_a^b (x-c) f'(x) dx \\ &= \frac{1}{b-a} \int_a^c (x-c) f'(x) dx + \frac{1}{b-a} \int_c^b (x-c) f'(x) dx \\ &\equiv A + B. \end{aligned}$$

By changing variables as $x = (1-\lambda)a + \lambda c$, ($0 < \lambda < 1$) in A and $x = (1-\lambda)c + \lambda b$ in B and applying Jensen's inequality, we have

$$\begin{aligned} A &\equiv \frac{1}{b-a} \int_a^c (x-c) f'(x) dx = \frac{(a-c)^2}{b-a} \int_0^1 (\lambda-1) f'((1-\lambda)a + \lambda c) d\lambda \\ &\leq \frac{(a-c)^2}{b-a} \int_0^1 (\lambda-1) [(1-\lambda) f'(a) + \lambda f'(c)] d\lambda \\ &= -\frac{(a-c)^2}{6(b-a)} [2f'(a) + f'(c)]; \end{aligned} \quad (22)$$

$$\begin{aligned} B &\equiv \frac{1}{b-a} \int_c^b (x-c) f'(x) dx = \frac{(b-c)^2}{(b-a)} \int_0^1 \lambda f'((1-\lambda)c + \lambda b) d\lambda \\ &\leq \frac{(b-c)^2}{(b-a)} \int_0^1 (\lambda(1-\lambda) f'(c) + \lambda^2 f'(b)) d\lambda \\ &= \frac{(b-c)^2}{6(b-a)} [f'(c) + 2f'(b)]. \end{aligned} \quad (23)$$

It follows from (22) and (23) that

$$A + B \leq \frac{1}{3} f'(b) \frac{(b-c)^2}{b-a} - \frac{1}{3} f'(a) \frac{(a-c)^2}{b-a} + \frac{1}{6} f'(c) (a+b-2c),$$

which completes the proof. \square

Remark 6. A simple calculation shows that the equality in (21) holds for the functions $f(x) = k(x-c)^2 + m$, ($k, m \in \mathbb{R}$).

Remark 7. In the "critical" cases $c = a$ or $c = b$, i.e. in the cases when f' is convex or concave on $[a, b]$ we have from (21)

$$f(b) - \frac{1}{b-a} \int_a^b f(x)dx \leq \frac{b-a}{6} [f'(a) + 2f'(b)]$$

and

$$f(a) - \frac{1}{b-a} \int_a^b f(x)dx \leq -\frac{b-a}{6} [2f'(a) + f'(b)],$$

respectively.

5. VARIOUS INEQUALITIES FOR FUNCTIONS HAVING CONVEX FIRST OR SECOND ORDER DERIVATIVES

The first moment of a function f about the center point $c = (a + b)/2$ is defined by $M_f = \int_a^b (x - \frac{a+b}{2}) f(x)dx$. In the following theorem we obtain some estimation from above and below for M_f , when f' is convex.

Theorem 7. Suppose that the derivative f' of the function $f : [a, b] \rightarrow \mathbb{R}$ is convex. Then the first moment of f about the center point $c = (a+b)/2$ satisfies the following inequality

$$A \leq \int_a^b \left(x - \frac{a+b}{2}\right) f(x)dx \leq B, \tag{24}$$

where

$$A = \frac{(a-b)^2}{8} (f(b) - f(a)) - \frac{(b-a)^3}{48} (f'(a) + f'(b))$$

and

$$B = \frac{(b-a)^3}{24} (f'(a) + f'(b)).$$

Proof. Integration by parts leads to

$$\begin{aligned} \int_a^b (x-a)(b-x)f'(x)dx &= \int_a^b (x-a)(b-x)df(x) \\ &= 2 \int_a^b \left(x - \frac{a+b}{2}\right) f(x)dx. \end{aligned}$$

Hence,

$$\begin{aligned} \int_a^b \left(x - \frac{a+b}{2}\right) f(x)dx &= \frac{1}{2} \int_a^b (x-a)(b-x)f'(x)dx \\ \text{(set } x &= (1-t)a + tb, (x-a)(b-x) = (b-a)^2 t(1-t), 0 \leq t \leq 1) \\ &= \frac{1}{2} (b-a)^3 \int_0^1 t(1-t)f'((1-t)a + tb)dt \\ &\leq \frac{1}{2} (b-a)^3 \int_0^1 t(1-t)[f'(a)(1-t) + f'(b)t]dt \end{aligned}$$

$$= \frac{(b-a)^3}{24}(f'(a) + f'(b)).$$

This proved the right hand side of (24).

Further, again using integration by parts we have

$$\int_a^b \left(x - \frac{a+b}{2}\right)^2 f'(x) dx = \frac{(b-a)^2}{4}(f(b) - f(a)) - 2 \int_a^b \left(x - \frac{a+b}{2}\right) f(x) dx,$$

and therefore,

$$\int_a^b \left(x - \frac{a+b}{2}\right) f(x) dx = \frac{(b-a)^2}{8}(f(b) - f(a)) - \frac{1}{2} \int_a^b \left(x - \frac{a+b}{2}\right)^2 f'(x) dx. \quad (25)$$

Furhermore, setting $x = (1-t)a + tb$, $\left(x - \frac{a+b}{2}\right)^2 = (b-a)^2 \left(t - \frac{1}{2}\right)^2$ and $dx = (b-a)dt$, ($0 \leq t \leq 1$), we get

$$\begin{aligned} \int_a^b \left(x - \frac{a+b}{2}\right)^2 f'(x) dx &= (b-a)^3 \int_0^1 \left(t - \frac{1}{2}\right)^2 f'((1-t)a + tb) dt \\ &\leq (b-a)^3 \int_0^1 \left(t - \frac{1}{2}\right)^2 [(1-t)f'(a) + tf'(b)] dt \\ &= (b-a)^3 \left[f'(a) \int_0^1 \left(t - \frac{1}{2}\right)^2 (1-t) dt + f'(b) \int_0^1 t \left(t - \frac{1}{2}\right)^2 dt \right] \\ &= \frac{(b-a)^3}{24}(f'(a) + f'(b)). \end{aligned}$$

Taking into account this in (25) we obtain the left hand side of inequality (24).

The proof is complete. \square

A straightforward calculation shows that the equality in both sides of (24) is attained for $f(x) = k(x^2 - (a+b)x) + n$, where k and n are arbitrary real numbers.

Theorem 8. Given $f : [a, b] \rightarrow \mathbb{R}$, let f'' be convex. Then the following inequality holds

$$A \leq \frac{f(a) + f(b)}{2} - \frac{1}{b-a} \int_a^b f(x) dx \leq B, \quad (26)$$

where

$$A = \frac{b-a}{8}(f'(b) - f'(a)) - \frac{(b-a)^2}{48}(f''(a) + f''(b))$$

and

$$B = \frac{(b-a)^2}{24}(f''(a) + f''(b)).$$

Proof. Integration by parts twice gives

$$\int_a^b (x-a)(b-x)f''(x) dx = (b-a)(f(a) + f(b)) - 2 \int_a^b f(x) dx.$$

Hence,

$$\begin{aligned} \frac{f(a) + f(b)}{2} - \frac{1}{b-a} \int_a^b f(x) dx &= \frac{1}{2(b-a)} \int_a^b (x-a)(b-x) f''(x) dx \\ &\quad (\text{Set } x = (1-t)a + tb, 0 \leq t \leq 1) \\ &= \frac{(b-a)^2}{2} \int_0^1 t(1-t) f''((1-t)a + tb) dt \\ &\leq \frac{(b-a)^2}{2} \int_0^1 t(1-t) [(1-t) f''(a) + t f''(b)] dt \\ &= \frac{(b-a)^2}{24} (f''(a) + f''(b)). \end{aligned}$$

The right hand side of (26) is proved.

Straightforward calculations show that, integration by parts twice yields

$$\begin{aligned} &\int_a^b \left(x - \frac{a+b}{2}\right)^2 f''(x) dx \\ &= \left(\frac{b-a}{2}\right)^2 (f'(b) - f'(a)) - 2(b-a) \left[\frac{f(a) + f(b)}{2} - \frac{1}{b-a} \int_a^b f(x) dx \right]. \end{aligned}$$

Hence,

$$\begin{aligned} &\frac{f(a) + f(b)}{2} - \frac{1}{b-a} \int_a^b f(x) dx \\ &= \frac{b-a}{8} (f'(b) - f'(a)) - \frac{1}{2(b-a)} \int_a^b \left(x - \frac{a+b}{2}\right)^2 f''(x) dx. \end{aligned} \quad (27)$$

Setting $x = (1-t)a + tb$, ($0 \leq t \leq 1$) and using the convexity of f'' , we have

$$\begin{aligned} \int_a^b \left(x - \frac{a+b}{2}\right)^2 f''(x) dx &= (b-a)^3 \int_0^1 \left(t - \frac{1}{2}\right)^2 f''((1-t)a + tb) dt \\ &\leq (b-a)^3 \left[f''(a) \int_0^1 \left(t - \frac{1}{2}\right)^2 (1-t) dt + f''(b) \int_0^1 \left(t - \frac{1}{2}\right)^2 t dt \right] \\ &= \frac{(b-a)^3}{24} (f''(a) + f''(b)). \end{aligned}$$

By making use of this in (27) we obtain the left hand side of inequality (26).

The proof is complete. □

It is easy to verify that the equality in both sides of (24) is attained for the functions $f(x) = k(2x^3 - 3(a+b)x^2) + mx + n$, with arbitrary real numbers k , m and n .

Remark 8. In the literature there are results of the type (24) and (26) under the condition of the convexity of $|f'|$ or $|f''|$ (see, e.g. [2, 5, 19]). As far as we know, the conditions and assertions of the theorems [7] and [8] completely differ from those known in the literature.

In the following theorem we give some estimations for the mean value of a function f whose first derivative is convex.

Theorem 9. Let $f : [a, b] \rightarrow \mathbb{R}$ be differentiable and its derivative f' be convex. Then

(a)

$$N \leq \frac{1}{b-a} \int_a^b f(x) dx \leq M, \quad (28)$$

where

$$N = \frac{1}{3}(f(a) + 2f(b)) - \frac{1}{6}f'(b)(b-a)$$

and

$$M = \frac{1}{3}(f(b) + 2f(a)) + \frac{1}{6}f'(a)(b-a);$$

(b)

$$\mathcal{N} \leq \frac{1}{b-a} \int_a^b f(x) dx \leq \mathcal{M}, \quad (29)$$

where

$$\mathcal{N} = f(a) + 2f\left(\frac{a+b}{2}\right) - \frac{4}{b-a} \int_a^{\frac{a+b}{2}} f(x) dx$$

and

$$\mathcal{M} = f(b) + 2f\left(\frac{a+b}{2}\right) - \frac{4}{b-a} \int_{\frac{a+b}{2}}^b f(x) dx.$$

Corollary 4.

$$\int_a^b f(x) dx - \int_a^{\frac{a+b}{2}} f(x) dx \leq \frac{1}{4}(b-a)(f(b) - f(a)). \quad (30)$$

Proof of Theorem 9. Since f' is convex, (HH) leads to

$$f'\left(\frac{a+x}{2}\right) \leq \frac{1}{x-a}(f(x) - f(a)) \leq \frac{f'(a) + f'(x)}{2}; \quad (31)$$

$$f'\left(\frac{x+b}{2}\right) \leq \frac{1}{b-x}(f(b) - f(x)) \leq \frac{f'(x) + f'(b)}{2}. \quad (32)$$

Multiplying the inequalities (31) by $(x-a)$ and integrating over $[a, b]$, after simple calculations we obtain

$$2(b-a)f\left(\frac{a+b}{2}\right) - 4 \int_a^{\frac{a+b}{2}} f(x) dx \leq \int_a^b f(x) dx - f(a)(b-a)$$

$$\leq \frac{1}{4}f'(a)(b-a)^2 + \frac{1}{2}(b-a)f(b) - \frac{1}{2} \int_a^b f(x)dx.$$

The above inequalities can be written as two separate inequalities:

$$\frac{1}{b-a} \int_a^b f(x)dx \leq \frac{1}{3}(2f(a) + f(b)) + \frac{1}{6}f'(a)(b-a) \tag{33}$$

and

$$\frac{1}{b-a} \int_a^b f(x)dx + \frac{4}{b-a} \int_a^{\frac{a+b}{2}} f(x)dx \geq f(a) + 2f\left(\frac{a+b}{2}\right). \tag{34}$$

In a similar way, multiplying inequalities (32) by $(b-x)$ and integrating over $[a, b]$, after some calculations we have the following two inequalities:

$$\frac{1}{b-a} \int_a^b f(x)dx \geq \frac{1}{3}(f(a) + 2f(b)) - \frac{1}{6}f'(b)(b-a) \tag{35}$$

and

$$\frac{1}{b-a} \int_a^b f(x)dx + \frac{4}{b-a} \int_{\frac{a+b}{2}}^b f(x)dx \leq f(b) + 2f\left(\frac{a+b}{2}\right). \tag{36}$$

Now, the inequalities (33) and (35) yields (28) and the inequalities (34) and (36) yields (29). The Corollary follows by subtracting (34) from (36).

The proof is complete. □

Example 3. For $f(x) = \ln x$, $0 < a < x < b < \infty$, the inequality (30) yields

$$a^{\frac{3a+b}{4(a+b)}} \cdot b^{\frac{a+3b}{4(a+b)}} \leq \frac{a+b}{2}. \tag{37}$$

Since $\alpha + \beta = 1$ for $\alpha = \frac{3a+b}{4(a+b)}$ and $\beta = \frac{a+3b}{4(a+b)}$, then by the generalized AM-GM inequality we have

$$a^\alpha \cdot b^\beta < \alpha \cdot a + \beta \cdot b = \frac{3a+b}{4(a+b)} \cdot a + \frac{a+3b}{4(a+b)} \cdot b. \tag{38}$$

A simple calculation shows that

$$\frac{a+b}{2} < \frac{3a+b}{4(a+b)} \cdot a + \frac{a+3b}{4(a+b)} \cdot b,$$

and therefore, the inequality (37) is better than (38).

Remark 9. In our opinion, most of the results in this article can also be examined for non-classical convexity types (abstract convexity, s -convexity, p -convexity, m -convexity, etc.). Necessary information about the mentioned convexity types can be found, for example, in [4, 5, 7, 13, 14, 20]

Author Contribution Statements The authors contributed equally. All authors read and approved the final copy of the paper.

Declaration of Competing Interests The authors declare that they have no competing financial interests and personal relationships that could have appeared to influence the work reported in this paper.

REFERENCES

- [1] Amrahov, S. E., A note on Hadamard inequalities for the product of the convex functions, *International J. of Research and Reviews in Applied Sciences*, 5(2) (2010), 168-170.
- [2] Alomari, M., Darus, M. and Dragomir, S. S., New inequalities of Hermite-Hadamard type for functions whose second derivatives absolute values are quasi-convex, *Tamkang J. Math.*, 41(4) (2010), 353-359.
- [3] Azpetia, A. G., Convex functions and the Hadamard inequality, *Revista Colombiana Mat.*, 28 (1994), 7-12.
- [4] Bakula, M. K., Özdemir, M. E. and Pecaric, J., Hadamard-type inequalities for m -convex and (α, m) -convex functions. *J. Ineq. Pure Appl. Math.*, 9(4) (2008), Article 96.
- [5] Chen, F., Liu, X., On Hermite-Hadamard type inequalities for functions whose second derivatives absolute values are s -convex, *ISRN Applied Mathematics*, (2014), 1-4, DOI 10.1155/2014/829158.
- [6] Dragomir, S. S., Pearce, C. E. M., Selected Topics on Hermite-Hadamard Inequalities and Applications, RGMIA Monographs, Victoria University, 2000.
- [7] Dragomir, S. S., On some new inequalities of Hermite-Hadamard type for m -convex functions, *Tamkang J. Math.*, 3(1) (2002).
- [8] El Farissi, A., Simple proof and refinement of Hermite-Hadamard inequality. *J. Math. Inequal*, 4(3) (2010), 365-369.
- [9] Fink, A. M., A best possible Hadamard inequality, *Math. Inequal Appl.*, 1 (1998), 223-230.
- [10] Florea, A., Niculescu, C. P., A Hermite-Hadamard inequality for convex-concave symmetric functions, *Bull. Soc. Sci. Math. Roum.*, 50(98) No:2 (2007), 149-156.
- [11] Hwang, D. Y., Tseng, K. L. and Yang, G. S., Some Hadamard's inequalities for co-ordinated convex functions in a rectangle from the plane, *Taiwanese J. Math.*, 11(1) (2007), 63-73, DOI 10.11650/twjm/1500404635.
- [12] Ion, D. A., On an inequality due to Amrahov, *Annals of University of Craiova, Math. Comp. Sci. Ser.*, 38(1) (2011), 92-95, DOI 10.52846/ami.v38i1.396.
- [13] Kemali, S., Yesilce, I., Adilov, G., B-Convexity, B-1-Convexity and Their Comparison, *Numerical Functional Analysis and Optimization*, 36(2) (2015), 133-146, 10.1080/01630563.2014.970641.
- [14] Kemali, S., Sezer, S., Tinaztepe, G., Adilov, G., s -Convex functions in the third sense, *Korean Journal of Mathematics*, 29(3) (2021), 593-602, DOI 10.11568/kjm.2021.29.3.593.
- [15] Mercer, A. M. D., A variant of Jensen's inequality, *J. Ineq. Pure and Appl. Math.*, 4(4) (2003), Article 73.
- [16] Mitrinovic, D. S., Pecaric, J. E. and Fink, A. M., Classical and New Inequalities in Analysis, Kluwer Academic, Dordrecht, 1993.
- [17] Niculescu C. P., Persson, L. E., Old and new on the Hermite-Hadamard inequality, *Real Anal. Exchange*, 29 (2003/2004), 663-686.
- [18] Niculescu C. P., Persson, L. E., Convex Functions and Their Applications, A Contemporary Approach, CMS Books in Mathematics, V.23, Springer-Verlag, 2006.
- [19] Sarikaya, M. Z., Saglam, A. and Yildirim, H., New inequalities of Hermite-Hadamard type for functions whose second derivatives absolute values are convex or quasi-convex, *International J. of Open Problems in Comp. Sci. and Math.*, 5(3) (2012), 1-14.

- [20] Sezer, S., Eken, Z., Tinaztepe, G., Adilov, G., p -Convex functions and some of their properties, *Numerical Functional Analysis and Optimization*, 42(4) (2021), 443-459, DOI 10.1080/01630563.2021.1884876.
- [21] Tseng, K. L., Hwang S. R. and Dragomir, S. S., On some new inequalities of Hermite-Hadamard-Fejer type involving convex functions, *Demons. Math.*, 40(1) (2007), 51-64, DOI 10.1515/dema-2007-0108.
- [22] Qi, F., Yang, Z. L., Generalizations and refinements of Hermite-Hadamard's inequality, *Rocky Mountain J. Math.*, 35 (2005), 235-251.



SOME BOUNDS FOR THE k -GENERALIZED DIGAMMA FUNCTION

Hesham MOUSTAFA¹, Mansour MAHMOUD² and Ahmed TALAT³

¹Mathematics Department, Mansoura University, Mansoura 35516, EGYPT

²Mathematics Department, King Abdulaziz University, P.O. Box 80203, Jeddah 21589, SAUDI ARABIA

³Mathematics and Computer Sciences Department, Port Said University, Port Said, EGYPT

ABSTRACT. We presented some monotonicity properties for the k -generalized digamma function $\psi_k(h)$ and we established some new bounds for $\psi_k^{(s)}(h)$, $s \in \mathbb{N} \cup \{0\}$, which refine recent results.

1. INTRODUCTION

The ordinary Gamma function is given by [1]:

$$\Gamma(h) = \lim_{s \rightarrow \infty} \frac{s! s^{h-1}}{h(h+1)(h+2) \cdots (h+(s-1))}, \quad h > 0$$

was discovered by Euler when he generalized the factorial function to non integer values. The digamma function is the logarithmic derivative of the ordinary gamma function and is given by [1]:

$$\psi(1+h) = -\gamma + \sum_{s=1}^{\infty} \frac{h}{s(h+s)}, \quad h > -1$$

where $\gamma = \lim_{m \rightarrow \infty} \left(\sum_{s=1}^m \frac{1}{s} - \log m \right) \simeq 0.577$ is the Euler-Mascheroni constant. In 2006, Kirchoff applied the polygamma functions in the field of physics [3] and many series involving polygamma functions appeared in Feynman calculations [8]. In 2021, Wilkins and Hromadka [16] use the digamma function, as well as new

2020 *Mathematics Subject Classification.* 33B15, 26A48, 26D07.

Keywords. Gamma function, digamma function, polygamma function, completely monotonic function, asymptotic expansion, inequalities.

¹ heshammoustafa14@gmail.com-Corresponding author; 0000-0002-2792-6239

² mansour@mans.edu.eg; 0000-0002-5918-1913

³ a_t_amer@yahoo.com; 0000-0001-7702-8093.

variants of the digamma function, as a new family of basis functions in mesh-free numerical methods for solving partial differential equations. polygamma functions are used to approximate the values of many special functions and have many applications in physics, statistics and applied mathematics [14].

Many mathematicians studied the completely monotonic (CM) of some functions including the digamma function to deduce some of its bounds. An infinitely differentiable function $L(h)$ on \mathbb{R}^+ is CM if $(-1)^s L^{(s)}(h) \geq 0$ for $s \in \mathbb{N} \cup \{0\}$. A theorem [15, Theorem 12b] stated the sufficient condition for $L(h)$ being CM on \mathbb{R}^+ as:

$$L(h) = \int_0^\infty e^{-hy} dv(y),$$

where $v(y)$ is non-decreasing and the integral converges for $h \in \mathbb{R}^+$.

In 2006, Muqattash and Yahdi [10] presented the following inequality:

$$\ln h < \psi(1+h) < \ln(1+h), \quad h \in \mathbb{R}^+. \quad (1)$$

In 2011, Batir [2] presented the following inequalities:

$$\ln \left(h^2 + h + e^{-2\gamma} \right) \leq 2\psi(h+1) < \ln \left(h^2 + h + \frac{1}{3} \right), \quad h \in [0, \infty) \quad (2)$$

$$\ln \left(\frac{2h+2}{e^{\frac{2}{h+1}} - 1} \right) < 2\psi(h+1) \leq \ln \left(\frac{2h + (e^2 - 1)e^{-2\gamma}}{e^{\frac{2}{1+h}} - 1} \right), \quad h \in [0, \infty) \quad (3)$$

and

$$\left(\frac{1+2h}{2} \right) e^{-2\psi(1+h)} < \psi'(1+h) < \left(\frac{\pi^2 e^{-2\gamma} + 6h}{6} \right) e^{-2\psi(h+1)}, \quad h \in (0, \infty). \quad (4)$$

In 2014, Guo and Qi [5] refined the inequality [1] by

$$\ln(h+1/2) < \psi(1+h) < \ln(e^{-\gamma} + h), \quad h \in \mathbb{R}^+. \quad (5)$$

Diaz and Pariguan [4] presented the k -generalized gamma function as:

$$\Gamma_k(h) = \lim_{s \rightarrow \infty} \frac{s! k^s (sk)^{\frac{h}{k}-1}}{h(k+h)(2k+h) \cdots ((s-1)k+h)}, \quad k, h \in \mathbb{R}^+.$$

Mansour [7] determined the Γ_k by a combination of some functional equations. The k -analogue of the digamma function is introduced by [11]

$$\psi_k(h) = \frac{-1}{k} (\gamma - \ln k) - 1/h - \sum_{s=1}^{\infty} \left(\frac{1}{sk+h} - \frac{1}{sk} \right), \quad k, h \in \mathbb{R}^+$$

and it has the following relations for $h, k \in \mathbb{R}^+$ and $s \in \mathbb{N} \cup \{0\}$

$$k\psi_k(h) - \psi\left(\frac{h}{k}\right) = \ln k, \quad \psi_k^{(s)}(k+h) = \frac{(-1)^s s!}{h^{s+1}} + \psi_k^{(s)}(h) \text{ and } \psi_k'(k) = \frac{\pi^2}{6k^2}. \quad (6)$$

In 2018, Nantomah, Nisar and Gehlot [12] introduced the following integral formulas:

$$\psi_k(h) = \int_0^\infty \left(\frac{2e^{-y} - e^{-ky}}{ky} - \frac{e^{-hy}}{1 - e^{-ky}} \right) dy, \quad h, k > 0 \tag{7}$$

and

$$\psi_k^{(s)}(h) = (-1)^{s+1} \int_0^\infty y^s \left(\frac{e^{-hy}}{1 - e^{-ky}} \right) dy, \quad h, k > 0; s \in \mathbb{N}. \tag{8}$$

Yin, Huag, Song and Dou [19] deduced the following inequality:

$$0 \leq \psi'_k(h) - \frac{1}{kh} \leq \frac{1}{h^2}, \quad h, k \in \mathbb{R}^+. \tag{9}$$

In 2020, Yildirim [17] deduced the following inequality:

$$-\frac{k}{12h^2} < \psi_k(h+k) - \frac{1}{k} \ln h - \frac{1}{2h} < 0, \quad h, k \in \mathbb{R}^+. \tag{10}$$

In 2021, Moustafa, Almuashi and Mahmoud [9] presented the following asymptotic formulas for $k > 0$:

$$\psi_k(h) \sim \frac{1}{k} \ln h - \frac{1}{2h} - \sum_{m=1}^\infty \frac{k^{2m-1} B_{2m}}{(2m) h^{2m}}, \quad h \rightarrow \infty \tag{11}$$

and for $s \in \mathbb{N}$,

$$\psi_k^{(s)}(h) \sim \frac{(-1)^{s-1} (s-1)!}{kh^s} - \frac{(-1)^s s!}{2h^{s+1}} + (-1)^{s+1} \sum_{m=1}^\infty \frac{(s+2m-1)! k^{2m-1} B_{2m}}{(2m)! h^{2m+s}}, \quad h \rightarrow \infty \tag{12}$$

and they also deduced the inequalities:

$$\frac{1}{k} \ln h + \frac{1}{h} - \frac{k}{2} \psi'_k(h) < \psi_k(k+h) < \frac{\ln h}{k} + 1/h - \frac{k}{2} \psi'_k\left(\frac{k+3h}{3}\right), \quad h, k > 0 \tag{13}$$

where the upper bound of [13] refines upper bound of [10] for all $h > \frac{k}{3}$, and for $s \in \mathbb{N}$, $h, k \in \mathbb{R}^+$

$$\frac{(s-1)!}{kh^s} + \frac{(-1)^s k}{2} \psi_k^{(s+1)}\left(h + \frac{k}{3}\right) < (-1)^{s+1} \psi_k^{(s)}(h) < \frac{(s-1)!}{kh^s} + \frac{(-1)^s k}{2} \psi_k^{(s+1)}(h). \tag{14}$$

Notes: All of the k -digamma function results allow us to make new conclusions about the classical digamma function or new proofs for some of its established conclusions when k tends to one, and likewise for the k -gamma function [6, 18, 20]. For extra information about Γ_k and ψ_k functions, see [4, 7, 9, 19] and the related references therein.

We will introduce two CM functions involving $\psi_k(h)$ and $\psi'_k(h)$ functions. Some new bounds for $\psi_k^{(s)}(h)$ functions ($s \in \mathbb{N} \cup \{0\}$) will be deduced, which generalize and refine some recent results. Also, we will study the monotonicity of two functions

containing the k -generalized digamma function and consequently, we will deduce some new best bounds for $\psi_k^{(s)}(h)$ functions ($s \in \mathbb{N} \cup \{0\}$).

2. AUXILIARY RESULTS

In [13], the following corollary was introduced:

Corollary 1. Assume that S is a function defined on $h > h_0$, $h_0 \in \mathbb{R}$ with $\lim_{h \rightarrow \infty} S(h) = 0$. Then for $\omega \in \mathbb{R}^+$, $S(h) > 0$, if $S(h + \omega) < S(h)$ for $h > h_0$ and $S(h) < 0$, if $S(h + \omega) > S(h)$ for $h > h_0$.

Using the monotonicity properties, we can conclude the following results:

Lemma 1.

$$\ln\left(\frac{h^2 + 3h + 3}{3}\right) < h, \quad \forall h \in \mathbb{R}^+, \tag{15}$$

$$\ln\left(\frac{1}{e^{-\gamma} + h} + 1\right) < \frac{1}{1+h}, \quad \forall h > \frac{e^{2\gamma} - e^\gamma - 1}{e^\gamma(2 - e^\gamma)} \simeq 1.00313 \tag{16}$$

and

$$\frac{2}{1+h} < \ln\left(\frac{2(1+h)}{h^2 + h + e^{-2\gamma}} + 1\right), \quad \forall h > \frac{1}{\sqrt{e^{2\gamma}(-3 + e^{2\gamma})}} - 1 \simeq 0.352938. \tag{17}$$

Proof. Let the function $L(h) = \ln\left(\frac{h^2+3h+3}{3}\right) - h$ and then $L'(h) = \frac{-h(1+h)}{3+3h+h^2} < 0$ for all $h > 0$ and then $L(h)$ is decreasing on $(0, \infty)$ with $\lim_{h \rightarrow 0^+} L(h) = 0$ and then $L(h) < 0$ for all $h > 0$ which proves (15). Secondly, we let the function $C(h) = \ln\left(\frac{1}{e^{-\gamma}+h} + 1\right) - \frac{1}{1+h}$. Then

$$C'(h) = \frac{1 + e^\gamma - e^{2\gamma} + e^\gamma(2 - e^\gamma)h}{(1+h)^2(1+e^\gamma h)(1+e^\gamma(1+h))} > 0, \quad h > h_1 = \frac{-1 - e^\gamma + e^{2\gamma}}{e^\gamma(2 - e^\gamma)} \simeq 1.00313.$$

Then $C(h)$ is increasing on (h_1, ∞) with $\lim_{h \rightarrow \infty} C(h) = 0$ and this proves (16). By the same way, we obtain (17). □

Lemma 2. For $k \in \mathbb{R}^+$, we have

$$k\psi_k(k+h) < \gamma + \ln\left(\frac{3}{\pi^2}\right) + \ln(2h+k), \quad \forall h > \frac{k}{2}. \tag{18}$$

Proof. Let the function $N_k(h) = \ln\left(\frac{3}{\pi^2}\right) + \gamma + \ln(2h+k) - k\psi_k(k+h)$. Then $N'_k(h) = \frac{2}{k+2h} - k\psi'_k(k+h)$ and by using (6), we obtain

$$N'_k(h) - N'_k(k+h) = \frac{k^3}{(3k+2h)(k+2h)(k+h)^2} > 0, \quad h, k > 0.$$

Using the asymptotic formula (12), we have $\lim_{h \rightarrow \infty} N'_k(h) = 0$ and then Corollary 1 gives us that $N'_k(h) > 0$ for $h > 0$ and $k > 0$. Then, we have $N_k(h)$ is increasing on \mathbb{R}^+ and by using (6) again, we get $N_k(h) > N_k\left(\frac{k}{2}\right) \simeq 0.0430254 > 0$ for all $h > \frac{k}{2}$ and $k > 0$. \square

Lemma 3. For $k > 0$, we have

$$e^{k\psi_k(h+2k)} < e^{k\psi_k(h+k)} + k, \quad \forall h > 0. \tag{19}$$

Proof. Set the function $B_k(h) = e^{k\psi_k(h+2k)} - e^{k\psi_k(h+k)} - k$. Then by using (6), we get

$$\frac{B_k(h+k) - B_k(h)}{e^{k\psi_k(h+k)}} = e^{\frac{k}{h+k} + \frac{k}{h+2k}} - 2e^{\frac{k}{h+k}} + 1 \doteq D_k(h).$$

Then

$$\frac{(h+k)^2}{ke^{\frac{k}{h+k}}} D'_k(h) = 2 - \frac{(5k^2 + 6kh + 2h^2)e^{\frac{k}{h+2k}}}{(2k+h)^2} \doteq f_k(h).$$

Then $f'_k(h) = \frac{k^3 e^{\frac{k}{h+2k}}}{(2k+h)^4} > 0$ for all $h, k > 0$ and hence $f_k(h)$ is increasing on \mathbb{R}^+ with $\lim_{h \rightarrow \infty} f_k(h) = 0$. Then $f_k(h) < 0$ for $h, k > 0$ and then $D_k(h)$ is decreasing on \mathbb{R}^+ with $\lim_{h \rightarrow \infty} D_k(h) = 0$. Then $B_k(h+k) - B_k(h) > 0$ for $h, k > 0$. Using the asymptotic formula (11), we have $\lim_{h \rightarrow \infty} B_k(h) = 0$ and then Corollary 1 gives us that $B_k(h) < 0$ for all $h, k > 0$. \square

Lemma 4. For $k > 0$, we have

$$e^{2k\psi_k(h+2k)} > e^{2k\psi_k(h+k)} + 2k(h+k), \quad \forall h > 0. \tag{20}$$

Proof. Set the function $m_k(h) = e^{2k\psi_k(h+2k)} - e^{2k\psi_k(h+k)} - 2k(h+k)$. Then

$$m_k(h+k) - m_k(h) = e^{2k\psi_k(h+3k)} - 2e^{2k\psi_k(h+2k)} + e^{2k\psi_k(h+k)} - 2k^2 \doteq t_k(h).$$

Then by using (6), we get

$$\frac{t_k(h+k) - t_k(h)}{e^{2k\psi_k(h+k)}} = e^{\frac{2k}{h+k} + \frac{2k}{h+2k} + \frac{2k}{h+3k}} - 3e^{\frac{2k}{h+k} + \frac{2k}{h+2k}} + 3e^{\frac{2k}{h+k}} - 1 \doteq s_k(h).$$

Then

$$\begin{aligned} \frac{(h+k)^2 s'_k(h)}{2ke^{\frac{2k}{h+k}}} &= -\frac{(49k^4 + 96k^3h + 72k^2h^2 + 24kh^3 + 3h^4)e^{\frac{2k}{h+2k} + \frac{2k}{h+3k}}}{(2k+h)^2(3k+h)^2} \\ &\quad + \frac{3(5k^2 + 6kh + 2h^2)}{(2k+h)^2 e^{\frac{-2k}{h+2k}}} - 3 \doteq u_k(h) \end{aligned}$$

Then

$$\frac{(2k+h)^4 u'_k(h)}{2k(3k^2+3kh+h^2)e^{\frac{2k}{h+2k}}} = \frac{379k^6 + 959k^5h + 1049k^4h^2 + 626k^3h^3 + 213k^2h^4}{(3k^2+3kh+h^2)(3k+h)^4 e^{\frac{-2k}{h+3k}}} + \frac{39kh^5 + 3h^6}{(3k^2+3kh+h^2)(3k+h)^4 e^{\frac{-2k}{h+3k}}} - 3 \doteq w_k(h).$$

Then

$$w'_k(h) = \frac{-2k^5 \left(129k^4 + 240k^3h + 172k^2h^2 + 56kh^3 + 7h^4\right) e^{\frac{2k}{h+3k}}}{(3k+h)^6(3k^2+3kh+h^2)^2} < 0, \quad h, k > 0$$

and hence $w_k(h)$ is decreasing on $(0, \infty)$ with $\lim_{h \rightarrow \infty} w_k(h) = 0$. Then $w_k(h) > 0$ for $h, k \in \mathbb{R}^+$ and then $u_k(h)$ is increasing on \mathbb{R}^+ with $\lim_{h \rightarrow \infty} u_k(h) = 0$. Then $s_k(h)$ is decreasing on \mathbb{R}^+ with $\lim_{h \rightarrow \infty} s_k(h) = 0$. Then $t_k(h+k) - t_k(h) > 0$ for $h, k \in \mathbb{R}^+$. Using the asymptotic formula (11), we have $\lim_{h \rightarrow \infty} t_k(h) = 0$ and then Corollary 1 gives us that $t_k(h) < 0$ for all $h, k \in \mathbb{R}^+$. Then $m_k(h+k) - m_k(h) < 0$ for $h, k \in \mathbb{R}^+$ with $\lim_{h \rightarrow \infty} m_k(h) = 0$ and then $m_k(h) > 0$ for all $h, k \in \mathbb{R}^+$. \square

3. SOME CM MONOTONIC FUNCTIONS

Theorem 1. Assume that $h, k > 0$. Then the function

$$U_{\beta,k}(h) = \psi'_k(h) - \frac{2}{kh} + \frac{2}{k^2} \ln \left(1 + \frac{\beta k}{h}\right)$$

is CM on \mathbb{R}^+ if and only if $\beta \geq \frac{1}{2}$.

Proof.

$$U'_{\beta,k}(h) = \psi''_k(h) + \frac{2}{kh^2} + \frac{2}{k^2} \left(\frac{1}{h + \beta k} - \frac{1}{h}\right)$$

and by using (8) and the identity $\frac{1}{h^l} = \frac{1}{(l-1)!} \int_0^\infty y^{l-1} e^{-hy} dy$ for $h > 0$, (see (1)), we have

$$U'_{\beta,k}(h) = \int_0^\infty \frac{2e^{-hy}}{k^2(e^{ky} - 1)} \phi_k(y) dy,$$

where

$$\phi_k(y) = (e^{ky} - 1)(e^{-\beta ky} - 1) + ky(e^{ky} - 1) - \frac{(ky)^2}{2} e^{ky}.$$

Let $\beta \geq \frac{1}{2}$. Then

$$\begin{aligned} e^{\frac{ky}{2}} \phi_k(y) &\leq e^{ky} - e^{\frac{3ky}{2}} + e^{\frac{ky}{2}} - 1 + ky \left(e^{\frac{3ky}{2}} - e^{\frac{ky}{2}}\right) - 1/2(ky)^2 e^{\frac{3ky}{2}} \\ &= \sum_{m=1}^\infty \frac{n(m)}{2^{m+2} (m+2)!} (ky)^{m+2} \end{aligned}$$

where

$$\begin{aligned} n(m) &= 2^{m+2} - 3^{m+2} + 1 + 2(m+2)(3^{m+1} - 1) - 2(m+2)(m+1)3^m \\ &= -2(m+2)\left((m-1)2^m + 1\right) - \sum_{s=1}^m \frac{(m+2)(m+1)(m-s)}{(m+2-s)} \binom{m}{s} 2^{m+1-s} \\ &< 0 \end{aligned}$$

and then $-U'_{\beta,k}(h)$ is CM on \mathbb{R}^+ and hence $U_{\beta,k}(h)$ is decreasing on \mathbb{R}^+ . Using the asymptotic formula (12), we have $\lim_{h \rightarrow \infty} U_{\beta,k}(h) = 0$ and then $U_{\beta,k}(h) > 0$. Then $U_{\beta,k}(h)$ is CM on \mathbb{R}^+ for $\beta \geq \frac{1}{2}$. On the other side, if $U_{\beta,k}(h)$ is CM, then by using again the asymptotic formula (12), we get $\lim_{h \rightarrow \infty} h U_{\beta,k}(h) = \frac{2\beta-1}{k} \geq 0$ and hence $\beta \geq \frac{1}{2}$. □

Theorem 2. Assume that $h, k > 0$ and $\lambda \in \mathbb{R}$. Then the function

$$F_{\lambda,k}(h) = \psi_k(h+k) - \frac{1}{k} \ln(h+\lambda k)$$

is CM on \mathbb{R}^+ if and only if $\lambda \leq \frac{1}{2}$. Also, the function $-F_{\lambda,k}(h)$ is CM on \mathbb{R}^+ if $\lambda \geq 1$.

Proof.

$$F'_{\lambda,k}(h) = -\frac{1}{k(h+\lambda k)} + \psi'_k(h+k) = \int_0^\infty \frac{e^{-hy}}{k(e^{ky}-1)} \varphi_k(y) dy,$$

where

$$\varphi_k(y) = ky - e^{-\lambda ky} (e^{ky} - 1).$$

Let $\lambda \leq \frac{1}{2}$, then we obtain

$$\begin{aligned} e^{\frac{ky}{2}} \varphi_k(y) &\leq 1 + ky e^{\frac{ky}{2}} - e^{ky} \\ &= -\sum_{l=2}^\infty \frac{(2^l - l - 1)(ky)^{1+l}}{2^l (1+l)!} \\ &= -\sum_{l=2}^\infty \frac{\left(\sum_{s=2}^l \binom{l}{s}\right) (ky)^{1+l}}{2^l (1+l)!} < 0 \end{aligned}$$

and consequently, $-F'_{\lambda,k}(h)$ is CM on \mathbb{R}^+ for $\lambda \leq \frac{1}{2}$ and hence $F_{\lambda,k}(h)$ is decreasing on \mathbb{R}^+ . Using the asymptotic formula (11), we obtain $\lim_{h \rightarrow \infty} F_{\lambda,k}(h) = 0$ and then $F_{\lambda,k}(h) > 0$. Hence $F_{\lambda,k}(h)$ is CM on \mathbb{R}^+ for $\lambda \leq \frac{1}{2}$. On the other hand, if $F_{\lambda,k}(h)$ is CM, then by using again the asymptotic formula (11), we obtain $\lim_{h \rightarrow \infty} h F_{\lambda,k}(h) = \frac{1}{2} - \lambda \geq 0$ and then $\lambda \leq \frac{1}{2}$. Now for $\lambda \geq 1$, we have $e^{ky} \varphi_k(y) \geq \sum_{l=1}^\infty \frac{l(ky)^{l+1}}{(l+1)!} > 0$

and consequently, $F'_{\lambda,k}(h)$ is CM on \mathbb{R}^+ for $\lambda \geq 1$ and hence $F_{\lambda,k}(h)$ is increasing on \mathbb{R}^+ with $\lim_{h \rightarrow \infty} F_{\lambda,k}(h) = 0$ and then $F_{\lambda,k}(h) < 0$. Then $-F_{\lambda,k}(h)$ is CM on \mathbb{R}^+ for $\lambda \geq 1$. □

4. SOME INEQUALITIES FOR THE ψ_k AND $\psi_k^{(s)}$ FUNCTIONS

Let us mention some important consequences of Theorems 1 and 2

Corollary 2. *Let $a \in (0, \infty)$. Then we have*

$$\frac{1}{kh} - \frac{1}{k^2} \ln\left(\frac{ak+h}{h}\right) < \frac{\psi'_k(h)}{2}, \quad k, h \in \mathbb{R}^+ \tag{21}$$

with the best possible constant $a = \frac{1}{2}$.

Proof. The inequality (21) at $a = \frac{1}{2}$ follows from $U_{\frac{1}{2},k}(h) > 0$ in Theorem 1 and the inequality (21) is equivalent that $h U_{a,k}(h) > 0$ which yields $a \geq \frac{1}{2}$ as stated when we proved Theorem 1. Then $a = \frac{1}{2}$ is the best in (21), since the logarithmic function is strictly increasing on \mathbb{R}^+ . □

Remark 1. *Using the identity $\ln(1+h) < h$ for all $h > -1$, (see 1) yields the lower bound of (21) refines the lower bound of (9) for all $h, k > 0$.*

Corollary 3. *Let $a \in (0, \infty)$ and $s = 1, 2, 3, \dots$. Then we have*

$$\frac{2s!}{kh^{s+1}} + \frac{2(s-1)!}{k^2} \left(\frac{1}{(h+ak)^s} - \frac{1}{h^s} \right) < (-1)^s \psi_k^{(s+1)}(h), \quad h, k \in (0, \infty) \tag{22}$$

with the best possible constant $a = \frac{1}{2}$.

Proof. The inequality (22) at $a = \frac{1}{2}$ follows from $(-1)^s U_{\frac{1}{2},k}^{(s)}(h) > 0$ in Theorem 1 and the inequality (22) is equivalent that $h^{s+1} (-1)^s U_{a,k}^{(s)}(h) > 0$. Using the asymptotic expansion (12), we have $\lim_{h \rightarrow \infty} h^{s+1} (-1)^s U_{a,k}^{(s)}(h) = \frac{s!}{k} (2a-1) \geq 0$ and hence $a \geq \frac{1}{2}$. Using the decreasing property of the function $\frac{1}{h^s}$ on $(0, \infty)$ for $s = 1, 2, 3, \dots$, we deduce that $a = \frac{1}{2}$ is the best possible constant in (22). □

Corollary 4. *Let $a \in [0, \infty)$. Then we have*

$$\ln(h+ak) < k\psi_k(k+h) < \ln(k+h), \quad k, h \in \mathbb{R}^+ \tag{23}$$

with the best possible constant $a = \frac{1}{2}$.

Proof. The inequality (23) at $a = \frac{1}{2}$ is deduced from $F_{\frac{1}{2},k}(h) > 0$ and $F_{1,k}(h) < 0$ in Theorem 2. The left-hand side of (23) is equivalent that $h F_{a,k}(h) > 0$ and this gives $a \leq \frac{1}{2}$ as stated when we proved Theorem 2. Then $a = \frac{1}{2}$ is the best in (23). □

Remark 2. • *Letting $k = 1$ and $a = 0$ in (23), we obtain (1).*

- Using (21), we deduce that the lower bound of (23) refines the lower bound of (13) for every $k, h \in \mathbb{R}^+$.

Corollary 5. Let $a \in [0, \infty)$ and $s = 1, 2, 3, \dots$. Then we have

$$\frac{s!}{h^{s+1}} + \frac{(s-1)!}{k(h+k)^s} < (-1)^{s+1} \psi_k^{(s)}(h) < \frac{s!}{h^{s+1}} + \frac{(s-1)!}{k(h+ak)^s}, \quad h, k \in (0, \infty) \quad (24)$$

with the best possible constant $a = \frac{1}{2}$.

Proof. The inequality (24) at $a = \frac{1}{2}$ is deduced from $(-1)^s F_{\frac{1}{2}, k}^{(s)}(h) > 0$ and $(-1)^s F_{1, k}^{(s)}(h) < 0$ in Theorem 2. The right-hand side of (24) is equivalent that $h^{1+s} (-1)^s F_{a, k}^{(s)}(h) > 0$. Using the asymptotic expansion (12), we have

$$\lim_{h \rightarrow \infty} h^{s+1} (-1)^s F_{a, k}^{(s)}(h) = s! \left(\frac{1}{2} - a \right) \geq 0$$

and hence $a \leq \frac{1}{2}$. Then $a = \frac{1}{2}$ is the best possible constant in (24). □

Remark 3. Using (22), we deduce that the upper bound of (24) refines the upper bound of (14) for every $s \in \mathbb{N}$ and $h, k > 0$.

Lemma 5. For $k > 0$, the function

$$T_k(h) = e^{k\psi_k(h+k)} - h \quad (25)$$

is strictly decreasing convex on $(-k, \infty)$ with $\lim_{h \rightarrow \infty} T_k(h) = \frac{k}{2}$ and $\lim_{h \rightarrow 0} T_k(h) = ke^{-\gamma}$.

Proof. Using (6), we have $\lim_{h \rightarrow 0} T_k(h) = ke^{-\gamma}$. Differentiating (25) yields

$$T'_k(h) = -1 + k\psi'_k(h+k)e^{k\psi_k(k+h)}$$

and

$$\frac{T''_k(h)}{k e^{k\psi_k(k+h)}} = k \left[\psi'_k(k+h) \right]^2 + \psi''_k(k+h) \doteq S_k(h).$$

Applying (6), we get

$$\frac{(k+h)^2}{2k} \left[S_k(k+h) - S_k(h) \right] = -\psi'_k(k+h) - \frac{2h^2 + 4kh + 2k^2 - 1}{2(h+k)^2} \doteq Q_k(h).$$

Applying (6) again, we get

$$Q_k(k+h) = Q_k(h) + \frac{A_k(k+h)}{2(k+h)^2(2k+h)^2},$$

where

$$A_k(h) = k^2 + 2kh + 2h^2 > 0, \quad h, k \in \mathbb{R}^+$$

and then $Q_k(k+h) > Q_k(h)$ for all $h > -k$ and by using the asymptotic formula (12), we have $\lim_{h \rightarrow \infty} Q_k(h) = 0$ and then Corollary 1 gives us $Q_k(h) < 0$ for every $h > -k$. Consequently, we have $S_k(k+h) < S_k(h)$ for all $h > -k$ and by using the

asymptotic expansion (12), we have $\lim_{h \rightarrow \infty} S_k(h) = 0$ and then $T_k''(h) > 0$ for every $h > -k$. Then $T_k'(h)$ is strictly increasing on $(-k, \infty)$. By using the asymptotic formulas (11) and (12), we have

$$\lim_{h \rightarrow \infty} T_k'(h) = 0 \text{ and } \lim_{h \rightarrow \infty} T_k(h) = k/2.$$

Then $T_k'(h) < \lim_{h \rightarrow \infty} T_k'(h) = 0$ and this finishes the proof. □

And consequently, we have the following Corollary:

Corollary 6. *Set a and b be positive real numbers. Then we have*

$$\ln(h + ak) < k\psi_k(h + k) < \ln(h + bk), \quad h, k \in \mathbb{R}^+ \tag{26}$$

where $a = \frac{1}{2}$ and $b = \frac{1}{e^\gamma} \simeq 0.56$ being the best.

Remark 4. • Letting $k = 1$ in (26), we obtain (5).

• The upper bound of (26) refines the upper bound of (23) for all $h, k > 0$.

Lemma 6. *For $h \geq 0$ and $k \in \mathbb{R}^+$,*

$$\ln\left(\frac{c k}{e^{\frac{k}{k+h}} - 1}\right) \leq k\psi_k(k + h) < \ln\left(\frac{d k}{e^{\frac{k}{k+h}} - 1}\right), \tag{27}$$

where the constants $c = e^{-\gamma}(e - 1) \simeq 0.965$ and $d = 1$ are the best possible.

Proof. Set

$$f_k(h) = T_k(k + h) - T_k(h) = -k + e^{k\psi_k(k+h)}\left(e^{\frac{k}{k+h}} - 1\right), \quad h \geq 0 \text{ and } k > 0.$$

Since $T_k'(h)$ is strictly increasing on $(-k, \infty)$, then $f_k(h)$ is strictly increasing on $[0, \infty)$ and by using (6) and the asymptotic expansion (11), we get

$$f_k(0) = -k + ke^{-\gamma}(e - 1) \leq -k + e^{k\psi_k(k+h)}\left(e^{\frac{k}{k+h}} - 1\right) < \lim_{h \rightarrow \infty} f_k(h) = 0$$

and this gives (27). □

Remark 5. *Using (16), we deduce that the upper bound of (27) refines the upper bound of (26) for all $h > 1.00313k$ and $k > 0$.*

Lemma 7. *For $h > 0$ and $k > 0$, we have*

$$g e^{-k\psi_k(h+k)} < k\psi_k'(k + h) < r e^{-k\psi_k(k+h)}, \tag{28}$$

where the constants $g = \frac{\pi^2 e^{-\gamma}}{6} \simeq 0.924$ and $r = 1$ are the best possible.

Proof. By using the increasing property of $T_k'(h)$ on $(-k, \infty)$, we have

$$T_k'(0) = -1 + k\psi_k'(k)e^{k\psi_k(k)} < -1 + k\psi_k'(k + h)e^{k\psi_k(k+h)} < \lim_{h \rightarrow \infty} T_k'(h) = 0.$$

Using (6) yields

$$\frac{\pi^2 e^{-\gamma}}{6} < k\psi_k'(k + h)e^{k\psi_k(k+h)} < 1,$$

which finishes the proof. □

Remark 6. Using (23) yields $e^{-k\psi_k(k+h)} < \frac{2}{2h+k}$ for every $h, k > 0$ and then the upper bound of (28) refines the upper bound of (24) at $s = 1$ for all $h, k > 0$.

Lemma 8. For $h > 0$ and $k > 0$,

$$1 - e^{-\frac{k}{h+k}} + \frac{k^2}{(h+k)^2} < k^2\psi'_k(h+k) < e^{\frac{k}{h+k}} - 1. \quad (29)$$

Proof. By applying the mean value theorem to T_k on the interval $[h, h+k]$, we obtain

$$\frac{-T_k(h) + T_k(k+h)}{k} = T'_k(h + \alpha_h), \quad 0 < \alpha_h < k.$$

By using the increasing property of $T'_k(h)$ on $(-k, \infty)$, we obtain

$$T'_k(h) < T'_k(h + \alpha_h) < T'_k(k+h), \quad 0 < \alpha_h < k.$$

Combining the last two relations yields

$$T'_k(h) < \frac{-T_k(h) + T_k(k+h)}{k} < T'_k(k+h)$$

and this gives us (29). \square

Remark 7. Using (19), we deduce that the upper bound of (29) refines the upper bound of (28) for every $h, k \in \mathbb{R}^+$.

Lemma 9. For $k > 0$, the function

$$W_k(h) = e^{2k\psi_k(h+k)} - h^2 - hk \quad (30)$$

is strictly increasing concave in $(-k, \infty)$ with $\lim_{h \rightarrow \infty} W_k(h) = \frac{k^2}{3}$ and $\lim_{h \rightarrow 0} W_k(h) = k^2e^{-2\gamma}$.

Proof. Using (6), we have $\lim_{h \rightarrow 0} W_k(h) = k^2e^{-2\gamma}$. Differentiating (30) yields

$$W'_k(h) = -2h - k + 2k\psi'_k(h+k)e^{2k\psi_k(k+h)},$$

$$\frac{1}{2}W''_k(h) = -1 + ke^{2k\psi_k(k+h)} \left[\psi''_k(k+h) + 2k(\psi'_k(k+h))^2 \right]$$

and

$$\frac{1}{2ke^{2k\psi_k(k+h)}} W'''_k(h) = \psi'''_k(k+h) + 6k\psi'_k(k+h)\psi''_k(k+h) + 4k^2(\psi'_k(k+h))^3 \doteq V_k(h).$$

Applying (6), we get

$$\begin{aligned} \frac{(h+k)^2}{2k} [V_k(k+h) - V_k(h)] &= -3\psi''_k(k+h) + \frac{6(h+2k)}{(h+k)^2} \psi'_k(h+k) \\ &\quad - 6k(\psi'_k(h+k))^2 - \frac{11k^2 + 12kh + 3h^2}{k(h+k)^4} \doteq U_k(h). \end{aligned}$$

Similarly, we get

$$\begin{aligned} \frac{(h+k)^2(h+2k)^2}{6k(3k^2+3kh+h^2)} [U_k(h+k) - U_k(h)] &= \psi'_k(h+k) \\ &- \frac{114k^5 + 298k^4h + 321k^3h^2}{6k(k+h)^2(2k+h)^2(3k^2+3kh+h^2)} \\ &- \frac{178k^2h^3 + 51kh^4 + 6h^5}{6k(k+h)^2(2k+h)^2(3k^2+3kh+h^2)} \\ &\doteq H_k(h). \end{aligned}$$

And finally, we get

$$H_k(k+h) - H_k(h) = -\frac{k^4 P_k(k+h)}{3(k+h)^2(2k+h)^2(3k+h)^2(3k^2+3kh+h^2)(7k^2+5kh+h^2)}$$

where

$$P_k(h) = 12k^4 + 36k^3h + 46k^2h^2 + 28kh^3 + 7h^4 > 0, \quad h, k \in \mathbb{R}^+$$

and then $H_k(h+k) < H_k(h)$ for all $h > -k$ and by using the asymptotic formula (12), we have $\lim_{h \rightarrow \infty} H_k(h) = 0$ and then Corollary 1 gives us $H_k(h) > 0$ for every $h > -k$. Consequently, we obtain $U_k(h+k) > U_k(h)$ for all $h > -k$ with $\lim_{h \rightarrow \infty} U_k(h) = 0$ and then $U_k(h) < 0$ for every $h > -k$ and similarly, we get $V_k(h) > 0$ for all $h > -k$. Then $W'_k(h)$ is strictly increasing on $(-k, \infty)$. By using the asymptotic formulas (11) and (12), we have

$$\lim_{h \rightarrow \infty} W''_k(h) = \lim_{h \rightarrow \infty} W'_k(h) = 0 \text{ and } \lim_{h \rightarrow \infty} W_k(h) = \frac{k^2}{3}.$$

Then $W''_k(h) < 0$ for all $h > -k$ and then $W'_k(h)$ is strictly decreasing on $(-k, \infty)$. Hence $W'_k(h) > \lim_{h \rightarrow \infty} W'_k(h) = 0$ and this completes the proof. \square

And consequently, we have the following Corollary:

Corollary 7. *Set $a, b \in \mathbb{R}^+$ and $k > 0$. Then we have*

$$\frac{1}{2k} \ln(h^2 + hk + ak^2) \leq \psi_k(h+k) < \frac{1}{2k} \ln(h^2 + hk + bk^2), \quad h \in [0, \infty) \quad (31)$$

where the constants $a = e^{-2\gamma} \simeq 0.315$ and $b = \frac{1}{3}$ are the best possible.

Remark 8. • Putting $k = 1$ in (31) yields (2).

- Using (15), we deduce that the upper bound of (31) refines the upper bound of (10) for $h, k > 0$.
- For $k > 0$, the upper and lower bounds of (31) refine the upper and lower bounds of (26) for $h > \left(\frac{\frac{1}{3} - e^{-2\gamma}}{2e^{-\gamma} - 1}\right)k \simeq 0.147224 k$ and $h > 0$ respectively.

Lemma 10. For $h \geq 0$ and $k > 0$, we have

$$\frac{1}{2k} \ln \left(\frac{2hk + ck^2}{e^{\frac{2k}{h+k}} - 1} \right) < \psi_k(h+k) \leq \frac{1}{2k} \ln \left(\frac{2hk + dk^2}{e^{\frac{2k}{h+k}} - 1} \right), \tag{32}$$

where $c = 2$ and $d = e^{-2\gamma}(e^2 - 1) \simeq 2.014$ are the best possible.

Proof. Set

$$M_k(h) = W_k(k+h) - W_k(h) = e^{2k\psi_k(k+h)} \left(e^{\frac{2k}{h+k}} - 1 \right) - 2hk - 2k^2, \quad h \geq 0, \quad k > 0.$$

Since $W'_k(h)$ is strictly decreasing on $(-k, \infty)$, then $M_k(h)$ is strictly decreasing on $[0, \infty)$ and by using (6) and the asymptotic expansion (11), we get

$$M_k(0) = k^2 e^{-2\gamma}(e^2 - 1) - 2k^2 \geq e^{2k\psi_k(h+k)} \left(e^{\frac{2k}{h+k}} - 1 \right) - 2hk - 2k^2 > \lim_{h \rightarrow \infty} M_k(h) = 0$$

and this gives (32). □

Remark 9. • Letting $k = 1$ in (32), we obtain (3).

- Using (17), we deduce that the lower bound of (32) refines the lower bound of (31) for $h > 0.352938k$.

Lemma 11. For $h > 0$ and $k > 0$, we have

$$\left(\frac{h}{k} + a \right) e^{-2k\psi_k(h+k)} < \psi'_k(h+k) < \left(\frac{h}{k} + b \right) e^{-2k\psi_k(h+k)}, \tag{33}$$

where the constants $a = \frac{1}{2}$ and $b = \frac{\pi^2 e^{-2\gamma}}{6} \simeq 0.519$ are the best possible.

Proof. Using the decreasing property of $W'_k(h)$ on $(-k, \infty)$ yields

$$W'_k(0) > 2k\psi'_k(h+k)e^{2k\psi_k(h+k)} - 2h - k > \lim_{h \rightarrow \infty} W'_k(h) = 0.$$

Using (6), we have

$$\frac{\pi^2 e^{-2\gamma} k}{3} > 2k\psi'_k(h+k)e^{2k\psi_k(h+k)} - 2h > k,$$

which finishes the proof. □

Remark 10. • Putting $k = 1$ in (33) gives (4).

- Using (18), we deduce that the lower bound of (33) refine the lower bound of (28) for $h > \frac{k}{2}$ and $k > 0$.

Lemma 12. For $h > 0$ and $k > 0$,

$$\begin{aligned} \frac{1}{2k^2} \left(e^{\frac{2k}{h+k}} - 1 - k^2 e^{-2k\psi_k(h+k)} \right) &< \psi'_k(h+k) \\ &< \frac{1}{2k^2} \left(\frac{2k^2}{(h+k)^2} + 1 - e^{-\frac{2k}{h+k}} + k^2 e^{-2k\psi_k(h+2k)} \right). \end{aligned} \tag{34}$$

Proof. By applying the mean value theorem to W_k on the interval $[h, h+k]$, we get

$$\frac{W_k(h+k) - W_k(h)}{k} = W'_k(h + \beta_h), \quad 0 < \beta_h < k.$$

Using the decreasing property of $W'_k(h)$ on $(-k, \infty)$ yields

$$W'_k(h+k) < \frac{W_k(h+k) - W_k(h)}{k} < W'_k(h)$$

and this gives us (34). \square

Remark 11. Using (20), we deduce that the lower bound of (34) refine the lower bound of (33) for $h, k \in \mathbb{R}^+$.

5. CONCLUSION

The main conclusions of this paper are stated in Theorems 1 and 2 and Lemmas 5 and 9. The authors proved the CM and the monotonicity properties of four functions containing the k -generalized digamma and polygamma functions, derived some new bounds for $\psi_k^{(s)}(h)$ functions ($s \in \mathbb{N} \cup \{0\}$). These bounds refine some recent results.

Author Contribution Statements The authors contributed equally to this article.

Declaration of Competing Interests The authors declare that they have no competing interest.

REFERENCES

- [1] Abramowitz, M., Stegun, I. A., Handbook of Mathematical Functions with Formulas, Graphs and Mathematical Tables, Dover, New York, 1965.
- [2] Batir, N., Sharp bounds for the psi function and harmonic numbers, *Math. Inequal. Appl.*, 14(4) (2011), 917-925. <http://files.ele-math.com/abstracts/mia-14-77-abs.pdf>
- [3] Coffey, M. W., One integral in three ways: moments of a quantum distribution, *J. Phys. A: Math. Gen.*, 39 (2006), 1425-1431. <https://doi.org/10.1088/0305-4470/39/6/015>
- [4] Díaz, R., Pariguan, E., On hypergeometric functions and k -Pochhammer symbol, *Divulg. Mat.*, 15(2) (2007), 179-192. <https://doi.org/10.48550/arXiv.math/0405596>
- [5] Guo, B.-N., Qi, F., Sharp inequalities for the psi function and harmonic numbers, *Analysis*, 34(2) (2014), 201-208. DOI 10.1515/anly-2014-0001.
- [6] Kokologiannaki, C. G., Krasniqi, V., Some properties of the k -gamma function, *Le Matematiche*, 68(1) (2013), 13-22. DOI 10.4418/2013.68.1.2
- [7] Mansour, M., Determining the k -generalized gamma function $\Gamma_k(x)$ by functional equations, *Int. J. Contemp. Math. Sciences*, 4(21) (2009), 653-660. <http://www.m-hikari.com/ijcms-password2009/21-24-2009/mansourIJCMS21-24-2009.pdf>
- [8] Miller, A. R., Summations for certain series containing the digamma function, *J. Phys. A: Math. Gen.*, 39 (2006), 3011-3020. DOI 10.1088/0305-4470/39/12/010
- [9] Moustafa, H., Almuashi, H., Mahmoud, M., On some complete monotonicity of functions related to generalized k -gamma function, *J. Math.*, 2021 (2021), 1-9. <https://doi.org/10.1155/2021/9941377>

- [10] Muqattash, I., Yahdi, M., Infinite family of approximations of the digamma function, *Math. Comput. Modelling*, 43(11-12) (2006), 1329-1336. <https://doi.org/10.1016/j.mcm.2005.02.010>
- [11] Nantomah, K., Iddrisu, M. M., The k -analogue of some inequalities for the gamma function, *Electron. J. Math. Anal. Appl.*, 2(2) (2014), 172-177.
- [12] Nantomah, K., Nisar, K. S., Gehlot, K. S., On a k -extension of the Nielsen's (beta)-function, *Int. J. Nonlinear Anal. Appl.*, 9(2) (2018), 191-201. <http://dx.doi.org/10.22075/ijnaa.2018.12972.1668>
- [13] Qi, F., Guo, S.-L., Guo, B.-N., Complete monotonicity of some functions involving polygamma functions, *J. Comput. Appl. Math.*, 233 (2010), 2149-2160. <https://doi.org/10.1016/j.cam.2009.09.044>
- [14] Qiu, S.-L., Vuorinen, M., Some properties of the gamma and psi functions with applications, *Math. Comp.*, 74(250) (2005), 723-742. DOI 10.1090/S0025-5718-04-01675-8
- [15] Widder, D. V., The Laplace Transform, Princeton University Press, Princeton, 1946.
- [16] Wilkins, B. D., Hromadka, T. V., Using the digamma function for basis functions in mesh-free computational methods, *Engineering Analysis with Boundary Elements*, 131 (2021), 218-227. <https://doi.org/10.1016/j.enganabound.2021.06.004>
- [17] Yildirim, E., Monotonicity properties on k -digamma function and its related inequalities, *J. Math. Inequal.*, 14(1) (2020), 161-173. <https://doi.org/10.7153/jmi-2020-14-12>
- [18] Yildirim, E., Ege, I., On k -analogues of digamma and polygamma functions, *J. Class. Anal.*, 13(2) (2018), 123-131. <https://doi.org/10.7153/jca-2018-13-08>
- [19] Yin, L., Huag, L. G., Song, Z. M., Dou, X. K., Some monotonicity properties and inequalities for the generalized digamma and polygamma functions, *J. Inequal. Appl.*, 1 (2018), 249. <https://doi.org/10.1186/s13660-018-1844-2>
- [20] Yin, L., Zhang, J., Lin, X., Complete monotonicity related to the k -polygamma functions with applications, *Ad. Diff. Eq.*, (2019), 1-10. <https://doi.org/10.1186/s13662-019-2299-6>



MISCELLANEOUS PROPERTIES OF STURM-LIOUVILLE PROBLEMS IN MULTIPLICATIVE CALCULUS

Güler Başak ÖZNUR¹, Güher Gülçehre ÖZBEY², Yelda AYGAR³, Rabia AKTAŞ KARAMAN⁴

¹Department of Mathematics, Gazi University, Ankara, TURKEY

²Middle East Technical University, Ankara, TURKEY

^{3,4}Department of Mathematics, Ankara University, Ankara, TURKEY

ABSTRACT. The purpose of this paper is to investigate some properties of multiplicative regular and periodic Sturm-Liouville problems given in general form. We first introduce regular and periodic Sturm-Liouville (S-L) problems in multiplicative analysis by using some algebraic structures. Then, we discuss the main properties such as orthogonality of different eigenfunctions of the given problems. We show that the eigenfunctions corresponding to same eigenvalues are unique modulo a constant multiplicative factor and reality of the eigenvalues of multiplicative regular S-L problems. Finally, we present some examples to illustrate our main results.

1. INTRODUCTION

Grossman and Katz established a new part of analysis by giving definitions of new kinds of derivatives and integrals in the period between 1967 and 1970, which is called non-Newtonian calculus [12, 13]. This calculus provides alternative approaches to the classical calculus developed by Newton and Leibniz. Non-Newtonian calculus has many subbranches as multiplicative, anageometric, biogeometric, quadratic, and harmonic calculus. One of the most popular of them is multiplicative calculus. Arithmetics, which are a complete ordered field on a subset of real numbers, play a substantial role in the construction of non-Newtonian calculus. It is well known that the system of real numbers is a classical arithmetic. Each

2020 *Mathematics Subject Classification.* 34A30; 34A99.

Keywords. Multiplicative calculus, multiplicative derivative, multiplicative integral, Sturm-Liouville equation.

¹ ✉ basakoznur@gazi.edu.tr; 0000-0003-4130-5348;

² ✉ gulcehre@metu.edu.tr; 0000-0002-1326-4545

³ ✉ yaygar@ankara.edu.tr-Corresponding author; 0000-0002-5550-3073

³ ✉ raktas@science.ankara.edu.tr; 0000-0002-7811-8610.

arithmetic yields one generator, the opposite of this is also true, i.e., each generator yields one arithmetic. For instance, usual arithmetic and geometric arithmetic are produced by the generators I (unit operator) and exp, respectively. Also, the function $\sigma(x) = \frac{e^x - 1}{e^x + 1}$ is a generator for sigmoidal arithmetic which characterizes sigmoidal curves that appear in the research of biological growth and population. There is a useful relationship providing advantages to each other between ordinary Newtonian calculus and multiplicative calculus. There are actually many reasons to investigate multiplicative analysis. For instance, it is not easy to find solutions of nonlinear differential equations in general, but this theory provides more advantages to get this kind of solutions [25]. The main difference of multiplicative calculus from the classical analysis is that it moves the roles of subtraction and addition in ordinary Newtonian calculus to division and multiplication, respectively. Since several events in the real world such as the magnitudes of earthquakes, the levels of sound signals and the acidities of chemicals change exponentially, geometric calculus which is defined as multiplicative calculus provides a great benefit. Multiplicative calculus is convenient for some problems, e.g., in applied mathematics [1, 3, 4, 6, 19, 28, 29], mathematical analysis [6, 15, 19, 21, 24, 30], spectral analysis [11, 14, 31], physics [10, 22], biology [16, 17], economics and finance [7, 8], medicine [9], pattern recognition in images [18] and signal processing [20]. In recent years, multiplicative calculus has received a lot of attention, and most of the published research has been interested in some problems of differential equation, integral equation, spectral analysis, mathematical analysis. Sturm-Liouville equations lead to the development of many problems in mathematics and physics [32]. Important results have been obtained on Sturm-Liouville equations by many researchers over the years. Recently, some spectral properties of Sturm-Liouville problems in multiplicative calculus have been studied by many authors [11, 14, 31]. In [11], the author has moved a special S-L problem in the usual case to multiplicative calculus in the aspect of spectral analysis. He has investigated asymptotic behaviors of eigenvalues and eigenfunctions of the given S-L problem.

General properties of multiplicative Sturm-Liouville problems which arise in many problems of mathematics, physics, engineering have not been studied in multiplicative analysis yet. In this paper, we deal with multiplicative Sturm-Liouville problems in general form. We give some general properties of multiplicative regular and periodic Sturm-Liouville problems.

The paper is organized as follows. In Section 2, we recall some main definitions and concepts in multiplicative analysis. In Section 3, we present orthogonality of different eigenfunctions corresponding to different eigenvalues of multiplicative Sturm-Liouville problems and we discuss the uniqueness with a constant factor difference of eigenfunctions corresponding to same eigenvalues. Also, we find that the eigenvalues of multiplicative regular S-L problems are real. Finally, we give some applications of our main problems in the last section.

2. PRELIMINARIES

In this section, we will recall some well-known fundamental definitions and theorems of the multiplicative calculus given in [2, 12, 13, 23].

Non-Newtonian calculus use different types of arithmetic and their generators. Let α be a bijection between subsets X and Y of the set of real numbers \mathbb{R} , with $\alpha : X \rightarrow Y \subset \mathbb{R}$. α defines an arithmetic if the following operators are satisfied:

$$\begin{aligned} x \oplus y &= \alpha (\alpha^{-1}(x) + \alpha^{-1}(y)) \\ x \ominus y &= \alpha (\alpha^{-1}(x) - \alpha^{-1}(y)) \\ x \odot y &= \alpha (\alpha^{-1}(x) \cdot \alpha^{-1}(y)) \\ x \oslash y &= \alpha (\alpha^{-1}(x) / \alpha^{-1}(y)). \end{aligned} \tag{1}$$

If we choose α as identity function and $X = \mathbb{R}$, then (1) reduces to standard arithmetic and we get the ordinary Newtonian calculus.

Throughout the paper, we fix $\alpha(x) = e^x$, $\alpha^{-1}(x) = \ln(x)$, and $X = \mathbb{R}^+$. Then, it follows from (1)

$$\begin{aligned} x \oplus y &= x \cdot y, \\ x \ominus y &= \frac{x}{y}, \\ x \odot y &= x^{\ln(y)}, \\ x \oslash y &= x^{\frac{1}{\ln(y)}}. \end{aligned}$$

Let $a, b, c \in \mathbb{R}^+$. The operation \odot satisfies the following properties (cf. Proposition 2.1 of [5, 24])

- i) $a \odot b = b \odot a$ (commutativity)
- ii) $a \odot (b \odot c) = (a \odot b) \odot c$ (associativity)
- iii) $a \odot e = a$ (Euler's number e is the neutral element for \odot)
- iv) If $a^{\{-1\}} = e \oslash a$, $a \neq 1$, then $a \odot a^{\{-1\}} = e$ (inverse element)
- v) $b \odot a^{\{-1\}} = b \oslash a$
- vi) $(a^{\{-1\}})^{\{-1\}} = a$
- vii) $\ln(a \odot b) = \ln(a) \oplus \ln(b)$
- viii) $(a \odot b)^{\{-1\}} = a^{\{-1\}} \oslash b^{\{-1\}}$.

In view of the mentioned properties, $(\mathbb{R}^+, \oplus, \odot)$ is a field (see [5]).

Let A be a set of positive functions defined on a subset of \mathbb{R} and let $\oplus : AxA \rightarrow A$ be an operation satisfying the following properties:

$$\begin{aligned} f \oplus g &= fg \\ f \ominus g &= \frac{f}{g} \\ f \odot g &= f^{\ln g} = g^{\ln f}. \end{aligned} \tag{2}$$

Then, the algebraic structure (A, \oplus) is called a multiplicative group and (A, \oplus, \odot) is a multiplicative ring [2]. This situation allows us to define different structures.

Definition 1. Let $S \subset A \neq \emptyset$ and $\langle, \rangle_*: S \times S \rightarrow \mathbb{R}^+$ be a mapping such that the following axioms are satisfied for each $f, g, h \in S$:

- i) $\langle f, f \rangle_* \geq 1$,
- ii) $\langle f, f \rangle_* = 1$ if $f = 1$,
- iii) $\langle f \oplus g, h \rangle_* = \langle f, h \rangle_* \oplus \langle g, h \rangle_*$,
- iv) $\langle e^\alpha \odot f, g \rangle_* = e^{\alpha \odot} \langle f, g \rangle_*$, $\alpha \in \mathbb{R}$,
- v) $\langle f, g \rangle_* = \langle g, f \rangle_*$.

This mapping is called multiplicative inner product on S and is denoted by \langle, \rangle_* . Also, the space (S, \langle, \rangle_*) is called the *inner product space [11].

Definition 2 (see [2]). Let $f: A \subseteq \mathbb{R} \rightarrow \mathbb{R}^+$ be a positive function. The multiplicative derivative of the function f , which is denoted by f^* , is defined as

$$f^*(x) = \lim_{h \rightarrow 0} \left[\frac{f(x+h)}{f(x)} \right]^{\frac{1}{h}},$$

if the above limit exists. Note that the multiplicative derivative is also called geometric derivative.

Since f is a positive function, we can write the multiplicative derivative in the following form

$$f^*(x) = e^{(\ln \circ f)'(x)}$$

by using the properties of the classical derivative. It is seen that there exists the following relation between the classical derivative and multiplicative derivative

$$f'(x) = f(x) \ln f^*(x),$$

where f is a positive function. Moreover, the second order multiplicative derivative of f is obtained by taking multiplicative derivative of the function f^* and it is represented by f^{**} . By taking n -times multiplicative derivative of the function f consecutively, we get n -th order multiplicative derivative of the function f at the point x as

$$f^{*(n)}(x) = e^{(\ln \circ f)^{(n)}(x)}.$$

Theorem 1 (see [2]). Assume that f, g are multiplicative differentiable functions and h is a classical differentiable function at the point x . Then, it follows

- i) $(cf)^*(x) = f^*(x)$,
- ii) $(fg)^*(x) = f^*(x)g^*(x)$,
- iii) $\left(\frac{f}{g}\right)^*(x) = \frac{f^*(x)}{g^*(x)}$,
- iv) $(f^h)^*(x) = f^*(x)^{h(x)} f(x)^{h'(x)}$,

$$\text{v)} (f \circ h)^*(x) = f^*(h(x))^{h'(x)},$$

$$\text{vi)} (f + g)^*(x) = f^*(x)^{f(x)/(f(x)+g(x))} g^*(x)^{g(x)/(f(x)+g(x))},$$

where c is a positive constant.

Definition 3 (see [2]). Let f be a positive bounded function on $[a, b]$ where $-\infty < a < b < \infty$. A multiplicative integral of the function f is defined by

$$\int_a^b f(x) dx = e^{\int_a^b (\ln f(x)) dx}$$

if f is Riemann integrable on $[a, b]$.

On the other hand, the multiplicative integral of f on $[a, b]$ shows that

$$\int_a^b f(x) dx = \ln \int_a^b (e^{f(x)}) dx.$$

This multiplicative integral has the following properties:

$$\text{i)} \int_a^b [f(x)^k] dx = \left[\int_a^b f(x) dx \right]^k,$$

$$\text{ii)} \int_a^b [f(x)g(x)] dx = \int_a^b f(x) dx \int_a^b g(x) dx,$$

$$\text{iii)} \int_a^b \left[\frac{f(x)}{g(x)} \right] dx = \frac{\int_a^b f(x) dx}{\int_a^b g(x) dx},$$

$$\text{iv)} \int_a^b f(x) dx = \int_a^c f(x) dx \int_c^b f(x) dx,$$

where f, g are multiplicative integrable functions, $k \in \mathbb{R}$ is a constant and $c \in [a, b]$.

Definition 4. Assume that y_1, y_2, \dots, y_n functions are positive functions which are multiplicative differentiable at least $(n-1)$ times and a matrix M with dimension $n \times n$ is defined as

$$M = \begin{pmatrix} \ln y_1 & \ln y_2 & \dots & \ln y_n \\ \ln y_1^* & \ln y_2^* & \dots & \ln y_n^* \\ \vdots & \vdots & \dots & \vdots \\ \ln y_1^{*(n-1)} & \ln y_2^{*(n-1)} & \dots & \ln y_n^{*(n-1)} \end{pmatrix}.$$

Then, the determinant W_n defined as

$$W_n (y_1, y_2, \dots, y_n) = \det M$$

is called the multiplicative Wronskian determinant of the functions $\{y_i\}_{i=1}^n$ [26].

Note that the space $L_2^* [a, b] = \left\{ f : \int_a^b [f(x) \odot f(x)]^{dx} < \infty \right\}$ is an *inner product space with multiplicative inner product

$$\langle, \rangle_* : L_2^* [a, b] \times L_2^* [a, b] \rightarrow \mathbb{R}^+, \quad \langle f, g \rangle_* = \int_a^b [f(x) \odot g(x)]^{dx},$$

where $f, g \in L_2^* [a, b]$ are positive functions. It is clear that the space $L_2^* [a, b]$ is the multiplicative analogue of the well-known $L_2 [a, b]$. Since this space is a linear space and the field that we study is a special field whose scalars are real numbers, it helps us to find the properties of eigenvalues of the problems. Hence, it is important to study in the field $(\mathbb{R}^+, \oplus, \odot)$ for our results.

Definition 5. i) The n -th order multiplicative linear differential expression is given by

$$T(y) = [y^{*(n)}]^{a_n(x)} [y^{*(n-1)}]^{a_{n-1}(x)} \dots y^{a_0(x)}.$$

Here $a_n(x), a_{n-1}(x), \dots, a_0(x)$ are continuous exponents on $[a, b]$ and $y(x) \in C^{*(n)}$, where $C^{*(n)}$ is the set of the functions which are n -th order multiplicative differentiable and continuous.

ii) A solution of $T(y) = y^\lambda$ which satisfies $y \neq 1$ and $y \in L_2^* [a, b]$ is called a multiplicative eigenfunction of the operator T and the corresponding value of λ is called a multiplicative eigenvalue of the operator T [11].

3. MAIN RESULTS

Let us start our discussion with the boundary value problem

$$L[y] = \left((y^*)^{p(x)} \right)^* y^{q(x)} = y^{-\lambda s(x)}; \quad p(x) > 0, s(x) > 0 \tag{3}$$

defined on (a, b) , which has the boundary conditions

$$(y(a))^{a_1} (y^*(a))^{a_2} = 1 \tag{4}$$

$$(y(b))^{b_1} (y^*(b))^{b_2} = 1,$$

where $a_i, b_i; i = 1, 2$ are given constants, $a_1^2 + a_2^2 \neq 0, b_1^2 + b_2^2 \neq 0, p(x), p^*(x), q(x)$ and $s(x)$ are to be assumed continuous for $x \in [a, b]$. This problem is called a multiplicative regular Sturm-Liouville problem.

Definition 6. Let $\{\psi_k\}$ be a sequence of multiplicative integrable functions and s be a positive function on $[a, b]$. If the following equation holds for $k \neq j$

$$\int_a^b \left(\psi_k(x)^{s(x) \ln \psi_j(x)} \right)^{dx} = 1, \quad (5)$$

then the sequence of functions $\{\psi_k\}$ is orthogonal with respect to the weight function s on $[a, b]$. In particular, the special case of this definition for $s = 1$ was given in [11].

Theorem 2. Let $\psi_j(x, \lambda_j)$ and $\psi_k(x, \lambda_k)$ be multiplicative eigenfunctions of the regular Sturm-Liouville problem (3)-(4) corresponding to different multiplicative eigenvalues λ_j and λ_k , respectively. Then, $\psi_j(x, \lambda_j)$ and $\psi_k(x, \lambda_k)$ are orthogonal with respect to the weight function s .

Proof. Since $\psi_j(x, \lambda_j)$ and $\psi_k(x, \lambda_k)$ are the solutions of the equation (3), we can write

$$\left(\psi_j^*(x)^{p(x)} \right)^* \psi_j(x)^{q(x)} = \psi_j(x)^{-\lambda_j s(x)} \quad (6)$$

$$\left(\psi_k^*(x)^{p(x)} \right)^* \psi_k(x)^{q(x)} = \psi_k(x)^{-\lambda_k s(x)}. \quad (7)$$

By using (6) and (7), we obtain

$$\frac{\left(\psi_j^*(x)^{p(x)} \right)^* \ln \psi_k(x)}{\left(\psi_k^*(x)^{p(x)} \right)^* \ln \psi_j(x)} = \frac{\psi_j(x)^{-\lambda_j s(x) \ln \psi_k(x)}}{\psi_k(x)^{-\lambda_k s(x) \ln \psi_j(x)}}. \quad (8)$$

On the other hand, we have

$$\frac{\left(\psi_j^*(x)^{p(x)} \right)^* \ln \psi_k(x)}{\left(\psi_k^*(x)^{p(x)} \right)^* \ln \psi_j(x)} = \frac{\left(\psi_j^*(x)^{p(x) \ln \psi_k(x)} \right)^*}{\left(\psi_k^*(x)^{p(x) \ln \psi_j(x)} \right)^*} = \left(\frac{\psi_j^*(x)^{p(x) \ln \psi_k(x)}}{\psi_k^*(x)^{p(x) \ln \psi_j(x)}} \right)^*. \quad (9)$$

From (8) and (9), it follows

$$\left(\frac{\psi_j^*(x)^{p(x) \ln \psi_k(x)}}{\psi_k^*(x)^{p(x) \ln \psi_j(x)}} \right)^* = \frac{\psi_j(x)^{-\lambda_j s(x) \ln \psi_k(x)}}{\psi_k(x)^{-\lambda_k s(x) \ln \psi_j(x)}}. \quad (10)$$

By taking the multiplicative integral from a to b in (10) and using the properties of multiplicative integrals given in previous section, the following equation is obtained

$$\frac{\psi_j^*(b)^{p(b) \ln \psi_k(b)} \psi_k^*(a)^{p(a) \ln \psi_j(a)}}{\psi_k^*(b)^{p(b) \ln \psi_j(b)} \psi_j^*(a)^{p(a) \ln \psi_k(a)}} = \left(\int_a^b \left(\psi_k(x)^{s(x) \ln \psi_j(x)} \right)^{dx} \right)^{\lambda_k - \lambda_j}. \quad (11)$$

By the help of the boundary conditions in (4) and the equation (11), we find

$$\left(\int_a^b \left(\psi_k(x)^{s(x) \ln \psi_j(x)} \right)^{dx} \right)^{\lambda_k - \lambda_j} = 1.$$

Since $\lambda_j \neq \lambda_k$, the proof of theorem is completed. □

Now, consider a multiplicative periodic Sturm-Liouville problem

$$L[y] = \left((y^*)^{p(x)} \right)^* y^{q(x)} = y^{-\lambda s(x)}, \quad x \in [a, b]$$

with the periodic boundary conditions

$$y(a) = y(b) \tag{12}$$

$$y^*(a) = y^*(b),$$

where $p(a) = p(b)$.

Theorem 3. *The multiplicative eigenfunctions of the multiplicative periodic Sturm-Liouville problem (3)-(12) are orthogonal with respect to the weight function s on $[a, b]$.*

Proof. Let $\psi_j(x, \lambda_j)$ and $\psi_k(x, \lambda_k)$ be multiplicative eigenfunctions corresponding to distinct multiplicative eigenvalues λ_j and λ_k , respectively. Since ψ_j and ψ_k satisfy the periodic boundary conditions, we have

$$\begin{aligned} \psi_j(a) &= \psi_j(b) & , & & \psi_j^*(a) &= \psi_j^*(b) \\ \psi_k(a) &= \psi_k(b) & , & & \psi_k^*(a) &= \psi_k^*(b). \end{aligned} \tag{13}$$

By using (3), we can easily find

$$\left(\frac{\psi_j^*(b)^{\ln \psi_k(b)}}{\psi_k^*(b)^{\ln \psi_j(b)}} \right)^{p(b)} \left(\frac{\psi_k^*(a)^{\ln \psi_j(a)}}{\psi_j^*(a)^{\ln \psi_k(a)}} \right)^{p(a)} = \left(\int_a^b \left(\psi_k(x)^{s(x) \ln \psi_j(x)} \right)^{dx} \right)^{\lambda_k - \lambda_j}.$$

Since $p(a) = p(b)$ is in the periodic Sturm-Liouville problem and by the help of (13), by taking into account multiplicative algebraic operations given by (2) it follows

$$\int_a^b \left(\psi_k(x)^{s(x) \ln \psi_j(x)} \right)^{dx} = 1$$

for $\lambda_j \neq \lambda_k$. □

Lemma 1. *All multiplicative eigenvalues of the multiplicative regular Sturm-Liouville problem (3)-(4) are real.*

Proof. Let $\lambda_j = \alpha + i\beta$ be a complex multiplicative eigenvalue of the problem (3)-(4) corresponding the eigenfunction $\psi_j(x, \lambda_j)$. Then, $\lambda_k = \alpha - i\beta$, which is the conjugate of the multiplicative eigenvalue of λ_j , is also the multiplicative eigenvalue for (3)-(4) corresponding to eigenfunction $\psi_k(x, \lambda_k)$. By means of Theorem 2

$$\left(\int_a^b \left(\psi_k(x, \lambda_k)^{s(x) \ln \overline{\psi_k(x, \lambda_k)}} \right)^{dx} \right)^{\lambda_k - \lambda_j} = 1, \tag{14}$$

from rule (i) in Definition 3, it follows

$$\int_a^b \left(\left(\psi_k(x, \lambda_k)^{s(x) \ln \overline{\psi_k(x, \lambda_k)}} \right)^{\lambda_k - \lambda_j} \right)^{dx} = 1.$$

By definition of the multiplicative integral, we obtain

$$2i\beta \int_a^b s(x) |\ln \psi_k(x, \lambda_k)|^2 dx = 0.$$

The last equation holds if and only if when $\beta = 0$. Because, $s(x)$ is a positive function and $\psi_k(x, \lambda_k)$ can not be equal to 1. This is a contradiction, i.e., all multiplicative eigenvalues of (3)-(4) are real. \square

Theorem 4. *If the functions $\psi_j(x)$ and $\psi_k(x)$ are any two solutions of (3) on $[a, b]$, then the following equation is verified*

$$p(x) W(x; \psi_j, \psi_k) = \mu,$$

where W is Wronskian and μ is a constant.

Proof. Since the functions $\psi_j(x, \lambda)$ and $\psi_k(x, \lambda)$ are solutions of the following equation on $[a, b]$

$$L[y] = y^{-\lambda s(x)},$$

it follows from (10)

$$\left(\frac{\psi_j^*(x)^{p(x) \ln \psi_k(x)}}{\psi_k^*(x)^{p(x) \ln \psi_j(x)}} \right)^* = 1. \quad (15)$$

By taking the multiplicative integral from a to x in (15), we find

$$\left(\frac{\psi_j^*(x)^{\ln \psi_k(x)}}{\psi_k^*(x)^{\ln \psi_j(x)}} \right)^{p(x)} \left(\frac{\psi_k^*(a)^{\ln \psi_j(a)}}{\psi_j^*(a)^{\ln \psi_k(a)}} \right)^{p(a)} = 1. \quad (16)$$

From the definition of Wronskian, we get

$$\begin{aligned} W(x; \psi_j, \psi_k) &= \ln \psi_k^*(x)^{\ln \psi_j(x)} - \ln \psi_j^*(x)^{\ln \psi_k(x)} \\ &= \ln \left(\frac{\psi_k^*(x)^{\ln \psi_j(x)}}{\psi_j^*(x)^{\ln \psi_k(x)}} \right). \end{aligned} \quad (17)$$

By using (16) and (17) the following can be easily seen

$$e^{-W(x; \psi_j, \psi_k)p(x)} e^{W(a; \psi_j, \psi_k)p(a)} = 1.$$

It is seen that

$$W(x; \psi_j, \psi_k)p(x) = W(a; \psi_j, \psi_k)p(a).$$

By the help of the last equality, the proof is completed. \square

Theorem 5. *The multiplicative eigenfunction corresponding to any multiplicative eigenvalue of the regular Sturm-Liouville problem given by (3)-(4) is unique with a constant factor difference.*

Proof. Let $\psi_j(x, \lambda)$ and $\psi_k(x, \lambda)$ be multiplicative eigenfunctions of (3) corresponding to multiplicative eigenvalue λ . From Theorem 4, we have

$$p(x)W(x; \psi_j, \psi_k) = \mu,$$

where $p > 0$. It is clear from this equation that for each any point $x_0 \in [a, b]$ if $W(x_0; \psi_j, \psi_k) = 0$, then for all $x_0 \in [a, b]$ it should be $W(x; \psi_j, \psi_k) \equiv 0$. On the other hand, by using the boundary condition (4), we obtain

$$\psi_j^*(a)^{a_2} = \frac{1}{\psi_j(a)^{a_1}}, \quad \psi_k^*(a)^{a_2} = \frac{1}{\psi_k(a)^{a_1}}. \quad (18)$$

Since a_1 and a_2 should not be zero at once, it follows from the definition of Wronskian

$$e^{-W(a; \psi_j, \psi_k)} = \frac{\psi_k^*(a)^{\ln \psi_j(a)}}{\psi_j^*(a)^{\ln \psi_k(a)}}.$$

By using (18) and the last equality, we get

$$e^{-W(a; \psi_j, \psi_k)} = \frac{\psi_j(a)^{\frac{a_1}{a_2} \ln \psi_k(a)}}{\psi_k(a)^{\frac{a_1}{a_2} \ln \psi_j(a)}} = 1,$$

which gives $W = 0$ at the point $x_0 = a \in [a, b]$. So, $W \equiv 0$ on $[a, b]$. This is a sufficient condition for ψ_j and ψ_k to be linear dependent. Therefore, one of these solution is a constant multiple of the other. \square

4. APPLICATIONS

In this section, we will give some examples of multiplicative Sturm-Liouville problems defined by (3)-(4) and (3)-(12).

Example 1. Consider the multiplicative eigenvalue problem

$$\begin{aligned} y^{**}y^\lambda &= 1, \quad 0 \leq x \leq \pi \\ y(0) &= y^*(\pi) = 1. \end{aligned} \quad (19)$$

Assume that $\lambda \leq 0$. We get the solution of (19) as follow

$$y(x) = e^{c_1 e^{\sqrt{-\lambda}x} + c_2 e^{-\sqrt{-\lambda}x}},$$

where c_1 and c_2 are real numbers. Since $y(0) = y^*(\pi) = 1$, $c_1 = c_2 = 0$ is found. Since for $\lambda \leq 0$ we have the trivial multiplicative eigenfunction $y(x, \lambda) = 1$ of the problem (19), there is no eigenvalue for $\lambda \leq 0$. Now, assume that $\lambda > 0$. We get the solution of (19)

$$y(x) = e^{l_1 \cos \sqrt{\lambda}x + l_2 \sin \sqrt{\lambda}x},$$

where l_1 and l_2 are real numbers. Using the condition $y(0) = y^*(\pi) = 1$, we obtain the multiplicative eigenfunctions

$$y_n(x) = e^{l_2 \sin\left(\frac{2n-1}{2}x\right)}$$

of (19) corresponding to eigenvalues

$$\lambda_n = \left(\frac{2n-1}{2}\right)^2; \quad n = 1, 2, 3 \dots$$

Without loss of generality, by taking $l_2 = 1$, we get the family of eigenfunctions

$$y_n(x) = e^{\sin\left(\frac{2n-1}{2}x\right)}.$$

Remark 1. Since different multiplicative eigenfunctions corresponding to different eigenvalues of (3)-(4) are orthogonal as a consequence of Theorem 2, the following result holds

$$\int_0^\pi \left(y_n(x)^{\ln y_m(x)}\right)^{dx} = \int_0^\pi \left(e^{\sin\left(\frac{2n-1}{2}x\right) \sin\left(\frac{2m-1}{2}x\right)}\right)^{dx} = 1.$$

Example 2. Let us consider the following multiplicative periodic eigenvalue problem

$$\begin{aligned} y^{**}y^\lambda &= 1, \quad 0 \leq x \leq \pi \\ y(0) &= y(\pi), \quad y^*(0) = y^*(\pi). \end{aligned} \quad (20)$$

Since we have trivial eigenfunction $y(x) = 1$ for $\lambda < 0$, there is no eigenfunction of S-L problem for $\lambda < 0$. For $\lambda = 0$, the nontrivial solution of the problem is obtained as $y(x) = e$. Now, suppose that $\lambda > 0$. Then, we find the solution of (20) as follow

$$y(x) = e^{k_1 \cos \sqrt{\lambda}x + k_2 \sin \sqrt{\lambda}x},$$

where k_1 and k_2 are real numbers. From $y(0) = y(\pi)$, $y^*(0) = y^*(\pi)$, we find

$$k_2 = -k_1 \sin \sqrt{\lambda}\pi + k_2 \cos \sqrt{\lambda}\pi, \quad k_1 = k_1 \cos \sqrt{\lambda}\pi + k_2 \sin \sqrt{\lambda}\pi,$$

from which it gives $k_1 = k_2 = 0$. So, we get only a trivial eigenfunction of (20) for $\lambda > 0$. Thus, it is seen that the nontrivial solution of the given multiplicative periodic eigenvalue problem is $y(x) = e$ corresponding to eigenvalue $\lambda = 0$.

Example 3. Consider the following multiplicative Sturm-Liouville problem

$$\begin{aligned} (y^{**})^{x^2} (y^*)^x y^\lambda &= 1 \\ y(1) &= 1, \quad y(e) = 1. \end{aligned} \quad (21)$$

It is known that the following equalities are provided when the substitution $x = e^t$ is applied [27]

$$\left(\tilde{D}y\right)^x = \tilde{D}_1y \quad \text{and} \quad \left(\tilde{D}^{(2)}y\right)^{x^2} = \left(\tilde{D}_1^{(2)}y\right) \left(\tilde{D}_1y\right)^{-1}, \quad (22)$$

where \tilde{D} is the multiplicative derivative operator of y with respect to x and \tilde{D}_1 is the multiplicative derivative operator of y with respect to t . By the help of (22), we write

$$(y^*)^x = (e^{D \ln y})^x = e^{D_1 \ln y} = \tilde{D}_1 y$$

$$(y^{**})^{x^2} = (e^{D^2(\ln y)})^{x^2} = e^{D_1(D_1-1) \ln y} = (\tilde{D}_1^{(2)} y) (\tilde{D}_1 y)^{-1}, \quad (23)$$

where D is the derivative operator of y with respect to x and D_1 is the derivative operator of y with respect to t . Then, from (21) and (23), we get

$$e^{(D_1(D_1-1)+D_1+\lambda) \ln y} = 1,$$

from which it follows $(D_1^2 + \lambda) \ln y = 0$. If $\lambda \leq 0$, then we get

$$y(x) = e^{m_1 e^{\sqrt{-\lambda} \ln x} + m_2 e^{-\sqrt{-\lambda} \ln x}},$$

where m_1 and m_2 are real numbers. By using the condition $y(1) = 1$, $y(e) = 1$, it is clear that $m_1 = m_2 = 0$. Since for $\lambda \leq 0$ we have the trivial multiplicative eigenfunction $y(x, \lambda) = 1$ of this example, there is no eigenvalue for $\lambda \leq 0$. If $\lambda > 0$, we find the solution of (21) as follow

$$y(x) = e^{v_1 \cos(\sqrt{\lambda} \ln x) + v_2 \sin(\sqrt{\lambda} \ln x)},$$

where v_1 and v_2 are real numbers. From the boundary condition $y(1) = 1$, $y(e) = 1$, we get the multiplicative eigenfunctions

$$y_n(x) = e^{v_2 \sin(n\pi \ln x)}$$

of (21) corresponding to eigenvalues

$$\lambda_n = (n\pi)^2,$$

where $n = 1, 2, 3, \dots$

Author Contribution Statements The authors contributed equally to this work. All authors read and approved the final copy of this paper

Declaration of Competing Interests The authors declare that they have no competing interest.

REFERENCES

- [1] Aniszewska, D., Multiplicative Runge-Kutta method, *Nonlinear Dynamics*, 50 (2007), 265-272. <https://doi.org/10.1007/s11071-006-9156-3>.
- [2] Bashirov, A. E., Mısırlı, E., Özyapıcı, A., Multiplicative calculus and its applications, *Journal of Mathematical Analysis and Applications*, 337(1) (2008), 36-48. <https://doi.org/10.1016/j.jmaa.2007.03.081>.
- [3] Bashirov, A. E., Mısırlı, E., Tandoğdu, Y., Özyapıcı, A., On modeling with multiplicative differential equations, *Applied Mathematics-A Journal of Chinese Universities*, 26(4) (2011), 425-438. <https://doi.org/10.1007/s11766-011-2767-6>.
- [4] Bashirov, A. E., Riza, M., On complex multiplicative differentiation, *TWMS Journal of Applied and Engineering Mathematics*, 1(1) (2011), 75-85.

- [5] Campillay-Llanos, W., Guevara, F., Pinto, M., Torres, R., Differential and integral proportional calculus: how to find a primitive for $f(x)=1/2\pi e(1/2)x^2$, *International Journal of Mathematical Education in Science and Technology*, 52(3) (2021), 463-476. <https://doi.org/10.1080/0020739X.2020.1763489>.
- [6] Çakmak, A. F., Başar, F., Some new results on sequence spaces with respect to non-Newtonian calculus, *Journal of Inequalities and Applications*, 1 (2012), 1-7. <https://doi.org/10.1186/1029-242X-2012-228>.
- [7] Filip, D., Piatecki, C., A non-Newtonian examination of the theory of exogenous economic growth, *Mathematica Aeterna*, 4(2) (2014), 101–117.
- [8] Filip, D., Piatecki, C., An overview on the non-Newtonian calculus and its potential applications to economics, *Applied Mathematics and Computation*, 187(1) (2007), 68-78. <https://hal.science/hal-00945788>.
- [9] Florack, L., Van Assen, H., Multiplicative calculus in biomedical image analysis, *Journal of Mathematical Imaging and Vision*, 42(1), (2012) 64-75. <https://doi.org/10.1007/s10851-011-0275-1>.
- [10] Frederico, G. S. F., Odziejewicz, T., Torres, D. F. M., Noether's theorem for non-smooth externals of variational problems with time delay, *Applicable Analysis*, 93 (2014), 153-170. <http://dx.doi.org/10.1080/00036811.2012.762090>.
- [11] Göktas, S., A New Type of Sturm-Liouville equation in the non-Newtonian calculus, *Journal of Function Spaces*, (2021), 8 pages. <https://doi.org/10.1155/2021/5203939>.
- [12] Grossman, M., An introduction to non-Newtonian calculus, *International Journal of Mathematical Education in Science and Technology*, 10(4) (1979), 525-528. <https://doi.org/10.1080/0020739790100406>.
- [13] Grossman, M., Katz, R., Non-Newtonian Calculus, Lee Press, Pigeon Cove, 1972.
- [14] Gülsen, T., Yılmaz, E., Göktas, S., Multiplicative Dirac system, *Kuwait Journal of Science*, (2021). <https://doi.org/10.48129/kjs.13411>.
- [15] Gurefe, Y., Kadak, Y., Misirli, E., Kurdi, A., A new look at the classical sequence spaces by using multiplicative calculus, *University Politehnica of Bucharest Scientific Bulletin, Series A: Applied Mathematics and Physics*, 78(2) (2016), 9-20.
- [16] Jost, J., *Mathematical Methods in Biology and Neurobiology*, Universitext, Springer, New York, 1972.
- [17] Lemos-Paiao, A. P., Torres, C. J., Venturino, D. F. M., Optimal control of aquatic diseases: A case study of Yemen's cholera outbreak, *Journal of Optimization Theory and Applications*, 185 (2020), 1008-1030. <https://doi.org/10.1007/s10957-020-01668-z>.
- [18] Mora, M., Cordova-Lepe, F., Del-Valle, R., A non-Newtonian gradient for counter detection in images with multiplicative noise., *Pattern Recognition Letter*, 33 (2012), 1245-1256. <https://doi.org/10.1016/j.patrec.2012.02.012>.
- [19] Özcan, S., Some integral inequalities of Hermite-Hadamard type for multiplicatively preinvex functions, *AIMS Mathematics*, 5(2) (2020), 1505-1518. <https://doi.org/10.3934/math.2020103>.
- [20] Özyapıcı, A., Bilgehan, B., Finite product representation via multiplicative calculus and its applications to exponential signal processing, *Numer. Algorithms*, 71(2) (2016), 475-489. <https://doi.org/10.1007/s11075-015-0004-8>.
- [21] Pinto, M., Torres, R., Campillay-Llanos, W., Guevara-Morales, F., Applications of proportional calculus and a non-Newtonian logistic growth model, *Proyecciones*, 39 (2020), 1471–1513. <http://dx.doi.org/10.22199/issn.0717-6279-2020-06-0090>.
- [22] Silva, C. J., Torres, D. F. M., Two-dimensional Newton's problem of minimal resistance, *Control Cybernet*, 35 (2006), 965-975. <https://doi.org/10.3390/axioms10030171>.
- [23] Stanley, D., A multiplicative calculus, *Primus*, 9(4) (1999), 310-326. <https://doi.org/10.1080/10511979908965937>.

- [24] Torres, D. F. M., On a non-Newtonian calculus of variations, *Axioms*, 10(3) (2021), 15 pages. <https://doi.org/10.3390/axioms10030171>.
- [25] Waseem, M., Muhammad, M., Aslam Noor, F., Ahmed Shah, F., Inayat Noor, K., An efficient technique to solve nonlinear equations using multiplicative calculus, *Turkish Journal of Mathematics*, 42(2) (2018), 679–691. <https://doi.org/10.3906/mat-1611-95>.
- [26] Yalçın, N., Çelik, E., Solution of multiplicative homogeneous linear differential equations with constant exponentials, *New Trends in Mathematical Sciences*, 6(2) (2018), 58–67. <http://dx.doi.org/10.20852/ntmsci.2018.270>.
- [27] Yalçın, N., Çelik, E., Multiplicative Cauchy-Euler and Legendre Differential Equation, *Gümüşhane Üniversitesi Fen Bilimleri Enstitüsü Dergisi*, 9(3) (2019), 373 - 382. <https://doi.org/10.17714/gumusfenbil.451718>.
- [28] Yalçın, N., The solutions of multiplicative Hermite differential equation and multiplicative Hermite polynomials, *Rendiconti del Circolo Matematico di Palermo Series 2*, 70(1) (2021), 9-21. <http://dx.doi.org/10.1007/s12215-019-00474-5>.
- [29] Yalçın N., Dedeturk, M., Solutions of multiplicative ordinary differential equations via the multiplicative differential transform method, *AIMS Mathematics*, 6(4) (2021), 3393-3409. <https://doi.org/10.3934/math.2021203>.
- [30] Yener, G., Emiroglu, İ., A q-analogue of the multiplicative calculus:q-multiplicative calculus, *Discrete and Continuous Dynamical System*, 8(6) (2015), 1435–1450.
- [31] Yılmaz, E., Multiplicative Bessel equation and its spectral properties, *Ricerche di Matematica*, (2021). <https://doi.org/10.1007/s11587-021-00674-1>.
- [32] Zettl, A., Sturm–Liouville Theory, American Mathematical Society, 2010.



SELF CENTERED INTERVAL-VALUED INTUITIONISTIC FUZZY GRAPH WITH AN APPLICATION

S. Angelin Kavitha RAJ¹, S. N. Suber BATHUSHA² and S. Satham HUSSAIN^{3,4}

¹Department of Mathematics, Sadakathullah Appa College, Affiliated to Manonmaniam Sundaranar University, Tamil Nadu, INDIA

²Research Scholar, Reg. No:20211192091007, Department of Mathematics, Sadakathullah Appa College, Affiliated to Manonmaniam Sundaranar University, Tamil Nadu, INDIA

³P.G. and Research Department of Mathematics, Jamal Mohamed College, Trichy, Tamil Nadu, INDIA

⁴School of Advanced Science, Division of Mathematics, Vellore Institute of Technology, Chennai-600127, INDIA

ABSTRACT. In comparison to conventional fuzzy sets, the idea of interval-valued intuitionistic fuzzy sets provides a more accurate definition of uncertainty. Defuzzification is the aspect of fuzzy control that requires the most processing. It has numerous applications in fuzzy control. In this paper, the concepts strength, length, distance, eccentricity, radius, diameter, centred, self-centered, path cover, and edge cover of an interval-valued intuitionistic fuzzy graph (IVIFG) are defined in this work. Further, we introduce the definition of a self-centered IVIFG and the necessary and sufficient conditions for an IVIFG to be self-centered are given. Moreover, we investigate some properties of self-centered IVIFG with an illustration and we have discussed applications in IVIFG.

1. INTRODUCTION

L.A. Zadeh [18] developed fuzzy sets in 1965 to solve the challenges of dealing with ambiguity in fuzzy sets. Various scholars have since investigated fuzzy sets and fuzzy logic in attempt to answer other real-world issues involving ambiguous and uncertain situations. Interval-valued fuzzy sets are an extension of fuzzy sets that the author first introduced in Turksen [16] in 1986. Instead than utilising numbers as the membership function, it includes the values of number intervals to account

2020 *Mathematics Subject Classification.* 03E72, 68R10, 68R05.

Keywords. Eccentricity, radius, diameter, self centered, applications in IVIFG.

¹ ✉ angelinkavitha.s@gmail.com; 0000-0003-0712-5351

² ✉ mohamed.suber.96@gmail.com-Corresponding author; 0000-0002-1147-2391

³ ✉ sathamhussain5592@gmail.com; 0000-0002-6281-6158.

for uncertainty. It is typically represented by the symbol $[\mu_{AL}^-(x), \mu_{AU}^+(x)]$. Use the equation $0 \leq \mu_{AL}^-(x) + \mu_{AU}^+(x) \leq 1$ to represent the degree of membership of the fuzzy set A . T. Atanassov added a non-membership function that is represented by intuitionistic fuzzy sets as an additional component to fuzzy sets. Additionally, he added interval valued intuitionistic fuzzy sets to the concept of intuitionistic fuzzy sets [2]. It is preferable to depict uncertainty using interval-valued intuitionistic fuzzy sets as opposed to traditional fuzzy sets. Defuzzification, which has several applications in fuzzy control, is the component that needs the most processing. For the purpose of interpreting the degree of true and false membership functions, it is defined as a pair of intervals $[\mu^-, \mu^+], 0 \leq \mu^- + \mu^+ \leq 1$ and $[\lambda^-, \lambda^+], 0 \leq \lambda^- + \lambda^+ \leq 1$ with $0 \leq \mu^+ + \lambda^+ \leq 1$. Rosenfeld [13] created fuzzy graph theory in 1975. examined the fuzzy graphs for which Kauffmann conceived of the fundamental concept in 1973. The interval-valued neutrosophic sets (IVNS) [14], an extension of the interval-valued intuitionistic fuzzy sets (IVIFS), offer a more accurate representation of uncertainty when compared to ordinary fuzzy sets. The list of components that make up IVIFS was expanded by the addition of the indeterminate-membership function, which is represented by IVNS. Fuzzy control uses it in a variety of ways. Only holding incomplete data is permitted by the aforementioned limitations, but processing uncertain information is still necessary. Let's take a hypothetical situation where there are ten to seventeen patients being tested for a pandemic. In that period, five to seven patients will have positive results, three to six will have negative results, and two to four will still be awaiting results. It can be written as $x([0.5, 0.7], [0.2, 0.4], [0.3, 0.6])$ using neutrosophic notions. In this work, self-centered IVIFG analyses the proportion of interval-valued true and false membership functions in our result. If the indeterminate-membership function, which is represented by IVNG, is added to the result, the result can then devolve into self-centered IVNG. Rashmanlou [9], [10], [11], [12] researched fuzzy graphs with irregular IVFGs. Furthermore, they defined balanced IVFGs, antipodal IVFGs, and some properties of highly irregular IVFGs. The concept of an interval valued fuzzy subset of a set was created by Zadeh [17] in 1975 as an extension of the idea of a fuzzy set, where the values of the membership degrees are intervals of numbers rather than real numbers. Akram and Dudec [6] proposed the concept IVFGs in 2011. In this article, we present the idea of an IVIFG and analyse the concepts of strength, length, distance, eccentricity, radius, and diameter as well as of self-centered and centered. We also investigate into some of the properties of an illustration of a self-centered interval-valued intuitionistic fuzzy graph. Moreover, IVIFG applications are used to identify instability in various aspects of human life. These applications' purpose is to enhance the country's defences to the degree of its vulnerabilities. We suggested reading this article so that researchers could investigate this idea further using fuzzy graph theory to measure centre point radius distance, eccentricity, radius, and diameter are analyses. An

interval-based membership structure is offered by this set theory to handle interval-valued intuitionistic fuzzy data. By recording their hesitation when determining membership values, users are able to more accurately represent the ambiguity and unpredictability of this data. This work advances various areas that are relevant to fuzzy graph architectures across all types of graphs by utilising a number of conceptual frameworks that include vertex point and edge will analysis. this can be used in a wide variety of fuzzy set condition analysis domains. Applications of this principle include spotting instability in all aspects of human life. The structure of this paper is as follows: Introducing the concept is covered in Section 1 of the lesson plan. Preliminaries provide the fundamental definitions required for Section 2. Section 3 important concepts An interval-valued intuitionistic fuzzy graph (IV-IFG)'s strength, length, distance, eccentricity, radius, diameter, self-centeredness, path coverage, and edge coverage are specified in this work.

2. PRELIMINARIES

The discussion of some fundamental definitions and properties in this section will help in the formulation of the research studies.[3, 8, 4, 7, 6]

A graph is indeed an ordered pair $G^* = (Q, R)$, where Q is the collection of vertex positions for G^* . If a, b are on an edge of G^* , then two vertices a and b are said to be adjacent in G^* . To represent $\{a, b\}$ in R , we write ab in R . A simple graph is considered complete if an edge connects each pair of unique vertices in it. Path $P : a_1a_2\dots a_{n+1}$ ($n > 0$) in G^* has a length of n . If $a_1 = a_{n+1}$ and $n \geq 3$, a path $P : a_1a_2\dots a_{n+1}$ in G^* is referred to as a cycle. It should be noted that any edge in the cycle graph C_n can be removed to provide the path graph P_n , which has $n - 1$ edges. An undirected graph G^* is considered to be linked if there is a path connecting every pair of distinct vertices. If every pair of different vertices in a connected graph G^* has a path between them, then the distance between two vertices a, b is equal to the length of the shortest path that connects them. Eccentricity $e(a) = \max\{d(a, b)/a \in Q\}$. A connected graph's radius is given by the formula $r(G) = \min\{e(a)/a \in Q\}$. The formula $d(G) = \max\{e(a)/a \in Q\}$ is used to determine the diameter of a connected graph G^* . The set of eccentricities in a graph is called the eccentric set (S). A graph's $C(G^*)$ centre is made up of the collection of vertices with the least amount of eccentricity. If all of a graph's vertices are in the middle, the graph is said to be self-centered. As a result, the eccentric set of a self-centered graph only includes one element, meaning that all of the vertices are equally eccentric. A graph with a diameter equal to its radius is equivalently said to be self-centered.

Map $\mu : X \rightarrow [0, 1]$ is referred to as a fuzzy subset λ on a set X . Map $\lambda : X \times X \rightarrow [0, 1]$ If $\lambda(a, b) \leq \min\{\mu(a), \mu(b)\}$ for all $a, b \in X$, called a fuzzy relation on X . A fuzzy relation λ is symmetric if $\lambda(a, b) = \lambda(b, a)$ for all $a, b \in X$.

An interval number D is an interval $[a^-, a^+]$ with $0 \leq a^- \leq a^+ \leq 1$. The interval

$[a, a]$ is identified with the number $a \in [0, 1]$ $D[0, 1]$ denotes the set of all interval numbers.

Definition 1. [1] An IFS R in the universe of discourse X is characterized by two membership functions given by $\lambda_R : X \rightarrow [0, 1]$ and $\mu_R : X \rightarrow [0, 1]$ respectively, such that $\lambda_R(a) + \mu_R(a) \leq 1$ for all $a \in X$. The IFS R denoted by $R = \{(a, \lambda_R(a), \mu_R(a)) / a \in X\}$

Definition 2. [15] An IFG is of form $\tilde{G} = (\mu, \lambda)$ which $\mu = (\mu_1, \mu_2)$ and $\lambda = (\lambda_1, \lambda_2)$ so that

(i) The function $\mu_1 : Q \rightarrow [0, 1]$ and $\mu_2 : Q \rightarrow [0, 1]$ denote the degree of membership and non membership of the element $a \in Q$ respectively, such that $0 \leq \mu_1(a) + \mu_2(a) \leq 1$ for all $a \in Q$

(ii) The function $\lambda_1 : Q \times Q \rightarrow [0, 1]$ and $\lambda_2 : Q \times Q \rightarrow [0, 1]$ are defined by $\lambda_1(a, b) \leq \min\{\mu_1(a), \mu_1(b)\}$, $\lambda_2(a, b) \leq \max\{\mu_2(a), \mu_2(b)\}$ such that $0 \leq \lambda_1(a, b) + \lambda_2(a, b) \leq 1, \forall ab \in R$.

TABLE 1. Abbreviations

Notation	Meaning
$\tilde{G} = (\mu, \lambda)$	IVIFG
μ_1	IVIF degree of membership
μ_2	IVIF degree of non membership
λ_1	IVIF degree of edge membership
λ_2	IVIF degree of edge non membership
S_p	Strength of the strongest path P
l_{λ_1, λ_2}	$\lambda_1 \lambda_2$ -length of a path P
$\delta_{\lambda_1, \lambda_2}(a_i, a_j)$	$\lambda_1 \lambda_2$ -distance
$e_{\lambda_1, \lambda_2}(a_i)$	eccentricity of a_i
$r_{\lambda_1, \lambda_2}(a_i)$	radius of \tilde{G}
$d_{\lambda_1, \lambda_2}(a_i)$	diameter of \tilde{G}

3. SELF CENTERED IVIFG

IVIFG is defined in this section, which also lists helpful terms for the concepts which were used to create the main findings. We use illustrations to discuss some of the self-centered IVIFG's properties.

Definition 3. An IVIFG of the form $\tilde{G} = (\mu, \lambda)$ which $\mu = (\mu_1, \mu_2) = ([\mu_1^-, \mu_1^+], [\mu_2^-, \mu_2^+])$ and $\lambda = (\lambda_1, \lambda_2) = ([\lambda_1^-, \lambda_1^+], [\lambda_2^-, \lambda_2^+])$ So that

(1) The function $\mu_1 : Q \rightarrow [0, 1]$ and $\mu_2 : Q \rightarrow [0, 1]$ denote the degree of membership and non membership of the element $a \in Q$ respectively, such that $0 \leq \mu_1^+(a) + \mu_2^+(a) \leq 1$ for all $a \in Q$

(2) The function $\lambda_1 : Q \times Q \rightarrow [0, 1]$ and $\lambda_2 : Q \times Q \rightarrow [0, 1]$ denote the degree of interval-valued membership and interval-valued non-membership of the edge $ab \in R$, respectively, are defined by

- (i) $\lambda_1^-(a, b) \leq \min\{\mu_1^-(a), \mu_1^-(b)\}$ and $\lambda_1^+(a, b) \leq \min\{\mu_1^+(a), \mu_1^+(b)\}$
- (ii) $\lambda_2^-(a, b) \leq \max\{\mu_2^-(a), \mu_2^-(b)\}$ and $\lambda_2^+(a, b) \leq \max\{\mu_2^+(a), \mu_2^+(b)\}$ such that $0 \leq \lambda_1^+(a, b) + \lambda_2^+(a, b) \leq 1, \forall ab \in R$.

Definition 4. An IVIFG $\tilde{G} = (\mu, \lambda)$ of a graph $G^* = (Q, R)$ is called a complete if (i) $\lambda_1^-(a, b) = \min\{\mu_1^-(a), \mu_1^-(b)\}$ and $\lambda_1^+(a, b) = \min\{\mu_1^+(a), \mu_1^+(b)\}$, (ii) $\lambda_2^-(a, b) = \max\{\mu_2^-(a), \mu_2^-(b)\}$ and $\lambda_2^+(a, b) = \max\{\mu_2^+(a), \mu_2^+(b)\}$.

Example 1. An IVIFG $\tilde{G} = (\mu, \lambda)$ of a graph $G^* = (Q, R)$ given figure 1 is a complete IVIFG $\tilde{G} = (\mu, \lambda)$ such that $\mu = \{u_1([0.3, 0.5][0.2, 0.4]), u_2([0.4, 0.6][0.3, 0.4]), u_3([0.1, 0.3][0.3, 0.6]), u_4([0.3, 0.4][0.4, 0.5])\}$.

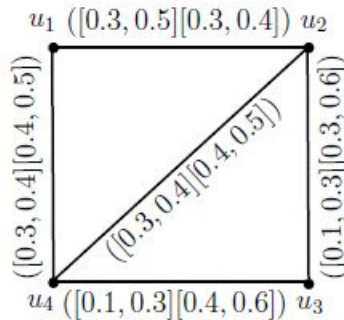


FIGURE 1. $\tilde{G} = (\mu, \lambda)$ is IVIFG of G_1^* is complete

Definition 5. A path P in IVIFG $\tilde{G} = (\mu, \lambda)$ of a graph $G^* = (Q, R)$ is a sequence of distinct vertices a_1, a_2, \dots, a_n such that either one of the following conditions is satisfied:

- (1) $\lambda_1^-(a, b) > 0, \lambda_2^-(a, b) = 0$ and $\lambda_1^+(a, b) > 0, \lambda_2^+(a, b) = 0$ for some $a, b \in R$
 - (2) $\lambda_1^-(a, b) = 0, \lambda_2^-(a, b) > 0$ and $\lambda_1^+(a, b) = 0, \lambda_2^+(a, b) > 0$ for some $a, b \in R$
 - (3) $\lambda_1^-(a, b) > 0, \lambda_1^+(a, b) = 0$ and $\lambda_2^-(a, b) > 0, \lambda_2^+(a, b) = 0$ for some $a, b \in R$
 - (4) $\lambda_1^-(a, b) = 0, \lambda_1^+(a, b) > 0$ and $\lambda_2^-(a, b) = 0, \lambda_2^+(a, b) > 0$ for some $a, b \in R$
- A path $P : a_1a_2\dots a_{n+1}$ in G^* is called a cycle if $a_1 = a_{n+1}$ and $n \geq 3$.

Definition 6. Let $P : u_1, u_2, \dots, u_n$ be a path in IVIFG $\tilde{G} = (\mu, \lambda)$ of graph $G^* = (Q, R)$. The λ_1^- -strength of all paths joining any two vertices and the expression a_i, a_j is represented by the symbol $(\lambda_{1ij}^-)^\infty$ and is defined as $\max(\lambda_1^-(a_i, a_j))$. The λ_1^+ -strength of all paths joining any two vertices and the expression a_i, a_j is represented by the symbol $(\lambda_{1ij}^+)^\infty$ and is defined as $\max(\lambda_1^+(a_i, a_j))$. The λ_2^- -

strength of all paths joining any two vertices and the expression a_i, a_j is represented by the symbol $(\lambda_{2ij}^-)^\infty$ and is defined as $\max(\lambda_2^-(a_i, a_j))$. The λ_2^+ – strength of all paths joining any two vertices and the expression a_i, a_j is represented by the symbol $(\lambda_{2ij}^+)^\infty$ and is defined as $\max(\lambda_2^+(a_i, a_j))$. If the same edge possesses every value of λ_1^- – strength, λ_1^+ – strength, λ_2^- – strength, λ_2^+ – strength, then it is the strength of the strongest path P and it is denoted by $S_P = ((\lambda_{1ij}^-)^\infty, (\lambda_{1ij}^+)^\infty), [(\lambda_{2ij}^-)^\infty, (\lambda_{2ij}^+)^\infty]$ for all $i, j = 1, 2, \dots, k$.

Definition 7. The IVIFG If any two vertices of $\tilde{G} = (\mu, \lambda)$ are connected by a path, they are said to be connected. That is, an IVIFG \tilde{G} is connected if $(\lambda_{1ij}^-)^\infty > 0$, $(\lambda_{1ij}^+)^\infty > 0$ and $(\lambda_{2ij}^-)^\infty > 0$, $(\lambda_{2ij}^+)^\infty > 0$.

Example 2. Consider a IVIFG $\tilde{G} = (\mu, \lambda)$ as shown in Figure-1 in Example-1. The path u_1u_4 has a length of 1 and a strength of $([0.3, 0.4][0.4, 0.5])$. The path $u_1u_2u_4$ has a length of 2 and a strength of $([0.3, 0.5][0.4, 0.5])$. The path $u_1u_2u_3u_4$ has a length of 3 and a strength of $([0.3, 0.5][0.4, 0.6])$.

Definition 8. Let $\tilde{G} = (\mu, \lambda)$ be a connected IVIFG of graph $G^* = (Q, R)$. The λ_1^- – length of a path $P : a_1a_2\dots a_n$ in G^* , $l_{\lambda_1^-}(p)$, is defined as $l_{\lambda_1^-}(p) = \sum_{i=1}^{n-1} \lambda_1^-(a_i, a_{i+1})$ and the λ_1^+ – length of a path $P : u_1u_2\dots u_n$ in G , $l_{\lambda_1^+}(p)$, is defined as $l_{\lambda_1^+}(p) = \sum_{i=1}^{n-1} \lambda_1^+(a_i, a_{i+1})$. The λ_2^- – length of a path $P : a_1a_2\dots a_n$ in G^* , $l_{\lambda_2^-}(p)$, is defined as $l_{\lambda_2^-}(p) = \sum_{i=1}^{n-1} \lambda_2^-(a_i, a_{i+1})$ and the λ_2^+ – length of a path $P : u_1u_2\dots u_n$ in G , $l_{\lambda_2^+}(p)$, is defined as $l_{\lambda_2^+}(p) = \sum_{i=1}^{n-1} \lambda_2^+(a_i, a_{i+1})$. The $\lambda_1\lambda_2$ – length of a path $P : u_1u_2\dots u_n$ in G , $l_{\lambda_1\lambda_2}(p)$, is defined as $l_{\lambda_1\lambda_2}(p) = (l_{\lambda_1^-}, l_{\lambda_1^+}), [l_{\lambda_2^-}, l_{\lambda_2^+}]$.

Example 3. Consider a connected IVIFG $\tilde{G} = (\mu, \lambda)$ as shown in Figure-1 in Example-1. Here, u_1u_4 is a path of length 1 and $l_{\lambda_1\lambda_2} = ([0.3, 0.4][0.4, 0.5])$, $u_1u_2u_4$ is a path of length 2 and $l_{\lambda_1\lambda_2} = ([0.6, 0.9][0.7, 0.9])$, $u_1u_2u_3u_4$ is a path of length 3 and $l_{\lambda_1\lambda_2} = ([0.5, 1.1][1.0, 1.6])$.

Definition 9. Let $\tilde{G} = (\mu, \lambda)$ be a connected IVIFG of graph $G^* = (Q, R)$. The λ_1^- – distance, $\delta_{\lambda_{1ij}^-}$, is the smallest λ_1^- – length of any $a_i - a_j$ path P in \tilde{G} , where $a_i, a_j \in Q$. That is, $\delta_{\lambda_{1ij}^-} = \delta_{\lambda_1^-}(a_i, a_j) = \min(l_{\lambda_1^-}(p))$ and λ_1^+ – distance, $\delta_{\lambda_{1ij}^+}$, is the smallest λ_1^+ – length of any $a_i - a_j$ path P in \tilde{G} , where $a_i, a_j \in Q$. That is, $\delta_{\lambda_{1ij}^+} = \delta_{\lambda_1^+}(a_i, a_j) = \min(l_{\lambda_1^+}(p))$. The λ_2^- – distance, $\delta_{\lambda_{2ij}^-}$, is the smallest λ_2^- – length of any $a_i - a_j$ path P in \tilde{G} , where $a_i, a_j \in Q$. That is, $\delta_{\lambda_{2ij}^-} = \delta_{\lambda_2^-}(a_i, a_j) = \min(l_{\lambda_2^-}(p))$ and λ_2^+ – distance, $\delta_{\lambda_{2ij}^+}$, is the smallest λ_2^+ – length of any $a_i - a_j$ path P in \tilde{G} , where $a_i, a_j \in Q$. That is, $\delta_{\lambda_{2ij}^+} = \delta_{\lambda_2^+}(a_i, a_j) = \min(l_{\lambda_2^+}(p))$. The distance, $\delta_{\lambda_1, \lambda_2}(a_i, a_j)$, is defined as $\delta_{\lambda_1, \lambda_2}(a_i, a_j) = ([\delta_{\lambda_{1ij}^-}, \delta_{\lambda_{1ij}^+}], [\delta_{\lambda_{2ij}^-}, \delta_{\lambda_{2ij}^+}])$.

Example 4. Consider a connected IVIFG $\tilde{G} = (\mu, \lambda)$ as shown in Figure-1 in Example-1. Here, $\delta_{\lambda_1^-}(u_1, u_4) = 0.3, \delta_{\lambda_1^+}(u_1, u_4) = 0.4$ and $\delta_{\lambda_2^-}(u_1, u_4) = 0.4, \delta_{\lambda_2^+}(u_1, u_4) = 0.5$. That is $\delta_{\lambda_1, \lambda_2}(u_1, u_4) = ([0.3, 0.4], [0.4, 0.5])$. Similarly, we calculate $\delta_{\lambda_1, \lambda_2}(u_1, u_2) = ([0.3, 0.5], [0.3, 0.4]), \delta_{\lambda_1, \lambda_2}(u_1, u_3) = ([0.4, 0.7], [0.6, 1.0]), \delta_{\lambda_1, \lambda_2}(u_2, u_3) = ([0.1, 0.3], [0.3, 0.6]), \delta_{\lambda_1, \lambda_2}(u_2, u_4) = ([0.2, 0.4], [0.4, 0.5]), \delta_{\lambda_1, \lambda_2}(u_3, u_4) = ([0.1, 0.3], [0.4, 0.6])$

Definition 10. Let $\tilde{G} = (\mu, \lambda)$ be a connected IVIFG of graph $G^* = (Q, R)$. For each $a_i \in Q$, the λ_1^- - eccentricity of a_i , denoted by $e_{\lambda_1^-}(a_i)$, is defined as $e_{\lambda_1^-}(a_i) = \max\{\delta_{\lambda_1^-}(a_i, a_j)/u_i \in Q\}$ and for each $a_i \in Q$, the λ_1^+ - eccentricity of a_i , denoted by $e_{\lambda_1^+}(a_i)$, is defined as $e_{\lambda_1^+}(a_i) = \max\{\delta_{\lambda_1^+}(a_i, a_j)/a_i \in Q\}$. For each $a_i \in Q$, the λ_2^- - eccentricity of a_i , denoted by $e_{\lambda_2^-}(a_i)$, is defined as $e_{\lambda_2^-}(a_i) = \max\{\delta_{\lambda_2^-}(a_i, a_j)/u_i \in Q\}$ and for each $a_i \in Q$, the λ_2^+ - eccentricity of a_i , denoted by $e_{\lambda_2^+}(a_i)$, is defined as $e_{\lambda_2^+}(a_i) = \max\{\delta_{\lambda_2^+}(a_i, a_j)/a_i \in Q\}$. For each $a_i \in Q$, the eccentricity of a_i , denoted by $e_{\lambda_1, \lambda_2}(a_i)$, is defined as $e_{\lambda_1, \lambda_2}(a_i) = ([e_{\lambda_1^-}(a_i), e_{\lambda_1^+}(a_i)], [e_{\lambda_2^-}(a_i), e_{\lambda_2^+}(a_i)])$.

Definition 11. Let $\tilde{G} = (\mu, \lambda)$ be a connected IVIFG of graph $G^* = (Q, R)$. The λ_1^- - radius of \tilde{G} is denoted by $r_{\lambda_1^-}(G)$ and is defined as $r_{\lambda_1^-}(G) = \min\{e_{\lambda_1^-}(a_i)/a_i \in Q\}$ and the λ_1^+ - radius of \tilde{G} is denoted by $r_{\lambda_1^+}(G)$ and is defined as $r_{\lambda_1^+}(G) = \min\{e_{\lambda_1^+}(a_i)/a_i \in Q\}$. The λ_2^- - radius of \tilde{G} is denoted by $r_{\lambda_2^-}(G)$ and is defined as $r_{\lambda_2^-}(G) = \min\{e_{\lambda_2^-}(a_i)/a_i \in Q\}$ and the λ_2^+ - radius of \tilde{G} is denoted by $r_{\lambda_2^+}(G)$ and is defined as $r_{\lambda_2^+}(G) = \min\{e_{\lambda_2^+}(a_i)/a_i \in Q\}$. The radius of \tilde{G} is denoted by $r_{\lambda_1, \lambda_2}(G)$ and is defined as $r_{\lambda_1, \lambda_2}(G) = ([r_{\lambda_1^-}(G), r_{\lambda_1^+}(G)], [r_{\lambda_2^-}(G), r_{\lambda_2^+}(G)])$.

Definition 12. Let $\tilde{G} = (\mu, \lambda)$ be a connected IVIFG of graph $G^* = (Q, R)$. The λ_1^- - diameter of \tilde{G} is denoted by $d_{\lambda_1^-}(G)$ and is defined as $d_{\lambda_1^-}(G) = \max\{e_{\lambda_1^-}(a_i)/a_i \in Q\}$ and the λ_1^+ - diameter of \tilde{G} is denoted by $d_{\lambda_1^+}(G)$ and is defined as $d_{\lambda_1^+}(G) = \max\{e_{\lambda_1^+}(a_i)/a_i \in Q\}$. The λ_2^- - diameter of \tilde{G} is denoted by $d_{\lambda_2^-}(G)$ and is defined as $d_{\lambda_2^-}(G) = \max\{e_{\lambda_2^-}(a_i)/a_i \in Q\}$ and the λ_2^+ - diameter of \tilde{G} is denoted by $d_{\lambda_2^+}(G)$ and is defined as $d_{\lambda_2^+}(G) = \max\{e_{\lambda_2^+}(a_i)/a_i \in Q\}$. The diameter of \tilde{G} is denoted by $d_{\lambda_1, \lambda_2}(G)$ and is defined as $d_{\lambda_1, \lambda_2}(G) = ([d_{\lambda_1^-}(G), d_{\lambda_1^+}(G)], [d_{\lambda_2^-}(G), d_{\lambda_2^+}(G)])$.

Example 5. From the above Examples-1,3,4 using standard calculations, it is easy to see that: $e_{\lambda_1^-}$ - eccentricity, $e_{\lambda_1^+}$ - eccentricity and $e_{\lambda_2^-}$ - eccentricity, $e_{\lambda_2^+}$ - eccentricity of each vertex is $e_{\lambda_1^-}(u_1) = 0.4, e_{\lambda_1^-}(u_2) = 0.3, e_{\lambda_1^-}(u_3) = 0.4, e_{\lambda_1^-}(u_4) = 0.3, e_{\lambda_1^+}(u_1) = 0.7, e_{\lambda_1^+}(u_2) = 0.5, e_{\lambda_1^+}(u_3) = 0.7, e_{\lambda_1^+}(u_4) = 0.4$ and $e_{\lambda_2^-}(u_1) = 0.6, e_{\lambda_2^-}(u_2) = 0.4, e_{\lambda_2^-}(u_3) = 0.6, e_{\lambda_2^-}(u_4) = 0.4, e_{\lambda_2^+}(u_1) = 1.0, e_{\lambda_2^+}(u_2) = 0.6, e_{\lambda_2^+}(u_3) = 1.0, e_{\lambda_2^+}(u_4) = 0.6$

eccentricity of each vertex is

$$e_{\lambda_1, \lambda_2}(u_1) = ([0.4, 0.7], [0.6, 1.0]), \quad e_{\lambda_1, \lambda_2}(u_2) = ([0.3, 0.5], [0.4, 0.6]),$$

$$e_{\lambda_1, \lambda_2}(u_3) = ([0.4, 0.7], [0.6, 1.0]), \quad e_{\lambda_1, \lambda_2}(u_4) = ([0.3, 0.4], [0.4, 0.6])$$

radius of \tilde{G} is $r_{\lambda_1, \lambda_2}(G) = ([0.3, 0.4], [0.4, 0.6])$ and

diameter of \tilde{G} is $d_{\lambda_1, \lambda_2}(G) = ([0.4, 0.7], [0.6, 1.0])$

Definition 13. A vertex $u_i \in Q$ is called a central vertex of a connected IVIFG $\tilde{G} = (\mu, \lambda)$ of graph $G^* = (Q, R)$, if $r_{\lambda_1^-}(G) = e_{\lambda_1^-}(u_i)$, $r_{\lambda_1^+}(G) = e_{\lambda_1^+}(u_i)$ and $r_{\lambda_2^-}(G) = e_{\lambda_2^-}(u_i)$, $r_{\lambda_2^+}(G) = e_{\lambda_2^+}(u_i)$ and $C(\tilde{G})$ stands for the set of all central vertices of an IVIFG.

Definition 14. IVIFG connected If every vertex in \tilde{G} is a central vertex, then the graph $\tilde{G} = (\mu, \lambda)$ is a self-centered IVIFG, that is $r_{\lambda_1^-}(G) = e_{\lambda_1^-}(u_i)$, $r_{\lambda_1^+}(G) = e_{\lambda_1^+}(u_i)$ and $r_{\lambda_2^-}(G) = e_{\lambda_2^-}(u_i)$, $r_{\lambda_2^+}(G) = e_{\lambda_2^+}(u_i) \forall u_i \in Q$.

Example 6. Consider a connected IVIFG $\tilde{G} = (\mu, \lambda)$ of graph $G^* = (Q, R)$ such that $\mu = \{u_1([0.2, 0.4], [0.3, 0.5]), u_2([0.4, 0.5], [0.3, 0.4]), u_3([0.3, 0.4], [0.2, 0.5])\}$ as shown in Figure 2. By routine computations, it is easy to

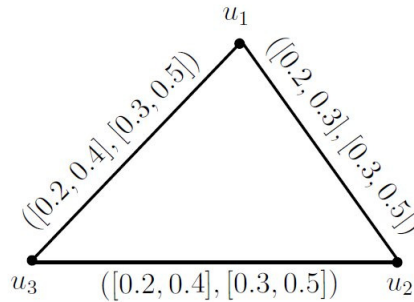


FIGURE 2. $\tilde{G} = (\mu, \lambda)$ is self centered IVIFG of G^*

see that:

(i) Distance $\delta_{\lambda_1, \lambda_2}(u_i, u_j)$ is

$$\delta_{\lambda_1, \lambda_2}(u_1, u_2) = ([0.2, 0.4], [0.3, 0.5]),$$

$$\delta_{\lambda_1, \lambda_2}(u_1, u_3) = ([0.2, 0.4], [0.3, 0.5]),$$

$$\delta_{\lambda_1, \lambda_2}(u_2, u_3) = ([0.2, 0.4], [0.3, 0.5])$$

(ii) Eccentricity $e_{\lambda_1, \lambda_2}(u_i)$ of each vertex is $([0.2, 0.4], [0.3, 0.5])$ for $i = 1, 2, 3$

(iii) radius of \tilde{G} is $r_{\lambda_1, \lambda_2}(G) = ([0.2, 0.4], [0.3, 0.5])$ and

diameter of \tilde{G} is $d_{\lambda_1, \lambda_2}(G) = ([0.2, 0.4], [0.3, 0.5])$

Hence, \tilde{G} is self centered IVIFG

Definition 15. A path cover of an IVIFG $\tilde{G} = (\mu, \lambda)$ of graph $G^* = (Q, R)$ is a set P of paths such that every vertex of \tilde{G} is incident to some path of P .

Example 7. Consider a connected IVIFG $\tilde{G} = (\mu, \lambda)$ of graph $G^* = (Q, R)$ such that $\mu = \{u_1([0.1, 0.3], [0.2, 0.4]), u_2([0.2, 0.4], [0.1, 0.3]), u_3([0.2, 0.3], [0.3, 0.5]), u_4([0.3, 0.4], [0.2, 0.5]), u_5([0.4, 0.5][0.2, 0.3]), u_6([0.2, 0.4], [0.3, 0.5])\}$ as shown in Figure-3. In this example, the some path covers of an IVIFG $\tilde{G} = (\mu, \lambda)$ are $M_1 =$

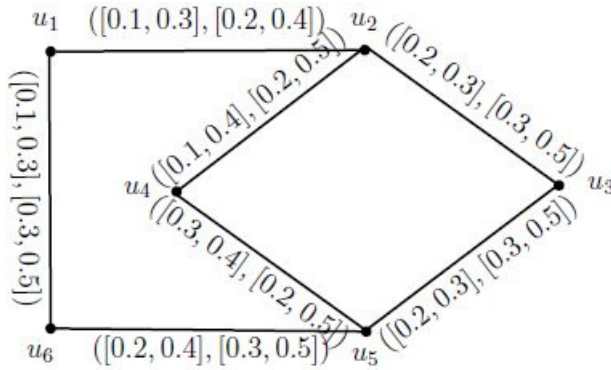


FIGURE 3. $\tilde{G} = (\mu, \lambda)$ is IVIFG of G^*

- $\{u_1u_2u_3u_5, u_4u_5u_6\},$
- $M_2 = \{u_1u_2u_4u_5, u_3u_5u_6\},$
- $M_3 = \{u_1u_2u_4u_5u_6, u_5u_3\},$
- $M_4 = \{u_1u_2u_4u_5u_6, u_2u_3\},$
- $M_5 = \{u_1u_2u_3u_5u_6, u_5u_4\},$
- $M_6 = \{u_1u_2u_3u_5u_6, u_2u_3\},$
- $M_7 = \{u_1u_2u_4, u_2u_3u_5u_6\},$
- $M_8 = \{u_1u_2u_3, u_2u_4u_5u_6\},$
- $M_9 = \{u_1u_6, u_2u_3u_5u_4\},$
- $M_{10} = \{u_1u_2, u_3u_5, u_4u_5u_6\},$
- $M_{11} = \{u_1u_2, u_4u_5, u_3u_5u_6\}$

Definition 16. An edge covers of an IVIFG $\tilde{G} = (\mu, \lambda)$ of graph $G^* = (Q, R)$ is a set E of edge such that every vertex of \tilde{G} is incident to some edge of E .

Example 8. In above Example-7, as shown in Figure-3. The some of the edge covers of an IVIFG $\tilde{G} = (\mu, \lambda)$ are

- $E_1 = \{(u_1, u_2), (u_2, u_3), (u_4, u_5), (u_5, u_6)\},$
- $E_2 = \{(u_1, u_6), (u_2, u_4), (u_3, u_5)\},$
- $E_3 = \{(u_1, u_2), (u_2, u_4), (u_3, u_5), (u_5, u_6)\},$
- $E_4 = \{(u_1, u_6), (u_2, u_3), (u_4, u_5)\},$
- $E_5 = \{(u_1, u_2), (u_2, u_3), (u_2, u_4), (u_5, u_6)\},$
- $E_6 = \{(u_1, u_6), (u_3, u_5), (u_4, u_5)\}$

Theorem 1. Every complete IVIFG $\tilde{G} = (\mu, \lambda)$ of graph $G^* = (Q, R)$ is a IVIFG and $r_{\lambda_1^-}(G) = \frac{1}{\mu_{1i}^-}$, $r_{\lambda_1^+}(G) = \frac{1}{\mu_{1i}^+}$ and $r_{\lambda_2^-} = \frac{1}{\mu_{2i}^-}$, $r_{\lambda_2^+} = \frac{1}{\mu_{2i}^+}$, where The lowest vertex membership is μ_{1i}^- and The largest vertex membership is μ_{1i}^+ and The lowest vertex membership is μ_{2i}^- and The largest vertex membership is μ_{2i}^+ .

Proof. Let $\tilde{G} = (\mu, \lambda)$ be a complete IVIFG. To prove that \tilde{G} is a self centered IVIFG. Therefore, we must demonstrate that each vertex is a central vertex. First we claim that \tilde{G} is a μ_{1i} -self centred IVIFG. Then $r_{\lambda_1^-}(G) = \frac{1}{\mu_{1i}^-}$ and $r_{\lambda_1^+}(G) = \frac{1}{\mu_{1i}^+}$, where The lowest vertex membership is μ_{1i}^- and The largest vertex membership is μ_{1i}^+ . Fix a vertex u_i in Q so that μ_{1i}^- is the value of \tilde{G} is lowest vertex membership and μ_{1i}^+ is the value of \tilde{G} is largest vertex membership.

Case1: Consider all the $u_i - u_j$ paths P of length n in \tilde{G} , $\forall u_j \in Q$.

(i) If $n = 1$, then $\lambda_{1ij}^- = \min\{\mu_{1i}^-, \mu_{1j}^-\}$. Therefore, $\lambda_1^- - length$ of $P = l_{\lambda_1^-}(P) = \frac{1}{\mu_{1i}^-}$ and $\lambda_{1ij}^+ = \min\{\mu_{1i}^+, \mu_{1j}^+\}$. Therefore, $\lambda_1^+ - length$ of $P = l_{\lambda_1^+}(P) = \frac{1}{\mu_{1i}^+}$.

(ii) (ii) One of the edges of P has the $\lambda_1^- - strength$ of μ_{1i}^- if $n > 1$ and hence, $\lambda_1^- - length$ of a $u_i - u_j$ path will exceed $\frac{1}{\mu_{1i}^-}$. So that, $\lambda_1^- - length$ of $P = l_{\lambda_1^-}(P) > \frac{1}{\mu_{1i}^-}$.

$$\text{Hence, } \delta_{\lambda_1^-}(u_i, u_j) = \min(l_{\lambda_1^-}(p)) = \frac{1}{\mu_{1i}^-}, \forall u_j \in Q. \tag{1}$$

Also one of the edges of P possesses the $\lambda_1^+ - strength$ of μ_{1i}^+ and hence, $\lambda_1^+ - length$ of P will exceed $\frac{1}{\mu_{1i}^+}$. that is, $\lambda_1^+ - length$ of $P = l_{\lambda_1^+}(P) > \frac{1}{\mu_{1i}^+}$.

$$\text{Hence, } \delta_{\lambda_1^+}(u_i, u_j) = \min(l_{\lambda_1^+}(p)) = \frac{1}{\mu_{1i}^+}, \forall u_j \in Q. \tag{2}$$

Case 2: Let $u_k \neq u_i \in Q$. Consider all $u_k - u_j$ paths X of length n in \tilde{G} , $\forall u_j \in Q$.

(i) If $n = 1$, then $\lambda_{1kj}^- = \min\{\mu_{1k}^-, \mu_{1j}^-\} \geq \mu_{1i}^-$, since μ_{1i}^- is the least. Hence, $\lambda_1^- - length$ (Q) = $l_{\lambda_1^-}(X) = \frac{1}{\lambda_1^-(u_k, u_j)} \leq \frac{1}{\mu_{1i}^-}$.

Also $\lambda_{1kj}^+ = \min\{\mu_{1k}^+, \mu_{1j}^+\} \leq \mu_{1i}^+$, since μ_{1i}^+ is the largest. Hence, $\lambda_1^+ - length$ (Q) = $l_{\lambda_1^+}(X) = \frac{1}{\lambda_1^+(u_k, u_j)} \geq \frac{1}{\mu_{1i}^+}$.

(ii) If $n = 2$, then $l_{\lambda_1^-}(X) = \frac{1}{\lambda_1^-(u_k, u_{k+1})} + \frac{1}{\lambda_1^-(u_{k+1}, u_j)} \leq \frac{2}{\mu_{1i}^-}$, Since, μ_{1i}^- is the lowest.

Also $l_{\lambda_1^+}(X) = \frac{1}{\lambda_1^+(u_k, u_{k+1})} + \frac{1}{\lambda_1^+(u_{k+1}, u_j)} \geq \frac{2}{\mu_{1i}^+}$, Since, μ_{1i}^+ is the largest.

(iii) If $n > 2$, then $l_{\lambda_1^-}(X) \leq \frac{n}{\mu_{1i}^-}$, since μ_{1i}^- is the lowest.

Also $l_{\lambda_1^+}(X) \geq \frac{n}{\mu_{1i}^+}$, since μ_{1i}^+ is the largest.

Hence, $\delta_{\lambda_1^-}(u_k, u_j) = \min(l_{\lambda_1^-}(X)) \leq \frac{1}{\mu_{1i}^-}$, $\forall u_k, u_j \in Q$. and

$$\delta_{\lambda_1^+}(u_k, u_j) = \min(l_{\lambda_1^+}(X)) \geq \frac{1}{\mu_{1i}^+}, \forall u_k, u_j \in Q. \tag{3}$$

From equation [1](#) and [3](#), we have,

$$e_{\lambda_1^-}(u_i) = \min(\delta_{\lambda_1^-}(u_i, u_j)) = \frac{1}{\mu_{1i}^-}, \forall u_i \in Q \text{ and}$$

$$e_{\lambda_1^+}(u_i) = \min(\delta_{\lambda_1^+}(u_i, u_j)) = \frac{1}{\mu_{1i}^+}, \forall u_i \in Q. \tag{4}$$

Hence, \tilde{G} is a λ_1^- and λ_1^+ self centered IVIFG.

Now, $r_{\lambda_1^-}(G) = \min(e_{\lambda_1^-}(u_i)) = \frac{1}{\mu_{1i}^-}$, since by [4](#) $r_{\lambda_1^-}(G) = \frac{1}{\mu_{1i}^-}$, where $\mu_{1i}^-(u_i)$ is the lowest and $r_{\lambda_1^+}(G) = \min(e_{\lambda_1^+}(u_i)) = \frac{1}{\mu_{1i}^+}$, since by [4](#) $r_{\lambda_1^+}(G) = \frac{1}{\mu_{1i}^+}$, where $\mu_{1i}^+(u_i)$ is the largest.

Next, we claim that \tilde{G} is a μ_{2i} -self centered IVIFG. Then $r_{\lambda_2^-}(G) = \frac{1}{\mu_{2i}^-}$ and $r_{\lambda_2^+}(G) = \frac{1}{\mu_{2i}^+}$, where μ_{2i}^- is the lowest and μ_{2i}^+ is the largest. Now fix a vertex $u_i \in Q$ such that μ_{2i}^- is lowest vertex membership value of \tilde{G} and μ_{2i}^+ is largest vertex membership value of \tilde{G} .

Case 1: Consider all the $u_i - u_j$ paths P of length n in \tilde{G} , $\forall u_j \in Q$.

(i) If $n = 1$, then $\lambda_{2ij}^- = \max\{\mu_{2i}^-, \mu_{2j}^-\} = \mu_{2i}^-$. Therefore, $\lambda_2^- - length$ of $P = l_{\lambda_2^-}(P) = \frac{1}{\mu_{2i}^-}$ and $\lambda_{2ij}^+ = \max\{\mu_{2i}^+, \mu_{2j}^+\} = \mu_{2i}^+$. Therefore, $\lambda_2^+ - length$ of $P = l_{\lambda_2^+}(P) = \frac{1}{\mu_{2i}^+}$.

(ii) If $n > 1$, then one of the edges of P possesses the $\lambda_2^- - strength$ of μ_{2i}^- and hence, $\lambda_2^- - length$ of a $u_i - u_j$ path will exceed $\frac{1}{\mu_{2i}^-}$. So that, $\lambda_2^- - length$ of $P = l_{\lambda_2^-}(P) > \frac{1}{\mu_{2i}^-}$.

$$\text{Hence, } \delta_{\lambda_2^-}(u_i, u_j) = \max(l_{\lambda_2^-}(p)) = \frac{1}{\mu_{2i}^-}, \forall u_j \in Q. \tag{5}$$

Also one of the edges of P possesses the $\lambda_2^+ - strength$ of μ_{2i}^+ and hence, $\lambda_2^+ - length$ of P will exceed $\frac{1}{\mu_{2i}^+}$. that is, $\lambda_2^+ - length$ of $P = l_{\lambda_2^+}(P) > \frac{1}{\mu_{2i}^+}$.

$$\text{Hence, } \delta_{\lambda_2^+}(u_i, u_j) = \max(l_{\lambda_2^+}(p)) = \frac{1}{\mu_{2i}^+}, \forall u_j \in Q. \tag{6}$$

Case 2: Let $u_k \neq u_i \in Q$. Consider all $u_k - u_j$ paths X of length n in \tilde{G} , $\forall u_j \in Q$.

(i) If $n = 1$, then $\lambda_{2kj}^- = \max\{\mu_{2k}^-, \mu_{2j}^-\} \geq \mu_{2i}^-$, since μ_{2i}^- is the least. Hence, $\lambda_2^- - length$ (Q) = $l_{\lambda_2^-}(X) = \frac{1}{\lambda_2^-(u_k, u_j)} \leq \frac{1}{\mu_{2i}^-}$.

Also $\lambda_{2kj}^+ = \max\{\mu_{2k}^+, \mu_{2j}^+\} \leq \mu_{2i}^+$, since μ_{2i}^+ is the greatest. Hence, $\lambda_2^+ - length$ (Q) = $l_{\lambda_2^+}(X) = \frac{1}{\lambda_2^+(u_k, u_j)} \geq \frac{1}{\mu_{2i}^+}$.

(ii) If $n = 2$, then $l_{\lambda_2^-}(X) = \frac{1}{\lambda_2^-(u_k, u_{k+1})} + \frac{1}{\lambda_2^-(u_{k+1}, u_j)} \leq \frac{2}{\mu_{2i}^-}$, Since, μ_{2i}^- is the least.

Also $l_{\lambda_2^+}(X) = \frac{1}{\lambda_2^+(u_k, u_{k+1})} + \frac{1}{\lambda_2^+(u_{k+1}, u_j)} \geq \frac{2}{\mu_{2i}^+}$, Since, μ_{2i}^+ is the greatest.

(iii) If $n > 2$, then $l_{\lambda_2^-}(X) \leq \frac{n}{\mu_{2i}^-}$, since μ_{2i}^- is the least.

Also $l_{\lambda_2^+}(X) \geq \frac{n}{\mu_{2i}^+}$, since μ_{2i}^+ is the greatest.

Hence, $\delta_{\lambda_2^-}(u_k, u_j) = \max(l_{\lambda_2^-}(X)) \leq \frac{1}{\mu_{2i}^-}$, $\forall u_k, u_j \in Q$. and

$$\delta_{\lambda_2^+}(u_k, u_j) = \max(l_{\lambda_2^+}(X)) \geq \frac{1}{\mu_{2i}^+}, \forall u_k, u_j \in Q. \tag{7}$$

From equation [5][6] and [7], we have,

$$e_{\lambda_2^-}(u_i) = \max(\delta_{\lambda_2^-}(u_i, u_j)) = \frac{1}{\mu_{2i}^-}, \forall u_i \in Q \text{ and}$$

$$e_{\lambda_2^+}(u_i) = \max(\delta_{\lambda_2^+}(u_i, u_j)) = \frac{1}{\mu_{2i}^+}, \forall u_i \in Q. \tag{8}$$

Hence, \tilde{G} is a λ_2^- and λ_2^+ self centered IVIFG.

Now, $r_{\lambda_2^-}(G) = \min(e_{\lambda_2^-}(u_i)) = \frac{1}{\mu_{2i}^-}$, since by [7] $r_{\lambda_2^-}(G) = \frac{1}{\mu_{2i}^-}$, where μ_{2i}^- is the least and $r_{\lambda_2^+}(G) = \max(e_{\lambda_2^+}(u_i)) = \frac{1}{\mu_{2i}^+}$, since by [8] $r_{\lambda_2^+}(G) = \frac{1}{\mu_{2i}^+}$, where μ_{2i}^+ is the largest.

From equation [4] and [8], every vertex of \tilde{G} is a central vertex. Hence \tilde{G} is a self centered IVIFG. \square

Corollary 1. Every complete IVIFG $\tilde{G} = (\mu, \lambda)$ of graph $G^* = (Q, R)$ is a self centered IVIFG and $r_{\lambda_1, \lambda_2}(G) = ([\frac{1}{\mu_{1i}^-}, \frac{1}{\mu_{1i}^+}], [\frac{1}{\mu_{2i}^-}, \frac{1}{\mu_{2i}^+}])$ where, μ_{1i}^- is the lowest vertex membership and μ_{1i}^+ is the largest vertex membership. μ_{2i}^- is the lowest vertex membership and μ_{2i}^+ is the largest vertex membership.

Proof. By above theorem-[1], every complete IVIFG $\tilde{G} = (\mu, \lambda)$ of graph $G^* = (Q, R)$ is a self centered IVIFG.

$$r_{\lambda_1, \lambda_2}(G) = (r_{\lambda_1}(G), r_{\lambda_2}(G)) = ([\min\{r_{\lambda_1^-}(G)\}, \min\{r_{\lambda_1^+}(G)\}], [\min\{r_{\lambda_2^-}(G)\}, \min\{r_{\lambda_2^+}(G)\}]).$$

$r_{\lambda_1, \lambda_2}(G) = ([\frac{1}{\mu_{1i}^-}, \frac{1}{\mu_{1i}^+}], [\frac{1}{\mu_{2i}^-}, \frac{1}{\mu_{2i}^+}])$, since μ_{1i}^- is the lowest membership value and μ_{1i}^+ is the largest membership value. μ_{2i}^- is the lowest membership value and μ_{2i}^+ is the largest membership value. \square

Remark 1. Converse of the above theorem-[1] is not true. By Example-[6]. Then \tilde{G} is self centered IVIFG but not complete.

Lemma 1. An IVIFG $\tilde{G} = (\mu, \lambda)$ of graph $G^* = (Q, R)$ is a self centered IVIFG if and only if $r_{\lambda_1^-}(G) = d_{\lambda_1^-}(G)$, $r_{\lambda_1^+}(G) = d_{\lambda_1^+}(G)$ and $r_{\lambda_2^-}(G) = d_{\lambda_2^-}(G)$, $r_{\lambda_2^+}(G) = d_{\lambda_2^+}(G)$.

Theorem 2. Let $\tilde{G} = (\mu, \lambda)$ is a connected IVIFG. Then for at least one edge $\max(\lambda_1^-(u_i, u_j)) = \lambda_1^-(u_i, u_j)$, $\max(\lambda_1^+(u_i, u_j)) = \lambda_1^+(u_i, u_j)$ and $\max(\lambda_2^-(u_i, u_j)) = \lambda_2^-(u_i, u_j)$, $\max(\lambda_2^+(u_i, u_j)) = \lambda_2^+(u_i, u_j)$

Proof. If $\tilde{G} = (\mu, \lambda)$ be a connected IVIFG. Consider a vertex u_i whose least membership value μ_{1i}^- and greatest membership value is μ_{1i}^+ and least membership value

μ_{2i}^- and greatest membership value is μ_{2i}^+ .

Case 1: Let μ_{1i}^- be the least value and $\mu_{1i}^+(u_i)$ be the greatest value and μ_{2i}^- be the least value and μ_{2i}^+ be the greatest value and in the vertex $u_i \in Q$. Let $u_i, u_j \in Q$, then $([\lambda_{1ij}^-, \lambda_{1ij}^+], [\lambda_{2ij}^-, \lambda_{2ij}^+]) = ([\mu_{1i}^-, \mu_{1i}^+], [\mu_{2i}^-, \mu_{2i}^+])$ and $([\max(\lambda_{1ij}^-), \max(\lambda_{1ij}^+)], [\max(\lambda_{2ij}^-), \max(\lambda_{2ij}^+)]) = ([\mu_{1i}^-, \mu_{1i}^+], [\mu_{2i}^-, \mu_{2i}^+])$. The strength of all the edges which are incident on the vertex u_i is $([\mu_{1i}^-, \mu_{1i}^+], [\mu_{2i}^-, \mu_{2i}^+])$. Since \tilde{G} is a connected IVIFG.

Case 2: Let μ_{1k}^- be the least value and μ_{1i}^+ be the greatest value and μ_{2k}^- be the least value and μ_{2i}^+ be the greatest value in the vertex $u_i, u_k \in Q$. Then $([\lambda_{1ik}^-, \lambda_{1ik}^+], [\lambda_{2ik}^-, \lambda_{2ik}^+]) = ([\mu_{1k}^-, \mu_{1i}^+], [\mu_{2k}^-, \mu_{2i}^+])$. Since, it is a connected IVIFG, there will be an edge between u_i and u_k , $\max(\lambda_{1ik}^-) = \mu_{1k}^-$, $\max(\lambda_{1ik}^+) = \mu_{1i}^+$ and $\max(\lambda_{2ik}^-) = \mu_{2k}^-$, $\max(\lambda_{2ik}^+) = \mu_{2i}^+$. \square

Theorem 3. Let $\tilde{G} = (\mu, \lambda)$ be a connected IVIFG of graph $G^* = (Q, R)$ with paths covers P_1 and P_2 of \tilde{G} . Then the necessary and sufficient condition for an IVIFG to be self centered IVIFG is $\delta_{\lambda_{1ij}^-} = r_{\lambda_1^-}(G), \forall (u_i, u_j) \in P_1, \delta_{\lambda_{1ij}^+} = d_{\lambda_1^+}(G), \forall (u_i, u_j) \in P_2$, and

$$\delta_{\lambda_{2ij}^-} = r_{\lambda_2^-}(G), \forall (u_i, u_j) \in P_1, \delta_{\lambda_{2ij}^+} = d_{\lambda_2^+}(G), \forall (u_i, u_j) \in P_2. \tag{9}$$

Proof. Necessary Condition: We now assume that $\tilde{G} = (\mu, \lambda)$ is a self centered IVIFG and we have to prove that equation 9 holds. Suppose equation 9 does not holds. then we have, $\delta_{\lambda_1^-}(u_i, u_j) \neq r_{\lambda_1^-}(G)$, for some $(u_i, u_j) \in P_1$ and $\delta_{\lambda_1^+}(u_i, u_j) \neq d_{\lambda_1^+}(G)$, for some $(u_i, u_j) \in P_2$ and $\delta_{\lambda_2^-}(u_i, u_j) \neq r_{\lambda_2^-}(G)$, for some $(u_i, u_j) \in P_1$ and $\delta_{\lambda_2^+}(u_i, u_j) \neq d_{\lambda_2^+}(G)$, for some $(u_i, u_j) \in P_2$. By using Lemma 1, the above inequality becomes $\delta_{\lambda_1^-}(u_i, u_j) \neq r_{\lambda_1^-}(G)$, for some $(u_i, u_j) \in P_1$ and $\delta_{\lambda_1^+}(u_i, u_j) \neq d_{\lambda_1^+}(G)$, for some $(u_i, u_j) \in P_2$ and $\delta_{\lambda_2^-}(u_i, u_j) \neq r_{\lambda_2^-}(G)$, for some $(u_i, u_j) \in P_1$ and $\delta_{\lambda_2^+}(u_i, u_j) \neq d_{\lambda_2^+}(G)$, for some $(u_i, u_j) \in P_2$. Then $e_{\lambda_1^-}(u_i) \neq r_{\lambda_1^-}(G)$, $e_{\lambda_1^+}(u_i) \neq r_{\lambda_1^+}(G)$ and $e_{\lambda_2^-}(u_i) \neq r_{\lambda_2^-}(G)$, $e_{\lambda_2^+}(u_i) \neq r_{\lambda_2^+}(G)$ for some $u_i \in Q$, which implies \tilde{G} is not self centered IVIFG, which is contradiction. Hence, $\delta_{\lambda_1^-}(u_i, u_j) = r_{\lambda_1^-}(G), \forall (u_i, u_j) \in P_1$ and $\delta_{\lambda_1^+}(u_i, u_j) = d_{\lambda_1^+}(G), \forall (u_i, u_j) \in P_2$ and $\delta_{\lambda_2^-}(u_i, u_j) = r_{\lambda_2^-}(G), \forall (u_i, u_j) \in P_1$ and $\delta_{\lambda_2^+}(u_i, u_j) = d_{\lambda_2^+}(G), \forall (u_i, u_j) \in P_2$.

Sufficient Condition: We now assume that equation 9 holds and we have to prove that \tilde{G} is a self centered IVIFG. If equation 9 holds, then we've $e_{\lambda_1^-}(u_i) = \delta_{\lambda_1^-}(u_i, u_j)$, for all $(u_i, u_j) \in P_1$, $e_{\lambda_1^+}(u_i) = \delta_{\lambda_1^+}(u_i, u_j)$, for all $(u_i, u_j) \in P_2$ and $e_{\lambda_2^-}(u_i) = \delta_{\lambda_2^-}(u_i, u_j)$, for all $(u_i, u_j) \in P_1$, $e_{\lambda_2^+}(u_i) = \delta_{\lambda_2^+}(u_i, u_j)$, for all $(u_i, u_j) \in P_2$. Which implies $e_{\lambda_1^-}(u_i) = r_{\lambda_1^-}(G)$, $e_{\lambda_1^+}(u_i) = r_{\lambda_1^+}(G)$ and $e_{\lambda_2^-}(u_i) = r_{\lambda_2^-}(G)$, $e_{\lambda_2^+}(u_i) = r_{\lambda_2^+}(G)$ for all $u_i \in Q$. Hence, \tilde{G} is self centered IVIFG. \square

Corollary 2. *If $\tilde{G} = (\mu, \lambda)$ is a connected IVIFG of graph $G^* = (Q, R)$ with an edge cover E of \tilde{G} . Then the necessary and sufficient condition for an IVIFG to be self centered IVIFG is $\delta_{\lambda_1^-}(u_i, u_j) = r_{\lambda_1^-}(G), \forall (u_i, u_j) \in E_1, \delta_{\lambda_1^+}(u_i, u_j) = d_{\lambda_1^+}(G), \forall (u_i, u_j) \in E_2$ and $\delta_{\lambda_2^-}(u_i, u_j) = r_{\lambda_2^-}(G), \forall (u_i, u_j) \in E_1,$*

$$\delta_{\lambda_2^+}(u_i, u_j) = d_{\lambda_2^+}(G), \forall (u_i, u_j) \in E_2. \tag{10}$$

Theorem 4. Embedding Theorem: *Let $\tilde{H} = (\mu', \lambda')$ is a connected self centered IVIFG. Then there exist a connected IVIFG \tilde{G} such that $\langle C(\tilde{G}) \rangle$ is isomorphic to \tilde{H} . Also $d_{\lambda_1^-}(G) = 2r_{\lambda_1^-}(G), d_{\lambda_1^+}(G) = 2r_{\lambda_1^+}(G)$ and $d_{\lambda_2^-}(G) = 2r_{\lambda_2^-}(G), d_{\lambda_2^+}(G) = 2r_{\lambda_2^+}(G)$.*

Proof. Given that $\tilde{H} = (\mu', \lambda')$ is a connected self centered IVIFG. Let $d_{\lambda_1^-}(H) = p_1, d_{\lambda_1^+}(H) = q_1$ and $d_{\lambda_2^-}(H) = p_2, d_{\lambda_2^+}(H) = q_2$. Then construct $\tilde{G} = (\mu, \lambda)$ from \tilde{H} as follows:

Take two vertices $u_i, u_j \in Q$ with $\mu_1^-(u_i) = \mu_1^-(u_j) = \frac{1}{p_1}, \mu_1^+(u_i) = \mu_1^+(u_j) = \frac{1}{2q_1}$ and $\mu_2^-(u_i) = \mu_2^-(u_j) = \frac{1}{p_2}, \mu_2^+(u_i) = \mu_2^+(u_j) = \frac{1}{2q_2}$ and join all the vertices of \tilde{H} to both u_i and u_j with $\lambda_{1ik}^- = \lambda_{1jk}^- = \frac{1}{p_1}, \lambda_{1ik}^+ = \lambda_{1jk}^+ = \frac{1}{2q_1}$ and $\lambda_{2ik}^- = \lambda_{2jk}^- = \frac{1}{p_2}, \lambda_{2ik}^+ = \lambda_{2jk}^+ = \frac{1}{2q_2}$ for all $u_k \in Q'$. Put $\mu_{1i}^- = (\mu_{1i}^-)', \mu_{1i}^+ = (\mu_{1i}^+)'$ and $\mu_{2i}^- = (\mu_{2i}^-)', \mu_{2i}^+ = (\mu_{2i}^+)'$ for all vertices in \tilde{H} . and $\lambda_{1ij}^- = (\lambda_{1ij}^-)', \lambda_{1ij}^+ = (\lambda_{1ij}^+)'$ for all edges in \tilde{H} and $\lambda_{2ij}^- = (\lambda_{2ij}^-)', \lambda_{2ij}^+ = (\lambda_{2ij}^+)'$ for all edges in \tilde{H} .

Claim: \tilde{G} is an IVIFG. First note that $\mu_{1i}^- \leq \mu_{1k}^-, \mu_{2i}^- \leq \mu_{2k}^-$ for all $u_k \in \tilde{H}$. If possible, let $\mu_{1i}^- > \mu_{1k}^-$ and $\mu_{2i}^- > \mu_{2k}^-$ for at least one vertex $u_k \in \tilde{H}$. Then $\frac{1}{p_1} > \mu_{1k}^-, \frac{1}{p_2} > \mu_{2k}^-$, that is $p_1 < \frac{1}{\mu_{1k}^-} \leq \frac{1}{\lambda_{1kl}^-}, p_2 < \frac{1}{\mu_{2k}^-} \leq \frac{1}{\lambda_{2kl}^-}$, where the last inequality holds for every $u_l \in Q'$, since \tilde{H} is an IVIFG. That is $\frac{1}{\lambda_{1kl}^-} > p_1, \frac{1}{\lambda_{2kl}^-} > p_2$ for all $u_k \in \tilde{H}$ which contradicts that $d_{\lambda_1^-}(\tilde{H}) = p_1, d_{\lambda_2^-}(\tilde{H}) = p_2$. Therefore $\mu_{1i}^- \leq \mu_{1k}^-, \mu_{2i}^- \leq \mu_{2k}^-$ for all $u_k \in Q'$ and $\lambda_{1ik}^- \leq \min\{\mu_{1i}^-, \mu_{1k}^-\} = \frac{1}{p_1}, \lambda_{2ik}^- \leq \max\{\mu_{2i}^-, \mu_{2k}^-\} = \frac{1}{p_2}$, similarly, $\lambda_{1jk}^- \leq \min\{\mu_{1j}^-, \mu_{1k}^-\} = \frac{1}{p_1}, \lambda_{2jk}^- \leq \max\{\mu_{2j}^-, \mu_{2k}^-\} = \frac{1}{p_2}$ for all $u_k \in Q'$. Note that $\mu_{1i}^+ \leq \mu_{1k}^+, \mu_{1j}^+ \leq \mu_{1k}^+$ and $\mu_{2i}^+ \leq \mu_{2k}^+, \mu_{2j}^+ \leq \mu_{2k}^+$ for all $u_k \in Q'$, since $d_{\lambda_1^+}(H) = q_1$ and $d_{\lambda_2^+}(H) = q_2$. Therefore $\lambda_{1ik}^+ \leq \min\{\mu_{1i}^+, \mu_{1k}^+\} = \frac{1}{2q_1}, \lambda_{2ik}^+ \leq \max\{\mu_{2i}^+, \mu_{2k}^+\} = \frac{1}{2q_2}$, similarly, $\lambda_{1jk}^+ \leq \min\{\mu_{1j}^+, \mu_{1k}^+\} = \frac{1}{2q_1}$ and $\lambda_{2jk}^+ \leq \max\{\mu_{2j}^+, \mu_{2k}^+\} = \frac{1}{2q_2}$. Hence, \tilde{G} is an IVIFG. Also, $e_{\lambda_1^-}(u_k) = p_1, e_{\lambda_1^+}(u_k) = p_2$ for all $u_k \in Q'$ and $e_{\lambda_1^-}(u_i) = e_{\lambda_1^-}(u_j) = \frac{1}{\lambda_{1ik}^-} + \frac{1}{\lambda_{1kl}^-} = 2p_1, r_{\lambda_1^-}(G) = p_1, d_{\lambda_1^-}(G) = 2p_1$ and $e_{\lambda_2^-}(u_i) = e_{\lambda_2^-}(u_j) = \frac{1}{\lambda_{2ik}^-} + \frac{1}{\lambda_{2kl}^-} = 2p_2, r_{\lambda_2^-}(G) = p_2, d_{\lambda_2^-}(G) = 2p_2$. Next, $e_{\lambda_1^+}(u_k) = q_1, e_{\lambda_2^+}(u_k) = q_2$ for all $u_k \in Q'$ and $e_{\lambda_1^+}(u_i) = e_{\lambda_1^+}(u_j) = \frac{1}{\lambda_{1ik}^+} = 2q_1, e_{\lambda_2^+}(u_i) = e_{\lambda_2^+}(u_j) = \frac{1}{\lambda_{2ik}^+} = 2q_2$ for all $u_k \in Q'$. Therefore, $r_{\lambda_1^+}(G) =$

$q_1, d_{\lambda_1^+}(G) = 2q_1$ and $r_{\lambda_2^+}(G) = q_2, d_{\lambda_2^+}(G) = 2q_2$. Hence, $\langle C(\tilde{G}) \rangle$ is isomorphic to \tilde{H} . \square

Theorem 5. *An IVIFG $\tilde{G} = (\mu, \lambda)$ is a self centered if and only if $\delta_{\lambda_1^-}(u_i, u_j) \leq r_{\lambda_1^-}(G), \delta_{\lambda_1^+}(u_i, u_j) \geq r_{\lambda_1^+}(G)$ and $\delta_{\lambda_2^-}(u_i, u_j) \leq r_{\lambda_2^-}(G), \delta_{\lambda_2^+}(u_i, u_j) \geq r_{\lambda_2^+}(G)$ for all $u_i, u_j \in Q$.*

Proof. We assume that $\tilde{G} = (\mu, \lambda)$ is a self centered IVIFG. That is, $e_{\lambda_1^-}(u_i) = e_{\lambda_1^-}(u_j), e_{\lambda_1^+}(u_i) = e_{\lambda_1^+}(u_j)$ and $e_{\lambda_2^-}(u_i) = e_{\lambda_2^-}(u_j), e_{\lambda_2^+}(u_i) = e_{\lambda_2^+}(u_j)$ for all $u_i, u_j \in Q, r_{\lambda_1^-}(G) = e_{\lambda_1^-}(u_i), r_{\lambda_1^+}(G) = e_{\lambda_1^+}(u_i)$ and $r_{\lambda_2^-}(G) = e_{\lambda_2^-}(u_i), r_{\lambda_2^+}(G) = e_{\lambda_2^+}(u_i)$ for all $u_i \in Q$. Now we wish to show that $\delta_{\lambda_1^-}(u_i, u_j) \leq r_{\lambda_1^-}(G), \delta_{\lambda_1^+}(u_i, u_j) \geq r_{\lambda_1^+}(G)$ and $\delta_{\lambda_2^-}(u_i, u_j) \leq r_{\lambda_2^-}(G), \delta_{\lambda_2^+}(u_i, u_j) \geq r_{\lambda_2^+}(G)$ for all $u_i, u_j \in Q$. By the definition of eccentricity, we obtain, $\delta_{\lambda_1^-}(u_i, u_j) \leq e_{\lambda_1^-}(u_i), \delta_{\lambda_1^+}(u_i, u_j) \geq e_{\lambda_1^+}(u_i)$ and $\delta_{\lambda_2^-}(u_i, u_j) \leq e_{\lambda_2^-}(u_i), \delta_{\lambda_2^+}(u_i, u_j) \geq e_{\lambda_2^+}(u_i)$ for all $u_i, v_i \in Q$. This is possible only when $e_{\lambda_1^-}(u_i) = e_{\lambda_1^-}(u_j), e_{\lambda_1^+}(u_i) = e_{\lambda_1^+}(u_j)$ and $e_{\lambda_2^-}(u_i) = e_{\lambda_2^-}(u_j), e_{\lambda_2^+}(u_i) = e_{\lambda_2^+}(u_j)$ for all $u_i, u_j \in Q$. Since, \tilde{G} is a self centered IVIFG, the above inequality becomes $\delta_{\lambda_1^-}(u_i, u_j) \leq r_{\lambda_1^-}(G), \delta_{\lambda_1^+}(u_i, u_j) \geq r_{\lambda_1^+}(G)$ and $\delta_{\lambda_2^-}(u_i, u_j) \leq r_{\lambda_2^-}(G), \delta_{\lambda_2^+}(u_i, u_j) \geq r_{\lambda_2^+}(G)$.

Conversely, we now assume that $\delta_{\lambda_1^-}(u_i, u_j) \leq r_{\lambda_1^-}(G), \delta_{\lambda_1^+}(u_i, u_j) \geq r_{\lambda_1^+}(G)$ and $\delta_{\lambda_2^-}(u_i, u_j) \leq r_{\lambda_2^-}(G), \delta_{\lambda_2^+}(u_i, u_j) \geq r_{\lambda_2^+}(G)$ for all $u_i, u_j \in Q$. Then we have to prove that \tilde{G} is a self centered IVIFG. Suppose that \tilde{G} is not self centered IVIFG. Then $r_{\lambda_1^-}(G) \neq e_{\lambda_1^-}(u_i), r_{\lambda_1^+}(G) \neq e_{\lambda_1^+}(u_i)$ and $r_{\lambda_2^-}(G) \neq e_{\lambda_2^-}(u_i), r_{\lambda_2^+}(G) \neq e_{\lambda_2^+}(u_i)$ for some $u_i \in Q$. Let us assume that $e_{\lambda_1^-}(u_i), e_{\lambda_1^+}(u_i)$ and $e_{\lambda_2^-}(u_i), e_{\lambda_2^+}(u_i)$ is the least value among all other eccentricity. That is, $r_{\lambda_1^-}(G) = e_{\lambda_1^-}(u_i), r_{\lambda_1^+}(G) = e_{\lambda_1^+}(u_i)$ and

$$r_{\lambda_2^-}(G) = e_{\lambda_2^-}(u_i), r_{\lambda_2^+}(G) = e_{\lambda_2^+}(u_i). \tag{11}$$

where $e_{\lambda_1^-}(u_i) < e_{\lambda_1^-}(u_j), e_{\lambda_1^+}(u_i) < e_{\lambda_1^+}(u_j)$ and $e_{\lambda_2^-}(u_i) < e_{\lambda_2^-}(u_j), e_{\lambda_2^+}(u_i) < e_{\lambda_2^+}(u_j)$ for some $u_i, u_j \in Q$ and $\delta_{\lambda_1^-}(u_i, u_j) = e_{\lambda_1^-}(u_j) > e_{\lambda_1^-}(u_i), \delta_{\lambda_1^+}(u_i, u_j) = e_{\lambda_1^+}(u_j) > e_{\lambda_1^+}(u_i)$ and $\delta_{\lambda_2^-}(u_i, u_j) = e_{\lambda_2^-}(u_j) > e_{\lambda_2^-}(u_i),$,

$$\delta_{\lambda_2^+}(u_i, u_j) = e_{\lambda_2^+}(u_j) > e_{\lambda_2^+}(u_i) \text{ for some } u_i, u_j \in Q. \tag{12}$$

Hence, from equation 11 and 12, we have, $\delta_{\lambda_1^-}(u_i, u_j) > r_{\lambda_1^-}(G), \delta_{\lambda_1^+}(u_i, u_j) > r_{\lambda_1^+}(G)$, and $\delta_{\lambda_2^-}(u_i, u_j) > r_{\lambda_2^-}(G), \delta_{\lambda_2^+}(u_i, u_j) > r_{\lambda_2^+}(G)$, for some $u_i, u_j \in Q$, which is a contradiction to the fact that $\delta_{\lambda_1^-}(u_i, u_j) \leq r_{\lambda_1^-}(G), \delta_{\lambda_1^+}(u_i, u_j) \geq r_{\lambda_1^+}(G)$ and $\delta_{\lambda_2^-}(u_i, u_j) \leq r_{\lambda_2^-}(G), \delta_{\lambda_2^+}(u_i, u_j) \geq r_{\lambda_2^+}(G)$ for all $u_i, u_j \in Q$. Hence, $\tilde{G} = (\mu, \lambda)$ is a self centered IVIFG. \square

4. APPLICATION OF IVIFG

Application in this paper are applied in detecting instability in human life and in all fields. The findings of this study can be used to prevent crime and foster peace in our nation. Using the security forces of our nation, we will defend the areas where the majority of unlawful operations occur. In order to stop illicit operations in our country, we will first deploy security forces there. Through the use of uncertainty values, we will determine the extent of unlawful activity in the cities of our nation and adjust the deployment of our security troops accordingly. Think of Q as the country and u_1, u_2, u_3, u_4 as the cities within Q . We shall examine this study using IVIFG. We define the most terrible terrorist crimes as μ_1^- , and let's define the special forces protecting the country from terrorist threats as μ_1^+ . Other criminal activity will be considered as μ_2^- by those involved. (Examples include the transfer of ill-gotten gains, the smuggling of precious metals, the smuggling of endangered species, and the illegal carrying of weapons). Let's treat troops who guard against other criminal actions as μ_2^+ . Let's have a look at the vertex set $Q = \{u_1, u_2, u_3, u_4\}$ in

TABLE 2.

Cities	[terrorist acts, protection]	[other illegal acts, other protection]
u_1	[0.3,0.5]	[0.2,0.4]
u_2	[0.4,0.6]	[0.3,0.4]
u_3	[0.1,0.3]	[0.3,0.6]
u_4	[0.3,0.4]	[0.4,0.5]

IVIFG. Any two city-connected highway that borders \tilde{G} is defined by R as $G^* = (Q, R)$. Let us consider the edge set $R = \{u_1u_2, u_2u_3, u_2u_4, u_3u_4, u_3u_5\}$ in G^* as shown in Figure-1. IVIFG calculates the value of the security forces, the value of the unlawful activities, and the value of the security forces from terrorist acts that take place on highways connecting two cities. used in the definition -9. We

TABLE 3.

highway	[terrorist acts, protection]	[other illegal acts, other protection]
u_1u_2	[0.3,0.5]	[0.3,0.4]
u_2u_3	[0.1,0.3]	[0.3,0.6]
u_2u_4	[0.3,0.4]	[0.4,0.5]
u_3u_4	[0.1,0.3]	[0.4,0.6]
u_1u_4	[0.3,0.4]	[0.4,0.5]

can estimate the cost of terrorist attacks spreading to other cities by using the symbols $d_{\lambda_{1ij}^-}$ and $d_{\lambda_{1ij}^+}$, respectively. We can also estimate the cost of security forces' protection by using the symbols $d_{\lambda_{2ij}^-}$ and $d_{\lambda_{2ij}^+}$. In the Example-1, we take

into consideration that u_1, u_2, u_3, u_4 are cities in Q and R is any two-city connected highway that is located on the boundaries of \tilde{G} . Let us consider the edge set $R = \{u_1u_2, u_2u_3, u_2u_4, u_3u_4, u_1u_4\}$ in G^* as shown in Figure-1 in Example-1. We

TABLE 4.

One city relation to distance between others city	$([d_{\lambda_{1ij}^-}, d_{\lambda_{1ij}^+}], [d_{\lambda_{2ij}^-}, d_{\lambda_{2ij}^+}])$
u_1u_4	$([0.3, 0.4], [0.4, 0.5])$
u_1u_2	$([0.3, 0.5], [0.3, 0.4])$
u_1u_3	$([0.4, 0.7], [0.6, 1.0])$
u_2u_3	$([0.1, 0.3], [0.3, 0.6])$
u_2u_4	$([0.2, 0.4], [0.4, 0.5])$
u_3u_4	$([0.1, 0.3], [0.4, 0.6])$

can estimate the impacts and protections a city has on others by comparing it to those cities. From the table-4 we find that $d_{\lambda_1, \lambda_2}(G) = ([0.4, 0.7], [0.6, 1.0])$ has

TABLE 5.

$e_{\lambda_1, \lambda_2}(u_i)$	maximum value of impacts and protection
$e_{\lambda_1, \lambda_2}(u_1)$	$([0.4, 0.7], [0.6, 1.0])$
$e_{\lambda_1, \lambda_2}(u_2)$	$([0.3, 0.5], [0.4, 0.6])$
$e_{\lambda_1, \lambda_2}(u_3)$	$([0.4, 0.7], [0.6, 1.0])$
$e_{\lambda_1, \lambda_2}(u_4)$	$([0.3, 0.4], [0.4, 0.6])$

the highest number of vulnerabilities and defenses and from the table-4 above we find that $r_{\lambda_1, \lambda_2}(G) = ([0.3, 0.4], [0.4, 0.6])$ has the lowest number of vulnerabilities and defenses. The purpose of these applications is to strengthen our country's defenses to the extent of it's vulnerabilities.

5. CONCLUSION

The researcher has developed the idea of an IVIFG in this study article. It has an impact on a lot of different industries. It is common for some features of a graph-theoretical problem to be unclear or ambiguous. This article analyses the concepts of strength, length, distance, eccentricity, radius, and diameter as well as self-centeredness and centeredness and introduces the idea of an IVIFG. We also investigate into some of the properties of a self-centered IVIFG with illustration. Finally, we investigated into an application in IVIFG.

Author Contribution Statements All authors have significant contributions to this paper.

Declaration of Competing Interests The authors declare no conflict of interest.

REFERENCES

- [1] Atanassov, K. T., Intuitionistic fuzzy sets, *Fuzzy Sets Syst*, 20(1) (1986), 87-96.
- [2] Atanassov, K. T., Gargov, G., Interval valued intuitionistic fuzzy sets, *Fuzzy Sets and Systems*, 31(3) (1989), 343-349.
- [3] Buckley, F., Self-centered graphs, graph theory and its applications *East and West. Ann. New York Acad. Sci*, 576 (1989), 71-78.
- [4] Karunambigai, M. G., Kalaivani, O. K., Self centered Intuitionistic fuzzy graph, *World Applied Sciences Journal*, 14(12) (2011), 1928-1936.
- [5] Akram, M., Dudek, W. A., Regular bipolar fuzzy graphs, *Neural Comput. Applic*, 21 (2012) (Suppl 1), 197-205, DOI 10.1007/s00521-011-0772-6.
- [6] Akram, M., Dudek, W. A., Interval-valued fuzzy graphs, *Comput. Math. Appl*, 61 (2011), 289-299, DOI 10.1016/j.camwa.2010.11.004.
- [7] Akram, M., Interval-valued fuzzy line graphs, *Neural Comput. Appl* 21, (2012), 145-150, DOI 10.1007/s00521-011-0733-0.
- [8] Akram, M., Yousaf, M. M., Dudek, W. A., Self centered interval-valued fuzzy graphs, *Afr. Mat*, 26 (2015), 887-898.
- [9] M. Pal and H. Rashmanlou, Irregular interval-valued fuzzy graphs, *Annals of Pure and Applied Mathematics*, 3(1) (2013), 56-66, DOI 10.1007/s13370-014-0256-9.
- [10] Rashmanlou, H., Pal, M., Antipodal interval-valued fuzzy graphs, *International Journal of Applications of Fuzzy Sets and Artificial Intelligence*, 3, (2013), 107-130.
- [11] Rashmanlou, H., and Pal, M., Balanced interval-valued fuzzy graph, *Journal of Physical Sciences*, 17 (2013), 43-57.
- [12] Rashmanlou, H., Pal, M., Some properties of highly irregular interval-valued fuzzy graphs, *World Applied Sciences Journal*, 27(12) (2013), 1756-1773.
- [13] Rosenfeld, A., Zadeh, L. A., Fu, K. S., Shimura, M. (Eds.), *Fuzzy Sets and Their Applications*, Academic Press, New York, pp.77-95, 1975.
- [14] Hussain, S. S., Rosyida, I., Rashmanlou, H., Mofidnakhai, F., Interval intuitionistic neutrosophic sets with its applications to interval intuitionistic neutrosophic graphs and climatic analysis, *Computational and Applied Mathematics*, 40:121 (2021), <https://doi.org/10.1007/s40314-021-01504-8>.
- [15] Shannon, A. , Atanassov, K. T., A first step to a theory of the Intuitionistic fuzzy graph, *Proceeding of FUBEST(D.Lako,ED.) sofia, sept* , 28-30 (1994), 59-61.
- [16] Turksen, I. B., Interval valued fuzzy sets based on normal forms. *Fuzzy Sets Syst*, 20 (1986), 191-210.
- [17] Zadeh, L. A., The concept of a linguistic and application to approximate reasoning I, *Inform. Sci*, 8 (1975), 199-249.
- [18] Zadeh, L. A., Fuzzy sets, *Inf. Control*, 8 (1965), 338-353.
- [19] Zhang, W. R., Bipolar fuzzy sets, *Proc. of FUZZ-IEEE*, (1998), 835-840.

VARIOUS RESULTS ON SOME ASYMMETRIC TYPES OF DENSITY

Nezakat JAVANSHIR¹ and Filiz YILDIZ²

¹Ankara Yıldırım Beyazıt University, Department of Mathematics, Ankara, TÜRKİYE
²Hacettepe University, Faculty of Science, Department of Mathematics, Beytepe, Ankara, TÜRKİYE

ABSTRACT. The structures of symmetric connectedness and dually, antisymmetric connectedness were described and studied before, especially in terms of graph theory as the corresponding counterparts of the connectedness of a graph and the connectedness of its complementary graph. By taking into consideration the deficiencies of topological density in the context of symmetric and antisymmetric connectedness, two special kinds of density in the theory of non-metric T_0 -quasi-metrics were introduced in the previous studies under the names symmetric density and antisymmetric density. In this paper, some crucial and useful properties of these two types of density are investigated with the help of the major results and (counter)examples peculiar to the asymmetric environment. Besides these, many further observations about the structures of symmetric and antisymmetric-density are dealt with, especially in the sense of their combinations such as products and unions through various theorems in the context of T_0 -quasi-metrics. Also, we examine the question of under what kind of quasi-metric mapping these structures will be preserved.

1. INTRODUCTION

In [11], symmetrically connected and dually, antisymmetrically connected T_0 -quasi-metric spaces were described and studied in detail. These theories were especially discussed in the sense of the notions peculiar to graph theory [1, 4, 10] as the suitable counterparts of the connectedness for a graph and complementary graph of it, respectively. In particular, it was shown that there were natural relationships

2020 *Mathematics Subject Classification.* 54B05; 11B05; 54E35; 54A05; 03E20; 05C38.

Keywords. T_0 -quasi-metric; connected graph; symmetrization topology; antisymmetric point; Star space; symmetrically-dense; antisymmetrically connected; complementary graph; isometric isomorphism; symmetric path.

¹ ✉ nezakat.javanshir@aybu.edu.tr;  0000-0002-1780-4684;

² ✉ yfiliz@hacettepe.edu.tr- Corresponding author;  0000-0002-2112-8949

between the theory of symmetrically connected - antisymmetrically connected T_0 -quasi-metric spaces and the theory of connected graphs - connected complementary graphs.

Following these theories, some new types of density specific to T_0 -quasi-metric subspaces in the asymmetric environment due to the apparent inadequacy of topological density in the transfer of properties symmetric and antisymmetric connectedness to the subspaces or superspaces are described in [9] under the names symmetric density and antisymmetric density.

As for the subject of this study, we observed some combinations of symmetrically / antisymmetrically-dense subspaces such as products, unions and intersections in the context of T_0 -quasi-metrics. With this viewpoint, it is also natural to inquire whether the images of symmetrically / antisymmetrically-dense subspaces under an isometric isomorphism have the same property or not. Hereby, we will also obtain some crucial and useful results within this framework.

In the light of all these considerations, the content of paper is as follows:

Some necessary background material for the remaining of paper is presented in Section 2. After recalling the preliminary information, as one of the purposes of the paper, in Section 3 we discussed some properties and new (counter)examples of the symmetric density theory in the context of asymmetric topology. In addition, we presented some observations about the products, unions, intersections... of the symmetrically-dense T_0 -quasi-metric subspaces and their preservation under the specific mappings peculiar to quasi-metrics.

Following these, in Section 4 some future properties and asymmetric aspects of antisymmetrically-dense subspaces are investigated with the help of many useful (counter)examples. The remainder of this section is devoted to discussing preservation of antisymmetric density under the specific mappings in the context of quasi-metrics as well as some combinations such as unions, products,... of the antisymmetrically-dense T_0 -quasi-metric subspaces.

Consequently, Section 5 as the last part of the paper gives a conclusion about the whole of the work.

2. BACKGROUND

This section will present some background material on T_0 -quasi-metrics and particularly, it consists of the required information related to the theories of symmetrically connected and antisymmetrically connected spaces as well as antisymmetric spaces which are a kind of opposite to metric spaces.

All preliminary information presented in this section is taken from the references [3, 5, 8, 12].

T_0 -quasi-metrics:

Definition 1. Let X be a set and $d : X \times X \rightarrow [0, \infty)$ be a function. Then d is called a T_0 -quasi-metric on X if

- (a) $d(x, x) = 0$
- (b) $d(x, y) = 0 = d(y, x) \Rightarrow x = y$
- (c) $d(x, z) \leq d(x, y) + d(y, z)$

whenever $x, y, z \in X$. Thus, (X, d) is called T_0 -quasi-metric space.

Here the notation τ_{d^s} will be used to denote the topology induced by the symmetrization metric $d^s = d \vee d^{-1}$ where $d^{-1}(x, y) = d(y, x)$.

Example 1. On \mathbb{R} , take

$$u(x, y) = \max\{x - y, 0\}$$

whenever $x, y \in \mathbb{R}$.

It is easy to prove that u satisfies the conditions of Definition 1 and u is called the standard T_0 -quasi-metric on \mathbb{R} .

Now, let us recall some important notions and (counter)examples related to the theories constructed in [11]:

Symmetrically connected spaces:

Definition 2. Let (X, d) be a T_0 -quasi-metric space.

- i) A pair $(x, y) \in X \times X$ is called symmetric pair if $d(x, y) = d(y, x)$.
- ii) A finite sequence of points in X , starting at x and ending with y , is called a (finite) symmetric path $P_{x,y} = (x = x_0, x_1, \dots, x_{n-1}, x_n = y)$ (where $n \in \mathbb{N}$) from x to y provided that all the pairs (x_i, x_{i+1}) are symmetric where $i \in \{0, \dots, n - 1\}$.

For a T_0 -quasi-metric space (X, d) , we take

$$Z_d = \{(x, y) \in X \times X : d(x, y) = d(y, x)\}$$

as the set of symmetric pairs in (X, d) . Note that this relation is reflexive and symmetric.

Incidentally, note that

$$d^s(x, y) = d(x, y) = d^{-1}(x, y)$$

for $(x, y) \in Z_d$.

Also,

$$Z_d(x) = \{y \in X \mid (x, y) \in Z_d\}$$

is called symmetry set of $x \in X$.

Definition 3. If (X, d) is a T_0 -quasi-metric space and $x, y \in X$ then $x \in X$ is symmetrically connected to $y \in X$ whenever there is a symmetric path $P_{x,y}$, starting at the point x and ending at the point y .

Clearly, “symmetric connectedness” is an equivalence relation on X , by definition.

Definition 4. *The equivalence class of a point $x \in X$ with respect to the symmetric connectedness relation is called the symmetry component of x .*

More clearly, if C_d denotes the *symmetric connectedness relation* then the symmetry component of $x \in X$ is

$$C_d(x) = \{y \in X : \text{there is a symmetric path from } x \text{ to } y\}.$$

We are now in a position to recall the following crucial notion:

Definition 5. *A T_0 -quasi-metric space (X, d) such that $C_d(x) = X$ for all $x \in X$, is called symmetrically connected.*

Therefore, (X, d) is symmetrically connected if and only if for all $x, y \in X$, x and y are symmetrically connected by Definition 3 obviously.

At this stage, we will turn our attention to the dual counterparts of some notions described above.

Antisymmetrically connected spaces:

Definition 6. *Let (X, d) be a T_0 -quasi-metric space, and $x, y \in X$. Then*

- i) $(x, y) \in X \times X$ is called antisymmetric pair if $d(x, y) \neq d(y, x)$
- ii) A finite sequence of points in X , starting at x and ending with y , is called a (finite) antisymmetric path $P_{x,y} = (x = x_0, x_1, \dots, x_{n-1}, x_n = y)$ (where $n \in \mathbb{N}$) from x to y provided that all the pairs (x_i, x_{i+1}) are antisymmetric where $i \in \{0, \dots, n-1\}$.

Definition 7. *In a T_0 -quasi-metric space (X, d) , two points $x, y \in X$ are called antisymmetrically connected if there is an antisymmetric path $P_{x,y} = (x = x_0, x_1, \dots, x_{n-1}, x_n = y)$, or $x = y$.*

Now, if we consider the relation

$$T_d := \{(x, y) \in X \times X : x \text{ and } y \text{ are antisymmetrically connected in } (X, d)\}$$

then T_d describes an equivalence relation on X , trivially.

Let us recall some other notions from 11:

Definition 8. i) *The equivalence class of a point $x \in X$ with respect to T_d is called the antisymmetry component and it is denoted by*

$$T_d(x) = \{y \in X : \text{there is an antisymmetric path from } x \text{ to } y\}.$$

- ii) *If $T_d(x) = X$ for each $x \in X$, then the space (X, d) is called antisymmetrically connected.*

Hence, (X, d) is antisymmetrically connected if and only if for all $x, y \in X$, x and y are antisymmetrically connected by Definition 7

Example 2. The T_0 -quasi-metric space (\mathbb{R}, u) given in Example 1 is antisymmetrically connected but not symmetrically connected.

Antisymmetric spaces:

The following notion is described in 11 as opposite to that of “metric” :

Definition 9. 11 A T_0 -quasi-metric space (X, d) is called antisymmetric if $Z_d = \{(x, x) : x \in X\} = \Delta_X$, that is, if $d(x, y) = d(y, x)$ then $x = y$, for all $x, y \in X$.

Symmetric-Antisymmetric points:

Definition 10. Let (X, d) be a T_0 -quasi-metric space and $x \in X$.

- i) x is called symmetric point if $d(x, y) = d(y, x)$ for each $y \in X$.
- ii) x is called antisymmetric point if $d(x, y) \neq d(y, x)$ for each $y \in X \setminus \{x\}$.

According to the above descriptions, the next statements will be obvious:

- Proposition 1.**
- a) A T_0 -quasi-metric space which has a symmetric point will be symmetrically connected and not an antisymmetric space.
 - b) A T_0 -quasi-metric space which has an antisymmetric point will be antisymmetrically connected and not a metric space.

3. SOME FURTHER PROPERTIES AND EXAMPLES OF SYMMETRIC DENSITY

Firstly, let us recall the following notion from 9.

Definition 11. Let (X, d) be a T_0 -quasi-metric space and $A \subseteq X$. If for $x \in X \setminus A$, there exists $a_x \in A$ such that $d(x, a_x) = d(a_x, x)$ then A is called symmetrically-dense in (X, d) .

Example 3. Let us define a T_0 -quasi-metric p on the set $X = \{1, 2, 3\}$ via the matrix

$$P = \begin{pmatrix} 0 & 9 & 8 \\ 9 & 0 & 1 \\ 10 & 1 & 0 \end{pmatrix}.$$

That is, $P = (p_{ij})$ where $p(i, j) = p_{ij}$ for $i, j \in X$. It is easy to prove that p is a T_0 -quasi-metric on X . Specifically, now we will check the triangle inequality:

$$\begin{aligned} p(1, 2) &= 9 \leq 8 + 1 = p(1, 3) + p(3, 2), & p(3, 1) &= 10 \leq 1 + 9 = p(3, 2) + p(2, 1) \\ p(1, 3) &= 8 \leq 9 + 1 = p(1, 2) + p(2, 3), & p(2, 1) &= 9 \leq 1 + 10 = p(2, 3) + p(3, 1) \\ p(2, 3) &= 1 \leq 9 + 8 = p(2, 1) + p(1, 3), & p(3, 2) &= 1 \leq 10 + 9 = p(3, 1) + p(1, 2). \end{aligned}$$

Thus p satisfies the triangle inequality.

Here also note that $p(1, 2) = p(2, 1)$. Therefore, the subset $A = \{2, 3\}$ of X is symmetrically-dense in X . In addition, the subset $B = \{1\}$ is not symmetrically-dense since $p(3, 1) \neq p(1, 3)$.

Proposition 2. *Let (X, d) be a T_0 -quasi-metric space with at least two-elements and let $x \in X$ be an antisymmetric point. Thus, the subsets $\{x\}$ and $X \setminus \{x\}$ are not symmetrically-dense in X .*

Proof. By Definition 10 ii), we have $d(x, y) \neq d(y, x)$ whenever $y \in X \setminus \{x\}$. Then, $\{x\}$ is not symmetrically-dense in X . Similarly, $y = x$ whenever $y \in X \setminus (X \setminus \{x\})$ and since x is antisymmetric point, $d(x, a) \neq d(a, x)$ for $a \in X \setminus \{x\}$. That is, $X \setminus \{x\}$ is not symmetrically-dense. \square

Example 4. *Let $Y = \{0\} \cup \{\frac{1}{2^n} : n \in \mathbb{N}\}$ and define $f : Y \rightarrow [0, \infty)$ as follows:*

$$f(x, y) = \begin{cases} |x - y| & ; x < y \text{ and } (x, y) \neq (\frac{1}{2^{n+1}}, \frac{1}{2^n}), \forall n \in \mathbb{N} \\ 2|x - y| & ; \text{otherwise} \end{cases}$$

for $x, y \in Y$.

The fact that f is a T_0 -quasi-metric on Y is proved in 5.

Also, because of the inequality $f(a, 0) \neq f(0, a)$ for each $a \in Y \setminus \{0\}$ the point 0 is antisymmetric point. Thus (Y, f) is antisymmetrically connected by Proposition 7. Additionally, the space (Y, f) has symmetrically-dense subsets $T_f(\frac{1}{2}), T_f(\frac{1}{4})\dots$ since they are antisymmetry components.

At this stage, we can compute $C_f(\frac{1}{2})$: For each $n \in \mathbb{N}$, we have that $\frac{1}{2^n} \in C_f(\frac{1}{2})$, since $(\frac{1}{2^n}, \dots, \frac{1}{2})$ is a symmetric path in (Y, f) from $\frac{1}{2^n}$ to $\frac{1}{2}$. But $0 \notin C_f(\frac{1}{2})$, since $f(0, \frac{1}{2^k}) = \frac{1}{2^k}$, $f(\frac{1}{2^k}, 0) = \frac{1}{2^{(k+1)}}$, for all $k \in \mathbb{N}$. Thus, $C_f(\frac{1}{2}) = Y \setminus \{0\} = V$, and so (Y, f) is not symmetrically connected. A similar argument shows that in V , $C_{f_V}(x) = V$ for every $x \in V$, and so (V, f_V) will be symmetrically connected.

Moreover, the subsets $\{0\}$ and V are not symmetrically-dense from Proposition 2.

Incidentally, we can recall from 9 the following characterization of the metrics via symmetric density, in the context of T_0 -quasi-metrics:

Proposition 3. *Each nonempty subset of a T_0 -quasi-metric space (X, d) is symmetrically-dense in X if and only if d is metric.*

As a result of Proposition 3 the next corollary is obvious.

Corollary 1. *Let (X, d) be a T_0 -quasi-metric space. If each nonempty subset of (X, d) is symmetrically-dense in X then (X, d) is symmetrically connected.*

The converse of Corollary 1 may not be true by virtue of the following space.

Example 5. *Consider the Star Space (X, d) constructed in 5, Example 2.12], as follows:*

On $X = [0, \infty)$, take

$$d(x, y) = \begin{cases} x - y & ; x \geq y \\ x + y & ; x < y \end{cases}$$

for each $x, y \in X$. Trivially, 0 is symmetric point since $d(x, 0) = d(0, x)$ for all $x \in X$, according to Definition 10. Thus, (X, d) is symmetrically connected by Proposition 7. Now consider the subset $B = \{1\}$ of X . Then it is easy to verify that B is not symmetrically-dense. Indeed, take $2 \in X \setminus B$, and note that $d(1, 2) = 3 \neq 1 = d(2, 1)$.

Incidentally, the fact that any subspace of an antisymmetric T_0 -quasi-metric space is antisymmetric is trivial by Definition 9. Nevertheless, a T_0 -quasi-metric space (X, d) may not be antisymmetric even though (X, d) has a symmetrically-dense and antisymmetric subspace, as the following example shows:

Example 6. It can be easily shown that Star Space (X, d) given in Example 5 is not antisymmetric by the fact that $d(1, 0) = d(0, 1)$. It is also easy to see $X \setminus \{0\}$ is symmetrically dense since 0 is a symmetric point. Moreover, $X \setminus \{0\}$ is an antisymmetric subspace since $x = y$ whenever $d(x, y) = d(y, x)$ for all $x, y \in (0, \infty)$.

We are now in a position to recall a T_0 -quasi-metric function described on the product of two T_0 -quasi-metric spaces:

Remark 1. Let (X, d) and (Y, q) be T_0 -quasi-metric spaces. The function defined by

$$D((x, y), (a, b)) = d(x, a) \vee q(y, b)$$

for each $(x, y), (a, b) \in X \times Y$ gives a T_0 -quasi-metric on the product set $X \times Y$.

The fact that D is a T_0 -quasi-metric can be verified since d and q are T_0 -quasi-metrics.

Proposition 4. Let $(X, d), (Y, q)$ be T_0 -quasi-metric spaces and $A \subseteq X, B \subseteq Y$. If A is symmetrically-dense in X and B is symmetrically-dense in Y then $A \times B$ is symmetrically-dense in $X \times Y$.

Proof. Take $(x, y) \in (X \times Y) \setminus (A \times B)$. Since A is symmetrically-dense in (X, d) and B is symmetrically-dense in (Y, q) , respectively there exist $a \in A$ and $b \in B$ such that $d(x, a) = d(a, x)$ and $q(y, b) = q(b, y)$. Now by the definition of product T_0 -quasi-metric D on $X \times Y$, we have

$$D((x, y), (a, b)) = d(x, a) \vee q(y, b) = d(a, x) \vee q(b, y) = D((a, b), (x, y))$$

that is $A \times B$ is symmetrically-dense in $X \times Y$. □

The following result will be trivial via induction by Proposition 4

Corollary 2. For a T_0 -quasi-metric space (X, d) , the finite product of symmetrically-dense subsets of X is symmetrically-dense.

Even though Proposition 4, we have the following example which states that if A is symmetrically-dense and B is not symmetrically-dense then $A \times B$ may not be symmetrically-dense.

Example 7. Let us consider Star Space (X, d) from Example 5. Clearly the set $A = \{0\}$ is symmetrically-dense, and the set $B = \{1\}$ is not symmetrically-dense in (X, d) . If we take the product T_0 -quasi-metric D given in Remark 1 as $D((x, y), (a, b)) = d(x, a) \vee d(y, b)$ on $X \times X$ then the product set $A \times B$ is not symmetrically-dense since $D((3, 5), (0, 1)) \neq D((0, 1), (3, 5))$ for $(3, 5) \in (X \times X) \setminus (A \times B)$ and $(0, 1) \in A \times B$.

At this stage, let us turn our attention to the following natural question:
Under which mappings is the symmetric density property preserved in the context of T_0 -quasi-metric spaces ?

Proposition 5. Let $(X, d), (Y, e)$ be T_0 -quasi-metric spaces and $f : X \rightarrow Y$ an isometric isomorphism. In this case, $A \subseteq X$ is symmetrically-dense in X if and only if $f(A)$ is symmetrically-dense in Y .

Proof. Take $y \in Y \setminus f(A)$. So we have $x \in X \setminus A$ such that $f(x) = y$ since f is onto. By considering the symmetric density of A in X , there exists $a \in A$ such that $d(x, a) = d(a, x)$. Clearly, $f(a) \in f(A)$. Also, we have $e(f(x), f(a)) = d(x, a) = d(a, x) = e(f(a), f(x))$ since f is an isometry. Thus, $f(A)$ is symmetrically-dense in Y .

Conversely, if $a \in X \setminus A$ then $f(a) \notin f(A)$ as f is one-to-one. In this case, there exists $b \in f(A)$ satisfying the equality $e(b, f(a)) = e(f(a), b)$ since $f(A)$ is symmetrically-dense. Thus, there exists $z \in A$ such that $f(z) = b$ via the fact that f is onto. Now, by considering the isometry property of f the expression $d(z, a) = d(a, z)$ is obtained. This shows that A is symmetrically-dense. \square

Proposition 6. Let (X, d) be a T_0 -quasi-metric space. If A is symmetrically dense in X and $B \subseteq X$ then $A \cup B$ is symmetrically-dense in X .

Proof. If $x \in X \setminus (A \cup B)$ then there exists $a \in A$ such that $d(x, a) = d(a, x)$ since A is symmetrically-dense in X . Thus, $A \cup B$ is also symmetrically-dense in X due to $A \subseteq A \cup B$. \square

As the consequence of Proposition 6 the following fact will be trivial.

Corollary 3. The union of all subsets of a T_0 -quasi-metric space which has at least one symmetrically-dense subset is symmetrically-dense.

Despite the above fact, we have:

Remark 2. The intersection of two symmetrically-dense subsets of a T_0 -quasi-metric space may not be symmetrically-dense.

Example 8. On the set $X = \{\frac{1}{2}, 1, 2, 3\}$ consider the Sorgenfrey (bounded) T_0 -quasi-metric $b : \mathbb{R} \times \mathbb{R} \rightarrow [0, \infty)$ as

$$b(x, y) = \begin{cases} \min\{1, x - y\} & ; x \geq y \\ 1 & ; x < y \end{cases} .$$

Now let us take $A = \{\frac{1}{2}, 1\} \subseteq X$. In this case, since $b(x, 1) = b(1, x)$ for each $x \in X \setminus A$ the set A is symmetrically-dense in X . Similarly, $b(x, 3) = b(3, x)$ for each $x \in X \setminus B$ where $B = \{\frac{1}{2}, 3\} \subseteq X$, and so the set B is symmetrically-dense in X . But the intersection set $A \cap B = \{\frac{1}{2}\}$ is not symmetrically-dense in X because of the facts that $b(1, \frac{1}{2}) \neq b(\frac{1}{2}, 1)$ and $1 \in X \setminus (A \cap B)$.

4. SOME FURTHER PROPERTIES AND EXAMPLES OF ANTISYMMETRIC DENSITY

Definition 12. [9] Let (X, d) be a T_0 -quasi-metric space and $A \subseteq X$. If for $x \in X \setminus A$, there exists $a_x \in A$ such that $d(x, a_x) \neq d(a_x, x)$ then A is called antisymmetrically-dense in (X, d) .

Example 9. Consider a T_0 -quasi-metric on the set $Y = \{1, 2, 3, 4\}$ by the matrix

$$Q = \begin{pmatrix} 0 & 8 & 4 & 1 \\ 9 & 0 & 6 & 7 \\ 4 & 6 & 0 & 5 \\ 3 & 7 & 5 & 0 \end{pmatrix}.$$

That is, $Q = (q_{ij})$ where $q(i, j) = q_{ij}$ for $i, j \in Y$. The function q will be a T_0 -quasi-metric on Y . Indeed, it satisfies the other conditions of Definition 1, so we will prove just the triangle inequality:

$$\begin{aligned} q(1, 2) &= 8 \leq 4 + 6 = q(1, 3) + q(3, 2), & q(1, 2) &= 8 \leq 1 + 7 = q(1, 4) + q(4, 2) \\ q(1, 3) &= 4 \leq 8 + 6 = q(1, 2) + q(2, 3), & q(1, 3) &= 4 \leq 1 + 5 = q(1, 4) + q(4, 3) \\ q(1, 4) &= 1 \leq 8 + 7 = q(1, 2) + q(2, 4), & q(1, 4) &= 1 \leq 4 + 5 = q(1, 3) + q(3, 4) \\ q(2, 3) &= 6 \leq 9 + 4 = q(2, 1) + q(1, 3), & q(2, 3) &= 6 \leq 7 + 5 = q(2, 4) + q(4, 3) \\ q(2, 4) &= 7 \leq 9 + 1 = q(2, 1) + q(1, 4), & q(2, 4) &= 7 \leq 6 + 5 = q(2, 3) + q(3, 4) \end{aligned}$$

.
.

.

Other cases can be shown in a similar way.

Now, let us consider the subset $B = \{1, 2, 3\}$ of Y . It is easy to verify that B is antisymmetrically-dense in Y : For each $y \in Y \setminus B$ we must find $b \in B$ such that $q(y, b) \neq q(b, y)$. Here, if $y \in Y \setminus B$ then $y = 4$, and clearly $q(1, 4) \neq q(4, 1)$ for $1 \in B$.

Proposition 7. Let (X, d) be a T_0 -quasi-metric space with at least two-elements and $x \in X$ a symmetric point. Then the subsets $\{x\}$ and $X \setminus \{x\}$ cannot be antisymmetrically-dense in X .

Proof. By the definition of symmetric point (see Definition 10 i), $d(x, y) = d(y, x)$ whenever $y \in X \setminus \{x\}$. Then, $\{x\}$ cannot be antisymmetrically-dense in X . In a similar way, clearly $y = x$ whenever $y \in X \setminus (X \setminus \{x\})$. Thus, $d(x, a) = d(a, x)$ whenever $a \in X \setminus \{x\}$ since x is symmetric point. That is, $X \setminus \{x\}$ is not antisymmetrically-dense. □

The following proposition will be very useful in this context.

Proposition 8. *Let (X, d) be a T_0 -quasi-metric space. If each nonempty subset of (X, d) is antisymmetrically-dense in X then (X, d) will be an antisymmetrically connected space.*

Proof. Assume that each nonempty subset of (X, d) is antisymmetrically-dense in X . Now we can prove that (X, d) is indeed an antisymmetrically connected space by showing that, for $x \in X$, if $y \in X$ and $y \notin T_d(x)$ then $y \in X \setminus T_d(x)$ and $y \neq x$. Thus there exists $a \in T_d(x)$ such that $d(y, a) \neq d(a, y)$ since $T_d(x)$ is antisymmetrically-dense in X . Now, if $a = x$ then $d(y, x) \neq d(x, y)$, that is $y \in T_d(x)$ contradiction. If $a \neq x$ then $x \in X \setminus \{a\}$. Also, note that the subset $\{a\}$ is antisymmetrically-dense by the hypothesis. Thus $d(x, a) \neq d(a, x)$. In this case, $P_{x,y} = (x, a, y)$ will be an antisymmetric path from x to y . That is, $y \in T_d(x)$ which is a contradiction. Finally, $T_d(x) = X$, so (X, d) will be antisymmetrically connected. \square

The converse of Proposition 8 is not true always. Example 10 below is a counterexample. For it, first of all let us recall the notion *asymmetric norm* by Cobzaş 2.

Definition 13. *Let X be a real vector space equipped with a given map $\|\cdot\| : X \rightarrow [0, \infty)$ satisfying the conditions:*

- (a) $\|x\| = \|-x\| = 0$ if and only if $x = \mathbf{0}$.
- (b) $\|\lambda x\| = \lambda \|x\|$ whenever $\lambda \geq 0$ and $x \in X$.
- (c) $\|x + y\| \leq \|x\| + \|y\|$ whenever $x, y \in X$.

Then $\|\cdot\|$ is called an *asymmetric norm* and $(X, \|\cdot\|)$ is said to be an *asymmetrically normed real vector space*. (Here, $\mathbf{0}$ denotes the zero vector of the vector space X .)

Obviously, an asymmetric norm induces a T_0 -quasi-metric on X with the equality $d_{\|\cdot\|}(x, y) = \|x - y\|$ for each $x, y \in X$, where $(X, \|\cdot\|)$ is an asymmetrically normed real vector space. But, naturally some T_0 -quasi-metrics may not be induced by an asymmetric norm.

Note also that each norm is an asymmetric norm. However, the function $\|\cdot\|$ described by the equality $\|(x_1, x_2)\| = x_1 \vee x_2 \vee 0$ on \mathbb{R}^2 , satisfies the above conditions and thus, it is an asymmetric norm which is not a norm.

Example 10. *Consider the plane \mathbb{R}^2 with the T_0 -quasi-metric d induced by the maximum asymmetric norm $\|(x, y)\| = x \vee y \vee 0$. It is easy to see that for each $(a_1, a_2) \in \mathbb{R}^2$ the symmetry component $C_d((a_1, a_2)) = \{(x+a_1, -x+a_2) \mid x \in \mathbb{R}\} \neq \mathbb{R}^2$ where $d = d_{\|\cdot\|}$ and so the space (\mathbb{R}^2, d) is not symmetrically connected by Definition 5. In this case, (\mathbb{R}^2, d) is antisymmetrically connected from 11, Proposition 58] which states the fact that a T_0 -quasi-metric space is symmetrically connected or antisymmetrically connected by virtue of graph theory.*

Now take the subset $G = \{(x, -x) \mid x \in \mathbb{R}\} \subseteq \mathbb{R}^2$. Clearly, the subspace (G, d_G) is a metric space, and so symmetrically connected. But it is not antisymmetrically connected. On the other hand, G is antisymmetrically-dense: if $(x, y) \in \mathbb{R}^2 \setminus G$ then $(x, y) \notin G$ and so $y \neq -x$, that is $x + y \neq 0$. Now, let us consider the point $(x, -x) \in G$. In this case $d((x, -x), (x, y)) = (x - x) \vee (-x - y) \vee 0 = -(x + y) \vee 0$ and $d((x, y), (x, -x)) = (x - x) \vee (x + y) \vee 0$, thus $d((x, -x), (x, y)) \neq d((x, y), (x, -x))$.

In addition, note that the point $(0, 0)$ is neither symmetric point nor antisymmetric point. Moreover, the singleton set $\{(0, 0)\}$ is neither symmetrically-dense nor antisymmetrically-dense in \mathbb{R}^2 .

It is well-known that any subspace of an antisymmetric space is antisymmetric. Nevertheless, a T_0 -quasi-metric space (X, d) may not be antisymmetric even though (X, d) has an antisymmetrically-dense and antisymmetric subspace, as the following example shows:

Example 11. Let us define a T_0 -quasi-metric on the set $X = \{1, 2, 3\}$ via the matrix

$$W = \begin{pmatrix} 0 & 9 & 8 \\ 7 & 0 & 1 \\ 6 & 1 & 0 \end{pmatrix}.$$

That is, $W = (w_{ij})$ where $w(i, j) = w_{ij}$ for $i, j \in X$. It is easy to prove that w is a T_0 -quasi-metric on X . Because of the fact that $w(2, 3) = w(3, 2)$, the space (X, w) is not antisymmetric. Consider the subset $B = \{1, 3\}$ of X . It is easy to show that B is antisymmetric subspace w.r.t the induced T_0 -quasi-metric w_B on B . In addition, B is antisymmetrically-dense: If take $x \in X \setminus B$ then $x = 2$. In this case, for $1 \in B$ we have $w(1, 2) = 9$ and $w(2, 1) = 7$. That is, $w(1, 2) \neq w(2, 1)$.

Incidentally, there is an extension space which has an antisymmetrically-dense subspace not antisymmetrically connected even though the space itself is antisymmetrically connected.

Example 12. Take a metric space (X, m) with at least two-elements. By [5, Corollary 3.4], (X, m) has an antisymmetrically connected T_0 -quasi-metric one-point extension (Y, v) such that $Y = X \cup \{\infty\}$, and ∞ is antisymmetric point. In this case, if we delete the added (antisymmetric) point, then the remaining metric space is no longer antisymmetrically connected. Moreover, X is antisymmetrically-dense in Y : if $y \in Y \setminus X$ then $y = \infty$. Also, because $X \neq \emptyset$ there is at least a $a \in X$. Clearly, $a \neq \infty$ and $v(\infty, a) \neq v(a, \infty)$ since ∞ is an antisymmetric point in Y .

Now we can turn our attention to the following natural question:

Under which mappings is the antisymmetric density property preserved in the context of T_0 -quasi-metric spaces ?

Proposition 9. Let $(X, d), (Y, e)$ be T_0 -quasi-metric spaces and $f : X \rightarrow Y$ an isometric isomorphism. Then $A \subseteq X$ is antisymmetrically-dense in X if and only if $f(A)$ is antisymmetrically-dense in Y .

Proof. If $y \in Y \setminus f(A)$ then there exists $x \in X \setminus A$ such that $f(x) = y$ since f is onto. On the other hand, there exists $a \in A$ such that $d(x, a) \neq d(a, x)$ since A is antisymmetrically-dense. Clearly, $f(a) \in f(A)$. Also, we have $e(f(x), f(a)) = d(x, a) \neq d(a, x) = e(f(a), f(x))$ as f is an isometry. Thus, $f(A)$ is antisymmetrically-dense in Y .

Conversely, if $a \in X \setminus A$ then $f(a) \notin f(A)$ as f is one-to-one. In this case, there exists $b \in f(A)$ satisfying the inequality $e(b, f(a)) \neq e(f(a), b)$ since $f(A)$ is antisymmetrically-dense. Thus, there exists $z \in A$ such that $f(z) = b$ via the fact that f is onto. Now, by considering the isometry property of f the expression $d(z, a) \neq d(a, z)$ is obtained. This shows that A is antisymmetrically-dense. \square

In contrast to Proposition 4 we have the following remark for antisymmetric density:

Remark 3. For any T_0 -quasi-metric spaces (X, d) , (Y, q) , the product of any antisymmetrically-dense subsets of X and Y may not be antisymmetrically-dense in $X \times Y$.

Actually, we have a counterexample:

Example 13. Consider the standard T_0 -quasi-metric space (\mathbb{R}, u) where $u(x, y) = \max\{x - y, 0\}$, given in Example 7 and the T_0 -quasi-metric space (\mathbb{R}, d) with the function

$$d(x, y) = \begin{cases} 0 & ; x \leq y \\ 1 & ; y < x \end{cases}$$

on \mathbb{R} .

If we take the subset $A = \{0\}$ of \mathbb{R} then A is antisymmetrically dense in (\mathbb{R}, u) because of the fact that $u(x, 0) \neq u(0, x)$ whenever $x \in \mathbb{R} \setminus A$.

Similarly, let us take the subset $B = \{1\}$ of \mathbb{R} . Clearly, B is antisymmetrically dense in (\mathbb{R}, d) since the inequality $d(x, 1) \neq d(1, x)$ holds whenever $x \in \mathbb{R} \setminus B$.

On the other hand, by taking into consideration the definition of product T_0 -quasi-metric D given in Definition 7 we have the following fact:

If we consider the product T_0 -quasi-metric space $(\mathbb{R} \times \mathbb{R}, D)$ then for $(1, 0) \in (\mathbb{R} \times \mathbb{R}) \setminus (A \times B)$ we have the equality

$$D((1, 0), (a, b)) = u(1, a) \vee d(0, b) = 1 \vee 0 = 1 = u(a, 1) \vee d(b, 0) = D((a, b), (1, 0))$$

whenever $a \in A$, $b \in B$, that is $a = 0$ and $b = 1$. It means that the subset $A \times B$ is not antisymmetrically-dense in $(\mathbb{R} \times \mathbb{R}, D)$ even though A is antisymmetrically-dense in (\mathbb{R}, u) and B is antisymmetrically-dense in (\mathbb{R}, d) .

Proposition 10. Let (X, d) be a T_0 -quasi-metric space. If A is antisymmetrically-dense in X and $B \subseteq X$ then $A \cup B$ is antisymmetrically-dense in X .

Proof. Take $x \in X \setminus (A \cup B)$. So, by the antisymmetric density of A , there exists $a \in A$ such that $d(x, a) \neq d(a, x)$. Thus, $A \cup B$ is antisymmetrically-dense in X as well, since $A \subseteq A \cup B$. \square

Hence, the following result will be trivial as a consequence of Proposition [10](#).

Corollary 4. *The union of all subsets of a T_0 -quasi-metric space which has at least one antisymmetrically-dense subset is antisymmetrically-dense.*

Despite the above result, we have:

Remark 4. *The intersection of two antisymmetrically-dense subsets of a T_0 -quasi-metric space may not be antisymmetrically-dense.*

There is a counterexample:

Example 14. *On the set $X = \{1, 2, 3, 4, 5\}$ consider the Sorgenfrey T_0 -quasi-metric as*

$$s(x, y) = \begin{cases} x - y & ; y \leq x \\ 1 & ; y > x \end{cases} .$$

Now let us take $A = \{1, 5\}$. In this case, since $s(3, 1) \neq s(1, 3)$, $s(1, 4) \neq s(4, 1)$ and $s(2, 5) \neq s(5, 2)$, the set A is antisymmetrically-dense in X . Similarly, the set $B = \{1, 4\}$ is antisymmetrically-dense in X . But the intersection set $A \cap B = \{1\}$ is not antisymmetrically-dense in X because of the facts that $s(1, 2) = s(2, 1)$ and $2 \in X \setminus (A \cap B)$.

5. CONCLUSION

As opposed to the negative result ([5](#), Example 2.11]) which occurs in case τ_{d^s} -density, a T_0 -quasi-metric space which has a symmetrically connected and symmetrically-dense subspace will be symmetrically connected by [9](#), Theorem 2.15]. That is, it is possible to carry the symmetric connectedness of the subspace to the space, provided that the subspace is symmetrically-dense in the space.

However, we have a counterexample in [9](#) showing that “any symmetrically-dense subspace of a symmetrically connected space need not be symmetrically connected”. Similarly, in this paper we have an example which shows that “any antisymmetrically-dense subspace of an antisymmetrically connected space need not be antisymmetrically connected”.

In the light of above considerations, for future work, let us state a few new questions using the notions introduced in [6](#) and [12](#), as follows.

If (X, d) is locally symmetrically connected and it has a symmetrically-dense subset A , then is the subspace (A, d_A) locally symmetrically connected? If (X, d) has a symmetrically-dense and locally symmetrically connected subspace then is the space (X, d) locally symmetrically connected?

Author Contribution Statements The authors contributed equally to this paper. All authors read and approved this paper's final form.

Declaration of Competing Interests The author declare that there is no conflict of interest regarding the publication of this paper.

Acknowledgement The authors gratefully thank the Editor and Referees for their all constructive comments and valuable recommendations which definitely helped to improve the readability and quality of the paper.

REFERENCES

- [1] Bondy, J.A., Murty, U.S.R., Graph Theory with Applications, North-Holland, New York, Fifth Printing, 1982.
- [2] Cobzaş, Ş., Functional Analysis in Asymmetric Normed Spaces, Frontiers in Mathematics, Springer, Basel, 2013.
- [3] Demetriou, N., Künzi, H.-P.A., A study of quasi-pseudometrics, *Hacet. J. Math. Stat.*, 46 (1) (2017), 33-52. <https://doi.org/10.15672/HJMS.2016.396>.
- [4] Hellwig, A., Volkman, L., The connectivity of a graph and its complement, *Appl. Math.*, 156 (2008), 3325-3328. <https://doi.org/10.1016/j.dam.2008.05.012>.
- [5] Javanshir, N., Yıldız, F., Symmetrically connected and antisymmetrically connected T_0 -quasi-metric extensions, *Top. and Its Appl.*, 276 (2020), 107179. <https://doi.org/10.1016/j.topol.2020.107179>.
- [6] Javanshir, N., Yıldız, F., Locally symmetrically connected T_0 -quasi-metric spaces, *Quaest. Math.*, 45 (3) (2022), 369-384. <https://doi.org/10.2989/16073606.2021.1882602>.
- [7] Künzi, H.-P.A., An introduction to quasi-uniform spaces, in: Beyond Topology, eds. F. Myrland and E. Pearl (Eds.), *Beyond Topology, in: Contemp. Math.*, 486 (2009), 239-304.
- [8] Künzi, H.-P. A., Yıldız, F., Extensions of T_0 -quasi-metrics, *Acta Math. Hungar.*, 153 (1) (2017), 196-215. <https://doi.org/10.1007/s10474-017-0753-z>.
- [9] Künzi, H.-P.A., Yıldız, F., Javanshir, N., Symmetrically and antisymmetrically-dense subspaces of T_0 -quasi-metric spaces, *Top. Proc.*, 61 (2023), 215-231.
- [10] Wilson, R. J., Introduction To Graph Theory, Oliver and Boyd, Edinburgh, 1972.
- [11] Yıldız, F., Künzi, H.-P.A., Symmetric connectedness in T_0 -quasi-metric spaces, *Bull. Belg. Math. Soc. Simon Stevin*, 26 (5) (2019), 659-679. <https://doi.org/10.36045/bbms/1579402816>.
- [12] Yıldız, F., Javanshir, N., On the topological locality of antisymmetric connectedness, *Filomat*, 37 (12) (2023), 3879-3886. <https://doi.org/10.2298/FIL2312883Y>.



A NEW MULTIDIMENSIONAL MODEL II REGRESSION BASED ON BISECTOR APPROACH

Cengiz GAZELOGLU¹, Asuman ZEYTINOGLU² and Nurullah YILMAZ³

¹Department of Statistics, Suleyman Demirel University, Isparta, TÜRKİYE

^{2,3}Department of Mathematics, Suleyman Demirel University, Isparta, TÜRKİYE

ABSTRACT. A new multidimensional Model II regression based on bisector point of view (BRM-II) is introduced for multivariate problems that may contain measurement error. The suggested method is constructed depending on using the bisector of the minor angle between two hyperplanes identified by linear regression. The performance of the proposed method are examined by simulations up to ten variables for different sample sizes and distribution types in terms of the Mean Square Error. Moreover, the BRM-II is applied to two real problems with two and three variables, and compared with the existing methods. The results indicate that the BRM-II is easy applicable and offers relatively better accuracy. The relevant method can be easily coded in any programming language provides convenience in its application. Thus, the proposed method provide powerful tool for prediction of relevant real life problems.

1. INTRODUCTION

Regression analysis is a statistical method used to determine the relationship between two or more variables that have a cause and effect relation and to make estimation or prediction about that subject by using this relationship [12]. The regression method, which dates back to the 1800s, was first used in astronomical events and social sciences. In classical regression, the regression model including two variables is defined as

$$\hat{Y} = \beta_0 + \beta_1 X + e_i \quad (1)$$

2020 *Mathematics Subject Classification.* Primary 05C38, 15A15; Secondary 05A15, 15A18.

Keywords. Model II regression, measurement error model, multidimensional regression, bisector.

¹ cengizgazeloglu@sdu.edu.tr; 0000-0002-8222-3384

² asumanzeytinoglu@sdu.edu.tr; 0000-0001-5102-2152

³ nurullahyilmaz@sdu.edu.tr-Corresponding author; 0000-0001-6429-7518.

while the model including more than two variables is given by

$$\hat{Y} = \beta_0 + \beta_1 X_1 + \beta_2 X_2 + \beta_3 X_3 + \cdots + \beta_m X_m + e_i, \quad (2)$$

where \hat{Y} represents dependent variable, e_i are uncontrollable errors and β_i are coefficients ($i = 1, 2, \dots, m$). It is well-known that the regression analysis depends on fundamental assumptions as follows: (i) the relationship between the variables is linear, (ii) the variables have no measurement errors, (iii) the expected value of error terms is zero, (iv) the error terms display the normal distribution, (v) there is no relation between and the error terms, (vi) there is no autocorrelation between error terms, (vii) the variance of error terms is constant for all values of the independent variables [14]. In the analysis of classical regression, assumption (ii) is the important one because of losing the validity of the model in case of not providing this assumption. Besides, it is nonrealistic that the variables do not contain the measurement error stemming from the measuring equipment, observer, incorrect records, etc. in the real data sets. For this reason, the Model II regression methods have been developed in cases where assumption (ii) may not be provided. Model II regression methods are based on the idea of constituting a regression model that regards the fact that all variables may contain errors. In the analysis of classical regression, assumption (ii) is the important one because of losing the validity of the model in case of not providing this assumption. Besides, it is nonrealistic that the variables do not contain the measurement error stemming from the measuring equipment, observer, incorrect records, etc. in the real data sets. Thus, the Model II regression approach is derived, based on the idea of constructing a regression model that regards the fact that all variables may contain errors. In Model I regression, in order to determine the functional relationship between the variables and to make prediction, linear regression is used while, in Model II, linear regressions for each variable are constructed because assigning the variables as dependent or independent could not be possible and corresponding regression equations are evaluated depending on the nature of the problem.

The idea of Model II regression, which dates back to the early 1900s, has been studied theoretically by Deming (1943) [5], York (1966) [29] and Passing and Bablok (1983) [18]. Also, to estimate of the functional relationship, the line that bisects the minor angle between the two model regressions is suggested by Sprent and Dolby (1980) [23]. One of the important Model II regression called geometric mean Model II has been used in the analysis of most field data by Laws and Archie (1981) [13] while a linear regression method without particular assumptions, regarding the distribution of the samples and the measurement errors, has been investigated by Passing and Bablok (1983) [18]. In the next years, major axis and standardized major axis, which are the most known Model II methods, have been discussed by Warton *et al.* (2006) [27] to describe the key properties of line-fitting techniques in order to estimate the relationship between two variables. While it is seen that all of these mentioned studies focused on bivariate problems, a method for estimating multivariate functional relationships between sets of measured data in different

fields is described for three or more variables in the studies of Stavn and Richter (2008) [24] and Richter and Stavn (2014) [20]. Besides of these theoretical developments, there are many studies focused on the application of Model II methods in the literature. A number of Model II methods have been examined in fishery studies and reviewed in biomechanics by Ricker (1973) [21] and Rayner (1985) [19], respectively. Isobe *et al.* (1990) [11] have discussed and applied five different methods to bivariate data with measurement errors in astronomical problems. Some Model II procedures have been reviewed comprehensively and compared the effectiveness of the methods on clinical and biomedical chemistry by Ludbrook (2010, 2012) [15, 16]. In several research areas such as natural sciences, biological researches, environmental sciences, fisheries, osteology and microbiology, etc., different types of Model II methods have been used in the literature [1, 4, 6, 10, 17, 25, 28]. On the other hand, when all model II regressions in the literature are examined, it is seen that all of them are derived for two or three variable problems, except the study of Richter and Stavn (2014) [20]. In their study, however, model II regression is defined only theoretically for problems with more than three variables, but it has not been applied to any real data or simulation calculations. Therefore, the Model II regression methods available in the literature are open to development when it is desired to model a problem with four or more variables. Accordingly, the novelty of this study is to develop a new Model II regression method for the problems with any number of variables. This new method, called Bisector Regression Model II (BRM-II), is constructed on the idea of computing the bisector of hyperplanes standing for the multidimensional regression models. The BRM-II method has the flexibility to be applied to many complex problems in the natural, medical, and social sciences since real-life problems are represented by multivariate models.

In this paper, the organization is follows: in Section 2, a new multidimensional BRM-II method is introduced in detail. Then, in order to demonstrate the validity and efficiency of the method, the proposed method is applied for both simulations which are up to ten variables for different sample sizes and distribution types and real data sets with two and three variables in Section 3. Finally, the concluding remarks are presented in the last section.

2. A NEW MULTIDIMENSIONAL BRM-II METHOD

Let we have a data set with m variables such as X_i ($i = 1, 2, \dots, m$). For instance, we decide X_1 as a dependent variable and set a linear regression with other $(m - 1)$ variables

$$X_1 = \beta_0 + \beta_1 X_2 + \beta_2 X_3 + \dots + \beta_{m-1} X_m.$$

From this point of view each linear regression is obtained and expressed as a system with the following form:

$$\left. \begin{aligned} H_1 : & \beta_{0,1} + \beta_{1,1}X_1 + \beta_{2,1}X_2 + \beta_{3,1}X_3 + \cdots + \beta_{m,1}X_m = 0 \\ H_2 : & \beta_{0,2} + \beta_{1,2}X_1 + \beta_{2,2}X_2 + \beta_{3,2}X_3 + \cdots + \beta_{m,2}X_m = 0 \\ H_3 : & \beta_{0,3} + \beta_{1,3}X_1 + \beta_{2,3}X_2 + \beta_{3,3}X_3 + \cdots + \beta_{m,3}X_m = 0 \\ & \vdots \\ H_m : & \beta_{0,m} + \beta_{1,m}X_1 + \beta_{2,m}X_2 + \beta_{3,m}X_3 + \cdots + \beta_{m,m}X_m = 0 \end{aligned} \right\} \quad (3)$$

where H_i for $i = 1, \dots, m$ represent the hyperplanes geometrically, $\beta_{i,j}$ for $i = 0, \dots, m$, $j = 1, \dots, m$ are unknown regression coefficients and $\beta_{i,i} = -1$ for $i = 1, \dots, m$. A bisector-hyperplane (BH_1) is found by considering the hyperplanes H_1 and H_2 in system (3), and then a new bisector-hyperplane (BH_2) is again found by using BH_1 and H_3 and so on (see Figure 1). The geometric observations of the bisector approach with two and three variables are given in Figure 2.

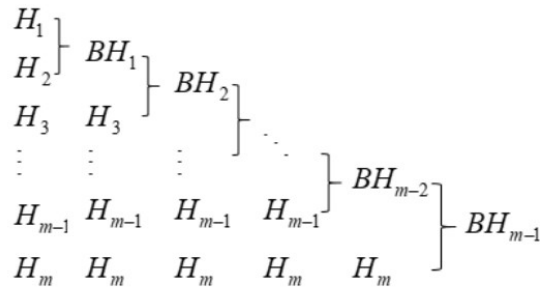
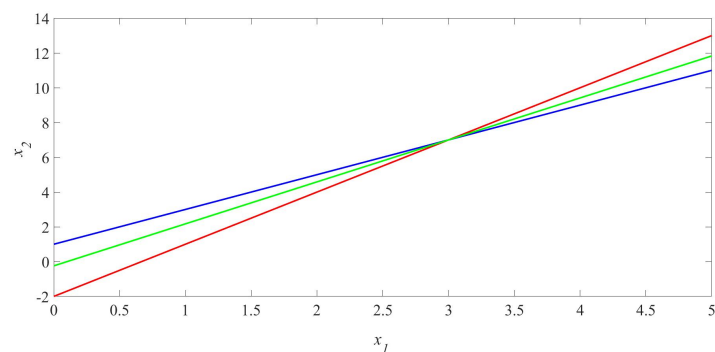


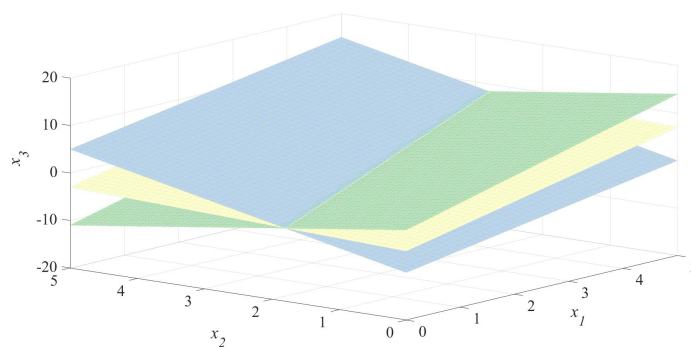
FIGURE 1. The schema of bisector hyperplanes

In order to carry out the bisector hyperplanes between each sequential hyperplanes, finding the normal vectors of the hyperplanes is needed. The matrix of normal vectors of the hyperplanes in the above system is defined by

$$\mathbf{A} = \begin{bmatrix} \beta_{1,1} & \beta_{2,1} & \beta_{3,1} & \cdots & \beta_{m,1} \\ \beta_{1,2} & \beta_{2,2} & \beta_{3,2} & \cdots & \beta_{m,2} \\ \beta_{1,3} & \beta_{2,3} & \beta_{3,3} & \cdots & \beta_{m,3} \\ \vdots & \vdots & \vdots & \ddots & \vdots \\ \beta_{1,m} & \beta_{2,m} & \beta_{3,m} & \cdots & \beta_{m,m} \end{bmatrix}. \quad (4)$$



(a)



(b)

FIGURE 2. The geometric observation of the bisector approach with (a) two variables (the red line: $\beta_{0,1} + \beta_{1,1}X_1 + \beta_{2,1}X_2 = 0$, the blue line: $\beta_{0,2} + \beta_{1,2}X_1 + \beta_{2,2}X_2 = 0$ and the green line is the bisector line) and (b) three variables (the blue plane: $\beta_{0,1} + \beta_{1,1}X_1 + \beta_{2,1}X_2 + \beta_{3,1}X_3 = 0$, the green plane: $\beta_{0,2} + \beta_{1,2}X_1 + \beta_{2,2}X_2 + \beta_{3,2}X_3 = 0$ and the yellow plane is the bisector plane)

Let us now obtain the first bisector hyperplane BH_1 using with the hyperplanes H_1 and H_2 . It is well-known that the equation of a bisector hyperplane is computed by

$$\frac{|\beta_{0,1} + \beta_{1,1}X_1 + \beta_{2,1}X_2 + \dots + \beta_{m,1}X_m|}{\|\tilde{n}_1\|} = \frac{|\beta_{0,2} + \beta_{1,2}X_1 + \beta_{2,2}X_2 + \dots + \beta_{m,2}X_m|}{\|\tilde{n}_2\|} \tag{5}$$

where $\|\cdot\|$ is Euclidean norm of the corresponding vector and \tilde{n}_1, \tilde{n}_2 are the normal vectors of H_1 and H_2 as follows

$$\tilde{n}_1 = [\beta_{1,1} \ \beta_{2,1} \ \beta_{3,1} \ \cdots \ \beta_{m,1}], \quad (6)$$

$$\tilde{n}_2 = [\beta_{1,2} \ \beta_{2,2} \ \beta_{3,2} \ \cdots \ \beta_{m,2}]. \quad (7)$$

Therefore, the matrix form of the normal vector of BH_1 is obtained

$$\tilde{n}_{BH_1} = \frac{\tilde{n}_1}{\|\tilde{n}_1\|} \mp \frac{\tilde{n}_2}{\|\tilde{n}_2\|}. \quad (8)$$

As can be seen from Eq. (8) there are two cases to determine the normal vector of BH_1 since there are two bisector hyperplane arising from two angles called the minor and major ones between the H_1 and H_2 . The bisector hyperplane stemming from the minor angle is preferred as BH_1 because of representing the data set meaningfully. The formulae of BH_1 is written as

$$BH_1: \tilde{\beta}_{0,1} + \tilde{n}_{BH_1}X = 0, \quad (9)$$

where $X = [X_1 \ X_2 \ X_3 \ \cdots \ X_m]^T$, $\tilde{n}_{BH_1} = [\tilde{\beta}_{1,1} \ \tilde{\beta}_{2,1} \ \tilde{\beta}_{3,1} \ \cdots \ \tilde{\beta}_{m,1}]$ and $\tilde{\beta}_{0,1} = \frac{\beta_{0,1}}{\|\tilde{n}_1\|} \mp \frac{\beta_{0,2}}{\|\tilde{n}_2\|}$. In a similar manner, the normal vectors of BH_1 and H_3 are taken as

$$\tilde{n}_{BH_1} = [\tilde{\beta}_{1,1} \ \tilde{\beta}_{2,1} \ \tilde{\beta}_{3,1} \ \cdots \ \tilde{\beta}_{m,1}], \quad (10)$$

$$\tilde{n}_3 = [\beta_{1,3} \ \beta_{2,3} \ \beta_{3,3} \ \cdots \ \beta_{m,3}]. \quad (11)$$

and the matrix form of the normal vector of BH_2 is obtained

$$\tilde{n}_{BH_2} = \frac{\tilde{n}_{BH_1}}{\|\tilde{n}_{BH_1}\|} \mp \frac{\tilde{n}_3}{\|\tilde{n}_3\|}. \quad (12)$$

Use the minor angle point of view,

$$BH_2: \tilde{\beta}_{0,2} + \tilde{n}_{BH_2}X = 0, \quad (13)$$

where $X = [X_1 \ X_2 \ X_3 \ \cdots \ X_m]^T$, $\tilde{n}_{BH_2} = [\tilde{\beta}_{1,2} \ \tilde{\beta}_{2,2} \ \tilde{\beta}_{3,2} \ \cdots \ \tilde{\beta}_{m,2}]$ and $\tilde{\beta}_{0,2} = \frac{\tilde{\beta}_{0,1}}{\|\tilde{n}_{BH_1}\|} \mp \frac{\beta_{0,3}}{\|\tilde{n}_3\|}$. The computation process is continued as the similar way, and the last bisector hyperplane BH_{m-1} is obtained as

$$BH_{m-1}: \tilde{\beta}_{0,m-1} + \tilde{n}_{BH_{m-1}}X = 0 \quad (14)$$

where $X = [X_1 \ X_2 \ X_3 \ \cdots \ X_m]^T$,

$\tilde{n}_{BH_{m-1}} = [\tilde{\beta}_{1,m-1} \ \tilde{\beta}_{2,m-1} \ \cdots \ \tilde{\beta}_{m,m-1}]$ and $\tilde{\beta}_{0,m-1} = \frac{\tilde{\beta}_{0,m-2}}{\|\tilde{n}_{BH_{m-2}}\|} \mp \frac{\beta_{0,m}}{\|\tilde{n}_m\|}$.

Thus, the process is completed, and the BH_{m-1} is called as the BRM-II model.

3. COMPUTATIONAL EXPERIMENTS

To demonstrate the applicability and efficiency of the multidimensional BRM-II, various simulations which are up to ten variables for different sample sizes and distribution types are performed in terms of the MSE

$$MSE = \sum_{i=1}^n \frac{(y_i - \hat{y}_i)^2}{n - k},$$

where y_i are real observation values, \hat{y}_i are estimated values, n is the sample size and k is the number of parameters. In addition to the simulations, the BRM-II is applied to two real problems with two and three variables, and compared with the existing methods in the literature.

3.1. Simulations. It is well-known that simulation is defined as imitating something in an artificial environment depending on time. In this study, the performance measurement of the BRM-II method is calculated on the computer by designing the simulation conditions. The corresponding simulations are organized by randomly selecting different sample sizes n such as 20, 30, 50, 100 and 200 from the data sets with a population size $N=5000$ with different distributions $t \sim 4$, $t \sim 10$ and $t \sim 30$. The MSE values of the simulations were calculated for up to 10 variables in this study (the number of variables can be increased further if desired). The simulations are repeated $100000/n$ times, and the arithmetic means of the results obtained are calculated after the processes are completed. The produced results are listed in Table 1 in details. According to these results, when the BRM-II method is ana-

TABLE 1. The MSE values of the BRM-II simulations using total population $N=5000$

Number of Variables (nv)	Sample Size (n)	The degrees of freedom of the distribution (df)			Number of Variables (nv)	Sample Size (n)	The degrees of freedom of the distribution (df)		
		$t \sim 4$	$t \sim 10$	$t \sim 30$			$t \sim 4$	$t \sim 10$	$t \sim 30$
3	20	6.96	5.22	4.82	5	20	8.20	5.98	5.30
	30	6.65	5.01	4.54		30	7.15	5.32	4.85
	50	6.15	4.66	4.37		50	6.68	4.96	4.66
	100	6.08	4.60	4.18		100	6.28	4.70	4.27
	200	6.00	4.55	4.15		200	5.94	4.66	4.25
4	20	7.02	5.36	5.11	10	20	12.60	9.00	8.64
	30	6.98	5.04	4.78		30	9.54	6.60	6.38
	50	6.36	4.89	4.45		50	7.51	5.56	5.23
	100	6.13	4.66	4.32		100	6.58	5.08	4.59
	200	6.11	4.62	4.22		200	6.32	4.66	4.36

lyzed with 3 variables, the MSE decreases in all sample sizes when the degrees of freedom of the distribution are increased. For instance, the MSE equals to 6.68 if nv , n and df are taken as 5, 50 and 4, respectively, while the MSE decrease to 4.96 and 4.66 if df is increased to 10 and 30 without changing the other parameters.

Besides, the MSE decreases as n is increased by keeping df and nv unchanged. It can be seen that the same behaviour is valid as nv is 4, 5 and 10. Note that the MSE is expected to increase as nv increases by keeping df and n unchanged. The relationship between the sample sizes and the degrees of freedom of distribution for different number of variables are shown in Figure 3.

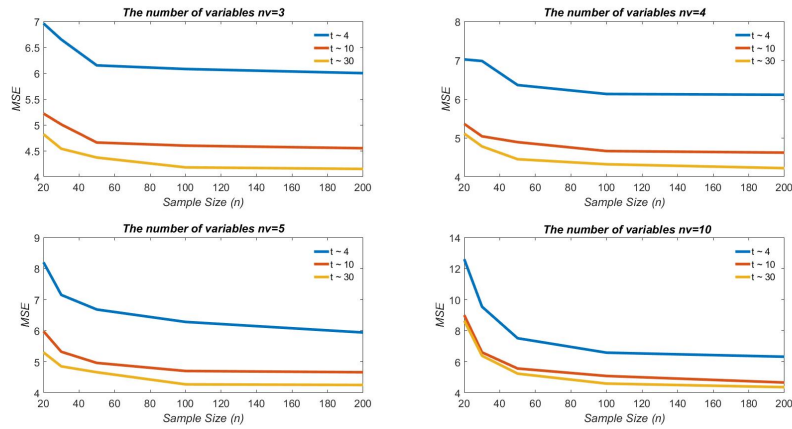


FIGURE 3. The relationship between the sample sizes and the degrees of freedom of distribution for different number of variables

Consequently, the performance of the BRM-II method draws attention in terms of supporting the theoretical expectation regarding the decreasing behaviour of MSE. Therefore, the proposed method is a powerful tool among the regression approaches.

3.2. Application to the real data sets. In this part, there are two real modeling processes with two and three variables including the oceanographic data sets are considered to demonstrate the performance of the BRM-II methods.

3.2.1. Example with two variables. As the first real application of proposed method with two variables is used the data that including weights of unspawned female cabezon (a California marine fish, *Scorpaenichthys marmoratus*) and the number of eggs subsequently produced for 11 fish are given as [22]:

TABLE 2. The biological oceanographic data set

Weight (to nearest 100g): X_1	14	17	24	25	27	33	34	37	40	41	42
Eggs (in thousands): X_2	61	37	65	69	54	93	87	89	100	90	97

It is desired to constitute a functional relationship between weight before spawning and number of egg produced because of both variables are subject to error.

In order to construct the BRM-II method, as the first step, the simple linear regression is applied for each variable with respect to the data in Table 2 as follows:

$$\beta_{0,1} + \beta_{1,1}X_1 + \beta_{2,1}X_2 = 0 , \tag{15}$$

$$\beta_{0,2} + \beta_{1,2}X_1 + \beta_{2,2}X_2 = 0 , \tag{16}$$

where X_1 and X_2 are dependent variables in Eqs. (15) and (16), respectively. The coefficients are computed as reported in Table 3.

TABLE 3. The coefficients of simple linear regressions

$\beta_{i,j}$	$i = 0$	$i = 1$	$i = 2$
$j = 1$	-1.5032	-1	0.4163
$j = 2$	19.7668	1.8700	-1

Then, the bisector line of these system is obtained by using the Eqs. (5)-(9) in proposed method mentioned above

$$-10.7093 - 1.8050 X_1 + 0.8559X_2 = 0. \tag{17}$$

The regression lines are illustrated in Figure 4. Moreover, in order to demonstrate the efficiency of the BRM-II, the results of MSE are compared with some previous studies in the literature, and given in Table 4. It can be seen from the results that the BRM-II method is outstanding in comparison with the study of Richter and Stavn (2014) (20). Moreover, the MSE of our method is even better than the MSE result in their study by using the standardized data.

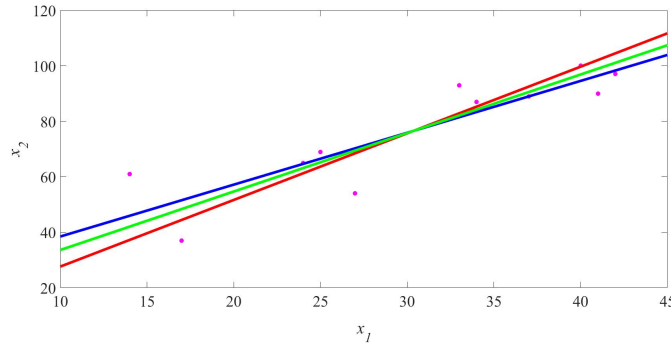


FIGURE 4. The data set and the regression lines in Example 1 (the red line: Eq. (3.1), the blue line: Eq. (16), and the green (bisector) line: Eq. (17))

TABLE 4. The results of MSE for the different regression models

Regression Model	MSE
BRM-II	109.01
[20]	122.62
[20] (with Standardized data)	109.47
[26]	109.54

TABLE 5. The oceanographic field data set

PIM: X_1	POM: X_2	b_{555} : X_3	PIM: X_1	POM: X_2	b_{555} : X_3
11.36	2.36	8.41	5.33	1.94	4.99
6.98	1.49	5.85	5.46	2.16	5.05
6.89	1.15	6.91	9.98	2.87	9.11
14.60	3.00	11.31	5.67	1.81	8.39
12.52	1.59	10.03	6.89	3.11	7.57
5.40	2.53	3.40	3.21	3.32	4.38
6.45	2.21	5.43	4.56	1.69	3.78
1.57	0.18	1.09	6.56	1.06	4.91
2.15	0.45	1.84	4.63	1.05	3.09
22.31	3.28	17.94	5.48	0.69	3.66
4.67	2.05	4.85	3.88	0.71	2.41
5.01	0.52	1.20	2.80	0.48	1.77

3.2.2. *Example with three variables.* The second application of proposed method with three variables is discussed the data sets that including the concentration of particulate inorganic matter [PIM (gm^{-3})], the particulate organic matter [POM (gm^{-3})] and the total scattering coefficient at a wavelength of 555 nm [b_{555} (m^{-1})] for 24 field stations at Mobile Bay, Alabama are given in Table 5 [20]:

In order to constitute a functional relationship among PIM, POM and b_{555} , the simple linear regressions for each variable are written with respect to the data in Table 4 similar to the previous example as follows:

$$\beta_{0,1} + \beta_{1,1}X_1 + \beta_{2,1}X_2 + \beta_{3,1}X_3 = 0, \quad (18)$$

$$\beta_{0,2} + \beta_{1,2}X_1 + \beta_{2,2}X_2 + \beta_{3,2}X_3 = 0, \quad (19)$$

$$\beta_{0,3} + \beta_{1,3}X_1 + \beta_{2,3}X_2 + \beta_{3,3}X_3 = 0, \quad (20)$$

where X_1 , X_2 and X_3 are dependent variables in Eqs. (18), (19) and (20), respectively. The coefficients are given in the following Table 6. The bisector line of these system is obtained

$$1.0225 - 0.8603 X_1 - 1.2936 X_2 + 1.2434X_3 = 0. \quad (21)$$

The regression planes are illustrated in Figure 5 and the MSE result of the BRM-II is compared with some previous studies in the literature (see Table 7).

TABLE 6. The coefficients of simple linear regression

$\beta_{i,j}$	$i = 0$	$i = 1$	$i = 2$	$i = 3$
$j = 1$	0.9066	-1	-0.6394	1.2322
$j = 2$	0.8042	-0.1404	-1	0.3310
$j = 3$	-0.4658	0.6897	0.8440	-1

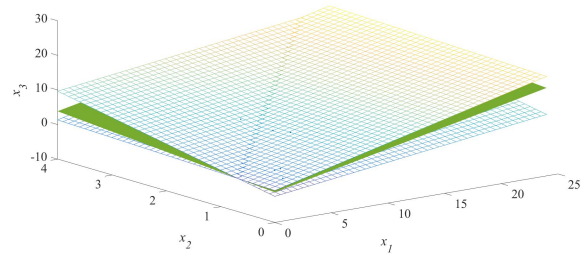
TABLE 7. The results of MSE for the different regression models

Regression Model	MSE
BRM-II	1.3336
[20]	2.2318
[20] (with standardized data)	1.3210

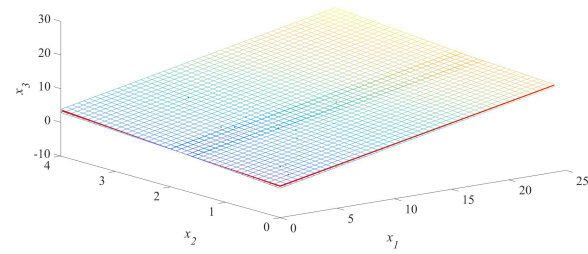
It can be said from the table that the BRM-II method is superior in comparison with the study of Richter and Stavn (2014) [20]. Also, the MSE of our method is competitive with the MSE of their study by using the standardized data.

4. CONCLUSION AND RECOMMENDATION

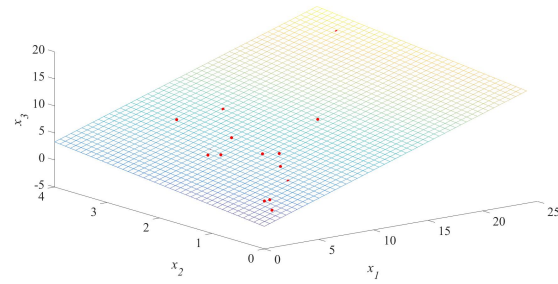
In this study, a new multidimensional BRM-II method is introduced for multivariate problems that may contain measurement error. In order to demonstrate the validity and efficiency, the proposed method is applied to simulations up to ten variables for different sample sizes and distribution types in terms of the Mean Square Error (MSE), and then implemented to two real problems with two and three variables. By comparing with the methods in the literature, it is observed that the BRM-II method is outstanding in comparison with the study of Richter and Stavn (2014) for both original and standardized data. So it can be deduced that the proposed method provides relatively higher accuracy. Besides, it is easy applicable and versatile tool for prediction of relevant real life problems. For the further studies, different forms of the BRM-II can be derived for more realistic phenomena.



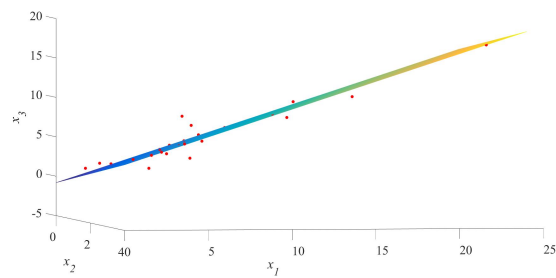
(a)



(b)



(c)



(d)

FIGURE 5. The data set and the regression planes in Example 2 (a) Eq. (18), Eq. (19) and the bisector-1; (b) Eq. (20), the bisector-1 and the bisector-2; (c) the final bisector plane: Eq. (21); (d) the final bisector plane: Eq. (21) in (c) with different perspective.

Author Contribution Statements The authors contributed equally to this work. All authors read and approved the final copy of this paper.

Declaration of Competing Interests The authors declare that they have no known competing financial interest or personal relationships that could have appeared to influence the work reported in this paper.

REFERENCES

- [1] Alexiades, A. V., Marcy-Quay, B., Sullivan, P. J., Kraft, C. E., Measurement error in angler creel surveys, *North American Journal of Fisheries Management*, 35 (2) (2015), 253–261, <https://doi.org/10.1080/02755947.2014.996689>.
- [2] Amado, A., Meirelles-Pereira, F., Vidal, L., Sarmento, H., Suhett, A., Farjalla, V., Cotner, J., Roland, F., Tropical freshwater ecosystems have lower bacterial growth efficiency than temperate ones, *Frontiers in Microbiology*, 4 (2013), <https://doi.org/10.3389/fmicb.2013.00167>.
- [3] Bradbury, J. W., Vehrencamp, S. L., Choice of regression model for isodar analysis, *Evolutionary Ecology Research*, 16 (2015), 689–704.
- [4] Chen, S.-C., Pahlevani, A. H., Malíková, L., Riina, R., Thomson, F. J., Giladi, I., Trade-off or coordination? correlations between ballochorous and myrmecochorous phases of diplochory, *Functional Ecology*, 33 (8) (2019), 1469–1479, <https://doi.org/10.1111/1365-2435.13353>.
- [5] Deming, W. E., Statistical Adjustment Of Data, J. Wiley & Sons, inc.; Chapman & Hall, ltd New York, London, 1943.
- [6] Downs, D. E., Cheng, Y. W., Length–length and width–length conversion of longnose skate and big skate off the pacific coast: Implications for the choice of alternative measurement units in fisheries stock assessment, *North American Journal of Fisheries Management*, 33 (5) (2013), 887–893, <https://doi.org/10.1080/02755947.2013.818080>.
- [7] Endo, H., Nishigaki, T., Yamamoto, Keigoand Takeno, K., Age- and size-based morphological comparison between the brown alga sargassum macrocarpum (heterokonta; fucales) from different depths at an exposed coast in northern kyoto, japan, *Journal of Applied Phycology*, 25 (6) (Dec 2013), 1815–1822, <https://doi.org/10.1007/s10811-013-0002-y>.
- [8] Fairchild, W., Hales, B., High-resolution carbonate system dynamics of neartars bay, or from 2014 to 2019, *Frontiers in Marine Science*, 7 (2021), <https://doi.org/10.3389/fmars.2020.590236>.
- [9] Formicola, V., Franceschi, M., Regression equations for estimating stature from long bones of early holocene european samples, *Am J Phys Anthropol*, 100 (1) (May 1996), 83–88.
- [10] Hou, A., DeLaune, Ronald D.and Tan, M., Reams, M., Laws, E., Toxic elements in aquatic sediments: Distinguishing natural variability from anthropogenic effects, *Water, Air, and Soil Pollution*, 203 (1) (Oct 2009), 179–191, <https://doi.org/10.1007/s11270-009-0002-3>.
- [11] Isobe, T., Feigelson, E. D., Akritas, M. G., Babu, G. J., Linear regression in astronomy. i., *apj*, 364 (Nov. 1990), 104, <https://doi.org/10.1086/169390>.
- [12] James, G., Witten, D., Hastie, T., Tibshirani, R., An Introduction To Statistical Learning, 1 ed., Springer texts in statistics, Springer, New York, NY, June 2013.
- [13] Laws, E. A., Archie, J. W., Appropriate use of regression analysis in marine biology, *Marine Biology*, 65 (1) (Nov 1981), 13–16, <https://doi.org/10.1007/BF00397062>.
- [14] Lewis-Beck, M. S., Applied Regression: An Introduction, Quantitative applications in the social sciences, SAGE, Newbury Park, London, 1980.
- [15] Ludbrook, J., Linear regression analysis for comparing two measurers or methods of measurement: But which regression?, *Clinical and Experimental Pharmacology and Physiology*, 37 (7) (2010), 692–699, <https://doi.org/10.1111/j.1440-1681.2010.05376.x>.

- [16] Ludbrook, J., A primer for biomedical scientists on how to execute model ii linear regression analysis, *Clinical and Experimental Pharmacology and Physiology*, 39 (4) (2012), 329–335, <https://doi.org/10.1111/j.1440-1681.2011.05643.x>.
- [17] Martínez, P. A., Bidau, C. J., A re-assessment of rensch's rule in tuco-tucos (rodentia: Ctenomyidae: Ctenomys) using a phylogenetic approach, *Mammalian Biology*, 81 (1) (2016), 66–72, <https://doi.org/10.1016/j.mambio.2014.11.008>.
- [18] Passing, H., Bablok, W., A new biometrical procedure for testing the equality of measurements from two different analytical methods. application of linear regression procedures for method comparison studies in clinical chemistry, part i, 709–720, <https://doi.org/10.1515/cclm.1983.21.11.709>.
- [19] Rayner, J. M. V., Linear relations in biomechanics: the statistics of scaling functions, *Journal of Zoology*, 206 (3) (1985), 415–439, <https://doi.org/10.1111/j.1469-7998.1985.tb05668.x>.
- [20] Richter, S. J., Stavn, R. H., Determining functional relations in multivariate oceanographic systems: Model ii multiple linear regression, *Journal of Atmospheric and Oceanic Technology*, 31 (7) (2014), 1663 – 1672, <https://doi.org/10.1175/JTECH-D-13-00210.1>.
- [21] Ricker, W. E., Linear regressions in fishery research, *Journal of the Fisheries Research Board of Canada*, 30 (3) (1973), 409–434, 10.1139/f73-072.
- [22] Sokal, R. R., Rohlf, F. J., Biometry, W.H. Freeman, New York, NY, Aug. 1969.
- [23] Sprent, P., Dolby, G. R., Query: The geometric mean functional relationship, *Biometrics*, 36 (3) (1980), 547–550.
- [24] Stavn, R. H., Richter, S. J., Biogeo-optics: particle optical properties and the partitioning of the spectral scattering coefficient of ocean waters, *Appl. Opt.*, 47 (14) (May 2008), 2660–2679, <https://doi.org/10.1364/AO.47.002660>.
- [25] Tao, J., Hill, P. S., Boss, E. S., Milligan, T. G., Evaluation of optical proxies for suspended particulate mass in stratified waters, *Journal of Atmospheric and Oceanic Technology*, 34 (10) (2017), 2203 – 2212, <https://doi.org/10.1175/JTECH-D-17-0042.1>.
- [26] Trujillo-Ortiz, A., Hernandez-Walls, R., gmregress: Geometric mean regression (reduced major axis regression). a matlab file. retrived august 10, 2021, <http://www.mathworks.com/matlabcentral/fileexchange/27918-gmregress>. Accessed, [Accessed 30-Mar-2023].
- [27] Warton, D. I., Wright, I. J., Falster, D. S., Westoby, M., Bivariate line-fitting methods for allometry, *Biological Reviews*, 81 (2) (2006), 259–291, <https://doi.org/10.1017/S1464793106007007>.
- [28] Yang, X., Lauzon, C. B., Crainiceanu, C., Caffo, B., Resnick, S. M., Landman, B. A., Biological parametric mapping accounting for random regressors with regression calibration and model ii regression, *NeuroImage*, 62 (3) (2012), 1761–1768, <https://doi.org/10.1016/j.neuroimage.2012.05.020>.
- [29] York, D., Least-squares of fitting of a straight line, *Canadian Journal of Physics*, 44 (5) (1966), 1079–1086, <https://doi.org/10.1139/p66-090>.



SHARP COEFFICIENT ESTIMATES FOR ϑ -SPIRALLIKE FUNCTIONS INVOLVING GENERALIZED q -INTEGRAL OPERATOR

Tuğba YAVUZ¹ and Şahsene ALTINKAYA²

^{1,2}Department of Mathematics, Istanbul Beykent University, Istanbul, TÜRKİYE

ABSTRACT. The aim of this article is to identify a new subfamily of spirallike functions and then to demonstrate necessary and sufficient conditions, sharp coefficients estimates for functions in this subfamily.

1. INTRODUCTION

Stand by \mathbb{A} the family of functions $f(\zeta) = \zeta + \sum_{k=2}^{\infty} a_k \zeta^k$ analytic in the open unit disk $\mathcal{D} = \{\zeta \in \mathbb{C} : |\zeta| < 1\}$ with the normalization condition $f(0) = 0 = f'(0) - 1$. A function $f \in \mathbb{A}$ is named univalent in \mathcal{D} provided that it does not take the same value twice. Stand by \mathbb{S} the subfamily of \mathbb{A} involving univalent functions. For analytic functions f_1 and f_2 in \mathcal{D} , we ensure that f_1 is subordinate to f_2 , expressed by $f_1 \prec f_2$, for a Schwarz function

$$\Lambda(\zeta) = \sum_{k=1}^{\infty} \kappa_k \zeta^k \quad (\Lambda(0) = 0, |\Lambda(\zeta)| < 1),$$

analytic in \mathcal{D} such that $f_1(\zeta) = f_2(\Lambda(\zeta))$ ($\zeta \in \mathcal{D}$).

Now, we shall deal with a subfamily of \mathbb{S} which is of special interest in its own right, namely the spirallike functions.

For $-\infty < t < \infty$ and $\vartheta \in (-\frac{\pi}{2}, \frac{\pi}{2})$, the logarithmic ϑ -spiral curve is expressed by $w = w_0 \exp(-e^{-i\vartheta} t)$, where w_0 is a nonzero complex number. We must mention here that 0-spirals are radial half-lines. For an analytic function, we can call it ϑ -spirallike provided that its range is ϑ -spirallike. Stand by \mathcal{S}_{ϑ} the family of ϑ -spirallike functions. Analytically, $f \in \mathbb{A}$ belongs to the family \mathcal{S}_{ϑ} iff

2020 *Mathematics Subject Classification.* 30C45.

Keywords. Spirallike function, coefficient estimate, subordination, q -integral operator.

¹ tugbayavuz@beykent.edu.tr-Corresponding author; 0000-0002-0490-9313;

² sahsenealtinkaya@beykent.edu.tr; 0000-0002-7950-8450.

$\Re \left(e^{i\vartheta} \frac{\zeta f'(\zeta)}{f(\zeta)} \right) > 0$ [17]. Libera [10] used this approach to ϑ -spirallike functions of order σ

$$\Re \left(e^{i\vartheta} \frac{\zeta f'(\zeta)}{f(\zeta)} \right) > \sigma \cos \vartheta$$

and asserted by $\mathcal{S}_\vartheta(\sigma)$. Clearly, $\mathcal{S}_\vartheta(\sigma) \subset \mathcal{S}_\vartheta$. Further, the general coefficient bounds for functions in $\mathcal{S}_\vartheta(\sigma)$ was proved:

$$|a_k| \leq \prod_{j=0}^{k-2} \left(\frac{|2(1-\sigma)e^{-i\vartheta} \cos \vartheta + j|}{j+1} \right) \quad (k \in \mathbb{N} \setminus \{1\}, \quad \mathbb{N} = \{1, 2, \dots\}).$$

This result is sharp. Finding sharp results for functions belonging to the different families of analytic functions is of special interest because of the geometric properties of such functions [12], [14], [20], [21].

The age of quantum calculus (q -calculus) is as old as calculus and because of its applications to wider disciplines from physical sciences to social sciences, it was revived during the last three decades. The first study on the q -calculus dates back to 1908 [8]. On the other hand, q -calculus is connection with function theory. The study of q -calculus in Geometric Function Theory was partially provided by Srivastava [18]. This application is still among the most popular subject of many mathematicians today [1], [2], [3], [5], [7], [15], [19].

In the course of the paper, suppose $0 < q < 1$ and the definitions deal with the complex-valued function f .

The q -derivative of f expressed by [8]:

$$D_q f(\zeta) = \begin{cases} \frac{f(\zeta) - f(q\zeta)}{(1-q)\zeta}, & \zeta \neq 0 \\ f'(0), & \zeta = 0 \end{cases}. \quad (1)$$

If f is differentiable at ζ , then $\lim_{q \rightarrow 1^-} D_q f(\zeta) = f'(\zeta)$.

The q -integral of f expressed by [9]:

$$\int_0^\zeta f(u) d_q u = \zeta(1-q) \sum_{k=0}^{\infty} q^k f(\zeta q^k),$$

provided the series converges.

Next, the q -gamma function is expressed by

$$\Gamma_q(u) = (1-q)^{1-u} \prod_{k=0}^{\infty} \frac{1-q^{k+1}}{1-q^{k+u}} \quad (u > 0),$$

which has the following properties

$$\Gamma_q(u+1) = [u]_q \Gamma_q(u), \quad \Gamma_q(u+1) = [u]_q!, \quad (2)$$

where $u \in \mathbb{N}$ and

$$[u]_q! = \begin{cases} [u]_q [u-1]_q \dots [2]_q [1]_q, & u \geq 1 \\ 1, & u = 0. \end{cases}$$

If we set $q \rightarrow 1^-$, we find $\Gamma_q(u) \rightarrow \Gamma(u)$ [8].

The q -beta function

$$B_q(u, s) = \int_0^1 \zeta^{u-1} (1 - q\zeta)_q^{s-1} d_q \zeta, \quad (u, s > 0) \tag{3}$$

is the q -analogue of Euler's formula [9] with

$$B_q(u, s) = \frac{\Gamma_q(u)\Gamma_q(s)}{\Gamma_q(u+s)}, \tag{4}$$

Next, the q -binomial coefficients are expressed by [6]

$$\binom{k}{n}_q = \frac{[k]_q!}{[n]_q! [k-n]_q!}. \tag{5}$$

In a recent study [11], the generalized q -integral operator $\chi_{\beta,q}^\alpha f : \mathbb{A} \rightarrow \mathbb{A}$ is expressed by

$$\chi_{\beta,q}^\alpha f(\zeta) = \binom{\alpha+\beta}{\beta}_q \frac{[\alpha]_q}{\zeta^\beta} \int_0^\zeta \left(1 - \frac{qu}{\zeta}\right)_q^{\alpha-1} u^{\beta-1} f(u) d_q u \quad (\alpha > 0, \beta > -1). \tag{6}$$

From [2], [3], [4] and [5], they arrive

$$\chi_{\beta,q}^\alpha f(\zeta) = \zeta + \sum_{k=2}^\infty \frac{\Gamma_q(\beta+n)\Gamma_q(\alpha+\beta+1)}{\Gamma_q(\alpha+\beta+n)\Gamma_q(\beta+1)} a_k \zeta^k. \tag{7}$$

For some special values, we find the following integral operators previously known.

(i) If $\alpha = 1$, the q -Bernardi integral operator $J_{\beta,q} f$ is obtained [13]

$$J_{\beta,q} f(\zeta) = \frac{[1+\beta]_q}{\zeta^\beta} \int_0^\zeta u^{\beta-1} f(u) d_q u = \sum_{k=1}^\infty \frac{[1+\beta]_q}{[n+\beta]_q} a_k \zeta^k.$$

(ii) If $\alpha = 1, q \rightarrow 1^-$, the Bernardi integral operator is obtained [4]

$$J_\beta f(\zeta) = \frac{1+\beta}{\zeta^\beta} \int_0^\zeta u^{\beta-1} f(u) du = \sum_{k=1}^\infty \frac{1+\beta}{n+\beta} a_k \zeta^k.$$

(iii) If $\alpha = 1, \beta = 0, q \rightarrow 1^-$, the Alexander integral operator is obtained [16]

$$J_0 f(\zeta) = \int_0^\zeta \frac{f(u)}{u} du = \zeta + \sum_{k=2}^\infty \frac{1}{n} a_k \zeta^k.$$

2. MAIN RESULTS

Firstly, we introduce the new subfamily $SC_{\beta,q}^\alpha(\sigma, \nu)$ of ϑ -spirallike functions inserting the function $\chi_{\beta,q}^\alpha f$.

Definition 1. A function $f \in \mathbb{A}$ is in $SC_{\beta,q}^\alpha(\sigma, \nu)$ if

$$\Re \left(\frac{e^{i\vartheta} \zeta \left(\chi_{\beta,q}^\alpha f(\zeta) \right)'}{\nu \zeta \left(\chi_{\beta,q}^\alpha f(\zeta) \right)' + (1 - \nu) \chi_{\beta,q}^\alpha f(\zeta)} \right) > \sigma \cos \vartheta,$$

where $|\vartheta| < \frac{\pi}{2}$, $0 \leq \sigma < 1$, $\alpha > 0$, $\beta > -1$, $0 \leq \nu \leq 1$.

Note that

1) Letting $q \rightarrow 1^-$ and $\alpha = 1$ in Definition 1, we arrive the class $SC_{\beta,q}^\alpha(\sigma, \nu) := SC_\beta(\sigma, \nu)$ involving Bernardi integral operator given in (ii).

2) Letting $q \rightarrow 1^-$, $\alpha = 1$ and $\beta = 0$ in Definition 1, we arrive the class $SC_{\beta,q}^\alpha(\sigma, \nu) := SC(\sigma, \nu)$ involving Alexander integral operator given in (iii).

This paper deals with the new class $SC_{\beta,q}^\alpha(\sigma, \nu)$ of ϑ -spirallike functions involving a generalized q -integral operator and its several properties.

Next, we get coefficient conditions and sharp bounds for functions in $SC_{\beta,q}^\alpha(\sigma, \nu)$.

Theorem 1. Assume $\chi_{\beta,q}^\alpha f(\zeta) \neq 0$ for $\zeta \in \mathcal{D} \setminus \{0\}$. Then, f is in $SC_{\beta,q}^\alpha(\sigma, \nu)$ if and only if

$$\sum_{k=2}^{\infty} \left[(k-1)(1 + e^{2i\vartheta})(1 - \sigma\nu + i(1 - \nu)\tan\vartheta) + 2(1 - \sigma)e^{2i\vartheta} - (k-1)(1 - e^{2i\vartheta})(1 - \sigma)\nu \right] \times \frac{\Gamma_q(\beta + k)\Gamma_q(\alpha + \beta + 1)}{\Gamma_q(\alpha + \beta + k)\Gamma_q(\beta + 1)} a_k \zeta^k \neq 0.$$

Proof. Let us put

$$\Delta(\zeta) = \chi_{\beta,q}^\alpha f(\zeta) = \zeta + \sum_{k=2}^{\infty} X_k \zeta^k \quad (\zeta \in \mathcal{D}),$$

where $X_n = \frac{\Gamma_q(\beta+k)\Gamma_q(\alpha+\beta+1)}{\Gamma_q(\alpha+\beta+k)\Gamma_q(\beta+1)} a_k$ with $X_1 = 1$. Now, consider the function

$$\Sigma(\zeta) = \frac{\left(\frac{\zeta \Delta'(\zeta)}{\nu \zeta \Delta'(\zeta) + (1 - \nu) \Delta(\zeta)} \right) e^{i\vartheta} \sec\vartheta - i \tan\vartheta - \sigma}{1 - \sigma}.$$

is an analytic, $\Sigma(0) = 1$ and $\Re\Sigma(\zeta) > 0$, then $f \in SC_{\beta,q}^\alpha(\sigma, \nu)$ iff

$$\Sigma(\zeta) \neq \frac{1 - e^{2i\vartheta}}{1 + e^{2i\vartheta}}$$

or, equivalently

$$\frac{e^{i\vartheta} \sec\vartheta \zeta \Delta'(\zeta) - (\sigma + i \tan\vartheta)(\nu \zeta \Delta'(\zeta) + (1 - \nu) \Delta(\zeta))}{(1 - \sigma)(\nu \zeta \Delta'(\zeta) + (1 - \nu) \Delta(\zeta))} \neq \frac{1 - e^{2i\vartheta}}{1 + e^{2i\vartheta}}.$$

Now, from the series expansion of $\Delta(\zeta)$, we arrive

$$\frac{\sum_{k=1}^{\infty} [(k - 1)(1 - \sigma\nu + i(1 - \nu)\tan\vartheta) + (1 - \sigma)] X_k \zeta^k}{(1 - \sigma) \sum_{k=1}^{\infty} (1 + (k - 1)\nu) X_k \zeta^k} \neq \frac{1 - e^{2i\vartheta}}{1 + e^{2i\vartheta}},$$

which yields for $\zeta \neq 0$

$$\begin{aligned} & \sum_{k=2}^{\infty} [(k - 1)(1 + e^{2i\vartheta})(1 - \sigma\nu + i(1 - \nu)\tan\vartheta) + 2(1 - \sigma)e^{2i\vartheta} \\ & - (k - 1)(1 - e^{2i\vartheta})(1 - \sigma)\nu] X_k \zeta^k \neq 0. \end{aligned}$$

□

Theorem 2. Let $\chi_{\beta,q}^\alpha f(\zeta) \neq 0$ for $\zeta \in \mathcal{D} \setminus \{0\}$. If f is in $SC_{\beta,q}^\alpha(\sigma, \nu)$, then

$$\begin{aligned} |a_k| \leq & \frac{\Gamma_q(\alpha + \beta + k)\Gamma_q(\beta + 1)}{\Gamma_q(\beta + k)\Gamma_q(\alpha + \beta + 1)(k - 1)!(1 - \nu)^{k-1}} \\ & \times \prod_{j=0}^{k-2} |j(1 - \nu) + 2(1 - \sigma)e^{i\vartheta} \cos\vartheta(1 + \nu j)|, \end{aligned} \tag{8}$$

where $k \in \mathbb{N} \setminus \{1\}$ with $a_1 = 1$. This result is sharp.

Proof. Since $f \in SC_{\beta,q}^\alpha(\sigma, \nu)$, we can use a Schwarz function $\Lambda(\zeta)$ such that

$$\left(\frac{\zeta (\chi_{\beta,q}^\alpha f(\zeta))'}{\nu \zeta (\chi_{\beta,q}^\alpha f(\zeta))' + (1 - \nu)\chi_{\beta,q}^\alpha f(\zeta)} \right) e^{i\vartheta} \sec\vartheta - i \tan\vartheta = \frac{1 + (1 - 2\sigma)\Lambda(\zeta)}{1 - \Lambda(\zeta)}.$$

If we put the function $\Delta(\zeta)$, we find

$$\begin{aligned} & \sum_{k=1}^{\infty} [ke^{i\vartheta} \sec\vartheta - (1 + i \tan\vartheta)(1 + (k - 1)\nu)] X_k \zeta^k \\ & = \left(\sum_{k=1}^{\infty} [ke^{i\vartheta} \sec\vartheta + (1 - 2\sigma - i \tan\vartheta)(1 + (k - 1)\nu)] X_k \zeta^k \right) \Lambda(\zeta). \end{aligned}$$

Now, for $k \in \mathbb{N}$, we can write

$$\begin{aligned} & \sum_{k=1}^m [ke^{i\vartheta} \sec\vartheta - (1 + i \tan\vartheta)(1 + (k - 1)\nu)] X_k \zeta^k + \sum_{k=m+1}^{\infty} b_k \zeta^k \\ & = \left(\sum_{k=1}^{m-1} [ke^{i\vartheta} \sec\vartheta + (1 - 2\sigma - i \tan\vartheta)(1 + (k - 1)\nu)] X_k \zeta^k \right) \Lambda(\zeta). \end{aligned} \tag{9}$$

For $m = 2, 3, \dots$, the LHS of (9) is convergent in \mathcal{D} . Since $|\Lambda(\zeta)| < 1$, it is easy to get by appealing to Parseval's Theorem that

$$\begin{aligned} & \sum_{k=1}^{m-1} |ke^{i\vartheta} \sec\vartheta + (1 - 2\sigma - itan\vartheta)(1 + (k - 1)\nu)|^2 |X_k|^2 \\ & \geq \sum_{k=2}^m |ne^{i\vartheta} \sec\vartheta - (1 + itan\vartheta)(1 + (k - 1)\nu)|^2 |X_k|^2 \end{aligned}$$

or

$$\sum_{k=1}^{m-1} 4(1 - \sigma)(1 + (k - 1)\nu)(k - \sigma(1 + (k - 1)\nu)) |X_k|^2 \geq \frac{(m - 1)^2(1 - \nu)^2}{\cos^2\vartheta} |X_m|^2, \tag{10}$$

where $X_1 = 1$. Now, we claim that

$$|X_k| \leq \frac{1}{(k - 1)!(1 - \nu)^{k-1}} \prod_{j=0}^{k-2} |j(1 - \nu) + 2(1 - \sigma)e^{i\vartheta} \cos\vartheta(1 + \nu j)|. \tag{11}$$

For $k = 2$, we find from (10)

$$|X_2| \leq \frac{2(1 - \sigma)\cos\vartheta}{1 - \nu},$$

which is equivalent to (11). The equation (11) is found for larger k from (10) by the principle of the mathematical induction.

Fix $k, k \geq 3$ and let the equation (8) holds for $n = 2, 3, \dots, k - 1$. From (10), we arrive

$$|X_k|^2 \leq \frac{4(1 - \sigma)\cos^2\vartheta}{(k - 1)^2(1 - \nu)^2} \left\{ 1 - \sigma + \sum_{n=2}^{k-1} X(n, j, \sigma) \right\}, \tag{12}$$

where

$$X(n, j, \sigma) = \frac{(1 + (n - 1)\nu)(n - \sigma(n - 1)\nu)}{((n - 1)!(1 - \nu)^{n-1})^2} \prod_{j=0}^{n-2} |j(1 - \nu) + 2(1 - \sigma)e^{i\vartheta} \cos\vartheta(1 + \nu j)|^2.$$

Now, we will indicate that the square of RSH of (11) is equal to RSH of (12), that is,

$$\begin{aligned} & \prod_{j=0}^{k-2} \frac{|j(1 - \nu) + 2(1 - \sigma)e^{i\vartheta} \cos\vartheta(1 + \nu j)|^2}{((k - 1)!(1 - \nu)^{k-1})^2} \\ & = \frac{4(1 - \sigma)\cos^2\vartheta}{(k - 1)^2(1 - \nu)^2} \left\{ 1 - \sigma + \sum_{n=2}^{k-1} X(n, j, \sigma) \right\} \end{aligned} \tag{13}$$

for $k = 3, 4, \dots$. After further calculations, we indicate that (13) is true for $k = 3$ and prove the claim. Assume the equation (13) is valid for all $n, 3 < n \leq (k - 1)$.

From (9) and (12), we find

$$\begin{aligned}
 |X_k|^2 &\leq \frac{4(1-\sigma)\cos^2\vartheta}{(k-1)^2(1-\nu)^2} \left\{ 1 - \sigma + \sum_{n=2}^{k-2} X(n, j, \sigma) + X(k-1, j, \sigma) \right\} \\
 &\leq \frac{4(1-\sigma)\cos^2\vartheta}{(k-1)^2(1-\nu)^2} \times \left\{ 1 - \sigma + \sum_{n=2}^{k-2} \frac{(1+(n-1)\nu)(n-\sigma(n-1)\nu)}{((n-1)!(1-\nu)^{n-1})^2} \right. \\
 &\quad \times \prod_{j=0}^{n-2} |j(1-\nu) + 2(1-\sigma)e^{i\vartheta}\cos\vartheta(1+\nu j)|^2 \\
 &\quad + \frac{(1+(k-2)\nu)(k-1-\sigma(k-2)\nu)}{((k-2)!(1-\nu)^{k-2})^2} \\
 &\quad \left. \times \prod_{j=0}^{k-3} |j(1-\nu) + 2(1-\sigma)e^{i\vartheta}\cos\vartheta(1+\nu j)|^2 \right\} \\
 &= \frac{\prod_{j=0}^{k-3} |j(1-\nu) + 2(1-\sigma)e^{i\vartheta}\cos\vartheta(1+\nu j)|^2}{((k-2)!(1-\nu)^{k-2})^2} \\
 &\quad \times \left\{ \frac{(k-2)^2}{(k-1)^2} + \frac{4(1-\sigma)\cos^2\vartheta(1+(k-2)\nu)(k-1-\sigma(k-2)\nu)}{(k-1)^2(1-\nu)^2} \right\} \\
 &= \frac{\prod_{j=0}^{k-3} |j(1-\nu) + 2(1-\sigma)e^{i\vartheta}\cos\vartheta(1+\nu j)|^2}{((k-1)!(1-\nu)^{k-1})^2} \\
 &\quad \times \left\{ (k-2)^2(1-\nu)^2 + 4(1-\sigma)\cos^2\vartheta(1+(k-2)\nu)(k-1-\sigma(k-2)\nu) \right\}
 \end{aligned}$$

yields

$$|X_k| \leq \frac{1}{((k-1)!(1-\nu)^{k-1})^2} \prod_{j=0}^{k-2} |j(1-\nu) + 2(1-\sigma)e^{i\vartheta}\cos\vartheta(1+\nu j)|^2.$$

Since

$$X_k = \frac{\Gamma_q(\beta+k)\Gamma_q(\alpha+\beta+1)}{\Gamma_q(\alpha+\beta+k)\Gamma_q(\beta+1)} a_k \quad (X_1 = 1),$$

we obtain the desired result.

To prove the estimate is sharp, we need following equality

$$\chi_{\beta,q}^\alpha f(\zeta) = \frac{\zeta}{(1+K\zeta)^{\frac{2(\sigma-1)e^{-i\vartheta}\cos\vartheta}{K}}}$$

where $K = (1-\nu) - 2\nu(1-\sigma)e^{-i\vartheta}\cos\vartheta$. □

3. CONCLUSIONS

It is obvious that the link between q -calculus and Geometric Function Theory presents original and interesting results. Hence, in the present work, we use a generalized q -integral operator to establish a new subfamily $SC_{\beta,q}^{\alpha}(\sigma, \nu)$ of ϑ -spirallike functions. We also derive sharp upper bounds for Taylor Maclaurin coefficients of functions in this family.

Letting $\alpha = 1$, we have coefficients bounds for functions defined by q -Bernardi integral operator.

Corollary 1. *Let $J_{\beta,q}f(\zeta) \neq 0$ for $\zeta \in \mathcal{D} \setminus \{0\}$. If f is in $SC_{\beta,q}(\sigma, \nu)$, then*

$$|a_k| \leq \frac{[\beta + k]_q}{[\beta + 1]_q (k-1)! (1-\nu)^{k-1}} \prod_{j=0}^{k-2} |j(1-\nu) + 2(1-\sigma)e^{i\vartheta} \cos\vartheta(1+\nu j)|,$$

where $k \in \mathbb{N} \setminus \{1\}$ with $a_1 = 1$. This result is sharp.

Letting $\alpha = 1$ and $q \rightarrow 1^-$, we obtain following coefficients bounds for functions given by Bernardi integral operator.

Corollary 2. *Let $J_{\beta}f(\zeta) \neq 0$ for $\zeta \in \mathcal{D} \setminus \{0\}$. If f is in $SC_{\beta}(\sigma, \nu)$, then*

$$|a_k| \leq \frac{(\beta + k)}{(\beta + 1)(k-1)! (1-\nu)^{k-1}} \prod_{j=0}^{k-2} |j(1-\nu) + 2(1-\sigma)e^{i\vartheta} \cos\vartheta(1+\nu j)|,$$

where $k \in \mathbb{N} \setminus \{1\}$ with $a_1 = 1$. This result is sharp.

If $\alpha = 1$, $\beta = 0$ and $q \rightarrow 1^-$, we have following result for functions given in terms of Alexander integral operator.

Corollary 3. *Let $J_0f(\zeta) \neq 0$ for $\zeta \in \mathcal{D} \setminus \{0\}$. If f is in $SC(\sigma, \nu)$, then*

$$|a_k| \leq \frac{k}{(k-1)! (1-\nu)^{k-1}} \prod_{j=0}^{k-2} |j(1-\nu) + 2(1-\sigma)e^{i\vartheta} \cos\vartheta(1+\nu j)|,$$

where $k \in \mathbb{N} \setminus \{1\}$ with $a_1 = 1$. This result is sharp.

Our consequences are also applicable for various subfamilies of analytic functions.

Author Contribution Statements The authors contributed equally to this work.

Declaration of Competing Interests The authors declare that they have no known competing financial interest.

REFERENCES

- [1] Ahuja, O. P., Çetinkaya, A., Use of quantum calculus approach in mathematical sciences and its role in geometric function theory, *AIP Conference Proceedings*, 2095 (1) (2019), 1-14.
- [2] Altinkaya, Ş., On the inclusion properties for ϑ -spirallike functions involving both Mittag-Leffler and Wright function, *Turkish J. Math.*, 46 (3) (2022), 1119-1131. <https://doi.org/10.55730/1300-0098.3147>
- [3] Aouf, M. K., Seoudy, T. M., Convolution properties for classes of bounded analytic functions with complex order defined by q -derivative operator, *Rev. Real Acad. Cienc. Exactas Fis. Nat. Ser. A-Mat.*, 113 (2) (2019), 1279-1288. <https://doi.org/10.1007/s13398-018-0545-5>
- [4] Bernardi, S. D., Convex and starlike univalent functions, *Trans. Amer. Math. Soc.*, 135 (1969), 429-446.
- [5] Bulut, S., Certain subclasses of analytic and bi-univalent functions involving the q -derivative operator, *Commun. Fac. Sci. Univ. Ank. Ser. A1 Math. Stat.*, 66 (1) (2017), 108-114. <https://doi.org/10.1501/Commua1-0000000780>
- [6] Gasper, G., Rahman, M., Basic hypergeometric series, second edition, Encyclopedia of Mathematics and its Applications, 96, Cambridge University Press, Cambridge, 2004.
- [7] Govindaraj, M., Sivasubramanian, S., On a class of analytic functions related to conic domains involving q -calculus, *Anal. Math.*, 43 (3) (2017), 475-487. <https://doi.org/10.1007/s10476-017-0206-5>
- [8] Jackson, F.H., On q -functions and a certain difference operator, *Earth and Environmental Science Transactions of the Royal Society of Edinburgh*, 46 (1908), 253-281. <https://doi.org/10.1017/S0080456800002751>
- [9] Jackson, F. H., On q -definite integrals, *Quart. J. Pure Appl. Math.*, 14 (1910), 193-203.
- [10] Libera, R. J., Univalent α -spiral functions, *Canadian Journal of Mathematics*, 19 (1967), 449-456.
- [11] Mahmood, S., Raza, N., Abujarad, E. S. A., Srivastava, G., Srivastava, H. M., Malik, S. N., Geometric properties of certain classes of analytic functions associated with q -integral operators, *Symmetry*, 11 (2019), 719.
- [12] Mustafa, N., Korkmaz, S., The Sharp Inequality for the coefficients of certain subclass of analytic functions defined by q -derivative, *Journal of Scientific and Engineering Research*, 7 (4) (2020), 209-218.
- [13] Noor, K. I., Riaz, S., Noor, M. A., On q -Bernardi integral operator, *TWMS J. Pure Appl. Math.*, 8 (1) (2017), 3-11.
- [14] Purohit, S. D., Raina, R. K., Certain subclasses of analytic functions associated with fractional q -calculus operators, *Mathematica Scandinavica*, (2011), 55-70.
- [15] Raza, M., Srivastava, H. M., Arif, M., Ahmad, K., Coefficient estimates for a certain family of analytic functions involving a q -derivative operator, *Ramanujan J.*, 55 (1) (2021), 53-71. <https://doi.org/10.1007/s11139-020-00338-y>
- [16] Shareef, Z., Hussain, S., Darus, M., Convolution operators in the geometric function theory, *J. Inequal. Appl.*, 2012 (2012), 213.
- [17] Spacek, L., Contribution a la theorie des fonctions univalentes, *Casopis Pro Pestovani Matematiky a Fysiky*, 62 (1933), 12-19.
- [18] Srivastava, H. M., Univalent functions, fractional calculus, and associated generalized hypergeometric functions, in *Univalent Functions, Fractional Calculus, and Their Applications* (H. M. Srivastava and S. Owa, Editors), Halsted Press (Ellis Horwood Limited, Chichester), John Wiley and Sons, New York, Chichester, Brisbane and Toronto, 1989.
- [19] Srivastava, H. M., Operators of basic (or q -) calculus and fractional q -calculus and their applications in geometric function theory of complex analysis, *Iran J Sci Technol Trans Sci.*, 44 (1) (2020), 327-344. <https://doi.org/10.1007/s40995-019-00815-0>

- [20] Xu, Q. H., Cai, Q. M., Srivastava, H. M., Sharp coefficient estimates for certain subclasses of starlike functions of complex order, *Appl. Mathe. Comput.*, 225 (2013), 43-49.
- [21] Yavuz, T., Coefficient estimates for certain subclass for spirallike functions defined by means of generalized Attiya-Srivastava operator, *Commun. Korean Math. Soc.*, 31 (4) (2016), 703-712.

INSTRUCTIONS TO CONTRIBUTORS

Communications Faculty of Sciences University of Ankara Series A1 Mathematics and Statistics (Commun. Fac. Sci. Univ. Ank. Ser. A1 Math. Stat.) is a single-blind peer reviewed open access journal which has been published biannually since 1948 by Ankara University, accepts original research articles written in English in the fields of Mathematics and Statistics. It will be published four times a year from 2022. Review articles written by eminent scientists can also be invited by the Editor.

The publication costs for Communications Faculty of Sciences University of Ankara Series A1 Mathematics and Statistics are covered by the journal, so authors do not need to pay an article-processing and submission charges. The PDF copies of accepted papers are free of charges and can be downloaded from the website. Hard copies of the paper, if required, are due to be charged for the amount of which is determined by the administration each year.

All manuscripts should be submitted via our online submission system <https://dergipark.org.tr/en/journal/2457/submission/step/manuscript/new>. Note that only two submissions per author per year will be considered. Once a paper is submitted to our journal, all co-authors need to wait 6 months from the submission date before submitting another paper to Commun. Fac. Sci. Univ. Ank. Ser. A1 Math. Stat. Manuscripts should be submitted in the PDF form used in the peer-review process together with the COVER LETTER and the TEX file (Source File). In the cover letter the authors should suggest the most appropriate Area Editor for the manuscript and potential four reviewers with full names, universities and institutional email addresses. Proposed reviewers must be experienced researchers in your area of research and at least two of them should be from different countries. In addition, proposed reviewers must not be co-authors, advisors, students, etc. of the authors. In the cover letter, the author may enter the name of anyone who he/she would prefer not to review the manuscript, with detailed explanation of the reason. Note that the editorial office may not use these nominations, but this may help to speed up the selection of appropriate reviewers.

Manuscripts should be typeset using the LATEX typesetting system. Authors should prepare the article using the Journal's templates (commun.cls and comun.cts). Manuscripts written in AMS LaTeX format are also acceptable. A template of manuscript can be downloaded in tex form from the link <https://dergipark.org.tr/en/download/journal-file/22173> (or can be reviewed in pdf form). The title page should contain the title of the paper, full names of the authors, affiliations addresses and e-mail addresses of all authors. Authors are also required to submit their Open Researcher and Contributor ID (ORCID)'s which can be obtained from <http://orcid.org> as their URL address in the format <http://orcid.org/xxxx-xxxx-xxxx-xxxx>. Please indicate the corresponding author. Each manuscript should be accompanied by classification numbers from the Mathematics Subject Classification 2020 scheme. The abstract should state briefly the purpose of the research. The length of the Abstract should be between 50 to 5000 characters. At least 3 keywords are required. Formulas should be numbered consecutively in the parentheses. All tables must have numbers (TABLE 1) consecutively in accordance with their appearance in the text and a legend above the table. Please submit tables as editable text not as images. All figures must have numbers (FIGURE 1) consecutively in accordance with their appearance in the text and a caption (not on the figure itself) below the figure. Please submit figures as EPS, TIFF or JPEG format. Authors Contribution Statement, Declaration of Competing Interests and Acknowledgements should be given at the end of the article before the references. Authors are urged to use the communication.bst style in BibTeX automated bibliography. If manual entry is preferred for bibliography, then all citations must be listed in the references part and vice versa. Number of the references (numbers in squared brackets) in the list can be in alphabetical order or in the order in which they appear in the text. Use of the DOI is highly encouraged. Formal abbreviations of the journals can be used. The Editor may seek the advice of two, or three referees, depending on the response of the referees, chosen in consultation with appropriate members of the Editorial Board, from among experts in the field of specialization of the paper. The reviewing process is conducted in strict confidence and the identity of a referee is not disclosed to the authors at any point since we use a single-blind peer review process.

Copyright on any open access article in Communications Faculty of Sciences University of Ankara Series A1-Mathematics and Statistics is licensed under a [Creative Commons Attribution 4.0 International License](https://creativecommons.org/licenses/by/4.0/) (CC BY). Authors grant Faculty of Sciences of Ankara University a license to publish the article and identify itself as the original publisher. Authors also grant any third party the right to use the article freely as long as its integrity is maintained and its original authors, citation details and publisher are identified. It is a fundamental condition that articles submitted to COMMUNICATIONS have not been previously published and will not be simultaneously submitted or published elsewhere. After the manuscript has been accepted for publication, the author will not be permitted to make any new additions to the manuscript. Before publication the galley proof is always sent to the author for correction. Thus it is solely the author's responsibility for any typographical mistakes which occur in their article as it appears in the Journal. The contents of the manuscript published in the COMMUNICATIONS are the sole responsibility of the authors.

Declarations/Ethics:

With the submission of the manuscript authors declare that:

- All authors of the submitted research paper have directly participated in the planning, execution, or analysis of study;
- All authors of the paper have read and approved the final version submitted;
- The contents of the manuscript have not been submitted, copyrighted or published elsewhere and the visual-graphical materials such as photograph, drawing, picture, and document within the article do not have any copyright issue;
- The contents of the manuscript will not be copyrighted, submitted, or published elsewhere, while acceptance by the Journal is under consideration.
- The article is clean in terms of plagiarism, and the legal and ethical responsibility of the article belongs to the author(s). Author(s) also accept that the manuscript may go through plagiarism check using iThenticate software;
- The objectivity and transparency in research, and the principles of ethical and professional conduct have been followed. Authors have also declared that they have no potential conflict of interest (financial or non-financial), and their research does not involve any human participants and/or animals.

Research papers published in **Communications Faculty of Sciences University of Ankara** are archived in the [Library of Ankara University](#) and in [Dergipark](#) immediately following publication with no embargo.

Editor in Chief

<http://communications.science.ankara.edu.tr>

Ankara University, Faculty of Sciences

06100, Besevler - ANKARA TURKEY

COMMUNICATIONS

FACULTY OF SCIENCES
UNIVERSITY OF ANKARA

DE LA FACULTE DES SCIENCES
DE L'UNIVERSITE D'ANKARA

Series A1: Mathematics and Statistics

Volume: 72

Number: 4

Year: 2023

Research Articles

Semra YURTTANÇIKMAZ, On the curves lying on parallel-like surfaces of the ruled surface in E^3	867
Süleyman ŞENYURT, Davut CANLI, Elif ÇAN, Sümeyye GÜR MAZLUM, Another application of Smarandache based ruled surfaces with the Darboux vector according to Frenet frame in E^3	880
Fatma TOKMAK FEN, Mehmet Onur FEN, Modulo periodic Poisson stable solutions of dynamic equations on a time scale.....	907
Thatayaone MOAKOFI, Broderick OLUYEDE, The type I heavy-tailed odd power generalized Weibull-G family of distributions with applications.....	921
Esra BAŞARIR NOYAN, Yılmaz GÜNDÜZALP, Quasi hemi-slant pseudo-Riemannian submersions in para-complex geometry.....	959
Jeevitha KANNAN, Vimala JAYAKUMAR, Sustainable method for tender selection using linear Diophantine multi-fuzzy soft set.....	976
Nurettin IRMAK, A Diophantine equation including Fibonacci and Fibonomial coefficients.....	992
Babar SULTAN, Mehvish SULTAN, Ferit GÜRBÜZ, BMO estimate for the higher order commutators of Marcinkiewicz integral operator on grand variable Herz-Morrey spaces.....	1000
Asia K, Shahid KHAN, Demonstration of the strength of strong convexity via Jensen's gap.....	1019
Melike KARTA, Numerical approximation with the splitting algorithm to a solution of the modified regularized long wave equation.....	1034
Yıldırım ÇELİK, Renewed structure of neutrosophic soft graphs and its application in decision-making problem.....	1055
Özgül İLHAN, Osman Raşit IŞIK, Simge BOZKURT, Numerical analysis of a time relaxation finite difference method for the heat equation.....	1077
Hazal CEYHAN, Ebru YANIK, Zehra OZDEMİR, Anholonomic co-ordinates and electromagnetic curves with alternative moving frame via Maxwell evolution.....	1094
Çağla SEKİN, Mehmet Emin TAMAR, İlham ALİYEV, New proofs of Fejer's and discrete Hermite-Hadamard inequalities with applications.....	1110
Hesham MOUSTAFA, Mansour MAHMOUD, Ahmed TALAT, Some bounds for the k-generalized digamma function.....	1126
Güler Başak ÖZNUR, Güher Gülçehre ÖZBEY, Yelda AYGAR KÜÇÜKEVCİLİOĞLU, Rabia AKTAŞ, Miscellaneous properties of Sturm-Liouville problems in multiplicative calculus.....	1141
Angelin KAVITHA RAJ, S. N. Suber BATHUSHA, Satham HUSSAIN, Self centered interval-valued intuitionistic fuzzy graph with an application.....	1155
Nezakat JAVANSHIR, Filiz YILDIZ, Various results on some asymmetric types of density.....	1173
Cengiz GAZELOĞLU, Asuman ZEYTİNOĞLU, Nurullah YILMAZ, A new multidimensional model II regression based on bisector approach.....	1187
Tuğba YAVUZ, Şahsene ALTINKAYA, Sharp coefficient estimates for \mathfrak{g} -spirallike functions involving generalized q-integral operator.....	1201